REPORT NO. F694
31 AUGUST 1967

PART B5 ALTERNATIVES, ANALYSES, SELECTION

3

VOYAGER CAPSULE PHASE B FINAL REPORT

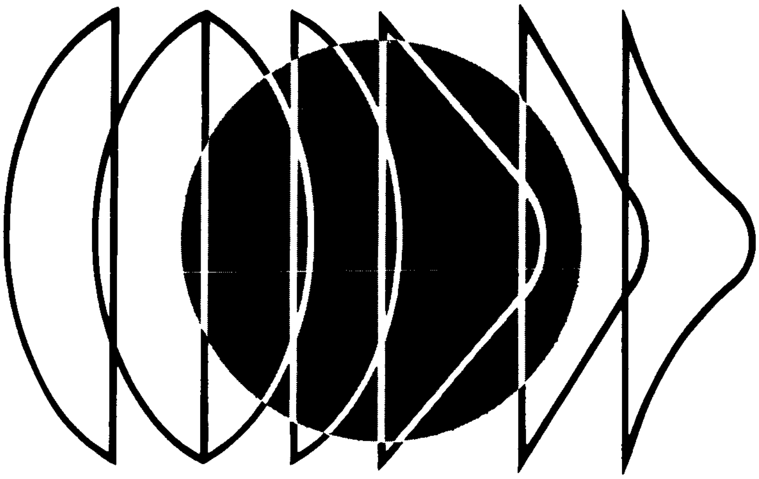

VOLUME II CAPSULE BUS SYSTEM

PREPARED FOR:
CALIFORNIA INSTITUTE OF TECHNOLOGY
JET PROPULSION LABORATORY
PASADENA, CALIFORNIA
CONTRACT NUMBER 952000

COPY NO. 47

MCDONNELL ASTRONAUTICS

REPORT ORGANIZATION

VOYAGER PHASE B FINAL REPORT

The results of the Phase B Voyager Flight Capsule study are organized into several volumes. These are:

Volume I	Summary
Volume II	Capsule Bus System
Volume III	Surface Laboratory System
Volume IV	Entry Science Package
Volume V	System Interfaces
Volume VI	Implementation

This volume, Volume II, describes the McDonnell Douglas preferred design for the Capsule Bus System. It is arranged in 5 parts, A through E, and bound in 11 separate documents, as noted below.

Part A	Preferred Design Concept	2 documents, Parts A_1 and A_2
Part B	Alternatives, Analyses, Selection	5 documents, Parts B_1, B_2, B_3, B_4 and B_5
Part C	Subsystem Functional Descriptions	2 documents, Parts C_1 and C_2
Part D	Operational Support Equipment	1 document
Part E	Reliability	1 document

In order to assist the reader in finding specific material relating to the Capsule Bus System, Figure 1 cross indexes broadly selected subject matter, at the system and subsystem level, through all volumes.

VOLUME II CROSS REFERENCE INDEX

SYSTEM/SUBSYSTEM	VOLUME II PARTS	PART A	PART B	PART C	PART D	PART E
		DESCRIPTION OF PREFERRED SYSTEM OBJECTIVES, MISSION, DESIGN, SUBSYSTEMS, OPERATIONS, SUPPORTING FUNCTIONS	ALTERNATIVES, ANALYSIS AND SELECTION – METHODS TRADE STUDIES, OPTIMIZATION STUDIES RESULTS	DETAILED DESCRIPTION OF SUBSYSTEM FUNCTIONS	OPERATIONAL SUPPORT EQUIPMENT – SYSTEM, SUBSYSTEM, LAUNCH COMPLEX, MISSION, HANDLING, SOFTWARE	RELIABILITY CONSTRAINTS, ANALYSIS, RESULTS, PROGRAM TESTING, CONTROL
CAPSULE BUS SYSTEM						
Mission	Objectives	1.1–Summary	2–Analysis	N/A	1–General	1–Constraints
	Profile	1.2–Summary	2–Analysis 2.4–Selection	N/A	N/A	3.1.1–Analysis
	Operations	4–Description by Phase	2.3–Analysis 2.3.7–Landing Site Select	N/A	4.4–LCE Description 4.5–MDE Description	3–Estimates
Design	General	2–Criteria Summary 3.1–Configuration	1–Study Approach 3–Functional Requirements	N/A	3.2–Concept 3.3–Summary 6.1–AHSE	4–Program Requirements 5–Component Reliability
	Standardization/Growth	2.5–Summary 11–Future	(See Specific Subsystem Below)	N/A	4.3.8-STC 4.4.8-LCE 4.5.8-MDE } Growth	N/A
	Weight	3.1.2.4–Summary 5–Breakdown	(See Specific Subsystem Below)	N/A	N/A	2.3.2–Reliability vs Weight
Interfaces (See Also Vol. V)		3.1–Summary 9.0–Operational	(See Volume V)	N/A	4.2.1,4.3.5,4.4.5, 4.5.5	N/A
Implementation (See Also Vol. VI)		10–Schedule 8.11–OSE	(See Volume VI)	N/A	(See Specific Subsystem Below)	N/A
Planetary Quarantine		7–General	(See Volume VI, C,7 Sterilization Plan)	N/A	None Required	N/A
O.S.E. (See Also Part D)		8–General (See Also–D1,D2, D3,D4)	(See D2.5-Selection Criteria, D9-Analysis, DIO - Alternatives)	(See D5-Subsystem Level Test Equipment, See Also D4, D6, D7)	Complete OSE Description	(See D4.3.6–STC D4.4.6–LCE D4.5.6–MDE)
SUBSYSTEMS						
Sterilization Canister		3.2.1.1–Description 3.1.2–Summary	5.1–Analysis	1.1	6.1.5.2,6.1.5.3, 6.1.5.6 6.1.5.8–AHSE 6.2.15–Servicing	(See Part C Sections 1.1.1.7 1.1.2.7 1.1.3.7)
Adapter		3.2.1.2–Description 3.1.2–Summary	5.2–Analysis	1.2	None Required	(See Part C, 1.2.7)
Aeroshell		3.2.1.3–Description	4.1–Configuration	1.3	None Required	(See Part C, 1.3.7)

Figure 1

	3.1.2–Summary	Selection 4.6–Separation 5.3.1–Structure 5.3.2–Heat Shield			
Lander	3.2.1.4–Description 3.1.2–Summary	4.2–Configuration Selection 5.4–Analysis	1.4	6.1.5.9–Fixture	(See Part C, 1.4.7)
Telecommunications	3.2.2.1–Description	4.9–In-Flight Monitoring 5.5–Analysis	2–Telemetry 3–Radio 4–Antenna 5–Data Storage 6–Command	4.3.9.1–STC Console 5.7–Test Set	(See Part C, Sections 2.1.7, 2.2.7, 2.3.7, 3.1.7, 3.2.7, 4.5, 5.1.7, 5.2.7, 6.1.7, 6.2.7)
Power	3.2.2.2–Description	5.6–Analysis	7	4.3.9.1–STC Console 5.3–Test Set	(See Part C, Sect. 7.7)
Sequencing and Timing	3.2.2.3–Description	5.7–Analysis	8	4.3.9.1–STC Console 5.4–Test Set	(See Part C Sections 8.1.7, 8.2.7)
Guidance and Control	3.2.2.4–Description	4.7–De-orbit Attitube Reqm't. 5.8–Analysis	9	4.3.9.1–STC Console 5.5–Test Set	(See Part C, 9.7)
Radar	3.2.2.5–Description	5.9–Analysis	10	4.3.9.1–STC Console 5.6–Test Set	(See Part C, Sections 10.1.7, 10.2.7)
Aerodynamic Decelerator	3.2.3–Description	4.4–Selection 5.10–Analysis	11	None Required	(See Part C, 11.7)
Pyrotechnics	3.2.4–Description	5.11–Analysis	12	4.3.9.1–STC Console 5.9–Test Set	(See Part C, 12.7.1)
Thermal Control	3.2.5–Description	5.12–Analysis	13	4.3.9.1–STC Console 5.8–Test Set	(See Part C, 13.6)
De-orbit Propulsion	3.2.6.1–Description	5.13.1–Analysis	14	5.10–Test Set 6.1.5.10–AHSE	(See Part B, 5.13.4.5) (See Part C, 14.7)
Reaction Control	3.2.6.2–Description	5.13.2–Analysis	15	5.10–Test Set 6.2–Servicing	(See Part B, 5.13.4.5) (See Part C, 15.7)
Terminal Propulsion	3.2.6.3–Description	4.3–Configuration Selection 4.5–Terminal Deceleration 5.13.3–Analysis	16	4.3.9.1–STC Console 5.10–Test Set 6.2–Servicing	(See Part B, 5.13.4.5) (See Part C, 16.7)
Packaging and Cabling	3.2.7–Description	5.14–Analysis	17	4.3.9.8–Special Purpose Complex Equipment	Not Required

Note: Parentheses Refer Reader to Volumes/Parts Outside of the Respective Notation

TABLE OF CONTENTS

Page

SECTION 5.10 AERODYNAMIC DECELERATOR SUBSYSTEM 5.10-1
- 5.10.1 Constraints 5.10-1
- 5.10.2 Analysis of Subsystem Sizing and Sequence 5.10-2
- 5.10.3 Summary of Subsystem Operational Environment And Performance 5.10-27

SECTION 5.11 PYROTECHNICS 5.11-1
- 5.11.1 Functional And Technical Requirements 5.11-1
- 5.11.2 Alternate Approaches 5.11-1
- 5.11.3 Standardization 5.11-11
- 5.11.4 Standardization Problem Areas 5.11-11
- 5.11.5 Standardization Alternatives 5.11-12
- 5.11.6 Recommended Design Approach 5.11-13

SECTION 5.12 THERMAL CONTROL 5.12-1
- 5.12.1 Thermal Control for Missions Utilizing Battery Power in SLS 5.12-1
- 5.12.2 Thermal Control for Mission Utilizing RTG Power in SLS 5.12-8

SECTION 5.13 PROPULSION 5.13-1
- 5.13.1 De-Orbit Propulsion 5.13-3
- 5.13.2 Attitude Control 5.13-42
- 5.13.3 Terminal Propulsion 5.13-72
- 5.13.4 Supporting Design Studies 5.13-113

SECTION 5.14 PACKAGING AND CABLING 5.14-1

SECTION 5.15 INDEPENDENT DATA PACKAGE 5.15-1
- 5.15.1 Mission Considerations and Constraints 5.15-10
- 5.15.2 IDP Operation Studies 5.15-13
- 5.15.3 Environmental Measurement Studies 5.15-24
- 5.15.4 IDP Electronic Subject Studies 5.15-32
- 5.15.5 IDP Mechanical Subject Studies 5.15-47

This Document Consists of the Following Pages:

Title Page
i through iii
5.10-1 through 5.10-35
5.11-1 through 5.11-14
5.12-1 through 5.12-14
5.13-1 through 5.13-178
5.14-1 through 5.14-7
5.15-1 through 5.15-79

5.10 AERODYNAMIC DECELERATOR SUBSYSTEM

- The conclusion reached in the aerodynamic decelerator trade study (Section 4.4) is that a parachute is the preferred type of aerodynamic decelerator for the VOYAGER Capsule Bus. However, that trade study was not concerned with how or when to deploy the parachute, nor did it treat the practical problems of a detailed system design. The purpose of the following analysis is to examine the practical design problems, constraints, and performance requirements in the depth required to arrive at a detailed parachute system design. The final system design should satisfy as many of these demands as possible; however, it should not allow any one of them to force the system into marginal operation over a significant portion of the operational envelope.

5.10.1 Constraints

- The constraints which must be considered are similar to those normally imposed on the design of an entry vehicle aerodynamic decelerator subsystem. Specifically, these constraints are:

a. Aerodynamic decelerator performance capabilities
b. Aerodynamic decelerator trigger performance
c. Entry trajectory constraints
d. Related subsystem constraints

5.10.1.1 Aerodynamic Decelerator Performance Capabilities

- The Mach number, dynamic pressure, and density envelopes in which an aerodynamic decelerator operates in a predictable and reliable manner defines its performance capabilities. Very little is known about the performance of large parachute canopies operating supersonically at very low densities and dynamic pressures. One of the goals of the NASA Planetary Entry Parachute Program (PEPP) is to investigate the behavior of large canopies (diameter greater than 20 ft.) under these flight conditions. Although the test program is presently in progress and results are not complete, the tests to date have successfully demonstrated the supersonic operational feasibility of three "solid type" parachutes. These tests are being conducted at speeds up to approximately Mach 1.6 at very high Earth altitudes (above 100,000 ft.). In these tests the low density and dynamic pressure conditions encountered (density on the order of 1.0×10^{-5} slugs/ft^3 and dynamic pressure on the order of 10 psf or less) are very similar to the parachute deployment conditions expected during entry into the Martian atmosphere. Because these tests have been so successful, McDonnell feels it is not unreasonable to design for maximum parachute deployment at Mach 2. It may well be that the parachute could operate beyond Mach 2, but we feel such an assumption cannot be made at this time without additional development test data.

The effective drag coefficient of parachutes having low geometric and cloth porosity generally exhibits the tendency to increase as air density decreases over the range of Earth altitudes from sea level to approximately 50,000 ft. Above this level there is very little data to substantiate the continuance of this increasing drag trend, since most parachutes tested in that region are usually of the type having high geometric porosity (drogue chutes). The parachute drag data from the NASA PEPP tests is the best current source of applicable information available at this time. Data extracted from References 5.10-1 through 5.10-3 are shown correlated in Figure 5.10-1. Here C_{D_o} is based on the nominal area (S_o) which includes the open slots or gaps included to provide the desired geometric porosity. This data is from three tests on Ringsail and Disk-Gap-Band type parachutes. The Ringsail parachutes tested in balloon launch 1 and rocket launch 5 (data not shown) did not exhibit satisfactory inflation characteristics. An investigation of the construction of these parachutes (Reference 5.10-4) concluded that they did not inflate properly as a result of excessive total canopy porosity. Although designed to have 15% geometric porosity, these canopies had a much higher total porosity due to the crown porosity and cloth porosity (approximately 700 $ft^3/ft^2/min.$). In addition, the PEPP parachutes had suspension line lengths on the order of one diameter (D_o), and experience indicates that a 5% to 10% increase in drag coefficient can be realized by using 1.2 to 1.4 D_o suspension lines. Therefore, it appears reasonable to use a parachute drag coefficient (C_{D_o}) of .6 for system sizing purposes. In addition to improving drag characteristics, the use of suspension lines which are longer than normal improves the terminal descent stability of the parachute-payload system.

Knowledge of a parachute's opening characteristics and its associated opening shock factor is needed to properly design an aerodynamic decelerator subsystem. Because of the lack of data and understanding of parachute behavior under the low density, high velocity environment of the VOYAGER Capsule Lander, it is necessary to estimate these characteristics with whatever data may be available. Historically (Reference 5.10-5), parachute opening shock factor (X) has been found to be very dependent on the canopy unit loading ($W/C_{D_o}S_o$) parameter. The shock factor (X) is defined at $X = F_o/F_{SS}$, where F_o is the peak opening force experienced, and $F_{SS} = C_{D_o}S_o\ q$ is the steady state drag force that would be expected for the parachute operating at that dynamic pressure. Thus, the peak opening shock load is $F_o = XC_{D_o}S_oq$. The canopy unit loading is determined with Earth weights since "in the opening shock process, canopy loading represents a mass effect and therefore does not change with the acceleration of gravity" (Reference 5.10-5).

PARACHUTE DRAG COEFFICIENT FROM PEPP TEST

15% GEOMETRIC POROSITY

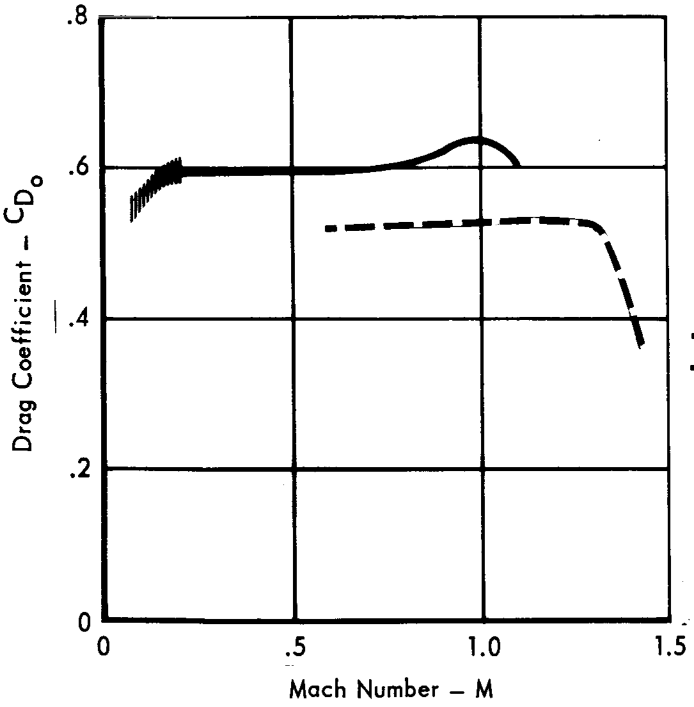

SYM	PARACHUTE	DIA–ft	PEPP TEST	REF.
▥	Ringsail	85.3	B/L 1	5.10–3
—	Ringsail	30.6	R/L 2	5.10–4
– –	Disk-Gap-Band	30.0	R/L 3	5.10–5

C_{D_o} Based on Nominal Area, S_o

S_o Includes all Slots, Vents, and Gaps

Figure 5.10–1

Figure 5.10-2 shows the opening shock factor computed from the opening load data from three PEPP tests plotted against the canopy unit loading. These data are for two different types of parachutes and for two major sizes. The two small (30 ft.) parachutes were not reefed; the large (85.3 ft.) parachute was reefed. Unfortunately, the 85.3 ft. parachute was reported to have poor opening characteristics so that the opening loads may have been lower than if it had opened properly. However, these are the only data available for use at this time, and the figure shows three curves drawn through the data points which will be used for preliminary estimates of the parachute opening shock loads. These estimated shock factors exhibit the same trend with increasing canopy loading as data from much lower altitude tests. These estimates will be revised as more test data becomes available from the PEPP tests.

5.10.1.2 Aerodynamic Decelerator Trigger Performance - The performance requirements of the device which triggers the deployment of a parachute is closely related to the performance capabilities of that parachute. This interdependency is in turn dependent on the known accuracy of the flight conditions to be encountered. Due to the wide latitude in the postulated VM atmospheric models, and the errors and uncertainties of the deorbit maneuver which requires the large design entry corridor, the expected atmospheric entry trajectories exhibit an extremely wide variation in their characteristics.

Throughout our VOYAGER studies we have examined several potential aerodynamic decelerator triggering devices. A few of the devices investigated include:

a. Accelerometers
b. Integrating accelerometers
c. Base pressure sensors
d. Time from a given acceleration (computer function)
e. Acceleration to maximum acceleration ratio (computer function)
f. Radar Altimeter

In general, we found that most of these devices exhibit a very large altitude-Mach number uncertainty that is so severe they become impractical. Other investigators have reached similar conclusions (Reference 5.10-6). As mentioned earlier we limited the maximum deployment Mach number to 2. Figure 5.10-3 shows, as a typical example, the aerodynamic decelerator deployment envelope for an integrating accelerometer trigger. This was one of the better triggering devices of those investigated in that it did control maximum deployment Mach number and minimum deployment altitude very well. However, it exhibited the usual tendency of allowing

OPENING SHOCK FACTOR DATA FROM PEPP TESTS

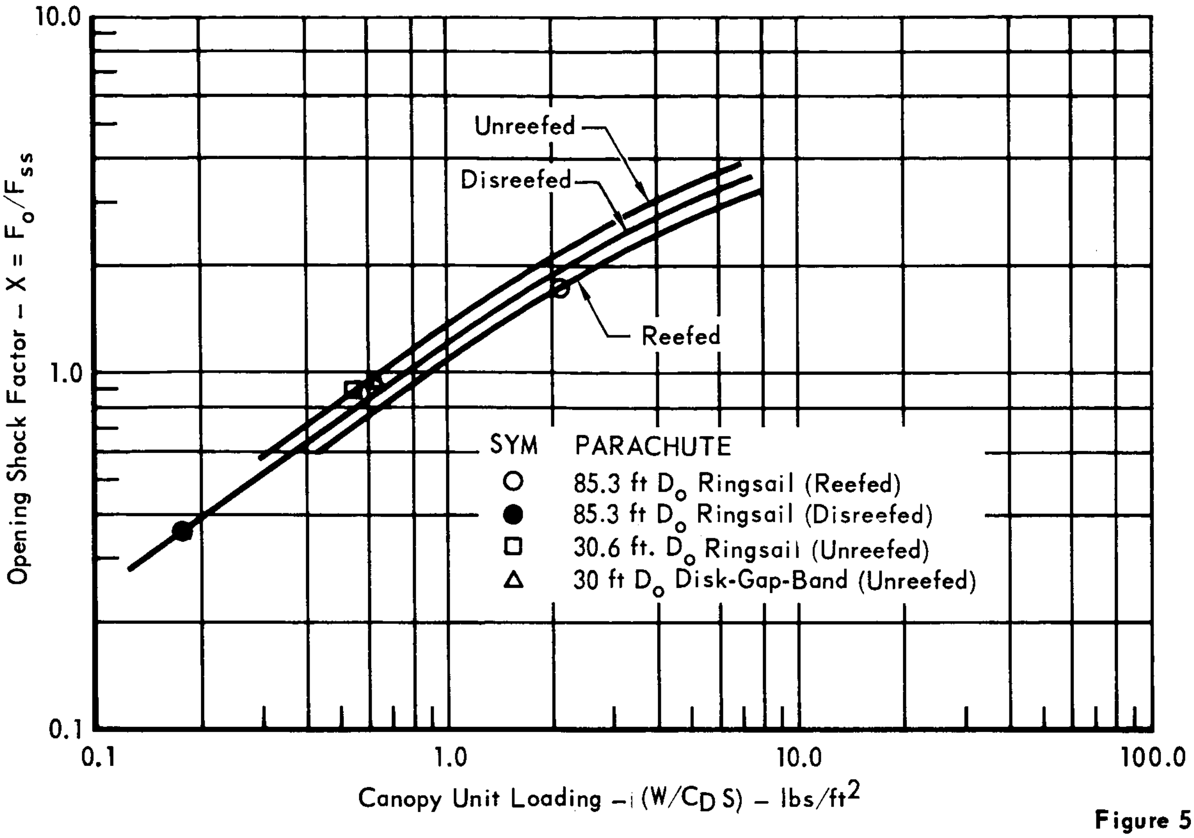

Figure 5.10-2

PARACHUTE DEPLOYMENT ENVELOPE FOR AN INTEGRATING ACCELEROMETER TRIGGER

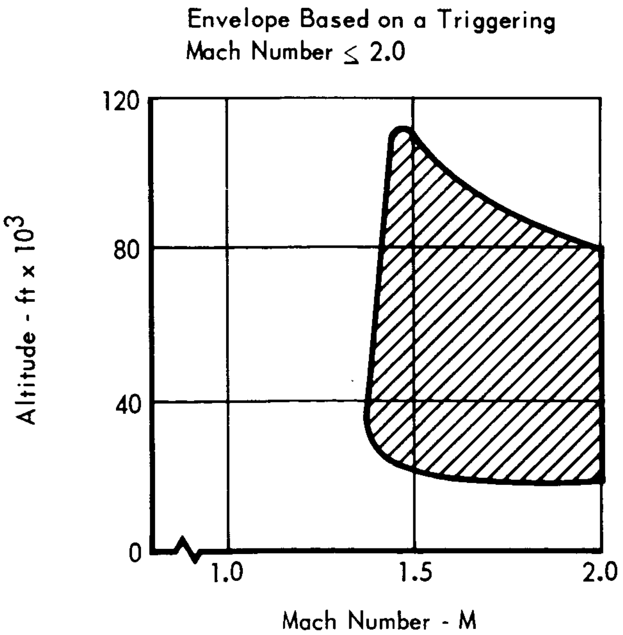

Figure 5.10-3

deployment at very high altitudes. This is undesirable because the excessively long descent time interferes with the post-landing data transmission requirement.

Preferred Trigger - Of all the devices investigated, the radar altimeter provides the best altitude-Mach number control at parachute deployment. It removes the large altitude spread and limits the maximum deployment Mach number, but it does have some Mach number uncertainty due to trajectory variations.

The radar altimeter has a distinct advantage over other triggers by guaranteeing that the parachute will be deployed at a preselected altitude above the local terrain. One drawback to this characteristic is that over highlands or mountainous regions, the parachute may be deployed beyond its Mach 2.0 limit. However, because a parachute is deployed above a given Mach number limitation, it does not necessarily mean the parachute will fail; it may not function as well as desired but may still perform its job.

For reasons outlined above, we believe that the radar altimeter is the best parachute triggering device, and we have based our aerodynamic decelerator subsystem design on its use.

Backup Trigger - For high mission success it is imperative that parachute deployment be initiated at the proper altitude by the signal from the radar altimeter. To insure operation of the radar altimeter we plan to provide internal redundancy in it. (See Section 5.9). If the altimeter fails to function properly, we plan to provide a backup trigger device to deploy the parachute. An integrating accelerometer (see Part A, Section 3.2.2.4) will be used to perform the backup function. Even though the integrating accelerometer is not a good primary trigger, it is a good backup and it improves the probability of successful landing. If the radar altimeter is functioning properly, the backup device is locked out to prevent it from generating the deployment signal before the altimeter.

5.10.1.3 Entry Trajectory Constraints - The basic characteristics of a ballistic atmospheric entry trajectory depend on the following parameters:

a. Atmospheric model
b. Entry conditions (altitude, V_e, and γ_e)
c. Vehicle ballistic parameter (m/C_DA)

Small perturbations on the basic characteristics can be caused by such things as the atmospheric winds, the vehicle's drag variation with Mach number, and the vehicle's angle of attack oscillations.

The entry altitude (800,000 ft) and the atmospheric models are specified in Reference 5.10-7, and the entry velocity and flight path angle corridor are shown in

Section 2.3.6. Basically, the entry corridor covers entry velocities from 13,000 to 15,000 ft/sec and entry flight path angles from vacuum graze to -20° from the horizontal.

The Capsule aerodynamic characteristics are shown in Section 2.3.6. With a Capsule diameter of 19 ft. and an entry weight of 3680 lbs, the entry ballistic parameter (m/C_DA) has a value of .266 slugs/ft^2.

Using the above parameters, our entry trajectory studies show that both the most severe Mach number and dynamic pressure conditions for parachute deployment occur for entry into the VM-8 atmosphere at 13,000 ft/sec and -20° flight path angle. The least severe conditions occur for entry into the VM-9 atmosphere at 13,000 ft/sec and at $\gamma_e = -20°$. These conditions, shown in Figure 5.10-4, define the extremes of the parachute deployment Mach number and dynamic pressure envelopes since all other entry conditions and atmospheres fall between these limits. The Mach number curve for VM-8 shows that, if the parachute is deployed at 23,000 ft or below, the Mach 2.0 limitation will not be exceeded.

5.10.1.4 Related Subsystem Constraints - The design of the aerodynamic decelerator subsystem has additional constraints imposed on it by the requirements or performance capabilities of other subsystems. These constraints are a result of the complete Capsule design and mode of operation. The related subsystems which affect the design and operation of the aerodynamic decelerator subsystem are:

a. Aeroshell/lander separation technique and timing

b. Terminal propulsion subsystems

Aeroshell/Lander Separation Technique and Timing - The preferred technique for separating the Aeroshell/lander uses the drag of the aerodynamic decelerator to extract the lander from the Aeroshell (see Section 4.6). This requirement establishes a minimum parachute size constraint since the parachute must have sufficient drag to extract the lander from the Aeroshell. This sizing is established by the drag-to-mass ratio of the Aeroshell and lander with parachute. For the parachute to provide good lander separation acceleration, the drag-to-mass ratio of the lander with parachute must exceed the drag-to-mass ratio of the Aeroshell. Figure 5.10-5 shows the effect of parachute size on the relative acceleration parameter "n" (in Earth g's) which defines the acceleration rate at which the two bodies separate. The parameter "n" is:

$$n = \frac{q}{W_L}\left[C_{D_o}S_o - (C_DS)_A \quad \frac{W_L}{W_A}\right]$$

where q = dynamic pressure at separation

PARACHUTE DEPLOYMENT ENVELOPE FOR THE PREFERRED FLIGHT CAPSULE

$m/C_DA = .266$ slugs/ft^2

$V_e = 13{,}000$ ft/sec, $\gamma_e = -20°$

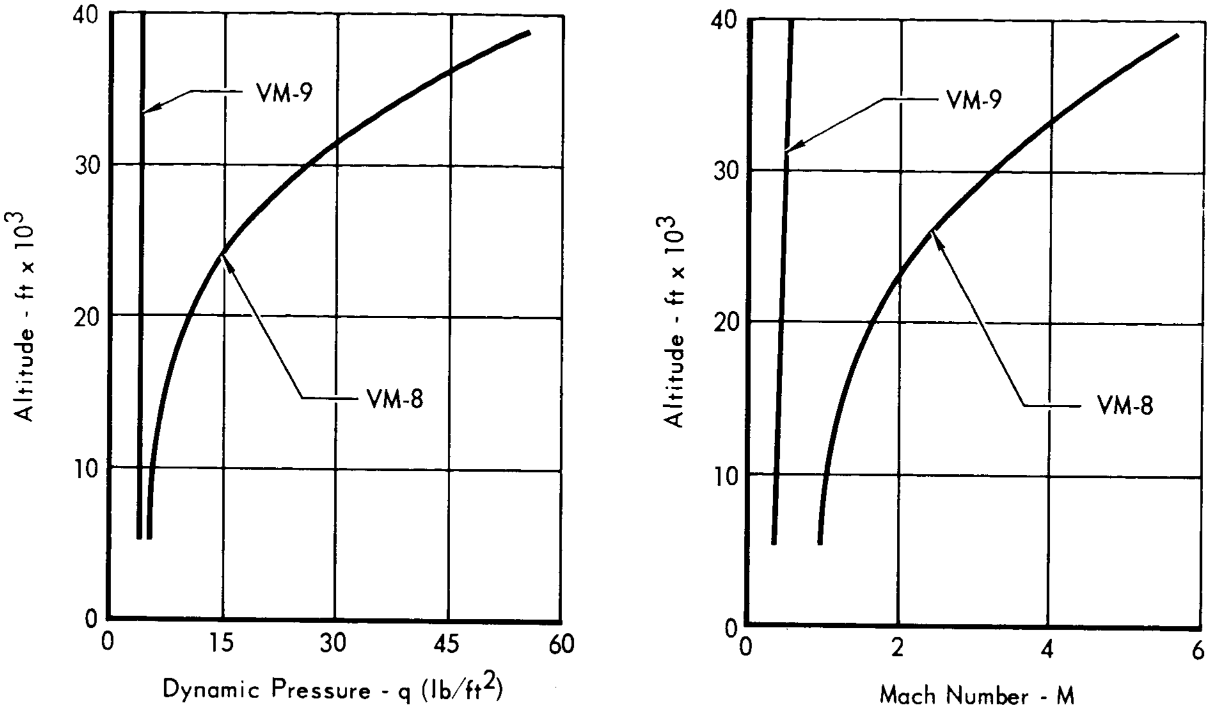

Figure 5.10-4

EFFECT OF PARACHUTE SIZE ON AEROSHELL/LANDER SEPARATION ACCELERATION

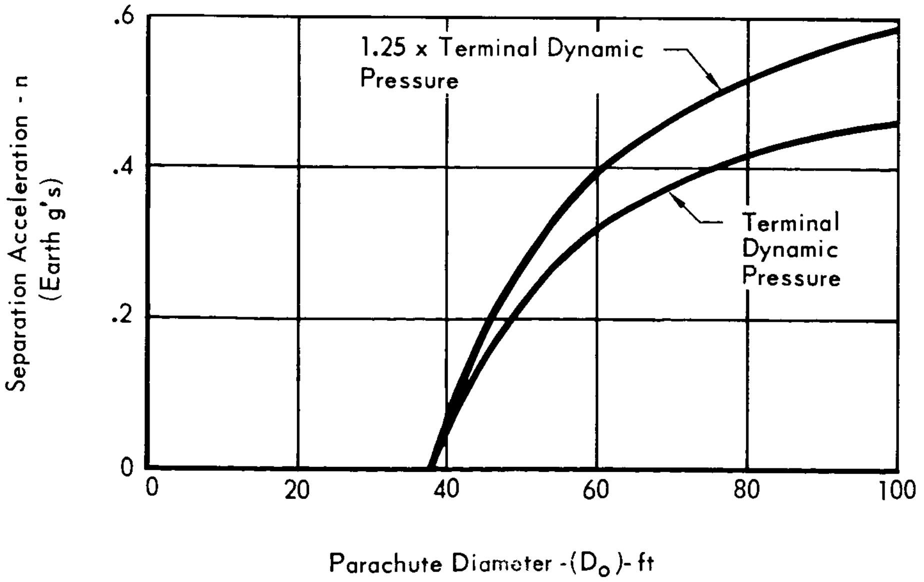

Figure 5.10-5

$C_{D_o}S_o$ = parachute drag area (ft^2)

$(C_DS)_A$ = Aeroshell drag area (ft^2)

W_L = weight of lander plus parachute (Earth lbs)

W_A = weight of Aeroshell (Earth lbs)

Note that Figure 5.10-5 is based on terminal descent dynamic pressure which defines the minimum separation dynamic pressure and thus the minimum parachute size. In this case the minimum parachute diameter is 38 ft. Parachutes smaller than this size will not effect separation. Note the curve labeled "1.25 dynamic pressure" shows that a smaller size parachute is required to attain a given level of separation acceleration. This trend indicates that the lander should be separated from the Aeroshell as soon as practical before the dynamic pressure reaches its terminal value. Therefore, a time delay should be used to release the Aeroshell/lander connection as soon as full parachute inflation is assured. As will be seen later, other constraints also require that Aeroshell/lander separation be initiated as soon after parachute deployment as possible.

Terminal Descent Subsystems - The terminal descent maneuver is accomplished by several systems working together to accomplish the goal of a controlled soft landing. The major subsystems contributing to this phase are the radar altimeter, terminal propulsion, guidance and control, and landing radar. Each of these, subsystems may contribute a constraint to the aerodynamic decelerator subsystem design because of a limitation peculiar to that subsystem design.

The radar altimeter imposes a constraint on the aerodynamic decelerator in that the Aeroshell should be as far from the lander as possible at the time the terminal descent phase begins. This is because the aft surfaces of the Aeroshell act like a reflector to return strong signals from it back to the radar altimeter (see Section 5.9). If the Martian surface is a poor reflector, the return signal from the Aeroshell may cause a false altitude indication in the radar altimeter and cause it to signal parachute release and to initiate the terminal descent phase. This constraint makes it highly desirable for the Aeroshell to have impacted on the surface before radar inputs are needed to initiate this phase. Because this is not always possible, our preferred radar altimeter subsystem will have the capacity to discriminate against the near return from the Aeroshell and to track the Martian surface.

The landing radar subsystem uses four velocity measuring beams and one range beam (see Section 5.9 for details of this subsystem). The velocity and range information from these measurements is supplied to the guidance and control subsystem

(Section 5.8) which controls the operation of the terminal propulsion subsystems (Section 5.13) during terminal descent. These three subsystems working together control the attitude and velocity of the Lander during the final phases of terminal descent (see Section 2.3.7 for details of the terminal descent operation). During this phase, the Lander is oriented so that its roll axis aligns with the relative velocity vector. In this way the thrust of the descent rocket motor is always aligned to cancel out the horizontal component of ground velocity caused by wind drift.

To function properly, the landing radar must receive signals from the surface for at least three of its four velocity beams. If the Lander is ever in a roll-pitch attitude such that the three velocity signals are not received, the landing radar cannot measure velocity and the Lander will stay in an attitude hold mode. There are two possible ways the Lander may get into this situation:

a. If at the time of parachute release, the Lander is experiencing violent oscillations on the parachute due to gusts, its roll axis may be too close to horizontal so that two or more velocity beams are not locked on the surface. Thus, after parachute release and going into the six second attitude hold, the landing radar may never acquire the surface and the vehicle will then pass beyond the terminal propulsion switching line without recognizing it, resulting in a landing failure.

b. If at parachute release the Lander vehicle has a high wind drift rate in relation to the descent rate, the landing radar may be locked onto the surface, but will command the vehicle to pitch to a very shallow attitude to align with the velocity vector. In doing so it may drive the vehicle beyond the point where three out of four velocity beams are still acquired. Thus, a failure similar to the first will occur.

There is little that can be done to prevent the first possibility except to design the parachute suspension system to attain the best possible descent stability. However, the second possibility can be avoided by constraining the minimum descent velocity and thus the maximum parachute size.

Figure 5.10-6 shows the boundaries of minimum roll axis pitch attitude angle for proper landing radar velocity and range beam operation based on 10° ground slope. Note that the velocity beam boundary is the most severe, and at the 5,000 ft. parachute release altitude it requires a roll axis angle (θ) greater than 36°. Thus, for a given mean wind velocity at the parachute release altitude, the velocity beam boundary limits the descent velocity to not less than V_D =

MINIMUM ROLL AXIS PITCH ATTITUDE FOR LANDING RADAR OPERATION

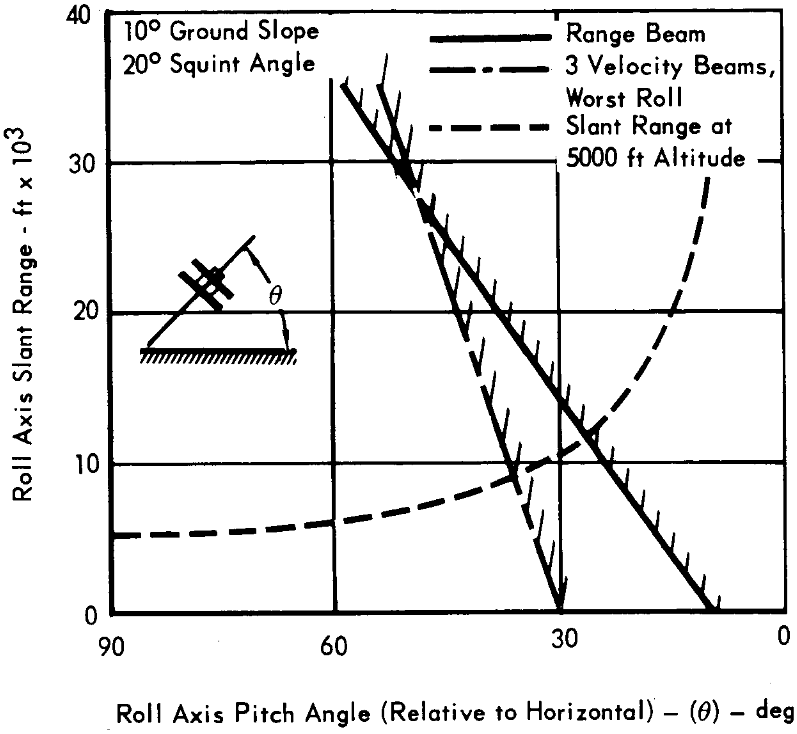

Figure 5.10-6

V_{wind} tan θ, where V_D is descent velocity and V_{wind} is the horizontal wind velocity component.

5.10.2 Analysis of Subsystem Sizing and Sequence - The constraints will now be considered simultaneously to determine which can be satisfied and where conflicts arise that require compromise.

5.10.2.1 Parachute Sizing Considerations - Parachute deployment is initiated at 23,000 ft by the radar altimeter. As previously discussed, this limits the Mach number to 2.0 in the VM-8 atmosphere for $V_e = 13{,}000$ ft/sec and $\gamma_e = -20^o$. To control the opening shock loads to a reasonable level, initial studies showed that the parachute should be reefed, and a reefed drag area ratio ($R = C_D S_{\text{ reefed}}/C_{D_o} S_o$) of approximately 25% for four seconds was assumed.

As previously discussed, it is desirable to release the Aeroshell and effect separation as soon as possible after parachute deployment. Therefore, it was assumed that the Aeroshell will be released as soon as the parachute is fully open. Waiting until the parachute is fully open is consistent with historically proven good recovery system practice, assures positive and rapid Aeroshell/lander separation characteristics, and lessens the chance of Aeroshell/lander collision or interference during separation.

Based on the above assumptions, Figure 5.10-7 shows the lander descent velocity at 5,000 ft just prior to parachute release for the VM-7, 8, and 10 atmospheres. The maximum parachute size boundaries are based on the constraints imposed by the landing radar velocity beam limitations in conjunction with mean wind velocities at 5,000 ft altitude. Note that the VM-8 atmosphere is the most restrictive in allowing a maximum parachute diameter of only 85 ft, while the VM-7 atmosphere would allow a parachute diameter up to 108 ft.

The lander altitude at the time the Aeroshell impacts the surface is shown in Figure 5.10-8. This figure shows that a 70 ft diameter parachute is the minimum size required in the most critical VM-7 atmosphere to insure that the Aeroshell has hit the surface before the landing radar begins operating (6 sec after initiation of terminal propulsion). In other atmospheres the Aeroshell impacts before the lander descends to 5,000 ft if a 70 ft parachute is used. Figure 5.10-9 shows the the time interval during which the landing radar may track the Aeroshell and shows that this only becomes a problem for parachute diameters less than 60 ft.

On the basis of the foregoing discussions a diameter of 70 ft was chosen for the parachute. A parachute of this size satisfies all the imposed constraints, and, in fact, allows some margin in all cases. Even in the landing radar Aeroshell

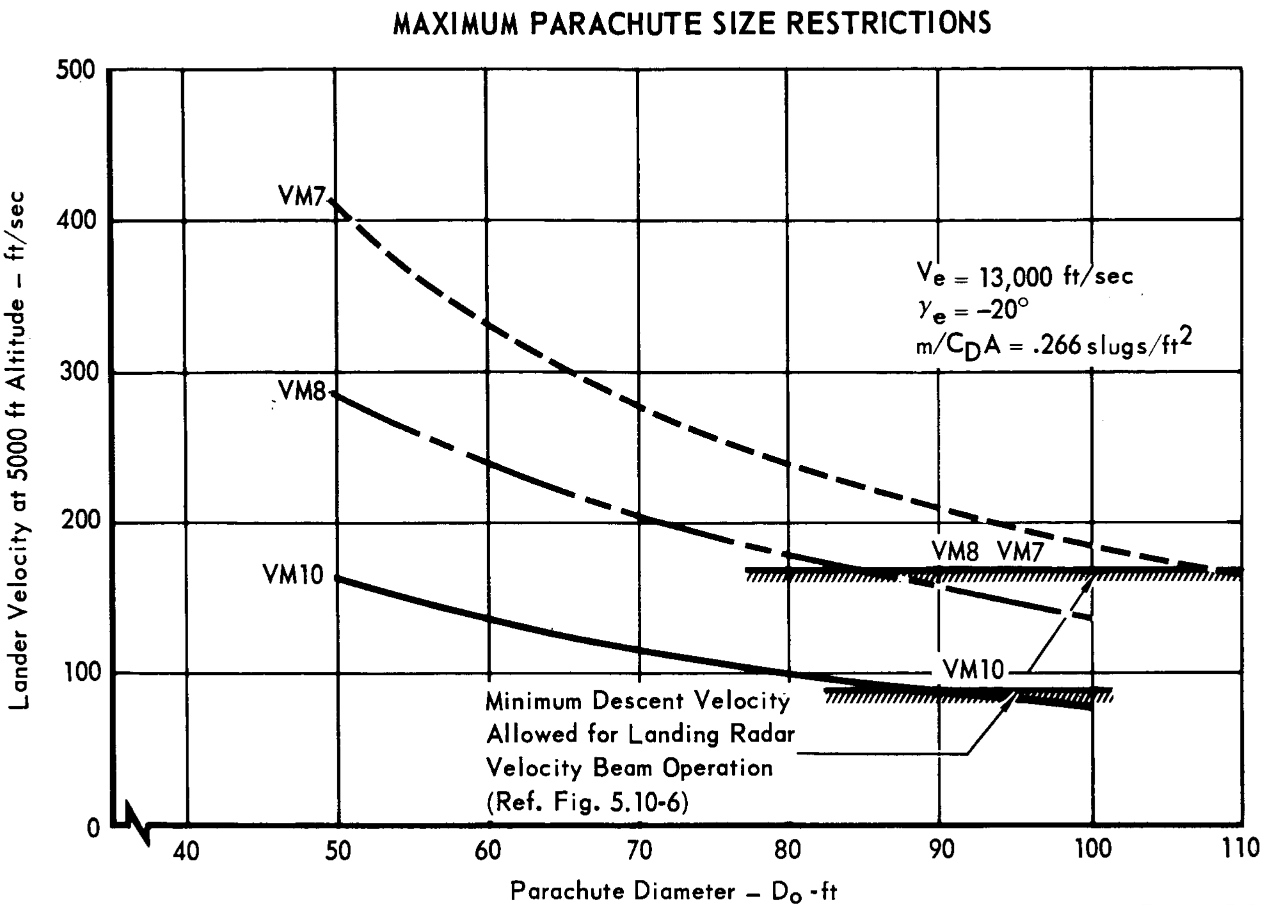

MAXIMUM PARACHUTE SIZE RESTRICTIONS

Figure 5.10–7

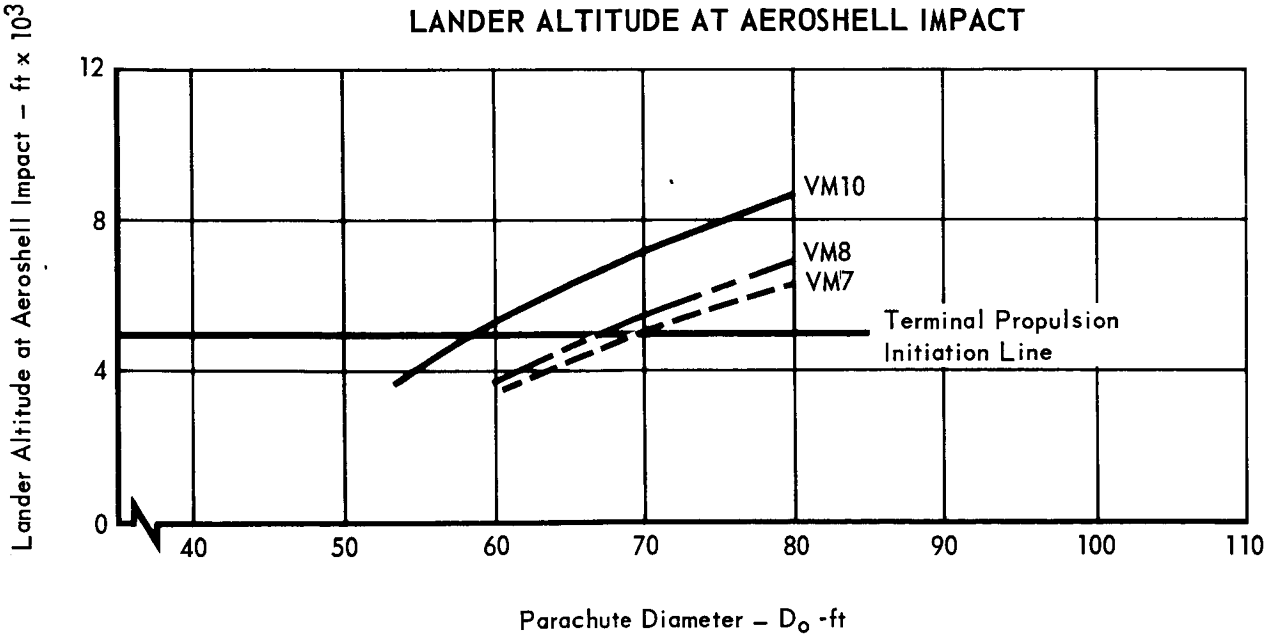

LANDER ALTITUDE AT AEROSHELL IMPACT

Figure 5.10–8

TIME INTERVAL OF POTENTIAL AEROSHELL TRACK

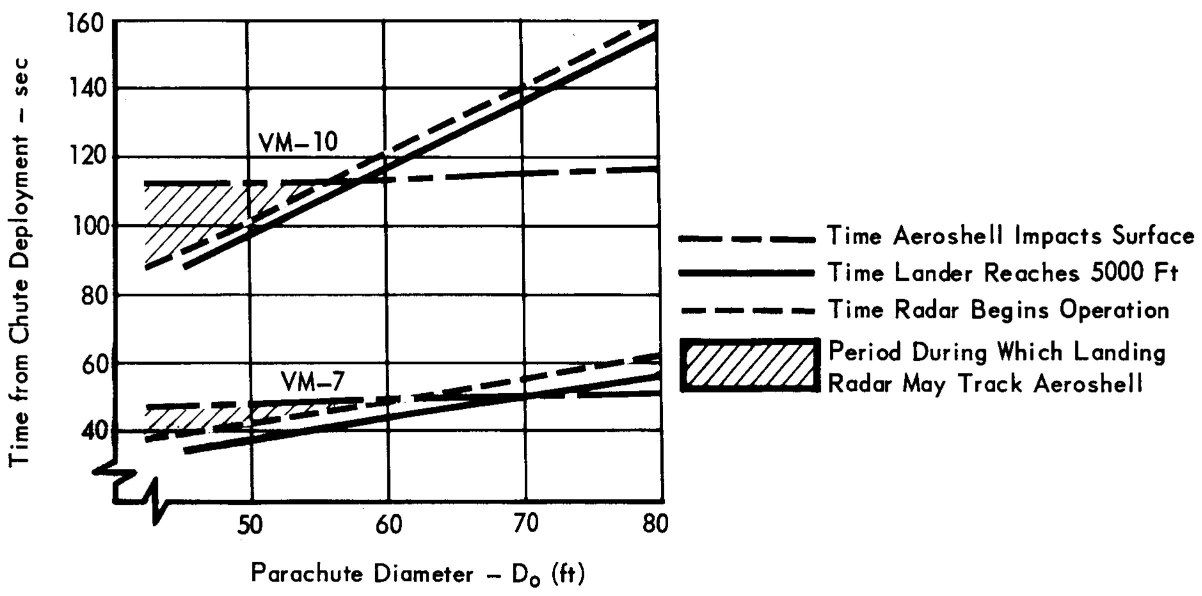

Figure 5.10–9

tracking problem, the 70 ft parachute allows a few seconds margin between Aeroshell impact and turning on the landing radar range beam.

5.10.2.2 Parachute Catapult Velocity - The parachute deployment bag will be forcefully ejected rearward from the Capsule by a pyrotechnically actuated catapult. McDonnell prefers a catapult over a mortar because in developing the parachute catapult for the F-111 A/B Crew Module we found that:

a. For the same muzzle velocity requirements a catapult weighs less than a mortar.

b. By using pre-crushed honeycomb in the mortar piston the catapult loads can be maintained to a nearly constant level, thereby avoiding transmission of large load spikes to the supporting structure.

c. Catapults can be designed to be self-snubbing to protect the parachute from potentially severe damage from flying debris (such as the sabot in a mortar).

d. Self-snubbing catapults have no pyrotechnic outgassing to contaminate experiment instrumentation.

Because the dynamic pressures are very low at parachute deployment, there will be negligible aerodynamic loads acting on the deployment bag to help carry it rearward from the capsule to effect parachute deployment. McDonnell's experience has shown that high muzzle velocities are required to guarantee complete parachute deployment under low airload conditions. Our estimate is that a muzzle velocity of 100 ft/sec will be required to strip the deployment bag completely from the canopy. During parachute development testing, static deployment of the parachute assembly by the catapult will be required to verify the correct muzzle velocity.

5.10.2.3 Parachute Strength/Weight Analysis - The strength/weight characteristics of an aerodynamic decelerator subsystem are intimately related to the operational environment, performance requirements, and other mission constraints that may be imposed on the subsystem. Because the present VOYAGER related parachute technology is in an early state of development, the effect of some of these factors on the parachute strength/weight characteristics cannot be fully assessed at this time. Additional testing and test data are required before a comprehensive and meaningful evaluation can be made.

a. Parachute Materials - One of the most significant factors which may affect parachute weight is the sterilization heat cycle imposed by the VOYAGER mission requirements. Conventional nylon, commonly used in parachute construction, cannot withstand the high temperatures required for sterilization, so other materials will be required. Dacron appears to be one of the more promising candidates, but there are indications that other materials may also be usable.

During Phase B McDonnell awarded a study contract to Northrop-Ventura to aid us in our aerodynamic decelerator subsystem studies. In Reference 5.10-8, Northrop-Ventura reported on the results of their tests with 330 nylon and the effects of a sterilization heat cycle on its material properties. The objective was "to investigate the extent to which fabric made from nylon 6-6 yarn, designated as Type 330 nylon yarn, will retain its characteristic properties after prolonged heating at 135°C in a nitrogen atmosphere." The investigation concluded that "the results of heating specimens of a 1.1 ounce ripstop fabric at 135°C for various periods of time up to 450 hours in nitrogen indicated that the fabric essentially retained its characteristic properties after exposures for periods of time up to 200 hours. After 450 hours there were noticeable changes in breaking strength and elongation at break." In view of these favorable findings, and until further evidence indicates otherwise, McDonnell recommends that the parachute assembly be constructed primarily of 330 nylon materials.

One of the major advantages of the 330 nylon is that it has the same weaving properties as conventional nylon and can be woven into light-weight controlled porosity cloths much easier than dacron. The advantages of 330 nylon no longer exist in the construction of heavy webbings and cords since weave porosity is not a factor. In major structural members such as risers and reefing lines, where stiffness and elongation are factors, dacron will be used. In the final analysis, it is recognized that additional testing is necessary to establish whether 330 nylon or dacron, which is used for the PEPP parachutes, is the best material for the VOYAGER parachute. In addition, extensive testing is required on sample seams and joints, and complete parachute assemblies in the packed condition, to evaluate the effects of the sterilization heat cycle on the dimensional stability of these candidate materials.

b. Opening Shock Loads - Accurate prediction of the parachute's opening shock load characteristics is mandatory to arrive at an efficient design. Lack of good shock load data will result in unrealistic load estimates, which in turn cause the parachute to be unnecessarily overweight.

It must be emphasized that the only parachute opening shock load data available which are applicable to the VOYAGER parachute design are the data from the PEPP tests. These data, summarized in Figure 5.10-2, are used in the following shock load analysis. The parachute design opening loads are established for the case having the highest dynamic pressure at deployment. This case occurs for the V_e = 13,000 ft/sec, $\gamma_e = -20^\circ$ entry into the VM-8 atmosphere, and at the 23,000 ft deployment altitude the dynamic pressure is 13.2 psf. There is an option of whether or not to release the Aeroshell/lander attachments just prior to deployment.

If the 70 ft diameter parachute ($C_{D_o} S_o = 2310$ ft^2) is opened unreefed, the opening shock loads are as follows:

Connected Aeroshell/lander: W = 3680 lbs

$C_D S = (C_D S)_A + (C_D S)_o = 1.48(284) + .6(3850) = 2730$ ft^2

$W/C_D S = \frac{2800}{2730} = 1.025$ lbs/ft^2

X = 1.65 (See Figure 5.10-2)

$F_o = X\, C_{D_o} S_o q = (1.65)\ (2310)\ (13.2) = \underline{50{,}400 \text{ lbs.}}$

Disconnected Aeroshell/lander: W = 2800 lbs

$W/C_D S = \frac{2800}{2730} = 1.025$ lbs/ft^2

X = 1.4

$F_o = X C_{D_o} S_o q = 1.4(2310)13.2 = \underline{42{,}700 \text{ lbs}}$

Opening loads of this magnitude are impractical for a 70 ft parachute, and, in addition, would impose a severe weight penalty on the parachute attachment support structure. For these reasons the parachute should be reefed.

The question of Aeroshell/lander disconnect prior to parachute deployment arises again. To separate the lander from the Aeroshell the parachute must produce drag sufficient to cause the drag area to weight ratio ($C_{D_o} S_o/W_L$, W_L = lander weight) of the lander and parachute to be no less than the Aeroshell drag to weight ratio ($C_D S/W_A$, $C_D S$ = Aeroshell drag area, W_A = Aeroshell weight). These equations have the following values:

C_D = 1.48 (Mach 2.0), S = 284 ft^2, W_A = 880 lbs

S_o = 3850 ft^2, W_L = 2800 lbs

Then, the minimum required reefed parachute drag coefficient (C_{DR}) to effect separation is:

$$C_{DR} = \frac{(C_D S)}{(W_A)} \; \frac{W_L}{S_o} = \frac{(1.48)\ (284)}{880} \; \frac{2800}{3850}$$

$$C_{DR} = .348$$

With this reefed drag coefficient the opening shock load would be:

$$\frac{W}{C_D S} = \frac{2800}{1.48(284) + .348(3850)} = 1.59 \text{ lbs/ft}^2$$

$$X = 1.45 \qquad \text{(See Figure 5.10-2)}$$

$$F_o = X(C_{DR} S_o)\ q = 1.45(.348)\ (3850)\ \ 13.2$$

$$F_o = \underline{25,600 \text{ lbs}}$$

Even a load of this magnitude is high for a light to medium weight parachute design. Thus, to minimize the subsystem weight and to maximize payload capability, lower opening shock loads must be attained. This goal negates the feasibility of releasing the Aeroshell/lander connections prior to parachute deployment, and hereafter Aeroshell/lander separation will be programmed to occur after the parachute is fully open.

It is generally accepted as good practice in parachute design to scale the reefing parameters (reefed drag area and reefed time) to approximately balance both the reefed and disreef shock load. The variation of reefed and disreef shock load is shown in Figure 5.10-10 as a function of the reefed drag area ratio. These curves are based on deceleration trajectory data and shock load calculations similar to above. On the basis of the opening shock load trends, trajectory analysis of the Aeroshell/lander separation, and subsystem weight, a design opening shock load of 20,000 lbs was selected as the best compromise for all these considerations. To obtain these opening loads requires that the parachute be reefed to a drag area ratio (R) of approximately 26 percent for 8 seconds. The 8.0 sec reefing time was chosen because pyrotechnic reefing cutters usually display a ±20% tolerance about their nominal time delay. For the nominal time delay the shock loads balance at approximately 19,000 lbs, but for the short side tolerance (6.4 sec) a 21,000 lb disreef opening shock load would be encountered. However, it must be remembered that this slight overload condition

PARACHUTE OPENING SHOCK LOADS

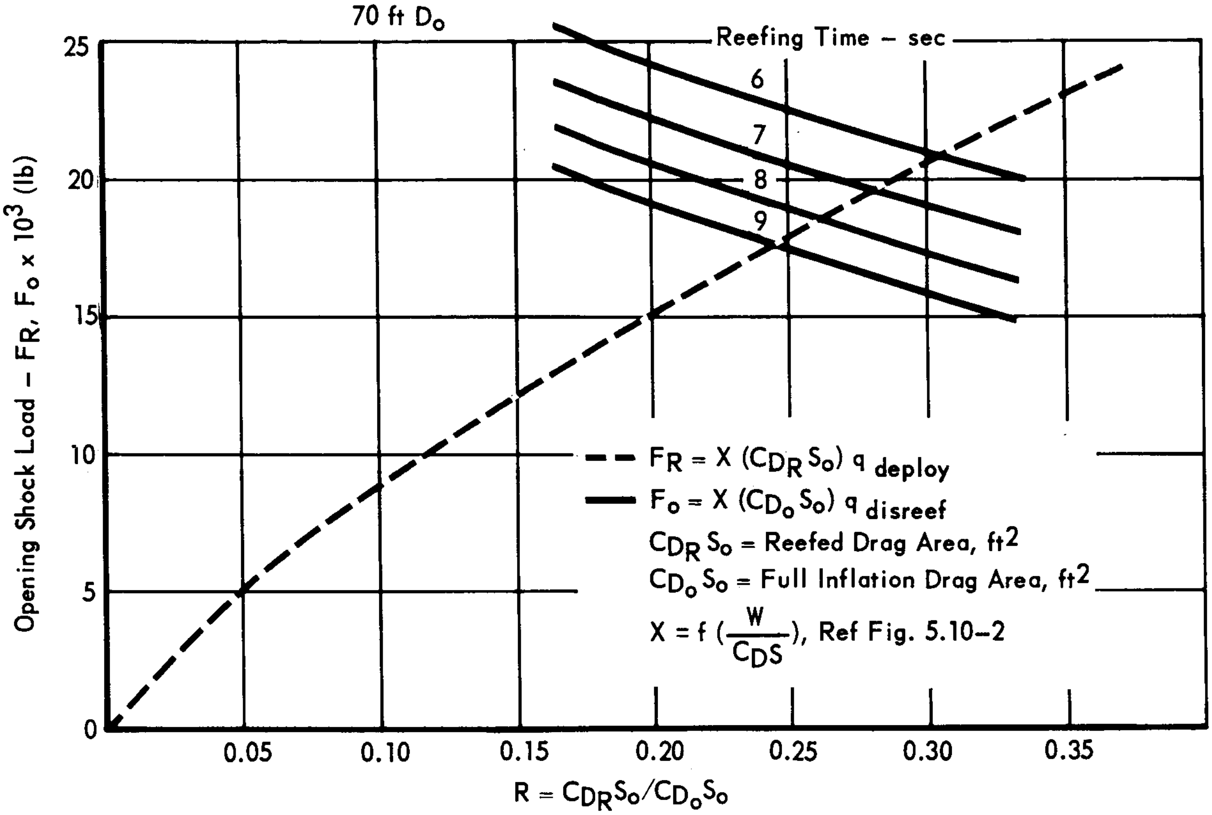

Figure 5.10–10

is only encountered for a single worst-on-worst-on-worst condition (atmosphere, entry conditions, cutter delay tolerance).

The Aeroshell/lander separation occurs 12 seconds after parachute deployment when the parachute has attained full open inflation, thus insuring good separation characteristics. In Figure 5.10-11 the Aeroshell/lander separation trajectories are compared for the worst case in VM-7 to show the effect of using either single stage or two stage reefing. The two stage reefing permitted balancing the opening shock loads to 18,000 lbs. Note that even though Aeroshell/lander separation can be initiated sooner with the two stage reefing, the separation trajectories are very similar and no strong advantage appears for the two stage reefing case. Two stage reefing is more complicated and less reliable than single stage. Therefore, single stage reefing is the best choice for mission success.

With single stage reefing Figure 5.10-11 shows the Aeroshell to be at 1200 ft altitude when the Lander is at 5,000 ft and the terminal propulsion is initiated. It is not necessary for the landing radar to acquire the surface until 6 seconds after the 5,000 ft mark; therefore, this delay allows the Aeroshell to impact several seconds prior to the time landing radar signal is required. Thus, there should be no danger of the landing radar receiving false signals from the Aeroshell. The 70 ft diameter parachute provides some margin in the worst case.

c. Parachute Assembly Weight - Accurate weight prediction of a parachute which is required to operate in a given environment and to certain loading conditions is difficult at best. There is no acceptable method of parachute stress analysis which will predict with good accuracy the cloth pressure loadings and distribution. For these reasons parachute weight predictions must rely on empirical data, past experience and engineering judgment. Our 70 ft diameter parachute, operating with 20,000 lb shock loads, is the same diameter and has the same design loading as the 70 ft diameter Ringsail parachute used so successfully in the McDonnell F-111A/B Crew Module. That parachute, designed to operate at dynamic pressures up to 360 psf in the low Earth atmosphere, weighs 110 lbs.

Based on a simple parachute loading analysis similar to that outlined in Reference 5.10-9, the crown portion of the 70 ft D_o canopy (one half of the diameter) will require moderate weight 330 nylon cloth (2.25 oz/yd^2) to withstand the high pressure loads experienced in that area during the reefed

COMPARISON OF SINGLE AND DOUBLE REEFED PARACHUTE TRAJECTORIES

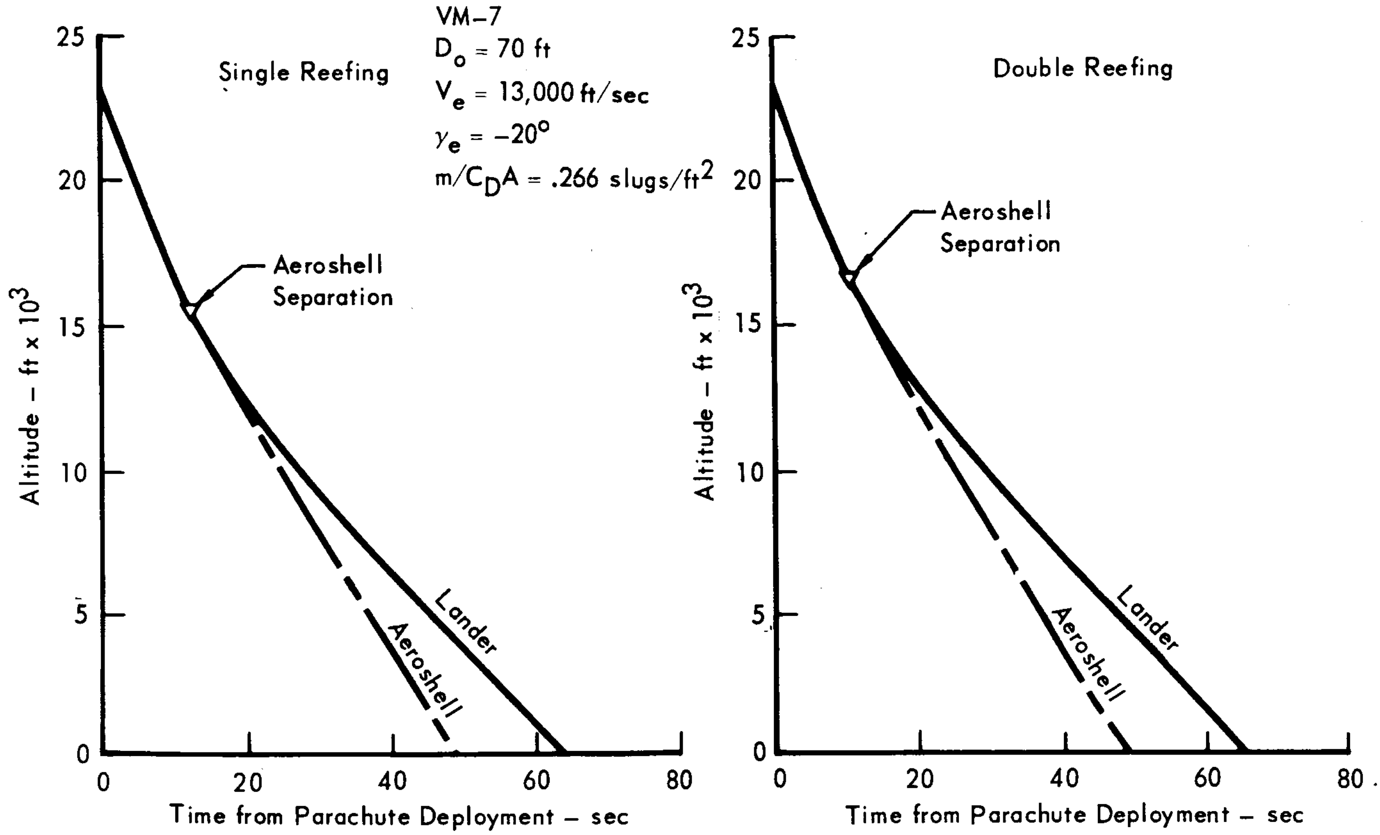

Figure 5.10-11

opening interval. The remainder of the canopy is constructed of the lightweight 1.1 oz/yd^2 330 nylon cloth. There will be 60 gores and suspension lines, and the suspension lines will have a 750 lb tensile strength. A weight breakdown for that portion of the parachute to be packed in the deployment bag (from the confluence of the suspension lines upward) is as follows:

2.25 oz/yd^2 cloth; 965 ft^2	15.1 lbs
1.1 ox/yd^2 cloth; 2,885 ft^2	22.1 lbs
Suspension lines; 750 lb strength; 1,990 yd	39.8 lbs
2 layers 525 lb radial tapes; 1,310 yd	24.6 lbs
Skirt band; 1,000 lb strength 330 nylon; 72 yd	2.3 lbs
Reefing line; 1,000 lb strength dacron; 13 yd	.3 lbs
Miscellaneous hardware (reefing cutters, rings, links)	4.5 lbs
TOTAL	108.7 lbs

The complete riser assembly, from the end of the suspension lines to the Capsule attachment, is constructed of multiple layers of 10,000 lb dacron webbing. At the upper end, where the riser divides into four branches for attachment of the parachute suspension lines, each branch is made of two layers of the webbing. The four lower legs of the riser, which attach to the Capsule are made of three layers of webbing. The estimated weight of the complete riser assembly is 17 lbs.

5.10.2.4 Subsystem Contingencies - In most subsystem design analyses there are points where a decision is required but there is little or no data to aid the decision making process. Parachute system design encounters many problems of this nature, so in many cases engineering judgement and experience are all that can be relied upon. The purpose here is to identify those areas where new information or data can have significant effects on the subsystem weight, detail design, and operation. These subsystem characteristics can be significantly affected by results of the PEPP tests or by investigations of the effect of sterilization on materials.

a. Influences of PEPP Tests - The results of the PEPP tests should make it possible to select the best parachute canopy configuration for the VOYAGER application. However, there are needed data which this program probably will not furnish. One of the needed items is reefed and disreef opening shock factors for higher canopy unit loading. Present scaling requires extrapolation of opening shock factor data to the point where a high degree of uncertainty exists. These uncertainties directly affect design loads and subsystem weight, which in turn can affect sizing consideration and systems operation.

The selection of the best canopy design may itself require new development in some areas. For instance, the Cross parachutes which are presently being tested are not reefed, but, if chosen for VOYAGER, reefing will probably be required. The construction of the Cross canopy is such that a unique reefing concept will have to be developed for it.

In summary, as the results of the PEPP tests become available they must be examined closely to determine their impact on the aerodynamic decelerator subsystem design. For instance, the PEPP tests could demonstrate that the operation of large parachutes is restricted to the vicinity of Mach 1.5 and our assumption of a Mach 2.0 operational capability is not feasible. The effect of lowering the Mach number limitation below Mach 2 is illustrated in Figure 5.10-12. As the deployment Mach limit, and thus altitude, is lowered the problem of the landing radar tracking the Aeroshell becomes more serious. In the same vein, tests may show that the upper operational limit is beyond Mach 2.0, and the problems discussed above are reduced.

b. Effects of Sterilization on Materials - An extensive investigation into the effect of sterilization on parachute materials is needed. There are several candidate materials such as Dacron, Nomex, and 330 Nylon, which show potential for use in the parachute. However, these materials have different strength to weight characteristics and the sterilization heat cycle affects each in a different manner. If the sterilization cycle appreciably degrades the load capabilities of these materials or if a low strength-to-weight ratio material is needed to withstand the cycle, a serious weight penalty will be imposed on the parachute design. Therefore, the importance of early materials investigations cannot be overemphasized.

c. Related Subsystems - The aerodynamic decelerator subsystem design is closely related to the capabilities and limitations of other subsytems. The development of these related subsystems must be watched closely, so that changes in their performance can be examined to determine the effect on the aerodynamic decelerator subsystem. In particular, this applies to the aerodynamic decelerator triggering system, landing radar, terminal propulsion, and guidance and control subsystems.

EFFECT OF MAXIMUM PARACHUTE DEPLOYMENT MACH NUMBER ON DESCENT TRAJECTORIES

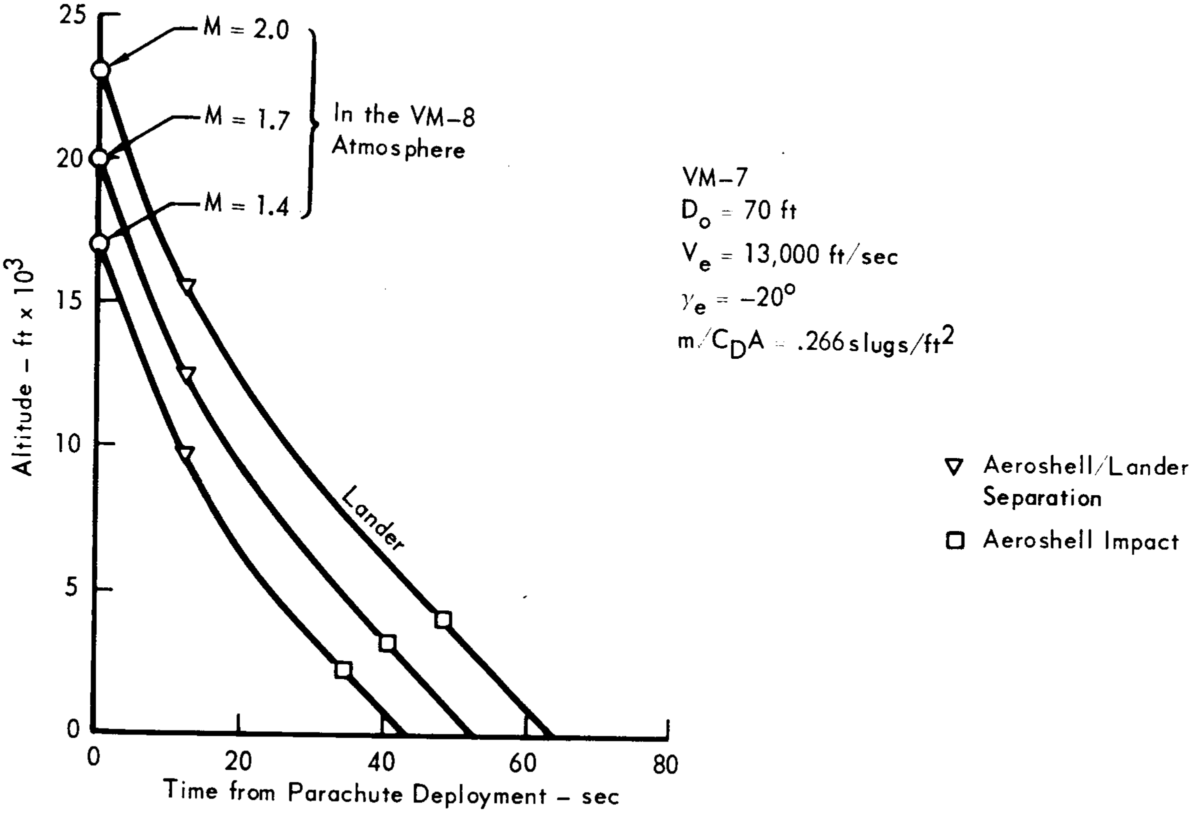

Figure 5.10-12

5.10.2.5 Subsystem Sequencing - Sequencing of the aerodynamic decelerator subsystem is initiated by a signal from the radar altimeter to fire the parachute catapult at 23,000 ft. The complete subsystem sequencing through Aeroshell/lander separation is shown in Figure 5.10-13 in block diagram form.

At 5,000 ft above the Martian surface, an altitude marking radar signal initiates the terminal propulsion rocket motors. This sequence is also shown in Figure 5.10-13. After an 0.5 second delay, if the rocket motors have all ignited and are functioning properly, and terminal propulsion status detector indicates proper operation and sends an electrical signal to initiate the parachute disconnect, the parachute is released from the Lander, which continues its descent to the Martian surface under the control of the terminal descent subsystems.

In case one or more of the terminal propulsion rocket motors fail to operate properly, the terminal propulsion status detector sends a signal to shut down the rocket motors. The parachute is not released in this malfunction mode and the lander continues to descend to the Martian surface with the parachute attached. Depending on the density of the Martian atmosphere encountered, the Lander could impact at a velocity as low as 112 ft/sec.

McDonnell feels there are valuable benefits to retaining the parachute until proper operation of the terminal propulsion subsystem is assured. These advantages include:

a. Release of the parachute followed by terminal propulsion subsystem failure results in the lander probably going into a violently tumbling descent. In this case, all experiment data will be lost, quality picture taking will be impossible, and data communications with the orbiting spacecraft will cease. The resulting surface impact will destroy the lander and all instrumentation.

b. Malfunction of the terminal propulsion with the parachute retained results in the lander impact velocity being higher than the 25 ft/sec design velocity, but it may be low enough that some instrumentation may survive the impact. In the final analysis, it may be advantageous to allot a portion of the weight contingency toward additional impact attenuation for high value experiment instrumentation.

c. Retention of the parachute, in case of a propulsion malfunction, is favorable for picture taking of the Martian surface during the final 5,000 ft descent. Without the parachute, impact could occur as soon as 14 sec after the propulsion malfunction, whereas, if the parachute is retained, as much as 43

AERODYNAMIC DECELERATOR SUBSYSTEM SEQUENCING

A – PARACHUTE DEPLOYMENT SEQUENCE

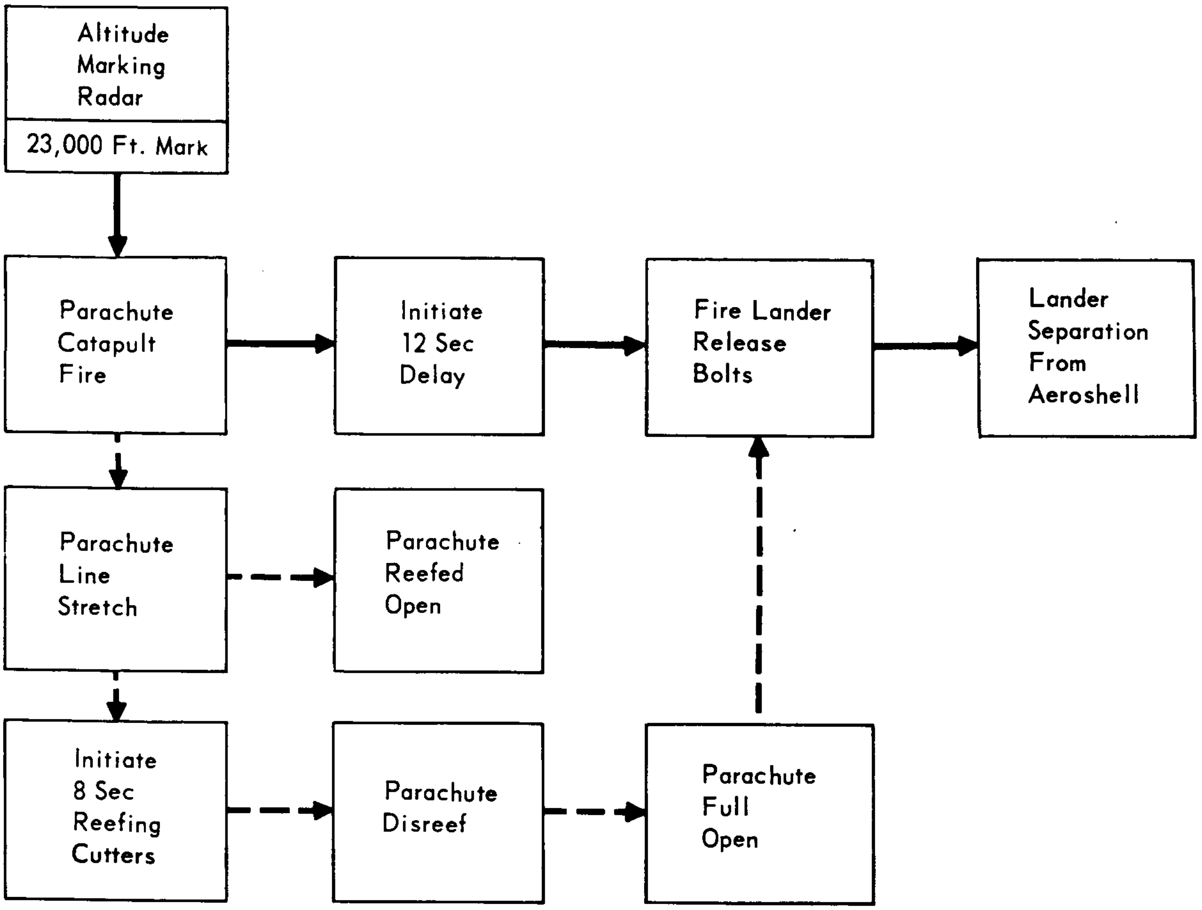
Altitude Marking Radar
23,000 Ft. Mark
Parachute Catapult Fire
Initiate 12 Sec Delay
Fire Lander Release Bolts
Lander Separation From Aeroshell
Parachute Line Stretch
Parachute Reefed Open
Initiate 8 Sec Reefing Cutters
Parachute Disreef
Parachute Full Open

B – PARACHUTE DISCONNECT SEQUENCE

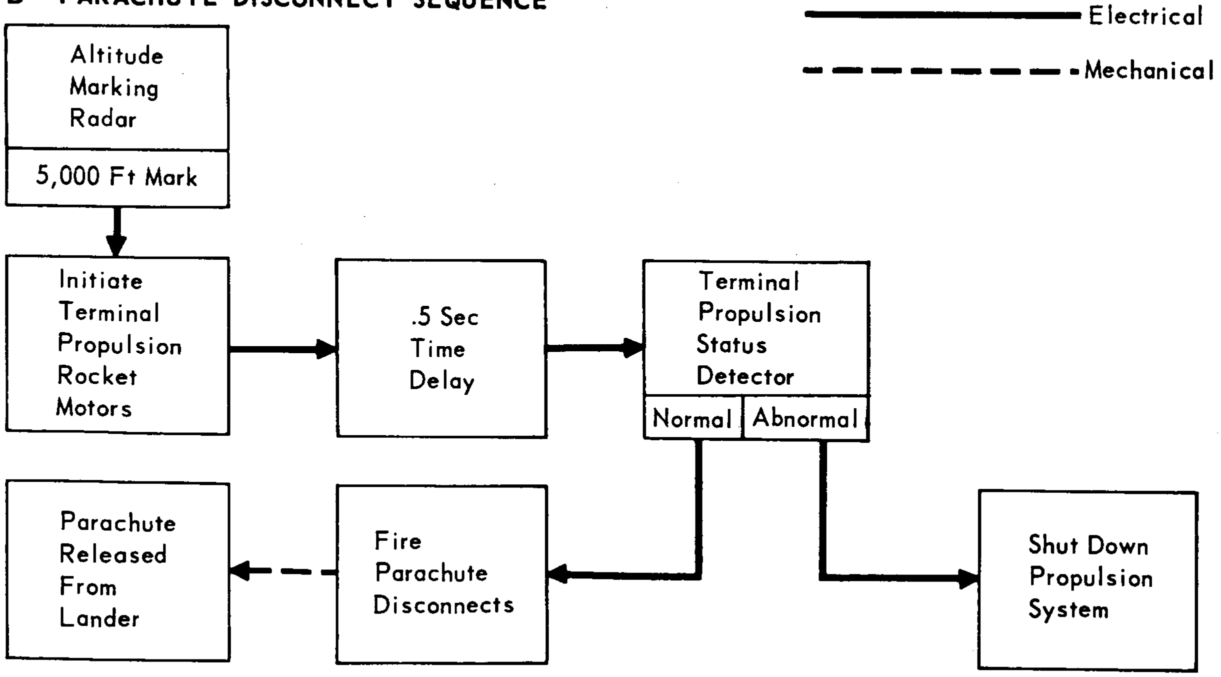
Electrical
Mechanical
Altitude Marking Radar
5,000 Ft Mark
Initiate Terminal Propulsion Rocket Motors
.5 Sec Time Delay
Terminal Propulsion Status Detector
Normal
Abnormal
Parachute Released From Lander
Fire Parachute Disconnects
Shut Down Propulsion System

Figure 5.10–13

seconds additional data transmission time may be available in a dense atmosphere. This increased time increases the probability of getting good low altitude pictures of the surface prior to impact.

5.10.3 Summary of Subsystem Operational Environment and Performance - In Figure 5.10-14 the pertinent parameters of the subsystem performance are summarized to show maximum/minimum values. The entry conditions and atmospheric model which impose the maximum/minimum values are also shown.

5.10.3.1 Time Histories for Normal Subsystem Operation - Three altitude time histories of the lander and Aeroshell are shown in Figure 5.10-15 for the atmospheres which impose maximum/minimum conditions on the aerodynamic decelerator subsystem. Comparison plots showing altitude versus velocity and parachute force versus time are shown in Figures 5.10-16 and 5.10-17, respectively.

The VM-7 case is critical from the aspect of minimum time to descend to 5,000 ft and represents the worst case in the potential problem area of the landing radar tracking the Aeroshell. Note in Figure 5.10-15 that our subsystem does avoid this problem since the Aeroshell has hit the surface a few seconds prior to starting the landing radar. The VM-10 case is the best in this respect as the Aeroshell is on the surface 14 seconds before the lander descends to 5,000 ft.

The VM-8 case has the highest Mach number and dynamic pressure at parachute deployment and imposes the maximum parachute opening loads as shown in Figure 5.10-17.

The VM-10 case represents the opposite extreme to the VM-7 case since it displays the lowest lander velocity at 5,000 ft, as seen in Figure 5.10-16. In Figure 5.10-17, this case also imposes the lowest opening loads on the parachute.

5.10.3.2 Allowable Terrain Height - The Capsule design uses a radar altimeter to initiate parachute deployment 23,000 ft above the local Martian surface. The parachute is designed for the worst atmosphere (VM-8) and entry conditions (V_e = 13,000 ft/sec and $\gamma_e = -20^o$) and for terrain heights no higher than surface level. When high terrain levels are considered with these worst entry conditions the assumed Mach 2.0 limit and the design dynamic pressure at parachute deployment will be exceeded. However, this deficiency of the radar altimeter in the worst case is far outweighed by its obvious advantage in all other cases. By deploying the parachute a given altitude increment above the surface it guarantees sufficient altitude for proper operation of the parachute and terminal descent phase for a successful landing. Figure 5.10-18 shows the allowable terrain height for a successful landing based on the assumption that the parachute fails if deployed above Mach 2.0 or its design dynamic pressure. These boundaries are shown for the odd numbered and even numbered

SUMMARY OF AERODYNAMIC DECELERATOR SUBSYSTEM OPERATIONAL ENVIRONMENT AND PERFORMANCE

PARAMETER	VALUE MAXIMUM MINIMUM	ENTRY CONDITIONS WHICH DETERMINES CRITICAL VALUE (VM–; Ve; γ_e)
Parachute Deployment Altitude (ft)	23,000	Constant for all Entry Conditions
Mach Number at Parachute Deployment	2.0	VM–8; 13,000; –20°
	0.43	VM–9; 13,000; –20°
Dynamic Pressure at Parachute Deployment (lb/ft^2)	13.2	VM–8; 13,000; –20°
	3.65	VM–9; 13,000; –20°
Parachute Catapult Velocity (ft/sec)	100	Constant for all Entry Conditions
Parachute Reefed Opening Shock Load (lb)	18,300	VM–8; 13,000; –20°
	6,200	VM–10; 13,000; –20°
Parachute Full Open Shock Load (lb)	18,300	VM–8 13,000; –20°
	9,200	VM–10 13,000; –20°
Time from Parachute Deployment to Aeroshell/Lander Separation (sec)	12.0	Constant
Altitude at Aeroshell/Lander Separation (ft)	18,900	VM–10; 13,000; –20°
	15,600	VM–7; 13,000; –20°
Altitude at Parachute Release (ft)	5,000	Constant
Lander Velocity at 5,000 ft Terminal Propulsion Initiation (ft/sec)	283	VM–7; 13,000; –20°
	116	VM–10; 13,000; –20°
Lander Altitude When Aeroshell Impacts Martian Surface (ft)	6700	VM–10; 13,000; –20°
	4170	VM–7; 13,000; –20°
Lander Surface Impact Velocity Descending with Parachute (Terminal Propulsion Malfunction (ft/sec)	271	VM–7; 13,000; –20°
	112	VM–10; 13,000; –20°

Figure 5.10–14

DESCENT TRAJECTORIES AFTER PARACHUTE DEPLOYMENT

$V_e = 13{,}000$ ft/sec
$\gamma_e = -20^\circ$
$m/C_DA = .266$ slugs/ft^2

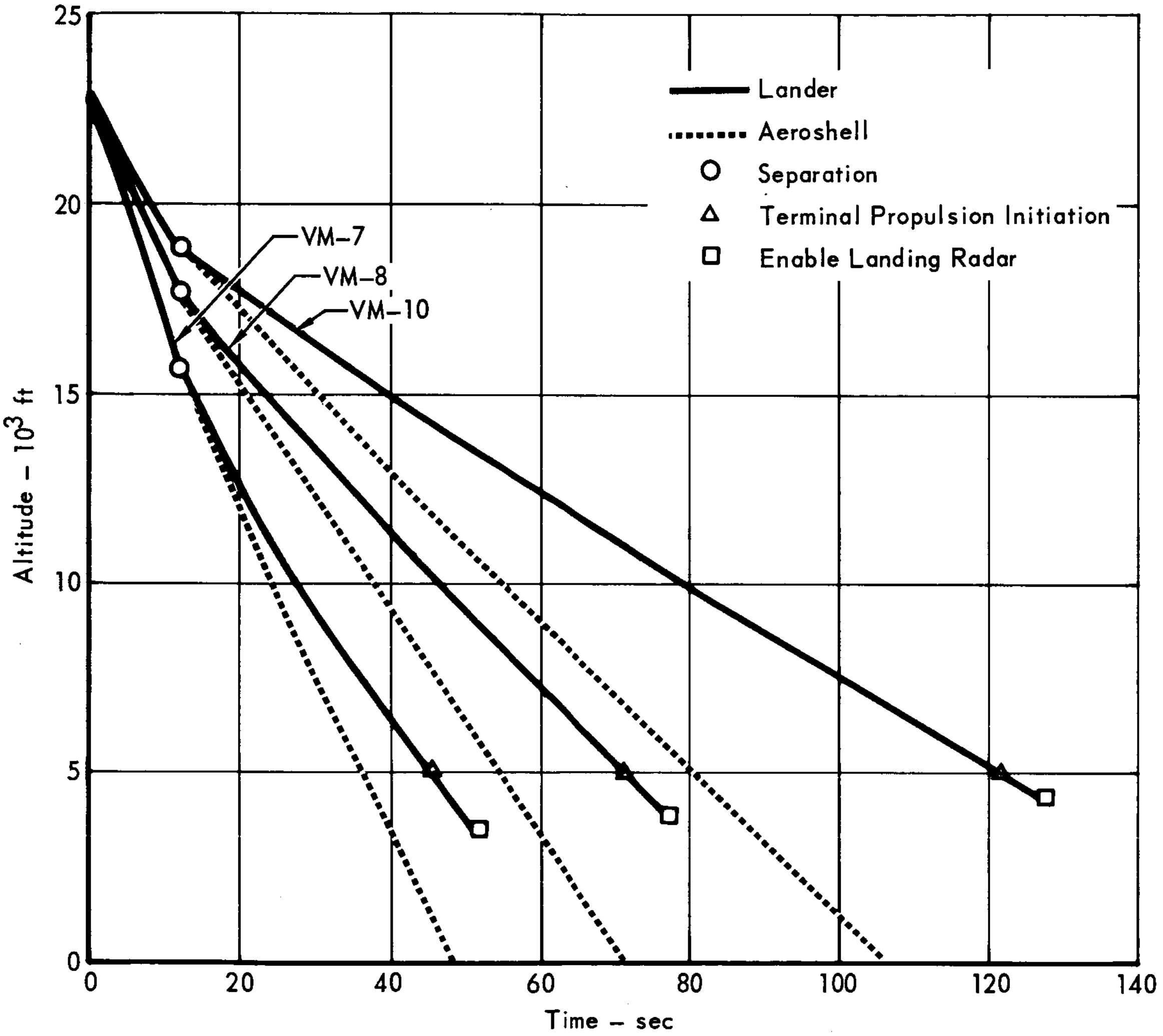

Figure 5.10-15

AEROSHELL/LANDER ALTITUDE – VELOCITY CHARACTERISTICS

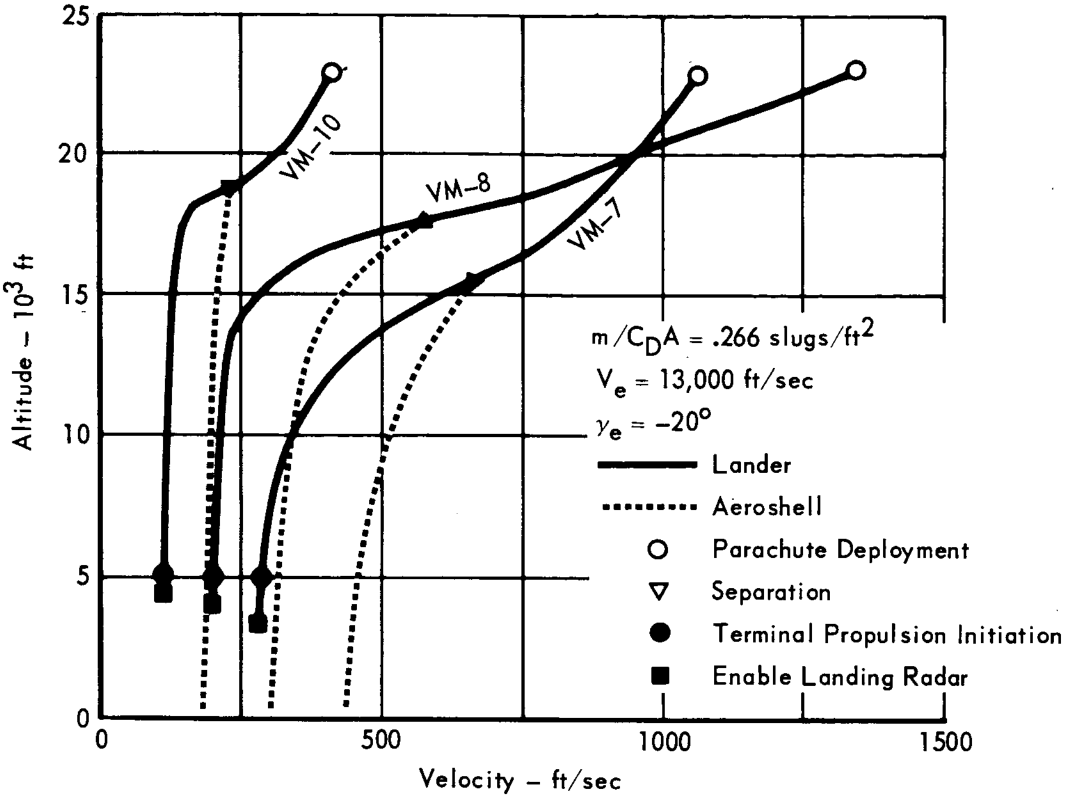

Figure 5.10–16

EFFECT OF ATMOSPHERE ON PARACHUTE SHOCK LOADS

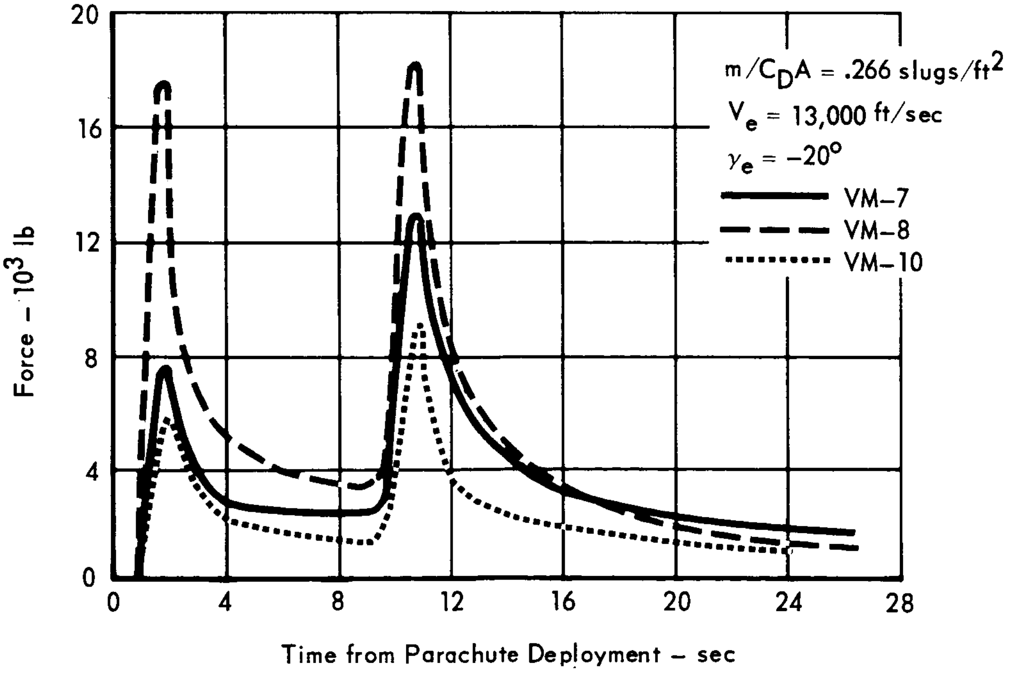

Figure 5.10–17

ALLOWABLE TERRAIN HEIGHT FOR SUCCESSFUL LANDING OPERATIONS

Notes:

1. Terrain Height is Measured Above Reference Spheroid
2. Assumes Failure of Parachute if Deployment is Initiated Above Mach 2.0 or Design Dynamic Pressure

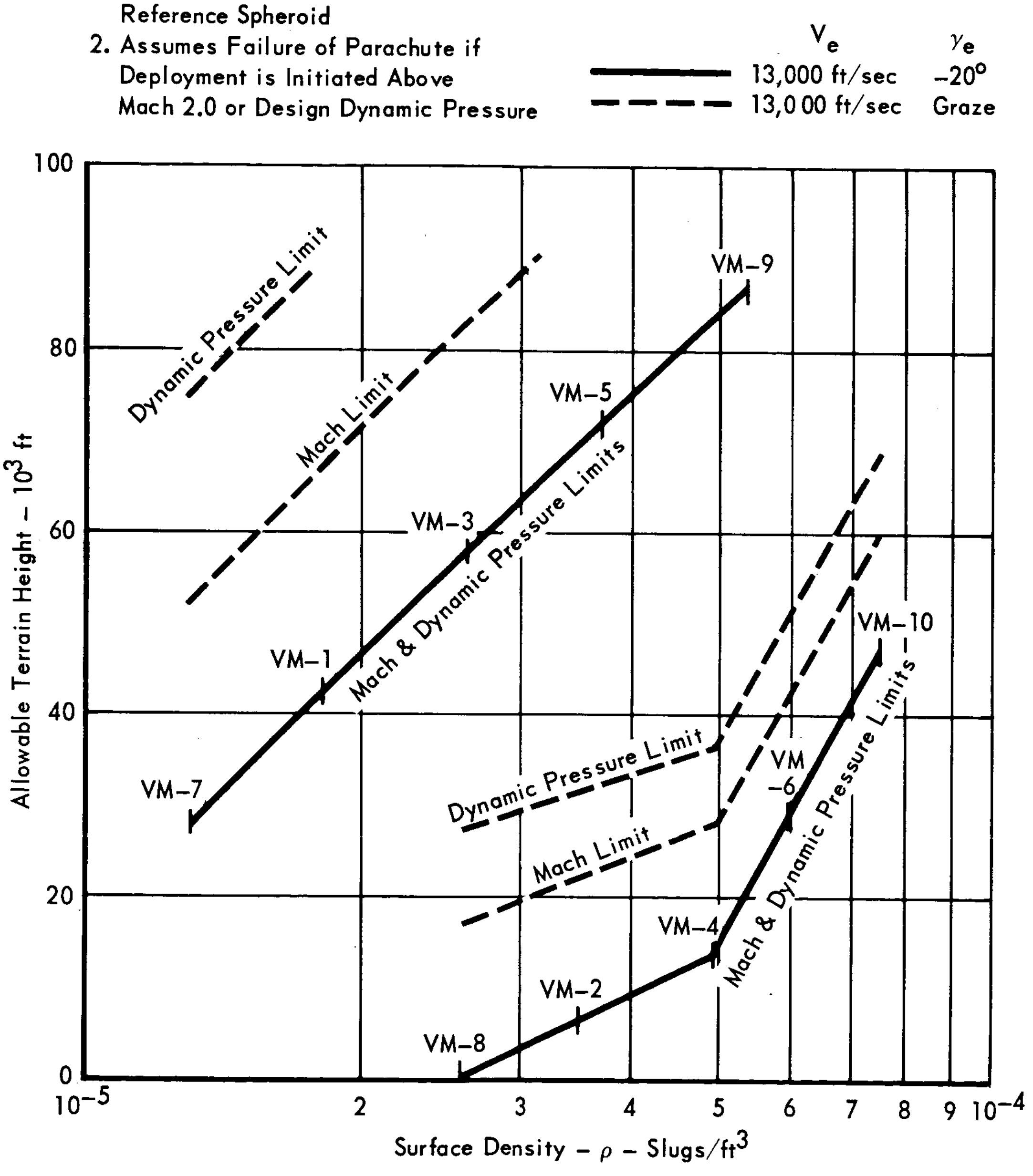

Figure 5.10-18

VM atmosphere families, and they are shown for the 13,000 ft/sec entry velocity since that is the most sensitive entry velocity for terrain height considerations. Thus, the radar altimeter trigger offers a very good chance of successful landing in all cases except a few combination worst cases.

5.10.3.3 Response to Gusts During Parachute Descent - During the Northrop-Ventura studies (reported in Reference 5.10-7), a broad range of parachute size and payload weight combinations were examined. Computer program simulation studies of the parachute system stability under the influence of wind shears and moderate (50 ft/sec) sharp edged gusts showed good stability and damping characteristics.

The time histories shown in Figures 5.10-19 (a) and (b) from the computer simulation are shown for our subsystem encountering sharp edged gusts of 200 ft/sec in VM-7 and 100 ft/sec in VM-10. The VM-7 case exhibits the best damping characteristics. Note the maximum angular change experienced in the first half cycle after the disturbance is on the order of 50 degrees for both cases, and both encounter peak angular rates on the order of 30 deg/sec. The two examples shown are for sharp edged gusts of large amplitude (which is consistent with the JPL constraints), but we feel that gusts of this type and magnitude are unrealistic and are not consistent with Earth experience or natural law. We recommend that ramp type gusts, having a reasonable onset rate based on Earth experience, be used for gust analyses of the parachute system.

The mathematical model used in this study to simulate the parachute-payload combination is very complete in that it includes payload aerodynamics, parachute aerodynamics, suspension system geometry and spring constant, payload and parachute physical properties, model atmosphere, and parachute apparent and included air mass. However, past experience indicates it is very difficult to predict the response of a parachute system to a given disturbance, and generally the system's stability and damping characteristics are better than that predicted by the mathematical model. These limitations of the model may be due to sources of error such as the parachute's aerodynamic characteristics (estimated on the basis of wind tunnel test data obtained using small-scale rigid parachute models) and the damping characteristics of the payload and the parachute (usually poorly defined). In addition, the lifelike behavior of a parachute as it constantly changes shape, attitude, and loading, as it attempts to adjust itself to its instantaneous environment, causes complex damping forces which cannot be predicted, such as the energy absorbed within the cloth and structural members due to friction between material fibers. Nevertheless, mathematical models of this type are useful to optimize the system

TIME HISTORIES OF LANDER DEVIATION FROM VERTICAL AND PITCH RATE DURING PARACHUTE DESCENT

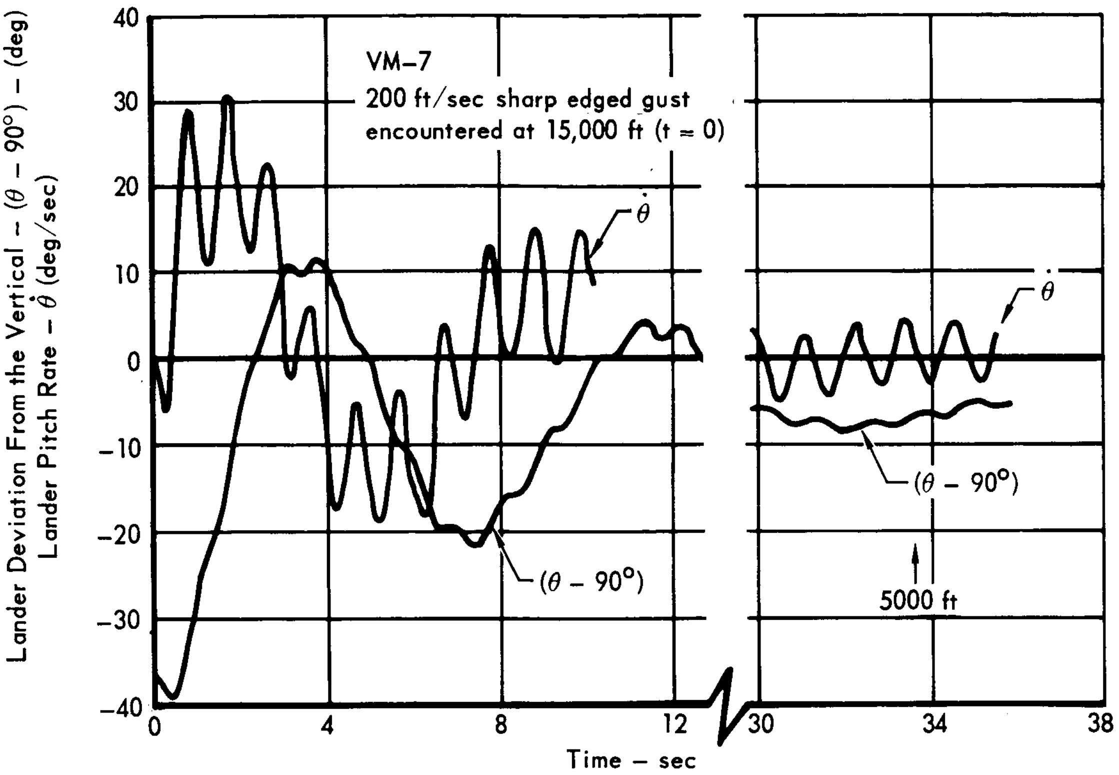

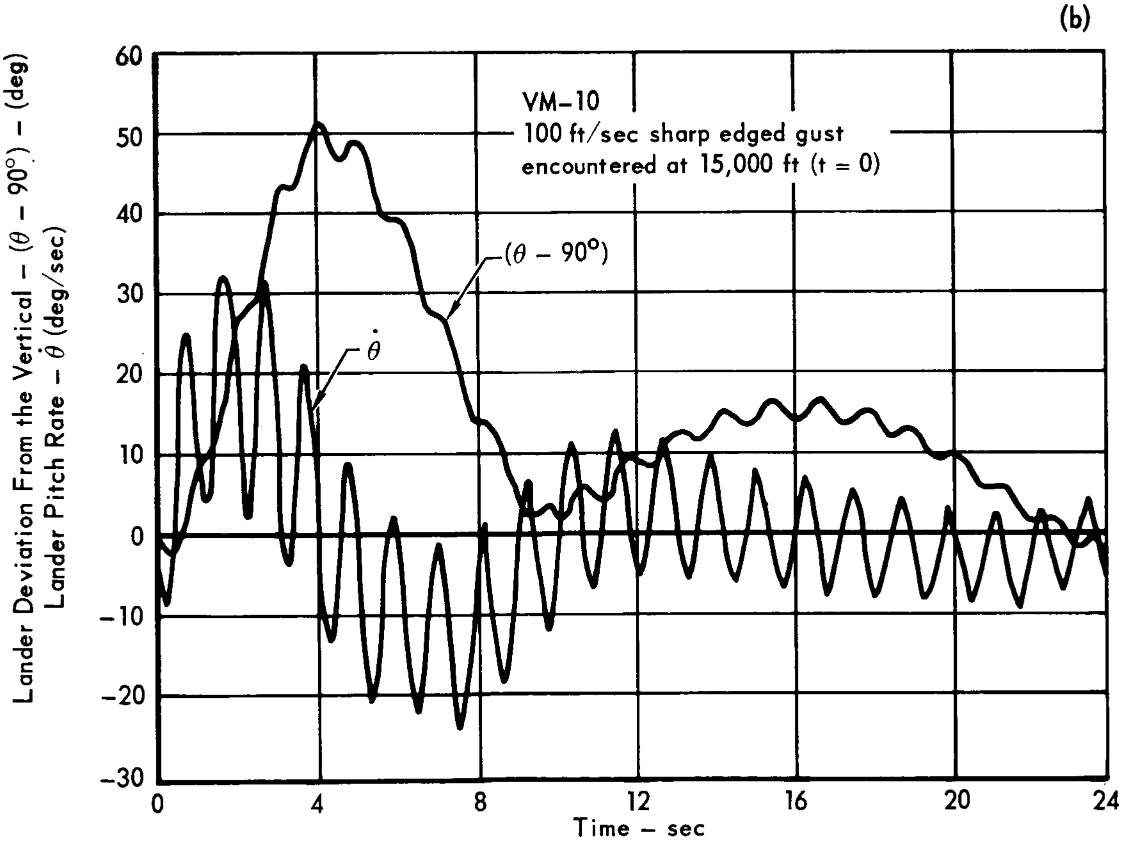

Figure 5.10-19

sizing, geometry, and spring constants to obtain the best system stability characteristics for a given disturbance.

As pointed out previously, for wind shears and sharp-edged gusts of moderate magnitude, the system stability is better than that illustrated. In the final analysis it must be realized, however, if high velocity winds and gusts are encountered in the lower Martian atmosphere, TV pictures of the surface may encounter smearing and be of poor quality during the parachute descent phase.

REFERENCES

5.10-1 Charles H. Whitlock, Richard J. Bendura, and Lucille C. Coltrane, Performance of a 26-Meter-Diameter Ringsail Parachute in a Simulated Martian Environment, NASA TM X-1356, March 1967.

5.10-2 Harold N. Murrow, Eight-Week Report of Data Analysis from PEPP-Rocket, Flight 2, Memorandum to Associate Director Langley Research Center, January 20, 1967.

5.10-3 Harold N. Murrow, Eight-Week Report of Data Analysis from PEPP-Rocket Flight 3, Memorandum to Associate Director Langley Research Center, February 24, 1967.

5.10-4 C. V. Eckstrom and H. N. Murrow, Recommended Changes for PEPP Program Ringsail Parachute Design Based on Evidence from Flight Tests R/L 2 and 5 and B/L 1, Langley Research Center, PEPP Files, May 29, 1967.

5.10-5 Final Report VOYAGER Aerodynamic Decelerator Study, NVR-6018; Northrop Corporation, Ventura Division, July 1967.

5.10-6 Fred E. Mickey and Jay W. Stuart, Jr., Sensing Techniques for Initiating Parachute Deployment on a Mars Lander Vehicle, AIAA Paper No. 67-2-2, January 23-26, 1967.

5.10-7 1973 Voyager Capsule Systems Constraints and Requirements Document, Revision 2, SE003BB002-2A21, 12 June 1967

5.10-8 W. F. DeMario and R. V. Lashbrook, Effects of Heat on a Nylon Fabric, NVR-4028, Northrop Corporation, Ventura Division, March 1966.

5.10-9 Performance of and Design Criteria for Deployable Aerodynamic Decelerators, USAF Technical Report ASD-TR-61-579, December 1963.

5.11 PYROTECHNICS - The pyrotechnic subsystem supports the Capsule Bus by non-repetitive sequencing of major mission events through controlled explosive or pyrotechnic actuations in devices. The firing circuit functions between the firing energy source, the event controllers and the pyrotechnic devices. The pyrotechnic firing circuit design is typical for each pyrotechnic sequence performed and is based on firing three electro-explosive devices (EED) simultaneously from the EED bus supplied by this energy source. Monitor and checkout requirements are incorporated as they affect the type of component selected.

This study evaluates and selects the preferred components for performing the CBS pyrotechnic initiation functions. The circuit selected is shown in Figure 5.11-1. A more detailed schematic of the typical EED firing circuit is shown in Figure 5.11-2 showing the monitor and test provisions required for firing three EED's simultaneously for a single pyrotechnic event.

5.11.1 Functional and Technical Requirements - The VOYAGER Flight Capsule requires a different approach to the pyrotechnic firing circuit checkout and EED connection procedures than previously used, due to the constraints imposed by sterilization. Conventional pyrotechnic firing circuit designs permit final connections of the firing circuit flight harness to the EED as late in the countdown as possible. The procedure is to install the EED in the device and to connect a shorting plug as close to the EED as possible prior to movement of the spacecraft to the launch pad. During the final checkout and launch countdown, the complete firing circuit including harness is checked out on the launch pad. The shorting plug is then removed and is replaced with the firing circuit harness. Resistance checks are then made from test connectors on the fire control panel to verify that the final connections and the subsystem are ready for launch. At no time after the live EED is connected to the firing circuit is any of the circuitry sequenced.

Application of this checkout procedure to the VOYAGER Flight Capsule pyrotechnic subsystem is not possible because the installed EED's and firing control modules are not accessible after installation of the sterilization canister. Without this capability it will be necessary to design remote shorting and checkout provisions into the EED firing circuitry to provide checkout of the firing circuit with the live EED installed and connected.

5.11.2 Alternate Approaches - The functional block diagram illustrated in Figure 5.11-3 represents the necessary circuit elements to satisfy the requirements that are applicable to the pyrotechnic firing circuitry. This block diagram shows a separate power source connected to the EED bus through a safe/arm device to permit

CBS PYROTECHNIC MAJOR ELEMENTS FUNCTIONAL SCHEMATIC

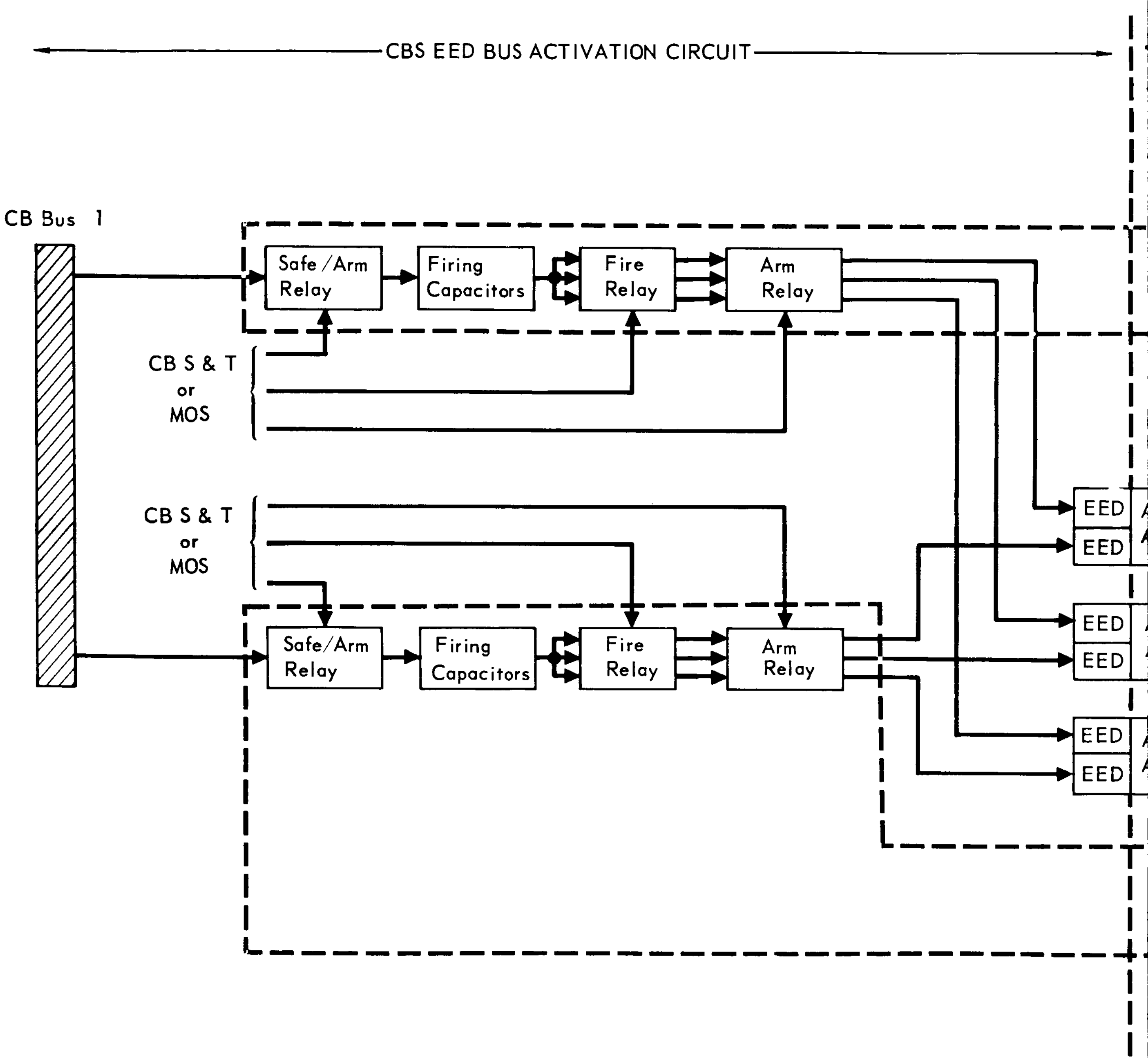
CBS EED BUS ACTIVATION CIRCUIT
CB Bus 1
Safe /Arm Relay
Firing Capacitors
Fire Relay
Arm Relay
CB S & T or MOS
CB S & T or MOS
Safe/Arm Relay
Firing Capacitors
Fire Relay
Arm Relay
EED
EED
EED
EED
EED
EED

Figure 5. 11-1

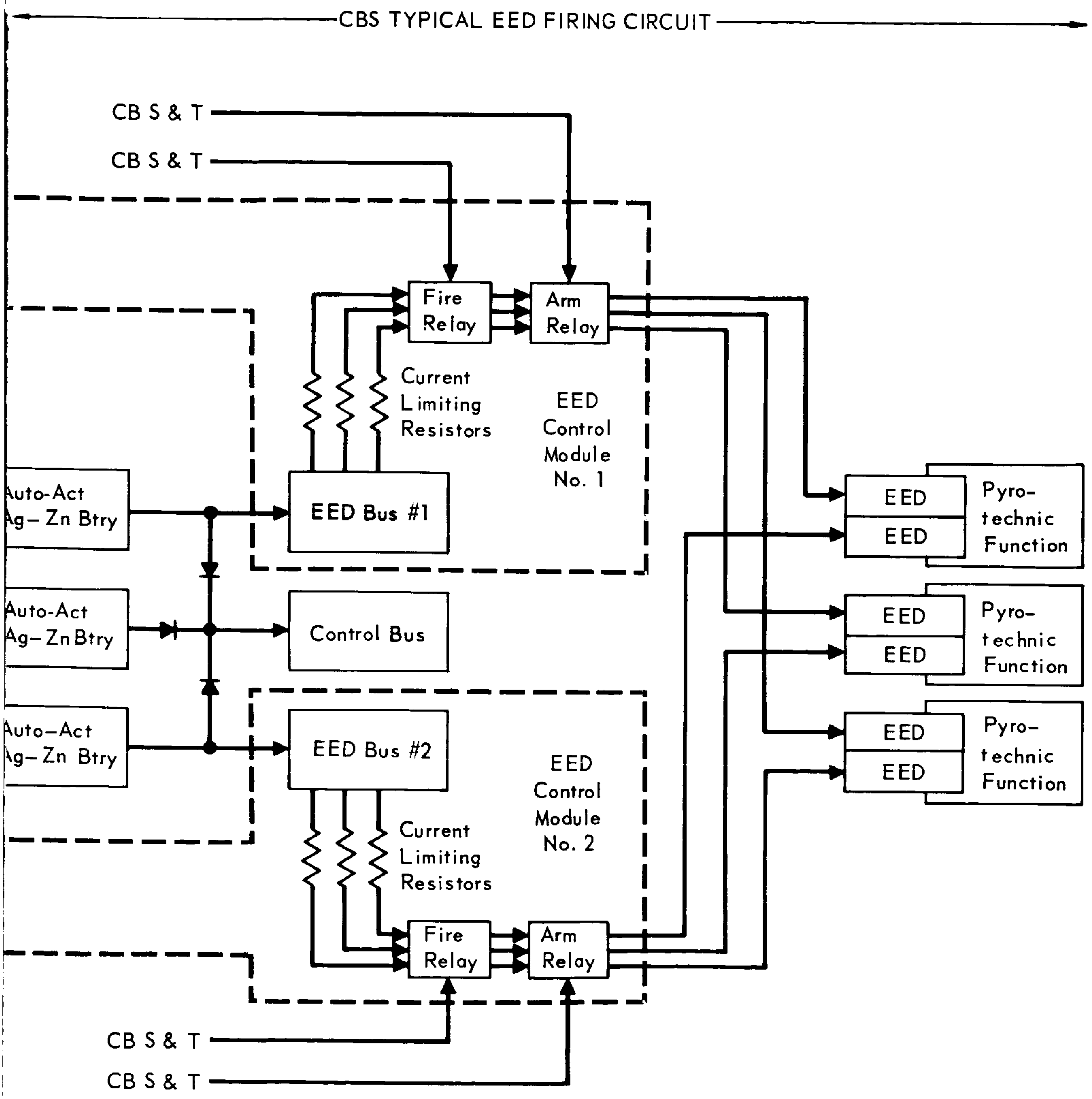
CBS TYPICAL EED FIRING CIRCUIT
CB S & T
CB S & T
Fire Relay
Arm Relay
Current Limiting Resistors
EED Control Module No. 1
uto-Act
g– Zn Btry
EED Bus #1
Auto–Act
Ag–Zn Btry
Control Bus
uto–Act
g– Zn Btry
EED Bus #2
EED Control Module No. 2
Current Limiting Resistors
Fire Relay
Arm Relay
CB S & T
CB S & T
EED
EED
Pyro-technic Function
EED
EED
Pyro-technic Function
EED
EED
Pyro-technic Function

SELECTED CBS EED FIRING CIRCUIT

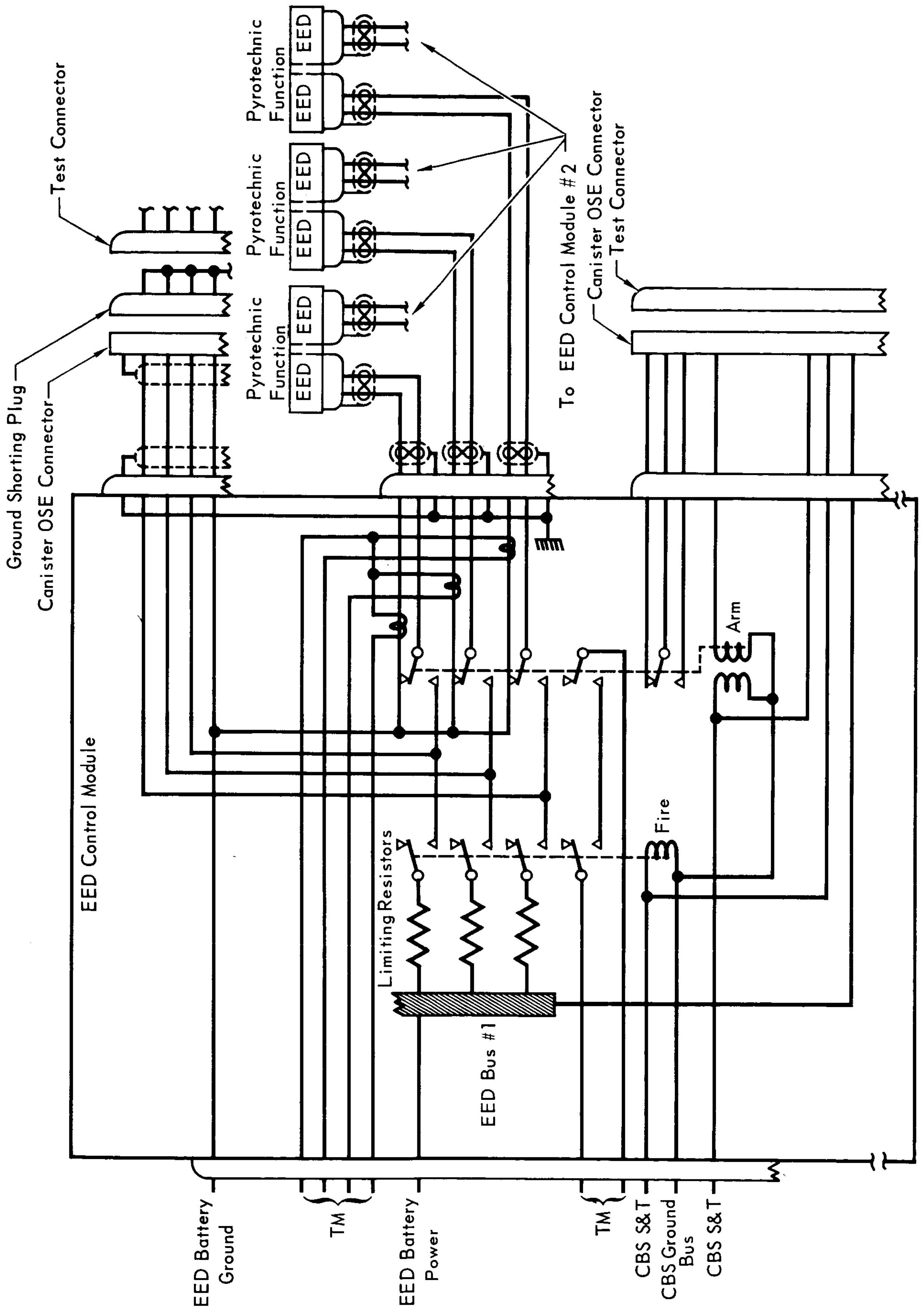
Test Connector
Ground Shorting Plug
Canister OSE Connector
Pyrotechnic Function
EED
EED
Pyrotechnic Function
EED
EED
Pyrotechnic Function
EED
EED
To EED Control Module #2
Canister OSE Connector
Test Connector
EED Control Module
Arm
Fire
Limiting Resistors
EED Bus #1
EED Battery Ground
TM
EED Battery Power
TM
CBS S&T
CBS Ground Bus
CBS S&T

Figure 5. 11-2

FUNCTIONAL SCHEMATIC OF PYROTECHNIC FIRING CIRCUIT

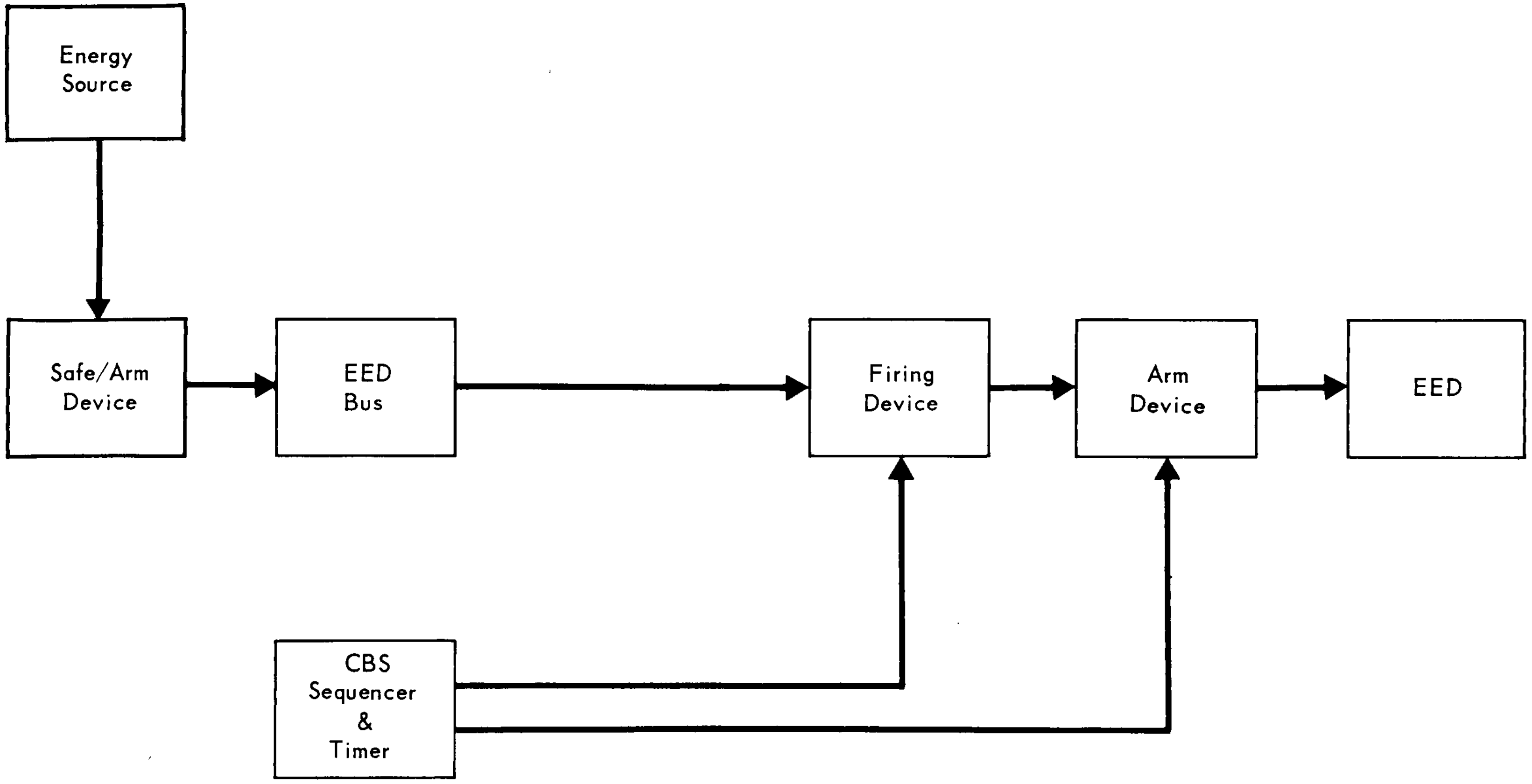
Energy Source
Safe/Arm Device
EED Bus
Firing Device
Arm Device
EED
CBS Sequencer & Timer

Figure 5.11–3

disarming the bus for maximum safety. The firing and arming devices, both controllable from separate sequencer commands, meet the necessary single point failure criterion that, "no single or common failure mode (including procedural deviation) shall both arm and command the pyrotechnic subsystem". In addition, the arm device will short and ground the installed EED.

5.11.2.1 Energy Sources - Use of separate energy sources for pyrotechnic firing, isolated from other subsystem uses, requires either separate batteries or capacitors charged from the main dc power bus to supply power to the pyrotechnic buses, EED's require large surges of current and reflect large voltage transients while firing. In addition, the inherently high probability of EED shorting, after firing due to the carbon deposits bridging between the pins, can cause even greater transients while the fault is being cleared, These transients can cause adverse effects on other more sensitive subsystem components if they are operating from the same energy source.

5.11.2.2 Separate Batteries - All of the pyrotechnics associated with the Capsule Bus are activated within a six hour period nearing the end of the mission. Manually activated silver zinc batteries to supply this energy would be required to have a long wet stand capability; therefore, this type of battery would be necessarily oversized to provide the high power requirements for EED firing. An automatically activated silver-zinc battery requiring a wet stand life of only eight hours has a much higher discharge rate and results in a considerable weight savings. Two 2 lb batteries of the auto-activated type could provide the necessary energy to fire just the Capsule Bus pyrotechnics. However, the energy for pyrotechnic devices and for solenoid loads are supplied by three 8 lb batteries.

5.11.2.3 Capacitors - Capacitors can be charged from the main DC power bus and will provide the necessary high rate energy discharge required for pyrotechnic firing. Adequate isolation can be provided by limiting the charging current, with resistors, to a small value. This has the advantage that, if the EED short-circuits after firing, the capacitor will completely discharge so that the remaining current to the shorted EED will be reduced to the low charging current of the capacitor, minimizing the interrupt requirements of the firing device.

The capacitor, being inefficient as a low voltage energy source, will increase in size the further it is from the EED because of the energy dissipated in the firing line. In order to keep the capacitor as small as possible it must be located close to the EED. In addition, parallel firing of EED's requires that the resistance in the firing lines be balanced to insure adequate energy to each EED.

The pyrotechnics on Mariner C were fired by capacitors charged to 30 Vdc by a transformer rectifier operating from the main ac bus. A wet foil tantalum capacitor was required to fire each bridgewire and had a capacity of 1800 μf, weighed 125 grams, and was encased in a hermetically sealed container 1.27 in. x .69 in. x 2.5 in. It was manufactured by General Electric Company and would withstand a temperature of 125°C. General Electric's Capacitor Division indicates they could make the capacitor sterilizable by going to dry foil. This would increase the weight and volume by approximately 25%. Four capacitor banks each capable of firing four EED's would simultaneously fire all of the Capsule Bus EED's in the proper sequence and would weigh 5 lb.

5.11.2.4 Preferred Concept - The control bus supplies energy to the CBS attitude control and terminal propulsion high power loads. McDonnell has found from past experience that other subsystem components such as thrust chamber solenoids and motors should also be separated from the energy source supplying the more sensitive subsystems components. This approach resulted in fewer EMI problems when the various subsystems were integrated into a complete spacecraft system.

- Power - Use of auto-activated silver-zinc batteries to provide the high discharge rate requirements for operating such items as the Capsule Bus reaction control valves, the terminal propulsion engine control valves, and other high current consuming devices is selected in Section 5.6. These same batteries are selected for firing the Capsule Bus EED's since they have the necessary high rate discharge required and entail little weight increase because of the small amount of energy required.

  Three batteries are used, any two of which can supply the necessary attitude control and terminal propulsion valve power requirements. They are arranged as shown in Figure 5.11-4 which is a successful method of integrating EED firing and other intermittent high power loads from the same energy sources. This concept of three interconnected batteries to supply high rate solenoid loads and fire redundant pyrotechnics was used on all Gemini Spacecraft. Since the EED's can be fired using these batteries without increasing their size, this integrated configuration is the lightest method of supplying the required energy for firing the Capsule Bus pyrotechnics. It is selected as the preferred concept. These batteries are activated by capacitors charged from the CB bus No. 1.

INTEGRATED ENERGY SOURCE ARRANGEMENT SELECTED FOR CBS EED FIRING

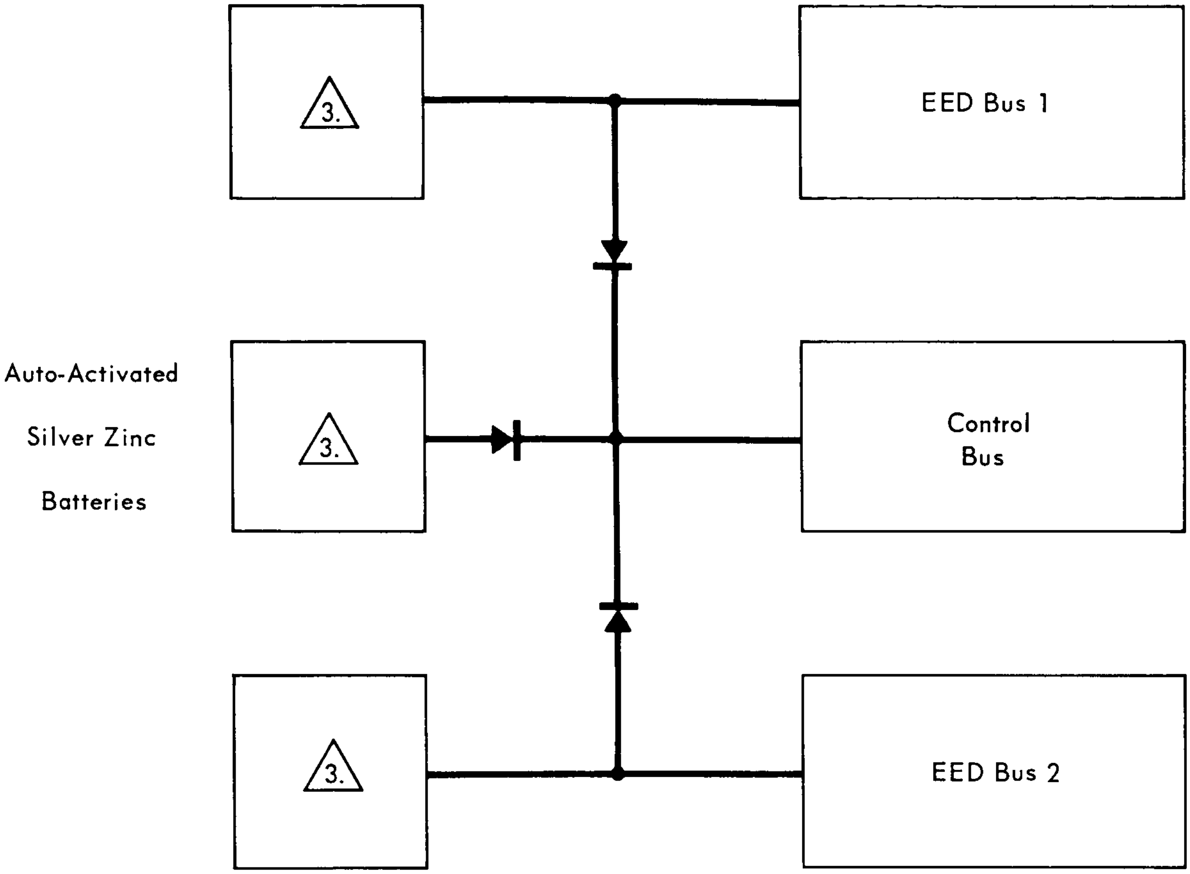
3.
EED Bus 1
Auto-Activated
Silver Zinc
Batteries
3.
Control
Bus
3.
EED Bus 2

1. The control bus supplies energy to the CBS attitude control and terminal propulsion high power loads.
2. The two EED buses are for supplying energy to separate redundant pyrotechnic firing subsystems.
3. All three batteries are the same and are sized to supply all of the energy requirements for one EED bus and 1/2 the energy requirements of the control bus.

Figure 5.11-4

- Safe/Arm Device - The requirement to disconnect the energy sources from the EED buses can best be satisfied by the use of a relay because it provides physical separation and can be controlled and monitored remotely. The use of auto-activated batteries precludes the need for a safe/arm device between these batteries and their buses; however, it is required for the auto-activated battery initiation circuit.
- Current Limiting Device - The EEDs used in the VOYAGER Flight Capsule pyrotechnic subsystems require a 5 ampere all-fire current and have a nominal resistance of 1 ohm. To this resistance is added the firing circuit resistance, consisting of the firing and arming devices, connectors, and firing loads. This resistance ranges between .3 and 1 ohm depending mostly on the length of the firing loads. The firing current is determined by the circuit resistance plus the EED resistance while the short circuit current is determined by the circuit resistance only, because the 1 ohm EED resistance is reduced to zero when short-circuited. A graphical representation of resistance and current for the EED battery maximum and minimum voltage limits is shown in Figure 5.11-5 with a circuit resistance of 1 ohm. The firing current ranges between 12.1 and 17.6 amperes and the short-circuit current ranges between 24.2 and 35.2 amperes. These high currents impose excessive requirements on the EED battery and firing device. Addition of a 1.5 ohm resistor to each firing circuit would result in a circuit resistance variation of from 1.8 to 2.5 ohms. This still allows a minimum firing current of 7 amperes while limiting the short-circuit current to a maximum of 20 amperes. The short-circuit currents are conservative in that the maximum voltage of the battery will not be maintained under short-circuit conditions.

  A resistor is selected as a current limiting device to provide protection against excessive firing current surges and to limit the short-circuit current, thus assuring that the firing device will reliably disconnect the EED after firing.
- Fire and Arm Device - Relays and semiconductor switches were evaluated as alternates for performing the arm and fire functions. Figure 5.11-6 shows the operational and environmental requirements for these devices. In addition, the characteristics of semiconductor switches and relays are included to compare the relative merits of each device in meeting these requirements.

RESISTANCE VS. CURRENT FOR MAXIMUM AND MINIMUM EED BATTERY VOLTAGES

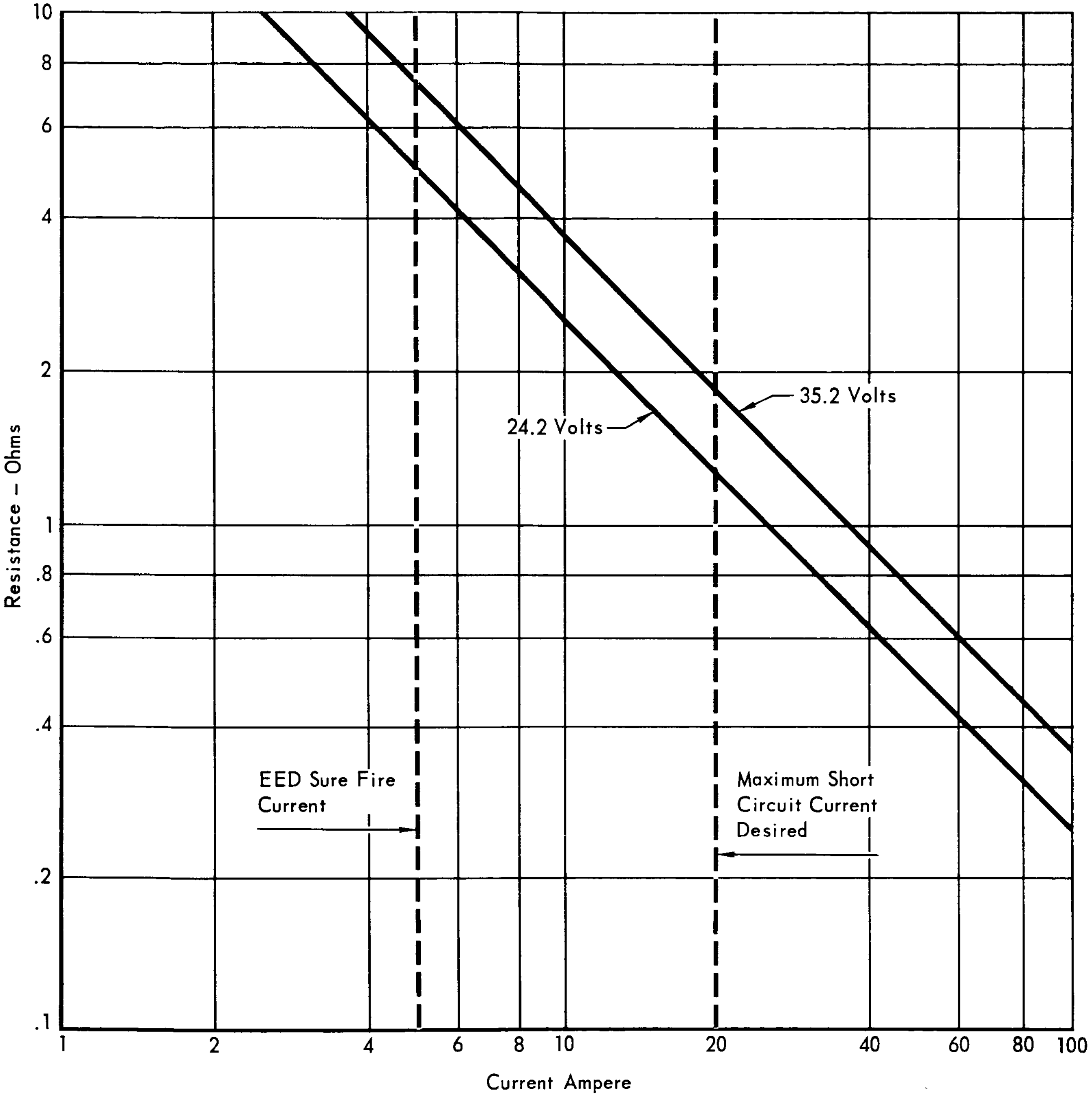

Figure 5.11–5

ARM & FIRE DEVICE COMPARISON

COMPARISON FACTOR	ARM & FIRE SWITCH REQUIREMENTS	SEMICONDUCTOR SWITCH CHARACTERISTICS	RELAY CHARACTERISTICS	REMARKS
Resistance "OFF" State	High Resistance	Allows leakage currents that vary with temperature	For all practical purposes: Infinity	Leakage current through EED after arming not desirable.
Resistance "ON" State	Low Resistance	Approx. 1 ohm	Approx. .010 ohm	Less energy dissipated in relay.
Isolation of control and switch circuit	Isolation of control and switch circuits	Auxiliary circuitry required to achieve isolation	Complete isolation but inductive relay coil requires buffering to protect driver circuit	Reliability would be affected by addition of auxiliary circuitry.
Multi-circuit switch capabilities	4 to 6 circuit configuration	One switching circuit per device equivalent to a S.P.S.T. arrangement	Small size relays, up to 10A contact rating, have from 2 to 6 separate D.P.D.T. switching circuits	Complexity of multi-circuit semiconductor switch much greater and reliability is lower.
Switching speed	.030 seconds adequate	Microsecond range no bounce	.003 seconds min with contact bounce in the order of .0001 sec	Either device would be adequate.
Circuit transients	Insensitive	Very sensitive to voltage transients	Relatively insensitive	Protection can be designed into semiconductor switch.
Life	Less than 50 cycles at rated load	Unlimited life if maximum ratings are not exceeded	50,000 cycles	Either device would be adequate.
Vibration & shock tolerance	Low	High	Low	Either device would be adequate.
Radiation tolerance	Insensitive	Sensitive	Relatively Insensitive	Either device would be adequate.
Maximum storage temperature	135 C	200 C	200 C	Either device would be adequate.

Figure 5. 11–6

Multipole relays are preferred to semiconductor switches for performing the arm and fire functions because of these advantages:

(1) Provides physical in-line separation.

(2) Lower "ON" state resistance.

(3) Electrical isolation between the coil and the contacts of the relays.

(4) 2 to 6 separate D.P.D.T. switching circuits per relay.

(5) Insensitive to voltage transients.

5.11.3 Standardization - With the increasing complexity of spacecraft and increasing severity of mission environments, more frequent use of pyrotechnics to perform many of the required spacecraft functions creates an obvious need for standardization of the initiating electroexplosive devices. The pyrotechnic industry has ascertained by test that gas generating compositions, such as Boron Potassium Nitrate and Aluminum Potassium Perchlorate, and explosive compositions such as HNS, Dipam and Nona are capable of surviving dry heat sterilization cycles without detrimental degradation. Use of these high temperature resistant compositions significantly reduces the sterilization problems on the Flight Capsule. All too frequently the vehicle under development will be furbished with EED's supplied by several different pyrotechnic vendors. Although these devices will meet all the mandatory range requirements, such as the 1 amp, 1 watt, no-fire and others, they also display a considerable variation in their "all-fire" characteristics as determined by Bruceton analysis. They also demonstrate other minor differences in other electrical characteristics. These variations are due to the use of different bridgewire materials, possible differences in bridgewire lengths and/or diameters, different ignition mixes in contact with the bridgewire, variations in consolidation pressure of the ignition mixes and variation of heat sink materials surrounding the ignition mix.

5.11.4 Standardization Problem Areas - In an attempt to overcome this problem at the inception of the Apollo Program, NASA developed a standardized EED, known as the Apollo Standard Initiator (ASI). This modular EED is the basic energy conversion unit for all Apollo/LM pyrotechnic systems. It can be used individually as a small pressure cartridge to actuate small mechanical devices, or it can serve as the basic ignition source when assembled into higher level devices such as detonators. This system has performed satisfactorily, but as of this writing, there is only one qualified vendor.

5.11.5 Standardization Alternatives - Standardization can be accomplished by any one of three principal alternatives, namely:

a. Select the Single Bridgewire Apollo Standard Initiator (SBASI) and base all pyrotechnic designs on the use of this initiator.
b. Procure all the initiators to be used in the program from one vendor which would essentially establish a fair degree of standardization.
c. Set forth a basic design specification covering the bridgewire/ignition interface of the EED's, and then procure the initiators from several vendors, who would incorporate these details in their overall design, thereby establishing a uniform set of electrical characteristics.

5.11.5.1 SBASI Approach - In the case of the ASI, one of its principal advantages was that through the development, qualification and subsequent test firings of several thousand cartridges, an extremely high reliability and confidence level has been established. However, in order to meet the relatively new NASA 25,000 volt static discharge requirement it became necessary to redesign the ASI from the dual-bridge circuit into a single bridge circuit EED, known as the SBASI. As a result of this change a considerably reduced quantity of EED's have been tested to date and though the SBASI is fully qualified it does not have the equivalent breadth of test data.

Several studies by various companies in the pyrotechnic industry have been run in the last three years to determine the ability of EED's to survive dry heat sterilization. Since these studies did not include the ASI as a candidate EED, McDonnell undertook a test program designed to answer this question. It has been found that the ASI will successfully survive the immediate effect of dry heat sterilization. Testing, however, is being continued to determine that the ASI's performance will not degrade during the post sterilization long term storage, as it applies to the VOYAGER cruise phase. Since the SBASI contains the same pyrotechnic components as the ASI, test data gained on the latter can be applied to the former.

5.11.5.2 The Single Vendor Approach - The second alternative where all the EED's would be procured from a single vendor has one major disadvantage. It requires that other vendors building mating hardware, such as thrusters, pin pullers, valves, etc., must determine theoretically the output charges necessary to operate these devices and this information must be fed back to the EED vendor. Since slight changes are often required in output loads during development, this would introduce a formidable procurement headache.

5.11.5.3 Basic Design and Specification Approach - The third alternative allows each vendor to manufacture his own EED's as is generally the case in the pyrotechnic industry. By tightly controlling the specification and design of the pin spacing, the bridgewire, the ignition mix, the alumina or beryllia cup for the ignition mix and the closure disk for this mix as shown in Figure 5.11-7, a high degree of standardization can be achieved between the EED's manufactured by any of the vendors. By single-source procurement of the most critical components, such as the ignition mix, and supplying it to each vendor a degree of standardization closely approximating the ASI/SBASI can be achieved.

5.11.6 Recommended Design Approach - The lightest, most reliable method of supplying energy to the CBS pyrotechnic subsystem is to use the same auto-activated silver zinc batteries that supply the attitude control and terminal propulsion loads. It is concluded that the lightest, most reliable method of activating these batteries is to charge capacitors from the CBS manually activated, silver zinc batteries. Relays are preferred for use in the pyrotechnic firing circuitry because they provide better isolation than semiconductor switches. In addition, they provide the capability to short and ground each installed EED until time for firing.

The selection of the preferred EED is based on the above considerations and strongly favors the use of the SBASI. Additional testing must be performed to determine that the SBASI conforms to all of the VOYAGER environments and design constraints. Should the SBASI be found unacceptable for VOYAGER use, then the basic design and specification approach discussed in section 5.11.5.3 above is the alternate approach.

STANDARDIZED ELECTRO-EXPLOSIVE DEVICE

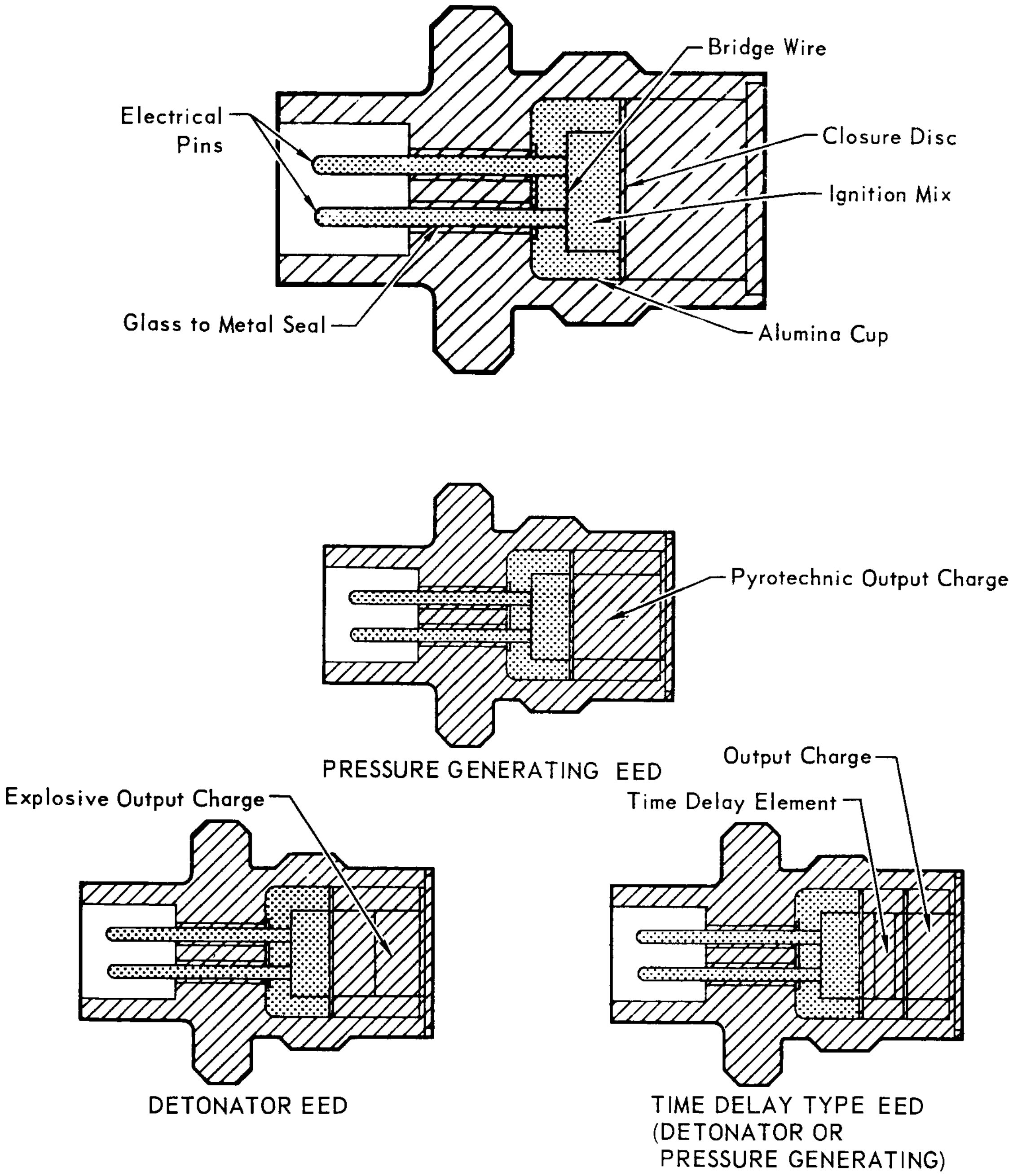
Bridge Wire
Electrical Pins
Closure Disc
Ignition Mix
Glass to Metal Seal
Alumina Cup
Pyrotechnic Output Charge
Explosive Output Charge
Output Charge
Time Delay Element

PRESSURE GENERATING EED

DETONATOR EED

TIME DELAY TYPE EED
(DETONATOR OR
PRESSURE GENERATING)

▒ Design Area Specified to All Vendors

▨ Vendor Design Responsibility

Figure 5.11–7

5.12 THERMAL CONTROL - The problem of thermal control of the Capsule Bus during all mission phases is largely dependent on whether the SLS is powered with batteries or a radiosotope thermoelectric generator (RTG). In the 1973 preferred design concept, batteries are used, hence, the thermal control problem is mainly one of retaining internally generated heat during the steady state cold environment of the cruise mission phase. In later missions, which utilize RTG developed electrical power in the SLS, the large amounts of heat rejected by the RTG must be dissipated efficiently if acceptable Capsule Bus temperatures are to be maintained.

5.12.1 Thermal Control for Missions Utilizing Battery Power in SLS - The long term, steady state cold environment of the cruise mission phase is the design condition for determining thermal control power requirements. During this mission phase the Flight Capsule is in the shade of the Spacecraft and its solar panels. As a result no external heating is available and an acceptable equilibrium condition must be maintained by generating heat internally at the same rate that heat is lost by radiation to space. Since the available power is limited, a multilayer insulation blanket is used to minimize heat loss.

The design condition for determining the location of the insulation blanket and the canister separation timing is the orbital descent mission phase. Canister separation has a strong interface with Capsule Bus thermal control because of the possibility of mounting the multilayer insulation blanket to the canister.

5.12.1.1 Thermal Control During the Cruise Mission Phase - The Surface Laboratory internal equipment temperature range during the cruise phase is limited to a range of 40°F to 125°F. Temperatures will be maintained within this range by the heat released during the SLS battery charging process. This is a continuous process except during the short mid-course maneuver periods when Spacecraft supplied power is not available. The design objective for the minimum structural temperature is -150°F. This is to avoid possible degradation of the heat shield ablator. Analytical results indicate that these temperatures can be maintained with the power available by using a multilayer insulation blanket.

The required multilayer insulation blanket will completely surround the Capsule Bus and can be placed either inside or outside the sterilization canister as discussed in Section 5.12.1.2. The blanket will be constructed of from 16 to 35 sheets of Mylar coated with aluminum. The sheets will be either crinkled or dimpled to minimize contact between layers. The blanket will be approximately .5 inches thick and will have a protective cover sheet to protect it from ground handling damage. Thermal performance testing has been performed on various blanket configurations by General Electric under JPL Contract No. 951537. These tests yielded the following vacuum thermal conductance data:

Configuration	Effective Thermal Conductivity BTU-ft/hr-ft^2-°F
35 sheets wrinkled, aluminized 1/4 mil Mylar	3.2×10^{-5} to 5.7×10^{-5}
16 sheets dimpled, aluminized 1/2 mil Mylar	10.5×10^{-5} to 13.1×10^{-5}
35 sheets wrinkled, aluminized 1/4 mil Mylar (with joint and support post)	4.08×10^{-5} to 6.26×10^{-5}
16 sheets dimpled, aluminized 1/2 mil Mylar (with support post and stitching)	13.5×10^{-5} to 27.6×10^{-5}

These test results indicate that multilayer insulation blankets with effective thermal conductivities of less than 1×10^{-4} BTU-ft/hr-ft^2-°F can be fabricated using wrinkled aluminized Mylar. Although this test data shows higher values for the dimpled Mylar blankets, it is felt that effective conductivities of less than 1×10^{-4} BTU-ft/hr-ft^2-°F can be obtained by using additional layers of the dimpled material. Additional testing is required before the optimum material and configuration for the blanket can be selected. However, the test data indicates that an effective thermal conductivity of 1×10^{-4} BTU-ft/hr-ft^2-°F is a realistic goal and this value was used in all calculations.

The possibility of a change in the preferred design concept which would locate the multilayer insulation blanket inside the Sterilization Canister must be considered. The previously referenced General Electric test report indicates that aluminized Mylar and ETO are incompatible except at very low humidity. Therefore, McDonnell is presently performing feasibility tests of gold coated Kapton as described in Volume VI, Part B, Section 1.0.

The analytical study of the CBS was performed using the 44 node thermal model shown in Figure 5.12-1, the McDonnell T-154 General Heat Transfer Program, and the McDonnell 149T Radiant Interchange Within an Enclosure Program. The T-154 is a general program coded in Fortran for the IBM 7094 computer and for the CDC-6400. The program is used to determine two- and three- dimensional temperature distributions in structure and insulation for transient and steady state heating. The thermal model is defined by any combination of, or in either, a rectangular, cylindrical, spherical, or conical coordinate system. The transient solution of the energy balance equations is achieved either by the forward, mid, or backward finite difference techniques, using a maximum of 4000, 600, or 600 temperature nodes, respectively. A forward difference equation is most rapidly solved by the machine. However, a mathematical model of metallic structure with thin gauges requires an

REPRESENTATIVE VOYAGER THERMAL MODEL
30° CONICAL SEGMENT

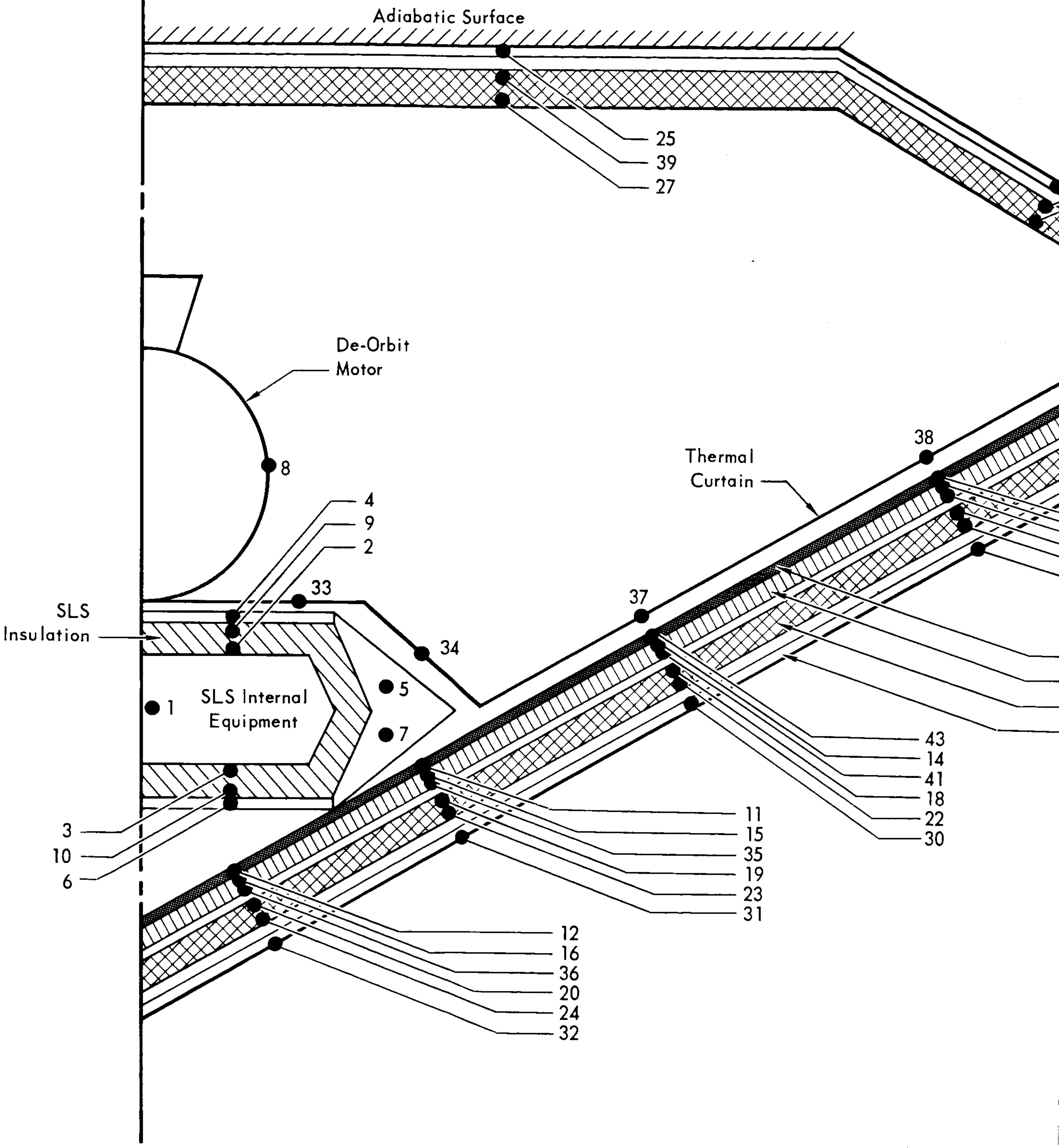

Adiabatic Surface
25
39
27
De-Orbit
Motor
8
Thermal
Curtain
38
4
9
2
33
SLS
Insulation
37
34
1
SLS Internal
Equipment
5
7
43
14
41
18
22
30
3
10
6
11
15
35
19
23
31
12
16
36
20
24
32

Figure 5.12-1

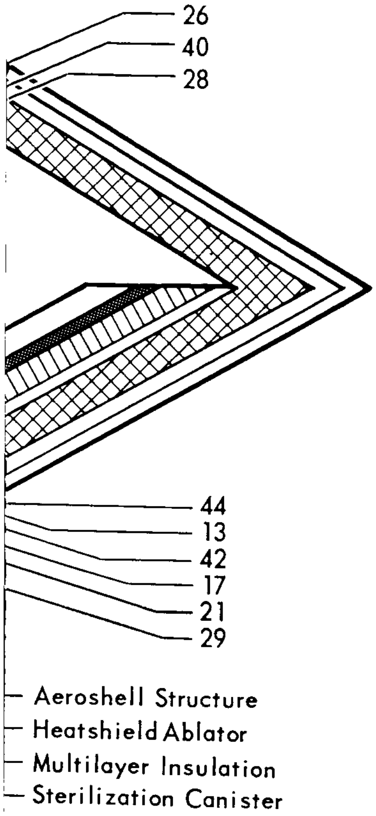
26
40
28
44
13
42
17
21
29
Aeroshell Structure
Heatshield Ablator
Multilayer Insulation
Sterilization Canister

CRUISE PHASE TEMPERATURE DISTRIBUTION

Battery Powered SLS

SLS Insulation k/x = .006 BTU/hr-ft^2-°F

- SLS internal equipment and de-orbit motor controlled to 40°F.
- Power Required = 148 watts

Node No.	Temperature (°F)
1	40*
2	40
3	40
4	-114
5	-115
6	-147
7	-149
8	40*
9	-114
10	-147
11	-151
12	-152
13	-138
14	-138
15	-151
16	-152
17	-141
18	-141
19	-153
20	-155
21	-302
22	-302
23	-304
24	-304
25	-118
26	-327
27	-118
28	-122
29	-331
30	-331
31	-331
32	-331
33	-110
34	-119
35	-151
36	-152
37	-121
38	-122
39	-118
40	-299
41	-138
42	-139
43	-138
44	-138

- SLS internal equipment and de-orbit motor controlled to 100°F.
- Power Required = 176 watts

Node No.	Temperature (°F)
1	100*
2	100
3	100
4	-47
5	-48
6	-99
7	-101
8	100*
9	-47
10	-99
11	-102
12	-103
13	-65
14	-66
15	-102
16	-103
17	-67
18	-68
19	-104
20	-106
21	-290
22	-290
23	-293
24	-294
25	-50
26	-318
27	-49
28	-53
29	-321
30	-321
31	-321
32	-321
33	-43
34	-50
35	-102
36	-104
37	-52
38	-53
39	-50
40	-287
41	-66
42	-65
43	-66
44	-65

*Controlled Temperatures

excessive number of time steps for a stable solution. Mid or backward difference equations, which are much more stable, often are more desirable, because fewer nodes are needed and time intervals can be greatly increased, thus reducing the number of intervals required to complete the solution. Extensive error checks are built into the program to provide a high degree of confidence in the computations.

The 149T program uses a simplified input of surface boundary coordinates and emittances. This program calculates configuration factors and energy exchange (radiosity) within an enclosure with up to 100 radiating surfaces. Several surfaces can be combined into larger equal temperature surfaces to simplify setup on the T-154. Thus, three functional steps are combined in radiant analysis: configuration factor analysis, radiosity analysis, and reduction in the number of nodes required to accurately solve the problem. The results from the 149T program are then used as input to the T-154 program.

The T-154 program allows the user the option of specifying the temperatures of certain nodes and the program then computes the heater power which must be supplied to those nodes to maintain the specified temperature. The amount of heat required to maintain the equipment within the SLS in a 40°F to 100°F temperature range is a function of the SLS insulation performance. This performance is indicated by the value of the k/x parameter, where (k) is the insulation thermal conductivity, and (x) is the insulation thickness. The smaller the value of k/x parameter, the greater the thermal resistance provided by the insulation. It is undesirable, however, to have the k/x parameter for the SLS insulation too small because this prevents sufficient heat from leaving the SLS to keep Aeroshell ablator temperatures above -150°F. This is an important consideration since the heat leak from the SLS is a significant portion of the heat required for CBS thermal control.

Figure 5.12-2 shows the relationship between SLS internal equipment and deorbit motor temperature, power required, k/x of SLS insulation, and minimum ablator temperature. The value of the SLS insulation k/x parameter is determined by post-landing thermal control requirements and is approximately .006 BTU/hr-ft^2-°F in the vacuum cruise environment. Examination of Figure 5.12-2 shows that a value of k/x = .006 BTU/hr-ft^2-°F would allow the deorbit motor and the SLS internal equipment to be maintained at 60°F with 131 watts of power. This power requirement includes 55 watts which is required for temperature control of equipment mounted to the CBS. The total power requirement for this condition is obtained by adding a 20% contingency factor thus bringing the total to 157 watts.

CRUISE PHASE THERMAL CONTROL

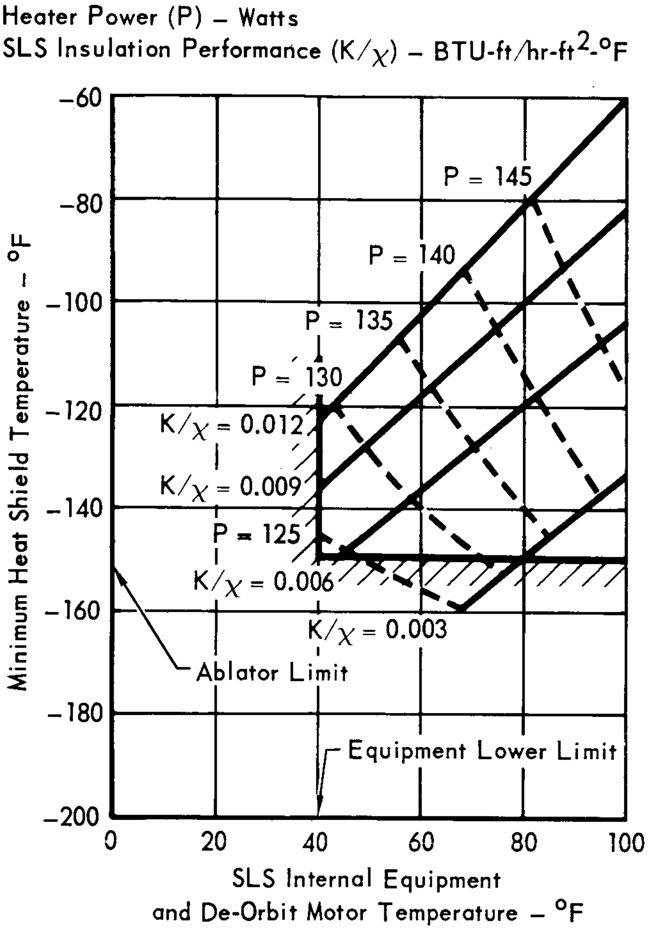

Figure 5.12–2

As previously mentioned, the analysis of the CBS made use of the thermal model shown in Figure 5.12-1. Also shown in the figure are the thermal model temperature distributions for two cruise thermal control conditions. In one case, the SLS internal equipment and deorbit motor are being controlled to 40°F and in the other to 100°F. The total power required for the former is 148 watts and the latter is 176 watts. It can be seen that the higher power condition results in higher Aeroshell structural temperatures while there is little change in temperatures external to the multilayer insulation blanket. It should be noted here that the thermal model shows the multilayer insulation blanket placed within the Sterilization Canister while the preferred design, discussed in Part A, locates the multilayer insulation blanket external to the Sterilization Canister. This difference in location has no effect on the total power requirement because the canister structure offers little thermal resistance.

5.12.1.2 Thermal Control During Mars Orbital Descent - The thermal control methods utilized during the Mars orbital descent mission phase are critical because they determine the multilayer insulation blanket location and the Sterilization Canister separation timing. All the alternatives considered with respect to the above are shown in Figure 5.12-3.

Orbiting the canister allows placing the insulation blanket on the external surface of the canister. The blanket is then separated with the forward canister section, thereby eliminating the requirement for a separate blanket separation sequence. In addition, the blanket would not be subjected to the sterilization cycle and the possible deteriorating effects to blanket metallic coatings if humidity is not properly controlled. Canister materials and separation devices would be kept at a temperature of about -150°F rather than the -330°F which would exist if the blanket were placed inside. External placement would, however, subject the insulation to potential micrometeoroid damage and to possible damage from Spacecraft attitude control system exhaust. These are not considered to be serious effects.

Separation of the Sterilization Canister from the Planetary Vehicle prior to Mars orbit insertion forces the use of a multilayer insulation blanket over the heat shield. A blanket is required because thermal control cannot be maintained with the allotted power during Mars orbit with the large heatshield surface area exposed to space. An insulation blanket over the heat shield is undesirable because: (a) windows must be provided for the various sensors since the blanket is metallic; (b) the blanket must be separated prior to entry to preclude sensor damage due to molten or vaporized metal deposits from the blanket coatings; and (c) the

THERMAL CONTROL TRADEOFFS FOR FLIGHT PHASES

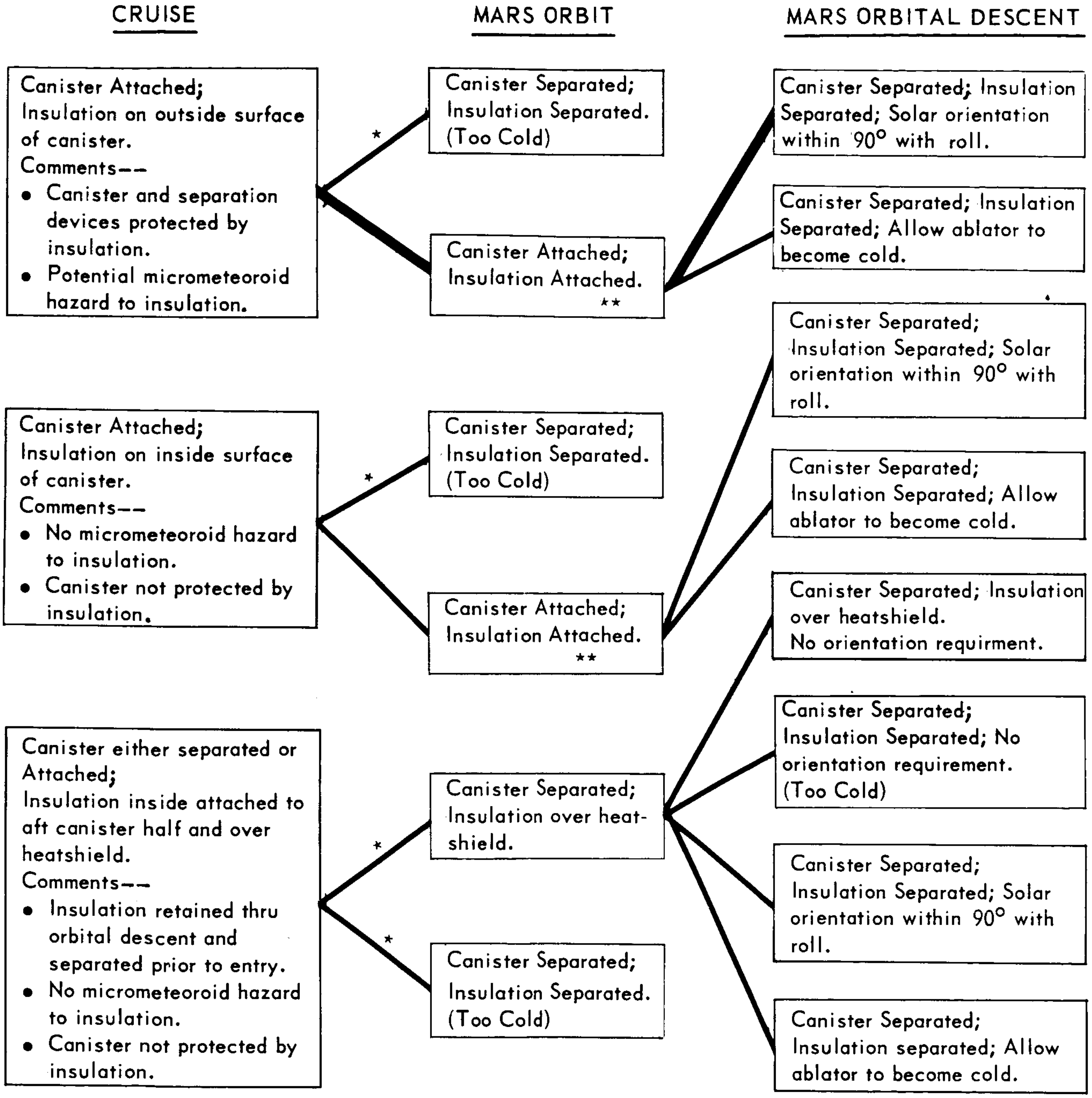
CRUISE
MARS ORBIT
MARS ORBITAL DESCENT
Canister Attached; Insulation on outside surface of canister. Comments-- • Canister and separation devices protected by insulation. • Potential micrometeoroid hazard to insulation.
*
Canister Separated; Insulation Separated. (Too Cold)
Canister Attached; Insulation Attached. **
Canister Separated; Insulation Separated; Solar orientation within 90° with roll.
Canister Separated; Insulation Separated; Allow ablator to become cold.
Canister Attached; Insulation on inside surface of canister. Comments-- • No micrometeoroid hazard to insulation. • Canister not protected by insulation.
*
Canister Separated; Insulation Separated. (Too Cold)
Canister Attached; Insulation Attached. **
Canister Separated; Insulation Separated; Solar orientation within 90° with roll.
Canister Separated; Insulation Separated; Allow ablator to become cold.
Canister either separated or Attached; Insulation inside attached to aft canister half and over heatshield. Comments-- • Insulation retained thru orbital descent and separated prior to entry. • No micrometeoroid hazard to insulation. • Canister not protected by insulation.
*
Canister Separated; Insulation over heatshield.
*
Canister Separated; Insulation Separated. (Too Cold)
Canister Separated; Insulation over heatshield. No orientation requirment.
Canister Separated; Insulation Separated; No orientation requirement. (Too Cold)
Canister Separated; Insulation Separated; Solar orientation within 90° with roll.
Canister Separated; Insulation separated; Allow ablator to become cold.

▬ Preferred Approach

* Canister Separation prior to attaining Mars Orbit.

** Canister Separation just prior to deorbit.

Figure 5.12-3

means of separation is complicated by the blanket's lack of rigidity. Thus, it is highly desirable to eliminate these difficulties by retaining the canister into Mars orbit.

If the Sterilization Canister is taken into orbit, the current planetary quarantine specification requires that it have an orbit lifetime of at least 10 years. Figure 5.12-4 shows the periapse-apoapse-ballistic coefficient relationships for 10 year orbital lifetimes. As discussed in Section 2.3.1, the current canister design has an m/C_DA of .02 slugs/ft^2 as a randomly oriented orbiting body. Thus, a periapse altitude of at least 720 km is required to comply with the quarantine constraint.

Separation of the multilayer insulation with the Sterilization Canister before deorbit requires that a solar orientation be assumed during the orbital descent if ablator temperatures are to be maintained above -150°F. During this time, heat loss from the backside of the Aeroshell is kept to a minimum by the thermal curtain. Figure 5.12-5 shows the allowable tolerance on the solar orientation. It can be seen that the angle between the Capsule Bus roll axis and the Sun line can be as large as 50 degrees before the ablator at the coldest point drops below -150°F. If the Capsule Bus is given a modest roll rate of 3 to 4 rev/hour during the orbital descent period, this tolerance on solar orientation may be extended up to an angle of 90 degrees.

The selected approach to insulation blanket location and canister separation is to attach the insulation to the external surface of the canister and provide canister separation after orbital insertion but prior to the deorbit maneuver. Deorbit thermal control will then be provided by maintaining a solar angle of 90 degrees or less and providing a 3 to 4 rev/hour roll rate.

5.12.2 Thermal Control for Missions Utilizing RTG Power in SLS - Utilization of RTG power in the SLS would require different thermal control methods than those utilized with a battery powered SLS. In this case the large amounts of heat rejected by the RTG must be dissipated efficiently to keep temperatures at acceptable levels. As a result, the multilayer insulation blanket discussed previously would not be required except at the Spacecraft/CBS interface. This is to prevent any of the RTG rejected heat from being transferred to the Spacecraft. Also, time of canister separation and the capsule attitude during orbital descent are not influenced by thermal control constraints.

5.12.2.1 Thermal Control During Launch and Earth Orbit - The launch and Earth orbit mission phases are the most critical with respect to high temperatures existing

ORBITAL SIZE TO PROVIDE 10 YEAR ORBIT LIFE EXTENDED VM-3 ATMOSPHERE

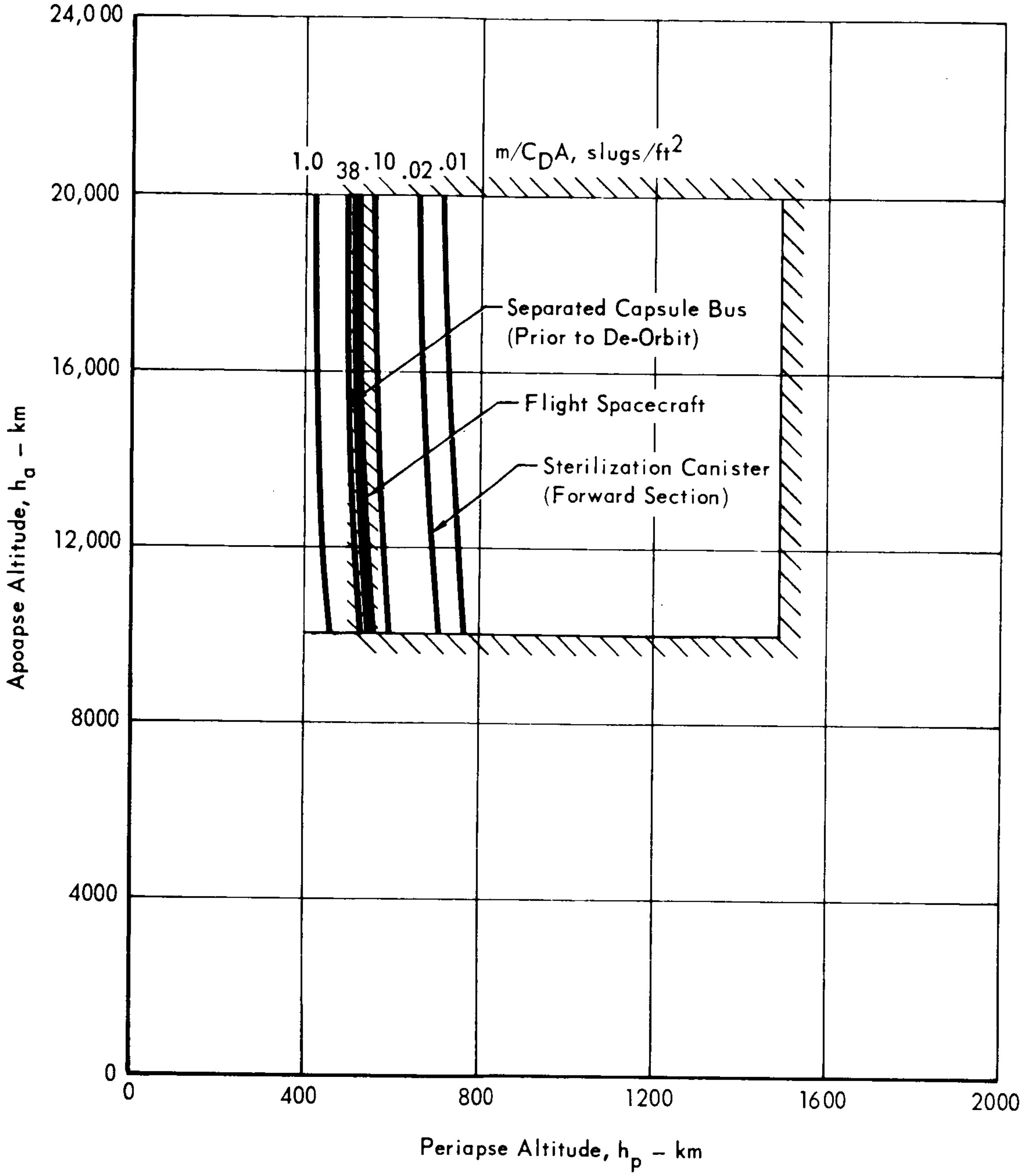

Figure 5.12–4

ABLATOR TEMPERATURES AT END OF ORBITAL DESCENT

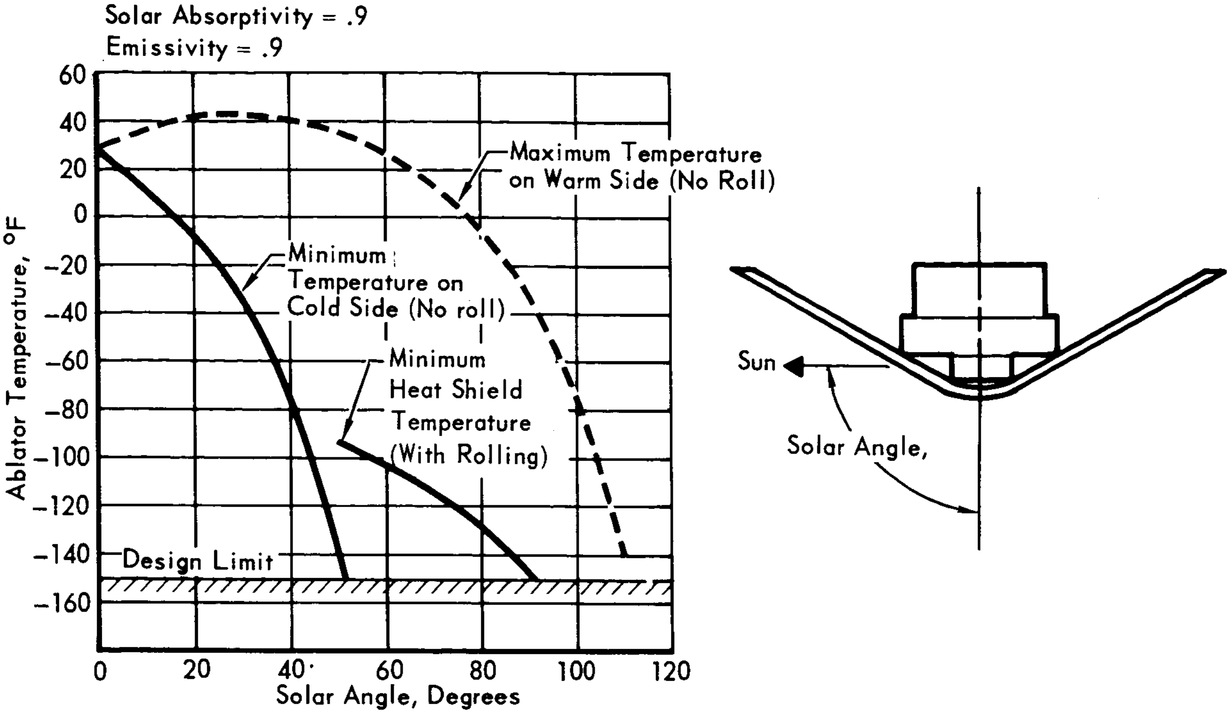

Figure 5.12-5

within the Capsule Bus. This is due to the launch shroud, which inhibits radiant heat rejection, being in place over the two Planetary Vehicles and the aerodynamic heat input during launch.

A transient temperature analysis was conducted using a 49 node, two-dimensional thermal model representing the Capsule Bus with RTG and the launch shroud. RTG heat rejection rates from 4.5 to 10 kilowatts were considered. The results of the study, as shown in Figures 5.12-6 and 5.12-7 indicate that 10 kilowatts of RTG rejected heat could be dissipated through the launch shroud at a sufficient rate to keep temperatures within acceptable limits during the entire launch and Earth orbit periods.

5.12.2.2 Thermal Control During Cruise Mission Phase - The long time spent in the cruise mission phase would require that the RTG heat rejection system be designed to function efficiently under that environment even though it is less severe with respect to temperature than is the launch and Earth orbit mission phase. A study was made to determine the effective RTG radiator area and operating temperature required to reject the RTG generated heat. The results of this study for various RTG heat rejection rates are shown in Figure 5.12-8. A low RTG radiator temperature is desirable in that it increases the RTG efficiency. However, Figure 5.12-8 shows that the required radiator area increases rapidly for a given heat load as lower temperatures are selected.

Figure 5.12-9 shows typical Capsule Bus temperatures which will exist during the Earth-Mars cruise for various RTG heat rejection rates. Surface 1 represents the internal face of the insulation required to thermally insulate the Flight Capsule from the Spacecraft. Surface 2 is the aft portion of the Sterilization Canister through which most of the heat is rejected to space. Surface 3 is the thermal curtain required to protect the internal surfaces of the Aeroshell during Mars entry. Surface 4 represents the forward portion of the Sterilization Canister. It should be noted that all Capsule Bus temperatures are below the sterilization temperature.

AFT CANISTER AND SHROUD TEMPERATURES DURING LAUNCH AND ONE EARTH ORBIT

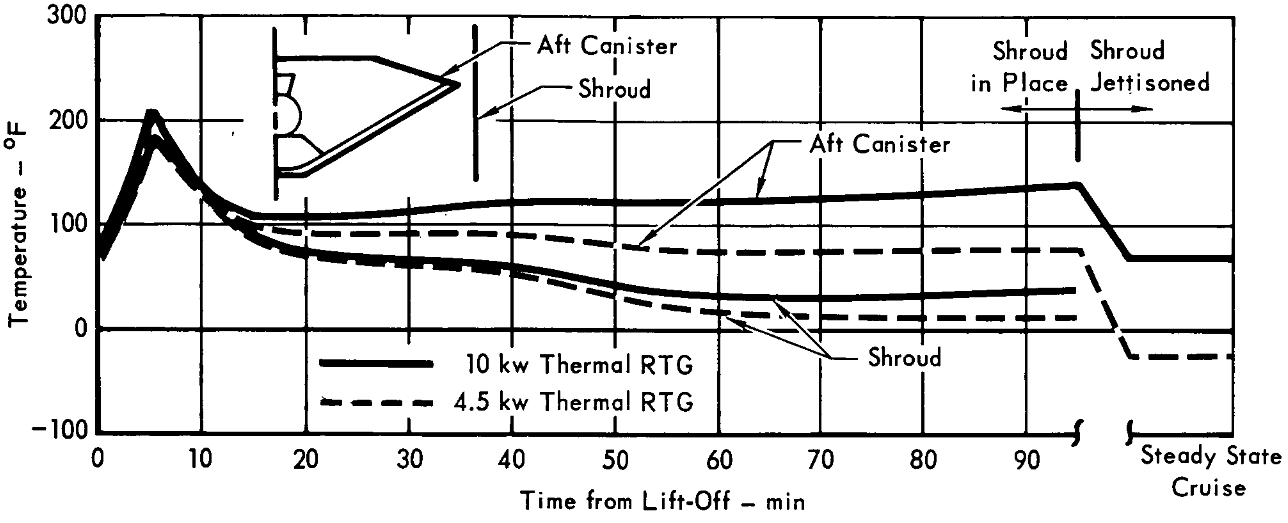

Figure 5.12-6

INSULATION SURFACE TEMPERATURE DURING LAUNCH AND ONE EARTH ORBIT

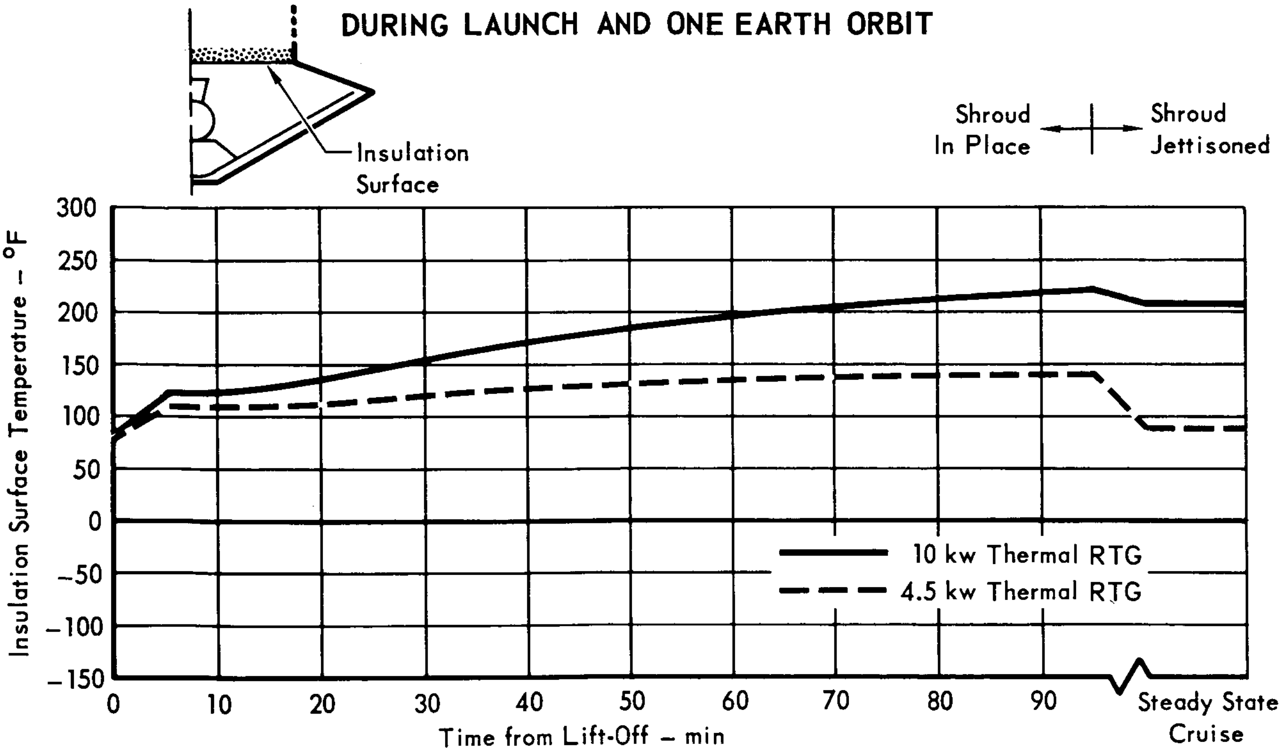

Figure 5.12-7

VOYAGER RTG RADIATOR TEMPERATURES DURING INTERPLANETARY CRUISE

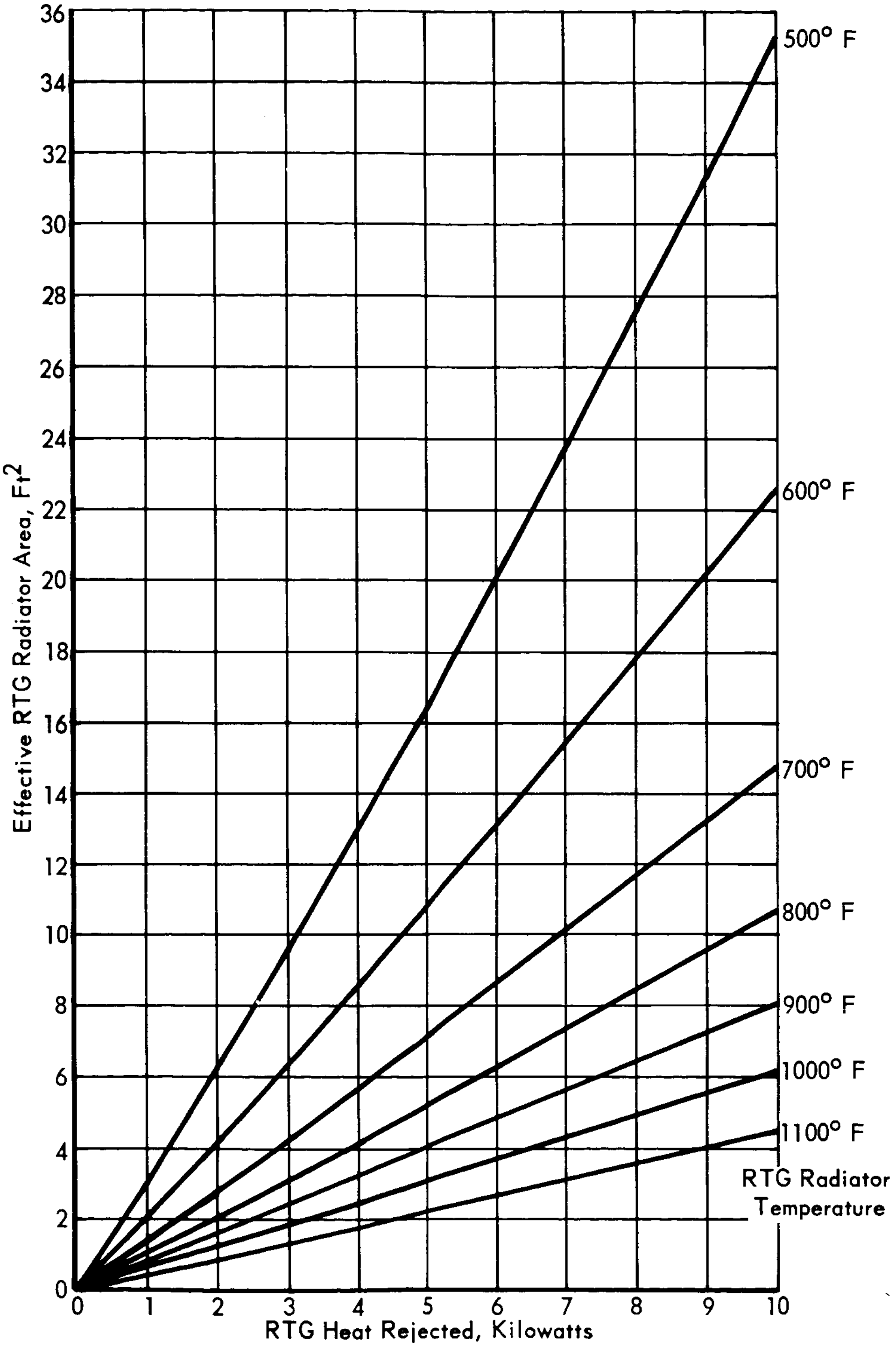

Figure 5.12-8

VOYAGER FLIGHT CAPSULE TEMPERATURES DURING INTERPLANETARY CRUISE

RTG POWER SYSTEM

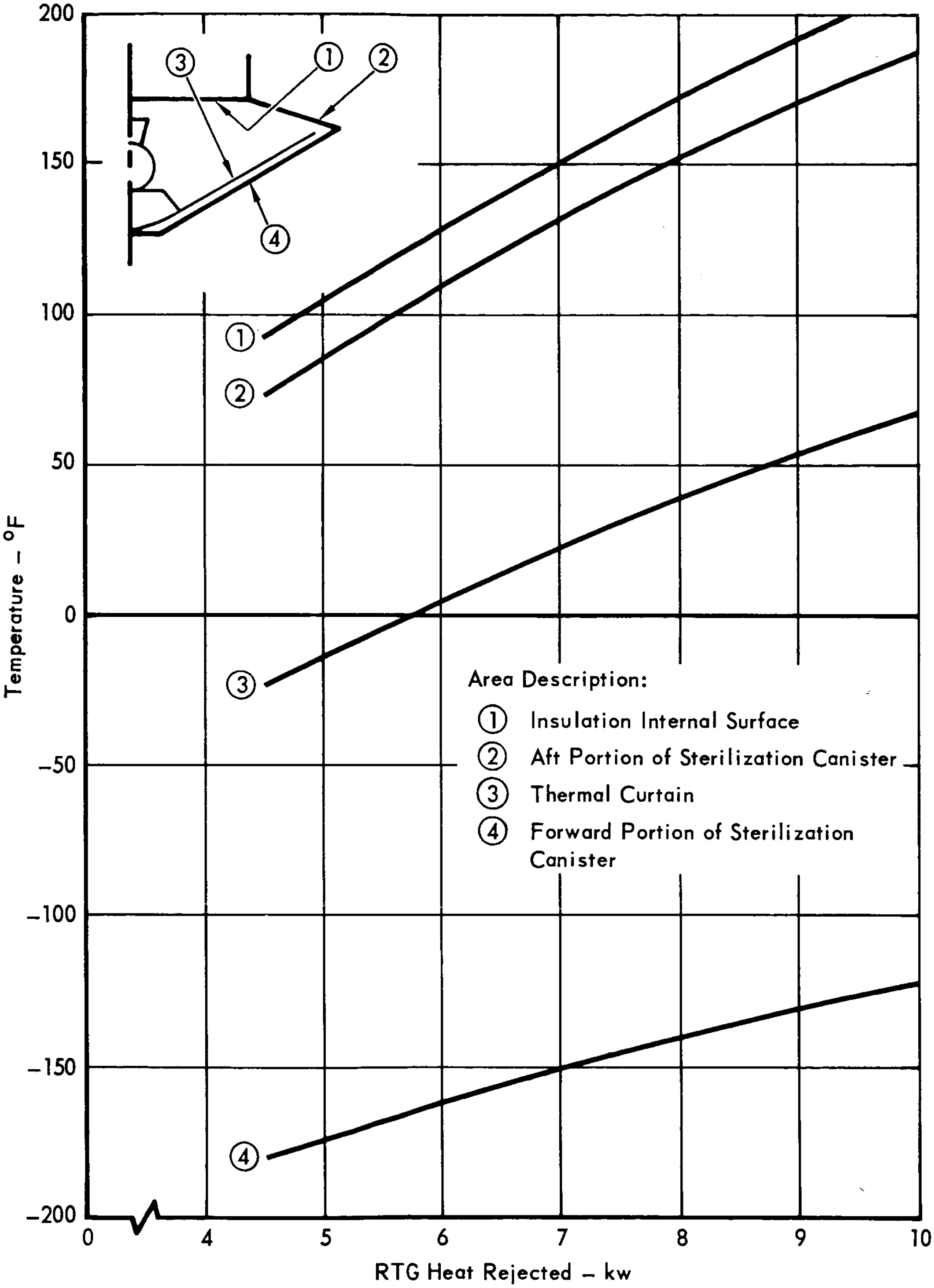

Figure 5.12-9

5.13 PROPULSION - The Capsule Bus requires propulsion for attitude control, de-orbit and terminal descent. The propulsion subsystem types which can potentially meet the VOYAGER sterilization requirements and have achieved a development status sufficient to indicate successful qualification for the 1973 launch, have been evaluated to establish the best combination of subsystems for accomplishing these functions. Specifically, cold gas, monopropellant, bipropellant and solid propellant subsystems were considered where applicable to the various mission phases. In addition, thrust vector control (TVC) devices were evaluated for the powered phases of the mission, viz., de-orbit and terminal descent.

For each of the mission phases, the applicable subsystems were evaluated and compared; the following subsystems were selected for the functions indicated:

a. Attitude Control - Monopropellant (hydrazine)

b. De-orbit - Solid propellant (polybutadiene/ammonium perchlorate)

c. Terminal Descent - Bipropellants (nitrogen tetroxide/monomethyl hydrazine)

The attitude control subsystem utilizes eight thrust chambers, located on the perimeter of the Capsule Bus, to achieve control during the de-orbit and unpowered flight phases of the mission. Four uncoupled and aft-pointing chambers provide pitch and yaw control; two coupled pairs, tangentially oriented, effect roll control.

A single rocket motor was chosen for the de-orbit function.

The preferred terminal propulsion subsystem consists of four engines, located at the corners of a rectangle and spaced approximately 44.0 inches from the capsule center line. Attitude control during terminal descent is accomplished by differential throttling of the engines. Roll control is made possible by tangentially canting the engines to provide roll forces by differential throttling.

Several propulsion subsystem combinations were considered before establishing our preferred design. One combination, consisting of a solid propellant rocket de-orbit motor, a cold gas reaction control and a bipropellant terminal descent subsystem, was attractive. Identical with the preferred design, except for the attitude control subsystem, this subsystem combination offers low development risk and greater reliability at the expense of increased weight and decreased versatility. The present lack of entry wind shear data and precise Capsule stability definition, which could modify RCS requirements,made subsystem versatility a particularly important aspect of evaluating this combination.

From the standpoint of development risk, a configuration consisting of a liquid bipropellant rocket for de-orbit, a cold gas RCS, and bipropellant for terminal descent propulsion is attractive. This would require the development of only two subsystem types, and one of these, cold gas, presents a minimum of development problems. The major disadvantage of the design is the weight penalty (approximately 100 lbs for the 1973 mission) associated with the use of the bipropellant subsystem in place of the solid rocket.

Another possible combination of subsystems consists of a solid propellant rocket de-orbit motor, a monopropellant hydrazine RCS and a monopropellant hydrazine terminal descent subsystem. It requires the development of only two subsystem types and provides a design which has relatively high generic reliability. The primary objection to this concept is the risk associated with the design, development, and qualification of a monopropellant hydrazine engine at the required thrust level (1650 pounds). Currently, the largest hydrazine engine under development is a 300 pound thrust unit. A hydrogen peroxide engine with 600 pounds of thrust is the largest monopropellant ever developed in this country. Thus, the feasibility of a 1650 pound thrust monopropellant hydrazine engine has not been demonstrated. Furthermore, such an engine design, based on current engine technology, is heavy, and results in a subsystem weight penalty of approximately 120 pounds over a bipropellant design. Although the use of a new chamber design concept promises to eliminate this penalty, it would introduce an even greater development risk than the conventional chamber design.

Selection of the propulsion subsystems for our preferred design is based on detail trade studies and supporting analyses. These studies have been confirmed and supplemented by information from propulsion subsystem vendors. Study of the effect of sterilization and decontamination on propulsion subsystem elements was supported by our laboratory testing.

5.13.1 De-orbit Propulsion - The de-orbit subsystem must provide the velocity increment required to deflect the Capsule Bus from a Mars orbit to a trajectory intersecting the surface at a predetermined landing site. Solid propellant, monopropellant, and bipropellant subsystems were all considered as suitable candidates for this function. Various configurations based upon these subsystems were evaluated on the basis of reliability, development status, weight and performance, versatility in meeting changes in mission requirements, and interactions with other subsystems. As a result of these studies a solid motor with thrust termination capability was selected as the preferred concept. Subsequent to this selection, vendor data were gathered to aid in formulating the preferred design. The requirements, trade studies, concept selection, and vendor design evaluation are presented below.

5.13.1.1 Requirements - Certain requirements must be met by the de-orbit subsystem in order to fulfill mission objectives. The maximum velocity increment needed to de-orbit the Flight Capsule from its Mars parking orbit has been established at 950 ft/sec. The minimum value is 350 ft/sec. Thrust termination is desired to provide a flexibility in choice of orbits and landing sites within the total impulse capability of the motor. While this is not a major consideration in early missions, the ability to land at the selected site or to change sites, once committed to a reference orbit, is paramount in later missions. In any case, however, the ΔV control accuracy must be within a 3σ value of $\pm$ .75%. In addition to the above capability it is desired that the de-orbit propulsion subsystem possess adequate performance flexibility for use on all VOYAGER Missions through 1979.

5.13.1.2 Subsystem Candidates - The de-orbit performance requirements may be met by various types of propulsion subsystems. In this study, consideration was given to solid propellant, monopropellant, and bipropellant subsystems.

Numerous configurations based upon these three subsystems are available for study. The five configurations selected for evaluation are shown schematically in Figures 5.13-1 through 5.13-5. In each case, the selected arrangement is the one best suited to the type of subsystem involved. For the composite bipropellant subsystem, where the same propellant supply is used for both de-orbit and terminal propulsion (Section 5.13.3), consideration was given to the use of either a common or separate engine.

Each candidate subsystem possesses certain inherent qualities which influence the de-orbit configuration. One significant difference between the solid and liquid propellant subsystems is the thrust level chosen. Our dispersion analyses, presented in Section 2.3.3, show that this is not a critical parameter, so the

SOLID PROPELLANT DE-ORBIT PROPULSION SUBSYSTEM

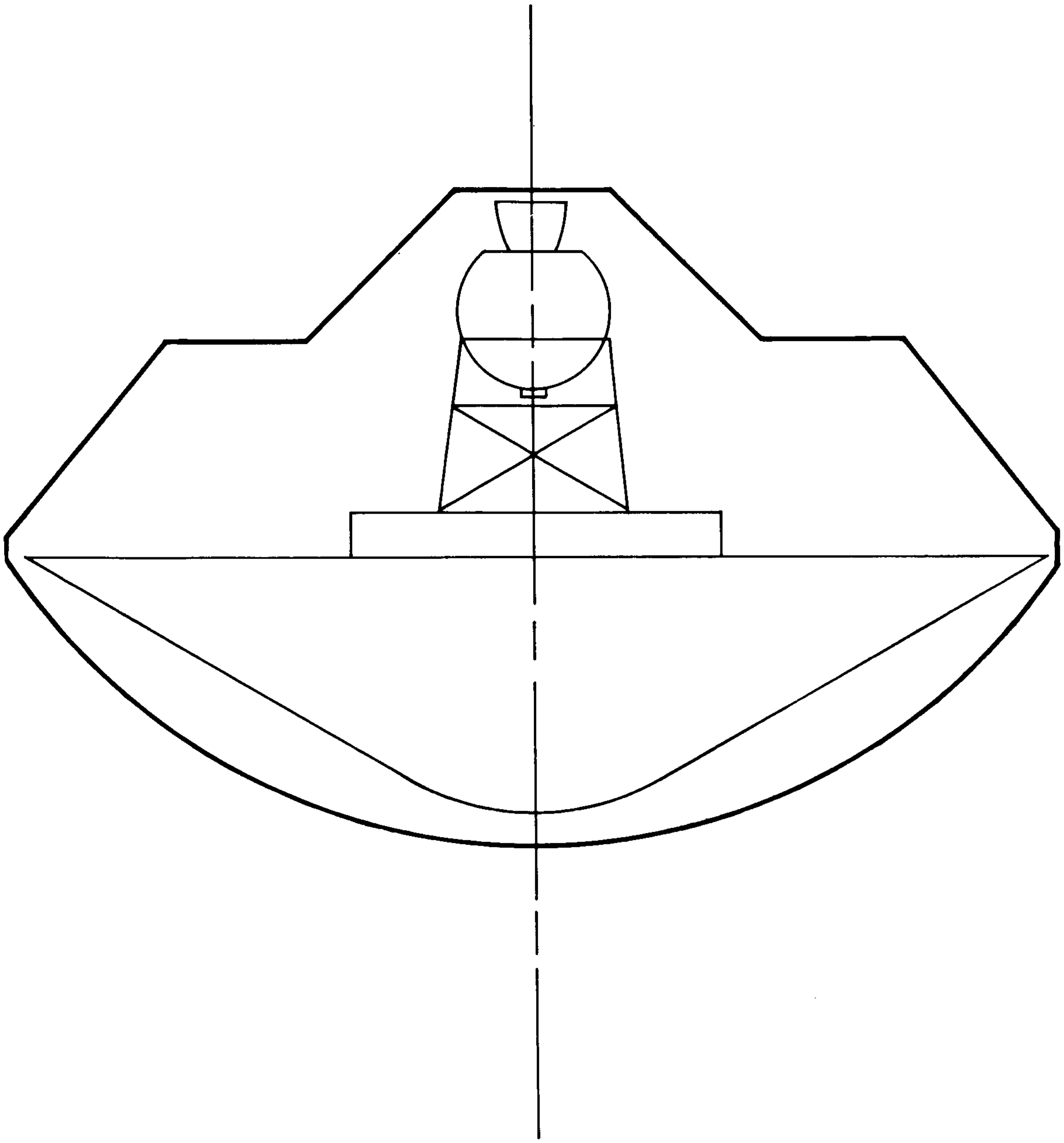

Figure 5.13-1

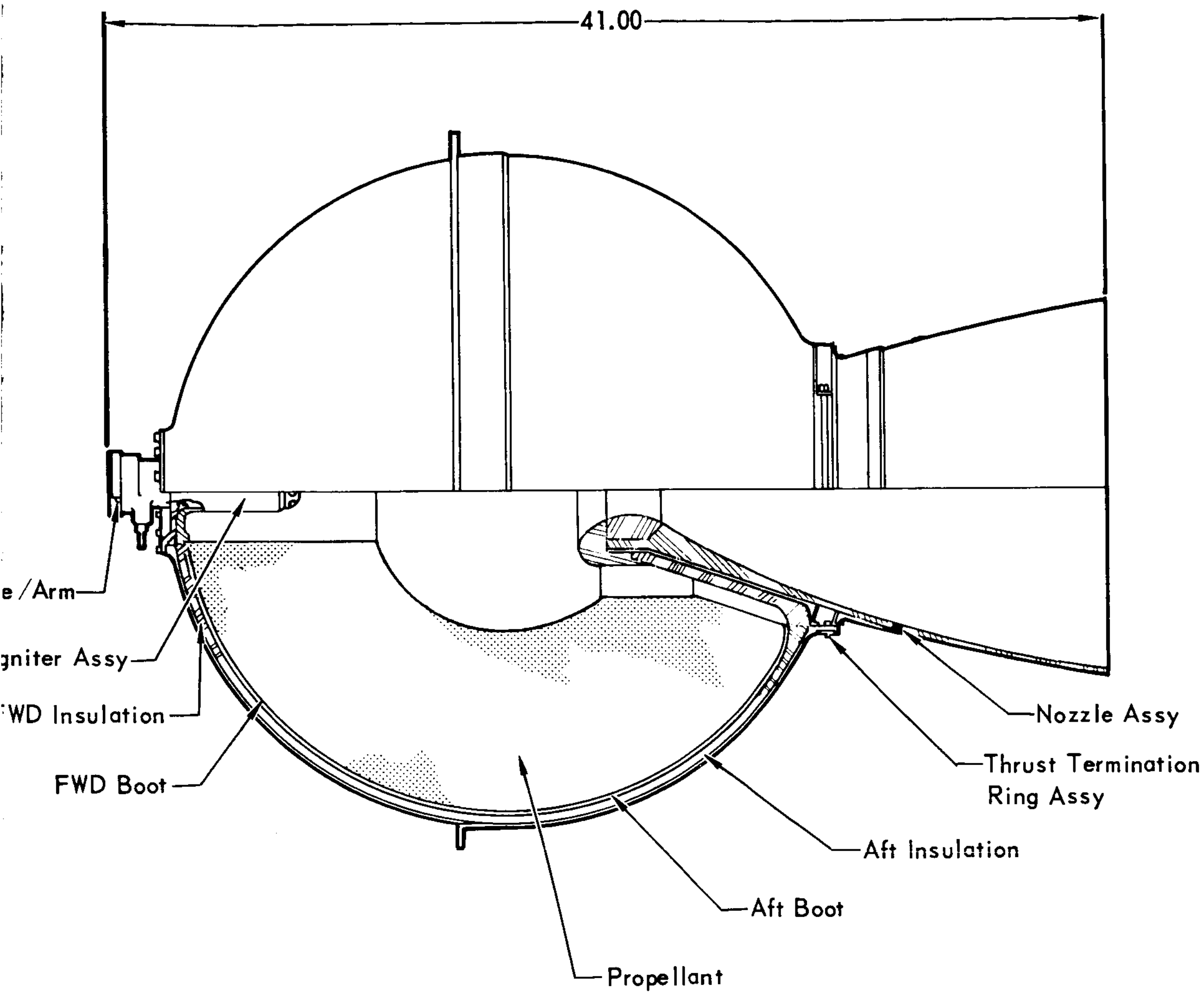
41.00
e /Arm
gniter Assy
WD Insulation
FWD Boot
Propellant
Aft Boot
Aft Insulation
Thrust Termination Ring Assy
Nozzle Assy

5.13-4-2

MONOPROPELLANT PROPULSION SUBSYSTEM

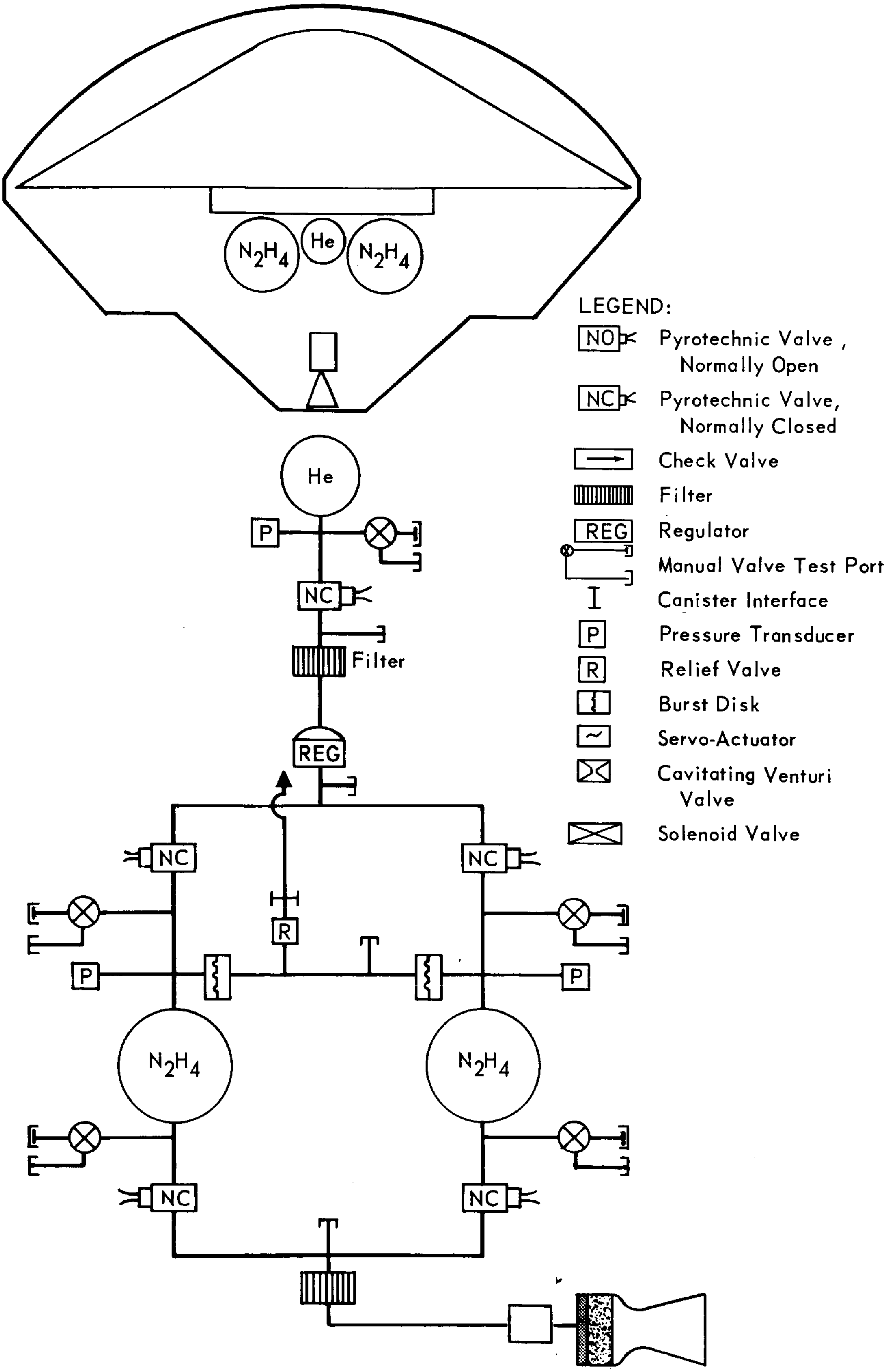
N_2H_4
He
N_2H_4
He
P
NC
Filter
REG
NC
NC
R
P
P
N_2H_4
N_2H_4
NC
NC
LEGEND:
NO Pyrotechnic Valve, Normally Open
NC Pyrotechnic Valve, Normally Closed
Check Valve
Filter
REG Regulator
Manual Valve Test Port
Canister Interface
P Pressure Transducer
R Relief Valve
Burst Disk
Servo-Actuator
Cavitating Venturi Valve
Solenoid Valve

Figure 5.13-2

SINGLE BI PROPELLANT DE-ORBIT SUBSYSTEM

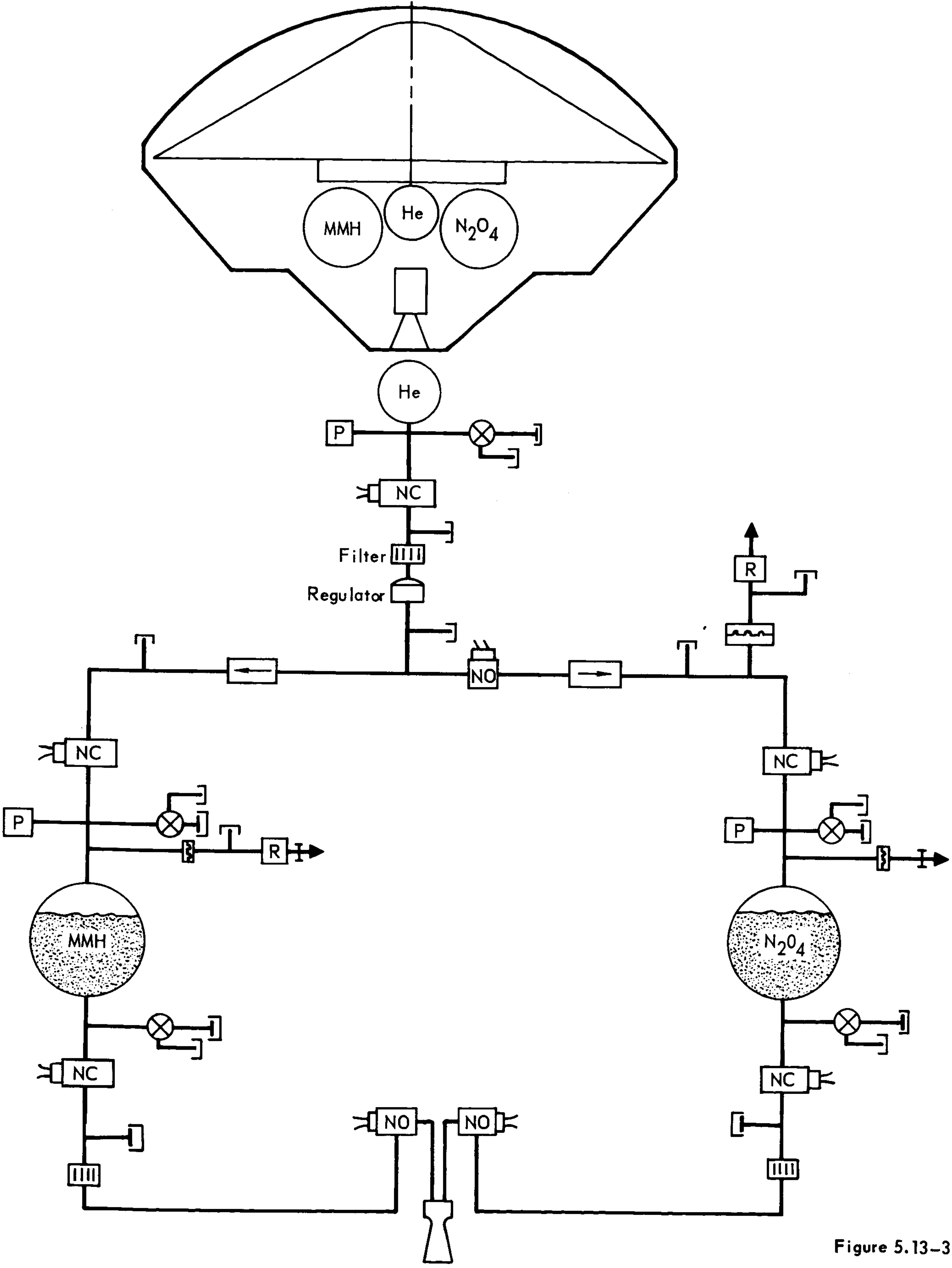
MMH
He
N_2O_4
He
P
NC
Filter
Regulator
NO
R
NC
P
R
MMH
NC
NO
NO
NC
P
N_2O_4
NC

Figure 5.13-3

COMPOSITE TERMINAL/DE-ORBIT SUBSYSTEM
COMMON TANKS

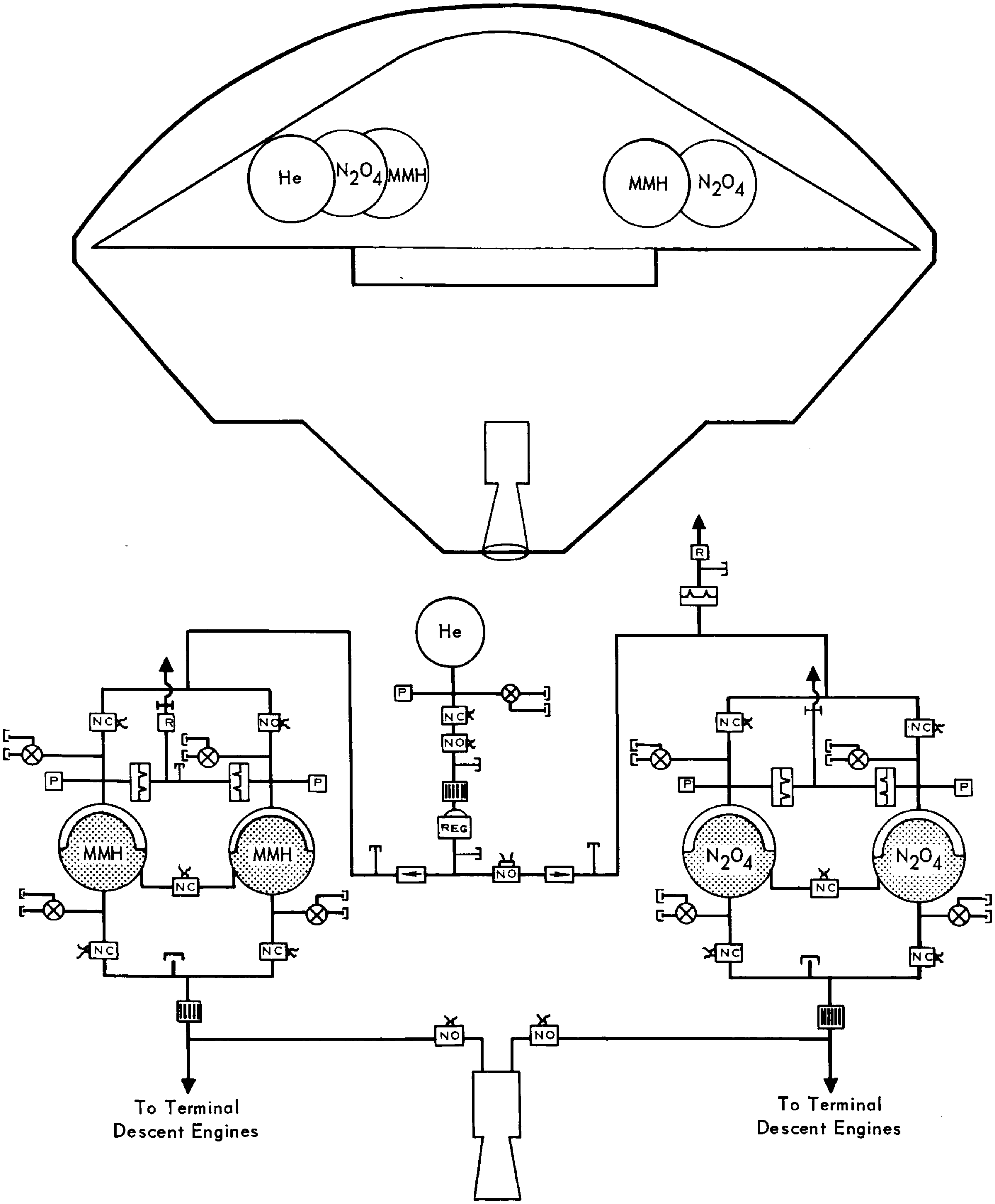
He
N_2O_4
MMH
MMH
N_2O_4
He
P
NC
NO
REG
R
NC
NC
P
P
MMH
MMH
NC
NC
NC
NO
NO
N_2O_4
N_2O_4
To Terminal Descent Engines
To Terminal Descent Engines

Figure 5.13-4

COMPOSITE TERMINAL/DE-ORBIT SUBSYSTEM
COMMON TANKS AND ENGINES

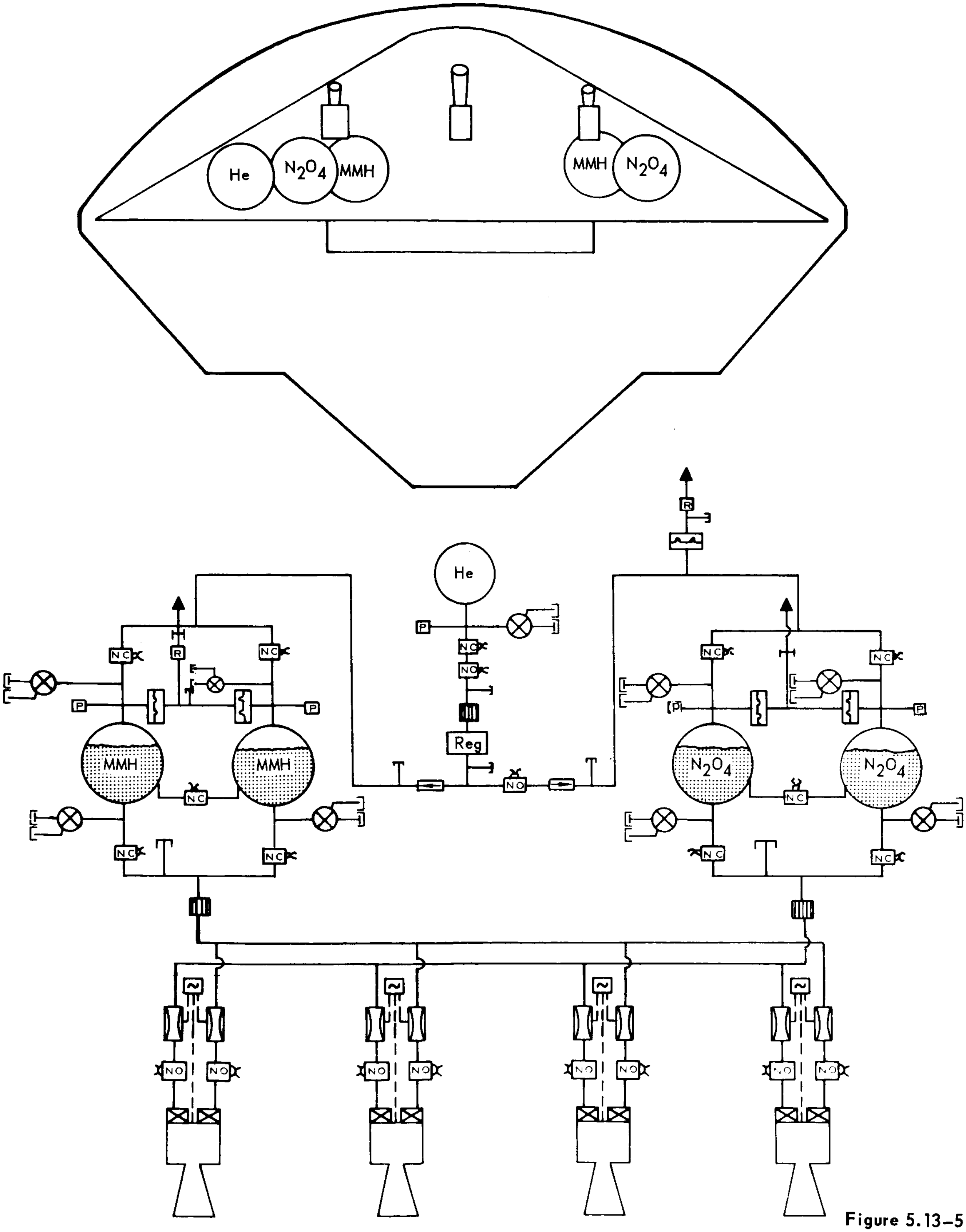
He
N_2O_4
MMH
MMH
N_2O_4
He
P
NC
NO
Reg
R
MMH
MMH
N_2O_4
N_2O_4
NC
NO

Figure 5.13-5

thrust level was selected to provide the greatest advantage to the subsystem.

For the solid propellant subsystem no particular advantage is gained by a choice of thrust level. However, the maximum thrust level is established by Capsule design g limits imposed by mission constraints. The Flight Capsule acceleration loads may be as high as 4.9 g's during Earth launch. This corresponds to an equivalent de-orbit thrust level of approximately 21,000 lbs. For the purpose of this study the solid motor thrust level was established at a nominal 6000 lbs. This selection is consistent with the motor size under consideration and the propellant burn rates which appear to be applicable. This level will impose a nominal 1.5 g load on a 4000 lb Capsule Bus (1973 mission), but the load can be 3 - 6 times as great as a result of the thrust spike associated with rapid depressurization thrust termination. Low weight is the primary advantage with selecting a low thrust level for the liquid propellant subsystem. For example, the weight saving between a 6000 lb thrust ablative and a 300 lb thrust radiative engine, with appropriate life time capability, is approximately 88 lbs.

Low thrust also allows closer control over the variation in total impulse. Excluding velocity sensor errors, the improved 3σ total impulse repeatability, with thrust termination, available at the 300 lb thrust levels is 0.001%, compared to 0.12% for 6000 lb thrust. For comparison purposes the same accuracy for a 6000 lb thrust solid propellant subsystem with thrust termination is 0.3%. A thrust level of 300 lb was selected for the liquid propellant subsystems.

In each configuration, a single thrust chamber was selected. There are no significant advantages to the use of multiple engines and several disadvantages. The latter include increased weight, greater thrust malalignment, and potential base heating problems. The gain in reliability possible by designing for engine-out capability cannot be justified against increased weight penalties. This is particularly true in the case of the solid rocket where the penalty may be one-fifth to one-third of the subsystem weight depending upon the final number of motors selected. In the case of liquid subsystems, no significant reliability gains are possible with multiple engines since the basic chamber is highly reliable and redundancy may be provided in valves and moving parts within the subsystem.

The preferred Flight Capsule design arrangement constrains the length of the de-orbit propulsion subsystem to approximately 41 inches. In this study this constraint has been respected in all candidate subsystems, except the composites, where the tanks are stored in the Capsule Lander.

Thermal considerations were found to be comparable for each subsystem and are not considered in detail in this analysis.

The inert propulsion subsystem weight remaining after the de-orbit maneuver is designed to be jettisoned in each case, except for the composite bipropellant subsystem. With the composite, this is not possible; but where a separate engine is used for de-orbit, its location will permit jettisoning when desirable.

Any of the configurations are adaptable to various thrust vector control techniques, which are discussed in Section 5.13.4.4.

5.13.1.3 Subsystem Trade Studies - In proceeding from the various propulsion subsystems and configuration arrangements discussed above to a preferred subsystem, each was evaluated using the factors listed in Section 5.13.

5.13.1.3.1 Reliability - Since mission success is primary, reliability is the most significant factor in selection of the de-orbit propulsion subsystem. The reliability of each of the candidate de-orbit propulsion subsystems has been evaluated. The complete analysis can be found in Section 5.13.4.5. A summary of the results is provided in Figure 5.13-6. The basic subsystems are considered separate from the thrust vector control techniques to permit individual selection of the latter.

5.13.1.3.2 Development Status - The de-orbit propulsion subsystems under consideration are essentially state-of-the-art, except for the sterilization and decontamination requirements. These, however, present major development problems which must be solved before a reliable subsystem can be assured.

The capability of either solid or liquid propellant subsystems to withstand sterilization has not yet been demonstrated. Available solid propellants have exhibited surface hardening, swelling, cracking, and decomposition exotherms during sterilization heating. The main result is a degradation in physical properties. The storable liquid propellants are incompatible (catalytic or corrosive) with many of the materials commonly used in propellant subsystems at sterilization temperatures. In some cases the high propellant vapor pressure associated with the sterilization temperature also introduces high tank weight penalties. Since many of the components are not exposed to the propellant at sterilization temperature, they present somewhat less of a problem. In fact, certain regulators and valves have been qualified for temperatures above that required for sterilization. Less is known about the capability of these to withstand exposure to the decontaminant, ethylene oxide. Questionable items include ablative chambers , radiative chamber coatings and brazed joints. Despite these difficulties, sufficient sterilization testing has been accomplished to indicate that either liquid or solid propellant subsystems can be exploited for VOYAGER applications.

RELIABILITY ASSESSMENTS

SUBSYSTEM	SOLID PROPELLANT	MONO-PROPELLANT	BIPROPELLANT	BIPROPELLANT COMPOSITE: COMMON TANKS	BIPROPELLANT COMPOSITE: COMMON TANKS AND ENGINES
Reliability (No Redundancy)	.9950	.9940	.9918	.9926(1)	.9869(1)

(1) Reliability Apportionment for De-orbit Function.

Figure 5.13–6

Sterilization of Solid Propellant Rocket Motors - The requirement of sterilizing a solid propellant subsytem by heating the entire motor assembly for 6 cycles at 275°F has caused serious degradation of current off-the-shelf propellants, liners, and insulations. Material incompatibilities also exist because of differences in thermal expansion between the different materials. Testing has been performed on modifications of existing propellant formulations as well as on new candidate formulations developed specifically to withstand the thermal environment of sterilization. Also, subsystem components such as liners, insulation, O-rings, nozzle and igniters have been investigated. Among the techniques which have been developed to reduce the amount of thermal degradation of propellants are the removal of low molecular weight compounds from the polymer raw material by vacuum stripping, the use of anti-oxidants in the propellant formulation, recrystallization of the ammonium perchlorate oxidizer to stabilize the crystals, and the elimination of plasticizers.

Appreciable effort has been spent in recent years to develop high energy propellants with increased solids loading and tailored to withstand low temperature strain requirements. The addition of plasticizers, water content in the raw materials, and a low curing agent-to-polymer ratio are not detrimental to the physical properties of propellants at low temperature. However, at elevated temperature, 275°F, all of these conditions have adverse effects on the cured propellant. These conditions can be eliminated to enhance the high temperature stability if the low temperature requirement is removed. This is accomplished on VOYAGER by maintaining active thermal control during the space transfer orbit to Mars. The development status and major design considerations in sterilizable solid rocket subsystems are discussed in detail in Section 5.13.4.3.

Sterilization of Liquid Propellant Subsystems - The heat sterilization and decontamination requirements for liquid propulsion subsystems introduce unique problems in the area of equipment design. Containment of the current storable propellants during sterilization requires materials of construction which are unusually inert. The propellants under consideration are nitrogen tetroxide oxidizer, monomethyl hydrazine fuel, and hydrazine monopropellant.

Nitrogen tetroxide is extremely corrosive at the sterilization temperature and titanium is the only metal, known suitable for component use, which can resist its attack. Hydrazine does not attack stainless steels or titanium, but it has been observed to decompose when in contact with these metals at sterilization temperature. Titanium is more passive than stainless steel; hence it is again preferred.

Monomethyl hydrazine has the greater thermal stability of the two fuels and is compatible with construction materials, including titanium and stainless steel.

The limited choice of construction materials which are compatible with the propellants at sterilization temperature suggests a subsystem design wherein the propellant is isolated from fluid control components during exposure to heat. This calls for new design techniques to overcome shortcomings in the physical properties of propellant-compatible materials.

High temperature effects on non-wetted components must also be considered. Although metals are not particularly affected, elastomeric seals, particularly Teflon, usually are. Teflon is the only known soft seal material compatible with nitrogen tetroxide.

Ethylene oxide also has some known deleterious effects on subsystem materials. For example, it has been found that the currently most satisfactory hydrazine catalyst, Shell 405, is poisoned by ethylene oxide exposure. As a result, it is necessary to isolate this material from the decontaminant by sealing the monopropellant thrust chamber.

Detail discussion of the development status of sterilizable liquid propellant subsystems is provided in Section 5.13.4.2.

5.13.1.3.3 Weight and Performance - The primary factors which determine the deorbit propulsion subsystem weight are: (1) maximum required velocity increment (950 ft/sec), (2) type of propellant and/or propulsion subsytem, and (3) inaccuracies associated with each subsystem, such as thrust termination, total impulse, mixture ratio control, etc. The weight and performance characteristics of each configuration are discussed below.

Solid Propellant - The propellant formulation assumed contains 84% total solids consisting of 16% aluminum and 68% ammonium perchlorate. To provide reasonable assurance that sterilization requirements will be satisfied, a hydrogen-saturated polybutadiene binder is used. An 8% performance gain is available through the use of aluminized propellants. The use of an aluminized propellant to save subsystem weight was justified after a study of the motor exhaust showed that the alumina presented no serious problems to the Flight Spacecraft. The results of this study are discussed in this section under Subsystem Interactions.

Preliminary calculations established the total impulse requirements for the 4200 lb (1973) and 6200 lb (1979) Capsules at 117,000 lb-sec and 172,000 lb-sec respectively. The 117,000 lb-sec requirement may be met either by off-loading the 172,000 lb-sec design or by designing specifically for this requirement. Chamber pressure was optimized for the heavy Capsule Bus at 600 psia, as shown in Figure 5.13-7. To satisfy the length restriction of 41 inches, an expansion ratio of 53:1 was found to result in minimum motor weight for the 6200 lb Capsule Bus (See Figure 5.13-8). In this study a nozzle submergence of 35% was assumed. Using the data from Figure 5.13-9, the vacuum specific impulse was estimated at 287 sec for a reasonably conservative solids loading of 84%.

To achieve the desired flexibility of de-orbit total impulse control, a solid rocket motor requires a thrust termination device. Of the techniques available, only nozzle ejection is considered applicable. Water quench, the only other serious candidate termination technique, weighs 50% more, decreases the reliability, and provides no significant performance advantages. A nozzle ejection mechanism is estimated to weigh 4 lbs. A schematic diagram of the two schemes is shown in Figure 5.13-10. The release ring for nozzle jettison is hinged to the aft closure assembly to preclude damage to the Capsule Bus from ejected debris.

Figure 5.13-11 summarizes the weight and dimensional characteristics of the solid motor propellant de-orbit subsystem. These are given for the 1973 and 1979 designs and for the 1979 design with propellant off-loaded for the 1973 requirements.

Monopropellant - The hydrazine monopropellant subsystem offers several advantages, such as sterilization feasibility, simple and accurate thrust termination and subsystem reliability. The major disadvantage of this concept is its comparatively low specific impulse and specific gravity, resulting in a relatively high weight and volume subsystem.

The basic data used in the analysis are shown in Figure 5.13-12. A maximum thrust level of 300 lbs was selected, with a single-start burn time of approximately ten minutes to provide the design total impulse of 172,000 lb-sec. Attitude control is provided with a separate reaction control subsystem (RCS), selected as the preferred technique from studies reported in Section 5.13.2. In addition, the RCS is used to position the propellant by simultaneously firing aft-directed pitch and yaw thrust chambers prior to ignition of the de-orbit engine, thus eliminating the need for positive expulsion devices. A chamber pressure of 75 psia was selected as providing near-optimum propulsion subsystem weight, as shown in Figure 5.13-13.

The monopropellant design utilizes two propellant tanks designed for the impulse requirements of the 1979 mission and off-loaded for the 1973 mission. The weight penalty involved in off-loading is 23 lbs. The arrangement of tanks is somewhat arbitrary but must include the following considerations: (1) length which is constrained by the preferred Flight Capsule design - approximately 41 inches,

CHAMBER PRESSURE OPTIMIZATION FOR SOLID PROPELLANT SUBSYSTEM

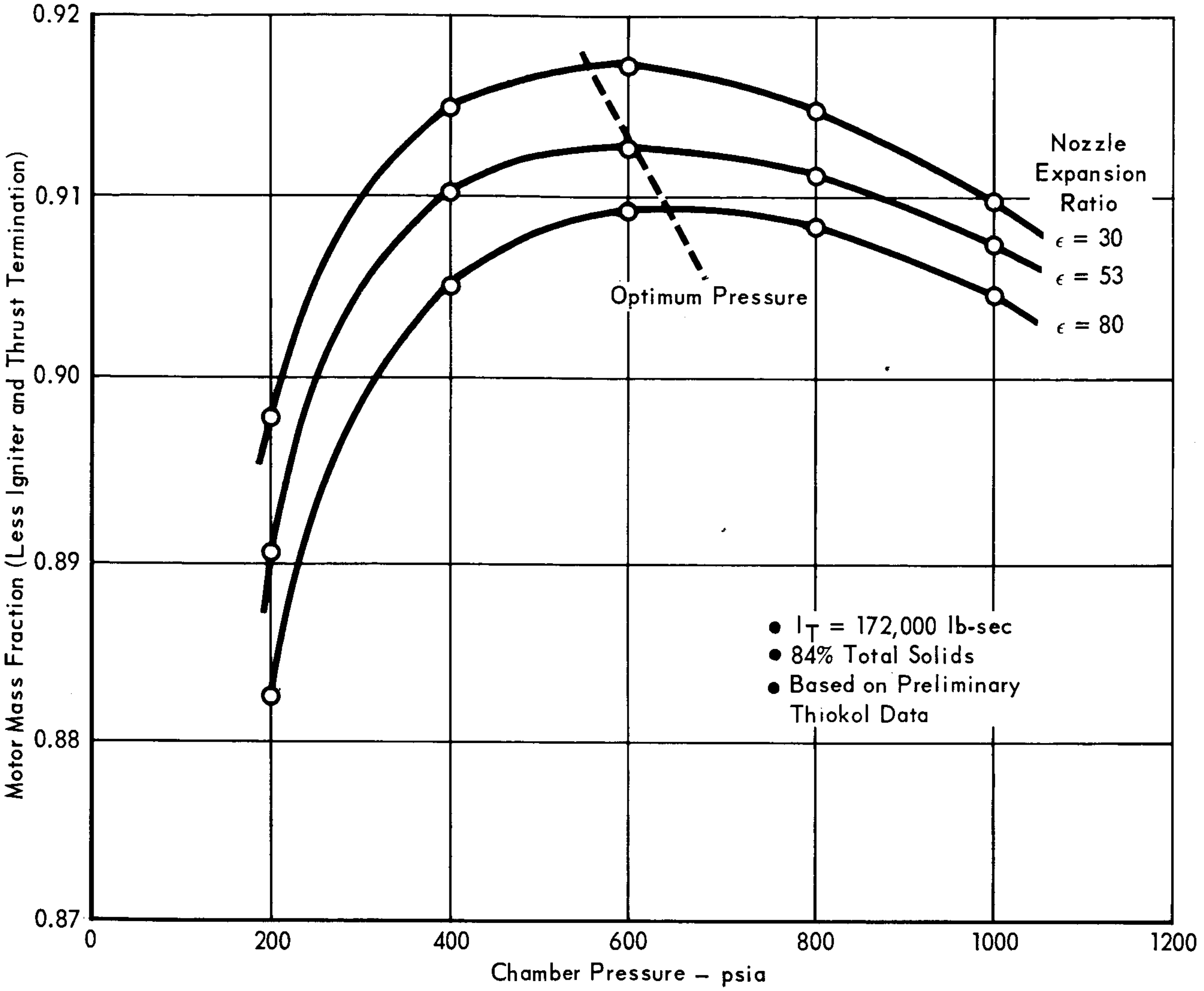

Figure 5.13-7

PERFORMANCE TRADE FOR MOTOR LENGTH AND EXPANSION RATIO

SPHERICAL MOTOR – 35% SUBMERGED NOZZLE

ΔV = 950 FT/SEC

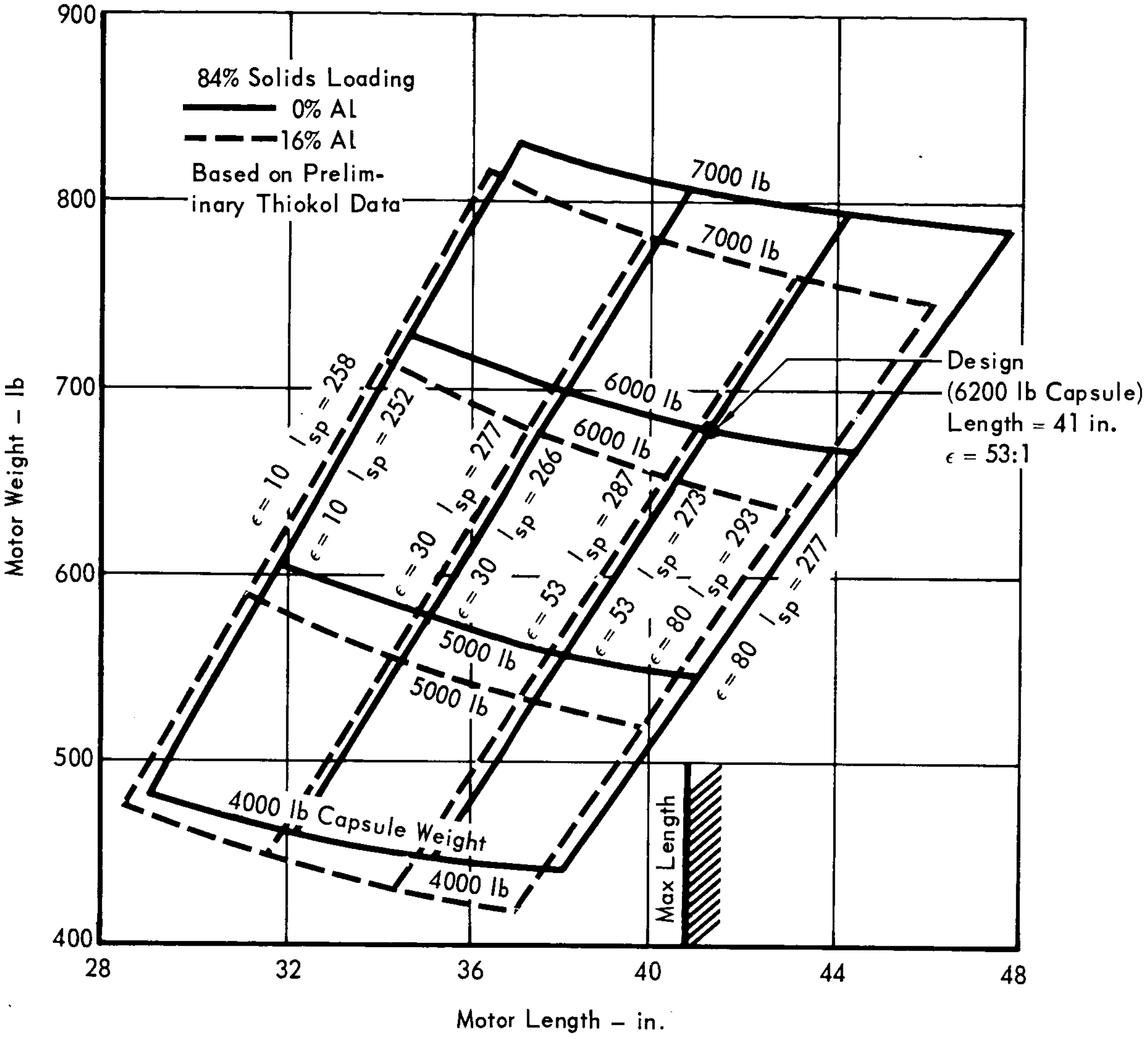

Figure 5.13–8

THE EFFECT OF TOTAL SOLIDS CONTENT ON VACUUM SPECIFIC IMPULSE

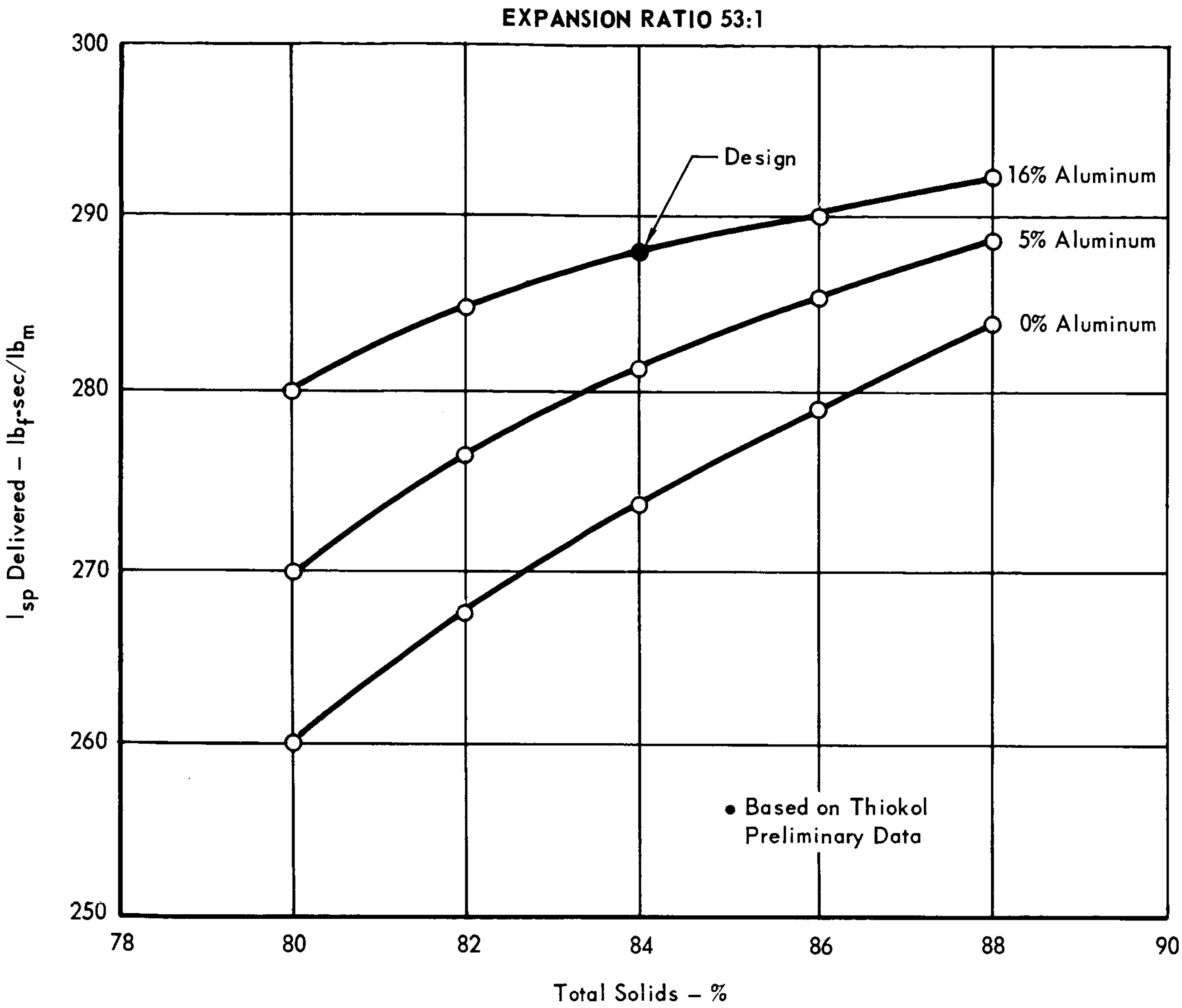

Figure 5.13-9

THRUST TERMINATION TECHNIQUES

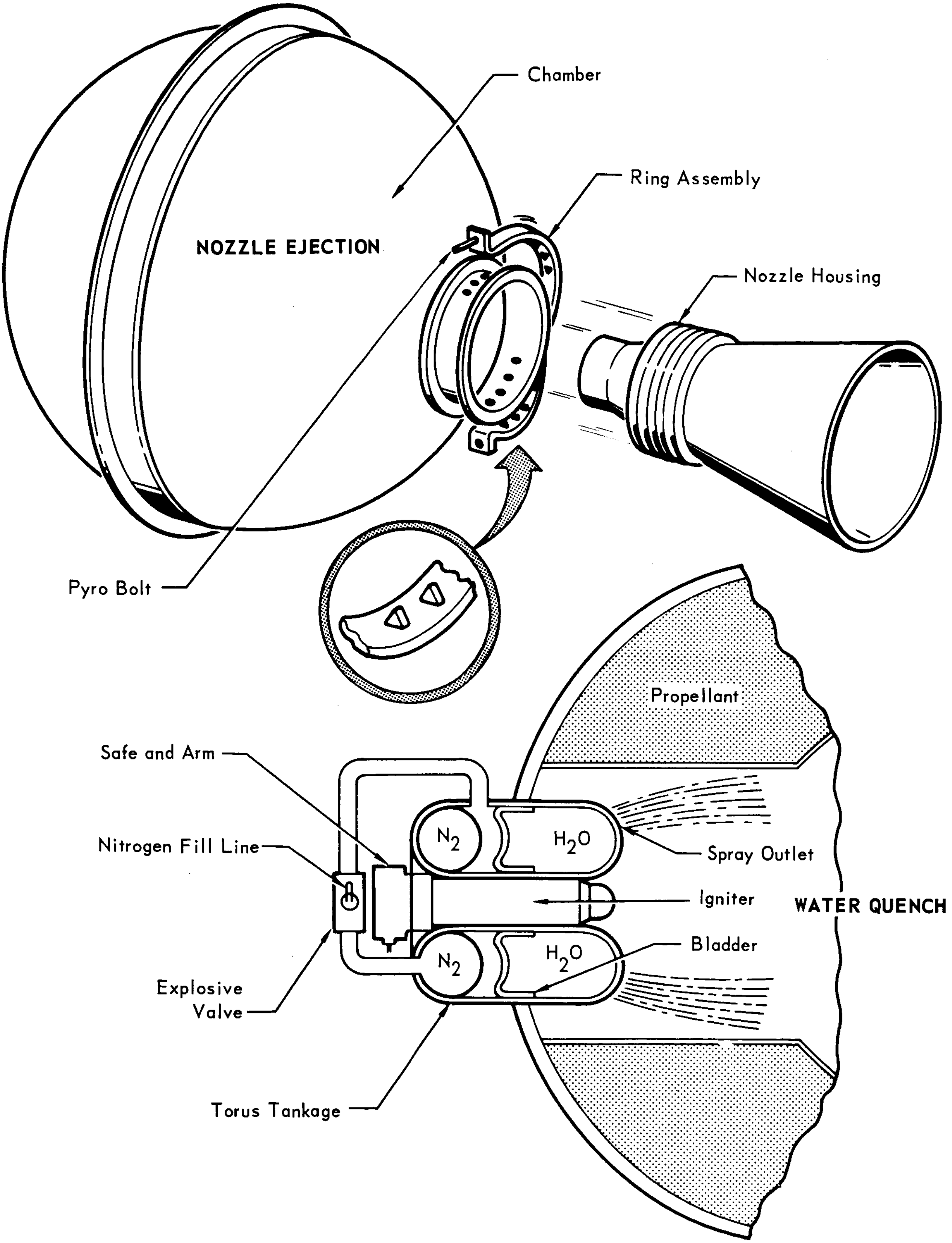
Chamber
Ring Assembly
NOZZLE EJECTION
Nozzle Housing
Pyro Bolt
Propellant
Safe and Arm
Nitrogen Fill Line
N_2
H_2O
Spray Outlet
Igniter
WATER QUENCH
Bladder
N_2
H_2O
Explosive Valve
Torus Tankage

Figure 5.13-10

SOLID PROPELLANT SUBSYSTEM
PHYSICAL CHARACTERISTICS

MISSION	SUBSYSTEM WEIGHT, lb	PROPELLANT WEIGHT, lb	MASS FRACTION	CASE OUTSIDE DIA, in.	MOTOR LENGTH, in.
1973	460	407	.885	25.0	35.0
1973 1979 Off-Loaded	477	407	.855	30.0	41.0
1979	678	608	.898	30.0	41.0

Figure 5.13-11

MONOPROPELLANT DE-ORBIT PROPULSION SUBSYSTEM

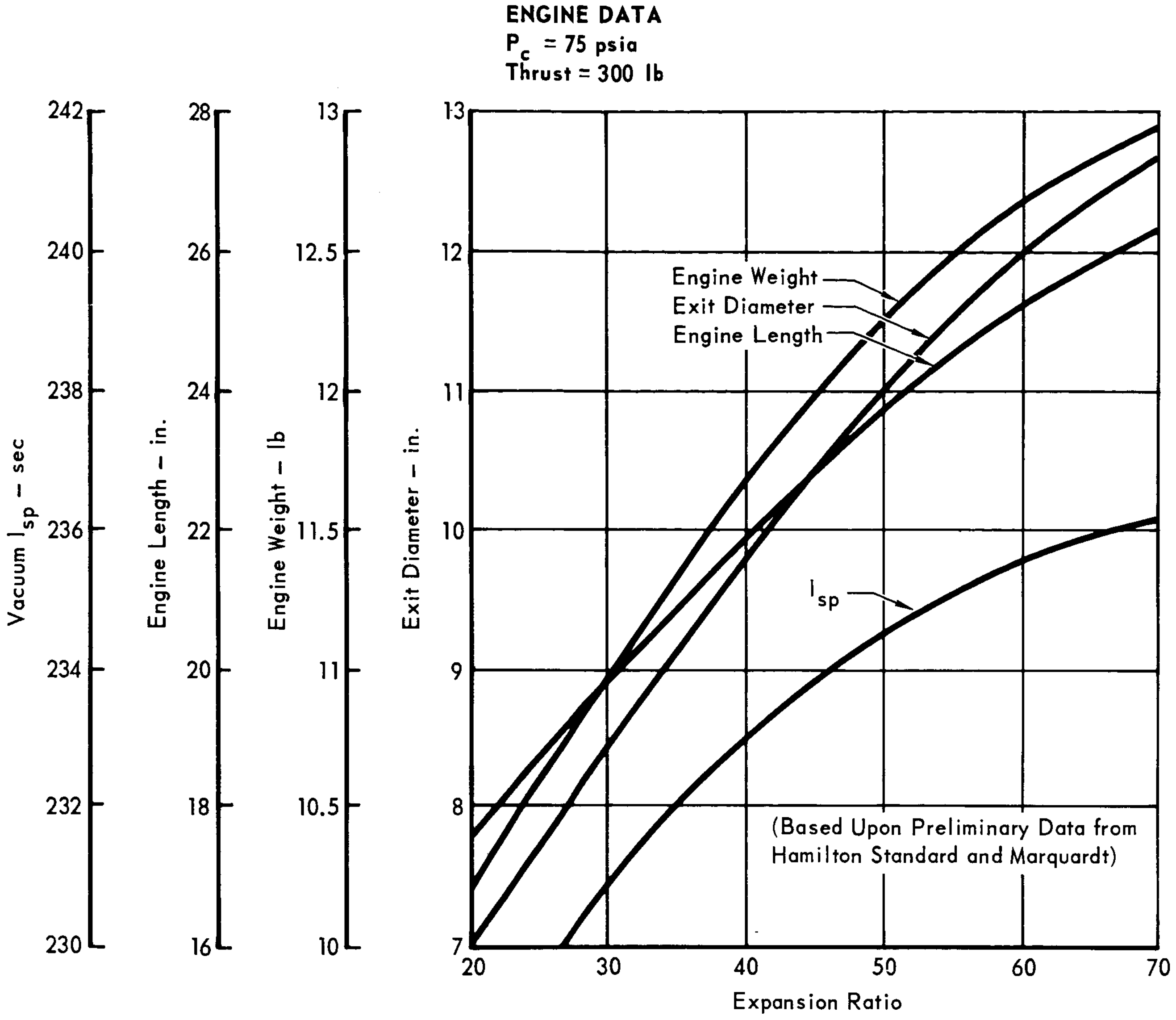

Propellant – N_2H_4
Pressurant – He

Pressure Factors:	Proof	Burst
Pressurant Tank	1.25	1.5
Propellant Tank	1.5	2.22
Lines, Fittings	2.0	4.0

Unavailable Propellant – 6%
Loading Accuracy (3σ) – 0.5%
Shut-Down Impulse Accuracy (3σ) – 0.2 lb-sec.
Materials:
  Tanks – 6A1–4V Titanium

Figure 5.13–12

CHAMBER PRESSURE EFFECTS ON HYDRAZINE DE-ORBIT SUBSYSTEM WEIGHT

1979 MISSION

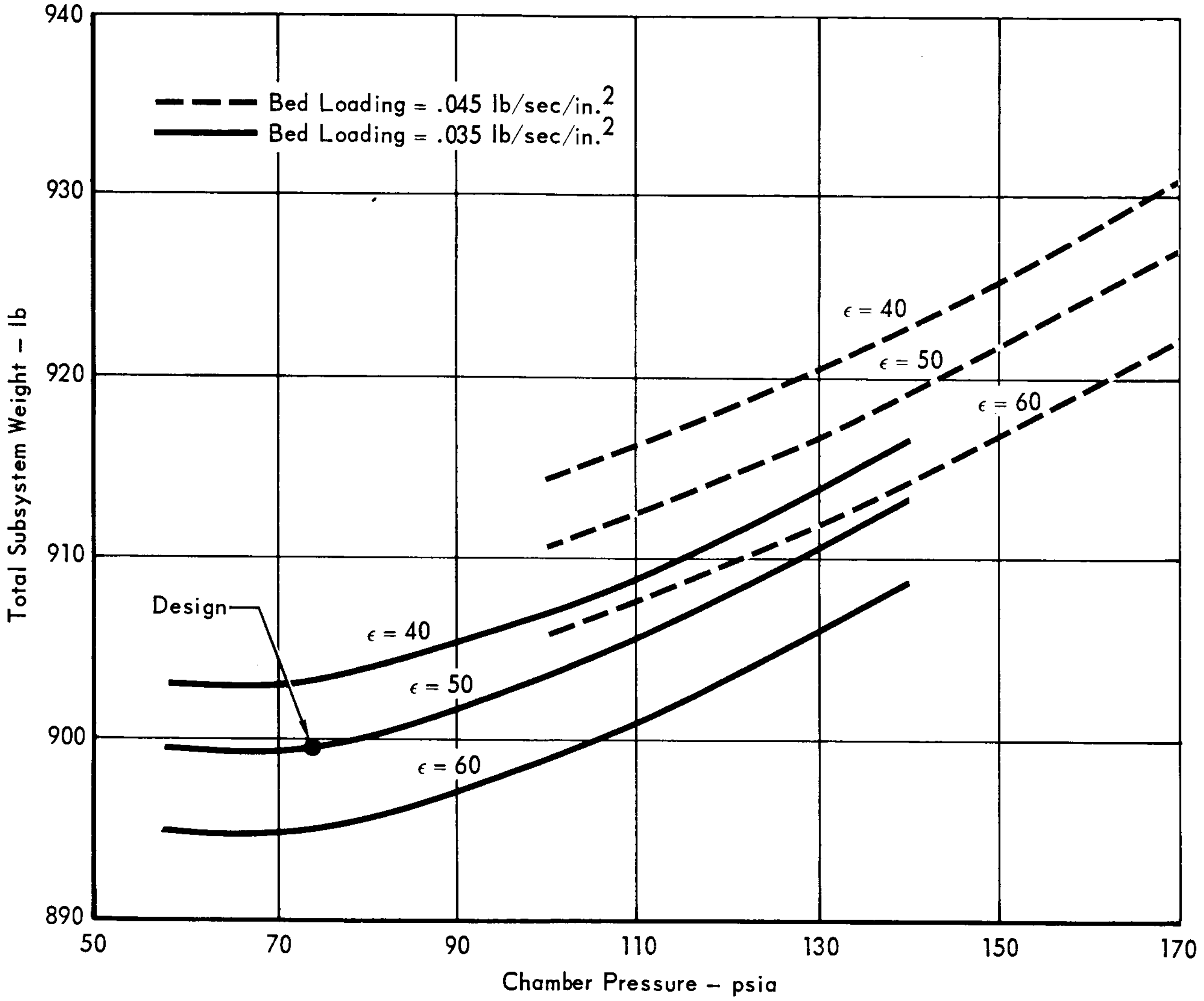

Figure 5.13–13

and, (2) flexibility in application from 1973 to 1979 missions.

Figure 5.13-14 summarizes the significant weight and dimension characteristics of hydrazine de-orbit propulsion subsystems capable of providing the required ΔV for the Capsule Bus weights anticipated for the 1973 and 1979 missions.

FIGURE 5.13-14

MONOPROPELLANT SUBSYSTEM
PHYSICAL CHARACTERISTICS

MISSION	SUBSYSTEM WEIGHT, LB	PROPELLANT WEIGHT, LB	MASS FRACTION	SUBSYSTEM LENGTH, IN.
1973	632	525	.830	39.0
1973 (1979 Off-Loaded)	655	525	.802	41.0
1979	900	770	.855	41.0

Figure 5.13-14

Bipropellant - The relatively high performance associated with storable liquid bipropellants is attractive for the de-orbit propulsion subsystem. Nitrogen tetroxide (N_2O_4) and monomethyl hydrazine (MMH) were selected as the propellant combinations. Nitrogen tetroxide is the most energetic of the storable oxidizers and has been found to be compatible with titanium. Monomethyl hydrazine was chosen simply because, with N_2O_4, it provides performance comparable to other hydrazine blends and it offers greater thermal stability than neat hydrazine. In addition, it has a low freezing point and low vapor pressure.

A schematic diagram of the subsystem design is presented in Figure 5.13-3. The propellant tanks are mounted off the roll axis to satisfy the centerline length constraint. To minimize radial c.g. travel during operation, the oxidizer tank and fuel tank are mounted 180° apart and at radial distances in inverse proportion to the design mixture ratio, 1.6:1.

The basic subsystem data used in the analysis are provided in Figure 5.13-15. Thrust termination for bipropellant subsystems is simple and accurate. The propellant orientation method and envelope restrictions are identical with those of the monopropellant subsystem discussed earlier. A chamber pressure of 65 psi was selected as optimum for the 300 lb thrust engine, as shown in Figure 5.13-16.

Figure 5.13-17 summarizes the significant weight and dimensional characteristics of a bipropellant de-orbit propulsion subsystem capable of meeting the required ΔV for the Capsule Bus weights anticipated for the 1973 and 1979 missions.

BIPROPELLANT DE-ORBIT PROPULSION SUBSYSTEM

ENGINE DATA
$P_c = 65$ psia
Thrust = 300 lb

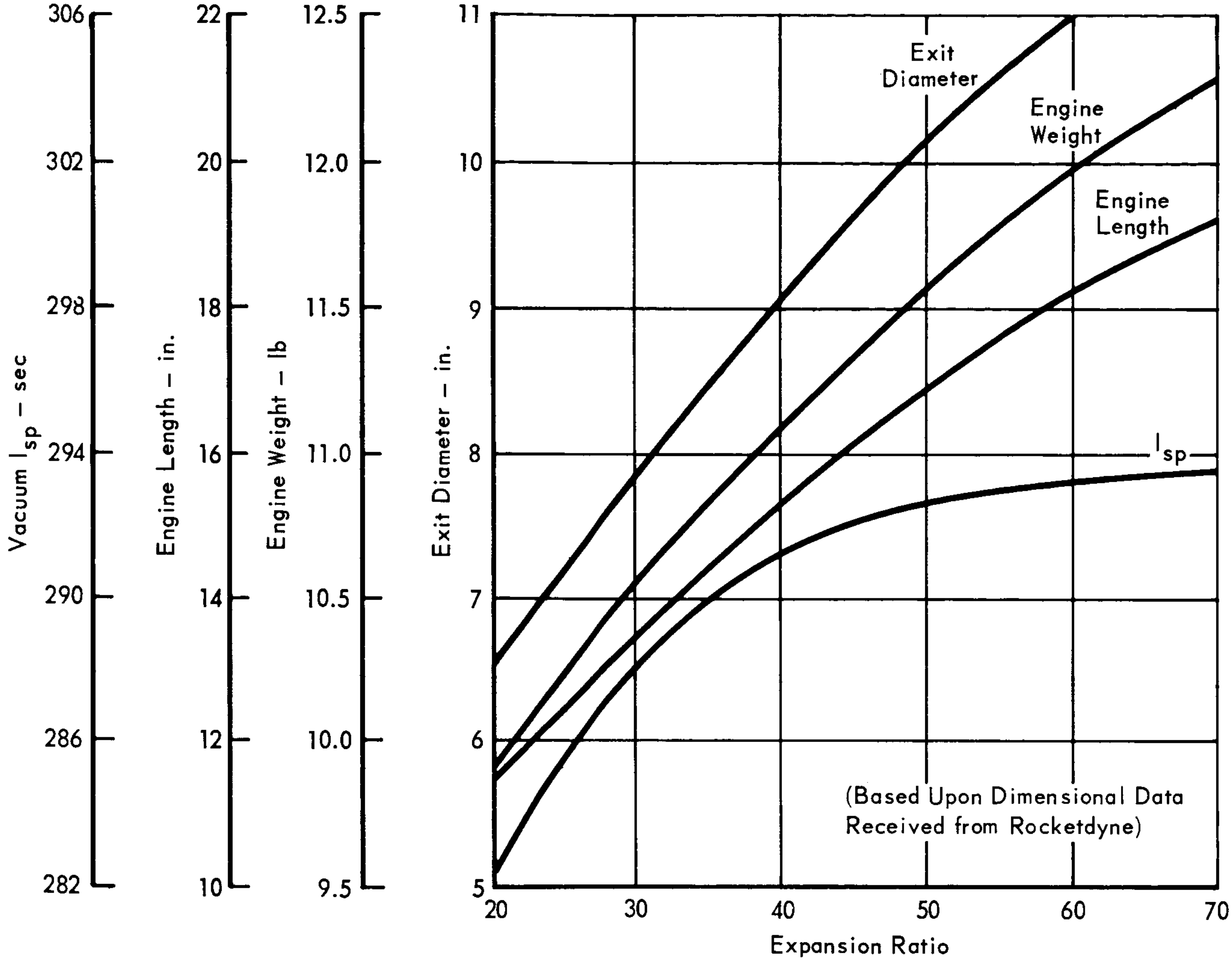

Propellants – N_2O_4/MMH
Pressurant – He

Pressure Factors:	Proof	Burst
Pressurant Tank	1.25	1.5
Propellant Tanks		
N_2O_4	1.25	1.5
MMH	1.5	2.22
Lines, Fittings	2.0	4.0

Unavailable Propellant – 6%
Loading Accuracy (3σ) – 0.5%
Shut-Down Impulse Accuracy (3σ) – 0.25 lb.-sec.
Materials:
Tanks – 6Al 4V Titanium

Figure 5.13–15

CHAMBER PRESSURE OPTIMIZATION FOR BIPROPELLANT SUBSYSTEM

- 1979 MISSION
- $\Delta V = 950$ fps
- Expansion Ratio = 50:1

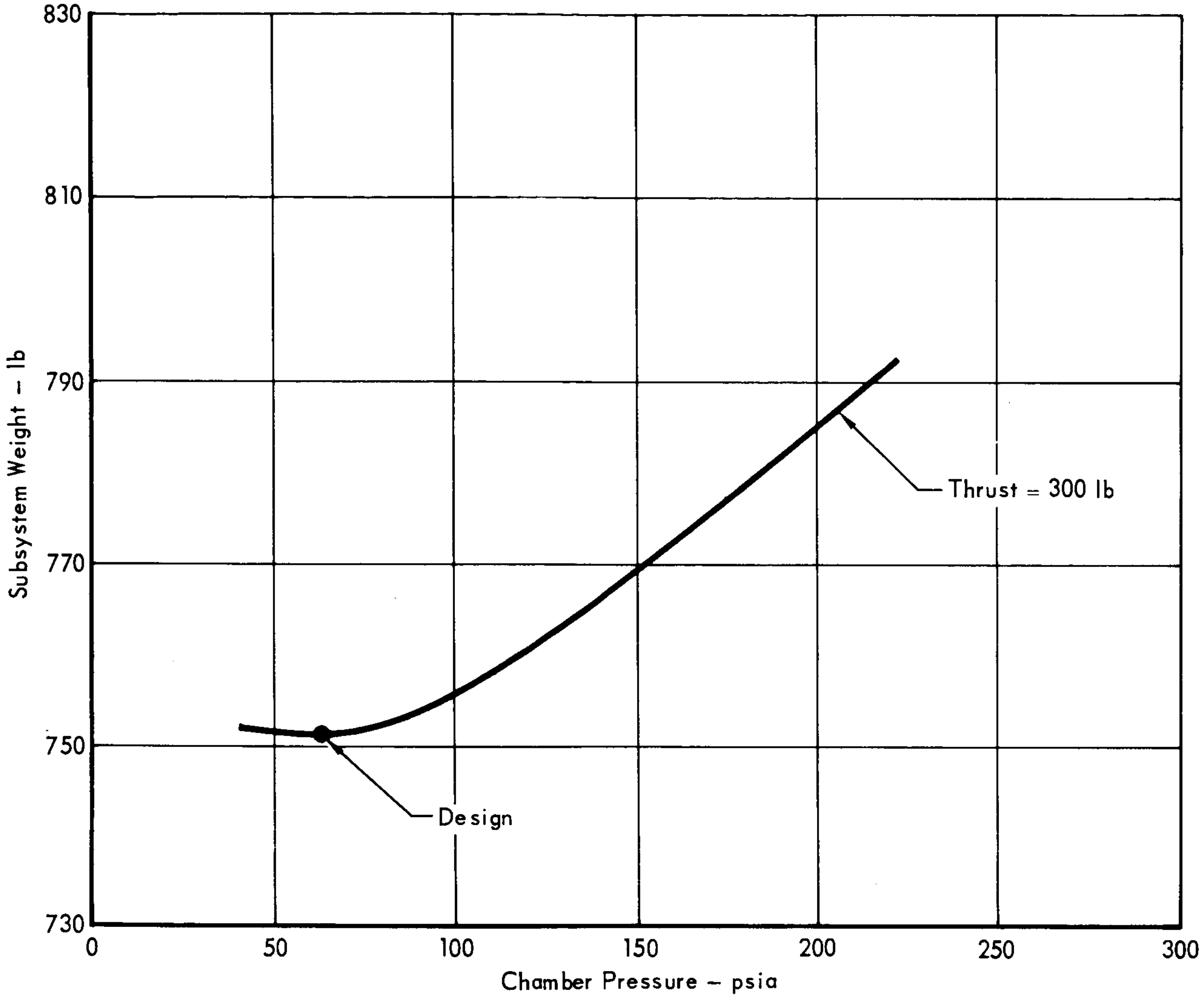

Figure 5.13-16

FIGURE 5.13-17

BIPROPELLANT SUBSYSTEM

PHYSICAL CHARACTERISTICS

MISSION	SUBSYSTEM WEIGHT, LB	PROPELLANT WEIGHT, LB	MASS FRACTION	ENGINE LENGTH, IN.
1973	533	425	.798	34.5
1973 (1979 Off-Loaded)	552	425	.770	36.5
1979	752	625	.832	36.5

Composite Bipropellant - Intuitively, there would appear to be certain weight advantages associated with combining the de-orbit and terminal propulsion functions into one subsystem. In addition, the number of subsystems requiring development would be reduced to one. Two alternatives are available. The engines may be common to both functions or a separate engine may be used for the de-orbit maneuver which eliminates the need for mechanical covers over the Aeroshell vent ports.

The arrangement and schematic of a subsystem design employing only one set of engines are shown in Figure 5.13-5. The propellants selected are monomethyl hydrazine and nitrogen tetroxide as required for terminal descent and discussed in Section 5.13.3. The thrust level is only 80% of the design rated thrust for the terminal subsystem, permitting 20% margin for attitude control by differential throttling during de-orbit burn. Thrust termination is easily achieved with propellant shutoff valves. To eliminate the need for positive propellant expulsion, the reaction control subsystem, included for de-orbit orientation and aerodynamic damping during entry, is used to position propellants prior to engine ignition.

The weight and performance characteristics of the terminal propulsion subsystem are presented in Section 5.13.3. Figure 5.13-18 presents those physical characteristics of the subsystem chargeable to the de-orbit function. The subsystem weight includes the weight of the Aeroshell porting mechanisms.

FIGURE 5.13-18

COMPOSITE DE-ORBIT/TERMINAL PROPULSION SUBSYSTEM

COMMON TANKS AND ENGINES

PHYSICAL CHARACTERISTICS

MISSION	WEIGHT CHARGEABLE TO DE-ORBIT SUBSYSTEM, LB.	DE-ORBIT PROPELLANT WEIGHT, LB.	EQUIVALENT MASS FRACTION
1973	598	417	.698
1973 (1979 Off-Loaded)	648	417	.645
1979	841	610	.725

Figure 5.13-18

The inherent development advantage of a composite subsystem could be maintained with only a minor weight increase over the subsystem arrangement just discussed, if a separate engine is added for the de-orbit maneuver. Offsetting this weight increase is the elimination of the requirement for mechanical covers over the Aeroshell vent ports, the attendant single point failure modes introduced by them, or the added development testing required to assure that open vent ports would not cause blockage of injector orifices and/or contribute to aerodynamic instability of the Aeroshell during atmospheric entry.

The arrangement and schematic drawings of the separate engine de-orbit subsystem design evaluated are shown in Figure 5.13-4. As before, the propellants selected were monomethyl hydrazine and nitrogen tetroxide. The engine has a design thrust level of 300 lb and a chamber pressure of 100 psia.

Realization of proper propellant orientation during engine operation is more difficult to achieve than in the previous arrangement. The problem arises because the application of thrust loads during the de-orbit and terminal deceleration functions are opposite in direction. To orient the propellants before burn by auxiliary means and maintain them in that position during engine operation would require multiple tank outlets, i.e., outlets on each end of the propellant tanks. Positive expulsion with reinforced metallic diaphragms were selected as a more practical approach, at least for the concept trade studies.

Figure 5.13-19 summarizes the weight and dimensional characteristics, pertinent to this de-orbit subsystem, in which only the propellant tankage is common to the Terminal Propulsion Subsystem.

FIGURE 5.13-19

COMPOSITE DE-ORBIT/TERMINAL PROPULSION SUBSYSTEM

COMMON TANKS

PHYSICAL CHARACTERISTICS

MISSION	WEIGHT CHARGEABLE TO DE-ORBIT SUBSYSTEM - lb.	DE-ORBIT PROPELLANT WEIGHT-LB.	EQUIVALENT MASS FRACTION
1973	607	425	.700
1973 (1979 Off-Loaded)	659	425	.647
1979	854	620	.728

Figure 5.13-19

5.13.1.3.4 Versatility - One of the major considerations in the formulation of a design is that changes to the Capsule Bus from one launch opportunity to the next be kept to a minimum. Major components and/or subsystems must therefore be standardized for projected capsule growth and must have sufficient flexibility to allow for late changes in mission planning. Versatility of the solid and liquid subsystems is discussed below:

Solid Propellant De-Orbit Propulsion - The solid propellant subsystem offers considerable versatility in meeting changing requirements and providing reasonable growth. Designed to meet the 1979 mission requirements, the subsystem can perform less demanding missions without introducing significant weight penalties simply by off-loading propellant. For example, use of the motor designed for the 1979 mission, off-loaded for the 1973 mission, results in a weight penalty of only 17 lbs over a motor designed specifically for the latter.

The thrust termination device provided in the preferred design offers great versatility in velocity control. Any velocity increment from Zero to maximum (950 ft/sec, for a 6200 lb Capsule weight) may be achieved. Thus, if desired, off-loading need not be considered for the early missions if weight is not a problem.

Liquid Propellant De-orbit Propulsion - The liquid propellant subsystem is inherently very versatile. The total impulse load for a mission is easily changed by off-loading or by adding or removing tanks, as was done extensively in the Gemini program. However, in the composite subsystems it is difficult to package the large propellant tanks within the Capsule lander. It was found that 1979 tanks off-loaded for the 1973 mission did not fit in our 1973 lander arrangement. Thus, tank sizes must be changed for these configurations, involving additional development time. Propellant volumetric requirements are shown in Figure 5.13-20.

PROPELLANT VOLUME REQUIRED FOR COMPOSITE TERMINAL/DE-ORBIT SUBSYSTEMS

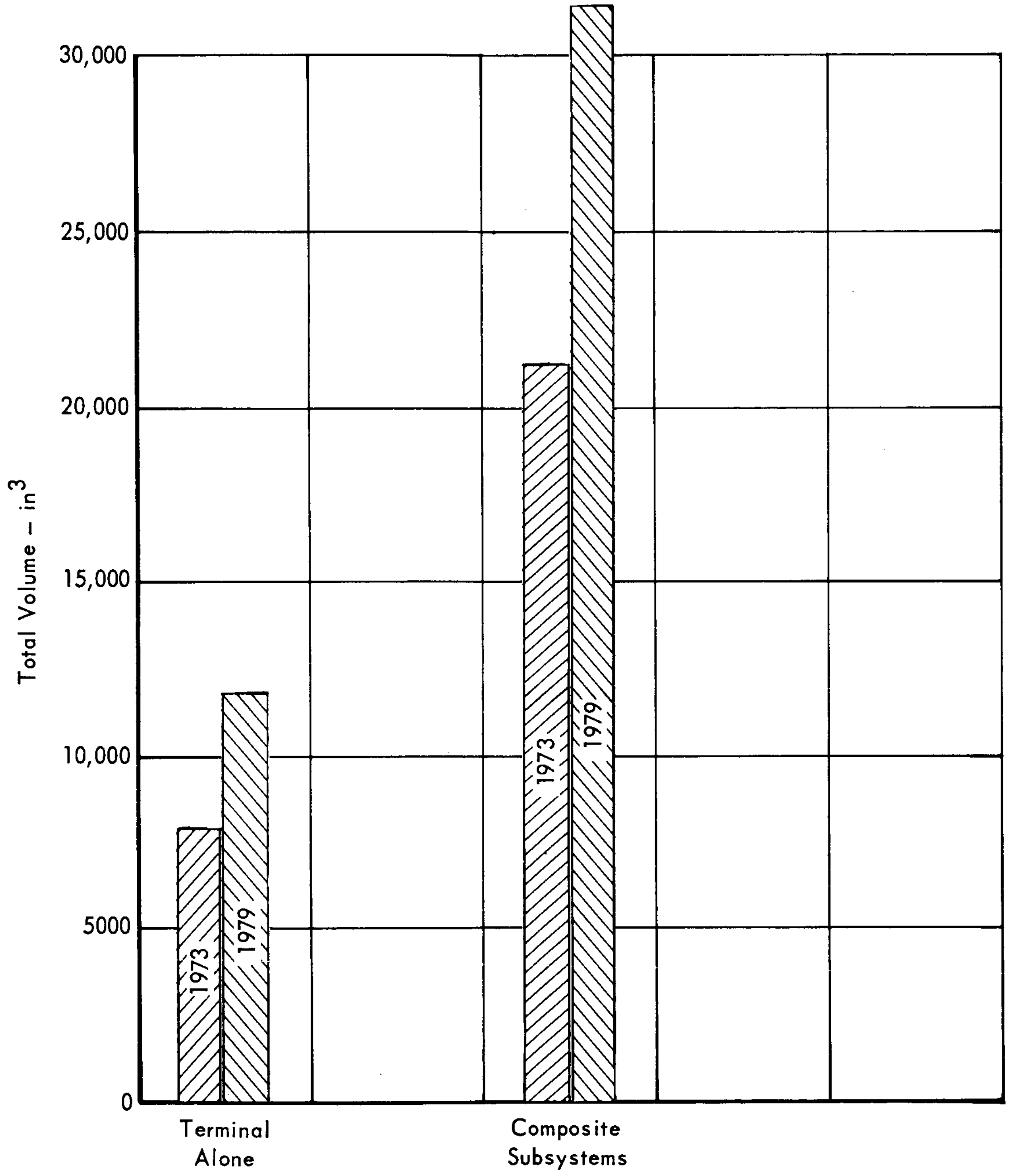

Figure 5.13–20

Thrust chambers which have a finite life limit restrict the extension of ΔV capability without thrust chamber modification. This appears to present a significant problem only in the case of the composite subsystem, where extending the chamber life may unduly penalize an engine development already complicated by the terminal propulsion requirements. Life-limited ablative chambers are a strong candidate for the high chamber pressure, short duration terminal propulsion subsystem while radiation chambers are desirable for extended endurance. The longest burn time studied for the de-orbit function is 600 seconds. The Marquardt R4D (Apollo Service Module, LM), a bipropellant engine, has a demonstrated life of 2000 seconds. Monopropellant hydrazine engines operate at a much lower temperature and can be expected to provide long life capability.

5.13.1.3.5 Subsystem Interactions - The major interactions between the Capsule Bus de-orbit propulsion and Flight Spacecraft subsystems are related to engine exhaust effects during de-orbit burn.

The present constraint of 300 meters separation distance between the Capsule Bus and Flight Spacecraft at de-orbit ignition serves to alleviate problems associated with exhaust plume impingement on solar cells, optics or other sensitive surfaces on the Flight Spacecraft. McDonnell studies on the Apollo Experiment Pallet (AEP) indicate that the liquid propellant subsystem will not present a problem to the Flight Spacecraft at this distance, neither from surface contamination nor from upsetting blast impingement loads. The introduction of solid products in the exhaust, however, requires careful consideration of separation distances and de-orbit "look angles". Of particular interest is the effect of aluminum oxide particles in the exhaust of high energy solid propellants. Because of the high performance gains available with aluminized solid propellants (approximately 8%), the de-orbit space-time relations between the Capsule Bus and Flight Spacecraft were investigated for the 1973 mission. While the analyses are not complete, the preliminary results, discussed in Section 2.3.3, indicate that the minimum "look angle", between the Flight Spacecraft and exhaust nozzle centerline is approximately 40 degrees. Considering that the aluminum oxide in the exhaust is confined within a 15 degree conical half angle about the nozzle centerline, direct impingement on the spacecraft is avoided. Also, the "look angle" can be increased appreciably with only minor restrictions on the de-orbit attitude of the Capsule Bus. In any case, the desired entry conditions can be achieved with proper choice of de-orbit anomaly and the de-orbit velocity increment.

At 300 meters the alumina in the exhaust will have solidified and the concentration will have become so low that, even if the de-orbit motor exit cone were pointed directly at the Flight Spacecraft, interference effects would be negligible. However, as pointed out above, this possibility is precluded by the relative positions and attitude of the two vehicles during operation of the de-orbit subsystem.

Alumina interference with the Spacecraft star tracker, if it occurred, would persist only for the short duration of the de-orbit burn. The alumina particles should not intersect succeeding orbits of the Spacecraft since the particles leave the nozzle with a velocity approximately equal to the maximum escape velocity (low orbit) of 8500 ft/sec.

An additional problem arose when nozzle blow-off was examined as a thrust termination technique. It was feared that the ejection velocity of the nozzle imposed a problem of potential recontact with the Flight Spacecraft. However, the maximum ΔV imparted to the nozzle is only 150 ft/sec, while the Capsule Bus undergoes a minimum de-orbit ΔV of 350 ft/sec in the opposite direction. The nozzle in effect picks up a minimum net ΔV of 200 ft/sec away from the Spacecraft. Consequently, there is no possibility of the nozzle hitting the Spacecraft.

5.13.1.4 Preferred Concept Selection - The pertinent quantities of the five de-orbit propulsion candidate subsystems evaluated are summarized in Figure 5.13-21. Of these, the solid propellant subsystem provides greater reliability, based on its general characteristics, than the other subsystems. Each of the other subsystems may achieve reliability improvement by adding redundancy, but this can be done only with considerable weight additions. The solid motor is also the lightest of the subsystems. The superior mass fraction of the solid is primarily responsible for this advantage. Although an aluminized propellant was chosen as the preferred design, a significant weight advantage is retained over other subsystems even with non-aluminized propellants.

Equipped with a thrust termination device, a solid propellant de-orbit subsystem provides significant flexibility in total impulse control. It does not have the flexibility of a liquid subsystem with respect to adding and removing propellant unless designed specifically for this purpose. Fortunately, the mass fraction of the solid propellant motor is such that only a small weight penalty accrues from adding unused volume. For example, a motor designed for the 1979 mission, off-loaded for the 1973 mission, results in a weight penalty over an ideal design of only 17 pounds.

Extensive solid propellant development and testing have been conducted during the past year. While many problems remain to be solved, indications are that a

DE-ORBIT PROPULSION SUBSYSTEM COMPARISON SUMMARY CHART

TYPE SYSTEM	PROPELLANTS	RELIABILITY	DEVELOPMENT STATUS	WEIGHT			VERSATILITY
				1973	1979	1973 Off-Loaded	
Solid Propellant	CTPB/AP/AL	.9950	Low - Requires propellant development and full scale demonstration	460	678	477	Very versatile with thrust termination. The 1979 design can be off-loaded with minimum penalty.
Monopropellant	Hydrazine	.9940	Good – N_2H_4 and storage tank compatibility requires development for 275°F. Catalyst bed and ETO compatibility must be resolved.	632	900	655	Very versatile. Termination easily effected. Off-loading propellant for 1973 results in low penalty.
Bipropellant	NTO/MMH	.9918	High – More propellant/mat'ls compatibility testing req'd but NTO/MMH propellants are thermally stable @275°F.	533	752	552	Very versatile. Termination easily effected. Off loading propellant for 1973 results in low penalty.
Composite – Common Tanks	NTO/MMH	.9926	Same as Bipropellant	607	854	–	Versatile. Termination easily effected. However seperate tanks must be designed for 1973 and 1979. Positive expulsion req'd.
Composite – Common Tanks and Engine	NTO/MMH	.9869	Same as Bipropellant	598	841	–	Same as Composite above.

Figure 5.13-21

sterilizable solid propellant motor can be developed, as discussed in Section 5.13.4.3. However, significantly more development work with propellants and full-scale motors is required to reach this objective.

The monopropellant subsystem rates high in versatility and development status. Thrust termination is readily achieved by a small propellant shut-off valve, propellant may be off-loaded to suit total impulse or ΔV requirements, and the long-life thrust chamber permits propellant loads up to almost any requirement conceivable. In the development area, the major problems are concerned with compatibility between storage tank material and the monopropellant hydrazine at sterilization temperatures and compatibility of the Shell 405 catalyst with ETO.

The bipropellant subsystem approaches the monopropellant design in versatility, but, because of the higher combustion temperatures, has more limited thrust chamber life. Tank changes to achieve versatility will present a slightly greater problem, but this is not considered a major factor. The primary bipropellant development problems are associated with compatibility of tank materials and propellants.

From these results, a solid propellant de-orbit propulsion subsystem is the obvious choice. As shown in Figure 5.13-21 the solid propellant motor is highest in weight, performance and reliability. In addition, thrust termination provides the solid propellant motor with an impulse control flexibility competitive with the liquid propellant subsystems. To achieve versatility for the 1973 and 1979 missions, the rocket motor must be sized for the 1979 misison. This introduces a small wieght penalty. The resulting weight is still less than for the other subsystems considered.

Perhaps the greatest problem associated with all the subsystems evaluated is development to meet the sterilization requirement. At this point, it appears that the solid propellant rocket motor may offer more difficulty than the liquid propellant subsystems. However, this is a qualitative rating and could change with improved understanding.

The significant fact here is that even though the versatility and development status of the solid propellant rocket motor are rated relatively low, it still is the obvious choice. Unfortunately, even this choice presents problems. To insure that the solid propellant rocket motor is available with the weight, reliability and performance required for VOYAGER, additional feasibility testing should begin immediately. Work should be continued on propellants, liners, insulation, nozzle and cases. Work should also be initiated on full scale testing, since essentially no development for sterilization has been conducted in this area. In

Section C-14, the preferred de-orbit propulsion subsystem is defined in detail.

5.13.1.5 Preferred Design - The foregoing studies were based upon preliminary information received from industry sources. To confirm the adequacy of a baseline design stemming from these trade studies, four companies were asked to submit designs for a sterilizable solid propellant rocket motor satisfying the following requirements. Written requests for technical information (RFTI's) were sent to Aerojet, Hercules, Thiokol and United Technology. The responses from these companies are presented below following by an evaluation of each design. The requests are summarized here:

General Design Characteristics

o Total impulse (vac) - design, lb-sec	185,000
- off-loaded, lb-sec	117,000
o Web burn time, sec	30. (min)
o Thrust termination - impulse accuracy, percent	±.3 (3σ)
o Thrust vector deflection (TVC) - maximum, degrees	±2.
- average, degrees	±.25
o Propellant	Aluminized
o Safe and Arm	Electromechanical, Position Monitor, one watt, one amp.

Design and Operational Constraints

o Overall length, inches	42
o Thrust vector alignment - angular, mrad	±2.
- offset, inch	± .01
o Electroexplosives	AFETRM 127-1
o Environments	McDonnell Rpt. E191

5.13.1.5.1 Vendor Design Solutions - Responses were received from four manufacturers. The major design and performance characteristics presented in these replies are summarized in Figure 5.13-22. As a result of refinements made to the McDonnell Capsule Bus design following de-orbit concept selection, the vendor designs do not reflect the most up-to-date envelope and performance requirements. The over-all motor length was reduced from 42 to 41 inches and the total impulse was reduced from 185,000 to 172,000 lb-sec for 1979. De-orbit TVC was carried as a candidate in the attitude control trade studies of Section 5.13.3, but was not selected. Although these changes were incorporated in an iteration of our own concept trade studies, it was decided not to perturb the vendor designs. Sufficient

SUMMARY OF VENDOR DESIGN CHARACTERISTICS

	AEROJET GENERAL	HERCULES POWD
SCHEMATIC	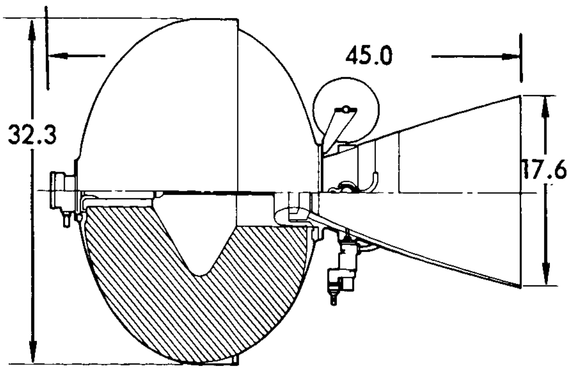	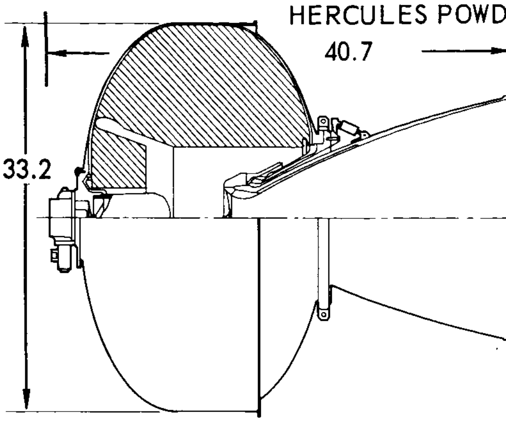
GENERAL DESCRIPTION		
Propellant Formulation	Saturated HTPB, 85% solids (16% Al)	CTPB binder, 85% solids (7% Al)
Grain	Slotted (2)	Conocyl perforate
Case/Nozzle	Titanium/wrapped silica phenolic	Titanium/silica phenolic
Igniter	Two designs, BPN and rocket type	Rocket-type, 2-SBW initiators
Thrust Termination	Nozzle separation, shaped charge	Nozzle separation, split-ring
Safe/Arm	Electro-mechanical	Electro-mechanical
Thrust Vector Control	Secondary injection (FREON 114B-2) – 20.6 lb	Flexible seal movable nozzle – 12 lb
PERFORMANCE CHARACTERISTICS		
Propellant	ANB-3289-2	HERCOPEL AC-1
Delivered Isp (sec)	286	281
Propellant Weight (lb)	646.8	662
Subsystem Weight Less TVC (lb)	729.0	727
Mass Fraction	0.890	0.912
Average Thrust (lb))	5500	4450
Average Chamber Pressure (psia)	500	404
Burn Time (sec)	33.3	41.9
DESIGN CHARACTERISTICS		
Case Diameter (in.)	32.3	33.2
Motor Length (in.)	42.0	38.0
Expansion Ratio	40:1	41.5:1
DEVELOPMENT SCHEDULE – months	36	21

Figure 5.13–22

ER	THIOKOL CHEMICAL	UNITED TECHNOLOGY CENTER
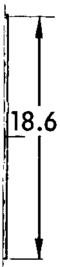	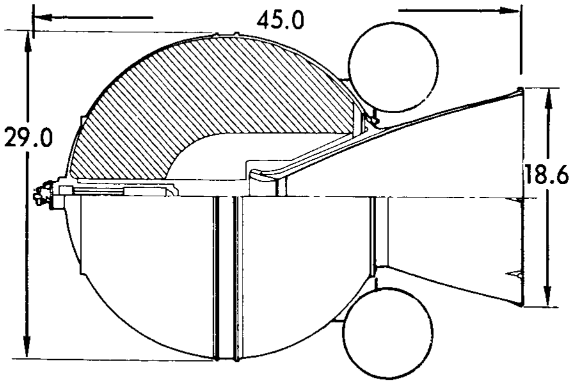	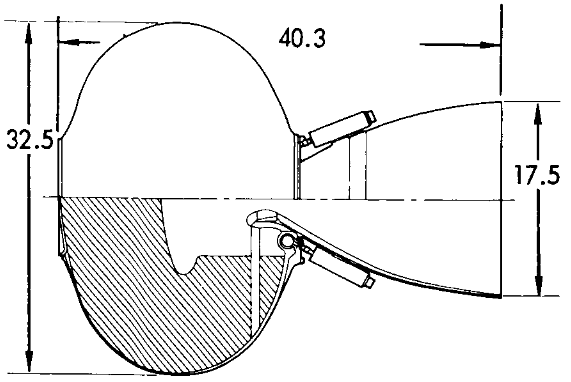
	CTPB binder, 82% solids (15% Al)	Saturated CT isobulylene, 83% solids (16% Al)
	Eight point star	Slotted
	Titanium/carbon cloth rosette	Fiberglass/tape wrapped silica microballoon
	Pyrogen with two initiators	Ring-shaped rocket type
	Nozzle separation, split-ring	Nozzle separation, shaped charge
	Electro-mechanical	Electro-mechanical
	Secondary injection (N_2O_4) – 65 lb	Secondary injection ($SnClO_4$) – 22 lb
	Modified HC–434	UTP 7794
	281	292
	673.8	642.3
	735	702.4
	0.917	0.918
	5675	3200
	600	544
	32.6	58.0
	29.0	32.5
	42.0	40.3
	53:1	80:1
	37	38

5,13-34-2

data were available to evaluate the effect of these changes on the performance and physical characteristics of each design. The propellant, performance and component selections of the four designs are discussed and evaluated below. Primary consideration is given to sterilization compatibility.

Propellants and Performance - The most critical heat sterilization effects on the solid propellant system are those which affect the physical properties: tensile strength, modulus and elongation at maximum stress. These properties determine the temperature transients associated with cure and subsequent sterilization as well as those induced during processing, handling and operation.

The physical property changes during thermal cycling of each of the proposed propellant systems, as reported by the rocket manufacturer, are shown in Figure 5.13-23. Each of the propellants exhibits sufficiently good physical properties for high performance motor designs but varying degrees of safety margins are provided. The Hercules AC-1, in particular, showed severe degradation during sterilization, with only 24 percent elongation after 6 cycles. However, visco-elastic stress analyses performed by that company shows that the maximum strain in their motor design is only 10%.

It is of interest to note that the four companies are equally split in their approach to the development of a sterilizable propellant. Hercules and Thiokol chose to modify existing formulations to achieve greater thermal stability while Aerojet and UTC elected to proceed with a new binder system.

Aerojet's propellant, ANB-3289-2, employs a saturated hydroxy-terminated polybutadiene binder, cured with isocyanates. Aerojet was also the only company to indicate that a problem exists from decomposition of the ammonium perchlorate (AP) oxidizer at sterilization temperatures. For this reason the AP in their formulation is recrystallized to remove impurities.

Both Hercules and Thiokol proposed carboxy-terminated polybutadiene propellants which are modifications of existing formulations. Hercules uses an epoxy cure; Thiokol did not specify the curing agent.

The UTC propellant contains a carboxy-terminated polyisobutylene binder which has all double bonds saturated with an epoxy-aziridine curative. Unreacted sites are avoided by saturation of the prepolymer and oxidation is reduced with an anti-oxidant additive.

No large motor testing has been conducted to date by any of these companies and questions remain as to susceptibility to propellant slump, alteration of the propellant/liner, liner/insulation and insulation/case bond systems, and the magnitude of any exotherm.

MECHANICAL PROPERTIES OF CANDIDATE PROPELLANTS

- PULL DATA AT -77°F

PROPELLANT	AEROJET GENERAL ANB-3289-2*				HERCULES AC-1				THIOKOL MOD-HC-1**				UTC UTP 7794 (UTREZ)***			
STERILIZATION CYCLES (TOTAL 6 @ 275F FOR 53 HR/CYCLE)	AFTER CURE	1	3	6	AFTER CURE	1	3	6	AFTER CURE	1	3	6	AFTER CURE	1	3	6
Initial Modulus, psi	1190	-	754	745	486	379	370	615	1400	-	-	1710	Not Available			
Elongation at Break %	29	-	44	45	55	52	38	24	47	-	-	38	40	33	-	30 ± 3
Maximum Tensile Strength, psi	183	-	167	161	102	63	73	86	143	-	-	244	275	440	-	371

* Mechanical properties of ANB-3289-2 up

* Mechanical properties of ANB-3289. The mechanical properties of ANB-3289-2 upon optimization are expected to be equivalent.

** Mechanical properties of 81% total solids content; however formulation similar to MOD-HC-1.

*** UTX 9539 non-aluminized 75% solids level UTREZ formulation.

Figure 5.13-23

Chemical decontamination with ETO/Freon-12 is similar to the thermal effect in that the reagent may add to terminal groups, causing swelling of the surface polymer. While only limited testing has been performed in this area, it is not expected that the bulk mechanical properties will be affected by this surface reaction unless the condition is complicated by subsequent thermal cycling.

Exclusive of the TVC subsystems, the total motor weights for the Aerojet, Hercules, Thiokol and UTC designs are 729 lbs, 726.8 lbs, 734.3 lbs and 702.4 lbs, respectively. These values correspond to a 185,000 lb-sec total impulse requirement. All of the propellants deliver comparable performance. The weight advantage on the UTC design stems from their selection of case material and high expansion ratio, as discussed below.

Pyrotechnically-actuated nozzle separation was unanimously proposed as the best approach to thrust termination.

The off-loading requirement to deliver 117,000 lb-sec of total impulse for the 1973 mission is met in each case by machining the propellant or by using larger core tooling during propellant casting.

Components and Materials - Case insulation materials are subject to many of the same mechanisms of thermal degradation as the propellant systems. Selection was based primarily on previous vendor experience and compatibility of the insulation with the propellant. Most have been subjected to heat sterilization, and found to be acceptable from the standpoint of weight loss, hardness, modulus and tensile strength. The selected insulations were: Aerojet - epoxy-cured polybutadiene (SD-850); Hercules - Buna-S; Thiokol - asbestos-filled polyisoprene; and UTC - silica and asbestos-filled butyl rubber.

Titanium was the preferred case material in all but the UTC design, where a fiberglass case was selected. Aerojet rejected a glass fiber case due to the contribution of the material's low modulus to high propellant gain strains during motor operation. UTC, on the other hand, cites the weight advantage of fiberglass and points to the use of an elastomer coating on the case following proof pressure testing and prior to thermal cycling to maintain the physical properties under high temperature and humidity. Titanium was selected for the McDonnell baseline design. While propellant strain during motor operation can be reduced by curing a fiberglass case while under pressure, little is known about the relaxation tendencies of this material under the sterilization environment.

All four companies provided pyrogen igniter designs. However, Aerojet reserved selection between a pyrogen and a boron potassium nitrate (BPN) hot-particle igniter pending completion of in-house sterilization testing.

Filled phenolics were chosen for nozzle components of all designs. Aerojet data indicates that, other than thermal expansion, the primary effect of sterilization on typical silica-phenolic nozzle insulation materials is a change in char regression rate. The extent of this change is unclear, however, due to the scatter of test data. Testing by JPL indicates that filled phenolics and graphite materials are not affected by heat sterilization.

5.13.1.5.2 Definition of Selected Subsystem - The important aspects of the subject designs are presented in Figure 5.13-24. The preferred design characteristics are indicated in each of the three categories: development status, weight and performance, and design complexity.

Despite the relative advantages of one design over another, the basis of vendor selection is contingent on the availability of a characterized propellant formulation with superior thermal stability. It is recognized that the full characterization of a newly-developed propellant formulation entails a lengthy development and testing period and, yet, the extent to which the thermal stability of existing propellants can be improved is unknown. For our preferred design, the modification of a current binder system was adjudged to be the more prudent approach. A propellant system consisting of a carboxy-terminated polybutadiene binder and ammonium perchlorate oxidizer was selected for this purpose. A slotted tube grain design was chosen because of its low stress concentrations, high loading efficiency and good processing characteristics.

The basic purpose of the vendor information was to provide added credence and validity to the preferred de-orbit propulsion subsystem design. As shown in Figure 5.13-25, excellent correlation exists between vendor design (as adjusted for subsystem trade iteration) and the preferred subsystem values.

5.13.1.6 Conclusion and Recommendations - Results from studies which have included solid propellant, monopropellant, and storable bipropellant de-orbit propulsion subsystems demonstrate our preference for the solid propellant subsystem. The basic data used in the parametric studies were provided by various rocket manufacturers. Thus the results are considered to be quite valid. However, to add additional credence to the validity of the results, motor designs were solicited from interested rocket companies. The characteristics of the proposed designs compare favorably with those used in this study and justify selection of the solid propellant motor for the de-orbit subsystem.

Even though the solid propellant de-orbit subsystem selection is obvious, the

SUMMARY OF EVALUATION CONSIDERATIONS

	DEVELOPMENT STATUS	WEIGHT AND PERFORMANCE	DESIGN COMPLEXITY
Aerojet-General	● Propellant (1) ● New Formulation – In Development ● Very Good Sterilization Compatibility ● 3 Year Development and Testing Schedule ✓	● Moderate Weight ● Moderate Isp ● High Solids Loading ● Short Burn Time	● Titanium, Ellipsoidal Case ● Fair Fabrication Cost and Ease ● Good Compatibility–High Modulus ● Grain Design ● Processing–Fair ● Stress–Good
Hercules Powder	● Propellant ● Modification of Commercial Formulation – Fully Developed ● Fair Sterilization Compatibility ● 2 Year Development and Testing Schedule	● Moderate Weight ● Low Isp ● High Solids Loading ● Moderate Burn Time	● Titanium, Ellipsoidal Case ● Fair Fabrication Cost and Ease ● Good Compatibility–High Modulus ● Grain Design ● Processing–Good ● Stress–Good ✓
Thiokol Chemical	● Propellant (2) ● Modification of Commercial Formulation – In Development ● Very Good Sterilization Compability ● 3 Year Development and Testing Schedule ✓	● Moderate Weight ● Low Isp ● Low Solids Loading ● Short Burn Time	● Titanium, Spherical Case ● Good Fabrication Cost and Ease ● Good Compatibility–High Modulus ● Grain Design ● Processing–Poor ● Stress–Good
United Technology Center	● Propellant ● New Formulation – In Development ● Good Sterilization Compatibility ● 3 Year Development and Testing Schedule	● Low Weight ● High Isp ● Low Solids Loading ● Low Burn Time ✓	● Fiberglas, Ellipsoidal Case ● Very Good Fabrication Cost and Ease ● Poor Compatability-Low Modulus ● Grain Design ● Processing–Good ● Stress–Good

(1) Better Thermal Stability of the New Formulations
(2) Better Thermal Stability of the Modified Formulations

✓ Indicates Best Candidate

Figure 5.13–24

COMPARISON OF SELECTED SUBSYSTEM CHARACTERISTICS WITH VENDOR DESIGNS

		ADJUSTED VENDOR DESIGN SPREAD
PERFORMANCE		
Thrust (Average), lb 1973	6000 max	3238–3720
Thrust (Average), lb 1979	6000 max	3200–5675
Pressure (Average) psi 1973	600 max	395–560
Pressure (Average) psi 1979	600 max	404–600
Total Motor Weight, lb 1973	477	461–491
Total Motor Weight, lb 1979	678	655–692
Vacuum Total impulse, 1973	117,000	117,000
Vacuum Total Impulse, 1979	172,000	172,000
PROPELLANT		
Type	CTPB(16-A1,68-AP)	281–292
Delivered Vacuum Isp	287	
Density, lbm/in^3	.063	.0612–.0626
Propellant Weight, lb 1973	407	401–417
Propellant Weight, lb 1979	608	595–620
Grain Configuration	Slotted Tube	Slotted, Star
CASE		
Type	Spherical	Spherical, Ellipsoidal
Material	6Al – 4V Titanium	6Al – 4V Titanium & Fiberglass
Weight lb	29	12.6–29.5
NOZZLE		
Type	Ablative	Ablative
Configuration	Contoured	Contoured
Weight lb	24	21.5–25
Throat Dia, in.	2.65	1.96–2.88
Exit Diameter, in	19.24	17.52–18.54
Expansion Ratio	53:1	40–80
IGNITER		
Type	Pyrogen	Pyrogen, Hot-particle
Weight lb	4	4–11.8
INSULATION		
Type	Rubber	Rubber
Weight lb	12	7–23.6

Figure 5.13–25

difficulty of developing a highly reliable sterilizable solid propellant rocket motor must not be minimized. Before this goal is achieved, much more work must be done on basic propellant development. Development work must also be pursued on liners, insulation, O-rings, nozzles and igniters, as well as motor cases. Of course, the ultimate test of motor adequacy will be the successful firing of a full scale unit subsequent to sterilization and vacuum exposure.

The task is a formidable one and will require high engineering competance, careful planning and efficient program management to reach the objective of a qualified motor within the three years required.

5.13.2 Attitude Control - The Capsule Bus requires active attitude control for all phases of the mission from Flight Spacecraft separation to landing, except for a brief interval during parachute deceleration. Specifically, the attitude control subsystems must provide for accurate delivery of the de-orbit velocity increment, limited vehicle angle-of-attack excursions upon atmospheric entry, a stable platform for entry science measurements, and attitude control and stabilization during terminal deceleration. With proper choice of engine orientation and arrangement, the subsystem which provides this attitude control can also be used to separate the Capsule Bus from the Flight Spacecraft. The objective of this section is to summarize the functional requirements during each mission phase and to establish the types of attitude control subsystems best suited to the VOYAGER Capsule Bus. Trade studies were performed to select the type of control subsystem, taken singly or in combination, best suited for unpowered flight, de-orbit motor firing and terminal deceleration. The study was conducted in two phases. The initial phase was broad in scope, considered many alternatives and was used to support the selection studies for the de-orbit and terminal propulsion subsystems. The final phase was conducted to select final attitude control techniques based on the preferred de-orbit and terminal propulsion subsystems. As a result of these studies, the preferred selections for attitude control are:

a. A reaction control subsystem (RCS), using monopropellant hydrazine, provides attitude control from separation until parachute deployment. This subsystem also provides ΔV for Capsule Bus separation from the Flight Spacecraft.

b. During terminal descent, attitude control is obtained from the deceleration engines themselves by differentially throttling four canted engines to provide the required control torques.

The attitude control subsystems requirements, analyses of candidate subsystems and study results are provided in the following paragraphs.

5.13.2.1 Requirements - Attitude control and stabilization requirements established for this study are summarized and presented by mission phase in Figure 5.13-26.

Separation - The relative velocity increment for Capsule Bus/Flight Spacecraft separation was established in a separate trade study, summarized in Part B, Section 2.3.2. Use of a reaction control subsystem for this function would involve the simultaneous firing of aft-directed pitch and yaw thrust chambers to impart a translational impulse. Control during this maneuver can be effected

ATTITUDE CONTROL AND STABILIZATION REQUIREMENTS
•1973 MISSION

MISSION PHASE	CONTROL DEADBAND	REACTION CONTROL THRUST REQUIRED (LB)	CONTROL IMPULSE (LB SEC)	DESIGN CONSIDERATIONS	REFERENCE
Separation	±2 deg	Negligible	163	• 1.25 ft/sec separation velocity • Guidance accuracy limitation	IIB 2.3.2 IIB 5.8
De-orbit				• 20 minutes between separation and de-orbit	IIB 2.3.2
(Solid propellant de-orbit)	±1/4 deg	22 lb (pitch, yaw) 2 lb (roll)	400	• Thrust malalignment • De-orbit point error	IIB 5.13.4 IIB 5.8
(Liquid propellant de-orbit)		.7 lb (all axes)	400	• 8.8 ft moment arm	IIA 3.2.6
Coast	±2 deg	Negligible	Less than 85 depend-on subsystem type	• Guidance accuracy limitations	IIB 5.8
Atmospheric entry	±3 deg/sec	2	197 (2 lb thrust) 333 (22 lb thrust)	• Aeroshell neutral stability • Entry TV image smear • Control of oscillations induced at maximum q • 8.8 ft moment arm	IIB 2.3.6 IVD 4.5 IIB 2.3.6 IIA 3.2.6
Terminal descent	± 5.9 deg	200 (pitch, yaw) 56 (roll)	1111 (pitch, yaw) 892 (roll)	• Thrust vector alignment with velocity vector • 4.8 ft moment arm with Aeroshell separated	IIB 2.3.6 IIA 3.2.1

Figure 5.13-26

by "OFF" logic, wherein the thrust chamber(s) producing a torque in the direction of the attitude disturbance are momentarily shut off.

De-Orbit - During de-orbit, the attitude must be maintained within ±1/4 degree to limit the maximum de-orbit pointing error to .86 degree. The disturbance torques generated during de-orbit thrusting are based on a thrust vector-center of gravity malalignment of ±.273 inch (3σ). Error sources contributing to this malalignment are presented in Section 5.13.4.4.

Coast - The capsule attitude during separation and coast must be maintained within ±2 degrees to avoid excessive drift in the guidance and attitude reference. A design separation distance of 300 meters is provided between the Capsule Bus and the Flight Spacecraft at de-orbit initiation.

Atmospheric Entry - Current data from wind tunnel simulations of atmospheric entry conditions have exhibited a wide scatter in dynamic stability coefficients ($C_{mq + \dot{\alpha}}$) for representative Capsule Bus configurations and a strong sensitivity to c.g. location. Moving the c.g. forward of the Aeroshell base enhances vehicle stability but the results are clouded by scale effects and data spread, particularly at the low Mach numbers. In the absence of complete Capsule Bus stability data, rate damping by reaction jets during atmospheric entry was considered in the study. This approach is conservative but it is deemed necessary at this time based on the results of entry computer studies, discussed in Section 2.3.4. For this study, a neutrally stable Capsule was assumed, and control capability provided to accomodate sharp-edged wind gusts in the worst-case VM-10 atmosphere.

Terminal Deceleration - Attitude control during terminal deceleration is required to counteract aerodynamic disturbances, engine thrust unbalances and torques induced by vehicle center of gravity shift during propellant usage. As discussed in Section 2.3.6 the attitude must be maintained within 5.9 degrees of the velocity vector to insure successful completion of the terminal deceleration maneuver.

5.13.2.2 Subsystem Candidates - Various combinations of attitude control techniques consisting of reaction control subsystems (RCS), thrust vector control (TVC) and differential throttling (multiple engines), are applicable to the VOYAGER Capsule Bus. Control of the thrust vector is only applicable during powered de-orbit and terminal mission phases. The RCS, on the other hand, is a candidate for all mission phases and a single RCS capable of performing all the required control functions is a definite possibility. However, preliminary studies indicated that the latter mechanization is not competitive from weight and design stand-points and was not considered further. This result precludes any attitude control subsystem commonality between the terminal and other mission phases. Consequently, to simplify analyses, the subsystem candidates have been divided into two categories consisting of those applicabale to: (1) De-Orbit and unpowered flight phases, and (2) Terminal descent phase.

The candidate subsystems synthesized for evaluation are shown in Figures 5.13-27 through 5.13-29.

The reaction control subsystem types selected for study are cold gas-nitrogen, monopropellant-hydrazine, and bipropellants-nitrogen tetroxide and monomethyl hydrazine.

Nitrogen was selected because it has been used extensively in cold gas subsystems. Other cold gas propellants are also available, but the weight and performance advantages are considered too small to justify additional analyses.

It appears that hydrazine (N_2H_4) is capable of withstanding heat sterilization and is the only monopropellant offering adequately high performance.

Monomethylhydrazine (MMH) and nitrogen tetroxide (N_2O_4) were selected as propellants for the bipropellant subsystem to take advantage of the sterilization technology which must be developed for the Terminal Propulsion Subsystem.

Each liquid propulsion RCS includes positive propellant expulsion, except where propellant was supplied by the main propulsion subsystem tank, as was the case for terminal descent. All subsystem candidates utilized component arrangements defined in Section 5.13.4.1.

5.13.2.2.1 De-Orbit and Unpowered Mission Phases - All reaction control subsystems considered for the de-orbit and/or unpowered mission phases utilize the same thrust chamber arrangement. The engine locations were chosen primarily to take advantage of the maximum possible moment arm. Four chambers are provided for coupled roll control, with four additional aft firing chambers used for uncoupled pitch and yaw plus separation from the Flight Spacecraft. To provide pure coupled pitch and yaw control, four additional forward firing chambers would be required. However, such a configuration would possess several undesirable characteristics. The exhaust gases would have to expand counter to the supersonic free stream, creating disturbance torques due to non-uniform pressure distributions at the edge of the Aeroshell. Furthermore, the engines so placed would be exposed to high entry heating rates and the possibility of injector blockage from products of ablation.

Propellant tanks and pressurant tanks are located in the nose of the Aeroshell

CANDIDATE REACTION CONTROL SUBSYSTEMS UNPOWERED AND/OR DE-ORBIT MISSION PHASES

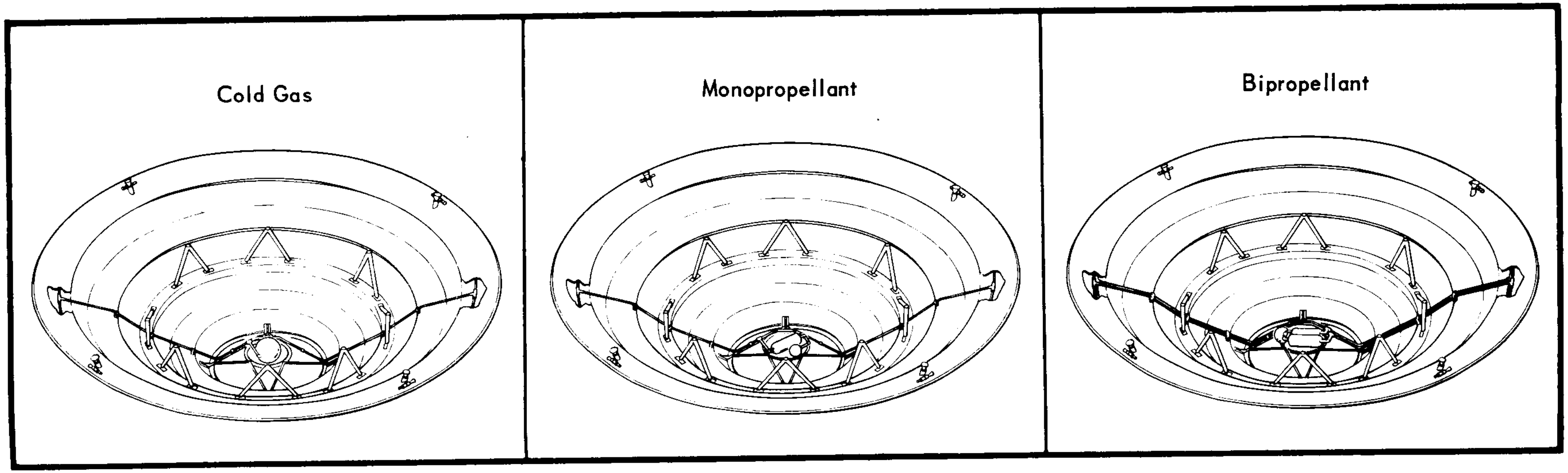

Cold Gas

Monopropellant

Bipropellant

Figure 5.13-27

DE-ORBIT MISSION PHASE
SELECTED THRUST VECTOR CONTROL SUBSYSTEM

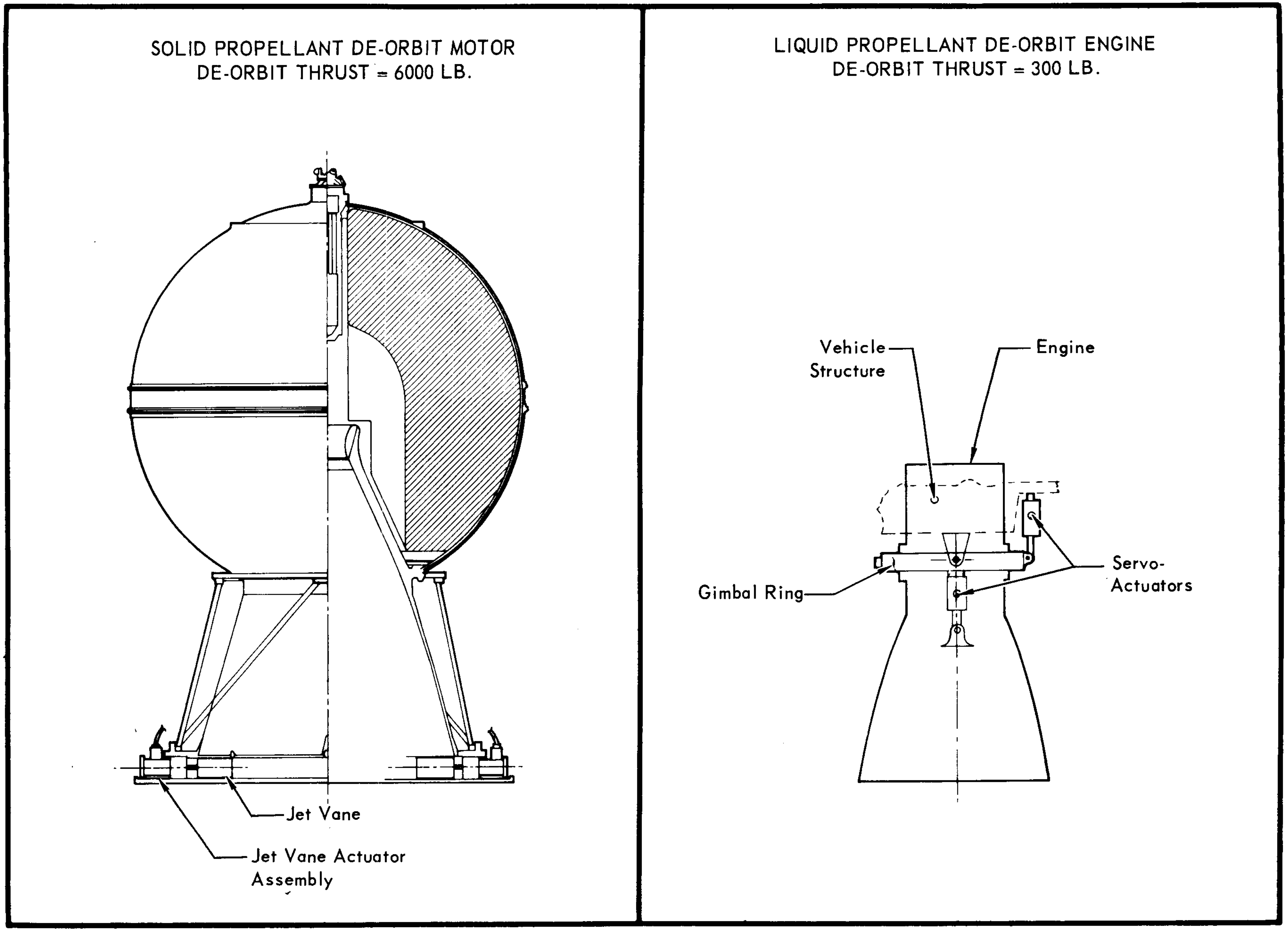

SOLID PROPELLANT DE-ORBIT MOTOR
DE-ORBIT THRUST = 6000 LB.

LIQUID PROPELLANT DE-ORBIT ENGINE
DE-ORBIT THRUST = 300 LB.

Jet Vane
Jet Vane Actuator Assembly
Vehicle Structure
Engine
Gimbal Ring
Servo-Actuators

Figure 5.13–28

TERMINAL DESCENT MISSION PHASE
CANDIDATE CONTROL SUBSYSTEMS

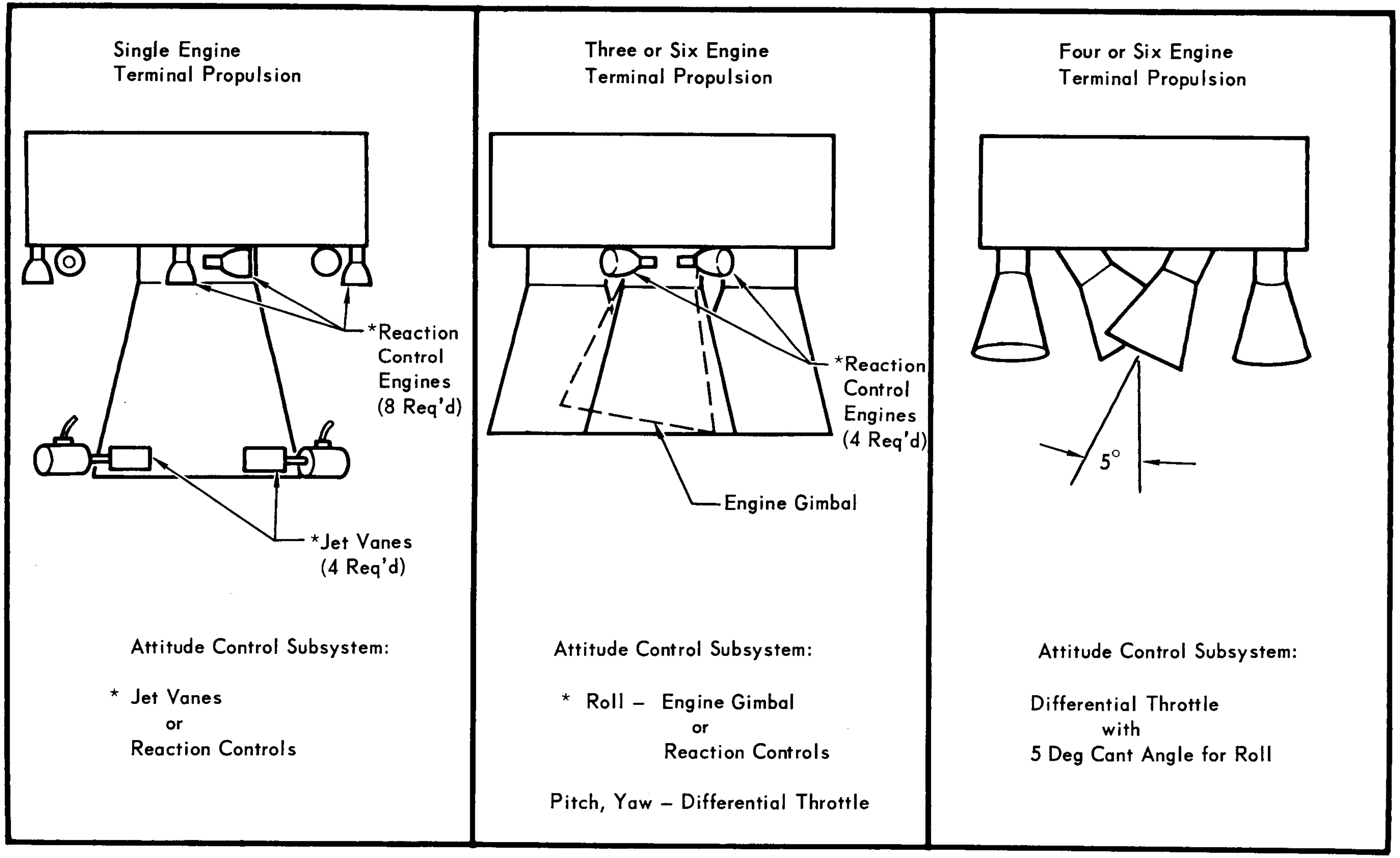
Single Engine
Terminal Propulsion
*Reaction
Control
Engines
(8 Req'd)
*Jet Vanes
(4 Req'd)
Attitude Control Subsystem:
* Jet Vanes
or
Reaction Controls
Three or Six Engine
Terminal Propulsion
*Reaction
Control
Engines
(4 Req'd)
Engine Gimbal
Attitude Control Subsystem:
* Roll – Engine Gimbal
or
Reaction Controls
Pitch, Yaw – Differential Throttle
Four or Six Engine
Terminal Propulsion
5°
Attitude Control Subsystem:
Differential Throttle
with
5 Deg Cant Angle for Roll

Figure 5.13–29

in order to provide: equal flow distribution to four thrust chamber groups; minimum c.g. shift during propellant utilization; and maximum use of Capsule Bus volume which cannot otherwise be utilized by Capsule Lander equipment, due to interaction with the landing radar. (The RCS is jettisoned with the Aeroshell prior to enabling the landing radar.)

The TVC concepts evaluated for de-orbit attitude control were selected from study results presented in Section 5.13.4.4. Jet vanes were chosen as best suited for the high thrust, short duration solid rocket, while gimballing was selected for use with the low thrust mono-propellant and bipropellant de-orbit engine.

5.13.2.2.2 Terminal Mission Phase - The RCS considered for the terminal phase utilizes engines directed downward for pitch and yaw. The reaction control jets thereby contribute to vehicle deceleration, minimizing losses due to control corrections. The use of propellant from the main tanks also decreases the weight penalty over that of a separate RCS.

Terminal propulsion subsystems using three engines can achieve pitch and yaw control by the technique of differential throttling, but require RCS or TVC for roll control. Four and six engine concepts can provide roll control, in addition to pitch and yaw, by canting alternate engines in opposite directions and differentially throttling adjacent engines to vary the net roll moment. The selection of TVC devices for this study are discussed in Section 5.13.4.4. The selections are jet vanes for all axis control of the single engine candidate and gimballing for roll control of multiple-engine candidates.

5.13.2.3 Candidate Subsystem Trades - The candidate attitude control concepts were compared on the basis of reliability, development status, performance, versatility, and interactions with other subsystems. The results of these considerations are presented below.

5.13.2.3.1 Reliability - The reliability of each candidate attitude control subsystem was evaluated using failure rate data from other programs. For reference, these data are present in Section 5.13.4.5.

De-orbit and Unpowered Mission Phase - The reliability of RCS designs and RCS plus TVC arrangements, suitable for the de-orbit and unpowered mission phase functions, was determined for configurations defined in Figures 5.13-27 and 5.13-28. For this mission, the highest reliability is achieved with a cold gas subsystem followed by monopropellant and bipropellant subsystems, in that order. The use of TVC, instead of RCS for de-orbit attitude control, results in minor changes in overall reliability. A summary of the reliability study results for the deorbit and unpowered mission phases are provided in Figure 5.13-30.

FIGURE 5.13-30

RELIABILITY OF CANDIDATES

(UNPOWERED AND DE-ORBIT MISSION PHASES)

RCS TYPE	RCS ONLY	RCS SOLID MOTOR JET VANE TVC (1)	RCS WITH LIQUID ENGINE GIMBAL TVC (1)
Cold Gas	.9967	.9961	.9962
Monopropellant	.9934	.9932	.9934
Bipropellant	.9898	.9902	.9903

(1) Reliability of RCS adjusted for decreased engine firing cycles.

Terminal Descent Mission Phase - Except for the six engine configuration, which contains TVC provisions for engine-out capability, the greatest attitude control reliability is associated with the four-engine, canted-nozzle system. There is only a small increment between this latter configuration and one using an engine gimbal. The reliability of each subsystem evaluated is provided in Figure 5.13-31.

5.13.2.3.2 Development Status - Development status of the candidate attitude control concepts is a particularly important consideration in achieving a flight qualified subsystem by 1973.

The basic technology of cold gas, monopropellant and bipropellant subsystems is well developed. Cold gas nitrogen subsystems were incorporated in Ranger, Mariner, Surveyor and Lunar Orbiter. Monopropellant hydrazine subsystems were also incorporated in Ranger and Mariner, and a hydrazine attitude control subsystem is being developed to replace a bipropellant subsystem for the Titan III - Transtage. Successful bipropellant applications include the Gemini OAMS and RCS, Surveyor, and Lunar Orbiter.

These programs have made available developed engines near the required thrust levels. However, the development is not totally applicable to VOYAGER and additional effort is required to meet mission requirements and to develop compatibility with the sterilization environment.

The cold gas subsystem is inherently simpler than monopropellant and bipropellant subsystems, requiring slightly less than one-half of the estimated 3 year

Figure 5.13-30

ATTITUDE CONTROL SUBSYSTEM RELIABILITY TERMINAL DESCENT MISSION PHASE

	TERMINAL PROPULSION CONFIGURATION			
	SINGLE ENGINE	THREE ENGINES	FOUR ENGINES	SIX ENGINES
Monopropellant Terminal Propulsion				
RCS	N/A	N/A	.9992(1)	.9992 (1)
TVC	N/A	N/A	.9994(1)	.9994 (1)
Differential Throttle	N/A	N/A	.9998	.9998
Bipropellant Terminal Propulsion				
RCS	.9979	.9988 (1)	.9988 (1)	.9988 (1)
TVC	.9991	.9994 (1)	.9994 (1)	.9998 (1)
Differential Throttle	N/A	N/A	.9998	N/A

(1) Reliability based on pitch and yaw control supplied by differential throttling, with roll control provided by the mechanism shown.

Figure 5.13-31

development time for the latter. In addition, heat sterilization of a cold gas subsystem will only affect the tank operating pressure, regulator, valves, and elastometers, and these are problems common to each subsystem.

The liquid propellants are highly reactive and present critical material compatibility problems. In addition, monopropellant hydrazine is sensitive to thermal decomposition. These problems are further complicated by the positive expulsion device required for the unpowered mission phases. In fact, the development of positive expulsion tankage will constitute a major development effort.

Testing directed at determining the feasibility of sterilizing liquid propellant subsystems is being sponsored by JPL. McDonnell has also completed sterilization testing of both monopropellants and bipropellants. Test results for each of these programs are described in detail in Section 5.13.4.2. The results of these tests indicate that the sterilization of liquid propellants is feasible if careful attention is given to material selection and processing. However, much more work must be done in this area. The material cleaning and passivation techniques must be verified. Propellant decomposition during sterilization results in gas evolution. Further testing is required to identify the amount of decomposition products formed, their solubility in the propellants at lower temperatures and operating pressures, and the effect of dissolved gases on thrust chamber response and performance.

A major milestone of the Surveyor Program was the successful development of the differential throttling concept of attitude control, and extension of this concept to the Capsule Bus should not require long development times or high risk potential.

The TVC devices considered in this study, i.e., gimbals and jet vanes, are highly developed except for the sterilization environment.

5.13.2.3.3 Weight and Performance - The performance data used in the study and shown in Figure 5.13-32 were obtained from the following sources: Nitrogen - Sterer; Monopropellant - Rocket Research, Hamilton Standard and Marquardt; Liquid bipropellant - Rocketdyne (Gemini). The nitrogen pressure levels used were established from subsystem weight optimization studies. The other pressure levels were accepted as nominal for the respective subsystem. Although, these data represent only approximations, they are considered to be sufficient to compare types.

De-orbit and Unpowered Mission Phases - Employing the above data the impulse requirements for the various reaction control subsystems were evaluated using computer techniques discussed in Section 2.3.3. The resulting total impulse requirements for the de-orbit and unpowered phases of the mission are

REACTION CONTROL SUBSYSTEM PERFORMANCE DATA

REACTION CONTROL SUBSYSTEM	THRUST (lb)	MINIMUM IMPULSE BIT (lb-sec)	VACUUM SPECIFIC IMPULSE (sec)		CHAMBER PRESSURE (psia)	REGULATED PRESSURE (psia)	STORAGE PRESSURE (psia)
			MINIMUM PULSE	STEADY STATE			
Cold Gas	2	.017	70	70	50	200	2750
	10	.082	70	65			
	22	.18	70	60			
Monopropellant	2	.02	115	220	150	300	3000
	10	.095					
	22	.23					
Bipropellant	2	.011	155	280	100	300	3000
	10	.056					
	22	.12					
	56	.285					
	200	1.0					

Figure 5.13-32

shown in Figure 5.13-33. These data are based on worst case wind shear profiles for the VM-10 atmosphere and an entry capsule with neutral dynamic stability. The variations in total impulse requirements with thrust, shown for the entry damping and coast mission phases, are due to rate limit cycle operation. The differences between subsystems result from the variations in minimum impulse bit characteristics.

The weight and performance of the jet vanes and gimbal systems used in each configuration analyzed are provided in Section 5.13.4.4.

The weight relationship of each of the RCS candidates with respect to total impulse and thrust level is shown in Figure 5.13-34. In each case the weights shown reflect sterilization considerations relative to tank design pressures and material selections. The specific component arrangements in each subsystem considered are those defined in Section 5.13.4.1, and the materials used are based on results reported in Section 5.13.4.2. Each liquid propellant subsystem is equipped with positive propellant expulsion devices.

A review of Figure 5.13-26 shows that RCS thrust level requirements vary from .7 to 22 lbs., depending upon the thrust level of the de-orbit rocket. The maximum thrust required for unpowered flight is for entry rate damping and is approximately 2 lbs. Thus, the use of a single, fixed-thrust subsystem, desired for simplicity, means compromising operating thrust levels during certain mission phases. The total impulse requirements shown in Figure 5.13-33 reflect the penalties associated with high thrust operation. For the low-thrust liquid de-orbit rocket, the penalty is small since the 2 lbs. thrust required for entry rate damping is not appreciably greater than the .7 lbs. needed for de-orbit. The large solid de-orbit motor, on the other hand requires 22 lbs. thrust, a value which is significantly greater than the 2 lb. necessary for entry. In this case, the penalty is appreciable and consideration was given to design modification. Two sets of thrust chambers are objectionable because of weight and complexity. The concept of bi-level thrust chambers, operating at high thrust during de-orbit and lower thrust during other phases, is attractive and has been considered in the following subsystem weight evaluation.

A summary of the configurations evaluated, along with their weights, is presented in Figure 5.13-35. In all cases the monopropellant hydrazine subsystem provides the minimum weight subsystem, followed by bipropellant and cold gas, in that order. Depending upon the thrust chamber combination selected, the pure cold gas reaction control is 11 to 25 lbs. heavier than the hydrazine RCS

TOTAL IMPULSE REQUIREMENTS
UNPOWERED PLUS DE-ORBIT MISSION PHASES

- 1973 Mission

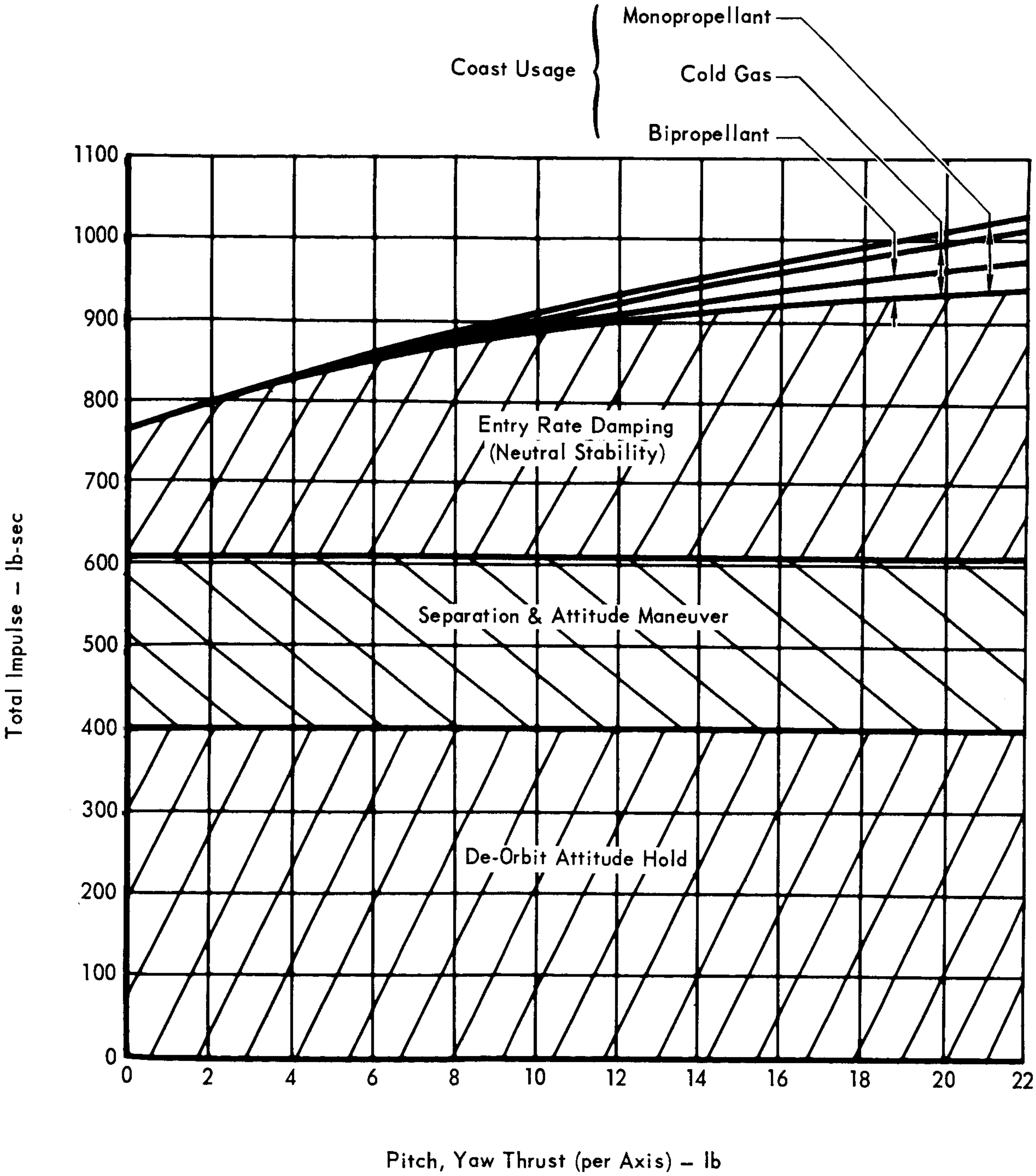

Figure 5.13-33

CANDIDATE REACTION CONTROL SUBSYSTEM WEIGHTS

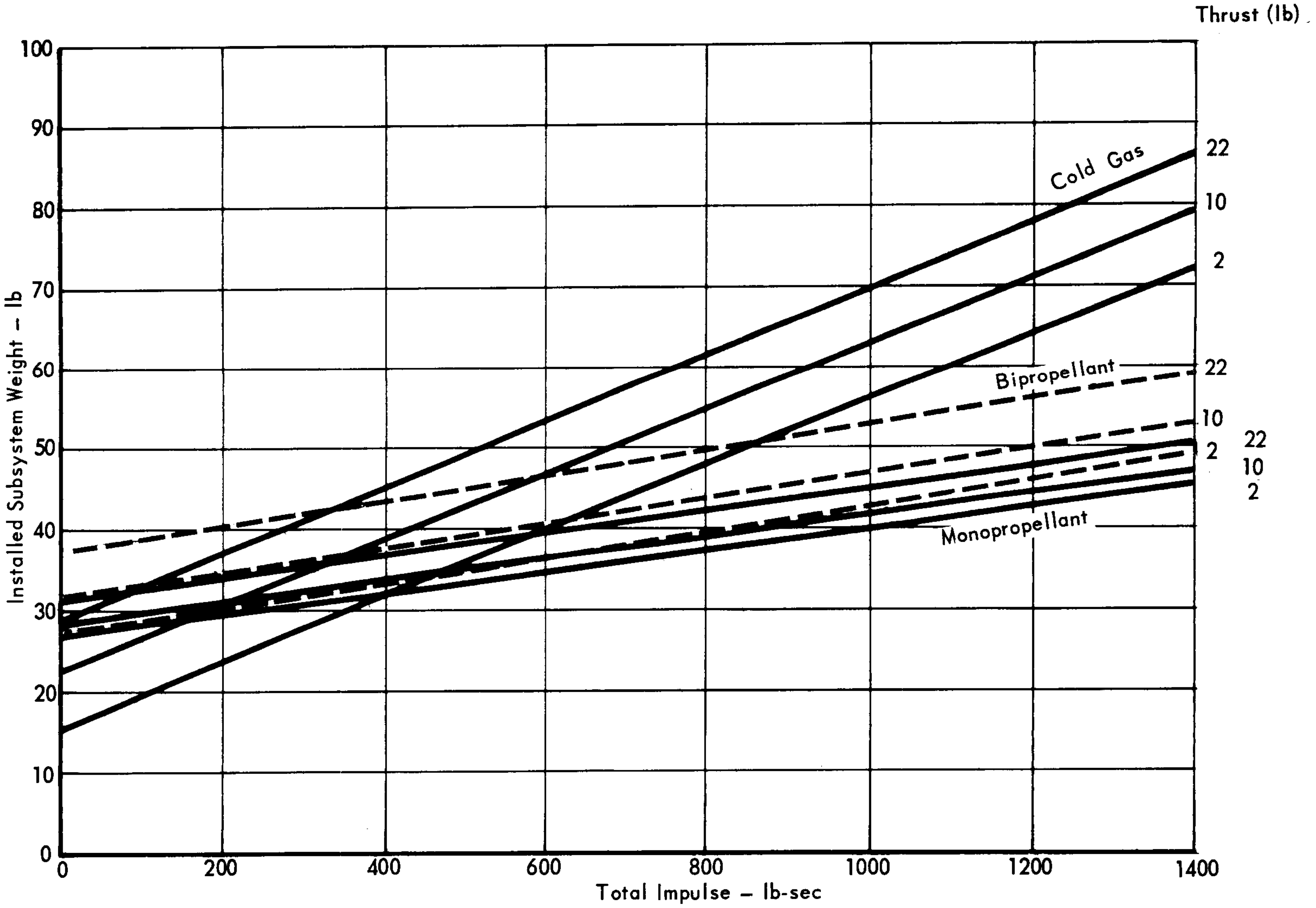

Figure 5.13–34

ATTITUDE CONTROL SUBSYSTEM WEIGHTS
DE-ORBIT AND UNPOWERED FLIGHT

TYPE DE-ORBIT ENGINE	ATTITUDE CONTROL CONFIGURATION			WEIGHT		
	RCS THRUST		TYPE DE-ORBIT TVC	COLD GAS	MONOPROPELLANT	BIPROPELLANT
	UNPOWERED FLIGHT (lb)	DE-ORBIT (lb)				
Liquid	2	2	–	48	37	40
Liquid	2	–	Gimbal	43	43	44
Solid	2	–	Jet Vanes	60	60	62
Solid	2	–	Freon Inj	61	61	63
Solid	*2	22	–	62	42	50
Solid	22	22	–	70	45	52

* Thrust Chamber is 22 lb thrust rating with bi-level step to 2 lb thrust during unpowered flight

Figure 5.13-35

designed for the same requirement. The use of TVC devices for de-orbit, in conjunction with cold gas for unpowered flight, improves the competitive weight position of a cold gas RCS.

Terminal Mission Phase - The attitude control requirement for terminal descent may be met with TVC, differential throttling, RCS, or combinations thereof. The weight of TVC subsystems to perform the required terminal functions were established under a separate study, and results are presented in Section 5.13.4.4.

The use of differential throttling introduces a penalty in engine weight since approximately 10% excess thrust is required to provide control margin. At a 1600 lb. thrust level, this amounts to approximately 9% of the engine weight (2 to 3 lb. per engine). The 5 degree engine cant angle used for roll control in the four-engine configuration introduces another weight penalty of about 3.5 lb.

The RCS weight was established using the basic data provided in Figure 5.13-32. The only RCS arrangements considered were those which utilize propellant from terminal subsystem tanks. The distinct advantages offered by this approach obviate evaluation of separate RCS designs. The propellant tankage penalty is small and the use of RCS engines directed downward provides deceleration forces, thereby reducing propellant consumption of the main propulsion subsystem. The weight penalties are, therefore, the increase in propellant weight due to the less efficient RCS engines, the propellant used in roll, and the weight of the dry engine, structure and propellant feed lines for the RCS engines. These weights have been evaluated for the applicable terminal subsystem and are provided in Figure 5.13-36 along with weights of the TVC and differential throttling techniques.

5.13.2.3.4 Versatility - Uncertainties in the atmospheric properties, especially wind shear and wind gust profiles, coupled with uncertainty in Aeroshell dynamic stability indicate the need for design flexibility in the attitude control subsystem to meet changing mission requirements. Growth potential, therefore, is an important consideration in the selection of the attitude control subsystem.

The TVC devices can provide growth capability for small changes in control levels and duty cycles.

The most versatile candidate subsystem is differential throttling. Since the propellants for control impulse are drawn from the main tanks fo the terminal propulsion subsystem, the control requirements may be greatly increased with small weight penalty. Also, additional differential control thrust can be obtained by reapportioning the thrust range between terminal deceleration and attitude control.

ATTITUDE CONTROL SUBSYSTEM WEIGHT TERMINAL DESCENT MISSION PHASE

	TERMINAL PROPULSION CONFIGURATION			
	SINGLE ENGINE	THREE ENGINE	FOUR ENGINE	SIX ENGINE
Monopropellant Terminal Propulsion				
RCS WT (lb)	N/A	N/A	29.8*	25.7*
TVC Wt (lb)	N/A	N/A	19.9*	11.8*
Differential Throttle Wt (lb)	N/A	N/A	11.8	9.5
Bipropellant Terminal Propulsion				
RCS Wt (lb)	40	30*	22.2*	32.1*
TVC Wt (lb)	52.2	21.4*	20.4*	30.4*
Differential Throttle Wt (lb)	N/A	N/A	14.4	N/A

*Weights are for roll control with pitch and yaw control supplied by differential throttle. Weights include terminal propulsion engine weight increase due to added thrust margins for control capability.

Figure 5.13-36

The reaction control subsystems can provide flexibility by adding propellant tankage. With a cold gas subsystem, tankage or service pressure modifications may be incorporated without seriously affecting subsystem development but the low specific impulse of this type of subsystem results in significantly larger storage volume and weight increases for the added capability.

5.13.2.3.5 Subsystem Interactions - Major subsystem interactions associated with the attitude control subsystem are thermal control and exhaust plume effects.

The bipropellant and monopropellant subsystems impose greater thermal control and exhaust plume interference problems than cold gas subsystems. The RCS liquid propellants must be maintained at a temperature above their freezing point, requiring radioisotope heaters or electrical power throughout the transit and entry portions of the mission. Thrust chamber insulation is required on the monopropellant subsystems to maintain catalyst bed temperatures for high thrust response during low duty cycle operation. On the other hand, valve stand-off must be provided to limit propellant valve temperatures to approximately 300°F during periods of continuous operation.

Potential exhaust plume interactions are heating of adjacent surfaces, electromagnetic attenuation and spacecraft upsetting moments introduced during Capsule Bus (CB)/Flight Spacecraft (FSC) separation. These effects are expected to be minor but require investigation.

Because of the small pulses and the relatively short total operating time the RCS is not expected to affect the relay communications link.

Although the RCS jets will impinge on the aft section of the sterilization canister during CB/FSC separation, disturbance moments due to uneven ignition response result in a negligible rotation of the SCS (approximately .2 milliradians in pitch and yaw during the separation burn). Contaminant deposition on the FSC sensitive surfaces from the exhaust plumes of the RCS is minimized by the aft portion of the sterilization canister which serves as a barrier.

The relative ranking of the reaction control subsystems in order of increasing interface complexity are cold gas, monopropellant and bipropellant.

The interactions of thrust vector control devices and differential throttling are presented in Sections 5.13.4.4 and 5.13.3, respectively.

5.13.2.4 Preferred Subsystem Selection - A comparison of the above evaluations has resulted in the selection of preferred subsystems. The rationale used in this selection is presented in the following paragraphs.

De-Orbit and Unpowered Mission Phases - As a result of the selection of a solid rocket motor for the de-orbit function, only a few of the mechanizations investigated are pertinent to this selection. Each, nevertheless, has been presented in Figure 5.13-37, in the interest of completeness. From those concepts studied, three are serious contenders. These are: cold gas RCS, because of development status and projected reliability; hydrazine monopropellant, because of light weight, relatively high reliability, and versatility; and cold gas RCS plus jet vanes (for de-orbit) because of weight (less than cold gas RCS) and development status relative to hydrazine monopropellant.

The cold gas design is the obvious choice except for weight and its lack of versatility and growth potential. Its weight has been estimated as 20 lbs. greater than the monopropellant hydrazine design and 2 lbs. greater than the design employing jet vanes for de-orbit and cold gas for other functions. Because of low specific impulse and the large volume required, changes necessary to the cold gas RCS to achieve growth involve significant increases in weight along with increased capsule packaging problems. The lack of the Mars environment definition plus the greater Capsule Bus weights planned for 1979, imply a need for versatility and growth not present in a cold gas RCS.

The weight penalty associated with the cold gas subsystem may be slightly reduced by using jet vanes during de-orbit, but the development is complicated by the use of two subsystems. Even more important is the requirement that jet vanes be developed in conjunction with the de-orbit motor, a program which is already faced with major development problems.

The major factor favoring the hydrazine monopropellant RCS, for the de-orbit and unpowered flight attitude control functions is weight. For the 1973 mission design a fixed thrust monopropellant subsystem is 17 lbs. lighter than the cold gas RCS and 15 lbs. lighter than the combined jet vanes - cold gas design. Also, because of its relatively high specific impulse and low volume storage, hydrazine monopropellant offers significant advantages in versatility and growth. In fact, a reasonable growth may be designed into the basic subsystem without major weight penalty. The primary problem with a hydrazine monopropellant design involves development to meet the sterilization requirements. Two major problems, not associated with the other designs discussed. are hydrazine/material compatibility, and catalyst poisoning by ethylene oxide exposure. Tests conducted at McDonnell during this study indicate that titanium may be used successfully for hydrazine storage. The thrust chamber must be sealed against ethylene oxide during decontamination to prevent catalyst bed poisoning. Additional work is required in each

ATTITUDE CONTROL SUMMARY COMPARISON
DE-ORBIT AND UNPOWERED MISSION PHASES

TYPE DE-ORBIT SUBSYSTEM	ATTITUDE CONTROL DEVICES				RELIABILITY
	TYPE RCS	TYPE TVC	RCS THRUST		
			UNPOWERED FLIGHT	DE-ORBIT	
Solid Rocket (F_N = 6000 lb)	Cold Gas	–	2*	22	.9967
		–	22	22	.9967
		Jet Vanes	2	None	.9961
Liquid Rocket (F_N = 300 lb)		–	2	2	.9967
		Gimbal	2	None	.9962
Solid Rocket (F_N = 6000 lb)	Monopropellant	–	2*	22	.9934
		–	22	22	.9934
		Jet Vanes	2	None	.9932
Liquid Rocket (F_N = 300 lb)		–	2	2	.9934
		Gimbal	2	None	.9934
Solid Rocket (F_N = 6000 lb)	Bipropellant	–	2*	22	.9898
		–	22	22	.9898
		Jet Vanes	2	None	.9902
Liquid Rocket (F_N = 300 lb)		–	2	2	.9898
		Gimbal	2	None	.9903

*2216 lb thrust engine restricted to produce two pounds of thrust.

Fig

5,13-62-1

WEIGHT	DEVELOPMENT STATUS	VERSATILITY AND GROWTH	INTERFACES
62 70 60 48 43	Cold gas subsystem relatively easy to develop. Estimated development time is 1½ years. Technology of TVC devices well developed except for sterilization.	Cold gas subsystem growth can be provided by additional tankage and/or storage pressure increases. TVC devices readily adjustable to changes in duty cycle.	Cold gas subsystem has minimal interactions. TVC devices complicate jettison and thrust termination of solid propellant motor.
42 45 60 37 43	Monopropellant engines well developed but subsystem development constrained by positive expulsion and sterilization effects. Estimated development time is three years. Technology of TVC devices is well developed except for sterilization.	Monopropellant subsystem growth can be provided by increased tankage. TVC devices readily adaptable to changes in duty cycle.	Monopropellant subsystem requires active thermal control. Surrounding components must be protected from high temperature engine and plume. TVC devices complicate jettison and thrust termination of solid propellant motor.
50 52 62 40 44	Bipropellant engines are well developed but subsystem development constrained by positive expulsion and heat sterilization effects. Estimated development time is three years. Technology of TVC devices is well developed except for sterilization.	Bipropellant subsystem growth can be provided by additional tankage. TVC devices readily adaptable to changes in duty cycle.	Bipropellant subsystem requires active thermal control. Surrounding components must be protected from high temperature engine and plume. TVC devices complicate jettison and thrust termination of solid propellant motor.

ure 5.13-37

[redacted]

5.13-62-2

of these areas to firmly demonstrate the feasibility of the hydrazine design for the VOYAGER mission.

A hydrazine monopropellant attitude control subsystem has been selected as the preferred design. The weight advantage, the relatively high reliability, and flexibility for growth, outweigh the sterilization disadvantages associated with its development.

Terminal Mission Phase - For purposes of completeness, the results of all terminal descent attitude control designs investigated are summarized in Figure 5.13-38. Since the main propulsion subsystem selected utilizes four bipropellant engines, the logical choice for attitude control is differential throttling.

Differential throttling offers advantages over TVC or RCS in each area investigated. Although this concept has not been employed for three axis control in previous programs it appears to present no major development problems, especially when compared to the development of an additional subsystem.

The attitude control subsystem choice for terminal descent is therefore differential throttling, employing canted engines for roll control.

5.13.2.5 Preferred Subsystem Design - The preferred attitude control subsystem design for the de-orbit and unpowered flight functions is shown schematically in Figure 5.13-39.

In selecting this configuration, special consideration was directed to component selection and arrangement, subsystem pressure levels propellant expulsion techniques, and engine design and performance. In case of the engine, assistance was obtained from the various manufacturers in defining geometry, weight, and performance.

Reliability was the primary factor considered in selecting component arrangement. Highly developed concepts were utilized and different arrangements were evaluated to establish the most reliable combinations. The final selection was based on study results presented in Section 5.13.4.1.

Positive propellant expulsion is required during the unpowered mission phases. Results of a study of the various concepts considered is presented in Figure 5.13-40. Elastomeric bladders were disqualified based primarily on undesirable material properties. Of the metallic devices considered, the bellows concept is preferred based on its flight proven reliability and high cycle life. Of the candidate bellows materials, A-70 titanium is preferred due to its demonstrated compatibility with hydrazine at sterilization temperatures. Bellows have been successfully manufactured from A-70 titanium by Sealol, Inc. An A-70 titanium bellows sample

ATTITUDE CONTROL SUMMARY COMPARISON
TERMINAL DESCENT MISSION PHASE

TERMINAL ENGINE CONFIGURATION	MAIN ENGINE PROPELLANT	ATTITUDE CONTROL			RELIABILITY	WEIGHT* lb	D
		DIFFERENTIAL THROTTLE	TVC	RCS			
Single	Bipropellant			Bipropellant	.9979	40	● Requires n
			Jet Vanes (Roll)		.9991	52.2	● Fully deve sterilizatio
3 Engines	Bipropellant	√		Bipropellant (Roll)	.9988	30.4	● Requires n
		√	Gimbal (Roll)		.9994	21.4	● Fully deve sterilizatio
4 Engines	Bipropellant	√			.9998	14.4	● Provided w
		√		Bipropellant (Roll)	.9988	22.2	● Requires n
		√	Gimbal (Roll)		.9994	20.4	● Fully deve sterilizatio
4 Engines	Monopropellant	√			.9998	11.8	● Provided w
		√		Monopropellant (Roll)	.9992	29.8	● Requires n
		√	Gimbal (Roll)		.9994	19.9	● Fully devel sterilizatio
6 Engines	Bipropellant	√		Bipropellant (Roll)	.9988	32.1	● Provided w
		√	Gimbal (Roll)		.9998	30.4	● Fully devel sterilizatio
Solid Motor with 6 Vernier Engines	Monopropellant	√			.9998	9.5	● Provided w
		√		Monopropellant (Roll)	.9992	25.7	● Requires n
		√	Gimbal (Roll)		.9994	11.8	● Fully devel sterilizatio

*Weights of differential throttling subsystems include engine cant angle pen

Figure 5.13–38

EVELOPMENT STATUS	VERSATILITY AND GROWTH	INTERACTIONS
w engine development. oped technology, except for n	● Growth capability provided by terminal propulsion tankage ● Most versatile, readily adaptable to thrust, duty cycle increases.	● High exhaust temperature requires engine isolation ● Minimal interactions
w engine development oped technology, except for n	● Growth capability provided by terminal propulsion tankage modification. ● Most versatile, readily adaptable to thrust, duty cycle increase.	● High exhaust temperature requires engine isolation ● Minimal interactions
th terminal propulsion development w engine development oped technology except for n	● Most versatile, terminal propulsion provides duty cycle flexibility. ● Growth capability provided by terminal propulsion tankage ● Readily adaptable to thrust, duty cycle increases	● Slightly increases thrust, throttle ratio,propellant weight ● High exhaust temperature requires engine isolation ● High exhaust temperature requires engine isolation
th terminal propulsion development w engine development oped technology, except for n	● Most versatile; terminal propulsion provides thrust, duty cycle flexibility. ● Growth capability provided by terminal propulsion tankage ● Readily adaptable to thrust, duty cycle increases	● Slightly increases thrust, throttle ratio propellant weight ● High exhaust temperature requires engine isolation ● Minimal
th terminal propulsion development oped technology except for n	● Growth capability provided by terminal propulsion tankage ● Readily adaptable to thrust, duty cycle increases	● High exhaust temperature requires engine isolation ● Minimal
th terminal propulsion development w engine development oped technology except for n.	● Most versatile, terminal propulsion provides thrust, duty cycle flexibility ● Growth capability provided by terminal propulsion tankage ● Readily adaptable to thrust, duty cycle increases.	● Slightly increases thrust, throttle ratio, propellant wt. ● High exhaust temperature requires engine isolation ● Minimal

lties and/or engine weight penalties associated with increased thrust requirements.

5.13-64-2

REACTION CONTROL SUBSYSTEM SCHEMATIC

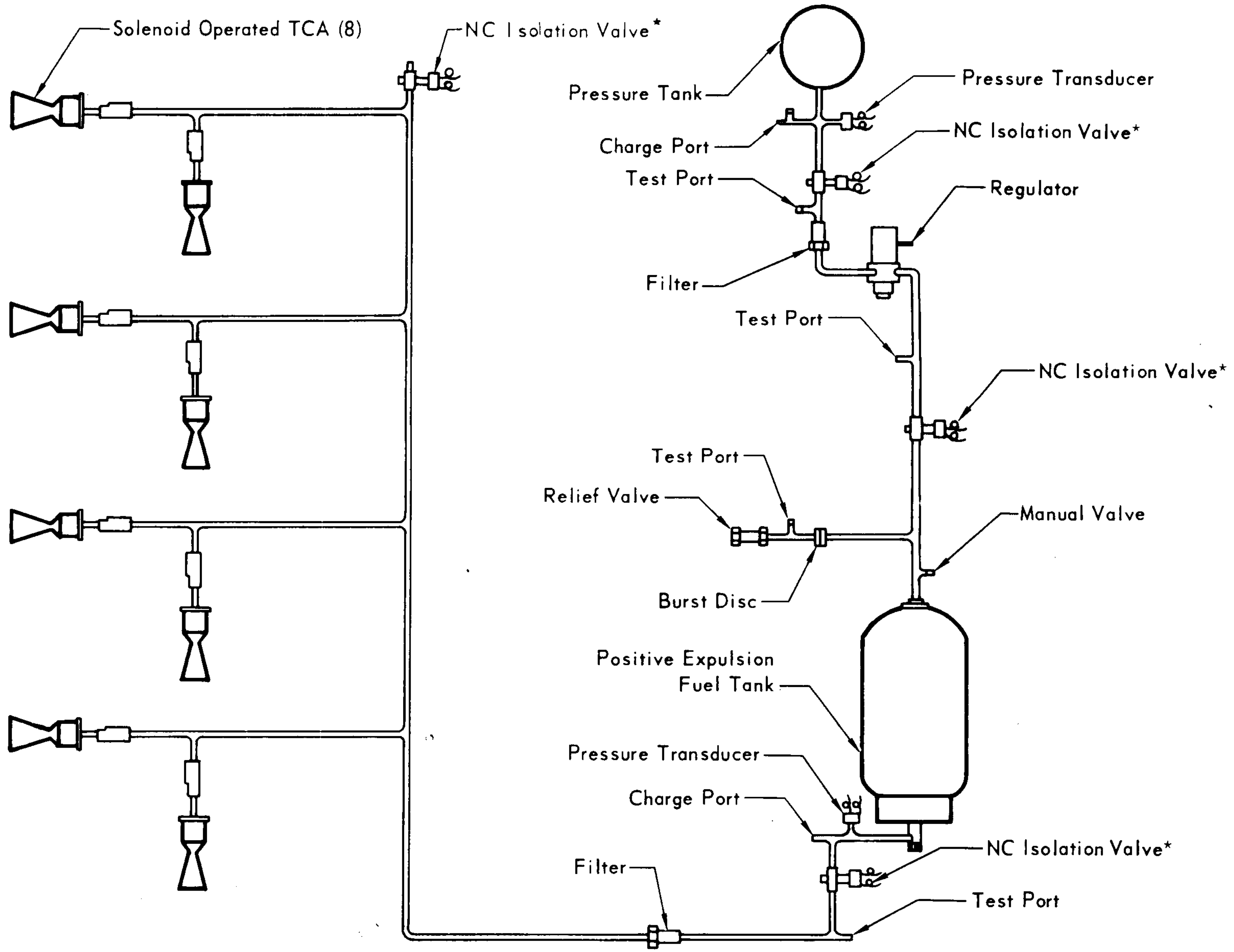
Solenoid Operated TCA (8)
NC Isolation Valve*
Pressure Tank
Pressure Transducer
Charge Port
NC Isolation Valve*
Test Port
Regulator
Filter
Test Port
NC Isolation Valve*
Test Port
Relief Valve
Manual Valve
Burst Disc
Positive Expulsion Fuel Tank
Pressure Transducer
Charge Port
NC Isolation Valve*
Filter
Test Port

*Indicates Pyro Initiator

Figure 5.13-39

POSITIVE EXPULSION TRADE STUDY

TYPE OF DEVICE	SCHEMATIC	STATE OF DEVELOPMENT	CYCLE LIFE	WEIGHT(1) (LB)	EXPULSION EFFICIENCY (%)	VOLUMETRIC EFFICIENCY (%)	RECOMMENDED MATERIALS	STERILIZATION COMPATIBILITY	PROPELLAN PRESSURAI PERMEABIL
1. Bellows a. Titanium	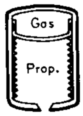	Demonstration Testing: Bell Aerosystems Co.; Sealol, Inc.	50–75	5.5	90–98	90–95	A55 Titanium A70 Titanium (Bellows)	Good probabilityA55 and A70 Ti are compatible with N_2H_4 at sterilization temp. N_2H_4 decomposition rate lower with titanium than with stainless steel.	None
b. Stainless Steel		Flight Proven: Gemini–Agena SPS Gemini–Agena Turbine Restart Tanks. Douglas S–IVB Auxillary Propulsion System.	200	13.2	90–98 (98% – Gemini/Agena SPS)	90–95 (92% – Gemini, Agena SPS)	347SS 321SS AM–350SS (347SS Preferred)	Explosions encountered at Bell with N_2H_4 in contact with 347SS at 290°F attributed to contamination rather than incompatibility. McDonnell test shows N_2H_4 decomposition greater in 321SS than in Titanium.	None
2. Piston	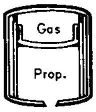	Qualification Testing – McDonnell BGRV Flight Proven: LTV Lance Missile	200	13.2	99	90–95	6AL–4V Ti 321SS 347SS	Tests at McDonnell indicate 6Al–4V Ti is compatible with N_2H_4 at sterilization temperature. Stainless steels cause significant N_2H_4 decomposition.	If a Shear Seal Incorporated Pressurant or pellant Leaka can Occur Unt System Armin
3. Metallic Diaphragm a. Wire Ring Re-enforced	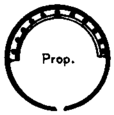	Current Programs: 1. Minuteman III LITVC Injectant Tank (Not Qualified) 2. Aerojet Post Boost Propulsion Propellant Tank (Not Qualified) Concept Developed by ARDE, Inc.	2	3.2	98–99	97–98	321SS 347SS (Diaphragm) 308SS (Wire Re-enforcement Rings)	When properly cleaned and passivated stainless steels are compatible with N_2H_4 but cause significant decomposition.	None
b. Piston Controlled Rolling	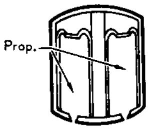	Flight Program: Thiokol, RMD, Bullpup Missile Feasibility Studies by Bell Aerosystems Co. Aircraft Armaments, Inc. has Fabricated Rolling Diaphragms Demonstration Test: NOTS Component Evaluation Propulsion System	1	5.5	95–99	90–95	1100–0 AL	N_2H_4 – excessive decomposition at 275°F (McDonnell).	None
c. Convoluted	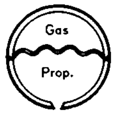	Bell Aerosystems Co. has Tested Convoluted Diaphragms. Rocketdyne, Douglas and ARDE have also Done Development Work		3.2	95–98	90–95	1100–0 AL	Same as Above	None
4. Collapsing Metal Bladder		Feasibility of Using Collapsing Aluminum Bladder has Been Demonstrated by Bell	1	4.0	95–98	95–98	1100–0 AL	Same as Above	None
5. Non-metallic Bladder (Elastomeric)	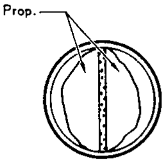	Most Common Positive Expulsion Technique Flight Proven: BOMARC RASCAL Ranger/Mariner ACS Gemini OAMS/RCS Agena SPS Surveyor VPS Apollo: Command; Service and Lunar Modules	5–50	4.0	98–99	97–99	Teflon	Teflon appears unaffected in contact with N_2H_4 at 275°F (McDonnell)	Teflon and Bladders ar Permeable Both Prope and Pressu
6. Non-Metallic Bladder, Metallic Foil Interlayer		Aluminum Foil Interlayer was Qualified for the Surveyor VPS. Flight Proven on Boeing's Lunar Orbiter	5–10 Estimated	4.0	98–99	97–99	Teflon 1100–0 AL (Foil)	(Same as 3b.)	1100–0 AL Slows Dowr Permeation Process

(1) Tank Sized for 10 Lb N_2H_4

Figure 5.13–40

NT NT TY	STORAGE LIFE	TANK SHAPE	FAILURE MODES	DEVELOPMENT RISK TIME	COST	ESTIMATED VOYAGER RELIABILITY	REMARKS
	Excellent	Cylindrical					Excellent response characteristics for pulse mode operation. Propellant storage within bellows eliminates requirement for non-metallic seals and bearing surfaces. A corrugated liner was incorporated between the bellows and tank wall on the Douglas S1VB APS to eliminate susceptability to lateral vibration. Low ΔP across bellows must be insured during sterilization. Propellant servicing must be accomplished under low feed pressures. Deservicing of propellant or test fluids requires vacuum drying.
	Excellent	Cylindrical	Bellows Distortion, Weld Fatigue, Leakage	Moderate Risk; Long Development Time	High	Excellent	
is lo Pro- ge il	Excellent	Cylindrical	Seal Leakage. Piston Sticking due to Interference Caused by Shell Distortion or Galling.	Moderate Risk, Moderate Development Time	High	High	A piston with skirt is less susceptable to vibration than other positive expulsion concepts. A pressure balanced dual wall tank design similar to McDonnell BGRV would eliminate critical tolerancing between piston and tank wall and maintain seal squeeze throughout stroke. A shear seal would provide an impermeable barrier between propellant and dynamic seal during sterilization and space storage. A shear seal was incorporated in the LANCE IRFNA tanks.
	Excellent	Spherical	Diaphragm Rupture. Failure at Weld. Local Buckling Instead of Desired Rolling.	Moderate Risk, Moderate Development Time.	Moderate	Fair	Wire ring re-enforced diaphragm provides impermeable barrier between propellant and pressurant. Tank halves and diaphragm are welded to form single unit, but visual weld inspection requires 2 diaphragm reversals, which reduces endurance life by 50%. Slow operation could induce local buckling instead of desired rolling. Problems have been encountered in forming the metal diaphragm, brazing re-enforcement rings to the diaphragm and welding tank halves and diaphragm. Should abort or subsystem failure require propellant deservicing, a new tank assembly would be required.
	Good	Cylindrical	Diaphragm Fatigue, and Rupture. Piston Binding and Cocking	Moderate Risk Moderate Development Time	Moderate	Fair	Piston sealing is not required and associated tolerances on fit are not critical. Large pistondiameter reduces circumferential stress in rolling diaphragm. Should diaphragm be permitted to roll and unroll during temperature cycling, fatigue failure could result. Early NOTS experiments indicated that a longitudinal center guide was required to prevent piston cocking. A second small diameter rolling metal diaphragm was used on this guide tube. Slow operation could induce local buckling instead of desired rolling. In the event propellant must be deserviced, a new tank assembly would be required.
	Good	Spherical	Diaphragm Ruture, Failure at Weld Seal. Local Buckling instead of Desired Rolling	High Risk, Moderate Development Time	Moderate	Fair	Tank halves and diaphragm welded to form single unit, but visual weld inspection would require 2 reversals. Slow operation could induce local buckling instead of desired rolling. A new tank assembly would be required if propellant is deserviced.
	Fair	Cylindrical or Spherical (Cylindrical Preferred)	Bladder Fatigue and Rupture. Unfavorable Flexure Pattern – 3 Corner Folding	High Risk, Moderate Development Time	Moderate	Low	Bladder sustains flexing and formation of three-corner folds during expulsion, slosh and vibration; and is susceptible to pin-hole and fracture development. Bladder may be stabilized against tank wall by evacuating pressurant side and allowing vapor pressure to position the bladder. If propellant must be deserviced a new tank assembly would be required.
EPR e o llants rant	Poor	Cylindrical or Spherical (Cylindrical Preferred)					Seal between Teflon bladder and tank which will withstand sterilization temperatures has not been developed. Bladder durability questionable below 40°F. Bladder sustains flexing and formation of three corner folds during expulsion, slosh and vibration; and is susceptible to pin hole and fracture development. Pressurant will permeate bladder and saturate propellants. Bladder may be temporarily stabilized against the tank wall by evacuating pressurent side and allowing vapor pressure to position the bladder. Permeation of propellant vapor will eventually free the bladder.
Foil the	Poor to Fair	Cylindrical or Spherical					

5113-66-2

has successfully undergone hydrazine compatibility testing at 275°F (See Section 5.13.4.2).

The engine chamber pressure was based on the rocket manufacturers' recommendations, and was established at 150 psia. The propellant tank pressure of 300 psia assures adequate injector pressure drop to aid engine stability and minimize dynamic coupling between engines and the propellant system. The pressurant subsystem pressure was set at 3000 psia.

The performance, geometry, and weight of the engines used in the study were obtained from various companies. To obtain these data, requests for information were sent to the following suppliers: Hamilton Standard, Walter Kidde, Marquardt, TRW, and Rocket Research, Inc.. The data requested is summarized below, followed by a summary of the data submitted by each supplier.

General Engine Characteristics

Thrust	22 lb.
Propellant (MIL-P-26536)	N_2H_4
Catalyst	Shell 405
Response	
Valve Signal on to 90% thrust	Approx 20 ms
Valve Signal off to 10% thrust	Approx 20 ms
Operating Life (pulsing and/or steady state)	200 sec
Minimum Impulse Bit	0.2 lb. sec. max.
Minimum Impulse Bit Repeatability	±10%

Environmental Conditions

Sterilization & Decontamination	McDonnell Report E191
Space Storage (unpressurized)	220 days

All vendors responded to the RFTI except Walter Kidde. The pertinent design and performance characteristics of these vendor designs are summarized in Figure 5.13-41.

The development of current engines furnished the basis for the proposed vendor designs. In order to satisfy the VOYAGER mission, high response and low minimum impulse bit capability is desirable. The valve should, therefore, be mounted close to the injector and the design should utilize high catalyst bed loading. The most promising vendor designs are those submitted by Hamilton Standard and Rocket Research. An engine selection has not been made since engine performance in accordance with the estimated VOYAGER mission duty cycle was not provided by the

VENDOR ENGINE DESIGN SUMMARY

	HAMILTON STANDARD	MARQUARDT CORP.	ROCKET RESEARCH CORP.	TRW SYSTEMS
Performance				
Steady State Specific Impulse (sec.)	230	224	233	232
Minimum Impulse Bit (lb.-sec)	Approx .2	.2 (± 10%)	.22 (± 5%)	–
Response from Valve ON to 90% P_c (ms)	15	14 to 27	10 to 17	33
Response from Valve OFF to 10% P_c (ms)	20	10 to 18	10 to 15	51 to 70
Design Characteristics				
Catalyst Bed Loading (lb./in.^{2}-sec)	.065	.032	.066	.035
Chamber Pressure (psia)	100	150	143	125
Expansion Ratio	40	34	50	50
Feed Pressure (psia)	225	245	279	300
Injector Pressure Drop (psi)	60	83	43	100
Catalyst Bed Pressure Drop (psi)	55	2	68	20
Valve Response (ms)				
Open	–	11	5	10
Closed	–	4	5	8
Valve Pressure Drop (psi)	10	10	27	55 (2 valves)
Valve Operating Power (watts)	–	35.7	30	67 (2 valves)
Physical Characteristics				
Length (in.)	7.0	7.25	8.75	11.10
Chamber Diameter (in.)	1.9	2.05	1.38	2.0
Exit Diameter (in.)	3.0	1.95	2.35	2.727
Weight (lb.)	2.05	1.56	2.58 (1 lb. insulation)	3.55 (2 valves)

Figure 5.13-41

vendors.

The duty cycle for VOYAGER contains short, widely spaced, pulses, with pulse duty cycles as low as 1/2 - 1%. The maximum propellant usage occurs during deorbit attitude hold, and performance approaches that of steady state operation. Each vendor has shown that specific impulse is degraded by low duty cycles wherein much of the propellant chemical energy is lost to heating the catalyst bed and chamber. This data must be extended to cover the VOYAGER duty cycle in order to accurately determine vacuum specific impulse, heat rejection rates and thrust response characteristics.

Although the engine designs received from the vendors have been extensively developed, their application to VOYAGER will require additional effort.

Additional consideration must be given to heat sterilization. The combustion chamber and nozzle are exposed to high temperatures during firing, and hence should be considered compatible with sterilization. However, the engine valve temperature is maintained at a relatively low level during firing and conclusions about the effects of sterilization on the valve cannot be drawn. In addition, the effect of potential hydrazine decomposition products on engine performance must be identified.

The significant features of the hydrazine reaction control subsystem are summarized in Figure 5.13-42. The total loaded weight shown reflects a weight contingency of 1.3 lb. Detailed subsystems descriptions are provided in Part A, Section 3.2.6.2 and Part C, Section 15.

Since attitude control during terminal descent is effected by differential throttling, control mechanization actually becomes part of the terminal propulsion subsystem. Additional description of this is therefore available under Section 5.13.3.

5.13.2.6 Conclusions and Recommendations - Attitude control for the Flight Capsule is best achieved by the use of two separate control subsystems. Control during deorbit and unpowered flight is best accomplished by use of a monopropellant hydrazine RCS. Differential throttling, using canted engines, provides the best attitude control concept for the selected four-engine terminal propulsion subsystem.

The choice between the cold gas RCS and the monopropellant RCS for the deorbit and unpowered flight portions of the mission is not obvious. The difficulty lies in assessing the importance of the weight and versatility advantage of hydrazine against the low risk development of a cold gas subsystem.

REACTION CONTROL SUBSYSTEM
PHYSICAL AND PERFORMANCE CHARACTERISTICS

Subsystem

Type – Monopropellant
  Propellant – Anhydrous Hydrazine
  Ignition – Catalyst, Shell 405
Pressurization – Stored Cold Gas, Regulated
  Pressurant – Nitrogen
Total Impulse, lb-sec – 1028

Thrust Chamber Assemblies

Total Number – 8
Type – Radiation Cooled, Fixed Thrust, Fixed Mount

Control Axis	PITCH	YAW	ROLL
No. of TCA's per Axis	2	2	4
No. of TCA's per Control Maneuver	1	1	2
Thrust per TCA, lb	22		2
Specific Impulse, Steady State, sec	220 min		
Minimum Impulse Pulse, lb-sec	0.22 max.		
Response, Start, Signal to 90% Thrust, sec	.020 max.		
Response, Shutdown, Signal to 10% Thrust, sec	.020 max.		
Area Ratio, ϵ	50:1		

Pressures –	CHARGE	STERILIZATION	OPERATION
Pressurant Tank	3000 psia @ 70°F	4400 psia @ 275°F	400–3000 psia
Regulator Inlet	14.7 psia	21 psia	400–3000 psia
Regulator Outlet	14.7 psia	21 psia	300 psia
Propellant Tank	14.7 psia	27 psia	300 psia
Combustion Chamber	14.7 psia	21 psia	150 psia

Burst Disc/Relief Valve Relief Pressure – 450 psia

Weights

Subsystem Total Weight, Loaded, lb – 46.6
Propellant Weight, Loaded, lb – 7.4
Propellant Weight, Usable, lb – 6.6
Pressurant Weight, lb – 0.4

Tankage

Propellant Tank – Positive Expulsion, Metal Bellows,
Cylindrical, Titanium
6.1 inch dia x 12.2 inch long
Pressurant Tank – Spherical, Titanium, 4.9 inch dia

TCA Envelopes	22 lb	2 lb
Length Overall (Including Valve)	9.3 in.	7.3 in.
Chamber Diameter	2.0 in.	1.0 in.
Nozzle Exit Diameter	2.7 in.	1.2 in.

Figure 5.13–42

The need for versatility is apparent since the requirements for the 1973 and future missions are not precisely defined. Of major significance is the active atmospheric entry damping requirement. The basic stability of the Flight Capsule can be defined by wind tunnel testing, but the actual Mars wind shear profile necessarily remains unknown. In addition, the growth of the Capsule Bus weight for future missions will undoubtedly require greater attitude control capability, but these requirements have not been firmly established. These factors favor a hydrazine subsystem which may be oversized for a small weight penalty or modified easily without introducing major cost, weight, and schedule problems.

The development of a hydrazine subsystem appears to be quite feasible. The hydrazine decomposition and the catalyst poisoning problems will require special attention but acceptable design solutions are achieveable.

Within the framework of the above discussion, the monopropellant hydrazine subsystem is preferred. Although there is significant technical risk involved in the development of this subsystem, the selection does not have to reflect as a technical risk to the VOYAGER program. The development time required for a cold gas subsystem is only about one-half that of the hydrazine subsystem. The most critical problems in development of the hydrazine design will arise within the first 18 months of the program. Adequate time remains at the end of 18 months to accomplish the design and development of a cold gas subsystem if development problems appear insurmountable.

Relaxation of any of the sterilization requirements would improve the position of hydrazine. Provision to permit filling the propellant tank after sterilization would eliminate most of the technical risks.

To insure confidence in the attitude control subsystem at the earliest date possible, work should begin immediately to establish the Capsule Bus aerodynamic characteristics. Work should also be initiated to further evaluate hydrazine decomposition in particular and hydrazine subsystem sterilization in general.

The use of canted engines in conjunction with differential throttling to achieve three axis control is a new concept. However, there appears to be no fundamental problem with this approach. Computer studies show excellent control characteristics. Thus, for our preferred four-engine terminal propulsion arrangement, the preferred attitude control concept is clearly differential throttling.

5.13.3 Terminal Propulsion - The Terminal Propulsion Subsystem (TPS) augments the aerodynamic decelerator(s) in the descent trajectory by providing the final braking required for soft landing the Capsule Lander on the surface of Mars.

The requirements of the terminal descent subsystem are inherently more complex than those encountered in previous space programs. Even the Surveyor program, with its VOYAGER similarity, did not require the complete automation imposed here by the communications time lag, the stringent heat and chemical sterilization, the subsequent nine-month period of deep space storage and a controlled descent through a poorly defined atmosphere. The parallels, though they exist, do not allow a simple selection of flight-proven Surveyor subsystem designs for VOYAGER. All feasible subsystems must be examined in detail to allow confident design selections.

The purpose of this study was to select a preferred concept to support the overall Capsule Bus trade studies, then to define the Terminal Propulsion Subsystem design best suited for the preferred Capsule Lander. As a result of these studies, the preferred selection for the Terminal Propulsion Subsystem is a pressure fed, storable hypergolic bipropellant subsystem. The subsystem utilizes four throttling engines positioned and oriented to provide differential throttling attitude control capability.

The Terminal Propulsion Subsystem requirements, the subsystem trade studies, the selection of the preferred concept, and the preferred subsystem design are presented in the following paragraphs.

5.13.3.1 Requirements - The TPS must provide the thrust and total impulse needed for the soft landing of a Capsule Lander weighing 2640 Earth pounds on the Mars surface in 1973. This must be accomplished from engine ignition at various conditions of altitude and velocity, depending upon the Mars environment and the guidance technique employed.

In the analysis reported in Section 2.3.7, the propulsion requirements were investigated for a practical range of ignition altitudes and velocities, namely, 5,000 to 15,000 feet and 285 to 1500 feet/sec. respectively. The following range of requirements were established.

- Total Impulse ranging from 65,000 to 170,000 lb/sec.
- Minimum thrust level of 660 lbs.
- Throttle ratic of 10:1

In addition to the operational requirements, the vehicle design and scientific measurements impose constraints on component sizing and placement within the vehicle. These are:

Subsystem design - The TPS must provide for:

- Minimum center of gravity shifts
- Flexibility to accommodate new data inputs from early missions
- Compatibility with the Capsule Lander design

Exhaust plume and products - The TPS exhaust must not:

- Degrade component reliability
- Have adverse effects on landing performance
- Excessively erode, heat or contaminate the surface near and under the capsule
- Interface with entry science package sensors

Engine Locations - Chamber Locations must not:

- Dominate the surface area of the Capsule to the exclusion of the radar antenna
- Obstruct heat rejection surfaces or devices
- Degrade scientific sensing
- Degrade the functioning of the impact attenuator.

5.13.3.2 Candidate Designs - The terminal landing function can be accomplished with various subsystems. Bipropellant, monopropellant and combined solid/liquid vernier subsystems were all evaluated for this mission phase.

The bipropellant subsystem was selected for evaluation because it offered significant weight advantages over alternate concepts. Also, bipropellant engines designed for similar applications, i.e., the Surveyor vernier and Lunar Module descent engine, have been flight-proven or have reached qualification status, thus forming a technological base for VOYAGER bipropellant subsystem development.

Of the monopropellants, only hydrazine offers sufficiently high performance to be considered for this application. The primary advantage of the monopropellant subsystem is its inherent high reliability. There are also some potential advantages in hydrazine subsystem development time and costs. However, this advantage depends upon solving the problems associated with the development of throttleable hydrazine engines, currently undemonstrated at the required thrust levels.

The combined solid/liquid concept was examined as a compromise design between the low weight of the bipropellant and the high reliability of the monopropellant.

In this concept a solid propellant rocket would be used to remove the major portion of the terminal velocity. Multiple monopropellant hydrazine engines are differentially throttled to provide attitude control during solid rocket burning and are used, after burnout of the solid, to decelerate the Capsule Lander during its low velocity descent to the Mars surface. Weight of this subsystem is competitive with the bipropellant subsystem because of the high mass fraction of the solid motor. The solid motor also reduces the required thrust level of the monopropellant engines and maintains the high level of reliability provided by the monopropellant subsystem. This permitted limiting the monopropellant engine size to the 300 lb. thrust class; the maximum size available under present state-of-the-art.

One subsystem type was used to evaluate combinations of engine number and arrangement. The bipropellant feed system was selected for this purpose. Arrangements of 1, 3, 4 and 6 engines are presented in the following paragraphs.

The selection of candidate designs span all reasonable subsystem arrangements from simplified single engines to multiple engines for differential throttling attitude control and engine-out capability.

The single engine was included to evaluate the simplicity of design of a single engine feed system with minimum manifolding and feed system components. In addition, the single engine permits maximum utilization of available Lunar Module Descent Engine (LMDE) hardware. Jet vanes were chosen for attitude control from a separate optimization discussed in Section 5.13.4.4.

A three-engine arrangement was included to evaluate differential throttling with the Surveyor type configuration, utilizing one gimballed engine for roll control. The four-engine configuration was selected to permit evaluation of three axis control with differential throttling. By tangentially canting alternate engines to provide opposing roll moments, 3 axis control can be achieved by differential throttling.

Another four-engine configuration was considered that provided engine-out capability by utilizing a centrally clustered arrangement which was gimballed through the center of gravity. With this arrangement, control is achieved by separate gimballing of the engines. Arranged in this manner, the four engines had to be canted 45 degrees resulting in a requirement for 2730 pounds of thrust increase and 29.3 percent total impulse increase to meet the descent requirements. Also, this arrangement could not be successfully packaged on the Lander and was dropped from further consideration.

A six-engine configuration was included to permit evaluation of one-engine-out capability with differential throttling control. All other factors could be achieved with fewer engines.

The candidate designs are shown schematically in Figures 5.13-43 through 5.13-45. In summary, six candidate designs were selected for evaluation. They were:

- Single engine bipropellant, with jet vane attitude control.
- Three-engine bipropellant with one-engine gimballed for roll control and differentially throttled for pitch and yaw control.
- Four-engine bipropellant with canted engines and differential throttling for attitude control.
- Six-engine bipropellant with two gimballed engines, differential throttling for attitude control, and one-engine-out capability.
- Four-engine monopropellant with canted engines and differential throttling for attitude control.
- Six-engine monopropellant vernier and a solid deceleration motor with two gimballed vernier engines, differential throttling for attitude control.

5.13.3.3 Trade Studies - The selection factors used in these studies in order of importance are reliability, development status, performance, versatility, and subsystem interactions with the Capsule Lander and the Martian surface.

Reliability - The basic failure rate data utilized in this study were obtained from other programs employing similar components and design arrangements. These data are provided in Section 5.13.4.5. The failure rates presented cannot be equated directly to VOYAGER because of the more stringent requirements imposed by sterilization and long term space storage. Furthermore, the failure rates employed in the analysis include failures of certain components to meet their specification requirements (degraded performance). While such failures certainly affect the mission, most of the variations in performance parameters, such as specific impulse response rates, and mixture ratio control can be sustained without a complete mission failure. For these reasons, the reliability numbers are not absolute, but are adequate for subsystem comparisons. Specific reliability values applicable to the various subsystem candidates are included in the concept summary comparison discussed later.

The unreliability of the solid/liquid and bipropellant are 1.67 and 1.8 times the monopropellant, respectively. Thus, a monopropellant hydrazine subsystem was selected for reliability.

SOLID/MONOPROPELLANT SUBSYSTEM SCHEMATIC

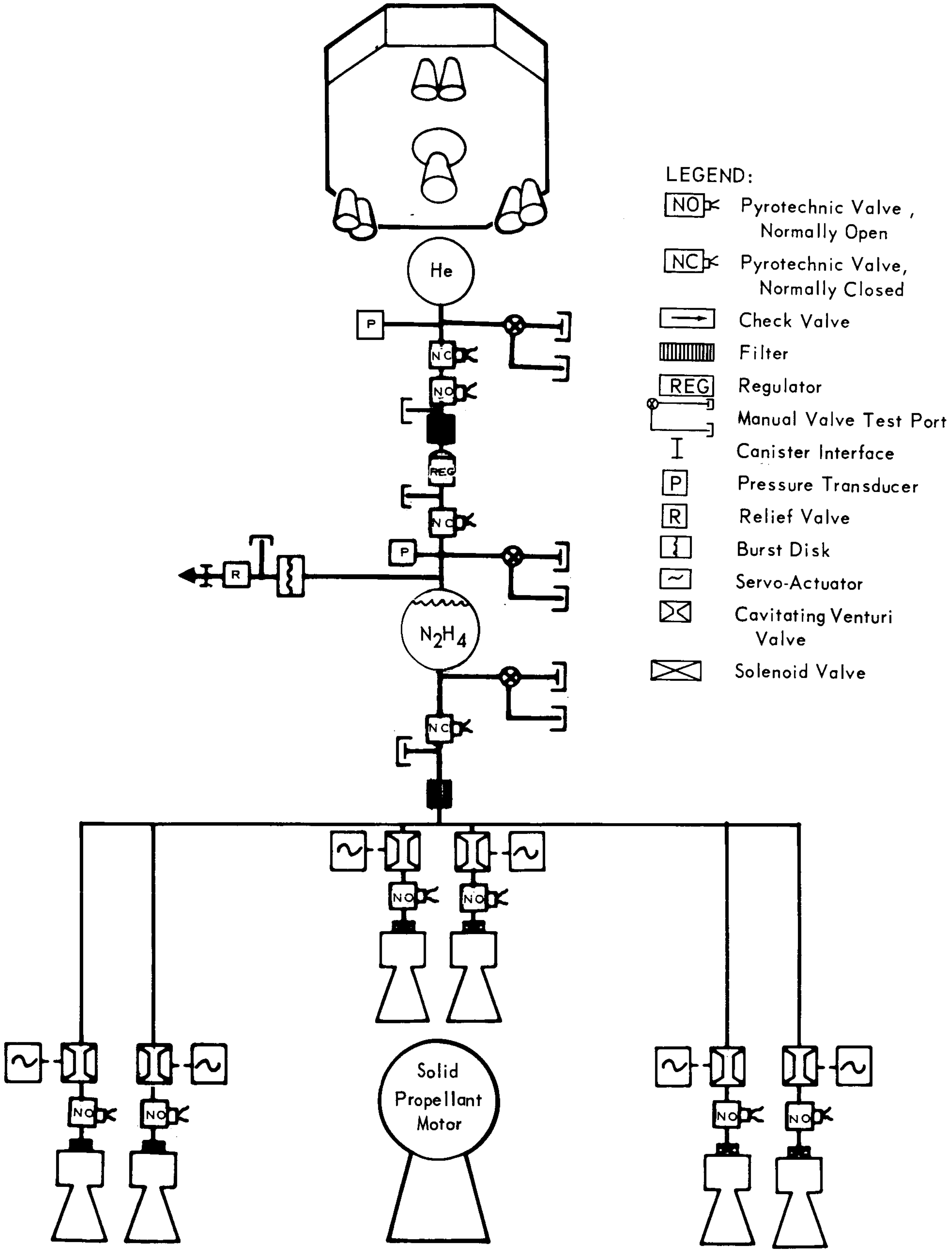
LEGEND:
NO Pyrotechnic Valve, Normally Open
NC Pyrotechnic Valve, Normally Closed
Check Valve
Filter
REG Regulator
Manual Valve Test Port
Canister Interface
P Pressure Transducer
R Relief Valve
Burst Disk
Servo-Actuator
Cavitating Venturi Valve
Solenoid Valve
He
P
NC
NO
REG
NC
P
R
N_2H_4
NC
NO
NO
NO
NO
NO
NO
Solid Propellant Motor

Figure 5.13–43

MONOPROPELLANT SUBSYSTEM

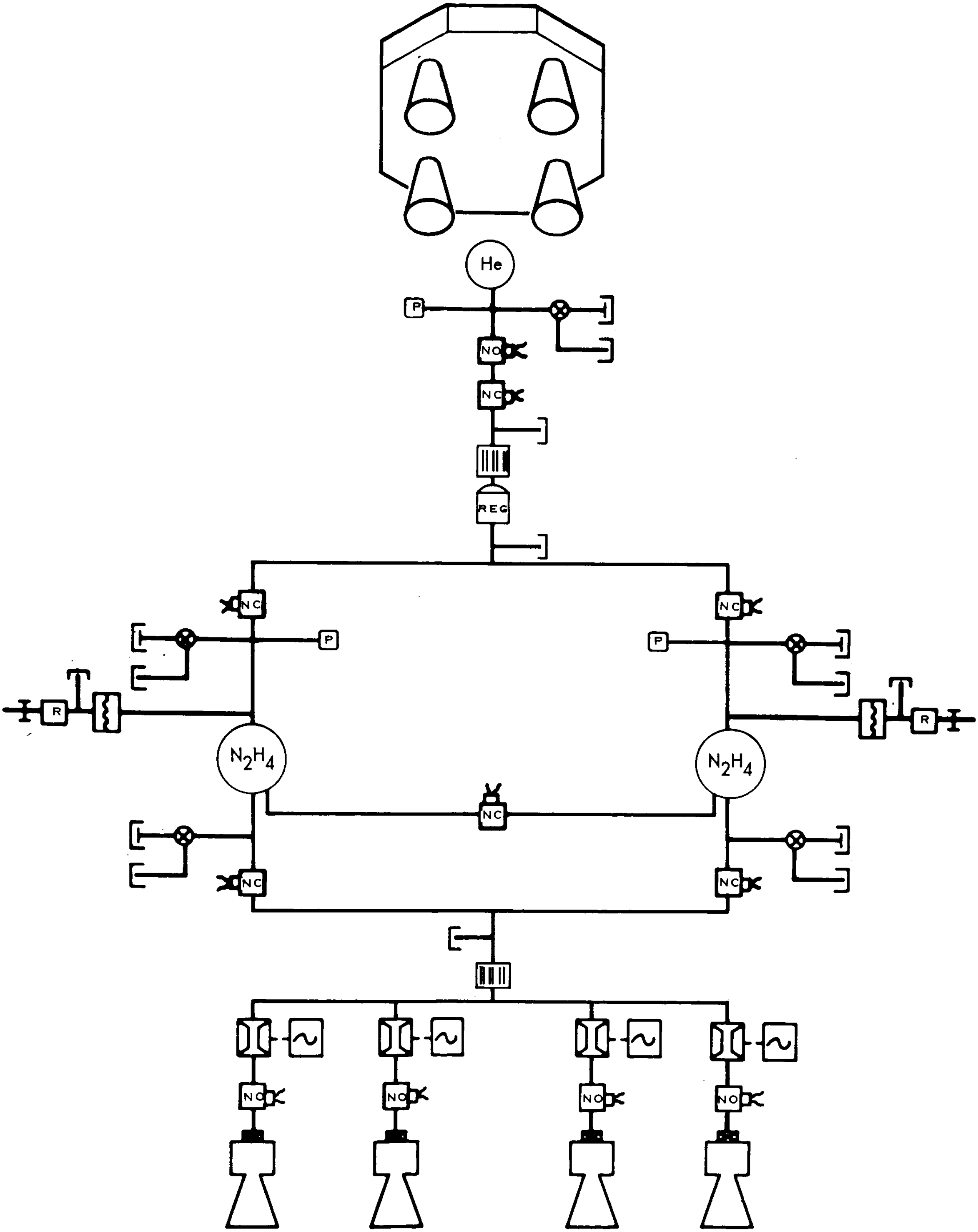
He
P
NO
NC
REG
NC
NC
P
P
R
R
N_2H_4
N_2H_4
NC
NC
NC
NO
NO
NO
NO

Figure 5.13-44

BIPROPELLANT SUBSYSTEMS

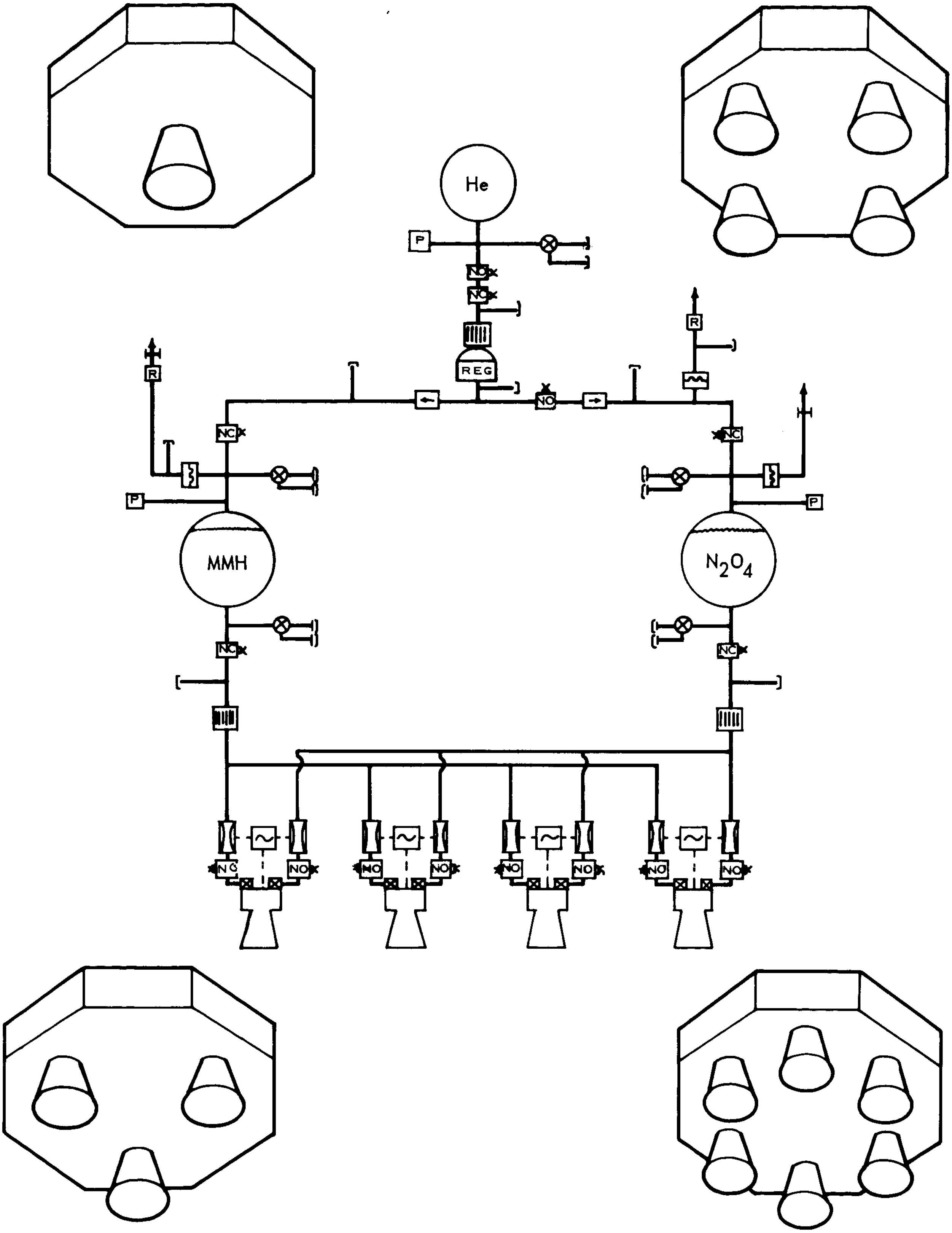
He
P
NO
NC
REG
NO
R
R
NC
NC
P
P
MMH
N_2O_4
NC
NC
NO
NO
NO
NO
NO
NO
NO
NO

Figure 5.13–45

Development Status - The terminal propulsion subsystem has been classified, in this study, as a long lead time item. The program requires complete qualification within approximately 3 years from go-ahead. With current VOYAGER estimates of Phase D go-ahead in 1969, slightly more than 3 years remain to meet a launch in 1973. In view of the 4-6 years required for development of the Surveyor and Apollo propulsion subsystems, this indicates a significant program restraint with little time available to recycle for modification and none for propulsion subsystem redesign. In this respect, there is no allowance for uncertainty of propulsion state-of-the-art technology advancement regardless of potential gain. New developments must be undertaken with care.

No developed propulsion hardware has been successfully subjected to the current sterilization environment. As such, evaluation of development status of sterilization is restricted to early Surveyor considerations and recent work with sterilization of subsystems candidate to VOYAGER. Sterilization testing to evaluate liquid propellant/materials compatibility has been done at JPL, Martin-Denver (JPL) and by McDonnell. Also JPL and various propulsion companies have investigated the sterilization capability of solid motors. Sterilization of liquid and solid propulsion subsystems is discussed in Sections 5.13.4.2 and 5.13.4.3, respectively. In general, isolated liquid storage appears to be a simpler sterilization design problem than solid motors.

Material compatibility and propellant decomposition are the major problems associated with liquid sterilization and storage. However, McDonnell and JPL sponsored testing indicates that nitrogen tetroxide, monomethyl hydrazine and neat hydrazine are each compatible with titanium containers. Nitrogen tetroxide and monomethyl hydrazine provides the most compatible bipropellant combination.

It has been demonstrated that solid propellants can be developed which retain adequate physical properties. Also, small motors have been sterilized, with some successes and some failures, to engender optimism of ultimate sterilizable design capability. However, solid motor design is an intricate marriage of grain, liner, insulation, case and nozzle design integration which requires full-scale testing for evaluation of strain relief, propellant slump, exothermic reactions, and propellant processing for final demonstration. No testing has been done with motors of the size required for this terminal descent function.

Aside from propellant sterilization, the throttleable engine represents the greatest development problem. Two throttleable bipropellant engines have reached qualification status, namely the LMDE and the LANCE. Neither of the two could be considered without modification. The LMDE requires slight head-end modification for higher pressures and a new chamber designed for 300 psi. The LANCE requires a new chamber design with extensive injector modification to permit use of nitrogen tetroxide and MMH and to allow acceptance firing.

Several throttling concepts, other than those used for the above, have been developed to various stages but each must be considered a new development engine within the context of this program. This factor represents a severe constraint in consideration of throttling concept plus engine definition and development.

Scaling of existing qualified engines is a more acceptable solution to new engine development, provided the engine scaling ratio is not large. Although scaling is not a simple problem, the experience gained in scaled engine development should be extremely valuable in the new engine program.

Cost estimates of bipropellant subsystems show small differences between a modified LMDE and a new engine development for the smaller, multiple engine configurations. Development time, however, is estimated to be one full year less for the single engine modified LMDE.

A monopropellant hydrazine engine may be even more difficult to develop. There is currently no known hydrazine engine development work at thrust levels in excess of 300 lbs. Multiples of three-hundred pound engines to provide the 6,600 thrust level required is not a practical consideration.

Consideration must then be given to the design and development of a throttleable engine of suitable thrust level. Rocket Research Corporation and Hamilton Standard have demonstrated 6:1 and 4:1 throttling, respectively, with low thrust monopropellant engines. This was accomplished by simple upstream flow control with fixed area injectors. This approach is not feasible for throttle ratios of 10:1.

Factors controlling monopropellant engine design are quite intricate, but the overall requirement is to maintain control of injection velocity and catalyst bed pressure drop. If injection velocity is too high, hydraulic milling of the catalyst occurs. If injection velocity is too low, the engine is susceptible to feed system-coupled instability. Hamilton Standard indicates that an injection velocity of 50 fps is required for stable operation. Since injection velocity varies directly with throttle ratio for simple upstream throttling, a maximum of 500 fps would occur. Hamilton Standard has encountered hydraulic catalyst bed milling at velocities far below this value. This indicates that some type of injection velocity control must be incorporated for throttle ratios of 10:1. Hamilton Standard and TRW systems have considered variable throat area designs for this purpose.

Rocket Research Corporation indicates that the catalyst bed pressure drop should not exceed 80 psi to avoid crushing the catalyst or complicating the catalyst retainer design. The catalyst bed pressure drop is a function of chamber pressure, bed loading, bed length, porosity of the catalyst bed, and Reynolds Number in the chamber. With a maximum allowable pressure drop, the problem of defining the optimum combination of the variables just defined appears difficult. All these factors complicate the high throttling ratio design.

To compound the problem, conventional monopropellant engine designs for the 1650 lb. thrust level are very heavy. Conceptual spherical shape designs proposed by Rocket Research Corporation offer significant weight improvements but these must yet be proven. Although monopropellant development has been relatively straightforward, development of the spherical chamber requires state-of-the-art extension of the design of an appropriately sized and throttling injector, catalyst bed, and catalyst bed retention. Therefore, the lack of demonstration and uncertainties of state-of-the-art extension severely limit serious consideration of a monopropellant TPS.

The solid/monopropellant configuration development schedule is controlled by the solid motor. Although monopropellant hydrazine development is in its infancy compared to bipropellants, it has been demonstrated that low thrust engines can be developed with low cost and short development times.

Development of a solid motor is controlled by design for sterilization. Without sterilization the solid motor design would be relatively straight-forward, utilizing the wealth of industry solid propellant experience. Although there is a requirment for thrust termination, such techniques as nozzle separation, utilized on the Titan II and Jupiter vernier motors, are available.

In view of extensive bipropellant experience, the lack of monopropellant demonstration at intermediate thrust levels and the unknowns in sterilizable solid propellant technology, the bipropellant system is the prime candidate from development status considerations.

Weight and Performance - The performance data and certain characteristics of the candidate subsystems are presented in Figure 5.13-46.

TERMINAL PROPULSION TRADE STUDY

PROPULSION SIZING PARAMETERS

Specific Impulse (5 millibar) (sec)	
Bipropellant – 100% Thrust	291
50% Thrust	285
10% Thrust	274
Monopropellant – 100% Thrust	231
50% Thrust	224
10% Thrust	204
Solid Motor	285
Propellant Contingency (%)	6
Ullage at 275°F (%)	3
Safety Factors – Tanks	
N_2H_4 and MMH at 77°F	2.22
He, N_2, and N_2O_4 at 275°F	1.50
Pressurant (He) Leakage Allowance (Gemini)	
Service Valves and Ports (SCCH)	10
Pressurant Tank (SCCH)	0.9

Figure 5.13–46

Propellant performance estimates were based on available data from existing programs. The bipropellant specific impulse was derived from the LMDE. This involved the following adjustments: fuel, Aerozine 50 to MMH; chamber pressure, 100 to 300 psia; expansion ratio, 46:1 to 20:1; and ambient pressure, vacuum to 5 millibars.

The monopropellant throttling specific inpulse was taken from extrapolated test data supplied by Marquardt and Rocket Research Corp. The solid propellant performance values are based on vendor supplied estimates of the performance of sterilizable solid propellant motors.

Subsystem operating pressures were selected from considerations of weight, capsule integration, engine design and sterilization. For the candidate subsystems, the engine chamber pressure for minimum weight was established at approximately 300 psia. Although this is appreciably greater than that used in current space engine designs, this pressure was selected because of the weight and volume advantage offered. Ablative chambers have operated successfully above 300 psia, but radiation and heat sink engines will require development for this pressure level.

With a 300 psia chamber pressure and pressure losses of 100, 100, and 25 psi for the injector, control valves, and lines, respectively, a tank pressure of 525 psia was derived. Gaseous helium, used for tank pressurization, was stored at 3000 psia initial pressure. The liquid feed systems were optimized for each subsystem type and were not perturbed during the type selection study. The detailed description of the feed system selection process is included in Section 5.13.4.1.

The weights derived include the components shown in the schematics, Figures 5.13-43 through -45, with additional engine and equipment support structure. No substantiated weight data were available for hydrazine engines at the thrust level required. A weight estimate of 50 lbs was used for the conventional engine design, excluding flow control valves. Extrapolated data from vendor sources varied from 50 to 80 pounds. The conceptual engine design weight of 20 lbs, excluding the flow control valves, was taken from data provided by Rocket Research Corporation.

The results of the candidate subsystem weight studies are provided in Figure 5.13-47 as a function of total impulse.

The lightest weight subsystem for the 1973 mission is the three-engine bipropellant configuration. Single engine arrangement is heavier by 37 pounds. The four and six engine configurations are heavier by 25 and 59 lbs, respectively.

CANDIDATE WEIGHT COMPARISON

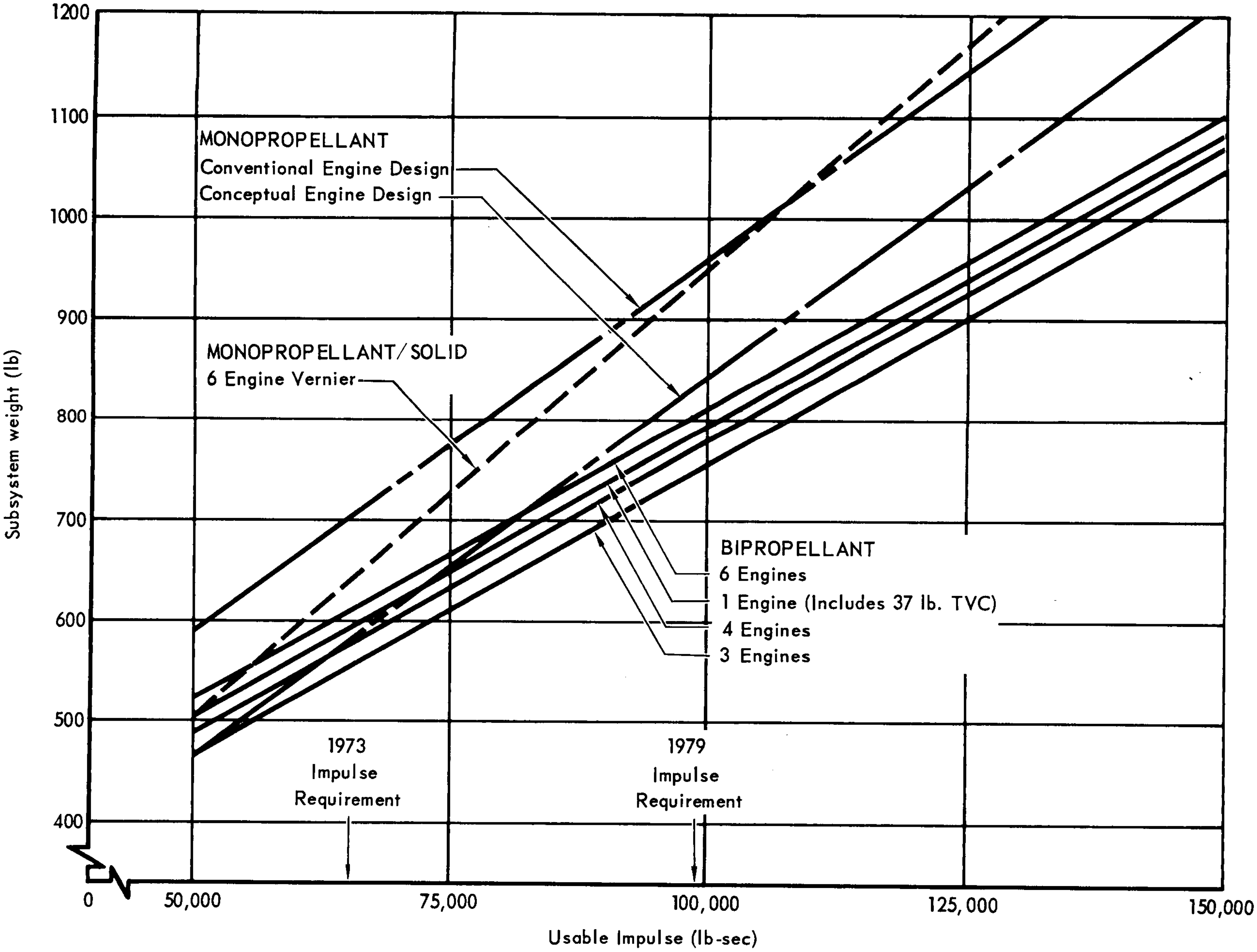

Figure 5.13-47

The four-engine monopropellant subsystem, based on current thrust chamber design technology, is 122 lbs heavier than the four-engine bipropellant configuration for the 1973 mission requirements. If the advanced concept monopropellant engine is considered, the weight of the four-engine configurations are essentially equal. However, the biopropellant design, due to higher specific impulse, provides improved growth capability even when compared to the monopropellant configuration employing the advanced concept engine.

The greatest effect on the solid/liquid subsystem is the propellant contingency which must be loaded to insure subsystem capability for both velocity extremes in the entry descent corridor. The solid rocket is sized by the high velocity; the liquid by the low velocity. For the case considered, the impulse penalty was 44%. This penalty was unfavorably influenced by the low thrust-to-weight capability of the monopropellant vernier.

Versatility - The later VOYAGER missions involve a Flight Capsule weight increase of 2000 pounds, approximately three-fourths of which is a direct increase in landed weight. Since schedule does not allow re-development of long lead time items, anticipation of the weight increase must be included in the 1973 designs. The effect of payload increase directly reflects itself in total impulse and thrust level requirements. Feed system control components present no difficulty as minimal oversizing can provide ample growth potential. Propellant and pressurant storage can use either multiples of vessels sized for early missions; tanks designed for the later mission, off-loaded for 1973; or new designs optimized for individual missions. The subsystem versatility then centers on engine thrust level and throttle ratio selection, and propellant performance to control engine and subsystem size.

To accomplish a successful landing, it is necessary to provide a minimum deceleration thrust level corresponding to 0.8 Martian g's and a suitable throttle ratio to compensate for the uncertainty introduced by the broad spectrum of postulated atmospheres. Additional capability is required to achieve standardization for the early and late missions and this can be accomplished in several ways:

- The engines can be designed for the 1973 mission with engines added for the 1979 mission to retain approximately the same thrust-to-weight.
- The engines can be designed for the 1979 thrust level and derated for the early flights.
- The engines can be designed with an operating range broad enough for 1973 and 1979 and can be used without change for all missions.

It has been determined that the last approach can be satisfied with a 10:1 throttle ratio. The method can be accomplished if the parachute is redesigned, to the then known atmospheric conditions, to provide the same descent velocity at engine ignition in 1973 and 1979. This is discussed further in Section 2.3.7.

The solid/liquid subsystem was designed for an off-loaded solid motor in the early missions. Since vernier thrust-to-weight is severly limited by maximum state-of-the-art monopropellant thrust level, additional engines are required to allow successful landing in 1979.

Figure 5.13-48 presents the characteristics of the 1973 systems considered when used for 1973 through 1979 missions; corresponding thrust-to-weight (T/W) and throttle ratios (TR) are included. From this figure, it is apparent that the high performance of the bipropellant subsystem results in maximum capability and flexibility of design necessary to satisfy all the VOYAGER Mars missions.

Subsystem Interactions - The major subsystem interactions affecting selection can be divided into Capsule Bus effects and landing site effects. The primary Capsule Bus interaction factors influencing subsystem selection and specific arrangement are packaging constraints, radar interference and base recirculation heating. Site interaction factors include exhaust contamination, site alteration and surface heating.

Figure 5.13-49 illustrates the Capsule Bus interaction problem as a function of engine arrangement and location. As can be seen, each configuration requires a crushable engine nozzle to be compatible with the landing impact energy attenuation mechanism.

Central packaging of the propulsion engines presents design integration problems, with respect to the surface laboratory and/or the energy attenuation mechanism.

Packaging of multiple engines about the periphery of the spacecraft presents no real problem and the need for accommodating a Rover type vehicle for the 1979 mission favors a four-engine arrangement.

The base surface area occupied by propulsion is significant as it affects radar antenna location, heat rejection devices, scientific sensors and landing subsystem design. The solid/liquid represents the worst configuration as it dominates the base area, with both central and peripheral engine emplacements. Centrally located engines force a split arrangement of the landing radar antennas.

CANDIDATE STANDARDIZATION AND GROWTH POTENTIAL

			MAX THRUST	TOTAL IMPULSE	MAX T/W CAPABILITY	TR*** USED	VOLUME ft^3	WEIGHT lb
1973	Bipropellant		6600	65,000	2:49	8.2:1	7.12	585
	Monopropellant		6600	65,000	2:49	8.2:1	13.44	707/587*
	Mono/Solid		2100/5600	93,600**	1.5/4.0	3.2:1	9.32	639
1979	Bipropellant	Standard Subsystem	6600	99,000	1.58	5.2:1	13.21	780
		Additional Engines	9900	99,000	2.37	7.8:1	13.73	852
	Monopropellant	Standard Subsystem	6600	99,000	1.58	5.2:1	21.36	958/838*
		Additional Engines	9900	99,000	2.37	7.8:1	24.12	1097/917*
	Mono/Solid	Standard Subsystem		Not Practical With Monopropellant Engines				
		Additional Engines	3150/5600	142,800**	1.6/2.86	3.0:1	14.33	941

Bipropellant and monopropellant analysis based on four engine subsystems

* Weight calculated for conceptual spherical chamber design

** Individual subsystems designed for differing velocities at ignition results in only 69.5% useable impulse

*** Throttle ratio available is limited by minimum landing weight.

Figure 5.13-48

ENGINE ARRANGEMENT PACKAGING COMPARISON

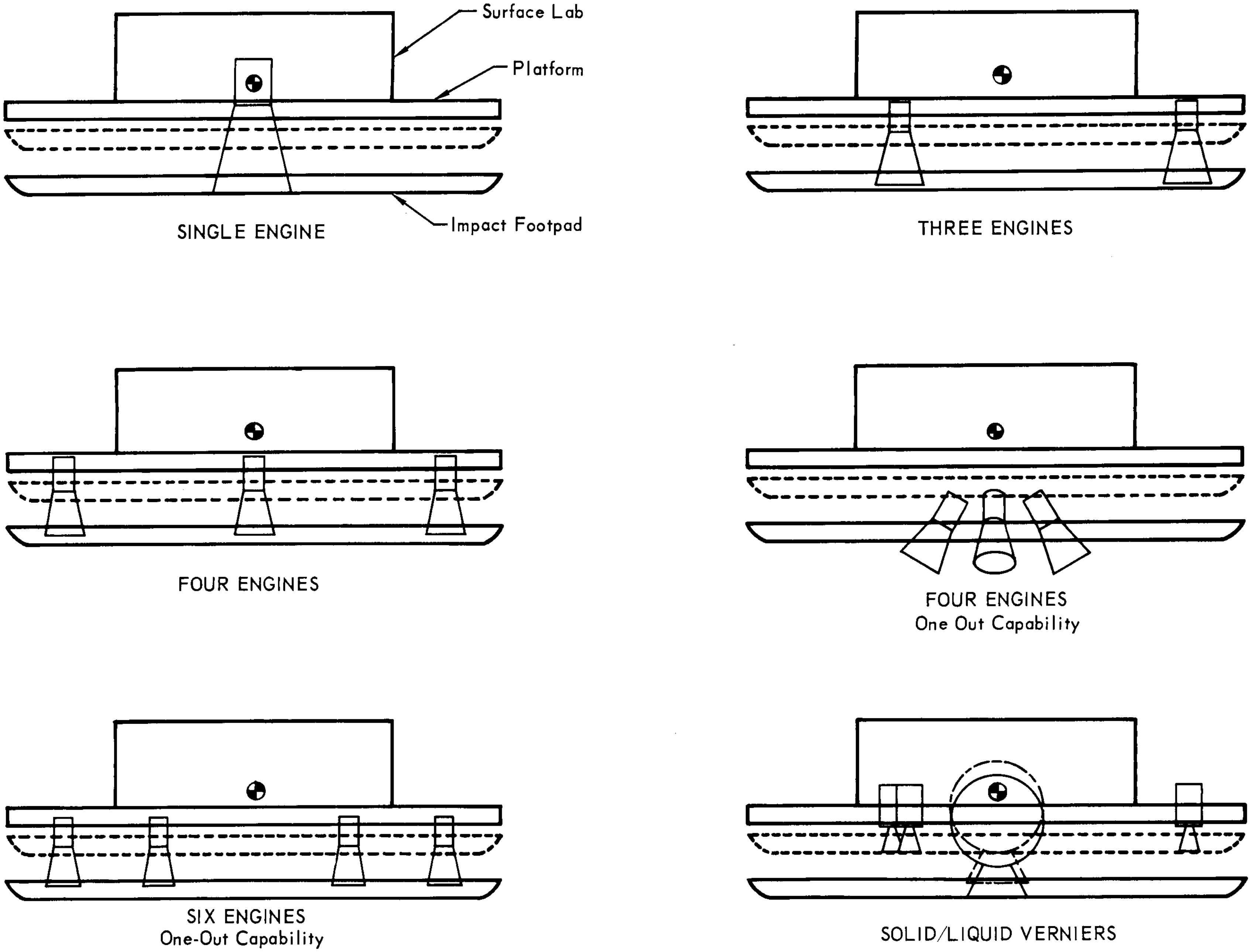
Surface Lab
Platform
Impact Footpad

SINGLE ENGINE

THREE ENGINES

FOUR ENGINES

FOUR ENGINES
One Out Capability

SIX ENGINES
One-Out Capability

SOLID/LIQUID VERNIERS

Figure 5.13-49

Attenuation of the radar signal was determined to be a minimal problem. The potential problem magnitude depends on electron density and collision frequencies in the exhaust products and exists due to trace contaminants of the alkali metals in the propellants, liners and chamber nozzle materials. The greatest offenders are solid motors and ablative chambers followed by monopropellant hydrazine with bipropellant N_2O_4/MMH presenting least attenuation potential. Detailed evaluations of attenuation effects appear in Sections 5.9.1 and 5.9.5.

In the engine arrangements considered, base recirculation does not appear to be a significant problem. Recirculation occurs when the exhaust jets from adjacent nozzles interact with one another. However, the diameter of the Capsule Lander permits favorable spacing between engines, and significant base heating due to adjacent nozzle plume impingement is highly unlikely. As can be seen, Capsule Lander integration considerations favor multiple engine arrangements.

While contamination, heating, and alteration of the landing site cannot be avoided, it is appropriate to consider how these are influenced by the subsystems using the various propellants. In each case, for similar configurations, the monopropellant subsystem presents the minimum problem. It produces slightly less erosion; there is no carbon in the exhaust; and the stagnation temperature is low (2000°F compared to 5000°F for bipropellants). The effects of the bipropellant, though appreciably greater, do not appear to be unacceptably severe. The analysis of bipropellant contamination is contained in Part B, Section 3.2.9.4.

From a subsystem interactions standpoint the above considerations show that a four-engine arrangement is preferred, and that the monopropellant hydrazine would cause the least amount of subsystem interaction.

5.13.3.4 Concept Selection - For comparison purposes the propulsion subsystem concepts evaluated above were divided into two groups, i.e., bipropellants and others. This permitted selection of the best bipropellant subsystem configuration for later comparison with the monopropellant and solid/monopropellant subsystem arrangements. This simplified somewhat the mechanics of concept selection.

The results of the bipropellant subsystems comparison are shown in Figure 5.13-50. The four engine concept was selected as the preferred bipropellant propulsion subsystem. This selection was influenced primarily by considerations external to the subsystem, notably integration into the preferred Capsule Bus design.

ENGINE ARRANGEMENT COMPARISON

NO. OF ENGINES	SUBSYSTEM COMPLEXITY	DEVELOPMENT STATUS	SUBSYSTEM PERFORMANCE	SUBSYSTEM FLEXIBILITY	SUBSYSTEM INTERACTIONS
Single Engine (TVC)	• Reliability – .9898 • Simplest Propellant Manifolding • Separate TVC Required	• Modified LMDE • 2.5 Year Development Time • TVC Development Required ✓	• 597 lb. Weight • 7.75 ft^3 Volume (65,000 lb–sec)	• Not Adaptable to Capsule Bus Design For 1979 Rover	• Worst Surface Effects • Lander Packaging Interference
Three Engines (Roll Gimbal)	• Reliability – .9790 • Complex Propellant System Manifolds • Inherent ACS With Gimballed Engine And Differential Throttling	• New Engine Required • 3.5 Year Development Time • Gimbal Development Required For TVC	• 560 lb. Weight • 7.22 ft^3 Volume (65,000 lb–sec) ✓	• Difficult to Integrate into Capsule Bus Design for 1979 Rover	• Minor Packaging Difficulty • High Electrical Power Usage Gimbal
Four Engines (Canted Engines) ✓	• Reliability – .9747 • Complex Propellant System Manifolds • ACS With Fixed Mount Engines and Differential Throttling	• New Engine Required • 3.5 Year Development Time • No Additional TVC Development Required	• 585 lb. Weight • 7.12 ft^3 Volume (65,000 lb–sec)	• Easily Located in Capsule Bus Design For 1979 Rover ✓	• Most Convenient Packaging • Low Engine Length • Lower Electrical Power Requirement ✓
Six Engines (Roll Gimbals)	• Reliability – .9960 * • Maximum Complexity • Two Gimbals • Complex Failure Detection for Engine–out Capability ✓	• New Engine Development • 3.5 Year Development for TVC • Gimbal Development for TVC	• 619 lb. Weight • 7.04 ft^3 Volume (65,000 lb–sec)	• Not Readily Adaptable to Capsule Bus Design for 1979 Rover • Increase Usable Throttle Ratio With Step From Three to Six Engines	• Least Surface Effects • Minimum Engine Length • Maximum Mount Points • Two High Electrical Power Usable Gimbals

☑ Indicates Preference as a Function of Selection Factor

* Generic Analysis Did Not Include Failure Rate of Failure Detection System

Figure 5.13–50

The subsystem with the highest reliability is the six engine arrangement by virtue of its engine-out capability. It must be noted, however, that the reliability estimate based upon generic failure rates does not include the effects of the failure detection subsystem. Automatic failure detection and correction is extremely complex, and implemetation is difficult to achieve. Considering the additional development effort required, and the weight penalty incurred, the single engine would appear to be a better selection. The disqualifying disadvantage of the single engine, however, is its incompatibility with the preferred Capsule Lander design. Emplacement of the engine in the center of the lander requires a split radar antenna, but more significantly, it seriously complicates equipment packaging for the 1979 Rover design. Therefore, the single engine, although propulsion-wise very attractive, must be discarded.

The three and four engine arrangements differ little in subsystem reliability. The comparative factors, therefore, reduce to the 25 pound weight advantage offered by three engines as opposed to the greater flexibility and more convenient packaging of four engines. The ease of integration and flexibility of the subsystem, coupled with the elimination of an engine gimbal development, offsets the weight and slight reliability advantage of three engines.

The results of the comparison of the selected four engines bipropellant with the four engine monopropellant and the solid/liquid arrangement is presented in Figure 5.13-51. The four engine bipropellant ranked highest in three of the five rating categories and was selected as the preferred concept. The superior development status, performance and flexibility of the bipropellant offset the potential reliability gain and minimum interface problems of the monopropellant subsystem. The technical risk entailed in the absence of throttling monopropellant engine development experience balances the potential reliability gain. Although surface interference problems are minimized, this factor was rated least and did not balance the bipropellant advantage. The solid/liquid subsystem was rated below the other candidates in all categories.

5.13.3.5 Preferred Subsystem Design - The propulsion subsystem data used in the preceeding analyses were sufficiently precise for the conceptual study conducted. However, for establishing the preferred Capsule Bus configuration a more refined definition of the terminal propulsion subsystem is necessary. In proceeding with the analytical refinements, special attention is given to basic component arrangements, subsystem pressure levels, mixture ratio, subsystem dynamic coupling and the

CANDIDATE COMPARISON

CANDIDATES	RELIABILITY	DEVELOPMENT STATUS	PERFORMANCE	FLEXIBILITY	INTERACTIONS
Bipropellant (N_2O_4/MMH) 4 Engines	• Least reliable subsystem from generic failure analysis • Most complex propellant feed • Greatest redundancy penalty	• Experience minimizes technical risk • Thermal stability of propellants minimizes sterilization risk • Two Throttleable engines have reached qualification status • Highest development cost • 3–1/2 year development • Sterilization capability not demonstrated. (* Preferred Candidate)	• Highest propellant performance • Low weight • Low volume eases packaging problems (* Preferred Candidate)	• Complete mission standardization allowed by 10:1 throttle ratio for the 1979 mission. • Weight and volume advantage improve for later missions • Two additional propellant tanks for 1979 (* Preferred Candidate)	• Highest site contamination, alteration and heating potential • Multiple engine packaging flexible to optimum equipment mounting • N_2O_4/MMH have lowest radar attenuation potential
Monopropellant (N_2H_4) 4 Engines	• Most reliable subsystem from generic failure analysis • Least complex subsystem • Low chamber temperature • Lack of engine experience limits confidence level at high thrust (* Preferred Candidate)	• No demonstrated engines in suitable thrust range • Development requires state-of-the-art extension • Indicated decomposition problem during sterilization • Potentially lowest development cost • 3 year development	• Lowest propellant performance • Highest weight • Higher volume than combined mono/solid • Lower weight can be achieved with spherical chamber design	• Complete mission standardization allowed by 10:1 throttle ratio for the 1973 mission. • Lower propellant performance limits growth potential	• Minimal site contamination, alteration and heating potential • Minimum packaging design integration problem (* Preferred Candidate)
Mono Solid (N_2H_4–HTPB NH_4ClO_4–16% Al) 1 Solid and 6 Vernier Engines	• Combined subsystems are complex • Effects of sterilized solid rocket unknown	• Development controlled by solid motor • Sterilizable solid motor not demonstrated • Solid motors require full-scale demonstration • Low thrust monopropellant demonstrated • Solid thrust termination demonstrated.	• Intermediate propellant performance • Lower weight than monopropellant • Higher volume than bipropellant.	• Requires off-loaded solid motor which requires precise establishment of 1979 impulse requirement • Monopropellant vernier requires additional engines for 1979 mission	• Lowest site contamination, alteration and heating potential. (Solid has negligible effect.) • Packaging dominates base area • Packaging interferes with preferred lander design • Solid has highest potential for radar attenuation

Figure 5.13–51

engine. For the design of the engine, assistance was solicited from various engine manufacturers. They were asked to evaluate throttling schemes, chamber cooling techniques, combustion stability, and performance capabilities.

Obviously, there is close interaction between each of the areas and it is not possible to isolate each for analysis. However, for purposes of simplicity, each item is discussed separately and interactions are mentioned as appropriate.

5.13.3.5.1 Component Selections and Arrangements - The primary considerations used in establishing the component arrangement was reliability. Emphasis was placed on highly developed concepts. The selection of the feed system components and component arrangements are presented in Section 5.13.4.1.

Propellant Tanks - The propellant supply must provide gas-free propellants to the main engine valves to ensure rapid and reliable ignition at subsystem initiation. This can be achieved with propellant traps, positive expulsion devices or techniques involving an induced g field. On VOYAGER, the drag deceleration loads encountered during atmospheric entry are ideally suited for this purpose, creating a force field which orients and settles the propellants at the tank discharge ports prior to activation of the terminal propulsion subsystem. Re-orientation of the propellants from their zero-g state begins early in the entry phase when atmospheric drag loads exceed propellant surface tension forces and continues as these applied loads slowly increase with descending altitudes. This gradual re-orientation minimizes propellant geysering, the primary contributor to the entrainment of ullage gases. Fluid behavior during propellant re-orientation is too complex to be handled by exact analytical methods, but drop test data and estimation techniques allow approximate calculation of re-orientation times and conditions for onset of propellant geysering. Application of these techniques show that propellant traps or positive explusion devices are not required, and that ample deceleration time exists (approximately 55 seconds) to settle and de-aerate the propellant before subsystem activation.

Additional fluid mechanics considerations which must be included in the propellant tank design are related to ingestion of gas into the propellant lines near propellant depletion. Gas may be ingested from the tanks by propellant vortexing or by suction dip resulting from inviscid fluid acceleration. The first of these will require a cross-type anti-vortex baffle at the tank discharge ports. Suction dip with this configuration presents a negligible restraint. Evaluation results show that gas ingestion is initiated when approximately 0.5% of the propellant is remaining. This quantity is considered negligible and no additional baffling is considered necessary.

In selecting the tank number and location, consideration was given to possible c.g. shifts. A study was undertaken to define the effects of selected tankage and arrangements. The results are presented in Section 5.13.4.1. In summary, a simple two tank arrangement, one for fuel and one for oxidizer, was selected for minimum weight and complexity. Packaging inconvenience was not severe and this selection permits maximum flexibility for growth to later missions.

Pressurization Systems - A regulated helium system was chosen for propellant tank pressurization. The regulated gas system has demonstrated high reliability. Essentially leak-tight pressurization systems have been developed by McDonnell for the Gemini systems. Service ports utilize redundant seals throughout the pressurant control system to insure seal integrity. Normally-closed and normally-open pyrotechnic valves provide pressurant isolation during sterilization and space storage, positive actuation for mission operation and isolation for non-interference of pressurant leakage with surface experimental measurements. Check valves and a normally-closed pyrotechnic valve protect against propellant mixing during sterilization, storage and operation. A normally-open pyrotechnic valve actuated after landing provides propellant isolation. Since the oxidizer pressure during sterilization is higher than operating pressure, a special high pressure burst disc is located downstream of the inlet isolation valve. Normally-closed pyrotechnic valves above and below the propellant tanks provide for minimum system exposure to propellant during sterilization and minimum leak potential during subsequent space storage.

Propellant Feed Lines - Although the design was too preliminary to adequately define sizing and geometry, the choice must be guided by the propellant hydraulic behavior during engine operation.

In the past, similar liquid propulsion systems have exhibited instability in the low to intermediate frequency ranges. This type of instability is characterized by coupling between the engine and propellant supply system. The coupling within the system may result from engine energy feedback through the propellant feed line, through the structure or through a propulsion subassembly.

Instability of this type has been encountered in the Titan II, Thor-Agena, Lance and Atlas programs and design modifications to these systems were required to correct the problem. The Titan II, Thor-Agena and Lance systems were coupled through the structure and the Atlas system was coupled through a pressurization subsystem. In those systems the problem was remedied by changing feed system frequency, to decouple the engine from the structure, or by increasing the intrinsic stability of the engine through increased injector pressure drop. The principal difficulty in these programs was that the problem was not uncovered until late in the development and thus correction was more difficult.

As a result of experience on past systems, the nature of supply system coupled instability and the parameters which affect stability are reasonably well understood. Analytical techniques have been developed which may be used as quantitative guides for design and evaluation of an integrated subsystem. However, functional testing of the integrated system is still the only valid check on subsystem stability, therefore, early simulation and test of the complete subsystem is mandatory.

Maximum Chamber Pressure - The choice of chamber pressure must take into account ambient pressure, subsystem weight, engine size, throttle ratio required, and expansion ratio. Of these, only ambient pressure and throttle ratios are fixed. Operation is required at both 5 and 20 millibar (mb) ambient pressures. The highest impulse requirement (65,000 lb-sec, 1973 mission) must be developed in the 5 mb atmosphere, but the chamber must operate satisfactorily, without nozzle flow separation, at 20 mb throttled 10:1. The relationship of chamber pressure to subsystem weight and expansion ratio is shown in Figure 5.13-52 for the 5 mb atmosphere. Also superimposed are the limiting expansion ratios for operation in a 20 mb atmosphere with the chamber throttled 10:1. The curves indicate that no nozzle flow separation will be encountered at expansion ratios of 32:1 or less, at a rated chamber pressure of 300 PSIA.

The nozzle geometry associated with the various chamber pressures is presented in Figure 5.13-53. To avoid structural heating problems by direct jet impingement, the engine must extend through the energy absorbing mechanism located beneath the Capsule Bus. The mechanism must stroke approximately 8 inches, thereby establishing minimum crushable nozzle length.

Examination of the above data shows that the best choice for weight and engine size is a chamber operating at 300 psi and with an expansion ratio of 30:1. Fortunately, as shown in Figure 5.13-52 the weight penalty for this selection is negligible; the 12-inch nozzle required for the 4-engine configuration may be designed for 8 inches of crush.

Tank Pressure - The operating tank pressure is established by chamber operating pressure, type of injector, the selected control valve, and basic line losses. Most

CHAMBER PRESSURE AND NOZZLE EXPANSION RATIO OPTIMIZATION

Total Impulse – 65,000 lb-sec
Ambient Pressure – 5 millibars

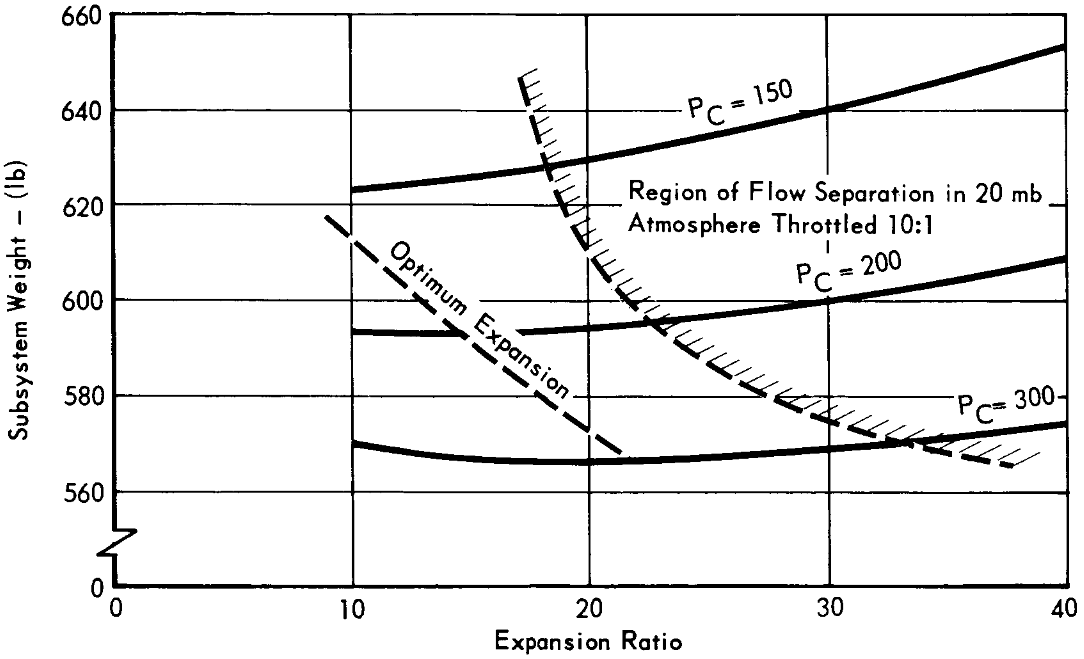

Figure 5.13–52

EFFECT OF EXPANSION RATIO
ON NOZZLE LENGTH

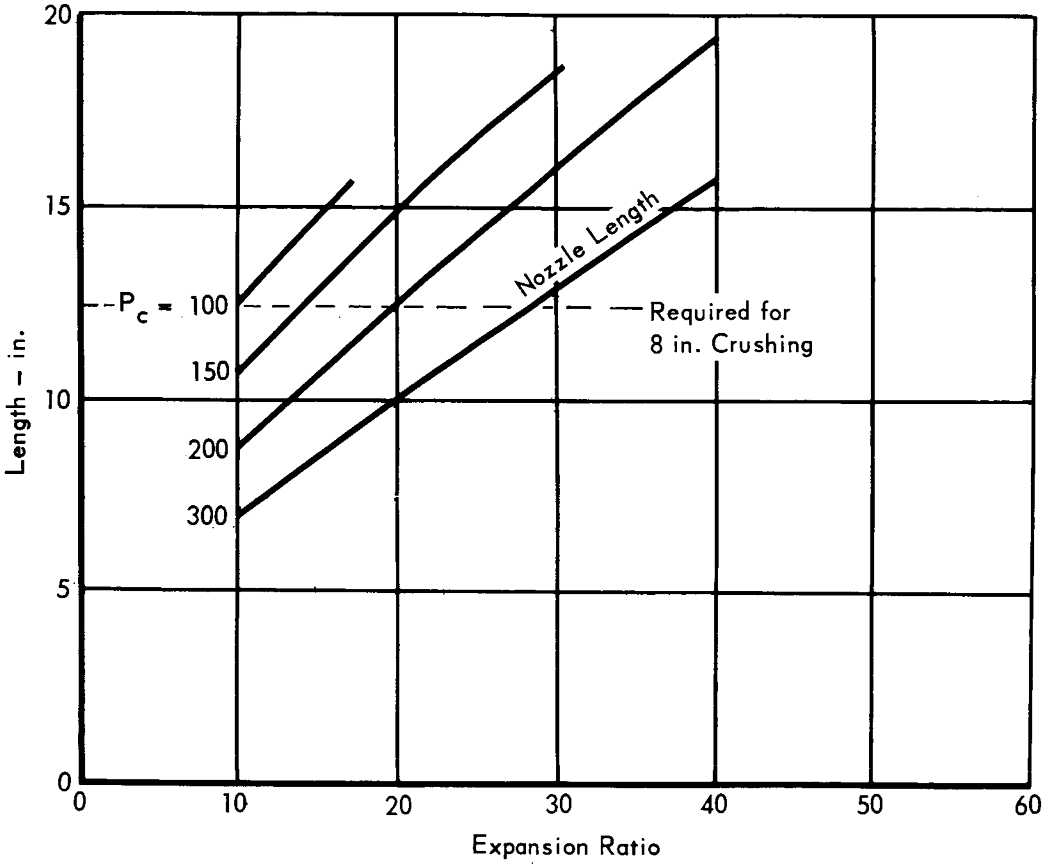

Figure 5.13–53

throttling engine concepts require an injector pressure drop of approximately 100 psi to ensure high performance. The preferred flow control concept, a cavitating venturi, introduces a 100 psi pressure drop. A reasonable line loss is 25 psi. The cummulative losses, therefore, are approximately 225 psi. For the design chamber pressure of 300 psi, the required tank pressure becomes 525 psia. This value has been used throughout this analysis.

Mixture Ratio - The mixture ratio selection involves numerous factors, including: engine performance, chamber cooling requirements, relationship of tank locations from c.g. and relative tank sizes.

The theoretically optimum mixture ratio for nitrogen tetroxide and monomethyl hydrazine propellant is near 2.0 at high expansion ratios. This is also true for nitrogen tetroxide and Aerozine-50. Extensive experience with the latter, however, shows that in practical designs the best performance is achieved near 1.6. Because of the similarity of the two propellant combinations, it is anticipated that the optimum mixture ratio will be near 1.6, for high expansion ratio nozzles. The physics and chemistry of this situation are not well understood. However, one contributing factor to this condition is engine fuel film cooling. In film cooled engines the gross mixture ratio, i.e., total oxidizer flow rate divided by the total fuel flow rate, is not meaningful in a theoretical sense. Performance will be degraded if the gross ratio is equal to the theoretical optimum because the flame core is operating higher and the boundary lower than the optimum mixture ratio. Therefore, central core performance is established at the optimum mixture ratio with fuel film cooling bringing the overall mixture ratio down to a lower value.

Realistically, it is not possible to establish exactly the optimum mixture ratio for the terminal engine at this time. This will depend upon the type of chamber used plus the terminal descent duty cycle. The duty cycle consisting of 50 to 70 seconds, with less than 5 seconds at full thrust, is not a particularly difficult one. The chamber pressure, of 300 psi, is greater than that in current engines and increases the cooling problem. Nevertheless, engine manufacturers indicate that a mixture ratio of 1.6 and performance consistent with current engines is feasible for the terminal propulsion subsystem.

It is desirable to avoid shifting of the c.g., as propellant is used, by proper tank location. This may be accomplished ideally if the tanks are located 180° apart at distances from the c.g. which are inversely proportional to the mixture ratio. Our preferred Flight Capsule design permits a maximum distance ratio of approximately 1.3; thus some shift in the c.g. will occur with a mixture ratio of 1.6. Calculations show, however, that for the preferred design this is negligible, requiring only 5% of the attitude control differential thrust capability.

Thus, the items of major significance are performance and chamber cooling, the latter of which is somewhat alleviated by the mild duty cycle. Since past experience has shown maximum performance at 1.6, this mixture ratio should be retained until more applicable studies and test data indicate a need for change.

Rocket Engine - The engine is the most significant single assembly in the propulsion subsystem. Thus, to ensure adequate consideration of this critical element, aid of the rocket industry was solicited. This was accomplished by requests for information from Aerojet, Bell, Marquardt, Rocketdyne, TRW, Thiokol and UTC. A summary of the information requested from each company is provided below, and the pertinent features of each proposed design are presented in Figure 5.13-54. Following these, the results of our comparative evaluation and engine selection are presented. The RFTI is summarized below:

General Engine Characteristics	
Throttle Ratio	10:1
Maximum Thrust Level	1650 lb
Maximum Chamber Pressure	300 psig
Mixture Ratio	1.6:1
Oxidizer (MSD-PPD-2)	N_2O_4
Fuel (MIL-P27404)	MMH
Maximum Expansion Ratio	20:1
Requirements and Conditions	
Nominal Propellant Temperature	70°F
Oxidizer Temperature Band	40° to 100°F
Fuel Temperature Band	40° to 100°F
Maximum Differential Temperature	±10°F
Response Time	
Min. to Max. and Max. to Min. Thrust	150 ms
Ignition Response	200 ms
Shutdown Response	200 ms
Storage Life	6 yrs
Sterilization	McDonnell Report E191

VENDOR ENGINE

AEROJET – PROPOSED DESIGN	GENERAL DESCRIPTION
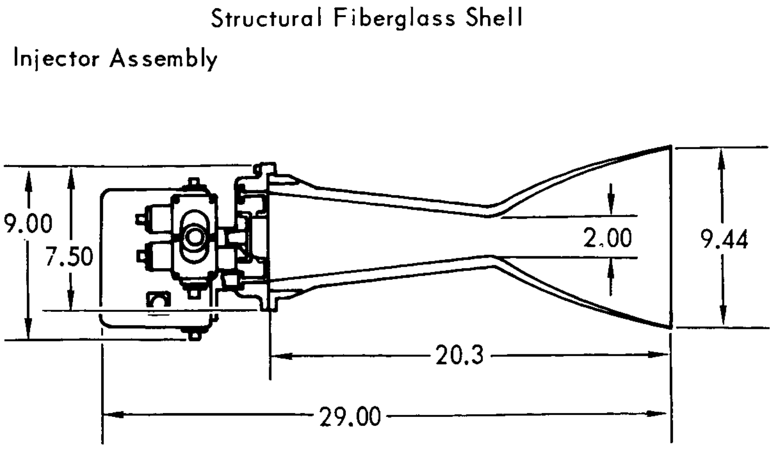 Structural Fiberglass Shell Injector Assembly 9.00 7.50 2.00 9.44 20.3 29.00 Engine Weight = 31.0 lb	The chamber design is a 45° oriented high silica/ phenolic ablative liner with a high temperature polyamide modified phenolic resin external fiberglass structural shell. The injector is a 16 element swirl cup design with momentum exchange throttling velocity control. Flow is controlled with variable area cavitating venturi bipropellant value, ball screw driven through a magnetic powder clutch by a .03 hp torque motor.
BELL – PROPOSED DESIGN	
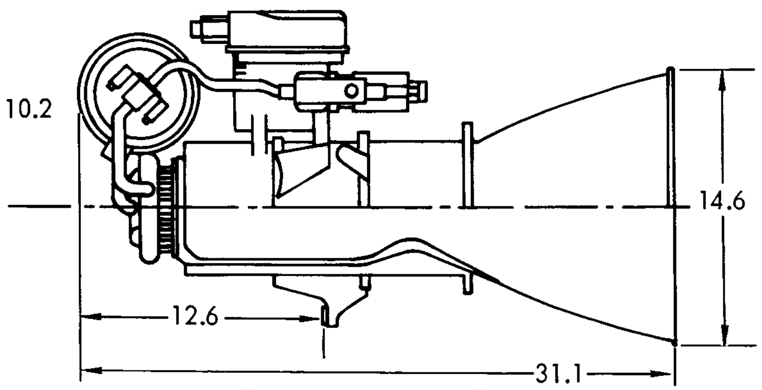 Engine Weight = 70 lb	The chamber design is a columbium lined ablative chamber with an ablative nozzle. The injector is a fixed geometry design with capillary stand-off injection tubes. Flow is controlled with variable area cavitating venturis, ball screw driven by a torque motor.
MARQUARDT – PROPOSED DESIGN	
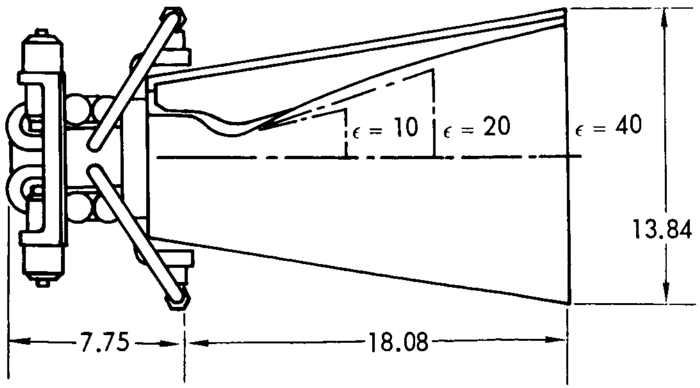 $\epsilon = 10$ $\epsilon = 20$ $\epsilon = 40$ 13.84 7.75 18.08 Engine Weight = 35 lb	The chamber design is a film cooled columbium radiation chamber. The injector is a fixed geometry dual doublet design with integral propellant pressure regulation and flow control. A variable area flow are scheduler is driven through a gear train by a DC motor.

(a) Development cost includes qualification (b) * indicates incomplete data submittal

Figure 5.13-54

DESIGN SUMMARY

PERFORMANCE CHARACTERISTICS	THROTTLING METHOD
• Chamber Pressure (psia) 300 • Feed Pressure (psia) 520 • O/F Weight Ratio 1.6 ± .03 • Specific Impulse – Max Thrust (sec) 295 ($P_\infty = 20$ mb) – 50% Thrust (sec) – – Min Thrust (sec) 228 • Transient Impulse – Ignition (0–90%) 30 – Shutdown (100–10%) 153 • Response – Ignition (0–90%) ms 0.076 – Shutdown (100–10%) ms 0.010 – Throttling (Min–Max) ms 0.125	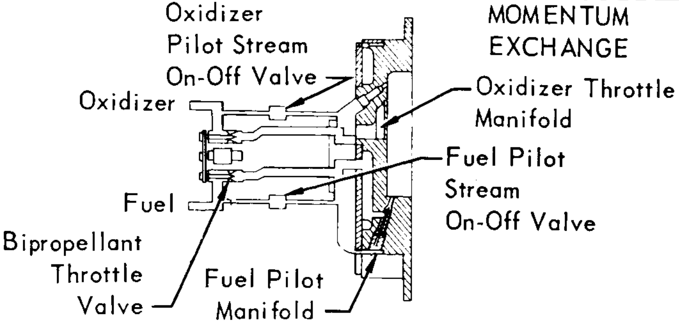 MOMENTUM EXCHANGE Oxidizer Pilot Stream On-Off Valve Oxidizer Oxidizer Throttle Manifold Fuel Pilot Stream On-Off Valve Fuel Bipropellant Throttle Valve Fuel Pilot Manifold • Description – high velocity pilot flow liquid – liquid momentum exchange injector with upstream flow control. • Applicable Program – LITE (Navy) • Development Time – 24 months • Development Cost – $13.5 M
• Chamber Pressure (psia) 130 • Feed Pressure (psia) 380 • O/F Weight Ratio $1.6 \pm^{.02}_{.04}$ • Specific Impulse – Max Thrust (sec) 286 – 50% Thrust (sec) 272 – Min Thrust (sec) 252 • Transient Impulse – Ignition (0–90%) * – Shutdown (100–10%) * • Response – Ignition (0–90%) ms * – Shutdown (100–10%) ms * – Throttling (Min–Max) ms *	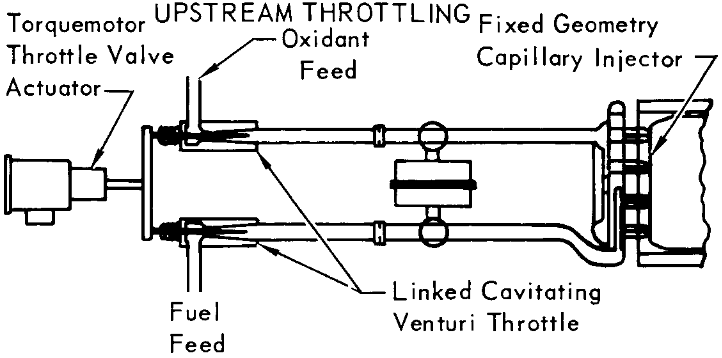 UPSTREAM THROTTLING Torquemotor Throttle Valve Actuator Oxidant Feed Fixed Geometry Capillary Injector Linked Cavitating Venturi Throttle Fuel Feed • Description – fixed geometry injector with cavitating venturi flow control valves. • Applicable Program – Bell – In-house • Development Time – * • Development Cost – *
• Chamber Pressure (psia) 300 • Feed Pressure (psia) • O/F Weight Ratio $1.6 \pm^{.02}_{.03}$ • Specific Impulse – Max Thrust (sec) 294 ($P_\infty = 20$ mb) – 50% Thrust (sec) 288 – Min Thrust (sec) 247 • Transient Impulse – Ignition (0–90%) * – Shutdown (100–10%) * • Response – Ignition (0–90%) ms * – Shutdown (100–10%) ms * – Throttling (Min–Max) ms *	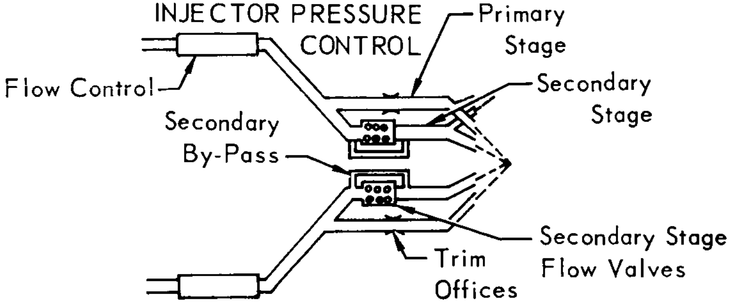 INJECTOR PRESSURE CONTROL Primary Stage Flow Control Secondary Stage Secondary By-Pass Secondary Stage Flow Valves Trim Offices • Description – fixed geometry injector with internal pressure and flow control. The design is a variation of the momentum exchange concept. • Applicable Program – BOMARC (Ramjet Fuel Control) • Development Time – * • Development Cost – *

VENDOR ENGINE DES

ROCKETDYNE – PROPOSED DESIGN

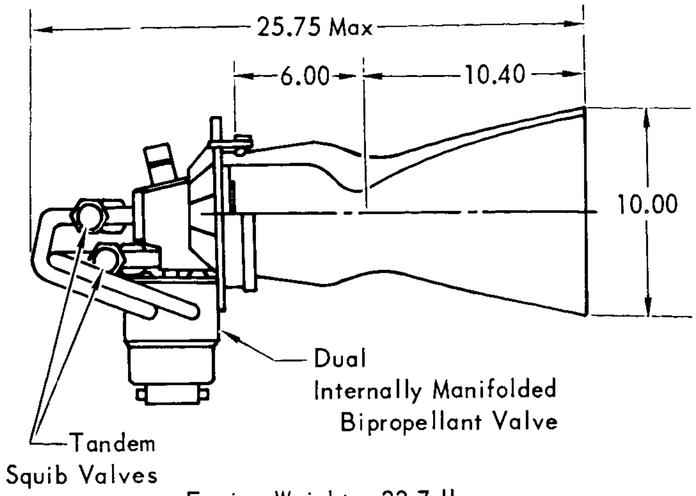
25.75 Max
6.00
10.40
10.00
Dual
Internally Manifolded
Bipropellant Valve
Tandem
Squib Valves

Engine Weight = 33.7 lb

GENERAL DESCRIPTION

A 2.5% fuel, film cooled beryllium chamber design is used for this engine. The injector is an annular design using a hydraulically driven servo actuator to drive a pintle sleeve which controls flow and injection velocity. The fuel is used for hydraulic actuation with the dump bled into the nozzle.

THIOKOL – PROPOSED DESIGN

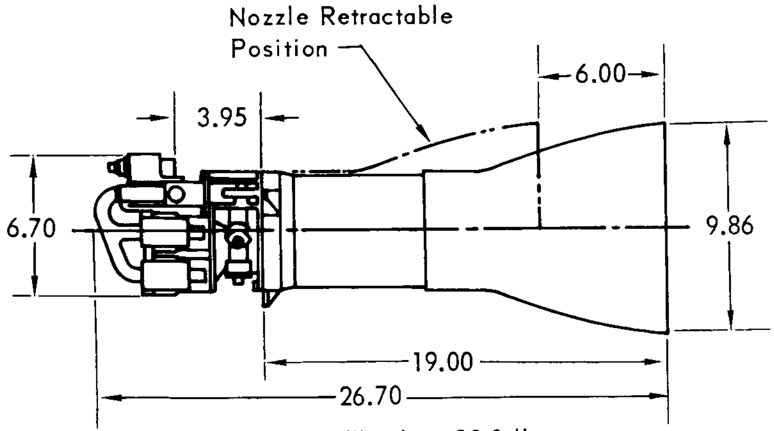
Nozzle Retractable
Position
6.00
3.95
6.70
9.86
19.00
26.70

Engine Weight = 30.0 lb

The chamber design is a silica phenolic soft throat ablator, tape-wrapped with a 6 Al 4V titanium shell. The injector is a dual manifold vortex injector based on Surveyor and C–1 engine designs. Flow control is obtained with cavitating venturis and area control by on-off manifold isolation valves. The proposed throttle valve actuator is hydraulic using the fuel as the fluid source.

TRW – PROPOSED DESIGN

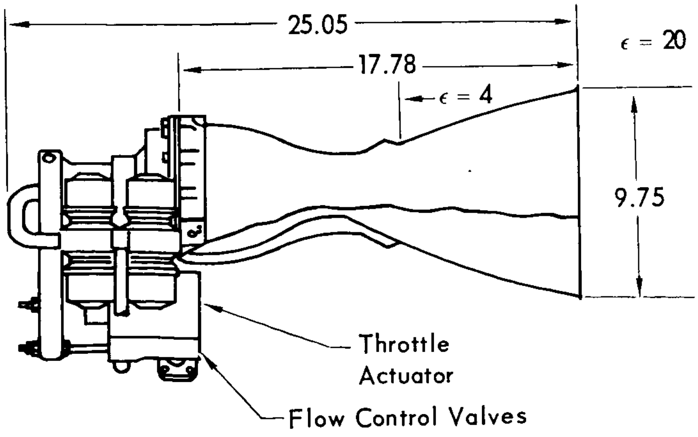
25.05
17.78
$\epsilon = 20$
$\epsilon = 4$
9.75
Throttle
Actuator
Flow Control Valves

Engine Weight = 34.4 lb

The chamber design is ablative contained within a titanium shell with a crushable nozzle skirt. The injector is a central coaxial element with a single movable sleeve to control injection momentum. Injector material is titanium. The flow control is achieved with variable area cavitating venturis driven by a ball screw from a trio of torque motors requiring nominal operating power of 100 watts.

(a) Development cost includes qualification (b) * indicates in complete data submittal

Figure 5.13–54 (Continued)

IGN SUMMARY (Continued)

PERFORMANCE CHARACTERISTICS		THROTTLING METHOD
• Chamber Pressure (psia) • Feed Pressure (psia) • O/F Weight Ratio • Specific Impulse – Max Thrust (sec) (P_∞ = 20 mb) – 50% Thrust (sec) – Min Thrust (sec) • Transient Impulse – Ignition (0–90%) – Shutdown (100–10%) • Response – Ignition (0–90%) ms – Shutdown (100–10%) ms – Throttling (Min–Max) ms	300 2500 1.6 ±.15 287 * * 1.6 8.4 80 9.4 *	VARIABLE – AREA INJECTOR 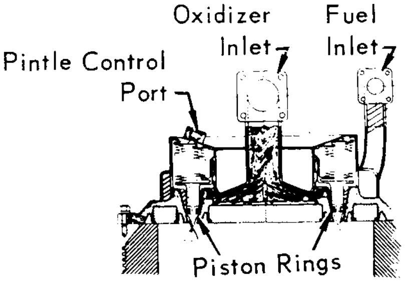 Oxidizer Inlet Fuel Inlet Pintle Control Port Piston Rings • Description – variable area injector velocity and flow control • Applicable Program – LANCE (Army) • Development Time – 24 Months • Development Cost – 8.5 M
• Chamber Pressure (psia) • Feed Pressure (psia) • O/F Weight Ratio • Specific Impulse – Max Thrust (sec) (Vacuum) – 50% Thrust (sec) – Min Thrust (sec) • Transient Impulse – Ignition (0–90%) – Shutdown (100–10%) • Response – Ignition (0–90%) ms – Shutdown (100–10%) ms – Throttling (Min–Max) ms	300 540 1.6 ±.048 296 287 278 5.0 130 115 53 165	DUAL MANIFOLD 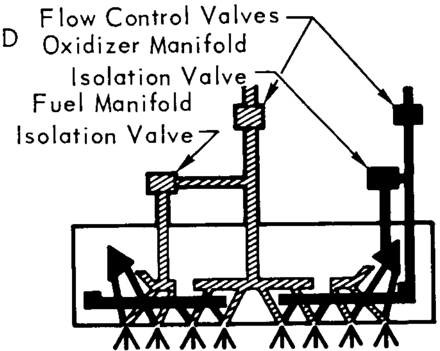 Flow Control Valves Oxidizer Manifold Isolation Valve Fuel Manifold Isolation Valve • Description – dual increment variable area injector with upstream flow control • Applicable Program – (In-house) • Development Time – 30 Months • Development Cost – 11.95 M
• Chamber Pressure (psia) • Feed Pressure (psia) • O/F Weight Ratio • Specific Impulse – Max Thrust (sec) (P_∞ = 20 mb) – 50% Thrust (sec) – Min Thrust (sec) • Transient Impulse – Ignition (0–90%) – Shutdown (100–10%) • Response – Ignition (0–90%) ms – Shutdown (100–10%) ms – Throttling (Min–Max) ms	300 520 $1.6\,^{+.032}_{\pm.048}$ 296 290 266 10 60+ 200 200 175	VARIABLE (PROPORTIONAL) AREA 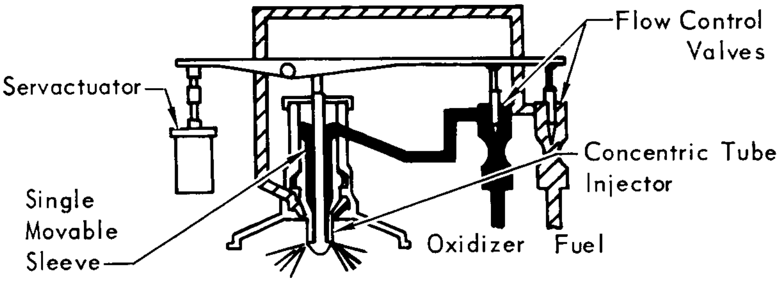 Flow Control Valves Servactuator Concentric Tube Injector Single Movable Sleeve Oxidizer Fuel • Description – variable area injector momentum control with upstream cavitating venturi flow control • Applicable Program – LMDE • Development Time – * x 42 months • Development Cost – * x 25.9 M

5,13-101-2

VENDOR ENGINE DESI

UTC – PROPOSED DESIGN	GENERAL DESCRIPTION
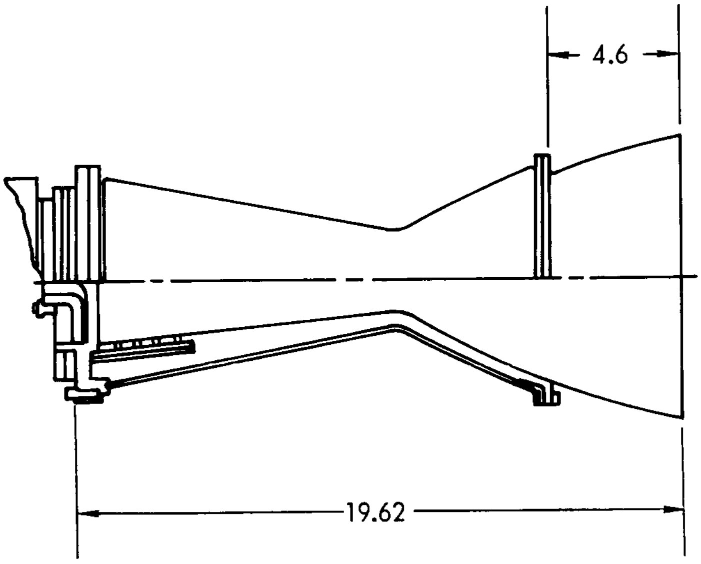 Engine Weight = 33.6 lb	The chamber assembly is glass wrapped ablatively cooled to an expansion of 10:1 with nozzle extension to 20:1. The liner is phenolic impregnated high silica cloth tape bias cut and wrapped at 45°. The chamber has an acoustic liner to damp high frequency instability. The injector is fixed area, flat faced with 56 duodoublet elements and 32 film coolant orifices. Flow is controlled by a bipropellant spool valve driven through a ball screw by a torque motor. Power requirement is 112 watts.

(a) Development cost includes qualification (b) * indicates incomplete data

Remarks

Development Status –
- The LMDE has significantly greater test experien
- The LANCE is a flight proven engine, but designe
- The aeration throttling method requires major deve
- The aerojet momentum exchange engine has under cept demonstration phase.
- Dual manifold methods have been tested on a dem
- Marquardt's momentum exchange dependent thrott ment to incorporate precise oxidizer in addition t
- 10:1 throttling has not been demonstrated with a

Significant Features –
- The LMDE has a complex injector but has demons
- The LANCE injector combines velocity and flow firing.
- Aeration requires no moving parts in the combust
- Momentum exchange requires close control of eac
- Dual manifold is simple extension of upstream th
- The Marquardt engine is very complex requiring
- The Bell method is very simple but very low inje and attendant possibility of combustion instabili

Figure 5.13–54 (Continued)

GN SUMMARY (Continued)

PERFORMANCE CHARACTERISTICS	
• Chamber Pressure (psia)	300
• Feed Pressure (psia)	545
• O/F Weight Ratio	1.6 ±*
• Specific Impulse – Max Thrust (sec)	300
(Vacuum) – 50% Thrust (sec)	293
– Min Thrust (sec)	272
• Transient Impulse – Ignition (0–90%) ms	*
– Shutdown (100–10%) ms	*
• Response – Ignition (0–90%) ms	120
– Shutdown (100–10%) ms	200
– Throttling (Min–Max) ms	90

THROTTLING METHOD

HELIUM AERATION

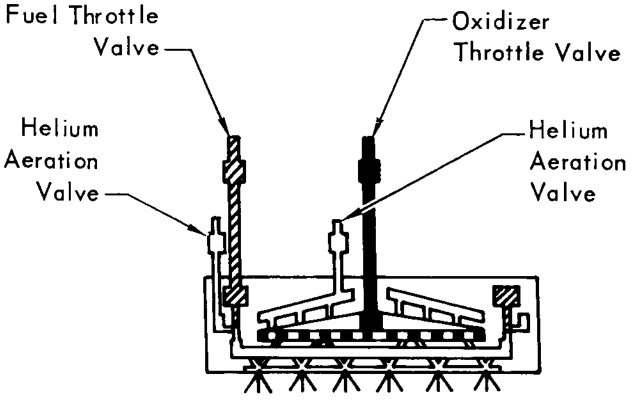

- Description – fixed area injector with helium aeration velocity control with upstream flow control
- Applicable Program – Retro-fit Transtage
- Development Time – 27 Months
- Development Cost – 9.7 M

submittal

ce than any other concept.
ed for high production and much less stringent requirements than space engines.
elopment to guarantee combustion stability.
gone significant development but cannot be considered to be far beyond a con-

onstration basis but have not undergone extensive examination.
ing is based on a ramjet throttle and is expected to require extensive develop-
fuel flow.
ixed area injector with cavitating venturi flow control.

strated high performance and extremely stable operation.
control at the injector face and heat soak distortion precludes acceptance

on zone but very careful design for uniform mixing.
h injector element and sufficient data is not available for complete optimization.
ottling but the step presents problems in absolute continuous throttling.
quid pressure regulators and precision calibration.
tion momentum at deep throttle contributes to low performance, poor mixing
y.

5,13-102-2

Cooling Method Alternates

Radiation

Heat Sink

Ablation

5.13.3.5.2 Evaluation of Proposed Engines - The factors used in evaluation the proposed engines are: development, performance, and reliability. The critical items influencing each of these are throtting capability, chamber design, specific impulse, combustion instability, and mixture ratio control.

Development Status of Throttling - Throttling is the most critical item to be considered in selection of the engine. Each proposed throttling concept could perform the terminal propulsion function. The TRW LMDE system is the most highly developed. The LMDE is, in fact, the only engine qualified for 10:1 throttling, using N_2O_4 - Aerozine 50, with demonstrated adaptability to N_2O_4-MMH. The Lance sustainer has been successfully throttled over a 50:1 ratio, but with IRFNA and UDMH. When operated with N_2O_4 - Aerozine 50, severe erosion of throat and pintle occurred in less than 30 seconds. Furthermore, the engine without extensive modification cannot be refired since heat soak back after shutdown warps the injector propellant flow control ring beyond use. For the VOYAGER application the Lance engine must be completely redesigned.

The helium injection technique of throttling has encountered combustion instability and as such has not been successfully developed. The Rocketdyne LMDE, using helium injection, was dropped in favor of the TRW engine. The combustion instability problems associated with this throttling technique are severe; instability has been encountered by Rocketdyne and more recently by UTC. A long development program is anticipated to effect a solution. The momentum exchange injector proposed by Aeroject is still in early development. The concept is promising but lacks the development maturity necessary for the VOYAGER program. The dual manifold injector proposed by Thiokol RMD is quite simple in design. The greatest apparent development uncertainty is attainment of stable throttling across the step. Sufficient test data, however, has not been generated to allow successful prediction of specific development problems. As such, it too lacks the development maturity needed in this project. The Marquardt and Bell proposed designs have not demonstrated capability. Considering all the factors, the TRW LMDE concept provides the lowest technical risk.

Chamber Design - Ablative, radiative and heat sink chambers are considered feasible for the terminal propulsion engine. Of the chamber types,only the ablative chamber has demonstrated capability at the 300 psia chamber pressure level. The LANCE engines, both sustainer and booster, operate at chamber pressures of 1000 psia. Ablative materials have been widely used in high chamber pressure solid rocket nozzles. There is no question concerning the chamber pressure capability of the ablator; however, two potential problems exist. The ablative chamber poses a site contamination hazard due to charred particles and pyrolysis products. No clear definition of site contamination limits is available, so this factor cannot be considered quantitatively. Laboratory analyses reported by Aerojet and TRW systems indicate that the products of pyrolysis remain as gases in the Martian atmosphere. Hence, the prime source of contamination is carbon particles dislodged from the charred chamber walls by erosion or impact loads.

The second potential problem is even more difficult to assess. It has not been conclusively demonstrated that the ablative chamber is compatible with chemical and heat sterilization. The data of Martin (JPL) and Hughes (JPL) has been reviewed. On the basis of this review and discussion with engine manufacturers, it appears that thermal and chemical sterilization compatibility can be attained. The results however are not conclusive and additional verification is indicated. TRW Systems is currently testing materials and more definitive data should be available within the next few months. A simple solution is available in the event that chemical sterilization presents a problem. Hermetic nozzle seals can be incorporated to prevent exposure of the ablative material to the ethylene oxide-Freon mixture.

No problems are expected with sterilization of the radiation cooled chamber. The only radiation engine qualified for nitrogen tetroxide and monomethyl hydrazine today is the Marquardt, 100-lb. thrust, 100 psia chamber pressure engine. The capability of radiation chambers to operate at 300 psia and 1650 lb thrust is yet to be demonstrated. The temperature of the chamber wall must be maintained several hundred degrees below that required by the ablative chamber. This requires a greater percent of fuel film cooling. The influence of throttling on radiation chamber film cooling is unknown. These factors indicate that significant development problems may be encountered.

Of the heat sink thrust chambers, engine manufacturers have considered beryllium and copper. The copper chamber weight is excessive and excludes it from consideration. The beryllium chamber is in an early development state. Rocketdyne has done considerable development work with beryllium and has developed several small thrust engines but no fully qualified engine is in existence. The adaptability of the beryllium chamber with a throttling injector is also questionable. The key to successful design is matching of stress and thermal profiles and controlling wall termperature to 1800°F or below. This makes the chamber design sensitive to injector characterization. The shifting injection conditions of throttling engines pose a major problem. Thus, the beryllium chamber proposed by Rocketdyne presents a serious development risk from the viewpoint of both chamber design and throttling.

Considering demonstrated capability, the ablation cooled chamber was chosen for the terminal engine. If, however, sterilization or site contamination presents prohibitive problems, it appears feasible to develop one of the other types. A parallel development program of a back-up chamber appears appropriate. Before a back-up type decision can be made, however, feasibility demonstration testing with throttling injectors should be conducted with both radiation and beryllium chambers.

Specific Impulse - Data which are directly applicable to terminal propulsion engines are meager. The preponderance of available data for storable propellants is for N_2O_4 - Aerozine 50, and chamber pressures in the range of 100 psia. Both tests and theory indicate very little performance difference between N_2O_4 - Aerozine 50 and N_2O_4 - MMH, so test data may be considered applicable to each. The specific impulse data presented by the various rocket engine manufacturers have, therefore, been based on N_2O_4 and both Aerozine 50 and MMH, then extended analytically to N_2O_4 and MMH at 300 psia chamber pressure. The techniques used in their analytical procedures are not clear and the accuracy may be open to question. Additional work is required to refine these data. For comparative purposes the data provided by the various companies were summarized. These were then compared with actual data from the TRW LMDE. These comparisons along with the data used for final sizing of the preferred propulsion are shown in Figure 5.13-55.

Combustion Instability - Combustion instability has been a primary cause of engine schedule delays. It appears, therefore, that because of the critical nature of the VOYAGER engine schedule major emphasis should be placed on eliminating combustion instability as a problem. The phenomemon of combustion instability is not readily amenable to analytical techniques, but it is known to be highly destructive under certain circumstances. Many rocket engines have been plagued with this problem, including the Rocketdyne F-1, Aerojet Apollo Service Propulsion engine,

EFFECT OF THROTTLING ON SPECIFIC IMPULSE

- N_2O_4/MMH
- MR = 1.6 0/F
- $P_{C(MAX)}$ = 300 psia
- $P_{AMBIENT}$ = 20 mb

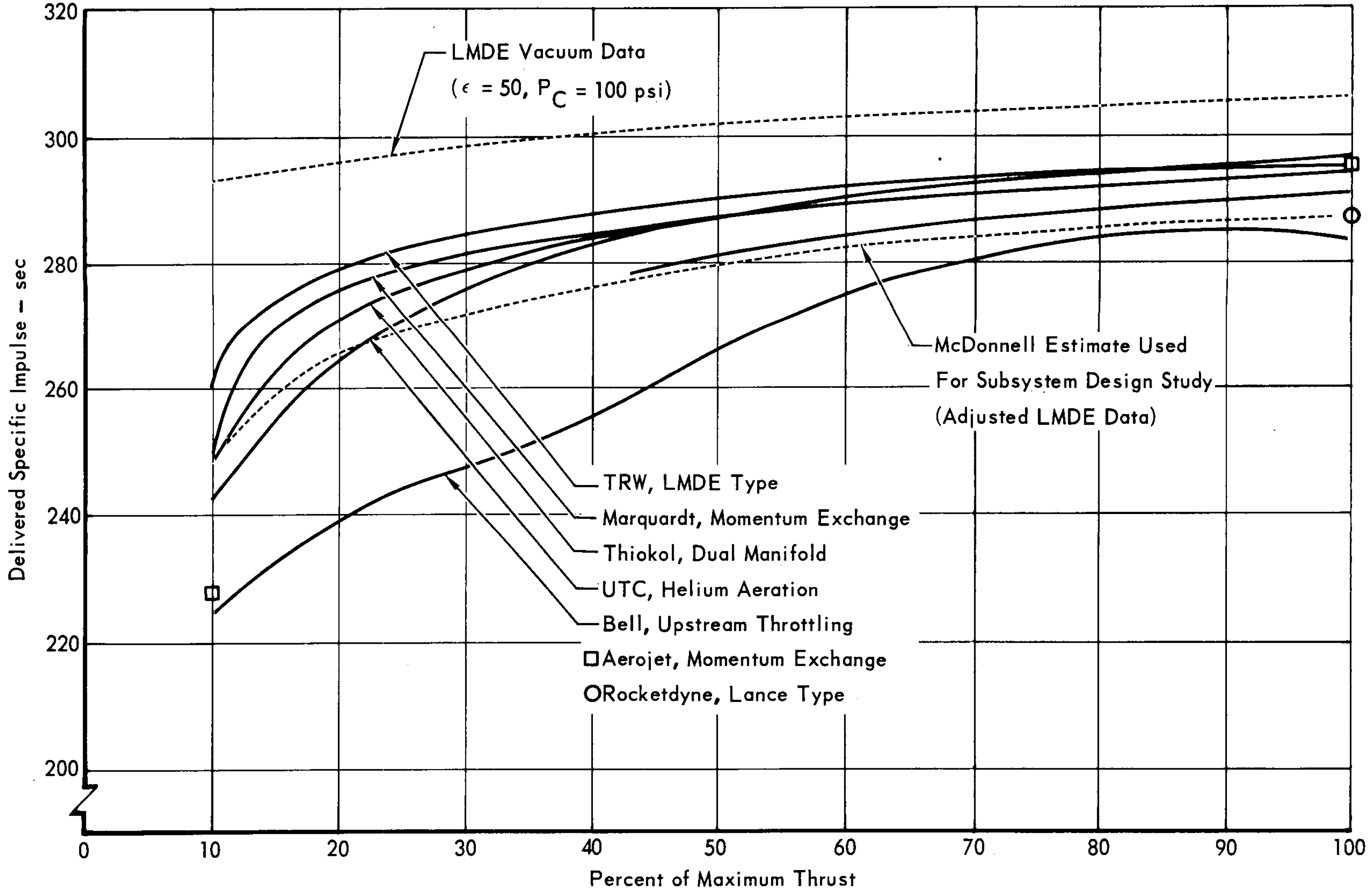

Figure 5.13–55

Rocketdyne LMDE, Bell LMAE, and the Aerojet Transtage.

Although various analytical techniques are available they are highly empirical and can only serve as stability indications. Experience has shown that flat face injectors are inherently less stable then centerbody injectors. The TRW LMDE which uses a centerbody type injector is remarkably stable. Even with 175% overpressure by "bomb devices" the engine has returned to stable operation over its complete range of throttled thrust levels. The LANCE sustainer, which also uses a centerbody type injector, has not presented combustion stability problems. It, however, has not been subjected to "bomb" overpressures. The Thiokol varitex and the Aerojet swirl cup injectors should also be stable but there are no substantiating data. Considering the factors discussed, the TRW LMDE centerbody injector has the best demonstrated stability characteristics.

Mixture Ratio Control - Variations in design mixture ratio can be attributed to two factors: (1) Changes in propellant supply conditions (pressure and temperature) and (2) Engine-to-engine tolerances in injector and/or flow control valves.

For equal changes in supply pressure (fuel and oxidizer) the effect on mixture ratio is small and can be ignored. Temperature changes, however, alter the relative densities and vapor pressures of the two fluids and are the major contributor to mixture ratio shifts. For our propellant temperature band of 40°F to 100°F and a maximum differential of 10°F between propellants, the maximum change in mixture ratio, due to temperature, is 2.5 percent.

Tolerances in the flow control valves include some degree of non-repeatability in mixture ratio, but this can be decreased appreciably during engine calibration firings, particularly if the flow control valves are mechanically interlinked. For example, TRW states that mixture ratio adjustments can be effected within .05 per cent.

In all designs except the Rocketdyne LANCE configuration, wherein flow control is accomplished with a variable area injector, the manufacturers report that the mixture ratio can be controlled within 3 percent. On the Rocketdyne design the mixture ratio variation is 9 percent.

Our preferred approach is to separate the flow control and injector velocity control functions. Mechanically linked cavitating venturis are selected for flow control to assure, among other things, close mixture ratio control.

Transient Performance Characteristics - The data received regarding response, impulse transients and repeatability are meager and of questionable accuracy. Since impulse transients and repeatability of response and impulse transients were not adequately considered by the engine manufacturers, these factors cannot be assessed. Therefore, no engine preference based on transient performance characteristics can be stated.

Design Complexity - Substantiated failure rate data, in the strictest sense, are not available for engine comparison. Only the LMDE and LANCE have accumulated enough run time to provide any reliability data. As such, ranking on the basis of reliability is predicated upon simplicity of design and operation. From this point of view the engine designs proposed are rated in this order of preference.

- Bell, simplest injector: moving parts- cavitating venturi
- Thiokol, fixed area injector requires manifold isolation valves: moving parts- on-off manifold valves, cavitating venturi
- Aerojet, fixed area injector with primary and secondary flow passages in each element: moving parts- secondary flow control on-off valves, cavitating venturi
- UTC, fixed area injector with helium injection manifolding, helium gas supply required; moving parts- helium on-off valves, cavitating venturi
- TRW, variable area injector with toleranced velocity control injector element close to hot combustion zone; moving parts- velocity control injector element and cavitating venturi,
- Rocketdyne, variable area injector has critically toleranced pintle for both velocity and propellant flow rate control close to hot combustion zone; moving parts- pintle
- Marquardt - Fixed area injector requires balanced check valves to control proportional primary and secondary flow rates, flow area schedules linked to spool valve controlled fluid pressure regulator: moving parts- check valves, area scheduler, sensing pot, spool valve.

5.13.3.5.3 Preferred Engine Design Selection - Figure 5.13-56 summarizes the significant characteristics of the proposed designs. The ranking of design preference indicates the best design for VOYAGER is the TRW LMDE type throttling engine. This design has been highly developed and has proven performance. It has demonstrated freedom from high frequency combustion instability. The cavitating venturi flow control effectively decouples the feed system, precluding low frequency instability. Due to these important factors the LMDE type throttling engine was chosen as the preferred design. As stated previously, the ablative chamber was chosen as the chamber concept, with a proposed parallel backup development.

ENGINE DESIGN SELE

MANUFACTURER	THROTTLING CONCEPT	CHAMBER TYPE	DEVELOPMENT STAT
• Aerojet	Momentum Exchange	Ablator X	• Major concept demonstr • Lacks complete data fo optimization.
• Bell	Upstream Throttling	Ablator with Columbium Chamber Liner	• Maximum demonstrated ratio is 8:1.
• Marquardt	Momentum Exchange	Radiation	• No demonstration.
• Rocketdyne	Variable Area	Beryllium	• Fully developed in hig version for LANCE Mis • Requires complete re-d Voyager and qualificati space.
• Thiokol	Dual Manifold	Ablator X	• Lacking complete conc demonstration. • No demonstration of ef manifold step on conti throttling.
• TRW	Variable Area – With Upstream Flow Control	Ablator X	• Most highly developed • Qualified for 10:1 thro X
• UTC	Helium Aeration	Ablator X	• Early parallel develop competition with TRW, • Major expended devel

5.13-109-1

CTION SUMMARY

US	PERFORMANCE	DESIGN COMPLEXITY
tion effort. full	● High specific impulse at maximum thrust, low at minimum thrust. ● Recessed, central swirl cup injection should be reasonably stable.	● Minimum moving parts but complex injector fabrication. ● No external fluid supply required.
hrottle	● Low specific impulse. ● likely to have low thrust instability problem.	● Least complex design. X
	● Potentially high specific impulse over complete throttle range.	● Most complex design.
production ile. sign for n for	● Average throttling specific impulse. ● Has no record of combustion instability. ● Susceptible to feed system coupled instability.	● Difficult design to provide flow and injection momentum control in combustion zone.
pt ect of ous	● High specific impulse at maximum thrust, low at minimum thrust. ● Vortex injector.	● Simple injector design.
oncept. ling.	● High specific impulse across throttle region. ● Demonstrated inherent stability. ● Good MR control. X	● Complex design but amenable to design features for reliability. ● Used on manned lunar mission.
ent LMDE . ment effort.	● Highest specific impulse at maximum thrust, low at minimum thrust. ● Repeatedly encountered combustion instability.	● Minimum moving parts but aeration manifolds designed into injector. ● Requires helium gas supply.

igure 5.13-56

5.13.3.6 Definition of Selected Subsystem - The significant characteristics of the preferred terminal propulsion subsystem are as follows:

Number of Engines	4
Propellants	N_2O_4/MMH
Thrust (lbs) per engine	1650
Type of thrust chamber	Ablative
Chamber pressure (psi.)	300
Nozzle expansion ratio	30:1
Mixture ratio	1.6:1
Tank pressure (psia.)	525
Throttling technique	Variable area injector with upstream flow control, LMDE type

A detailed physical description of the selected subsystem is defined in Part A, Section 3.2.6.3 and a functional description is presented in Section C 16.

5.13.3.7 Summary and Conclusions - A four-engine throttleable bipropellant subsystem was chosen as the preferred terminal propulsion subsystem concept.

The selection of four engines was influenced primarily by considerations of integration into the preferred Capsule Bus design. The alternate engine arrangements considered were six engines, one engine and three engines. The six engine arrangement offers engine-out capability but failure detection and isolation are difficult to implement. The single engine was discarded because it severely compromised equipment packaging for the 1979 Rover, a requirement specified in Reference 5.13-1. The three and four engine comparison revealed little difference in reliability and a 25-pound weight advantage of three engines was balanced by easier development and Capsule Bus integration. Elimination of the three-engine gimbal development and the convenient packaging of four engines led to its selection.

After comparison with monopropellant and solid/liquid subsystems, the four engine bipropellant subsystem was selected as the preferred concept. The superior development status, performance and flexibility of the bipropellant offset the potential reliability gain and minimum surface interface problems of the monopropellant. The solid/liquid subsystem was rated below the other candidates in all categories. Therefore, when the five selection factors of subsystem reliability, development status, performance, flexibility and interactions were considered, the

the bipropellant subsystem was selected as the best.

Following selection of the preferred concept, the study was refined to establish a preferred subsystem design. For the design analysis, special attention was given to basic component arrangements, subsystem pressure levels, mixture, ratio, subsystem dynamic coupling and engine design. Engine manufacturers provided assistance in evaluating throttling methods, chamber cooling techniques, combustion stability, performance and reliability.

The basic feed system; propellant storage, pressurization and fluids control and distribution components selection emphasized highly developed concepts. Prime consideration was given to sterilization compatibility. Based upon material compatibility testing at heat sterilization temperatures, titanium must be used in construction of all components wetted with propellant during sterilization.

The basic feed system selection consisted of a regulated helium pressurization system, one oxidizer and one fuel storage tank, and fluid flow control and isolation components. Significantly, the tanks do not require positive expulsion due to the favorable propellant orientation effects during entry and descent through the Martian atmosphere. The mixture ratio of 1.6 was chosen from considerations of performance and chamber cooling.

The selection of engine chamber pressure at 300 psia, to minimize subsystem weight and volume, established the propellant tank pressures at 525 psia. Helium storage pressure was selected as 3000 psia. The most significant single item in the subsystem is the engine. From a group of proposed designs supplied by engine manufacturers, the LMDE-type throttling injector coupled to an ablative chamber was selected. This selection is based on the successful throttling experience and demonstrated combustion stability characteristics of the centerbody type injector. The latter is of major significance, since solution of combustion stability problems has been a major cause of delay in previous engine programs. The 10:1 throttle ratio, state-of-the-art by virtue of the LMDE experience, provides an increase in flexibility needed for the 1979 mission. Since a 1973 throttle requirement of 9:1 was established, as described in Part B, Section 2.3.7, the increase to 10:1 provides adaptability to extremes of atmosphere. In addition, the engine design provides 50% greater life than required for 1973. This permits application to 1979 missions without introducing a new and expensive engine development program.

A major area of concern is the contamination problem associated with the ablative chamber selection. It is difficult to assess the importance of landing site contamination which may result from ablative chambers against the development problems associated with radiation and heat sink type thrust chambers. The contamination problem should be examined further, and the development of a metallic chamber should be pursued in parallel with the ablative chamber for the basic engine until either or both the contamination or metallic chamber development problems are resolved.

Of the many problems anticipated in the development of this complex subsystem, the prime problem area will be the new engine. The technical risk, however, is minimized by the subsystem design selection which allows maximum utilization of the background of experience developed for other space programs and a throttling concept offering inherent combustion stability. The problem of developing a sterilizable subsystem will require lengthy test verification but the technology exists which will allow accomplishment of this goal. Long term space storage, an additional area which has not been demonstrated, will require careful detail design and test verification.

Any subsystem designed for the stringent requirements established for the terminal propulsion function will encounter development difficulty. However, the analysis of all factors supports the selection of the four engine, throttling bipropellant subsystem. Therefore, this subsystem is best suited to perform the terminal propulsion subsystem function in the overall mission objective of the VOYAGER.

5.13.4 Supporting Design Studies - Various design studies were performed to assist in selection of the preferred De-orbit, Reaction Control, and Terminal Propulsion Subsystems. These studies were divided into a configuration analysis, an evaluation of sterilization and decontamination compatibility of liquid and solid propellant subsystems, a comparison of thrust vector control mechanizations and a reliability assessment of each of the candidate designs. These topics are discussed in this section.

5.13.4.1 Configuration Analysis - In the propulsion subsystem trade-off studies, both liquid and gaseous fluids were considered for various functions. Although the subsystems are designed for different requirements, the basic configurations are necessarily similar with respect to components, component arrangements and design criteria. Since these are essentially independent of the specific subsystem, studies were made to establish the best and most reliable combination for use in applicable propulsion subsystem trade studies. The studies are divided into two categories consisting of component arrangement and design criteria. These are discussed below. Engine arrangements are not included but are discussed in Sections 5.13.1, 5.13.2 and 5.13.3 for the de-orbit, reaction control, and terminal propulsion subsystems, respectively.

Component Arrangement - A number of propellant pressurization and control, configurations are suitable for VOYAGER liquid propulsion subsystems. Evaluation and selection of our preferred arrangements are presented below.

- Liquid Propellant Pressurization - Various pressurization concepts were evaluated to select the method most compatible with the Capsule Bus mission and constraints. Pressurization concepts which have been demonstrated or flight qualified include cryogenic and ambient stored cold gas subsystems, solid propellant gas generators, and liquid monopropellant or bipropellant gas generators. The primary constraints for the pressurization subsystem are sterilization, flight qualification by 1973 and growth provision for the 1979 mission. Reliability is considered to be the most important requirement.

  Based on demonstrated technology and the potential for surviving sterilization, only the ambient stored helium or nitrogen pressurization subsystem and a hydrazine bootstrap gas generator subsystem were evaluated for use in the Capsule Bus. The advantages of the cold gas subsystem are simplicity, ease of sterilization, and high reliability. Ambient stored cold gas subsystems have been utilized on our Mercury, ASSET and Gemini spacecraft, and many other systems. The inherent advantages of the bootstrap concept are reduced weight and elimination of gas leakage potential. Although the hydrazine bootstrap concept has been successfully demonstrated, no flight weight subsystems have been qualified, and development of the bootstrap concept for VOYAGER application would be complicated by the requirement for a sterilizable differential area bellows or piston tank to provide the required pressure amplification. In a bipropellant propulsion subsystem, an impermeable thermal barrier, such as a metallic diaphragm or bladder, is required to isolate the oxidizer from the fuel-rich gas generator products. The alternative is to use the gas generator to pressurize the fuel tanks only, with a separate helium or nitrogen supply used for pressurizing the oxidizer tanks. In this manner, the attributes of the bootstrap subsystem are degraded and the use of independent pressurant sources for the fuel and oxidizer tanks could result in a pressure imbalance giving rise to mixture ratio variations.

Based on its flight proven reliability, the cold gas pressurization concept was chosen for subsystem studies. A discussion of the preferred pressurant isolation, pressure control, and pressurant distribution functions is presented below. Several alternatives for the elimination of single point failures are discussed, but the preferred subsystem configurations evolve from the weight and reliability trade studies of Part E, Section 2.3.

o Pressurant Isolation - The pressurant is stored in a spherical tank isolated before use by a pyrotechnic valve immediately downstream, as shown in Figure 5.13-57. A manual access valve provides a means for pressurant servicing. The use of quick disconnects in propulsion subsystems was rejected in the Mercury and Gemini programs as a result of high leakage and low reliability. The crimp and weld technique is not recommended due to the difficulty in achieving a tight squeeze seal on high strength tubing, prior to welding. A pressure transducer is provided to monitor source pressure for telemetry. The transducer is referenced to absolute pressure and the flexible element is reinforced by a welded outer case which serves as a redundant external seal. A filter is provided downstream of the pyrotechnic valve to remove contamination induced by valve actuation, and test ports are provided for ground checkout.

The leakage rates exhibited by the Gemini pressurant tank, manual valve, and test port were maintained well within the specification limits of

PRESSURANT ISOLATION GROUP

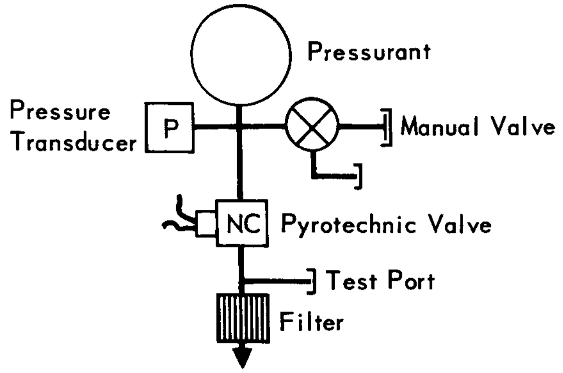
Pressurant
Pressure Transducer
P
Manual Valve
NC
Pyrotechnic Valve
Test Port
Filter

Figure 5.13-57

0.9 scc/hour, 10 scc/hour, and 10 scc/hour-helium, respectively, under a driving pressure of 3000 psi. Furthermore, since these components may be leak checked during ground tests prior to sterilization, and pressure decay may be monitored with the source pressure transducer following sterilization, installation of redundant pressurant tanks is therefore considered necessary. Protection against a failed pyrotechnic valve may be provided by incorporation of a redundant electro-explosive device (EED). Clogging of the filter element is considered improbable since only a small amount of contamination is induced by actuation of the pyrotechnic valve.

o Pressure Control - The concepts evaluated for the pressure control function included mechanical modulation (regulators), electro-mechanical bang-bang (pressure switch actuated solenoid valves), orifice blowdown, and simple blowdown without an orifice.

The orifice blowdown concept is most attractive for subsystems operating continuously at fixed thrust for a specified burn time. However, for the attitude control and terminal propulsion functions, engine duty cycles are not well defined, and if pressurant flow fails to equal propellant usage rates, wide excursions in propellant tank feed pressure could result. These fluctuations would be particularly unattractive in the terminal propulsion subsystem due to the sensitivity of cavitating venturi throttle valve operation to upstream pressure. Hence, for the purpose of insuring mission success, an orifice blowdown subsystem is not recommended.

The simple blowdown concept without orifice would be attractive for a spacecraft attitude control subsystem which requires maximum thrust at deorbit, and reduced thrust during entry. However, the Capsule Bus entry rate damping requirements are not well defined, and therefore, a regulated pressure control subsystem (modulating or bang-bang) is currently preferred.

In a subsystem with pressurant relief capability, failure of a normally open regulator or solenoid valve would not be catastrophic, but would cause the subsystem to operate in a blowdown mode with degraded performance.

Various regulator and bang-bang pressure control concepts are presented in Figure 5.13-58 and are compared on the basis of weight and reliability.

The electromechanical bang-bang concept would utilize relays to limit switch contact arcing and a zener diode for voltage surge suppression. Although this device would weigh less than a regulator, it has a wider control tolerance, and is slightly less reliable than a regulator. Based on our

PRESSURE CONTROL CONCEPTS

(1) REGULATOR

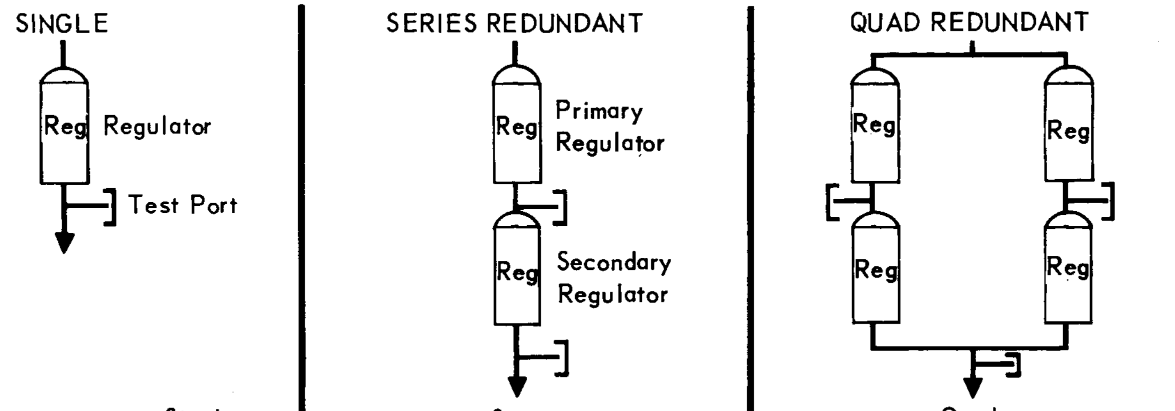
SINGLE
Reg
Regulator
Test Port
SERIES REDUNDANT
Reg
Primary Regulator
Reg
Secondary Regulator
QUAD REDUNDANT
Reg
Reg
Reg
Reg

	Single	Series	Quad
Relative Weight (lb)	4.5	9.0	17.5
Reliability	.998608	.999970	.9999981

(2) ELECTROMECHANICAL BANG-BANG

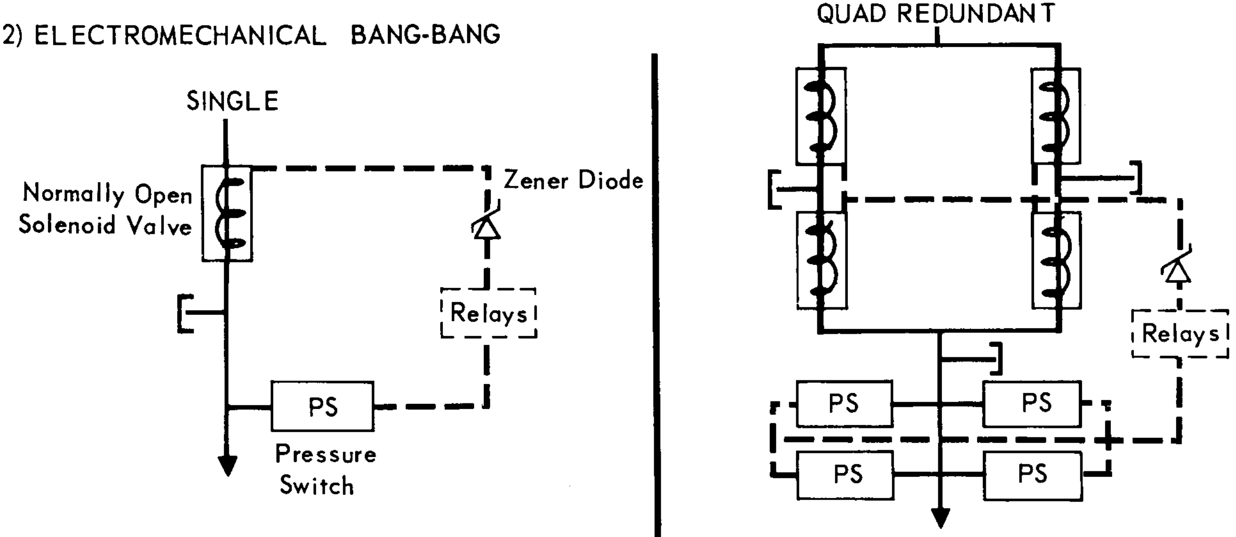
SINGLE
Normally Open Solenoid Valve
Zener Diode
Relays
PS
Pressure Switch
QUAD REDUNDANT
Relays
PS
PS
PS
PS

	Single	Quad
Relative Weight (lb)	3.25	12.5
Reliability	.99824	.9999974

(3) COMPOSITE

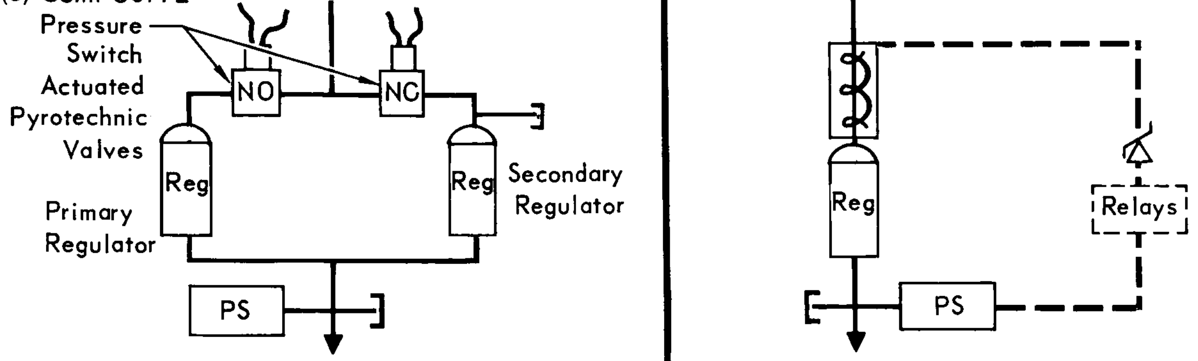
Pressure Switch Actuated Pyrotechnic Valves
NO
NC
Reg
Primary Regulator
Reg
Secondary Regulator
PS
Reg
Relays
PS

Relative Weight (lb)	13.75	7.25
Reliability	.9999966	.999701

Figure 5.13–58

experience with the use of regulators, their flight proven reliability, tight control band, and long life, we prefer a regulator for pressure control. The most common regulator failure mode is excessive internal leakage. Protection against this failure or a regulator failed full open may be provided by a series redundant regulator or one of the composite mechanisms illustrated in Figure 5.13-58. The series redundant regulator is preferred since it eliminates the requirement for electromechanical control components. In the series redundant arrangement, both regulators would be internal rather than ambient pressure referenced to prevent external leakage in the event of a bellows or diaphragm rupture. Furthermore, the secondary regulator would have a slightly higher lockup pressure than the primary and would remain open during normal subsystem operation. A failed closed regulator may be prevented by good design and for this reason we do not feel a backup for this failure mode is required. The only means by which a normally open regulator may fail closed is for the spring element to break or for the mechanical linkage to bind following regulator lockup. Spring failures would be eliminated by good quality control (including X-ray inspection) and insuring that the springs are not stressed beyond a small percentage of the material ultimate strength. Binding of the mechanical linkage is improbable with current regulator designs which exhibit large force margins for opening the poppet and low force margins for closing.

o Pressurant Distribution - Following the pressure regulator in a bipropellant subsystem, the pressurant flow divides and passes through check valves which isolate the fuel and oxidizer gas systems. (See Figure 5.13-59) A normally open pyrotechnic valve is located just upstream of the oxidizer check valve to prevent propellant vapor mixing in the pressurant lines following system shutdown. Protection against a failed closed check valve could be provided with incorporation of parallel redundant check valves. Furthermore, for the de-orbit or terminal deceleration maneuvers, system operation times are short and the normal flow of pressurant through a failed open valve would purge propellant vapor. The gas systems would be isolated during storage by a normally closed pyrotechnic valve just downstream of the check valves. Again, redundant EED's could be installed to eliminate a single point failure. Pressure transducers located in both the fuel and oxidizer subsystems are provided to sense regulated pressure during system operation, as well as tank pressure during sterilization. Pressure relief valves on

PRESSURANT DISTRIBUTION – BIPROPELLANT

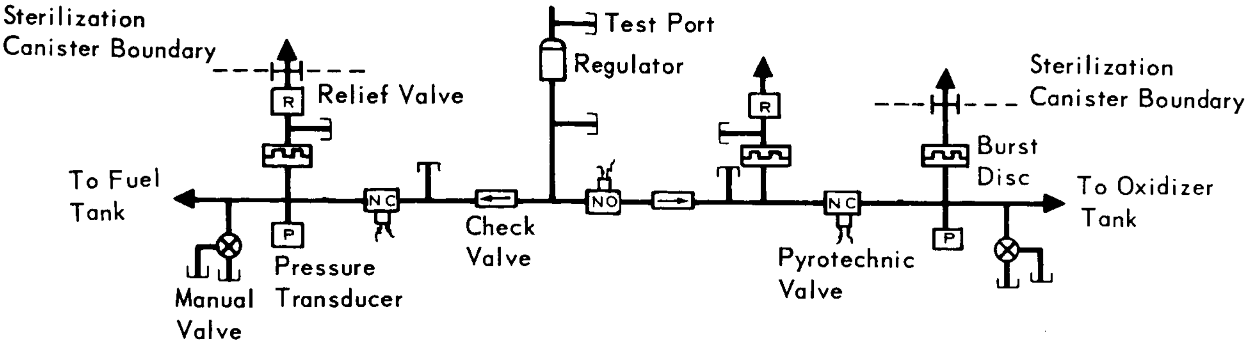
Sterilization Canister Boundary
Test Port
Regulator
Relief Valve
R
NC
NO
P
Sterilization Canister Boundary
Burst Disc
To Fuel Tank
To Oxidizer Tank
Check Valve
Pyrotechnic Valve
Manual Valve
Pressure Transducer

Figure 5.13–59

PRESSURANT DISTRIBUTION – MONOPROPELLANT

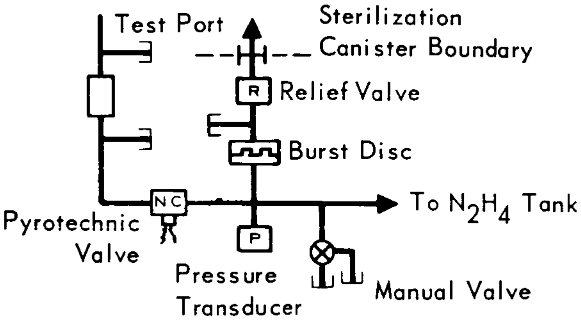
Test Port
Sterilization Canister Boundary
R
Relief Valve
Burst Disc
NC
P
To N_2H_4 Tank
Pyrotechnic Valve
Pressure Transducer
Manual Valve

Figure 5.13–60

both the fuel and oxidizer sides prevent propellant overpressure. These relief valves are isolated from the gas system by burst diaphragms which prevent failure due to relief valve leakage. Two burst diaphragms are incorporated on the oxidizer side since N_2O_4 vapor pressure during sterilization is considerably higher than nominal regulated pressure. The burst disc downstream of the normally closed valve protects the oxidizer tank from an overpressure condition during sterilization, whereas the burst disc upstream of the cartridge valve, designed to rupture at the same pressure as the fuel diaphragm, protects the oxidizer tank from an overpressure situation during subsystem operation. In this manner, if an overpressure condition is encountered during the mission, the fuel and oxidizer tanks would be relieved to nearly equal pressures, thereby maintaining near-nominal mixture ratio control. A manual valve is also provided for convenience during propellant servicing, and tests ports are provided for ground checkout of the individual components. Separate pressurant sources for the fuel and oxidizer tanks are not recommended since tolerances on pressurant regulation could result in off-nominal mixture ratio control.

The pressurant distribution components for a monopropellant subsystem are identical to the bipropellant subsystem with the exception that the normally open isolation valve and check valves are not required. The pressurant distribution grouping for the monopropellant subsystem is presented in Figure 5.13.60.

For a cold gas reaction control subsystem, the preferred gas storage, isolation and regulation groupings are identical to those selected for the liquid propellant groupings except, following regulation, gas is distributed directly to the thrust chambers.

o Liquid Propellant Tankage - Various monopropellant and bipropellant tankage arrangements were considered for the de-orbit, attitude control and terminal propulsion concepts. A primary consideration was minimum c.g. travel during propellant usage. Arrangements considered included two multi-tank concepts based on the Surveyor and Lunar Module (LM) propulsion subsystems, and a simple two-tank unequal moment arm concept. Schematics of these configurations are presented in Figure 5.13-61. Evaluations were based on weight and packaging considerations, and the probability of achieving mission success.

PROPELLANT TANKAGE CONCEPTS

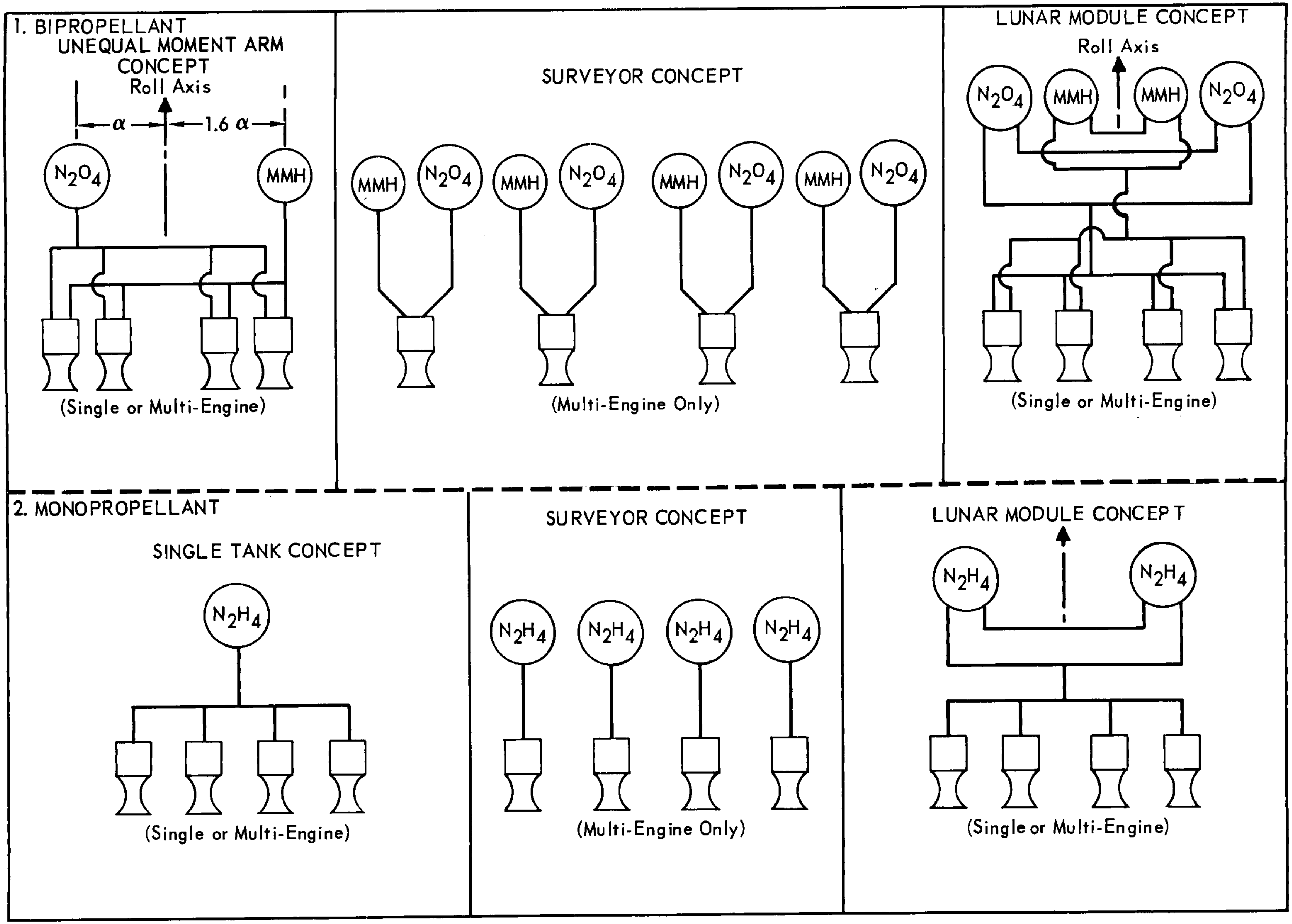
1. BIPROPELLANT
UNEQUAL MOMENT ARM CONCEPT
Roll Axis
α
1.6 α
N_2O_4
MMH
(Single or Multi-Engine)
SURVEYOR CONCEPT
MMH
N_2O_4
(Multi-Engine Only)
LUNAR MODULE CONCEPT
Roll Axis
N_2O_4
MMH
MMH
N_2O_4
(Single or Multi-Engine)
2. MONOPROPELLANT
SINGLE TANK CONCEPT
N_2H_4
(Single or Multi-Engine)
SURVEYOR CONCEPT
N_2H_4
(Multi-Engine Only)
LUNAR MODULE CONCEPT
N_2H_4
N_2H_4
(Single or Multi-Engine)

Figure 5.13-61

- Surveyor Concept - Manifolding of the propellant tanks was originally provided in the Surveyor Spacecraft to insure uniform propellant utilization, and thus minimize tipping moments. However, during engine firings it was observed that propellant would be drawn preferentially from the warmer tanks due to the lower viscosity and surface tension effects. Under some conditions the resulting propellant imbalance could become so great that the Vernier Propulsion Subsystem could not counteract the tipping moment. Furthermore, analysis revealed that, during zero g portions of the flight, propellant would migrate from the cooler tanks to the warmer tanks. It was found that the moment control capability could become insufficient during the main retro maneuver, since the propellant imbalance would not redistribute itself quickly enough. Hence, the propellant manifolds were removed and propellants were fed to each engine individually from tanks located above each engine. An advantage of this configuration is that, as an engine is throttled to counteract a disturbance torque, propellant is expended from the tanks directly above the engine, thereby reducing the control requirements. The disadvantage of removing the manifold is that additional propellant must be carried to provide for the extremes under which one engine would be fired at high thrust for longer periods than the others, or for the condition where the performance of one engine is considerably lower than the others. Due to this latter characteristic and the requirement for multiple tanks, the Surveyor configuration is the heaviest of those considered for the Capsule Bus. More importantly, however, individual engine duty cycles are difficult to estimate and possibility of premature propellant depletion from one pair of tanks degrades the probability of mission success.
- Lunar Module (LM) Concept - The Lunar Module configuration prevents preferential propellant usage during subsystem operation with the incorporation of a large diameter transfer manifold between tanks. Should some propellant be drawn preferentially from a warmer tank, the resulting hydraulic head differential under axial acceleration loads would cause propellant to be transferred from the cooler to the warmer tank through the low ΔP transfer manifold. In this manner, nearly equal propellant levels would be reestablished and propellant would be expended at equal rates. Propellant migration during the zero g cruise and orbit portions of the mission would be prevented by incorporation of a normally-closed pyrotechnic valve in the

propellant transfer manifold in order to limit the disturbance torque at de-orbit initiation. Similarly, propellant vapor migration and attending condensation during the same intervals would be prevented by installation of pyrotechnic actuated valves in the pressurant manifolds. A schematic of this concept is presented in Figure 5.13-62.

The Lunar Module configuration would weigh less than the Surveyor concept due to fewer tanks and the elimination of excessive propellant margins. Nevertheless, it is a complex arrangement due to the requirement for multiple components and possesses numerous single point failures which degrade the probability of mission success.

- Unequal Moment Arm Concept - This is the simplest and lightest of the configurations considered. In a bipropellant subsystem the fuel tank would have a larger moment arm and be diametrically opposite to the oxidizer tank to insure a nearly balanced propellant load during subsystem operation. The moment arms are established based on the propellant mixture ratio. For a mixture ratio of 1.6, the fuel tank would be installed at a moment arm nearly 1.6 times the oxidizer tank moment arm. In a monopropellant system only a single tank is required and it would have to be located near the roll axis of the vehicle to insure minimum center-of-gravity shift during propellant usage.

From a propulsion viewpoint, the bipropellant unequal moment arm and monopropellant single tank concepts are preferred. However, when required tank sizes and preferred locations are incompatible with packaging constraints, the LM arrangement is used in concept trade studies.

Design Criteria - Propellant requirements were estimated for all liquid subsystems included in the applicable trade studies by dividing total impulse by mission averaged specific impulse and providing a 6% margin to account for line and tank trapped propellant quantities and mixture ratio variances. For the RCS, trapped quantities were increased to 12% to account for proportionally larger line volumes. Propellant tank volumes were estimated assuming a 3% ullage at 275°F. Preliminary estimates of pressurant quantity were made assuming a polytropic expansion process midway between isothermal and isentropic. Hence, polytropic exponents of 1.2 and 1.335 were assumed for nitrogen and helium, respectively. Including the effects of sterilization, the near optimum storage pressures of helium and nitrogen pressurant are 6000 psia and 4000 psia at 70°F, respectively. However, since envelope constraints are not critical, storage at 3000 psia is recommended to mini-

LUNAR MODULE PROPELLANT TANKAGE CONCEPT

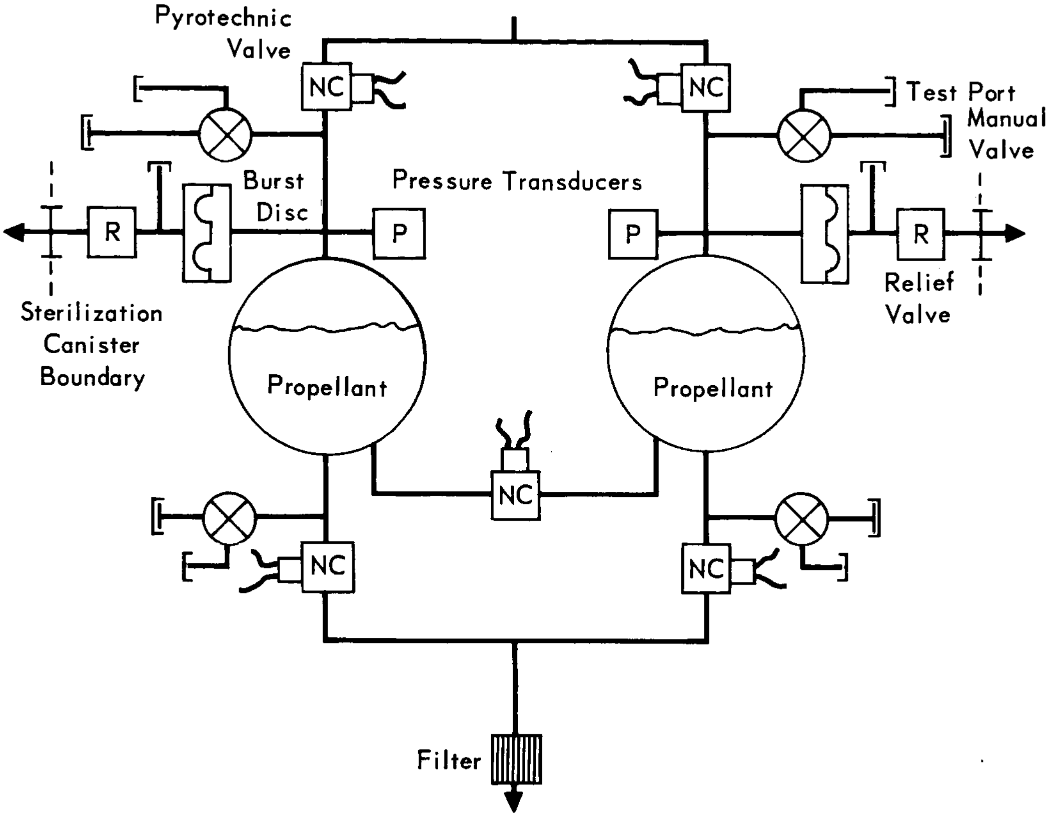
Pyrotechnic Valve
NC
NC
Test Port
Manual Valve
Burst Disc
Pressure Transducers
R
P
P
R
Sterilization Canister Boundary
Relief Valve
Propellant
Propellant
NC
NC
NC
Filter

Figure 5.13-62

mize leakage potential. The weight penalty incurred is very small, approximately 3 pounds (helium plus storage tank) for the 1979 high impulse TPS mission. An allowance for pressurant leakage was provided based on Gemini OAMS and RCS experience. The combined allowable leakage rate for the pressurant tank, manual valve and test port is 20.9 scc/hour (helium) under a driving pressure of 3000 psia. Therefore, the respective helium and nitrogen pressurant margins were .07 pounds and .19 pounds, based on a 1979 mission of approximately 400 days.

The design safety factor criteria presented in Part A, Section 2.3 were utilized to establish pressurant and propellant tank weights.

5.13.4.2 Liquid Propulsion Subsystem Sterilization - The sterilization requirement established for the Capsule Bus imposes stringent development demands on the liquid propulsion system. The high sterilization temperature specified and the required ethylene oxide exposure require designs which are currently beyond the state-of-the art. Considerable progress is now being made, however, in this area. Contracts funded by JPL, as well as privately supported efforts, are producing data applicable to the design of sterilizable systems.

By far, the most significant effort to date has been that accomplished under JPL Contract 951709, which is being conducted by Martin-Denver. Our in-house testing has confirmed some of the results reported in the JPL sponsored program. Additional work, particularly in hydrazine decomposition and ETO/catalyst compatibility, goes beyond the effort planned in the JPL program.

In this report the JPL program conclusions, through March 1967, are summarized and the McDonnell test results are presented. The implication of these results is discussed and component design considerations resulting from the sterilization requirements are presented. Finally, conclusions and recommendations are summarized.

5.13.4.2.1 Sterilization Tests - The test results of the JPL sterilizable liquid rocket propulsion system, through March 1967, are briefly summarized below. The McDonnell tests, not currently reported elsewhere, are discussed in greater detail.

JPL Sterilizable Liquid Rocket Propulsion System - The objective of this program is to demonstrate the feasibility of a heat sterilizable liquid bipropellant subsystem. The program consists of four phases as defined below:

- Subsystem design and component selection
- Component procurement and testing
- Materials investigation, parallel with the above design phase
- Assembly and test of complete propulsion subsystem

The last report issued, March 1967, extends through subsystem design/component selection and the material investigation (screening) phases. The conclusions to date, resulting from this work, which are pertinent to our investigation for sterilizable liquid propulsion subsystems for VOYAGER are presented below.

The recommended propellants are: Oxidizer - N_2O_4; Fuel - MMH.

For hardware in contact with propellants during sterilization the recommended materials are summarized in Figure 5.13-63. All metals evaluated were considered to be capable of withstanding the sterilization temperature, when not in contact with propellants.

METALS RECOMMENDED FOR HARDWARE EXPOSED TO PROPELLANTS DURING THERMAL STERILIZATION

PROPELLANTS	PROPELLANT TANKS	PLUMBING LINES	VALVE BODIES	BURST DISCS
N_2O_4	Titanium (6Al–4V)	Titanium (6Al–4V)	Titanium (6Al–4V) or Anodized Aluminum	Titanium (6Al–4V)
MMH	Titanium (6Al–4V) or Stainless Steel (17–4); or Aluminum (2014–T6 or 2219–T8)	Stainless Steel (304,304L, 321 or 347); or Aluminum (2014, 2219, 2024, or 6061)	Aluminum (2014, 2024 or 6061); or Stainless Steel (304, 304L, 321 or 347)	Aluminum (1100 or 6061); or Stainless Steel (304, 321, or 347)

Figure 5.13–63

Of the non-metals exposed to propellants at 275°F, only Teflon survived. It retained approximately 80% of its physical properties after 600 hours, in contact with nitrogen tetroxide. It was unaffected by monomethyl hydrazine.

No conclusions were made relative to the capabilities of adhesives; plastic and rubber sheet films; potting, encapsulating and sealing resins; and coatings and finishes, to withstand dry heat sterilization. The results presented indicate various degrees of degradation.

Most of the metals and non-metals commonly used in propulsion subsystem designs were reported as being compatible with the Ethylene Oxide-Freon 12 decontamination exposure.

McDonnell Propellant/Materials Compatibility Program - This program was initiated to obtain the data necessary to determine the feasibility of a sterilizable liquid propulsion subsystem. An industry and literature survey was made and various materials compatibility tests were conducted. Excepting the reports from the JPL program above, the literature survey revealed almost a complete lack of information on material compatibility with propellants at elevated temperatures. The results of this survey are summarized in Figure 5.13-64. Also found lacking were data on the effects of ethylene oxide on the Shell 405 catalyst, applicable to monopropellant hydrazine subsystems. The tests conducted to resolve these problems are discussed in the following sections.

Material Compatibility Test - This test consisted of a two hour test of the propellant alone in the test vessel, to measure vapor pressure at 275°F, followed by an eleven day exposure of selected materials to propellant, also at 275°F.

The propellants used conformed to the applicable MIL-Specifications, except that the N_2O_4 was "green" N_2O_4 per NASA Specification MSC-PPD-2 (0.4 to 0.8% NO added). The propellant and material combinations tested are summarized in Figure 5.13-65.

Testing was conducted in sealed, Teflon-lined, 321 SS pressure vessels fitted with pressure transducers. Following the vapor pressure test, it was found that the IRFNA had permeated through the Teflon vessel liner and attacked the vessel wall. Corrosion was sufficiently severe to cause cancellation of the materials compatibility portion of the IRFNA test.

The metal test specimens consisted of welded tensile test pieces and strips of unwelded material. Premabraze 130 braze filler alloy was coated onto a 304 tube section for the test. Teflon samples were strips of sheet stock. The different

LITERATURE SURVEY

COMPATIBILITY OF MATERIALS IN CONTACT WITH PROPELLANTS AT 275°F

PROPELLANT MATERIAL	N_2H_4	MMH	N_2O_4
1100 Al	No data at 275°	No attack at 275° No particle formation (4) (5) (C) (D) No data on pressure (G)	No attack at 275° No particles formed for 300° hr. test (4) Severe attack and corrosion products formed in 600 hr. test (5) No data on pressure (G)
2014-T6 Al	No data at 275°	No attack at 275° No particle formation (4) (5) (C) (D) No data on pressure (G)	
2219-T87 Al	No data at 275°	No attack at 275° No particle formation (4) (5) (C) (D) No data on pressure (G)	
6061-T6 Al	Satisfactory at 300° (1)	No attack at 275° No particle formation (4) (5) (C) (D) No data on pressure (G)	6061-T6 only Satisfactory at 300° (1)
7075 Al	Not recommended for use with N_2H_4 (8)	No data at 275°	Corrosion rate of 22 mpy at 160°(8)
7075 T6 Al	Satisfactory at 300° (1)(2)	No data at 275°	Satisfactory at 300° (1) Possible corrosion (A)
6Al-4V Ti	Satisfactory at 300°(1) Gas evolves faster with oxidized titanium than with unoxidized titanium (7)	No attack at 275° No particle formation (4) (5) (C) (D) No data on pressure (G)	Possible reaction (B) No attack at 275° No particle formation (4) (5) (C) (D) No data on pressure (G)
302 SS	No data at 275°	No data at 275°	No data at 275°
303 SS	No data at 275°	No data at 275°	No data at 275°
304 SS	No data at 275°	No attack at 275° No particle formation (4) (5) (C) (D) No data on pressure (G)	High corrosion at 275° Iron adducts formed (4) (5) (C) (D) No data on pressure (G)
304L SS	No data at 275°	No data at 275°	No data at 275°
316 SS	No data at 275°	No data at 275°	No data at 275°
317 SS	No data at 275°	No data at 275°	No data at 275°
321 SS	Satisfactory at 300° (1) Compatable at 275° (3) (E)	Satisfactory at 300° (1) No attack at 275° No particle formation (4) (5) (C) (D) No data on pressure (G)	High corrosion at 275° Iron adducts formed (4)(5)(C)(D) No data on pressure (G)

Figure 5.13-64

LITERATURE SURVEY (CONTINUED)

COMPATIBILITY OF MATERIALS IN CONTACT WITH PROPELLANTS AT 275°F

PROPELLANT MATERIAL	N_2H_4	MMH	N_2O_4
347 SS	Exploded at 290° at Bell due to improper cleaning (2)	Satisfactory at 300° (1) No attack at 275° No particle formation (4) (5) (C) (D) No data on pressure (G)	High corrosion at 275° Iron adducts formed (4) (5) (C) (D) No data on pressure (G)
17–4PH SS	No data at 275°	No attack at 275° No particle formation (4) (5) (C) (D) No data on pressure (G)	High corrosion at 275° Iron adducts formed (4) (5) (C) (D) No data on pressure (G)
17–7PH SS	No data at 275°	No attack at 275° No particle formation (4) (5) (C) (D) No data on pressure (G)	High corrosion at 275° Iron adducts formed (4) (5) (C) (D) No data on pressure (G)
Maraging Steel	No data at 275°	Unsuitable, but no high temperature tests conducted (F)	High corrosion at 275° Iron adducts formed (4) (5) (C) (D) No data on pressure (G)
Carpenter 20 Cb	No data at 275°	No attack at 275° No particle formation (4) (5) (C) (D) No data on pressure (G)	High corrosion at 275° Iron adducts formed (4) (5) (C) (D) No data on pressure (G)
Hastelloy C	Unsuitable, but no high temperature tests conducted (H)	No attack at 275° No particle formation (4) (5) (C) (D) No data on pressure (G)	High corrosion at 275° Iron adducts formed (4) (5) (C) (D) No data on pressure (G)
A–286	No data at 275°	No attack at 275° No particle formation (4) (5) (C) (D) No data on pressure (G)	High corrosion at 275° Iron adducts formed (4) (5) (C) (D) No data on pressure (G)
Teflon TFE	Satisfactory at 300° (1) Suitable for long time use at 500° (6) No data on pressure (G)	Satisfactory at 300° (1) Little attack at 275° No particle formation (4) (C) Fuel decomposition occurred (4)(C)	Satisfactory at 300° FEP better than TFE (1) Slight attack at 275° Small precipitate formed (4) (C) No data on pressure (G)
Teflon FEP	Satisfactory at 300° (1) Suitable for long time use at 500° (6) No data on pressure (G)	Satisfactory at 300° (1) Little attack at 275° No particle formation (4) (C) Fuel decomposition occurred (4)(C)	Satisfactory at 300° FEP better than TFE (1) Slight attack at 275° Small precipitate formed (4) (C) No data on pressure (G)

Figure 5.13–64 (Continued)

LITERATURE SURVEY (CONTINUED)

COMPATIBILITY OF MATERIALS IN CONTACT WITH PROPELLANTS AT 275°F

PROPELLANT / MATERIAL	N_2H_4	MMH	N_2O_4
Teflon TFE/FEP Laminate	No data at 275°	No attack at 275° No particle formation (5) (D) No data on pressure (G)	Slight attack at 275° No structure change Small particles formed (5) (D) No data on pressure (G)
Silastic Rubber	No data at 275°	No data at 275°	Dissolved at 275°(5) (D)
Ethylene Propylene Rubber	No data at 275°	No data at 275°	Excessive swelling, Lost all measureable physical properties at 275° (4) (5) (C) (D)
Kynar	No data at 275°	Severely attacked at 275° (5) (D) No data on particles No data on pressure (G)	Severely attacked at 275° (5) (D) No data on particles No data on pressure (G)

(A) DMIC predicts high corrosion
(B) NAA predicts possible problems with oxygen contamination.
(C) 300 hour test
(D) 600 hour test
(E) 72 hour test
(F) Unsatisfactory due to formation of iron oxide which reacts catalytically with MMH. Possible fuel ignition at 275 per Reference 4 and 5.
(G) No data available on pressure generation or gas evolution due to reaction or propellant decomposition.
(H) Not considered for use with N_2H_4 per Reference 4.
(1) Telephone conversation between JPL and McDonnell.
(2) Telephone conversation between Bell and McDonnell.
(3) Telephone conversation between Aerojet and McDonnell.
(4) The Martin Company, "Sterilizable Liquid Propulsion System," by F. Brady and C. Caudill. First quarterly progress report under JPL Contract 951709, January 1967. (Unclassified)
(5) The Martin Company, "Sterilizable Liquid Propulsion System," by F. Brady and C. Holt. Second quarterly progress report under JPL Contract 951709, April 1967. (Unclassified)
(6) Dedapper J.W. and Nadler M., "Non-Metallic Materials for Use With Liquid Rocket Propellants," North American Aviation Inc. Los Angeles, California, Report No. AL–692, May 1, 1951. (Unclassified)
(7) "Supporting Research and Advanced Development," JPL, Pasadena, California, October 31, 1965. Report No. SPS 37–35 Vol IV. (Unclassified)
(8) Liberto, R.R. "Research and Development on the Basic Design of Storable High Energy Propellant Systems and Components," Final Report TR 60–61 Bell Aerosystems Company, Buffalo, N.Y., 19 May 1961. (Unclassified)
(9) Berman, L.D. "Compatibility of Materials With Storage Propellants," The Martin Company, Denver, Colorado, paper presented at the 9th National SMMPE Symposium, Los Angeles, California, November 13–15, 1962. (Unclassified)

Figure 5.13–64 (Continued)

MATERIALS COMPATIBILITY TEST – MATERIALS TESTED

PROPELLANTS	MATERIALS
N_2O_4 MMH N_2H_4 *	Titanium 6Al–4V Aluminum 6061–T6 Aluminum 1100–0 Stainless Steel 304 Stainless Steel 321 Teflon TFE Teflon FEP Premabraze 130 (82% Gold, 18% Nickel)
IRFNA	Test Cancelled

*Test not completed

Figure 5.13–65

types of specimen were loaded into separate test tubes in a common pressure vessel. Propellant was added to each test tube and the entire assembly was sealed and heated. A temperature of 275°F was maintained for 264 hours, during which time the vessel pressure was monitored. The MMH and N_2O_4 tests were completed; the N_2H_4 vessel exploded 10 hours into its test.

- Test Results - the results of the N_2O_4 and MMH tests took the form of vapor pressure, decomposition pressure rise, tensile strength change, propellant composition change, specimen and propellant appearance change and weight change data.

  Vapor Pressure Test - Two of the vapor pressure measurements, N_2O_4 and MMH showed adequate correlation with published values, yielding pressures of 765 psi and 51 psia, respectively. A high value of vapor pressure was observed with IRFNA, resulting from gas evolved during the aforementioned corrosion reaction. The hydrazine pressure rose slowly but steadily throughout the test, obscuring vapor pressure measurements.

  MMH Materials Compatibility Test - All specimens, except 6061 Aluminum, were apparently unaffected by the 264 hour exposure to MMH at 275°F. One of the 6061 specimens was pitted; another showed a black deposit. Evidence of propellant decomposition was furnished by a pressure rise from 54 to 128 psig, during the test. Significant changes in MMH appearance and assay were observed in certain of the specimens as noted in Figure 5.13-66.

  Tensile test and weight change data show no effect from MMH exposure, within the accuracy of the test methods, for all samples except the 6061 Aluminum. The tensile test data from the 6061 Aluminum welded specimens showed a strength gain and elongation loss, presumably due to inadequate heat treat after welding.

  N_2O_4 Materials Compatibility Test - Nitrogen tetroxide proved to be a severe environment for the test samples. Inspection of the samples provided confirmation of reaction. Specific observations are tabulated in Figure 5.13-67.

- Conclusions - Of the metals tested, only 6Al-4V titanium and 321 stainless steel are suitable for containing MMH during sterilization. TFE and FEP Teflon are unaffected, and may be considered. All other materials tested resulted in undesirable changes to the propellant. Additional testing is required to assess the tendency of the above preferred candidate materials to catalyze MMH decomposition at sterilization temperature. Titanium is the only one of the metals tested considered suitable for N_2O_4 containment

MMH MATERIALS COMPATIBILITY TEST
POST-TEST PROPELLANT OBSERVATIONS

	APPEARANCE	ASSAY
Pre-test	Clear	99.64% MMH
Post-test		
Control *	Clear	97.21%
6061 Aluminum	Black residue	97.72% 96.92%
1100 Aluminum	Dark brown viscous liquid layer formed	–
304 Stainless Steel	Green viscous liquid layer formed	–
Premabraze 130 (304 tube)	Reddish brown solution	96.22%
TFE Teflon		96.89%

*Glass Container

Figure 5.13–66

POST-TEST MATERIAL SPECIMENS DATA
N_2O_4 MATERIALS COMPATIBILITY TEST

MATERIAL	TENSILE TEST	WEIGHT LOSS	APPEARANCE
6Al-4V Titanium	Yield and ultimate unchanged – 10% loss in elongation	None	No change
6061–T6 Aluminum	Data discarded – samples not properly heat-treated after weld	2.6%	Corroded – Dense, white crystalline formation on surface
1100 Aluminum	Yield and ultimate slightly reduced – 26% loss in elongation	5.7%	Corroded – Dense, white crystalline formation on surface
304 Stainless Steel	Minor change	3.2%	Corroded – Brown-black film formed on surface
321 Stainless Steel	Minor change	0.14%	Corroded – Brown-black film formed on surface
Premabraze 130	–	–	Corroded – 304 tube blackened. Braze filler detached from tube
TFE Teflon	–	–	No change
FEP Teflon	–	–	No change

Figure 5.13–67

during sterilization. Both TFE and FEP Teflon also appear to be suitable. Further testing of these materials in N_2O_4 is required to assess their capability for use.

Hydrazine Decomposition Test - This test was run to determine the compatibility of the materials listed in Figure 5.13-68 with hydrazine during six 64 hour cycles at 275°F, and to determine the decomposition rate of hydrazine at 275°F while in contact with these materials.

FIGURE 5.13-68

HYDRAZINE DECOMPOSITION TEST

MATERIALS TESTED

CONTAINER	SPECIMEN
6Al-4V Titanium Cylinder	Gemini OAMS "C" Package
6Al-4V Titanium Cylinder	A-70 Titanium Bellows
6Al-4V Titanium Cylinder	6Al-4V Titanium Tensile Specimens
6061-T6 Aluminum Cylinder	6061-T6 Aluminum Tensile Specimens
1100 Aluminum Cylinder	1100 Aluminum Tensile Specimens
321 Stainless Steel Cylinder	321 Stainless Steel Tensile Specimens

Each specimen was tested separately in its own container except the "C" package which was externally attached. Figure 5.13-69 illustrates the test set-up. All specimens exposed to hydrazine were passivated before test for 18 hours in a 25% aqueous solution of hydrazine at 175°F. Ullage volumes were set at about 10% at 275°F for the first heat cycle.

The 1100 Aluminum sample was removed from test six hours into the first cycle because of excessive pressure rise. The pressure rise rates of the other samples were also high. Between the first and second cycles, the ullages were increased to about 15% at 275°F. This was considered to be the maximum practical ullage for the VOYAGER application. The "C" package was excepted and loaded to a 275°F ullage of 45%. It was desired to gather six cycles of compatibility data on the various stainless steels and the glass-filled teflon in that component, without

TEST SET-UP – HYDRAZINE DECOMPOSITION TEST

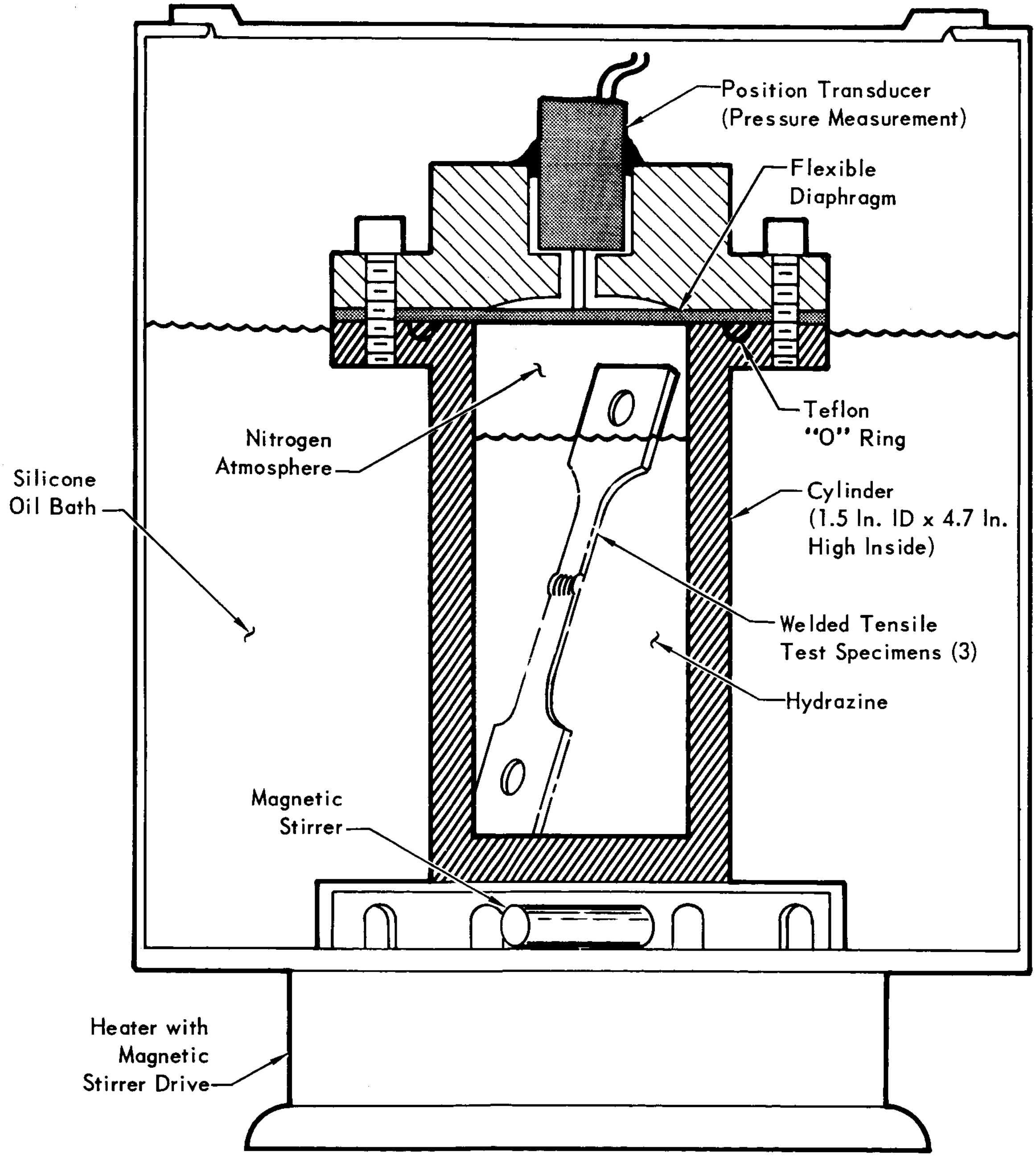
Position Transducer
(Pressure Measurement)
Flexible
Diaphragm
Teflon
"O" Ring
Nitrogen
Atmosphere
Silicone
Oil Bath
Cylinder
(1.5 In. ID x 4.7 In.
High Inside)
Welded Tensile
Test Specimens (3)
Hydrazine
Magnetic
Stirrer
Heater with
Magnetic
Stirrer Drive

Note: Cylinder and Diaphragm are of Same Alloy.

Figure 5.13–69

subsequent opening and venting. The cylinders and specimens were repassivated before being returned to test.

Two samples, the titanium bellows and 6061-T6 Aluminum, were unavailable for the first heat cycle, but were introduced in the second. As a result, the titanium bellows saw only five heat cycles. The 6061 Aluminum and 321 Stainless Steel samples were removed after one and three cycles respectively due to excessive pressure rise (exceeding 200 psig pressure).

The "C" package would have been removed from test for the same reason, had a leak not occurred around the container O-ring when cooled between cycles.

o Test Results - the test results were in the form of pressure rise, specimen, container and hydrazine appearance, and tensile test data. Pressure rise results are tabulated in Figure 5.13-70. Computations are based on the assumption that the pressure rise is the result of the addition of the products of hydrazine decomposition to the ullage volume, according to the reaction:

$$3\ N_2H_4 \rightarrow 4\ NH_3 + N_2$$

Gas evolution rates were computed using an average molecular weight from the reaction products in the ratio indicated. Evolution rates in titanium are seen to be the lowest for all materials tested. Aluminum induces an initial decomposition rate about one order of magnitude greater than titanium. Stainless steel appears to be three times as active as titanium.

One aluminum sample, 6061, became more passive with time, but the activity was unacceptably high even at the end of the test. Titanium became more passive with each succeeding cycle. The "C" package rate was inordinately high, possibly due to its comparatively rough interior finish.

Appearance of the aluminum samples all showed corrosion after exposure to hydrazine. In its six hour exposure period the 1100 Aluminum showed a light, white powdery film. The 6061 Aluminum, after being exposed a full 64 hours, showed pitting as well. The hydrazine samples from these tests both contained small quantities of white, gelatinous precipitate. The 321 Stainless Steel samples and the "C" package were unaffected. Small, black specks were noted in the hydrazine sample taken from the 321 stainless cylinder. The titanium samples were unaffected by the exposure. Of

HYDRAZINE DECOMPOSITION TEST RESULTS

DECOMPOSITION RATES AT 275°F – 64 HOUR HEAT CYCLES

	HEAT CYCLE NUMBER	ULLAGE (%)	PRESSURE RISE RATE (psi/hr)	GAS EVOLUTION RATE (SCC/hr)	GAS EVOLUTION RATE PER UNIT WETTED AREA (SCC/hr-in.^{2})
6Al–4V Titanium with Gemini OAMS "C" Package (304L, 321, 347, 17–7 PH St. Stl.; FEP Teflon, With and Without Glass Filler)	1	8.4	5.75	3.42	–
	2	46.5	.64	2.72	–
	3	46.5	.91	3.86	–
	4	46.5	1.21	5.15	–
	5	46.5	1.00	4.26	–
	6	46.5	1.11	4.72	–
6 Al–4V Titanium Cylinder, With A–70 Titanium Bellows	1	–	–	–	–
	2	16.3	.83	.86	.016
	3	16.3	.56	.58	.011
	4	16.3	.53	.55	.010
	5	16.3	.44	.45	.009
	6	16.3	.41	.42	.008
6Al–4V Titanium Cylinder, With 3 6Al–4V Titanium Tensile Test Specimens	1	6.32	.83	.33	.009
	2	12.4	.33	.26	.008
	3	12.4	.25	.20	.006
	4	12.4	.23	.18	.005
	5	12.4	.20	.16	.005
	6	12.4	.20	.16	.005
6061–T6 Aluminum Cylinder With 3 6061–T6 Aluminum Tensile Test Specimens	1	–	① –	–	–
	2	16.8	3.0/1.5②	3.1/1.55	.097/.049
	3	–	–	–	–
	4	–	–	–	–
	5	–	–	–	–
	6	–	–	–	–
1100 Aluminum Cylinder With 3 1100 Aluminum Tensile Test Specimens	1	11.4	4.7	3.27	.095
	2	–	–	–	–
	3	–	–	–	–
	4	–	–	–	–
	5	–	–	–	–
	6	–	–	–	–
321 Stainless Steel Cylinder, With 3 321 Stainless Steel Tensile Test Specimens	1	11.57	1.80	1.31	.038
	2	17.75	1.56	1.75	.056
	3	17.75	1.65	1.85	.059
	4	–	–	–	–
	5	–	–	–	–
	6	–	–	–	–

Note: Density of hydrazine at 275°F taken as 0.898 gm/ml.

① Average rate for first 27 hours.

② Average rate for final 37 hours.

Figure 5.13–70

particular interest was the 20% glass-filled Teflon seat seal in the "C" package manual valve, which had been tested in the full closed position. This seal showed some evidence of extrusion into the various clearances surrounding the seal, and it had taken on a brownish color. It had apparently retained the resistance to compression loading for which it was originally selected.

Tensile properties of the samples showed significant changes but weight changes were negligible.

o Conclusions - Titanium is the best known tank material for 275°F heat sterilization of hydrazine. It is unaffected by hydrazine and is the most passive. Stainless Steel, 321, is less passive, but it likewise is unaffected. Aluminum alloys 1100 and 6061 are unsatisfactory. FEP Teflon, with 20% glass filler, is durable under the hydrazine sterilization environment. Its activity with regard to hydrazine decomposition is unknown and should be investigated before use. The transition from smooth, regularly shaped test specimens to irregular equipment shapes of variable surface finish should be investigated relative to its effect on hydrazine decomposition rate.

Compatibility of Shell 405 Catalyst and Ethylene Oxide - This test was performed to determine whether the ethylene oxide decontamination process, specified for VOYAGER equipment, would affect the activity of Shell 405 hydrazine catalyst.

A monopropellant rocket engine, furnished by Hamilton Standard, was used to measure catalyst performance. As a control, the performance of the engine was mapped prior to decontamination. Following decontamination (and heat sterilization) engine performance was again measured to detect performance change. The engine firing tests were run at room temperature with altitude simulation; the combustion chamber and nozzle were insulated to simulate spacecraft installation. Decontamination cycles were performed in conformance with the requirements of JPL specification VOL 50503 ETS. Exposure consisted of 6 cycles, each 29 hours in length, with 26 hours at a stabilized temperature of 122°F. The atmosphere in the test chamber was 12% ethylene oxide, 88% Freon 12 and 50% relative humidity. Ethylene oxide concentration was 600 mg/liter. The ethylene oxide exposure was followed by an 18 hour desorption step, in air. The engine was then sterilized at 275°F, in a nitrogen atmosphere, for 64 hours. The propellant valve was removed during the exposure to ethylene oxide and sterilization temperature.

- Results - In the pre-exposure firings the performance of the engine was comparable to the manufacturer's data.

  There was no perceptible interaction between ethylene oxide and the Shell 405 catalyst during the decontamination cycles.

  In the post exposure firing attempts, the engine exhibited erratic performance. Degraded thrust was experienced on the first attempt. After an ignition delay of .16 second, thrust built up to 27% of rated in an additional .14 sec, at which time an automatic cutoff actuated. During three additional firing attempts over a one hour period the engine failed to ignite. Propellant flow to the chamber was verified by flow meters and, visually, by the accumulation of frozen propellant on the nozzle walls. The engine was allowed to stand overnight and firing attempts the following day resulted in ignition with thrust recovering from 50% to 100% of rated in four tests of 14 seconds accumulated time. A pressure overshoot accompanied the first ignition; performance returned to normal as burning time was accumulated on the engine.
- Conclusions - Shell 405 catalyst is poisoned by exposure to the ethylene oxide-Freon 12 decontaminating agent. Catalyst activity is restored after repeated firing attempts. It will be necessary to seal this catalyst from the environment during ethylene oxide decontamination or conduct additional tests to investigate recovery of catalyst activity under high vacuum and/or ambient exposure.

5.13.4.2.2 - Propulsion System Design Considerations - The test results and conclusions reported from the JPL and McDonnell test programs provide a good basis for initiating a sterilizable propulsion subsystem design. However, there are many items which require special consideration, and certain problems which must be resolved before a satisfactory sterilizable design can be completed.

The selection of N_2O_4 as the oxidizer for a bipropellant system is adequately justified on a performance basis, and if properly inhibited with NO it is definitely less active than IRFNA. The Apollo titanium tank failures experienced at Bell Aerosystems were traced to lack of NO inhibitor. The possibility that the failures resulted from chlorine-initiated stress corrosion has been disproven.

Monomethyl hydrazine possesses very desirable thermal characteristics and is compatible with most commonly used propulsion subsystem materials. Its decomposition characteristics, however, have not been defined for high temperature exposure to the various materials. This should be evaluated and the development of techniques for passivating materials for MMH need to be pursued. Compatibility tests conducted so far have included only corrosion effects during sterilization. Long term storage, 43 weeks, tests are mandatory to support final material selection for use with both N_2O_4 and MMH propellants.

Appreciable decomposition of hydrazine occurs when in contact with the most compatible materials (titanium) at sterilization temperature. Better passivation techniques need to be developed to minimize this problem. The effect of excessive decomposition may be minimized by increasing the design pressure requirement or increasing the ullage volume to reduce pressure rise during sterilization. However, if decomposition is appreciable in quantity the gas evolved may also affect engine performance.

Because no non-metallic materials have been found that are compatible with N_2O_4 for extended periods at 275°F, the system exposed to the propellant must be constructed entirely of titanium with possible deviations only in valve seals.

While not included in either of the tests reported, O-rings consisting of Teflon, Viton, some silicones, Kel-F, EPR and certain butyl rubbers are considered to be compatible with dry heat sterilization when used dry for static seals. For seals which are to be exposed ultimately to propellant, Teflon is best for N_2O_4 service, while EPR and some butyl rubbers have short term N_2O_4 compatibility. These materials may also be used with N_2H_4 and MMH. Carboxy nitroso rubber, a new product, has shown promise as a seal for N_2O_4 and will be investigated for sterilization survival.

The adhesives investigated in the JPL program, many of which are typical of those used in ablative thrust chambers, are compatible with the ethylene oxide decontamination procedure. However, each showed undesirable property changes when exposed to dry heat sterilization. This indicates the need for careful design study of ablative chambers, particularly in the areas of adhesive joints and external support for removal of vibration loads if ablative chambers are to be employed for the VOYAGER Capsule Bus.

Component Selection Considerations - Component designs are affected by the requirement to withstand sterilization and decontamination. The most severe impact is felt in the designs of components which are in contact with propellant during sterilization.

- Pressurant Subsystem - The pressurant subsystem presents no particular problem related to sterilization, except all materials must be stressed to allow for pressure increase and decreased materials stress capability at the higher temperatures. Pressure regulator, manual valve, burst disc, filter and check valve designs which will withstand the high temperature do not appear to present a problem.

- Propellant Subsystem - All metal components exposed to N_2O_4 during sterilization must be constructed of Titanium 6Al-4V, which is the only known compatible metal. The only feasible seal material for use with high temperature N_2O_4 is Teflon and additional exploration of the area is required. Stainless steels are not attacked by MMH and N_2H_4, but tests show that N_2H_4 decomposes more rapidly when exposed to these metals than when exposed to titanium. Data are not available for MMH but a similar result may be anticipated.

In the absence of better data, titanium should be used in storage tanks for N_2O_4, N_2H_4 and MMH. Positive expulsion devices should also be of titanium. Bellows have been fabricated successfully from titanium by Sealol, Inc., and this offers the best approach to positive expulsion at the present time.

Manual fill valves for N_2O_4 have to be constructed entirely of titanium. This presents a new design problem. The tendency of titanium to gall will present a problem for conventional V-threads. Surface hardening techniques such as cold rolling the threads may be effective. ACME threads may also be applicable. The practicality of using lubricants in this area is highly questionable. Fill and drain valves used with N_2H_4 and MMH systems may not have to be titanium since each is compatible with other materials, but the decomposition characteristics of these propellants may also dictate titanium on the wetted side. Teflon seals may be used at the valve stem, however, after final fill of the propellant tanks both the valve stem and outlet should be covered with closure caps and seal welded.

A burst diaphragm in which all exposed surfaces are titanium is not seen to present a serious problem. Current designs for this type of device are based on concepts which do not depend heavily upon the properties of the barrier material. Successful designs have been used in which the barrier is either self-supported or separately supported; this support fails or moves under the design pressure load and the barrier is then ruptured by an auxiliary cutter. The use of titanium in this device seems to present only routine development problems. Titanium burst diaphragms have been used successfully by the chemical process industry.

A pyrotechnic-actuated valve with a titanium inlet lends itself to a simple, unique solution. The valve developed and qualified for the Gemini propulsion systems was fabricated of stainless steel. Figure 5.13-71 depicts in cutaway the general configuration of that valve. Adaption of this proven design to incorporate titanium where it is needed is accomplished by replacing the inlet tube detail with one made of titanium, also shown in Figure 5.13-71. The problem of weld assembling the titanium inlet to the stainless valve body is solved by using a coextrusion of stainless steel and titanium and machining a weld lip in the stainless outer portion of the coextruded transition piece. The intermetallic bond is fully adequate in load capability and leakage, and remains so provided the interface is kept below 1400°F during weld assembly. The stainless shoulder provides sufficient distance between the stainless weld zone and the titanium to stainless transition to meet this restriction. The inlet will be welded to the titanium tankage. This valve modification will provide convenient transitions to stainless steel upstream and downstream feed systems, while providing a titanium surface in the propellant storage system. Relative to the pyrotechnic actuator portion of the valve, testing of the Apollo standard initiator at McDonnell (Reference Part C, Sec. 2.7) has successfully demonstrated compliance with sterilization, and development of an actuator to meet VOYAGER requirements should be accomplished relatively easily.

The design of a pressure transducer in which only titanium is exposed to the stored propellant presents significant problems. Transducers which utilize titanium sensing elements are unlikely candidates since the hysteresis characteristics of titanium are poor, based on instrument standards.

The approach which is most likely to be successful is that of interposing a flexible titanium barrier between the propellant system and the sensing element. Some penalties in accuracy are to be anticipated, but this is expected to be the most fruitful approach.

NORMALLY CLOSED PYROTECHNIC VALVE
(GEMINI CONFIGURATION)

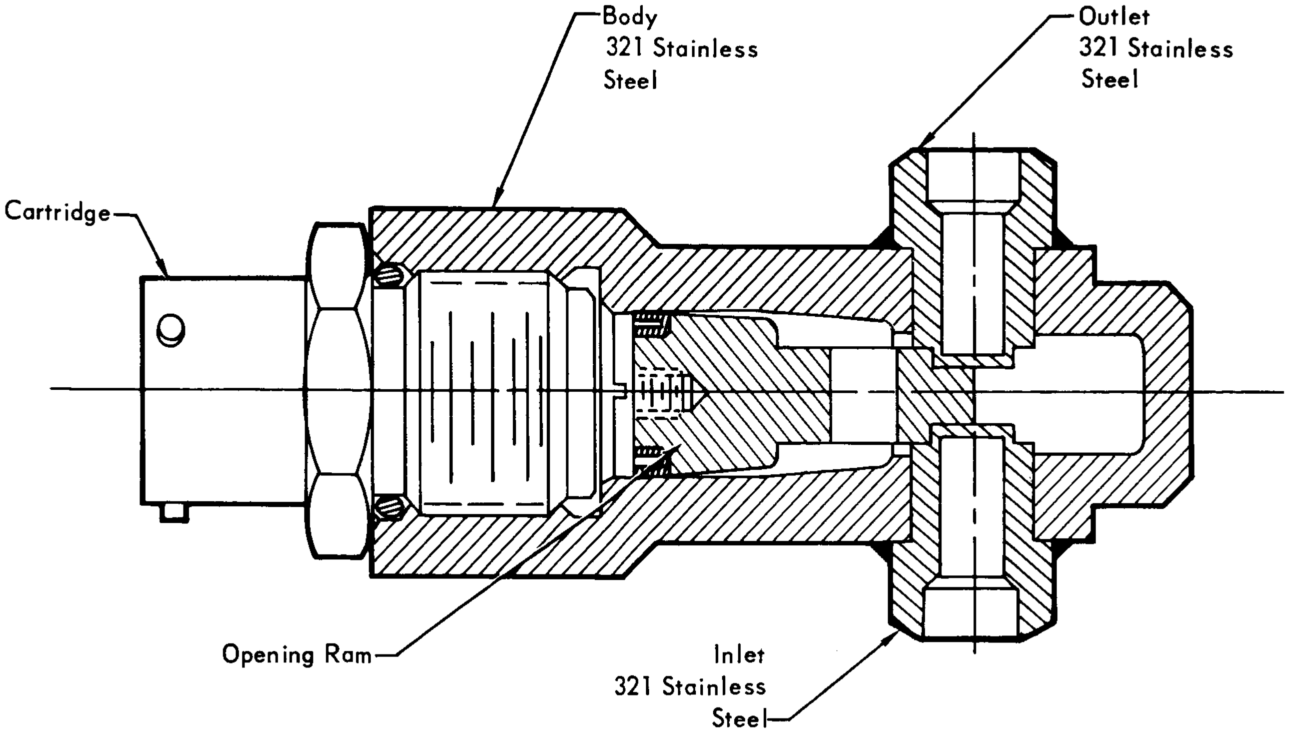
Body
321 Stainless
Steel
Outlet
321 Stainless
Steel
Cartridge
Opening Ram
Inlet
321 Stainless
Steel

NORMALLY CLOSED PYROTECHNIC VALVE
(VOYAGER CONFIGURATION)

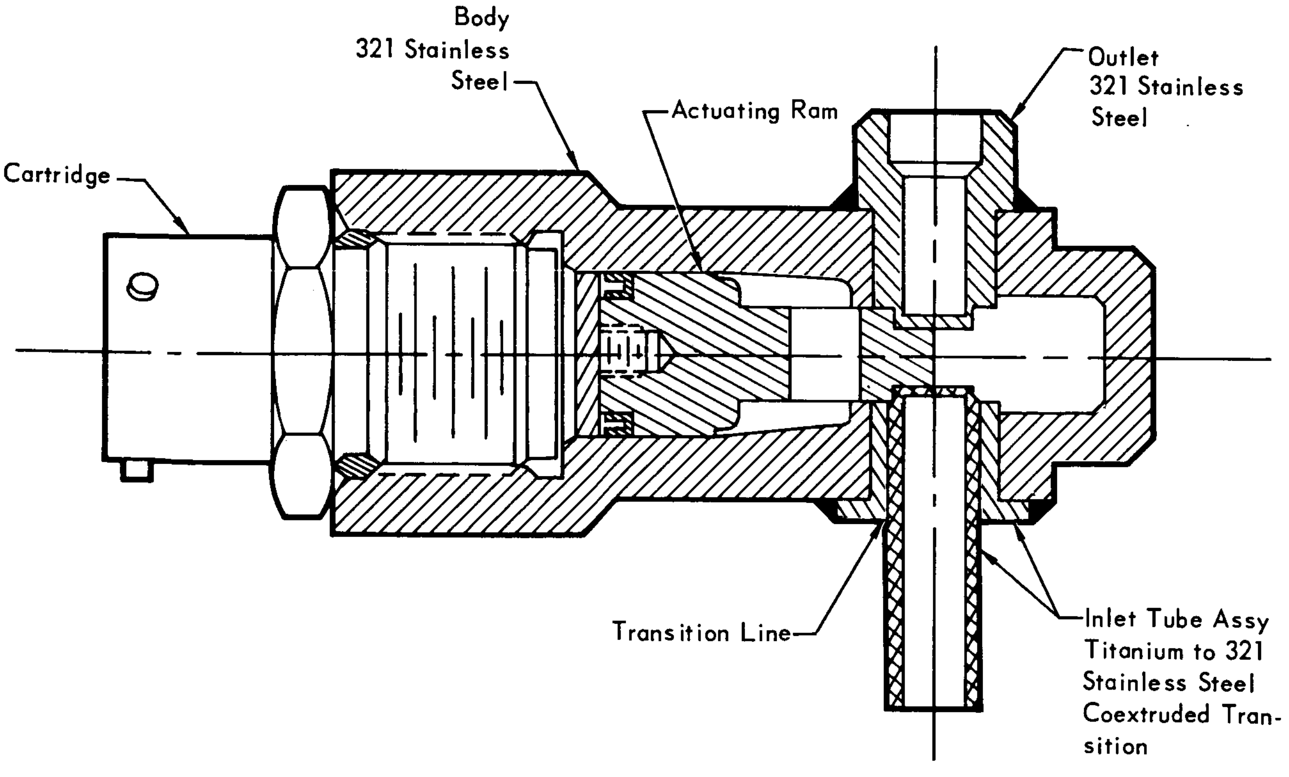
Body
321 Stainless
Steel
Actuating Ram
Outlet
321 Stainless
Steel
Cartridge
Transition Line
Inlet Tube Assy
Titanium to 321
Stainless Steel
Coextruded Transition

Figure 5.13-71

- Rocket Engine - Sterilization presents the same conditions to engine valves as for the other valves not wetted when sterilized, and as such, engine valves are not seen to present major problems. The only potential problem with the bipropellant rocket thrust chambers is degradation of ablative chamber properties from dry heat sterilization. Results, reported by various rocket manufacturers show this effect to be negligible, relative to the ability of the engine to meet the VOYAGER mission requirements.

  The N_2H_4 monopropellant engine catalyst is made inactive by exposure to ethylene oxide. It must, therefore, be sealed with a frangible diaphragm.

- Lines and Connectors - All lines exposed to propellants during sterilization should be titanium. These are required in the N_2O_4 system to assure material compatibility. In the N_2H_4 and MMH lines, titanium minimizes propellant decomposition. Other lines may be of aluminum or, preferably, stainless steel.

  Line connections may be welded or brazed if stainless lines are used. Aluminum lines must be welded. Transitions between aluminum, titanium and stainless may be accomplished using coextrusions of the two metals to be joined as applied on the Apollo LM Descent pressurant tank. Titanium lines must be welded; applicable braze fillers are not propellant compatible. Threaded connections will not be used since their leakage potential is excessive.

5.13.4.2.3 Conclusions and Recommendations - It is feasible to develop and qualify a liquid propulsion subsystem to meet the VOYAGER Capsule Bus sterilization requirements. The subsystems must utilize titanium in systems exposed to nitrogen tetroxide during sterilization. Titanium should also be used for N_2H_4 and MMH systems to minimize propellant decomposition. Titanium bellows offer the only really adequate positive expulsion technique. Elastomeric seals exposed to N_2O_4 during sterilization should be avoided. If seals are required, additional development work must be done. Teflon is the best candidate for seal material. Manual fills and drain valves for the N_2O_4 system introduce thread galling problems if designs of titanium are required for compatibility. Further study in this area is needed. The oxidizer pressure transducer, also requiring titanium construction, requires special design and testing work. The decomposition characteristics of N_2H_4 with various metals have been established. Similar data for MMH should be gathered. Although, many other component design and development problems are evident, the basic knowledge is available to assure solutions. The current JPL Sterilizable Liquid Propulsion System Program will provide additional information, valuable to the design, development and qualification of propulsion subsystems for the VOYAGER Capsule Bus. A program to carry an N_2H_4 system to the same degree of development should be initiated.

5.13.4.3 Sterilization Of Solid Propellant Rocket - The VOYAGER sterilization requirement imposes significant development demands on solid rocket motor design. The specified exposure of six cycles at 275°F far exceeds the technology employed in current solid rocket motors. Further, the need for a five year shelf life and nine month vacuum exposure capability introduces additional unknowns, which require investigation. It is essential to meet these requirements and maintain a high level of rocket performance.

Test data from various sources show that current propellants will not withstand the thermal sterilization exposure. Other available component materials such as liners, insulation, O-Rings, nozzles and igniters also appear to be inadequate. Current motor design techniques are applicable and will aid in the solution of the high temperature exposure problem.

Development work to overcome these problems has been underway by various industry and governmental organizations for well over two years. Specifically, J.P.L., Aerojet, Thiokol and UTC have made significant contributions in special areas. McDonnell has kept abreast with developments in this field to ensure that the technical risk involved is properly assessed in evaluating selection of solid rockets for applications to the VOYAGER Capsule Bus. These developments are discussed in the following paragraphs.

Propellants - The primary problem associated with the development of a sterilizable propellant is the degradation of initial physical properties during the required sterilization exposure cycles. The specific properties of concern are tangent modulus, maximum stress and strain at maximum stress.

The selected propellant must also have adequate processing properties to allow fabrication of a void-free motor assembly, low viscosity to allow good mixing and casting and good pot life to assure time to cast.

It is also desirable to have high energy to provide an efficient system with minimum volume and weight. This is usually achieved by a high solid loading in the candidate formulation. All of the above required and desired properties in a propellant are usually not compatible. Therefore, careful trade-offs must be made. The following sections discuss several specialized areas of current effort.

- Oxidizer - To date a preponderance of the industry development effort has been concentrated on the use of ammonium perchlorate as the oxidizer. Preliminary test data on small samples indicate that recrystallizing the oxidizer repurifies the material and makes it more stable at high temperatures. The standard grade as used in current off-the-shelf propellants tends to decompose at elevated temperature with consequent degradation of the propellant physical properties.

- Binders - Several different binder systems have been investigated in an effort to achieve stable propellant physical properties during the thermal sterilization heat cycles. The most promising candidates are: saturated carboxy-terminated polybutadiene, hydroxy-terminated polybutadiene both saturated and unsaturated, and saturated carboxy-terminated polyisobutylene. It appears from preliminary test data supplied by the propellant manufacturers that saturating the binder system with hydrogen to decrease the number of unstable double bonds improves the thermal stability. Figures 5.13-72 and 5.13-73 show the effect of saturating the binder on the propellant physical properties.
- Curing Agents - The accepted curing agent for modern carboxy-terminated polybutadiene propellants is a mixed curing system of MAPO, a trifunctional imine, and "ERLA", a trifunctional epoxide. In the past the stoichiometry or ratio of polymer to curing agent and the ratio of MAPO to ERLA has been deliberately tailored to give maximum elongation at low temperatures (-65°F) with maximum stability of aging at ambient storage (80°F - 100°F).

  These ratios are now being tailored in the other directions with promising results. The goal now for VOYAGER is to achieve thermal stability or strength during the heat cycles and maximum storage stability at ambient (0°F - 100°F) during transit from Earth to Mars.
- Plasticizers - In general, plasticizers are inert molecules that do not take part in the chemical reaction during cure and act somewhat as a lubricant between the long chain hydrocarbon molecules in the cured or polymerized propellant binder. These free molecules cause the propellant to be more flexible and have more elongation. It is generally added to formulations as an added ingredient and an aid in low temperature systems to increase elongation. At high temperatures these materials, which are not chemically attached, tend to migrate and concentrate at the propellant boundaries, i.e., the bond line between propellant and liner or insulation. Thus excess plasticizers tend to destroy the bond between propellant and liner.

  Again the reduction of plasticizer to very small quantities in the

STERILIZATION EFFECTS ON PROPELLANT

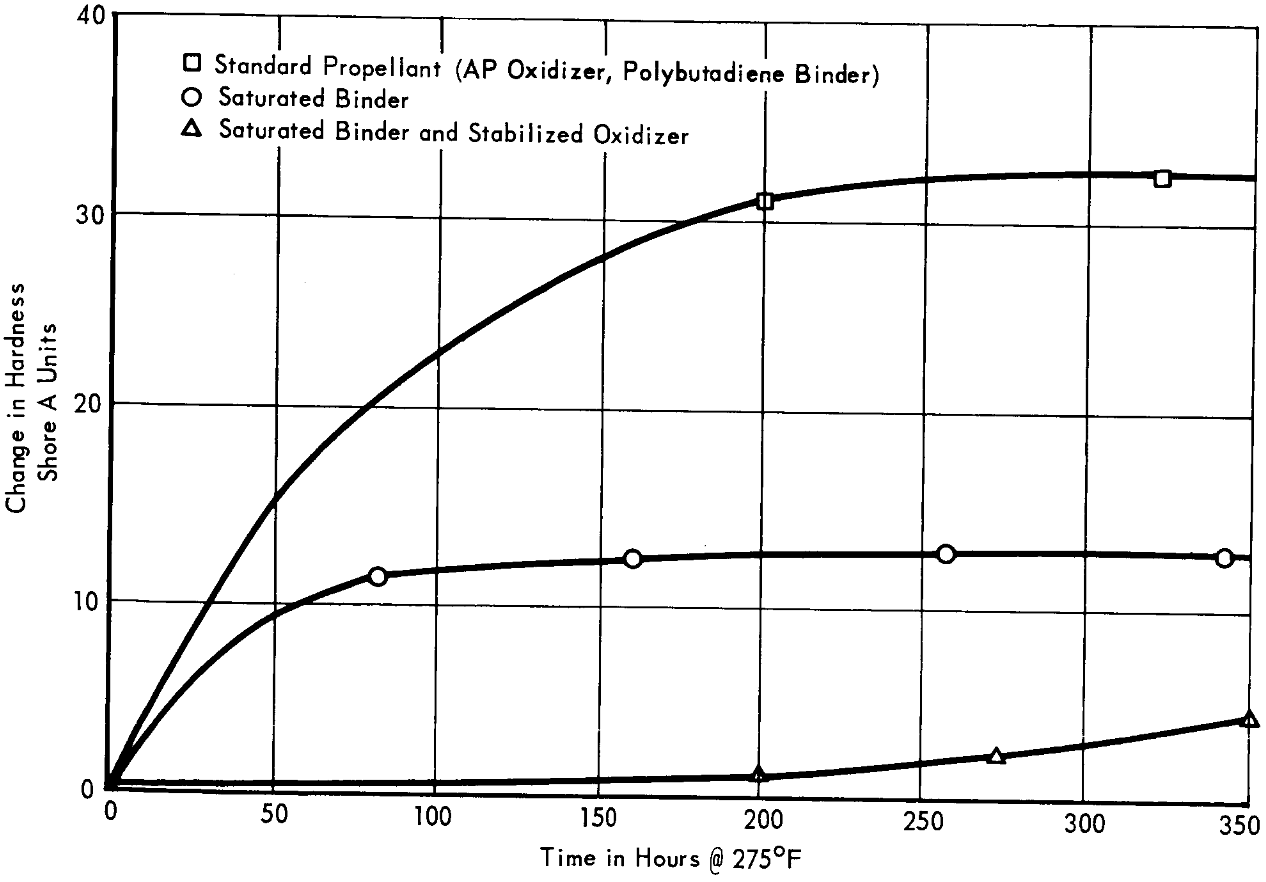

(From Aerojet-General Corporation)

Figure 5.13-72

STERILIZATION EFFECTS ON PROPELLANTS

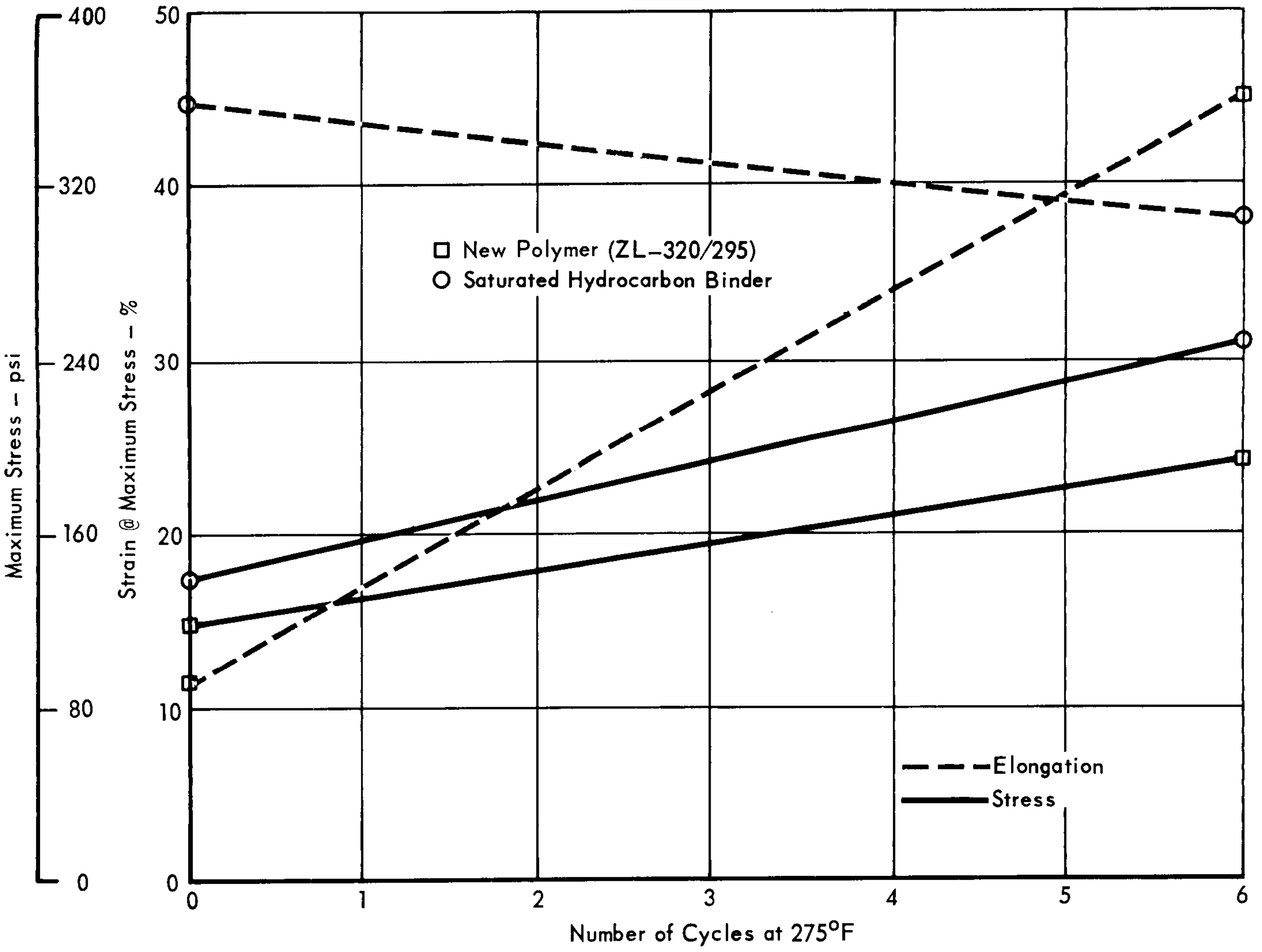

(Based on data from Thiokol Chemical Corp.)

Figure 5.13–73

basic propellant formulation for VOYAGER candidates or the elimination of plasticizers altogether is desirable if the necessary fluidity in the uncured propellant can be maintained.

- Vacuum Stripping Low Molecular Weight Compounds - Another technique which has been developed in an effort to improve the vacuum storage capability of propellants is the removal of low molecular weight compounds from the formulation. These light fractions tend to leave during vacuum exposure with corresponding weight loss, outgassing and swelling of the propellant. The elimination of these low molecular weight compounds prior to mixing the propellant by vacuum stripping of the raw materials has shown a significant increase in the stability of cured propellant samples. This same technique has also shown a significant increase in the thermal stability of cured propellant when subjected to the sterilization heat cycles.
- Anti-oxidants - The use of small amounts of stable anti-oxidants in the propellant formulations has significantly reduced the degradation of propellant physical properties in small samples subjected to the heat sterilization cycles. It is believed that small amounts of anti-oxidant will have no detrimental effects on other properties of the cured propellant such as would affect ballistics or performance. However, this is an unknown area and it would be desirable to avoid this addition if possible.

Liner and Insulation - Heat sterilization has resulted in an increase in the erosion rate of some flexible insulations, particularly BUNA-N rubbers filled with silica. Glass fibers or asbestos fibers appear to be stable. Additional thickness to allow for the increase in the erosion rate can be handled in the design of the de-orbit motor.

Liner materials are usually of the same basic polymer family as the propellant and are used primarily as a bond promoter between the propellant and the insulation or chamber. By the use of the same polymer and curing agent for the liner (in conjunction with a partial cure) a very good bond usually results during the propellant cure. In general, liners with high concentration of plasticizer appear to degrade during the heat sterilization cycles; plasticizer migration also causes bond failures between propellant and liner and between liner and insulation or chamber.

The same techniques discussed under propellants show a significant improvement in thermal stability of the liners, namely, plasticizer elimination, saturating the binder, changing the curing agent to polymer ratio and vacuum stripping the low molecular weight compounds out of the raw materials prior to use.

"O-Rings" - O-Rings of different materials have been tested at Aerojet and, while some materials showed severe degradation from the sterilization heat cycles, several candidates remained reasonably stable. Viton appeared particularly good, and appears to be an acceptable candidate.

Nozzles - Current plastic nozzles constructed of phenolics with glass tape or carbon cloth lay-up have not been optimized for best resins or optimum cure conditions to withstand heat sterilization. The only major problem appears to be an increase in char regression rate which can be compensated for in the basic design with very little weight penalty.

Igniter - The igniter is not considered to be a special problem since a pyrogen type would probably be used and thus employ the same propellant, liner and insulation as developed for the main motor. Squibs developed by Holex and Space Ordnance for other applications appear capable of withstanding the VOYAGER heat requirement. Furthermore, testing of the Apollo standard initiator at McDonnell successfully demonstrated acceptability for sterilization.

Motor Case - Aerojet reports that subjecting their glass chamber to the sterilization heating cycles increased the strength of the chamber and also appeared to anneal the aluminum bosses provided for nozzle and igniter attachment, yielding increased physical properties. However, metal chambers support the propellant grain during the firing loads (rapid pressurization) and, therefore, require a lower elongation in a candidate propellant by as much as 40%. Based on these reasons, a metal case is preferred. For the loading due to temperature (thermal changes during storage) the two chambers are very nearly the same. These curves are shown for glass and titanium chambers in Figure 5.13-74.

Other considerations - The current requirements for sterilization specifies the major portion of the atmosphere used for heating may be nitrogen. The use of nitrogen as the heating medium has shown a significant reduction in the amount of degradation exhibited by candidate formulations at Aerojet. This effect is shown for a typical propellant in both air and nitrogen in Figure 5.13-75.

Simplifying the grain geometry to lower the strain requirements and the use of "boots" in areas of high bond stresses are other methods available to the designer to help solve the overall problem. Significant reductions can be made in the physical property requirements of candidate propellants by these methods.

Conclusion - Much has been learned in the past two years about the sterilization characteristics of the various components which make up a complete rocket sub-

CHAMBER MATERIAL EFFECTS ON PROPELLANT STRAIN

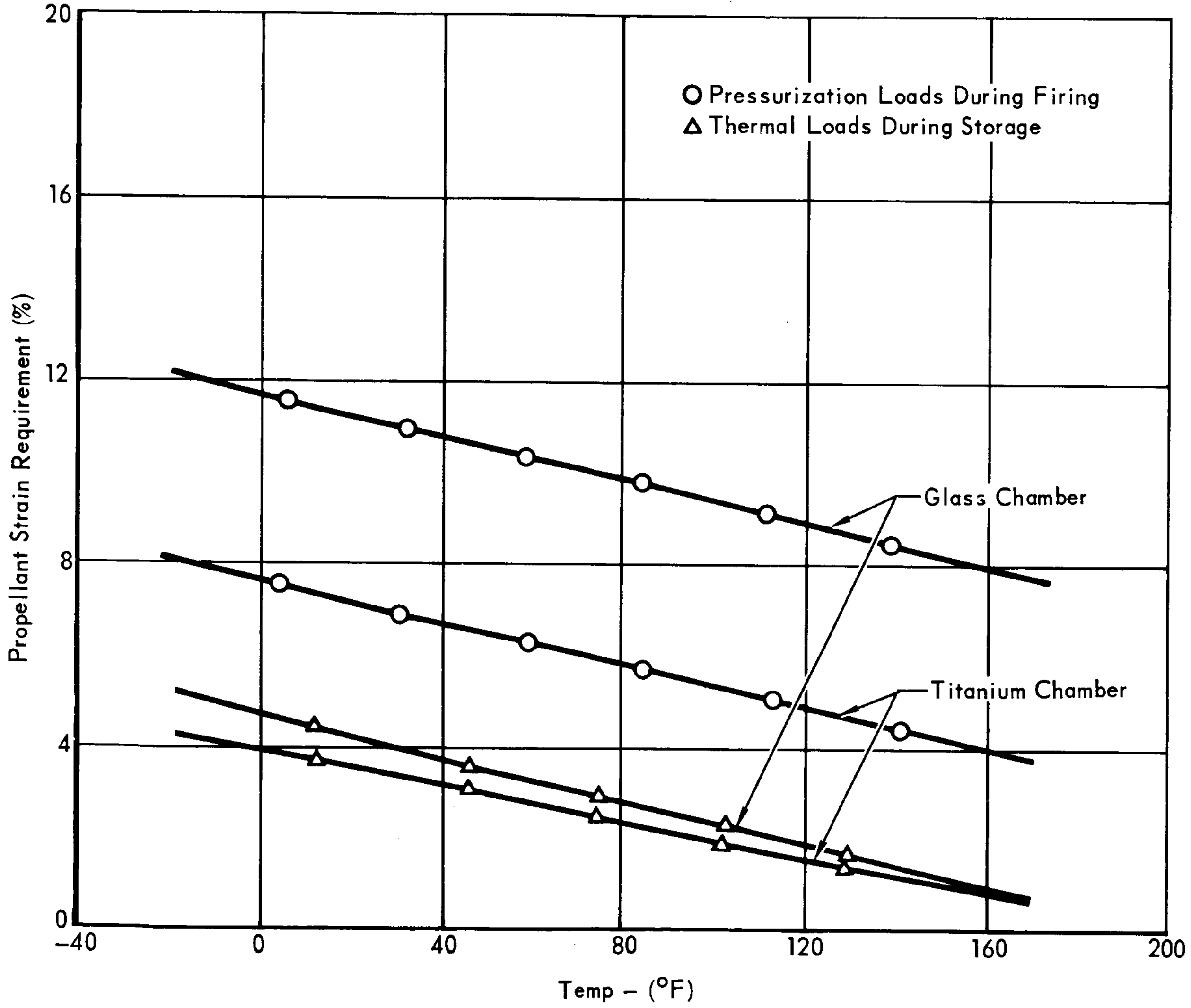

(From Aerojet-General Corporation)

Figure 5.13–74

EFFECT OF STERILIZING ATMOSPHERE ON PROPELLANT PHYSICAL PROPERTIES

PROPELLANT: TP-H-3105

TIME	STRESS		STRAIN		MODULUS	
(hr) AT 295°F	(psi)		(in/in)		(psi)	
	AIR	NITROGEN	AIR	NITROGEN	AIR	NITROGEN
0	128	128	0.27	0.27	918	918
40	187	183	0.26	0.24	1260	1390
80	151	160	0.06	0.21	5750	1100
108	53	175	0.03	0.28	3030	1070

(From Thiokol Chemical Corporation)
Pull Data @ 77°F

Figure 5.13-75

system. Results to date have been encouraging. In addition, small scale rockets have been tested with reasonable success. It is realized, however, that as the propellant stresses and strains develop, surface bond loading and other design considerations become significantly more critical as dimensions are increased to the scale required by the Flight Capsule de-orbit motor.

The major component development item is clearly the propellant and liner system. Several formulations have been investigated by various organizations and some warrant consideration for the sterilizable rocket. In this critical area, it is recommended that two or three propellant development programs be funded to evaluate different formulations.

At least one of these formulations should be based on current binder systems to minimize the unknowns introduced. A system consisting of polybutadiene carboxy terminated binder and ammonium perchlorate oxidizer is recommended. The following modifications should be considered:

- Saturate binder with hydrogen to improve its thermal stability.
- Eliminate the plasticizer to maintain bond integrity.
- Recrystallize oxidizer to improve its thermal stability.
- Vacuum strip low molecular weight components to reduce weight loss, outgassing and swelling and to improve stability.
- Sterilize in high nitrogen atmosphere to reduce oxidation.

The above changes to the basic propellant formulations should have no significant detrimental effect on aging, storage or performance. One additional change, which is not considered major, is adjustment of the ratio of curing agent to polymer and the ratio of imine to epoxy in the curing agent to permit optimization for the high sterilized temperature.

The other two propellant candidates should be chosen from new formulations, under investigation by various rocket companies, which appear to offer advantageous characteristics compared to the CTPB propellant.

The least explored area in rocket motor sterilization is the motor design. Full scale designs which minimize propellant grain stresses and strains, bond loading, etc. must be developed. Testing should proceed as soon as possible to ensure that design techniques are adequate for materials available.

The steps recommended above plus a concerted development and qualification effort should ensure the availability of a qualified solid rocket motor for the 1973 VOYAGER Mission.

5.13.4.4 Thrust Vector Control - The Capsule Bus requires attitude control throughout most of the mission. During unpowered phases reaction control subsystems are required. However, during the de-orbit and terminal deceleration phases, thrust vector control (TVC) may offer advantages over reaction control subsystems. Various TVC concepts have been evaluated to determine the best mechanization for each of the candidate de-orbit and terminal propulsion subsystems discussed in Sections 5.13.1 and 5.13.3. The requirements, analyses, selection criteria and the recommended TVC for each candidate propulsion subsystem studied are described in this section.

Requirements - Of the two propulsion maneuvers, de-orbit imposes the most straightforward control requirements, depending only upon the accuracy of thrust alignment through the vehicle c.g. Control demands during terminal deceleration, on the other hand, are influenced by thrust alignment accuracy, the preferred landing approach and Capsule Lander packaging constraints which contribute to adverse c.g. excursions during engine operation.

Attitude control is necessary during de-orbit thrusting to insure pointing accuracy of the velocity vector. The primary disturbing force results from thrust malalignment and, for our preferred Capsule Bus arrangement, this has been established as a $\pm 3\sigma$ value of .273 inch. The data used in deriving this error are shown in Figure 5.13-76. Based on this alignment error and a de-orbit ΔV of 950 ft/sec, the maximum estimated pitch/yaw torque impulse for VOYAGER missions is 5600 ft-lb-sec. Roll disturbances by the de-orbit motor are negligible.

Attitude control is also required during terminal propulsion deceleration to counteract c.g. shift during propellant usage, thrust malalignment and aerodynamic disturbances, and to align the roll axis of the Capsule Lander along the velocity vector. Control requirements for worst case atmospheric wind conditions and c.g. offsets were evaluated in conjunction with our preferred landing approach and have been conservatively established as 1000 ft-lb for pitch/yaw and 560 ft-lb for roll.

Error sources contributing to thrust malalignment and the c.g. shift with terminal propellant usage are presented in Figures 5.13-76 and 5.13-77, respectively. The shift in vehicle c.g. with propellant usage is a function of the tankage arrangement and the ratio of propellant weight to vehicle weight for the terminal deceleration maneuver. The tankage arrangements are similar for the 1973 and 1979 missions, wherein the fuel tank is mounted at a larger radius from the vehicle roll axis and diametrically opposite the oxidizer tank to insure a nearly balanced propellant load during subsystem operation. Ideally, the ratio of tank mounting radii

THRUST ALIGNMENT ERRORS

ERROR SOURCE	DE-ORBIT BURN		TERMINAL BRAKING	
	± VALUE in	$(\pm \text{VALUE})^2$	± VALUE-in	$(\pm \text{VALUE})^2$
1. C.G. Uncertainty	0.100	0.0100	0.100	0.0100
2. Thrust Vector				
– between mechanical and 'true' – 0°6'	0.115	0.0132	0.042	0.0018
– Variation during burning – 0° 10'	0.192	0.0369	0.070	0.0049
3. Aiming				
– Fixture	0.024	0.0006	0.024	0.0006
– Alignment	0.020	0.0004	0.020	0.0004
– Rocket Mounting	0.059	0.0035	0.040	0.0016
4. Structural Deflection	0.066	0.0044	0.386	0.1490
5. Fluids				
– Servicing	0.039 (RSS of de-orbit & terminal)	0.0016	0.036	0.0013
– During Usage (see Figure 5.13–77	–	–	0.550	(1)
– M.R. Control, 1.6±0.088	0.063	0.0040	0.120	0.0144
$\Sigma\,(\text{Value})^2 =$		0.0746		0.1840
Total Root Sum Square $\sqrt{\Sigma\,(\text{Value})^2} =$		0.273		0.429
				+ 0.550⁽¹⁾
Total Error , in.		0.273		0.979

(1) Directly additive, not an RSS value.

Figure 5.13–76

THRUST MALALIGNMENT DURING OPERATION OF TERMINAL PROPULSION SUBSYSTEM

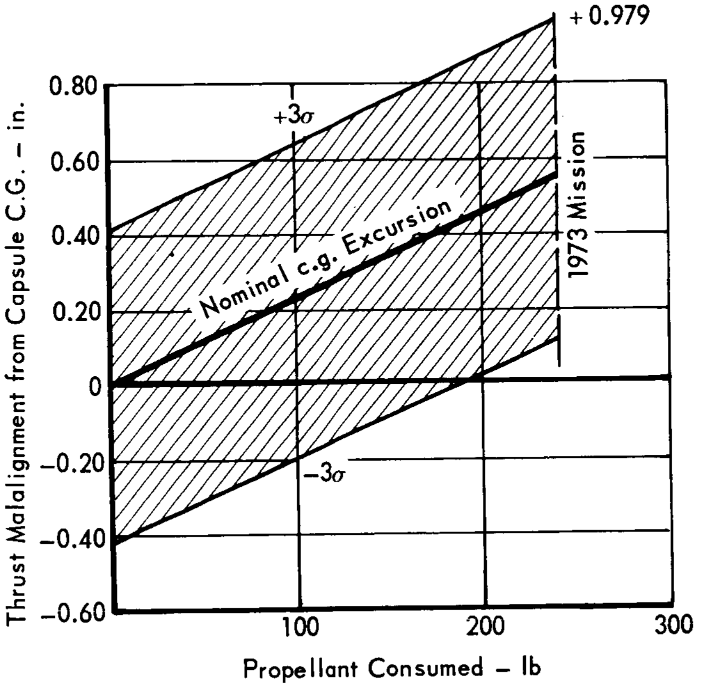

Figure 5.13–77

would be equal to the design mixture ratio of 1.6. However, the maximum ratio available with our arrangement is 1.3:1, causing a nominal vehicle c.g. shift of .55 inch, off the roll axis, at propellant depletion. The largest c.g. excursion occurs on the 1973 mission since it represents the maximum propellant-to-vehicle weight ratio.

The torque impulse required to counteract the resultant pitch/yaw terminal thrust disturbances is 5550 ft-lb-sec. A roll control moment of 560 ft-lbs is sufficient to cancel rates built up during parachute deceleration, within 3 seconds following chute release. For the multi-engine configuration, a torque impulse is required to counteract roll disturbances induced by engine malalignments of $\pm.25^{\circ}$. This impulse is a maximum of 2500 ft-lb-sec for the 6 engine configurations.

Candidate Subsystems - The TVC mechanizations considered in conjunction with the candidate de-orbit and terminal propulsion subsystems are presented in Figure 5.13-78. The following were evaluated: jet vanes, gimballed engine, swivel nozzle, and secondary liquid injection thrust vector control (LITVC). Schematics of these concepts are presented in Figure 5.13-79.

For the terminal propulsion multi-engine configurations, TVC is limited to roll control. For these configurations differential throttling control is inherent for pitch and yaw, and reliability is degraded only by the added actuation cycles on the throttle valves.

Subsystem Selection - The candidate subsystems were evaluated on the basis of reliability, development status, weight, performance, versatility and interactions with other subsystems.

- Reliability - A reliability estimate for each TVC concept was made based on the failure rates and analysis presented in Section 5.13.4.5 and the mission profile presented in Part E, Section 3.1. The results are presented in Figure 5.13-80. While reliability estimates are useful for quantitative ranking of each concept, component failure rates supplied by industry represent different levels of design maturity, and are not conclusive when comparing the widely divergent characteristics of the candidate designs. Therefore, consideration was given to such factors as capacity for post-sterilization checkout and basic subsystem complexity. Post-sterilization checkout of the TVC subsystem is predicted on the use of electromechanical servoactuators, except for the case of the single gimballed engine Terminal Propulsion Subsystem where this was impractical due to large actuator forces. For this subsystem, pressurized fuel hydraulic actuators were assumed.

CANDIDATE TVC SUBSYSTEMS

MISSION PHASE	MAIN PROPULSION	THRUST PER ENGINE (LB.)	ENGINE BURN TIME (SEC.)	GIMBAL ENGINES	SWIVEL NOZZLE	JET VANES	SEC LIQ INJ
De-Orbit	Single Solid	6000	20	–	√	√	√
	Single Monopropellant	300	600	√	–	√	–
	Single Bipropellant	300	600	√	–	*	√
Terminal	Solid +	5600		–	–		
	6 Monopropellant Verniers	350	70	**	–	**	**
	Single Bipropellant	6600	70	√	–	√	√
	3 Bipropellant	3200	70	**	–	**	**
	4 Bipropellant	1650	70	**	–	**	**
	4 Monopropellant	1650	70	**	–	**	**
	6 Bipropellant	1100	70	**	–	**	**

* Burn time too great for jet vanes.

** Technique considered only for roll control, i.e. single plane operation. Canted engines also considered for roll in case of 4 and 6 engines.

Figure 5.13–78

CANDIDATE TVC SUBSYSTEMS

GIMBALLED ENGINE

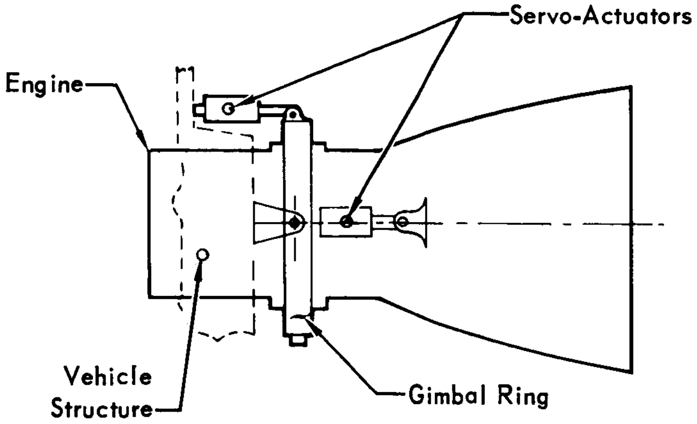
Servo-Actuators
Engine
Vehicle Structure
Gimbal Ring

JET VANE TVC

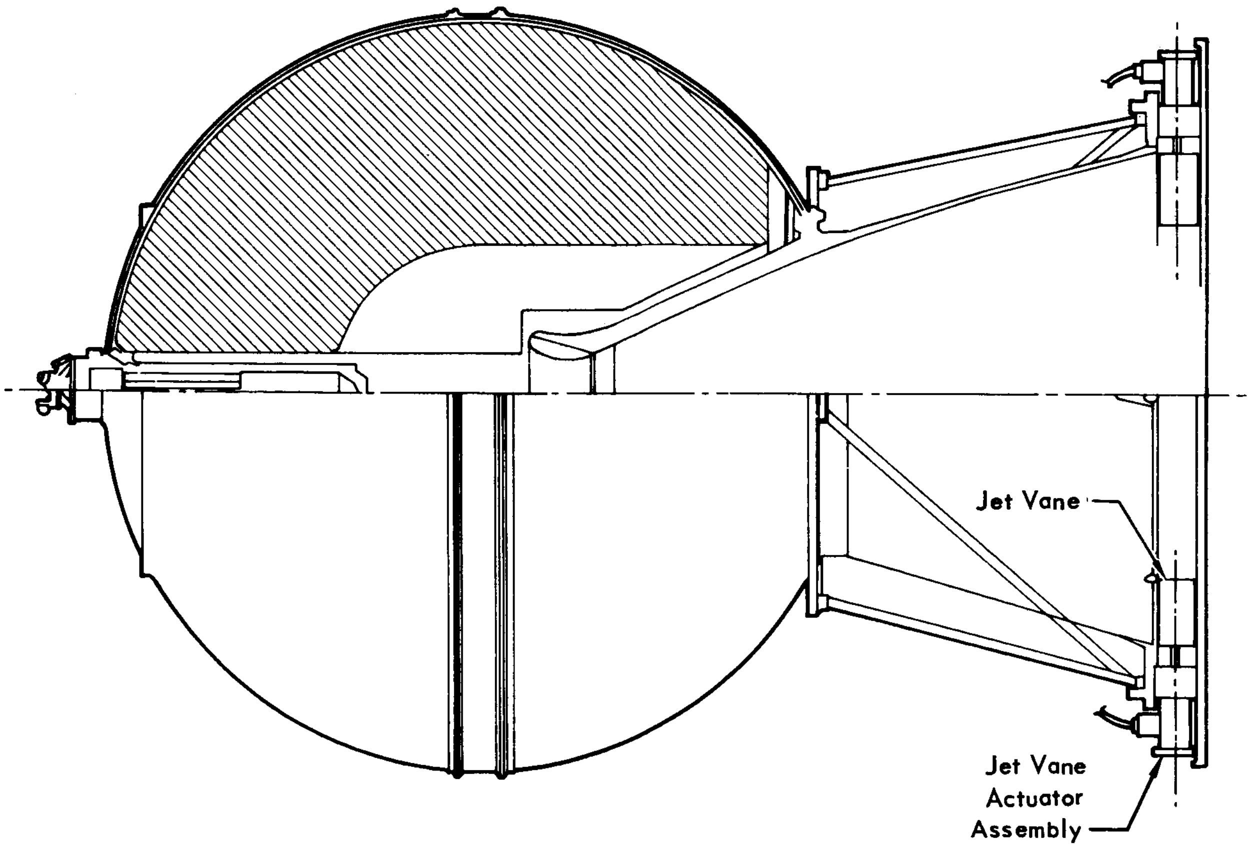
Jet Vane
Jet Vane Actuator Assembly

Figure 5.13-79

SWIVEL NOZZLE

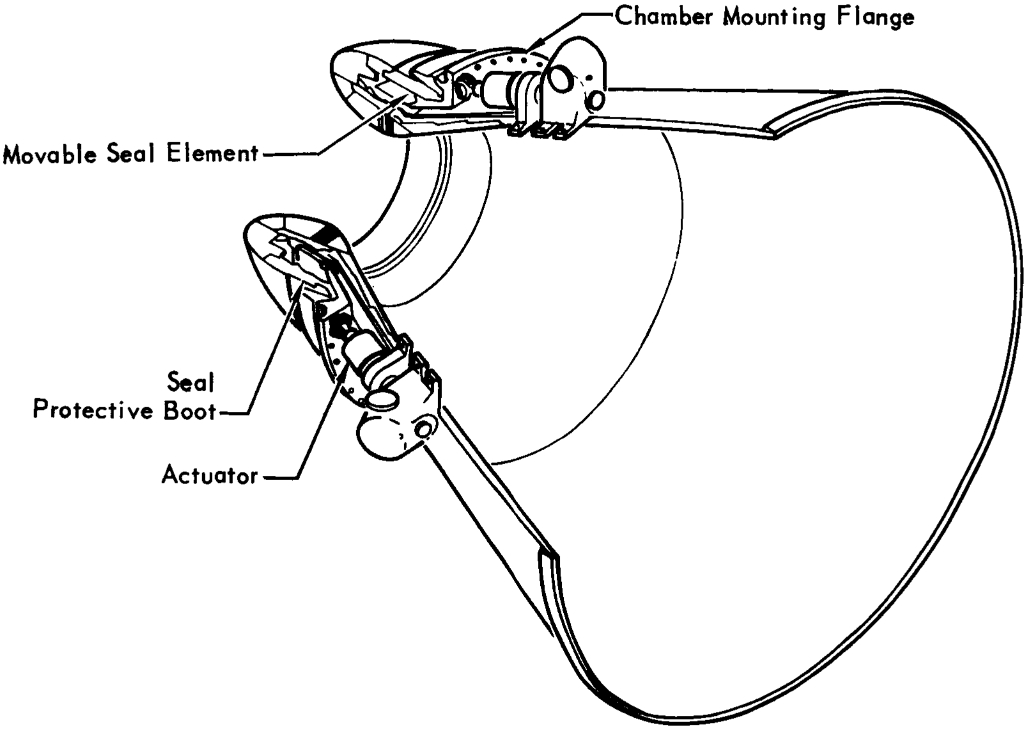
Chamber Mounting Flange
Movable Seal Element
Seal Protective Boot
Actuator

LIQUID INJECTION TVC

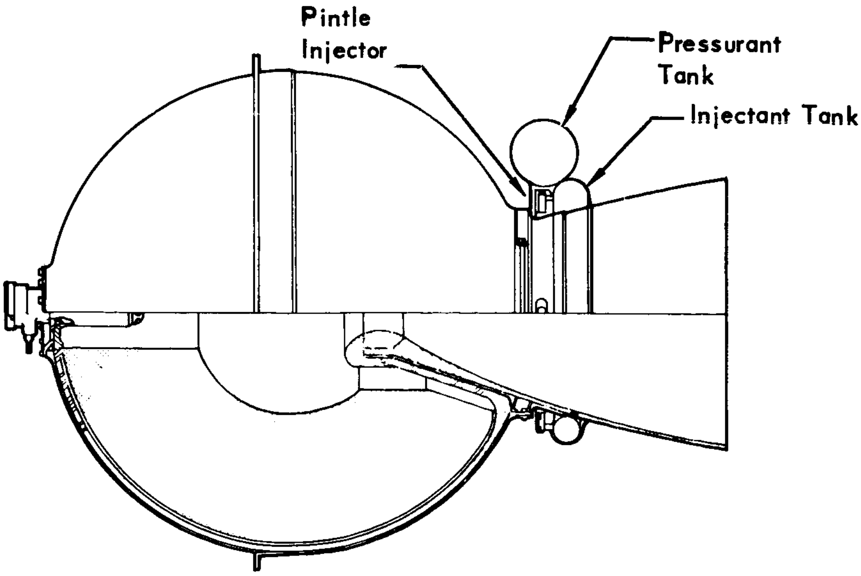
Pintle Injector
Pressurant Tank
Injectant Tank

5,13-162-2

TVC RELIABILITY ASSESSMENT

TVC CONCEPT	RELIABILITY		
	DE-ORBIT	TERMINAL DESCENT	
		2 AXIS – PITCH/YAW	1 AXIS – ROLL
Gimbal Engine			
– Electromechanical Actuator	.999254	–	.999540
– Hydraulic Actuator	–	.999386	–
Jet Vanes	.999064	.999064	.999532
Swivel Nozzle	.998428	–	–
Liquid Injection	.997590	.999328 (1)	.999664 (1)

(1) Injectant drawn from main oxidizer tank.

Figure 5.13–80

Functional verification of TVC mechanisms employing electrical actuators is achieved by attaching position transducers to the actuator linkage. With LITVC, checkout is limited to verification of modulating valve actuation.

The LITVC concept is inherently less reliable than the other concepts due to complexity associated with injectant and pressurant tankage, and attendant fluid plumbing and distribution components. Further complexity is added because positive expulsion of the injectant is required at the time of de-orbit rocket ignition. The swivel nozzle is complicated by the requirement for flexible seals which must survive sterilization and long term vacuum exposure.

When the above factors are considered, it is evident that jet vanes and electrically-powered engine gimbal concepts provide the highest inherent reliability.

- Development Status - A summary of current flight experience with the candidate TVC concepts is presented below.

TVC Concept	
Gimbal Engine	Atlas MA-3 Sustainer, Titan II and III, Saturn IB
Jet Vanes	Ranger, Mariner, Pershing, Sergeant, Scout
Swivel Nozzle	Minuteman, Polaris
Liquid Injection	Polaris, Minuteman, Titan III-C, Sprint

The primary development problem anticipated for the liquid injection and jet vane concepts is the selection of adequate materials. For the liquid injection subsystem, extensive sterilization testing must be performed to determine the compatibility of the preferred injectant fluid with candidate tankage, line, and component materials. For the jet vane concept, refractory metal vane designs using tungsten and molybdenum must be tested to establish performance losses and their resistance to the high temperature, erosive exhaust from a solid or bipropellant engine. However, this is not considered to be a severe problem. Two large solid rocket motors, viz., the Pershing and Scout first stages, have both utilized jet vane TVC subsystems in conjunction with highly aluminized propellant formulations and burn times of 40-50 seconds. The jet vane exhaust environments associated with these motors are more severe than any of the propulsion concepts considered for the VOYAGER Capsule Bus.

The primary difficulty associated with the gimbal engine and swivel nozzle designs is anticipated to be the development of complex drive mechanisms which can withstand sterilization and long term space storage.

- Weight and Performance - The weight and performance data used in this section were obtained from industry sources, including TRW Systems, Hercules, Pneumodynamics, Thiokol and Aerojet-General Corporation.

Current liquid injection TVC subsystems have primarily used N_2O_4 or freon injectants. Performance of N_2O_4 and Freon 114B2 injection fluids used in our studies is presented in Figure 5.13-81. Although a Strontium Perchlorate LITVC subsystem is being developed for Minuteman, use of this injectant was not considered due to the lack of flight experience. Nitrogen tetroxide delivers higher performance than Freon 114B2, and was used in the TVC analyses of the terminal propulsion bipropellant concepts. In these concepts positive expulsion devices are not required since the N_2O_4 injectant can be drawn from the main oxidizer tank. For the de-orbit function, which requires positive expulsion, Freon 114B2 was selected as the injectant for this study. It affords lower vapor pressure at the 275°F sterilization temperature (145 psia vs 760 psia for N_2O_4) and is more compatible with positive expulsion tankage and feed system materials.

Estimated performance losses to the propulsion subsystem by jet vanes, swivel nozzle, and Freon 114B2 injection is presented in Figure 5.13-82. Nitrogen tetroxide is a reactive injectant and produces a small increase in axial thrust. These performance changes for the basic propulsion subsystems are reflected in the TVC subsystem weight estimates.

The TVC subsystem must provide sufficient dynamic response during engine firing to adjust for dispersion of the thrust vector and to accommodate shift in vehicle center of gravity. Studies presented in Section 2.3.6 indicate that response times equivalent to a single order lag of .2 second time constant are adequate. Responses of the LITVC and jet vane concepts are highest. The response of the gimbal and swivel mechanisms is limited by the power requirements of the servoactuator.

Estimated weight of each de-orbit TVC mechanization is presented in Figure 5.13-83. For a solid de-orbit motor the swivel nozzle is lightest followed by jet vanes and LITVC. Motor gimballing was not considered for this concept due to excessive actuator requirements and associated weight penalty. The gimballed engine technique provides minimum weight in the cases of the monopropellant and bipropellant de-orbit rockets. Jet vanes were not considered for the bipropellant de-orbit engine because of high

CANDIDATE LSITVC PERFORMANCE

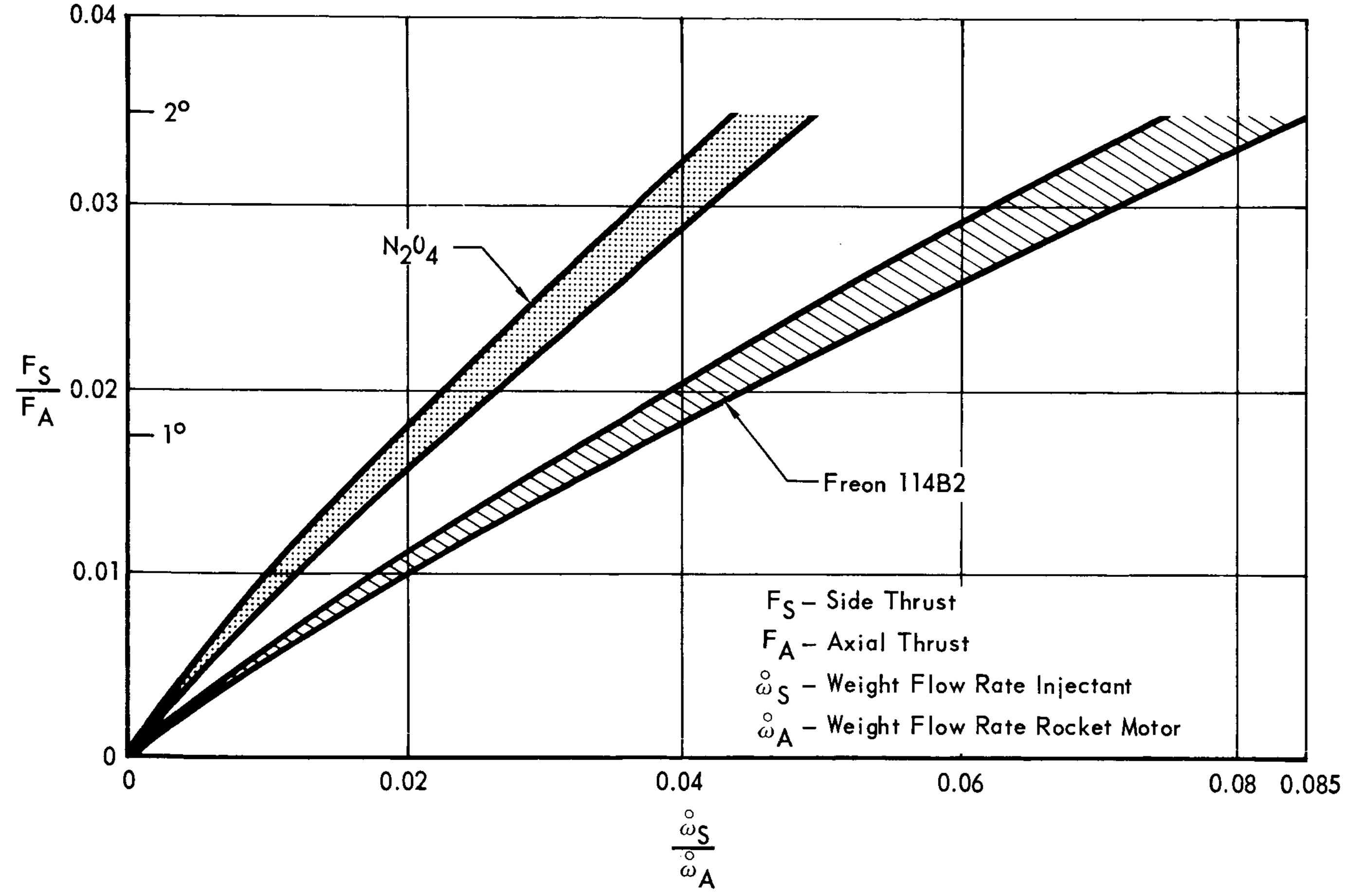

Figure 5.13-81

AXIAL THRUST LOSSES FOR CANDIDATE TVC SUBSYSTEMS

F_S = Side Thrust
F_A = Axial Thrust
ΔT = Thrust Decrement
T = Axial Thrust

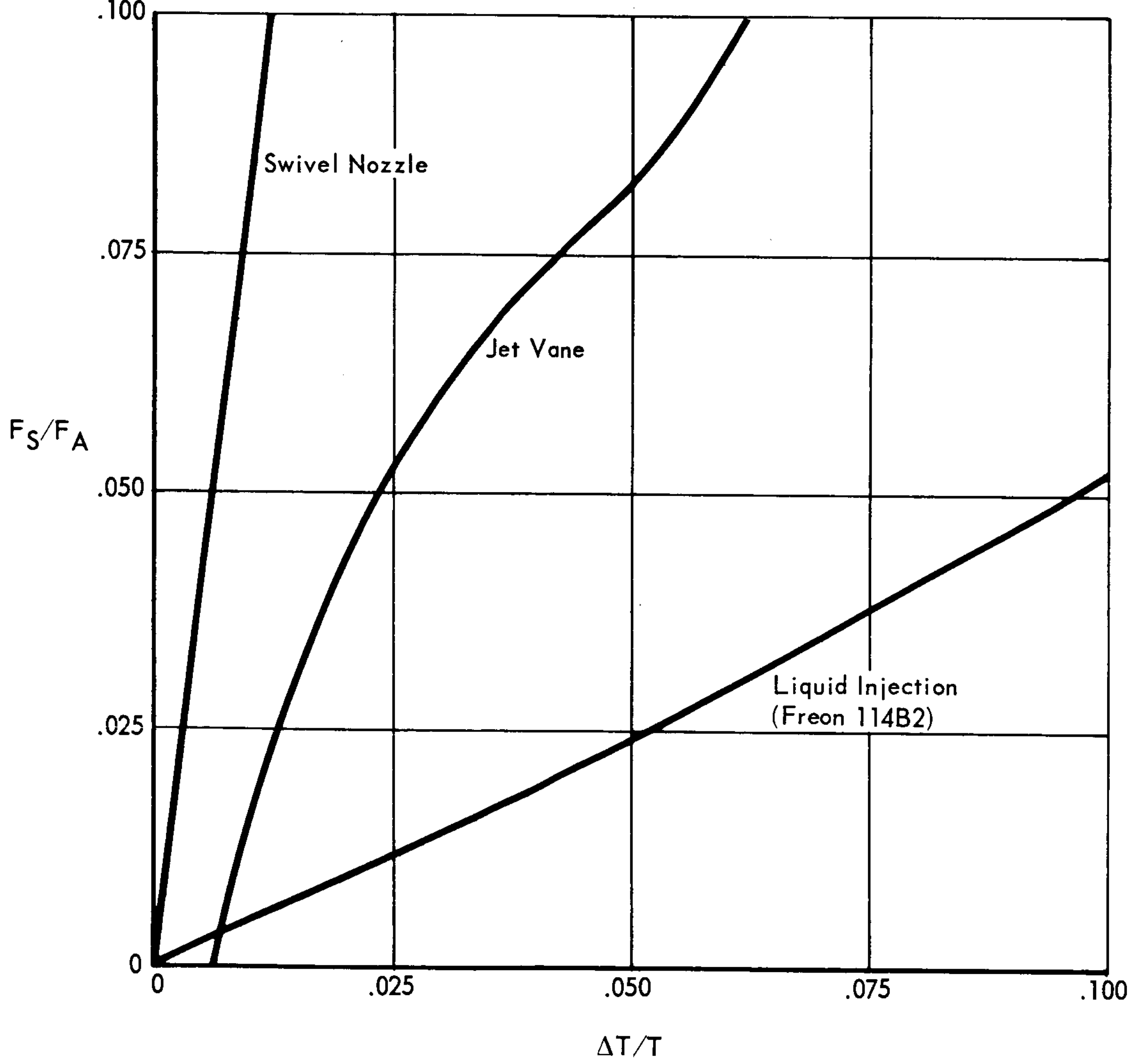

Figure 5.13-82

CANDIDATE TVC SUBSYSTEM WEIGHTS FOR DE-ORBIT MANEUVER

DE-ORBIT TOTAL IMPULSE – 172,000 LB-SEC

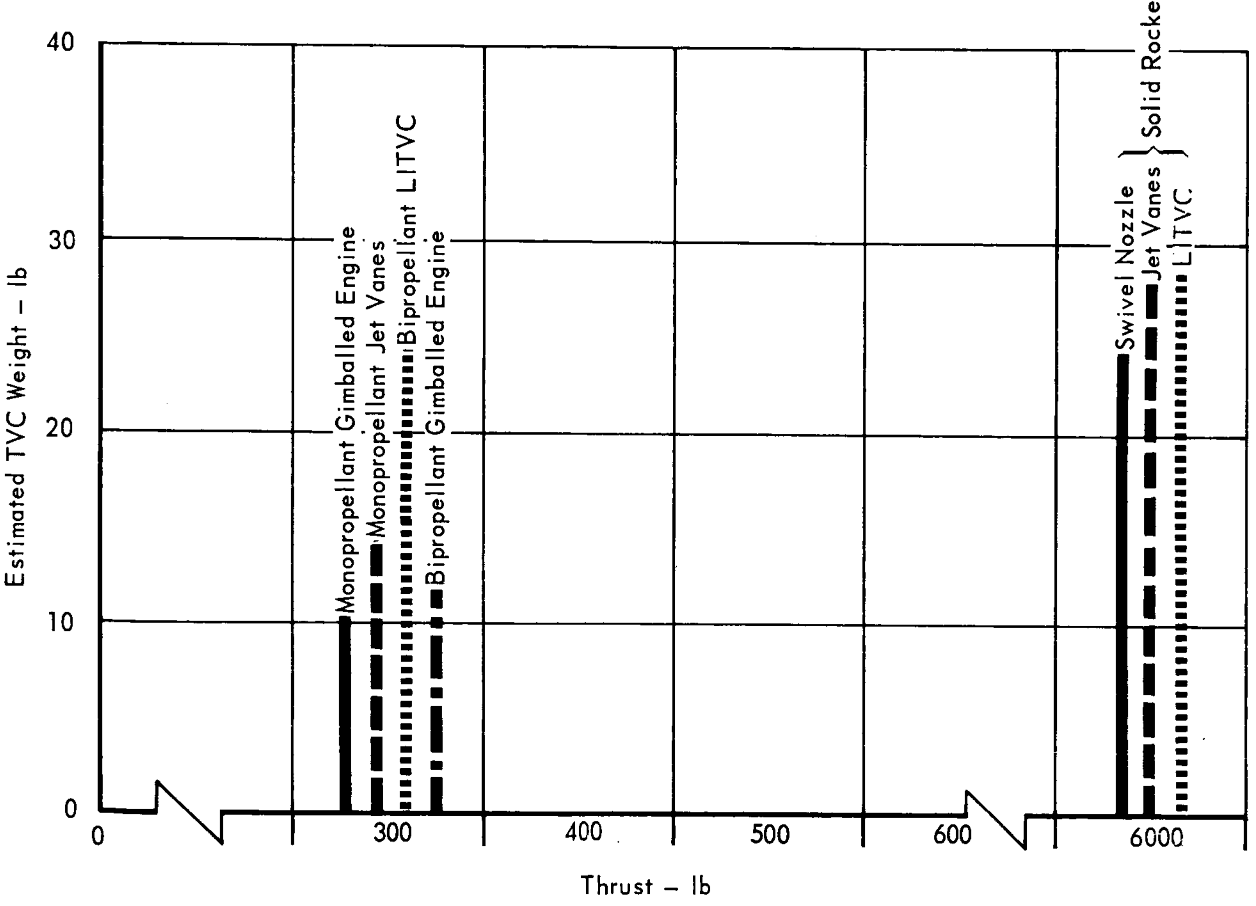

Figure 5.13-83

exhaust stagnation temperatures (above $5000^{o}R$) and long burn time (approximately 10 min).

Weight comparisons for the various terminal propulsion TVC mechanizations are presented in Figure 5.13-84. For the single bipropellant engine, the TVC weights represent 2 axis control except for the jet vanes which afford 3 axis control. Differential throttling provides distinct advantages over TVC mechanisms for pitch and yaw control for arrangements consisting of 3 or more engines. Differential control capability is inherent in development of the terminal propulsion subsystem and reliability is degraded only by the added actuation cycles on the throttle valves. Therefore, only roll control TVC was considered for multi-engine configurations. For the 4 and 6 engine configurations, roll control may also be provided by alternately canting the engines approximately 5 degrees to obtain a tangential thrust component. A net roll moment is achieved by differentially throttling adjacent engines.

o Versatility - The gimballed engine and swivel nozzle mechanisms offer the greatest flexibility of the candidate TVC concepts. These subsystems are sized based on actuator torque and response requirements and thus are insensitive to increased mission duty cycles.

The jet vane concept is limited by restrictions on burn time at high combustion flame temperatures.

Liquid injection TVC subsystems are sized for both torque and torque impulse requirements and are, therefore, limited in duty cycle extension by the quantity of injectant fluid.

o Subsystem Interactions - For the solid motor de-orbit concept, thrust termination is provided by nozzle release (see Section 5.13.1). This mechanization creates an obvious interaction with thrust vector control subsystem.

All three of the TVC concepts investigated for the solid de-orbit subsystem could be mounted directly to the nozzle assembly but this compromises weight, actuator power requirements and/or subsystem development (greater interaction with development of the propulsion subsystem). Designs for both LITVC and swivel nozzles, with provisions for thrust termination, are presented in Section 5.13.1, Vendor Design Solutions.

An interface also exists between the TVC and electrical subsystems. Power would be the greatest for the gimballed engine and swivel nozzle designs due to the large actuation forces required.

CANDIDATE TVC SUBSYSTEM WEIGHTS FOR TERMINAL DESCENT MANEUVER FOR A TOTAL IMPULSE OF 100,000 LB-SEC

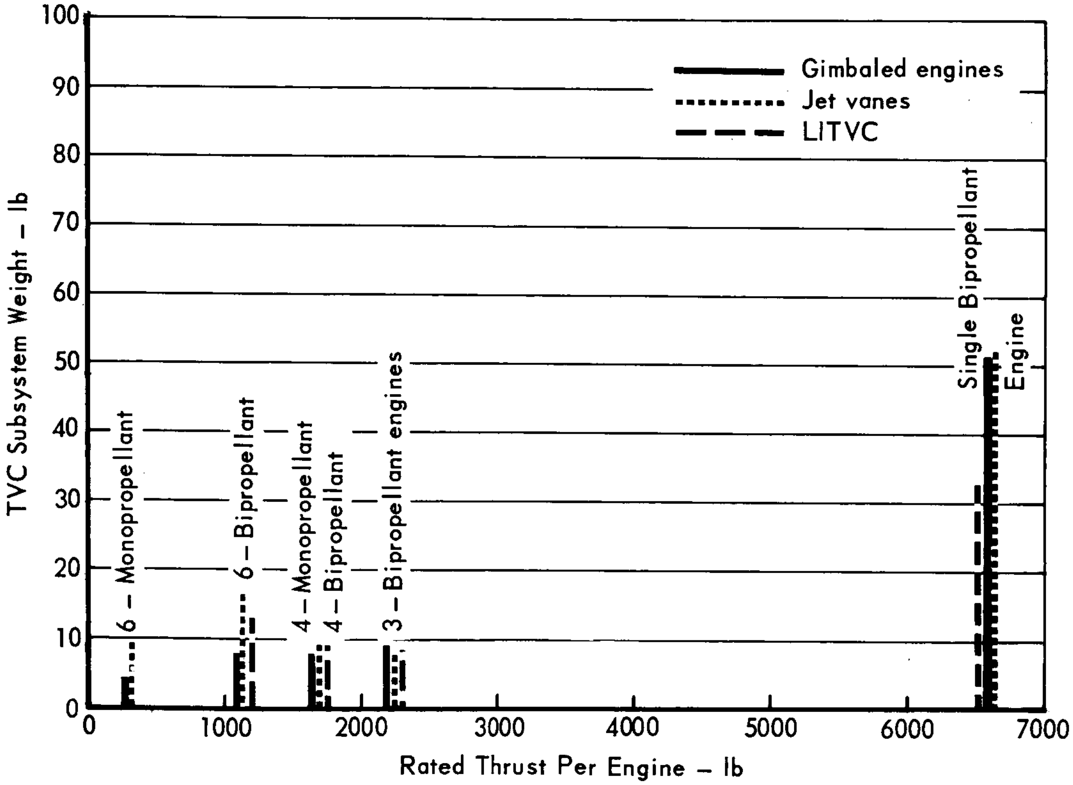

Figure 5.13-84

- Preferred TVC Subsystem Selection - Based on current technology, it is evident that any of the TVC concepts considered could be developed successfully for VOYAGER. Furthermore, few of the mechanisms considered display a significant advantage in terms of weight or reliability. Therefore, preferred subsystem selections have been based on assessments of probability of mission success, development risk, potential for satisfying extended mission duty cycles, and interactions with the propulsion subsystems. Two concepts, jet vanes and engine gimbal, were selected as the preferred approach, depending upon the mission function and propulsion subsystem arrangement. Jet vanes are preferred for the solid de-orbit rocket and the single engine terminal propulsion subsystem based on the following advantages.

  (1) 3-axis control
  (2) High generic reliability
  (3) Demonstrated technology: Scout and Pershing
  (4) Least vulnerability to sterilization and long term space storage
  (5) Capacity for post-sterilization checkout
  (6) Competitive weight

  Both jet vanes and gimbal mechanisms compared favorably for the liquid monopropellant and bipropellant de-orbit engines and multi-engine terminal configurations. However, the gimbal concept is preferred due to a weight advantage, lesser development problems for long de-orbit burn times and higher generic reliability. It too can be checked out following sterilization.

Summary and Conclusions - Results from evaluation of each TVC concept indicate preference for the jet vane subsystem, for the de-orbit phase in conjunction with the solid motor, and for the terminal mission with the single bipropellant engine. Multi-engine roll control requirements are best satisfied with the gimballed engine concept. The basic data used in reaching these conclusions were derived from industry sources.

Each of the TVC subsystems evaluated are considered adequate for mission performance, with no TVC subsystem exhibiting a clear cut advantage over the others. However, jet vane and gimballed engines represent low development risk and offer higher reliability than the others and for this reason are recommended for the respective de-orbit and terminal descent maneuvers.

5.13.4.5 Failure Rate Data and Reliability Analyses - As part of the Capsule Bus propulsion subsystem trade studies, reliability estimates were made for each of the candidate de-orbit, reaction control, and terminal propulsion subsystem concepts. The substantiated component failure rate data and the reliability studies performed are presented in this section.

To insure the integrity of reliability estimates substantiated failure rates were requested and received from industry. Based on these data, the failure rates of Figure 5.13-85 were selected for use in analyses of the various concepts. It is pointed out that some of the data showed no failures and in this case a failure was assumed to occur during the next cycle or time interval to arrive at a component failure rate. Although the resulting rates were pessimistic, this conservatism is counteracted by the fact that none of the failure rates were based on sterilizable component data. When generic failure rates were used in the analyses, failure rate modifying factors were applied as discussed in Part E, Section 3.

The reliability analyses based on the failure rates of Figure 5.13-85 are presented in Figures 5.13-86, -87, -88 for the de-orbit, reaction control and terminal propulsion subsystem concepts, respectively. Preferred thrust vector control mechanisms were selected independently, and the reliability analyses performed to assist these selections are presented in Figure 5.13-89. It is emphasized that, except for the case of the six-engine terminal propulsion subsystem, the component arrangements evaluated contained no redundancies. Since the six-engine terminal propulsion arrangement was evaluated only for the added capability of engine-out operation, this consideration was included in the reliability assessment of that concept.

PROPULSION SUBSYSTEM FAILURE RATE DATA

COMPONENT	FAILURE RATE $\lambda \times 10^6$	DATA SOURCE
Actuator, gimbal, electromechanical	28.6/cy	Aerojet General Corp. data
Actuator, jet vane electromechanical	23.4/cy	Compared to gimbal actuator by part count
Bearing, roller	0.5/hr	AVCO Reliability Engineering data series, failure rates, April 1962
Diaphragm, burst	10/cy	McDonnell estimate
Filter, pressurant	25.3/cy	Thiokol Chemical Corp. data – (YLR99)
Filter, propellant	52/cy	Thiokol Chemical Corp. data – (Surveyor)
Motor, solid propellant	5000/cy	JPL TM No. 33–219
Regulator, pressure	16/hr	AVCO Reliability Engineering data series, failure rates, April 1962
Seal, Flex or swivel nozzle	1000/ mission	McDonnell Estimate
Switch, pressure, helium control	6.6/hr	AVCO Reliability Engineering data series, failure rates, April 1962 – assumed complexity of pressure sensor
Tank, pressurant	.08/hr	AVCO Reliability Engineering data series failure rates, April 1962
Tank, Propellant, gravity expulsion	53.5/cy	Thiokol Chemical Corp. data – (LR–58 and LR–62)
Tank, propellant, metal bellows	357/cy	Bell Aerosystems Data – Program Model No. 825 and 8271
Throttling mechanism, bipropellant engine	100/sec	TRW Systems Data (Throttleable liquid engine)
Throttling mechanism monopropellant engine	50/sec	Estimate – assumed one-half the complexity of bipropellant throttling
Thrust chamber, ablative	10/sec	Thiokol Chemical Corp. data, Aerojet General Corp. data, Bell Aerosystems data
Thrust chamber, radiative	5.16/sec	Marquardt Corp. data (Bipropellant engines)
Valve, check	5/cy	AVCO Reliability Engineering data series, failure rates, April 1962. Conservative assumption that one-fifth of failures would restrict flow
Valve, motor operated	16.8/cy	Thiokol Chemical Corp. data – Surveyor
Valve, propellant shut-off pilot-operated	126.5/cy	Thiokol Chemical Corp. data – (YLR99)
Valve, pyrotechnic actuated normally closed	250/cy	McDonnell data and Holex Corp. data λ (Cartridge) $< 200 \times 10^{-6}$/cycle λ (Valve body) $= 50 \times 10^{-6}$/cycle (estimate)
Valve, pyrotechnic actuated normally open	250/cy	To function
	19.5/hr	To leak after closing. Aerojet-General Corp. data – (Able-star)
Valve, relief	42.2/cy	Thiokol Chemical Corp. data –(YLR99)
Valve, solenoid, hot gas thruster	0.84/cy	Marquardt Corp. data –(bipropellant engines)
Valve, solenoid, cold gas thruster	0.40/cy	Sterer Engineering and Manufacturing Co. data
Valve, solenoid, helium control	11.4/cy	Thiokol Chemical Corp. data – (Surveyor)

Figure 5.13–85

DE-ORBIT RELIABILITY ANALYSES

CANDIDATE SUBSYSTEM		MONOPROPELLANT			BIPROPELLANT		
COMPONENT	FAILURE RATE EACH COMPONENT $(\lambda)\cdot 10^{-6}$	NUMBER OF COMPONENTS (n)	DUTY CYCLE (Kt)	$n\cdot\lambda\cdot Kt\cdot 10^{-6}$	NUMBER OF COMPONENTS (n)	DUTY CYCLE (Kt)	$n\cdot\lambda\cdot K$
Pressurant Tank	.08/hr	1	5561 hr	445	1	5561 hr	44
Pressurant Filter	25/cy	1	1 cy	25	1	1 cy	2
Pressurant Regulator	16/hr	1	87 hr	1392	1	87 hr	13
Burst Diaphragm	10/cy				1	1 cy	10
Check Valves to Fail Open	4/cy						
Check Valves to Fail Closed	1/cy				2	50 cy	10
Propellant Tanks	53.5/cy	2	2 cy	214	2	2 cy	2
Propellant Tanks With Expulsion Bladder	357/cy						
Propellant Filter	52/cy	1	1 cy	52	2	1 cy	10
Pyrotechnic Valves N.C.	250/cy	6	1 cy	1500	5	1 cy	12
Pyrotechnic Valves N.O. to Operate	250/cy	1	1 cy	250	2	1 cy	5
Pyrotecnic Valves N.O. to Leak After Closing	19.5/hr	1	5 hr	98	2	5 hr	19
Engine Valves	127/sec						
Throttling Mechanism	100/sec						
Monopropellant TCA	5.1/sec	1	400 sec	2040			
Bipropellant TCA	10/sec				1	400 sec	4
Aeroshell Porting Mechanism	1000/cy						
Solid Rocket Motor	5000/cy						
$\Sigma\, n\cdot\lambda\cdot Kt\cdot 10^{-6}$				6016			8
Subsystem Reliabilify (R) $R = e^{-\Sigma n\cdot\lambda\cdot Kt}$		.9940			.9918		

(1) Reflects difference in unreliability due to replacement of two bladder-less tanks (terminal propulsion) with four tanks with bladders for the dual propulsion function (de-orbit and terminal)

Figure 5.13–86

	COMPOSITE COMMON TANKS			COMPOSITE COMMON TANKS AND ENGINES			SOLID		
t· 10^{-6}	NUMBER OF COMPONENTS (n)	DUTY CYCLE (Kt)	n·λ·Kt· 10^{-6}	NUMBER OF COMPONENTS (n)	DUTY CYCLE (Kt)	n·λ·Kt· 10^{-6}	NUMBER OF COMPONENTS (n)	DUTY CYCLE (Kt)	n·λ·Kt· 10^{-6}
5									
2	1	5 hr	80	1	5 hr	80			
				2	1 cy	10			
				2	50 cy	400			
0				2	50 cy	100			
4				2	2 cy	214			
	4	2 cy	$2642^{(1)}$						
4									
50				6	1 cy	1500			
0	2	1 cy	500						
5	2	5 hr	195						
				8	1 cy	1016			
				4	18.2 sec	7280			
00	1	400 sec	4000	4	18.2 sec	728			
				4	1 cy	4000			
							1	1 cy	5000
35			7417			13104			5000
	.9926			.9869			.9950		

5,13-174-2

REACTION CONTROL SUBSYSTEMS RELIABILITY ANALYSES

CANDIDATE SUBSYSTEM		COLD GAS		
COMPONENT	FAILURE RATE EACH COMPONENT $(\lambda)\times10^{-6}$	NUMBER OF COMPONENTS (n)	DUTY CYCLE (kt)	n.λ.ktx10
Tank, Pressurant or Cold Gas	.08/hr	1	5566 hr	445
Filter Pressurant or Cold Gas	25/cy	1	1 cy	25
Regulator, Pressurant or Cold Gas	16/hr	1	92 hr	1472
Propellant Tanks with Positive Expulsion	357/cy			
Propellant Filter	52/cy			
Pyrotechnic Valves N.C.	250/cy	1	1 cy	250
Propellant Valves	.84/cy			
Propellant Valves Cold Gas	.40/cy	8	350 cy	1120
Thrust Chamber	5.16/sec			
Σ n.λ.ktx10^{-6}				3312
Subsystem Reliability (R)		.9967		

Figure 5.13-87

	MONOPROPELLANT			BIPROPELLANT		
-6	NUMBER OF COMPONENTS (n)	DUTY CYCLE (kt)	$n.\lambda.kt\times10^{-6}$	NUMBER OF COMPONENTS (n)	DUTY CYCLE (kt)	$n.\lambda.kt\times10^{-6}$
	1	5566 hr	445	1	5566 hr	445
	1	1 cy	25	1	1 cy	25
	1	92 hr	1472	1	92 hr	1472
	1	2 cy	714	2	2 cy	1428
	1	1 cy	52	2	1 cy	124
	3	1 cy	750	5	1 cy	1250
	8	350 cy	2352	16	350 cy	4704
	8	20.8 sec	857	8	20.8	857
			6657			10,305
	.9934			.9898		

5,13-175-2

TERMINAL PROPULSION RELIABILITY ANALYSES

CANDIDATE SUBSYSTEM		FOUR ENGINE MONOPROPELLANT			SOLID/MONOPROPELLANT			ONE ENG
COMPONENT	FAILURE RATE EACH COMPONENT $(\lambda) \times 10^{-6}$	NUMBER OF COMPONENTS (n)	DUTY CYCLE (Kt)	$-\ln R \times 10^6$	NUMBER OF COMPONENTS (n)	DUTY CYCLE (Kt)	$-\ln R \times 10^6$	NUMBER COMPONE (n)
Pressurant Tank	.08/hr	1	5566 hr	445	1	5566 hr	445	1
Pressurant Filter	25/cy	1	1 cy	25	1	1 cy	25	1
Pressurant Regulator	16/hr	1	87 hr	1392	1	87 hr	1392	1
Check Valves	1/cy							2
Burst Diaphragm	10/cy							1
Propellant Tank	53.5/cy	2	2 cy	214	1	2 cy	107	2
Propellant Filter	52/cy	1	1 cy	52	1	1 cy	52	2
Pyrotechnic Valve N.C.	250/cy	6	1 cy	1500	3	1 cy	750	5
Pyrotechnic Valve N.O.	250/cy	1	1 cy	250				
Throttling Mechanism Monopropellant	50/sec	4	50 sec	10000	6	50 sec	15000	
Throttling Mechanism Bipropellant	100/sec							1
Engine Valve	127/cy	4	1 cy	508	6	1 cy	762	2
Thrust Chamber Monopropellant	5.16/sec	4	50 sec	1032	6	50 sec	1548	
Thrust Chamber Bipropellant	10/sec							1
Solid Rocket Motor	5000/cy				1	1 cy	5000	
Jet Vane Assembly	23.4/cy							4
Gimbal Assembly	1/hr							
Gimbal Actuator	28.6/cy							
$\Sigma n \cdot \lambda \cdot Kt = \ln RX10^6$		Total		15420	Total		25333	Total
Reliability (R)		.984			.975			

(1) Analyzed on basis of successful operation with 5 out of 6 engines.
(2) Analyzed on basis of 1 out of 2 gimbals.

Subsystem Reliability (R) $= \epsilon^{-\Sigma n \cdot \lambda \cdot Kt}$

Figure 5.13-88

Figure 5.13-88

INE BIPROPELLANT			THREE ENGINE BIPROPELLANT			FOUR ENGINE BIPROPELLANT			SIX ENGINE BIPROPELLANT		
OF NTS	DUTY CYCLE (Kt)	$-\ln R \times 10^6$	NUMBER OF COMPONENTS (n)	DUTY CYCLE (Kt)	$-\ln R \times 10^6$	NUMBER OF COMPONENTS (n)	DUTY CYCLE (Kt)	$-\ln R \times 10^6$	NUMBER OF COMPONENTS (n)	DUTY CYCLE (K+)	$-\ln R \times 10^6$
	5566 hr	445	1	5566 cy	445	1	5566 hr	445	1	5566 hr	445
	1 cy	25	1	1 cy	25	1	1 cy	25	1	1 cy	25
	87 hr	1392	1	87 hr	1392	1	87 hr	1392	1	87 hr	1392
	50 cy	100	2	50 cy	100	2	50 cy	100	2	50 cy	100
	1 cy	10	1	1 cy	10	1	1 cy	10	1	1 cy	10
	2 cy	214	2	2 cy	214	2	2 cy	214	2	2 cy	214
	1 cy	104	2	1 cy	104	2	1 cy	104	2	1 cy	104
	1 cy	1250	5	1 cy	1250	5	1 cy	1250	5	1 cy	1250
	50 sec	5000	3	50 sec	15000	4	50 sec	20000	6	50 sec	(1)
	1 cy	254	6	1 cy	762	8	1 cy	1016	12	1 cy	(1)
	50 sec	500	3	50 sec	1500	4	50 sec	2000	6	50 sec	Entire Engine Assembly 490(1)
	10 cy	936									
			1	87 hr	87				2	87 hr	0(2)
			1	10 cy	286				2	10 cy	0(2)
		16232	Total		21177	Total		26558	Total		4003
.990			.979			.974			.996		

5,13-176-2

TVC SUBSYSTEMS RELIABILITY ANA

DE-ORBIT SUBSYSTEMS, (2-AXIS) CONTROL P

CANDIDATE SUBSYSTEMS		GIMBALLED ENGINE			SWIVEL NOZZLE		
Component	Failure Rate Each Component $(\lambda) \cdot 10^{-6}$	No. of Components (n)	Duty Cycle (Kt)	$n \cdot \lambda \cdot Kt \cdot 10^{-6}$	No. of Components (n)	Duty Cycle (Kt)	$n \cdot \lambda \cdot Kt \cdot$
Gimbal Assembly	2/hr	1	87 hr	174			
Electromechanical Actuator	28.6/cy	2	10 cy	572	2	10 cy	57
Flexible Seal	100/cy				1	10 cy	100
Jet Vane Assembly	23.4/cy						
Pressurant Tank	.08/hr						
Pressurant Filter	25/cy						
Pyrotechnic Valve (N.C.)	250/cy						
Injectant Tank	357/cy						
Injectant Filter	52/cy						
Motor Operated Valve	16.8/cy						
$\Sigma n \cdot \lambda \cdot Kt = 10^{-6}$				746			15
Subsystem Reliability (R)		.9993			.9984		

$R = e^{-\Sigma n \cdot \lambda \cdot Kt}$

TERMINAL DESCENT SUBSYSTEMS

CANDIDATE SUBSYSTEMS		GIMBALLED ENGINE					
Component	Failure Rate Each Component $(\lambda) = 10^{-6}$	No. of Axes Control	No. of Components (n)	Duty Cycle (Kt)	$n \cdot \lambda \cdot Kt \cdot 10^{-6}$	No. of Axes Control	No. Compon (n
Gimbal Assembly	2/hr	1	1	87 hr	174 (174)		
Electromechanical Actuator	28.6/cy	1	1	10 cy	286	1 (2)	1
Hydraulic Actuator	22/cy	(2)	(2)	(10 cy)	(440)		
Jet Vane Assembly	23.4/cy					1 (2)	1
Motor Operated Valve	16.8/hr						
$\Sigma n \cdot \lambda \cdot Kt \cdot 10^{-6}$					460 (614)		
Subsystem Reliability (R)		.9995 (.9994)					

$R = e^{-\Sigma n \cdot \lambda \cdot Kt}$

Multi-Engine One Axis Control – Roll
(Two Axis Control – Pitch and Yaw)

Figure 5.13–89

LYSES

TCH AND YAW

	JET VANES			LIQUID INJECTION		
10−6	No. of Components (n)	Duty Cycle (Kt)	n·λ·Kt· 10−6	No. of Components (n)	Duty Cycle (Kt)	n·λ·Kt· 10−6
2	4	10 cy	1144			
)						
	4	10 cy	936			
				1	5566 hr	445
				1	1 cy	25
				2	1 cy	500
				1	2 cy	714
				1	1 cy	52
				4	10 cy	672
2			2080			2410
	.9979			.9976		

ET VANES			LIQUID INJECTION			
nts	Duty Cycle (Kt)	$n \cdot \lambda \cdot Kt \cdot 10^{-6}$	No. of Axes Control	No. of Components (n)	Duty Cycle (Kt)	$n \cdot \lambda \cdot Kt \cdot 10^{-6}$
l)	10 cy	286 (1144)				
l)	10 cy	234 (936)				
			1 (2)	2 (4)	10 cy	336 (672)
		520 (2080)				336 (672)
95 (.9979)			.9997 (.9993)			

5.13-177-2

REFERENCE

5.13-1 1973 VOYAGER Capsule Systems Constraints and Requirements Document - Revision 2, Jet Propulsion Laboratory, Pasadena, California, 12 June 1967

5.14 PACKAGING AND CABLING

5.14 PACKAGING AND CABLING - Fabrication, assembly and installation techniques for materials and components were studied to determine the most effective packaging and cabling for the Capsule Bus. The results are summarized in the following paragraphs.

5.14.1 Cable Studies - Efficient cabling interconnection requires integration with the structure, equipment form factors and equipment installation. The preferred wire and harnessing techniques provide the necessary integration with a reliable light weight design. Figure 5.14-1 lists the various materials and techniques studied and indicates the preferred approach. We prefer MIL-W-81381/1 (7 mil) "Kapton" insulated wire in round bundles. Sleeving is applied in areas where abrasion may occur and wire terminations are potted to provide environmental sealing and wire support.

5.14.2 Connector Studies - The cabling study was complemented by an evaluation of general purpose connectors. In some cases alternate cabling techniques were discarded because a reliable connector was not available. Figure 5.14-2 lists the connectors studied, summarizes the characteristics and parameters of each connector, and notes the selection for standardization of interconnects. The preferred MIL-C-38999 connector is circular, employs rear entry crimp contacts, has a quarter turn bayonet coupling, is environmentally sealed and has provisions for potting.

A study was performed to determine suitable devices for unattended in-flight disconnection of electrical circuits. The following ground rules were established to assist in evaluating the various disconnects:

a. Provide for redundant disconnection without the use of block redundancy methods.
b. Contain all gasses within pyrotechnically actuated devices.
c. Eject no loose pieces from individual devices or as a result of using multiple devices to effect redundancy.
d. Minimize reactant forces transmitted to the Capsule Bus during actuation or separation of the device.

Devices that satisfy these ground rules when used as individual devices or when combined with others in either a primary or backup/redundant capacity are:

a. Pyrotechnically actuated rotary disconnects
b. Guillotine wire bundle cutters
c. Hot wire actuated disconnects
d. Mechanically actuated lanyard disconnects.

CABLE STUDY SUMMARY

MATERIAL/ TECHNIQUE	ALTERNATES STUDIED	RATIONALE
Wire/Cable Type	**Round** Flat	Round wire fabricated into round wire bundles allows greater flexibility of circuit design, use of established fabrication, techniques and provides a greater background of development, testing, and experience of use in space flight. Flat cable concepts are limited in development of the basic wire, terminating devices, and fabrication techniques. Flat cable limits circuit design in a vehicle test and/or developmental program.
Wire Specifications	**MIL-W-81381/1 (7 mil) Kapton** MIL-W-81381/ (5 mil) Kapton MIL-W-16878 Type E MIL-W-81044/3 Kynar Raychem Thermorad	Only Kapton and Teflon (TFE) meet the initial constraints of compatibility with ETO and heat sterilization. Kapton 7 mil is selected over 5 mil because of limited test and development on the latter. Kapton is stronger and tougher than Teflon (TFE) and realizes up to 15.5% weight savings, to 12% volume savings, has 267% greater tensile strength, 87% less elongation, and has passed 284% greater cut through load tests.
Connector Wire Termination	**Crimp Contacts** Solder Contacts	Crimp contacts are considered the most reliable method to terminate wires in multi-pin connectors. Certified crimping tools provide uniform terminations with minimum dependence upon operator technique or capability. Replacement of individual wires and/or damaged contacts is possible without degradation and possible damage to adjacent contacts or replacement of the entire connector.
Wire Bundle Covering	**None** Sleeving Jacket	No covering external to the individual wires is provided for the interconnecting wiring, thus providing cables of less weight and volume, greater flexibility and ease of modification, and less susceptible to damage during change. Sleeving is provided in local areas where the possibility of abrasion and/or handling degradation may exist.
Wire Termination Sealing	**Potting Seal** Environmental Grommet Seal Non-environmental Grommet Seal	Potting has been selected to provide environmental sealing on all wire terminating devices. Potting provides excellent sealing without regard to grommet capabilities, is lighter and provides wire support for increased dynamic environmental resistance and handling without the use of heavy volume consuming accessories.
Multiwire Terminating Devices	**Terminal Junction Modules** Stud Terminal Strips	Terminal junction modules offer large savings in weight and volume. They provide flexibility for multiterminations of from 2 to 8 common terminations without additional weight for bussing and complete utilization of the terminating point wire capacity. The module is provided with grommet wire seals and capability for potting. Terminal identification is incorporated on the modules and they are easily assembled and/or changed.

Preferred Concept

Figure 5. 14-1

CONNECTOR CHARACTERISTICS SUMMARY

Connector Series / Characteristics	D	RE	126	SR	348	
Vendor Specification	Cannon, Cinch MIL-C-8384B	Deutsch	Amphenol	Bendix	Amphenol MIL-C-81511	Microdot MIL-C-38
Size Shape Coupling	Subminiature Rectangular Friction	Subminiature Rectangular Allen Hex Jackscrew	Miniature Rectangular Spring Loaded	Standard Rectangular Friction	Subminiature Circular Bayonet	Subminiat Circular Push-Pul Threaded
Number of Contacts	9 to 50	12 to 100	26 to 91	4 to 57	4 to 85	7 to 61
Wire Term. Contact (Size and Type)	#20 Solder or Crimp	#22 Crimp	#12, 16, 20 Solder	#4, 8, 16, 20 Solder	#22 Crimp	#12, 16 ar
Temperature	-65° F to +300° F	-65° F to +300° F	-85° F to +185° F	-67° F to +257° F	-67° F to +302° F	-85° F to
Inserts	Diallyl Phthalate Glass Fibre Filled Monobloc, Closed Entry Sockets, Grommet Seal or Potted	Hard Plastic Sockets, Silicone Interface and Rear Seal, Glass with Silicone Interface-Hermetics	Diallyl Phthalate Asbestos Filled, Potted Seal.	Resilient Insert, 16 & 20 Contacts Closed Entry Sockets, Potted Seal.	Retention Disc and Locking Nut Grommet Seal.	Diallyl P Silicone Ring and ing Inser Grommet
Past Usage	ASSET Mariner		F4			Gemini S
Hermetic Class [1]	Yes	Yes	None	None	Yes	Yes
Advantages	Rear Entry, Shape & Size	High Density, Rear Entry, Space & Weight, Environmental Seal, High Temperature, many Contacts	Rack and Panel	Rack and Panel	High Density, High Temperature	High De
Disadvantages	Only #20 Gage Contacts, Mounting and Alignment Difficult, Interface Sealing Difficult.	Mounting Only #22 Gage Contacts, Limited Development	Temperature Limitations, Only Solder Terminations, Interface Sealing Difficult, No Hermetic Class.	Solder Limitations, Heavy and Large, Interface Sealing Difficult, No Hermetic Class.	Only #22 Gage Contacts, Limited Development.	Many A Parts

[1] All Hermetic Classes – Solder Type Only.

[- - -] Prefered Connector

Figure 5.14–2

53	RTK	PT	PV	JC	JT	DBA
300	Deutsch MIL-C-26482	Bendix MIL-C-26482	Cannon NAS 1599	Bendix ZPH-2245-0300-B	Bendix MIL-C-38999	Deutsch NAS 1599
ure or	Subminiature Circular Push-Pull Bayonet	Miniature Circular Bayonet	Miniature Circular Bayonet	Miniature Circular Bayonet	Miniature Circular Bayonet	Miniature Circular Threaded, Bayonet or Push-Pull
	7 to 85	1 to 61	3 to 61	2 to 61	3 to 128	3 to 61
d 22 Crimp	#22 Crimp	#16, #20 Solder or Crimp	#16, #20 Crimp	#16, #20 Solder	#16, 20, 22, 22M Solder or Crimp	#12 thru # 20 Crimp
+257° F	-67° F to +300° F	-65° F to +257° F	-67° F to +392° F	-67° F to +257° F	-67° F to +302° F (392° F Crimp)	-100° F to +392° F
hthalate, "O" Float- t, Seal	Resilient Silicone Raised "Donut" Pins, Closed Entry Sockets, Silicone Interface and Rear Seal, Grommet Seal	Resilient Neoprene, Nut & Grommet, or Potting Seal.	Thermosetting Plastic or Glass, Raised "Donut" Pins, Closed Entry Sockets, Grommet Seal	Silicone Nut & Grommet, or Potting Seal.	Epoxy Resin Gaskets & Interface Seals, Silicone Rubber Closed Entry Raised "Donut" Pins, Nut & Grommet, or Potting Seal.	Hard Plastic Sockets, Silicone Pin Interface, Grommet Seal Closed Entry Sockets, Raised "Donut" Pins, Silicone Interface and Rear Seal, Grommet Seal
uit		F-4 ASSET BGRV Mariner Mercury Gemini	BGRV			BGRV
	Yes	Yes	Yes	None	Yes	Yes
nsity	High Density, Rear Entry, Environmental Seal, High Temperature	Proven Space Usage	Rear Entry, Environmental Seal, High Temperature	Thermal Sterilization, Extreme Vibration, Stringent Inspection, 32 hrs @ 240° F and Ethylene Oxide Gas	High Density Rear Entry, Space & Weight Low Silhouette, Environmental Seal, High Temperature	Rear Entry, Environmental Seal, High Temperature
ssembly	Low Voltage and Dielectric Rating, Limited Development	#22 Gage Contacts not Available	#22 Gage Contacts not Available	Only Solder Terminations, #22 Gage Contacts not Available		#22 Gage Contacts not Available

All the disconnects except the mechanically actuated lanyard type require similar auxiliary electrical initiation circuit control equipment, power sources, and test and checkout provisions. The selection of an electrically initiated disconnect device is more dependent upon weight, volume, and physical characteristics of the device than the requirements of the initiation circuit. Lanyard actuated disconnects provide a device free of electrical initiation controls but impart small disconnect unlatching and ejection forces to the structure during separation, since the device cannot be actuated prior to physical separation of the associated structures. The small forces resulting from the lanyard disconnect make it undesirable as the primary disconnect method, but the forces are not so large as to preclude its use as a backup device.

Isolation switches are required for circuit isolation with guillotine wire bundle cutters. Their use with other disconnect devices may be required to prevent voltage breakdown in the Mars atmosphere.

Deadfacing to prevent possible voltage breakdown in the Mars atmosphere, or during the cutting of wires by a guillotine, can be accomplished by electromechanical relays, pyrotechnically actuated switches, or motor-operated switches. Minimum weight and volume requirements, high reliability of operation and large capacity for multiple circuit switching are provided by pyrotechnically actuated switches. The use of pyrotechnically actuated disconnects does not impose added constraints to the Capsule Bus, since the pyrotechnic design techniques are used throughout the Capsule Bus for numerous other pyrotechnically actuated devices. A comparison of circuit capacity versus weight of disconnect is shown on the curves of Figure 5.14-3. The comparisons are made using existing hardware designs and as such do not show step changes that would occur when using multiple disconnect devices.

The pyrotechnically actuated rotary disconnect is selected for the Capsule Bus in-flight disconnect functions. It has sufficient capacity, in one device, for all disconnect requirements. It does not impart excessive forces to attaching structure, contains redundant pyrotechnic cartridges, the basic plug/receptacle components are qualified standards, it has low volume in comparison to other types of disconnects and, as shown in Figure 5.14-3, has circuit capacity/weight advantages over other types.

5.14.3 Equipment Packaging - Consistent with the critical VOYAGER objective of satisfactorily landing a Surface Laboratory System on the Martian surface, the Capsule Bus design is predicated upon maximizing the effectiveness of the Surface

DISCONNECT WEIGHT/CAPACITY COMPARISON

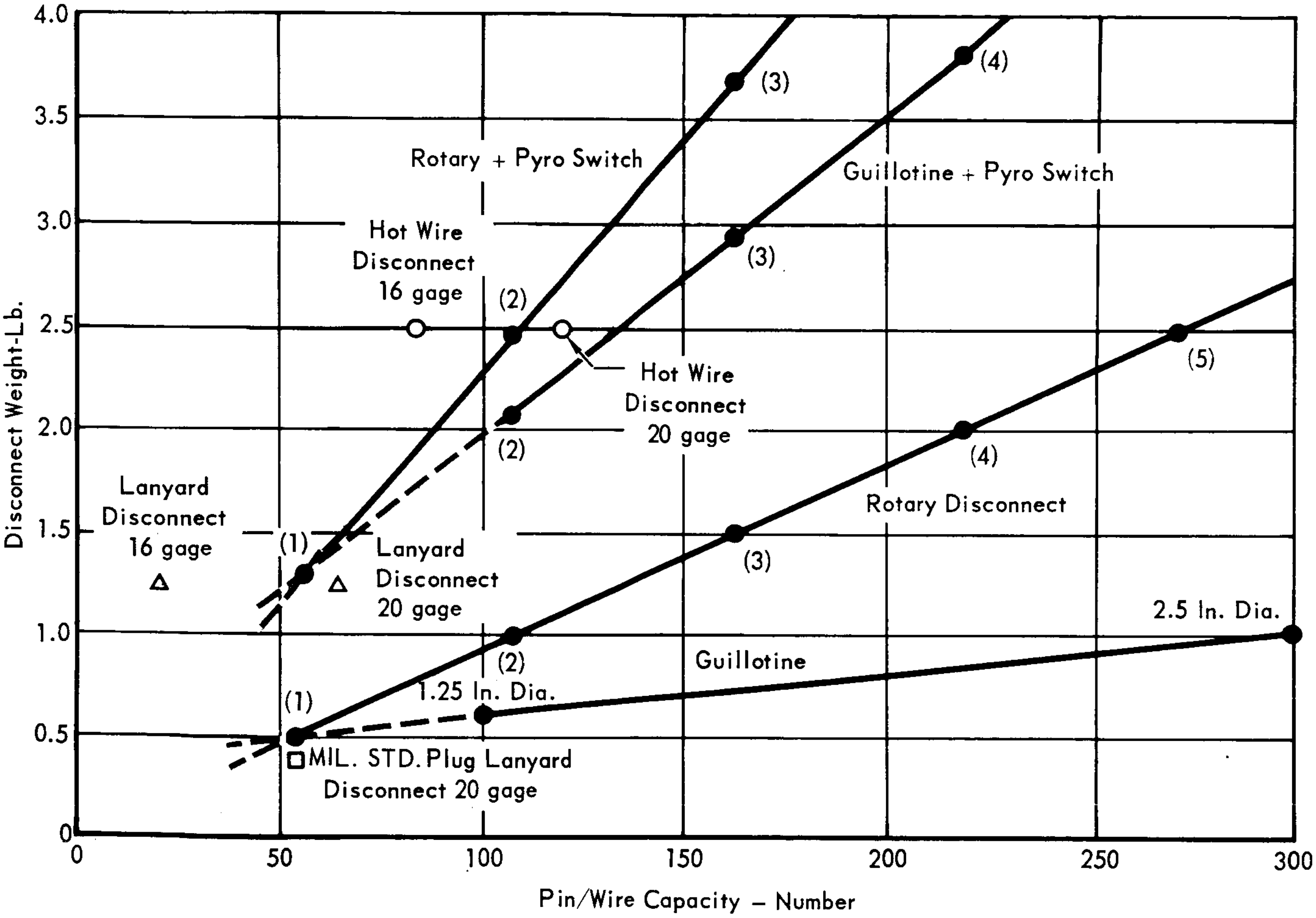

Notes:
1. Guillotine pin/wire numbers represent wire bundles containing MIL–W–81381/1 20 gage Wire – 70% shielded, 30% unshielded.
2. Hot wire and lanyard disconnects do not include deadfacing provisions.
3. ( ) indicates number of reference units (disconnects or pyro switches) to provide the required pin/wire capacity.

Figure 5.14–3

Laboratory. For example, the goal of maximizing the Surface Laboratory growth capabiltiy was considered of more fundamental importance than simplification and standardization of equipment installation in the Capsule Bus.

5.14.3.1 Equipment Form Factors - Since the Capsule Bus is to be utilized for multiple opportinities with little or no changes, accessibility and maintainability are of more importance than flexibility to facilitate design changes. The Capsule Bus equipment form factors are therefore predicated upon satisfactory equipment installation within the Capsule Bus structure, without compromising flexibility of the Surface Laboratory, while maintaining a high degree of accessibility for Capsule Bus equipment.

Thus, all equipment is of a controlled geometry consistent with the Capsule Bus structure. Some subassemblies are defined as black box units and some as modularized assembly elements, although the distinction is sometimes subtle.

a. Black Box - The black box approach consists of uniquely configured equipment elements. The equipment is packaged within a volume dictated by the size of internal functional elements and, in this case, within a volume consistent with the geometry available in the desired mounting location.

b. Modular Assembly - The modular assembly consists of subassemblies of standardized width and height and of variable length. The subassemblies of a given system are grouped in one assembly in which the required thermal insulation is provided by one enclosure for the entire assembly. All connectors are located on the top of the assembly for ease of mating and checkout. The modular assemblies can be interchanged within the Capsule Bus structure should this appear desirable.

5.14.3.2 Form Factor Selection - In assessing the two techniques it is apparent that the modularized assembly differs from the black box approach in that it provides an ordered regularity. The regularity improves flexibility and permits structural correlation between subassemblies. The modularized assembly is preferred for equipment which has a fair amount of location flexibility while the black box approach is selected for the Guidance and Control Subsystem equipment and for the UHF Radio because a position requirement dominates.

5.14.3.3 Internal Packaging - The successful management approach to assure reliable electronic equipment requires selection of equipment suppliers on the basis of proven capability with emphasis on design and production competence. Therefore, McDonnell does not dictate particular packaging approaches. From experience, we know that particular attention must be devoted to those areas where a critical operation or process can degrade the reliability of each packaging technique. This system management approach was verified on the relatively complex Gemini electronic subsystems which included practically every known packaging technique and termination device in use today. Typically, the following broad approaches are recommended and considered appropriate to VOYAGER designs.

a. Circuit Board Modules - This approach is primarily applicable to integrated circuit modules utilizing either series or parallel gap welding or resistance solder reflow for component interconnection. For both techniques the process must be closely monitored and a high level of cleanliness maintained. If welding is employed, weld schedules must be critically established and periodically verified. In either case, single or double sided circuit boards and conformal coating with or without embedment is preferred.

b. Embedded (Cordwood) Modules - Applicable to either integrated circuit, discrete component or combinations of these components, this approach can be satisfactorily applied by several techniques. The preferred interconnection method is by welding, either to comb or ribbon interconnects. Critical attention to embedment materials, thermally induced stresses and rigorous process controls are necessary. Satisfactory heat sinking is a design complication requiring attention.

c. Modular Interconnection of Modules - Minimization of friction contacts is desired. Thus, either fabricated multilayer boards (continuous conductors and risers or risers welded to conductors) or matrix interconnects are preferred as the modular interconnect technique. Module to board connections can be either welded or wire wrapped. The wire wrap technique has the advantage of easier module replacement and its disadvantage of requiring more space is mitigated by the requirement to incorporate additional space for a second weld if module replacement is necessary.

d. Radio Frequency Packaging - The preferred approach is to utilize functional elements inserted into a metallic compartmentized chassis. This permits individual module operation for test and facilitates shielding.

5.15 Independent Data Package - In Section 4.8, allocation of weight resources to devices other than an Independent Data Package (IDP) is recommended as the best way to improve probability of mission success. However, substantial analysis of the IDP concept was performed to investigate feasibility and to select a preferred configuration. The Independent Data Package was conceived to provide the VOYAGER 1973 with an independent capability to gather basic surface environmental data. The 100 pound IDP subsystem would monitor critical Flight Capsule engineering data; separate from the Capsule early in the descent sequence; descend to the surface via parachute; survive omni-directional impact at a velocity from 50 to 250 ft/sec; stabilize in one of two possible orientations deploy atmospheric sensors; and finally transmit scientific data direct to Earth. The general characteristics of the subsystem and the basic science instrument complement are tabulated in Figure 5.15-1. The design constraints, optimization studies and supporting analyses which were conducted to establish this configuration are presented in the subsequent paragraphs of this section.

The preferred IDP concept employs a separable, hard landing, disk-shaped capsule which is deployed near Aeroshell separation. Figure 5.15-2 shows the essential elements of the subsystem as they would appear installed on the Capsule during entry. These hardware elements are grouped by their performance functions in Figure 5.15-3. The landing sequence is depicted in Figure 5.15-4. A view of the internal packaging arrangement is shown in Figure 5.15-5. The installation of the protective balsa wood impact limiter and the payload functional block diagram are shown in Figures 5.15-6 and 5.15-7 , respectively. A weight statement for the 100 pound IDP subsystem is presented in Figure 5.15-8.

The payload is a complete self-contained assembly consisting of a science instrument complement; an 800 bit data acquisition, handling, and storage system; a 20 Watt TWT Amplifier S-band transmitter with MFSK modulation; six sequentially driven 110° beamwidth antennas; a 25 watt-hour per pound AgZn battery power supply; a structure; a protective balsa wood impact limiter; and all necessary support hardware. The concept employs selective deployment of dual atmospheric sensor masts to accommodate uncertainties in landed orientation. Omni-directional data communication is accomplished by sequential transmissions over six antennas, conceptually located on the faces of a cube. The approach effectively counters all terrain uncertainties, and allows pressure, water vapor, and atmospheric composition data to be gathered and transmitted without necessitating either antenna selection or instrument mast extension.

INDEPENDENT DATA PACKAGE GENERAL CHARACTERISTICS

BASIC CONFIGURATION

- Disk: 38 Inches Diameter x 14 Inches High
- Omnidirectional Impact Protection
- 250 ft/sec Design Impact Velocity
- 3100g Peak Impact Deceleration
- Parachute Descent Retardation
- 100 Pounds Gross System Weight
- Payload Size: 15.6 Inches Diameter x 5 Inches High
- Payload Weight Fraction 0.5 (Nominal)
- Balsa Wood Impact Limiter (6 lb/ft^3)
- Two Atmospheric Sensor Masts (Selective Deployment)
- Six Fixed Cavity-Backed Cross Slot Antennas
- 4π Steradian Data Transmission
- 24 Hour Surface Operating Lifetime
- Silver-Zinc, 25 Watt-Hour/Pound, Battery
- Direct MFSK Telecommunication Link
- 20 Watts Transmitter Output Power, 1.2 BPS
- 800 Bit Magnetic Core Memory

BASIC INSTRUMENTS

- Vibrating Diaphragm Pressure Transducer
- Gas Chromatograph for Atmospheric Composition
- Hygroscopic Sensor for Water Vapor Detection
- Hot-Wire Anemometer for Wind Velocity
- IDP/CB Diagnostic Sensors

Figure 5.15-1

INDEPENDENT DATA PACKAGE INTERFACES

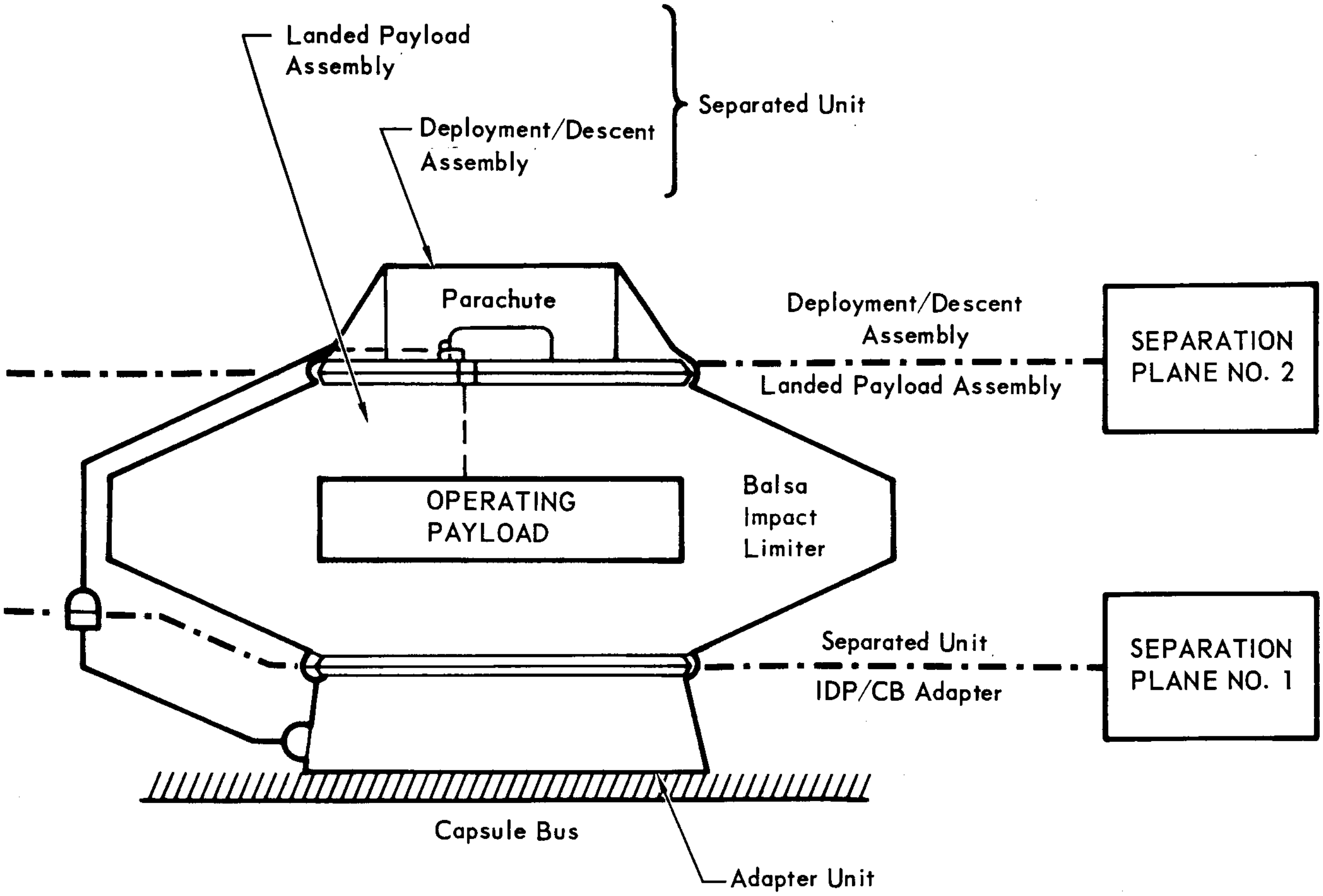
Landed Payload Assembly
Deployment/Descent Assembly
Separated Unit
Parachute
Deployment/Descent Assembly
Landed Payload Assembly
SEPARATION PLANE NO. 2
OPERATING PAYLOAD
Balsa Impact Limiter
Separated Unit
IDP/CB Adapter
SEPARATION PLANE NO. 1
Capsule Bus
Adapter Unit

Figure 5.15-2

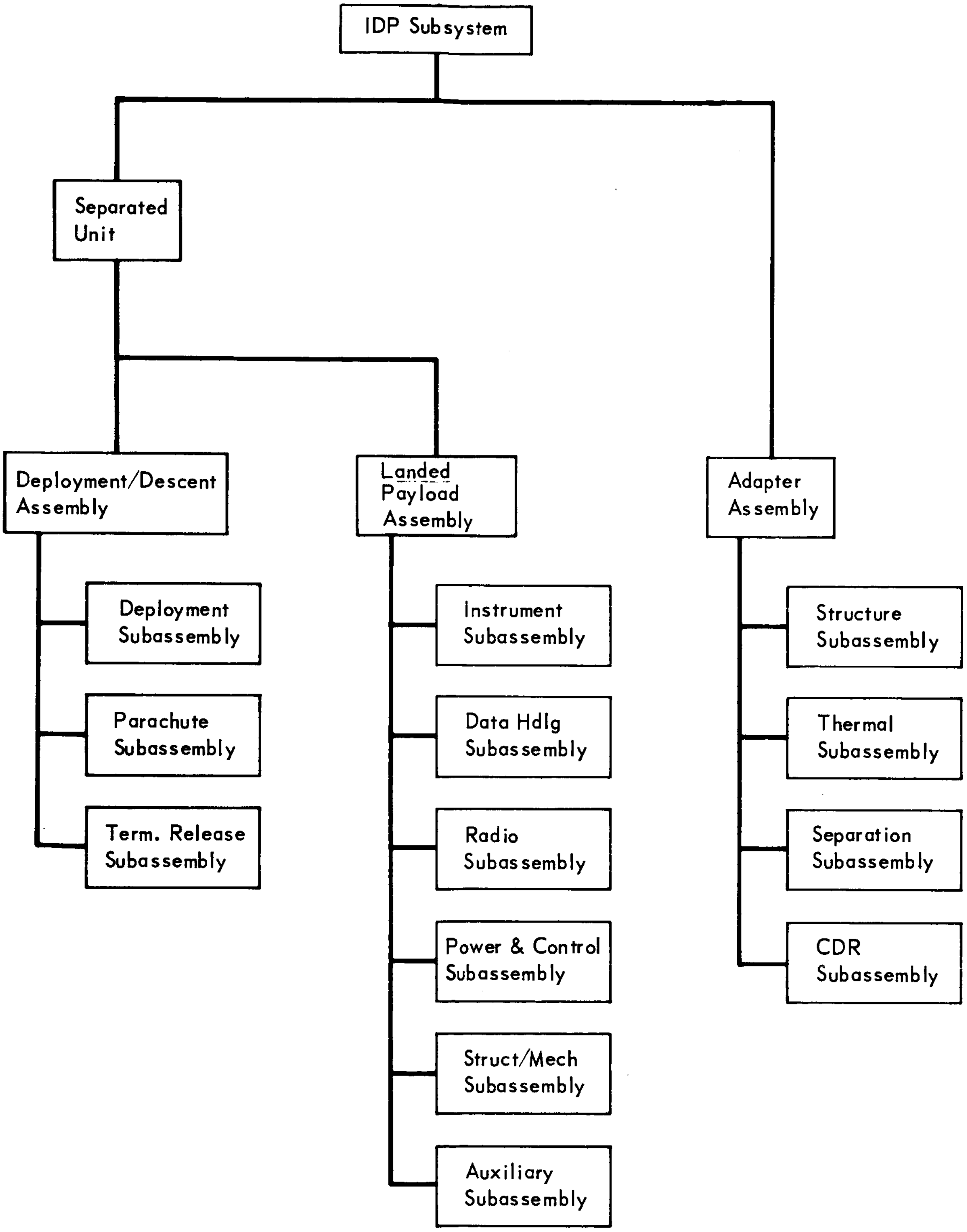
IDP Subsystem
Separated Unit
Deployment/Descent Assembly
Landed Payload Assembly
Adapter Assembly
Deployment Subassembly
Parachute Subassembly
Term. Release Subassembly
Instrument Subassembly
Data Hdlg Subassembly
Radio Subassembly
Power & Control Subassembly
Struct/Mech Subassembly
Auxiliary Subassembly
Structure Subassembly
Thermal Subassembly
Separation Subassembly
CDR Subassembly

IDP CONFIGURATION DEFINITION

Figure 5.15-3

INDEPENDENT DATA PACKAGE LANDING SEQUENCE

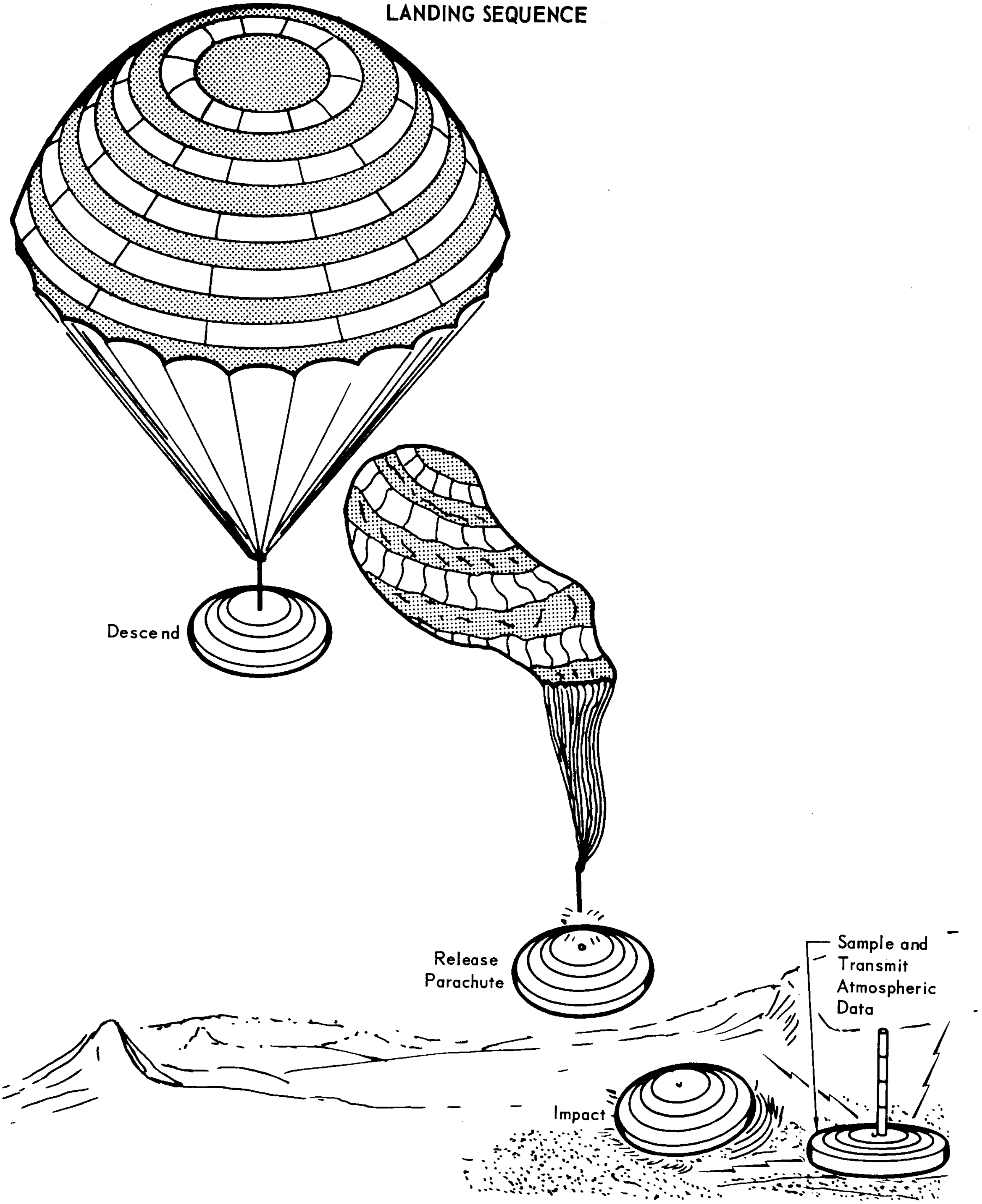
Descend
Release Parachute
Sample and Transmit Atmospheric Data
Impact

Figure 5.15-4

INDEPENDENT DATA PACKAGE PAYLOAD

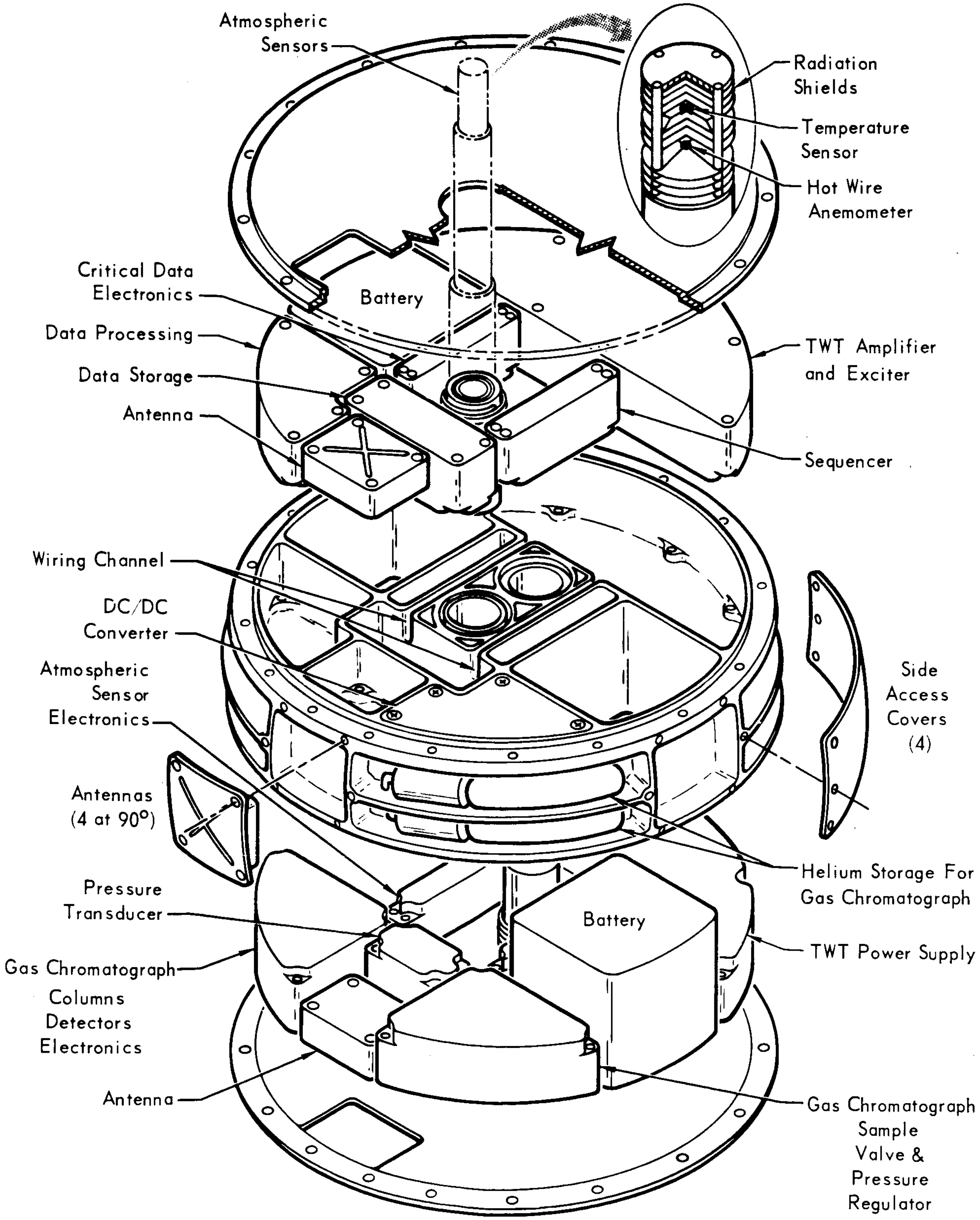
Atmospheric Sensors
Radiation Shields
Temperature Sensor
Hot Wire Anemometer
Critical Data Electronics
Battery
Data Processing
TWT Amplifier and Exciter
Data Storage
Antenna
Sequencer
Wiring Channel
DC/DC Converter
Atmospheric Sensor Electronics
Side Access Covers (4)
Antennas (4 at 90°)
Helium Storage For Gas Chromatograph
Pressure Transducer
Battery
TWT Power Supply
Gas Chromatograph
Columns
Detectors
Electronics
Antenna
Gas Chromatograph Sample Valve & Pressure Regulator

Figure 5.15-5

INDEPENDENT DATA PACKAGE IMPACT LIMITER

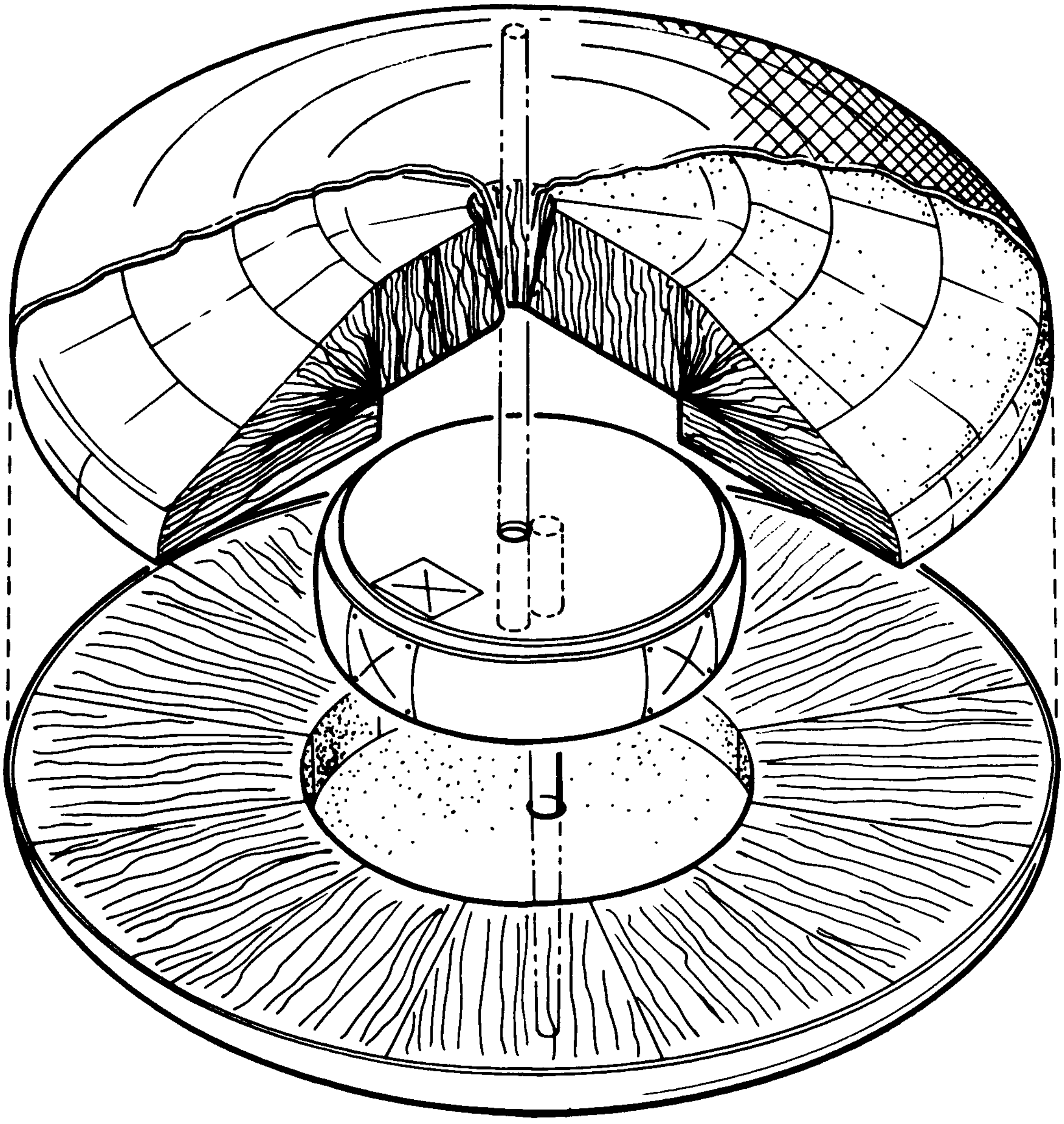

Figure 5.15-6

FUNCTIONAL BLOCK DIAGRAM – – INDEPENDENT DATA PACKAGE

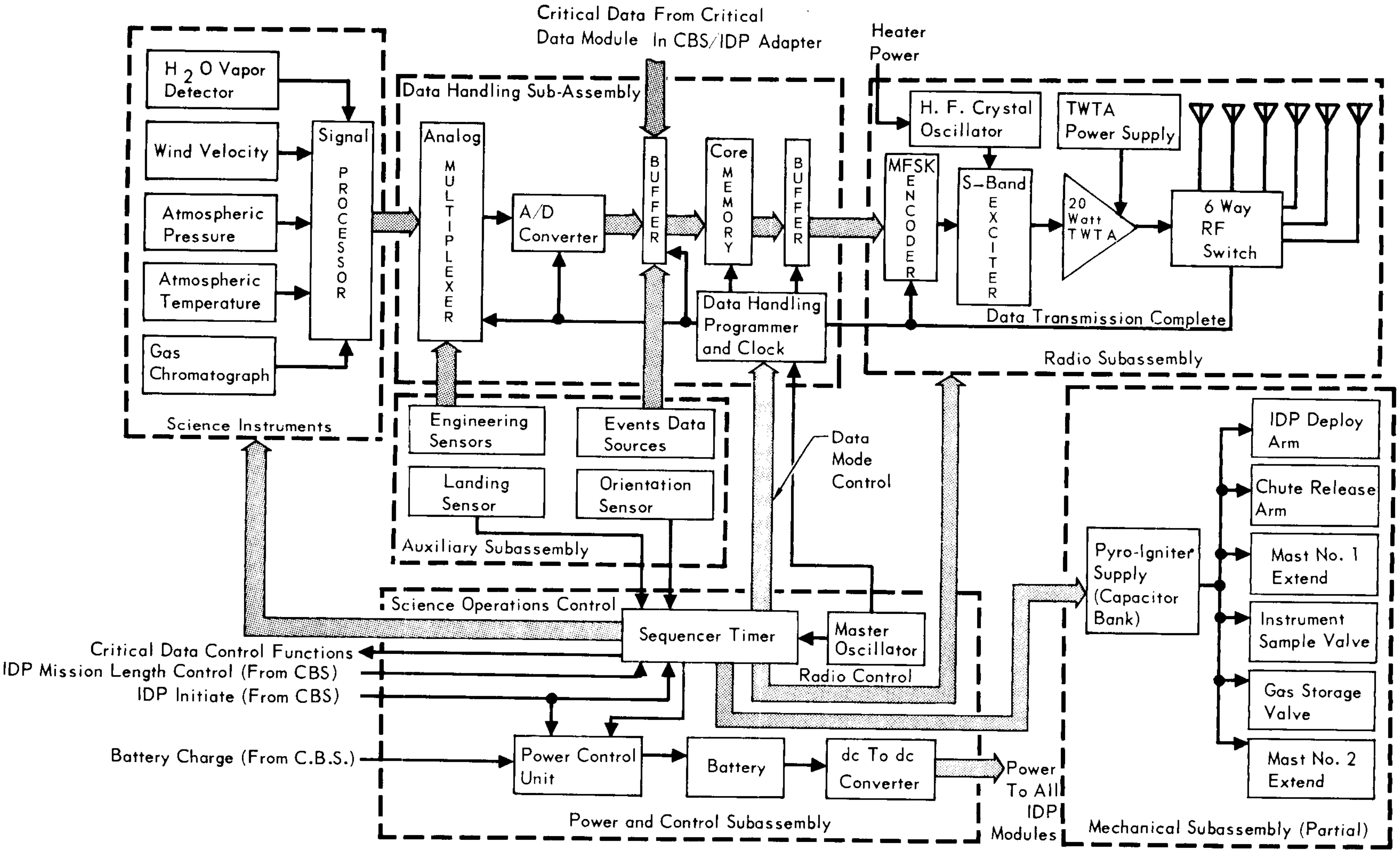

Critical Data From Critical Data Module In CBS/IDP Adapter
Heater Power
H_2O Vapor Detector
Wind Velocity
Atmospheric Pressure
Atmospheric Temperature
Gas Chromatograph
Signal PROCESSOR
Science Instruments
Data Handling Sub-Assembly
Analog MULTIPLEXER
A/D Converter
BUFFER
Core MEMORY
BUFFER
Data Handling Programmer and Clock
Engineering Sensors
Events Data Sources
Landing Sensor
Orientation Sensor
Auxiliary Subassembly
H. F. Crystal Oscillator
TWTA Power Supply
MFSK ENCODER
S–Band EXCITER
20 Watt TWTA
6 Way RF Switch
Data Transmission Complete
Radio Subassembly
Data Mode Control
Science Operations Control
Sequencer Timer
Master Oscillator
Radio Control
Critical Data Control Functions
IDP Mission Length Control (From CBS)
IDP Initiate (From CBS)
Battery Charge (From C.B.S.)
Power Control Unit
Battery
dc To dc Converter
Power To All IDP Modules
Power and Control Subassembly
Pyro-Igniter Supply (Capacitor Bank)
IDP Deploy Arm
Chute Release Arm
Mast No. 1 Extend
Instrument Sample Valve
Gas Storage Valve
Mast No. 2 Extend
Mechanical Subassembly (Partial)

Figure 5.15–7

INDEPENDENT DATA PACKAGE
WEIGHT STATEMENT

WEIGHT & VOLUME	WEIGHT(LBS)	VOLUME(IN^3)
Instruments		
Atmospheric Sensors (Temp. & Wind Velocity)	0.2	3
Pressure Sensor	0.2	3
Water Vapor Sensor	0.1	1
Gas Chromatograph (Including Electronics & Gas Supply)	3.4	75
Subtotal (Instruments)	3.9	82
Electronics		
TWT/Exciter/Filter	7.0	80
TWT Power Supply	4.0	80
Data Storage	1.0	14
Data Processing	2.0	25
Sequencer	0.5	7
DC/DC Converter	1.5	25
Critical Data Electronics	0.5	10
Atmospheric Sensor Electronics:		
Temperature	0.3	3
Wind	0.4	4
Pressure	0.4	6
Water Vapor	0.5	8
Antennas (6)	2.0	40
Batteries	10.0	130
Cabling & Potting	1.8	20
Subtotal (Electronics)	31.9	452
Mechanical		
Structure	8.2	80
Extension Systems (2)	1.3	10
Subtotal (Mechanical)	9.5	90
Voids		100
Internal Payload Total	453	724
Impact Limiter		
Balsa	32.0	9215
Resin	2.5	36
External Cover	5.0	70
Subtotal (Impact Limiter)	39.5	9,321
Capsule Total	84.8	10,045
Support Equipment		
Parachute Assembly	8.0	535
CBS Adapter Assembly	5.0	
Pyrotechnic Disconnects	2.0	
Subtotal (Support Equipment)	15.0	
IDP System Total	99.8	535

Figure 5.15-8

Near surface meteorological data will be gathered during the IDP's entire 24 hour operational lifetime. These measurements will consist of:

a. Atmospheric pressure
b. Atmospheric temperature
c. Atmospheric composition
  - Non-aqueous gases
  - Water vapor
d. Near-surface wind velocity.

The data will be retained within a self contained 800 bit magnetic core data storage unit for subsequent transmission direct to the DSN. The basic science data load including IDP/CB engineering diagnostic measurements, and necessary synchronization and parity data is summarized in Figure 5.15-9. Six successive transmissions of this data will be made at the rate of 1.2 bits per second for a total transmission period of 1.8 hours.

5.15.1 Mission Considerations and Constraints - Early separation of the IDP from the Capsule is recommended to minimize interactions and thereby maximize the probability of obtaining basic surface environmental data. However, parachute deployment should occur after subsonic speeds have been reached to ensure reliability in a relatively unknown atmosphere. These considerations dictate that IDP/CB separation should occur at, or near Aeroshell separation. This early separation approach will additionally provide a relatively large separation distance between the IDP and the CB thereby allowing for the acquisition of remote site meteorological data to supplement Surface Laboratory experimentation.

The time duration of landed operation will, in general, be governed by the landing time. This effect is demonstrated by Figure 5.15-10(a) where it is seen, that for a landing 30° from the evening terminator, a 24 hour mission duration will be required, for data transmission. With a near morning terminator landing, data communication can be achieved immediately therby requiring only a minimum 4 hour mission duration. This requires two modes of operation to be accommodated by the IDP sequencer design: 1) 4 hours for a short duration AM landing mission and (2) 24 hours for a long duration PM landing mission. The design concept accommodates the limiting 24 hour mission case.

The expected landing dates for 1973 dictate a maximum communication distance of 1.9 A.U. as a design constraint. The direct link communication parameters are summarized in Figure 5.15-10(b). For a single antenna, beamwidth requirements are determined by transmitting time errors, landing trajectory dispersions, vertical

IDP DATA LOAD – PREFERRED CONCEPT

MEASUREMENT	BITS/SAMPLE	NO. OF SAMPLE	TOTAL DATA BITS
1. Pressure (1X)	7	5	35
2. Temperature (1X)	7	5	35
3. Wind Velocity (1X)	7	4	28
4. H_2O Sensor (Hygroscopic)	7	4	28
5. Gas Chromatograph (1X)	200	2	400
EXPERIMENT SUBTOTAL			526
6. Data SYNC + Parity			80
7. IDP Summary			
Battery Volts	7	6	42
Temperature	7	6	42
Events	1	20	20
8. CDR Summary			
Events	1	20	20
Critical Parameters (10)	7	1	70
IDP/CDR, SYNC SUBTOTAL			274
	TOTAL		800

Figure 5.15-9

COMMUNICATION CONSTRAINTS

a) TYPICAL IDP LANDED MISSION PROFILES

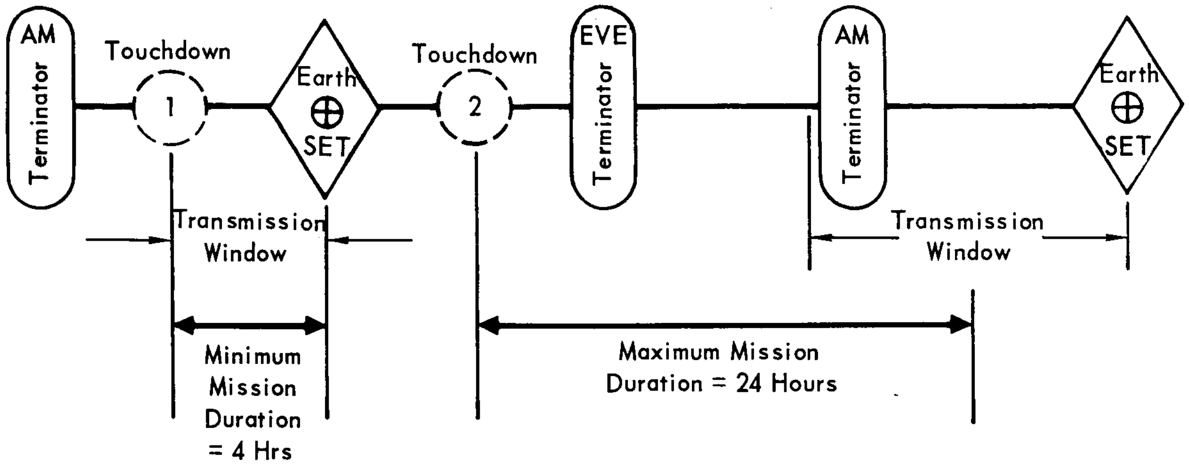
AM
Terminator
Touchdown
1
Earth
SET
Touchdown
2
EVE
Terminator
AM
Terminator
Earth
SET
Transmission Window
Minimum Mission Duration = 4 Hrs
Maximum Mission Duration = 24 Hours
Transmission Window

b) DIRECT LINK COMMUNICATION PARAMETERS

Landing Date	3–20–74 Early	3–25–74 Nominal	4–16–74 Late
Communication Range	1.6 A.U. 2.38×10^8 km	1.63 A.U. 2.43×10^8 km	1.9 A.U. 2.83×10^8 km
Elevation of Site from Equator	-5.7°	-5.1°	$+1.1^\circ$
One-Way Communication Transit Time	13.2 Min.	13.4 Min.	15.8 Min.

Above data for McDonnell T8 Trajectory – Baseline

Alternate trajectory T10 is also accommodated by these values, as these represent maximum excursions for landing latitude between 10°N and 40°S, 8°S nominal.

Figure 5.15–10

erection errors, and landing site displacement from the sub-Earth latitude. Timing errors are considered negligible since data transmission time is less than half the available view time. Latitude pointing error however, can be significant. A preliminary analysis indicated that a single antenna, oriented normal to the surface, must have a minimum beamwidth of 150°. An alternate preferred concept is to provide full spherical antenna coverage.

The derived mission constraints peculiar to the IDP are summarized in Figure 5.15-11.

5.15.2 IDP Operation Studies - Trade studies were made to investigate several variations in the IDP basic operating concept. The question of when during the descent sequence to have the IDP separate from the Capsule Bus was analyzed. As a related subject, consideratinn was given to using the IDP to monitor critical engineering parameters in the Capsule Bus prior to landing.

5.15.2.1 Separation Mode Analysis - An IDP lander separation mode analysis was conducted to establish the optimal point in the CB descent sequence where the IDP should be separated. Initial studies were made to select a few candidate separation modes from a spectrum of many. This was achieved by evaluating the effect of a number of different separation modes on IDP lander performance and reliability. This evaluation reduced the alternatives to three classes. Additional rationale was then called upon to narrow the selection to a single, preferred choice.

Approach - For the initial investigation two parallel studies were conducted. One from the functional performance and design standpoint and the other from the probability of mission success standpoint. Both approaches adopted a common baseline descent sequence and operational phase. The performance and reliability evaluation parameters were established based upon preliminary constraints; numerical evaluators were then assigned to these parameters for each separation mode considered; and finally weighting and ranking numerics were employed to estimate separation mode effects on the Capsule lander and IDP system performance. For the final selection of a preferred concept, "independence" from the lander was adopted as the most important factor.

IDP/Lander Performance and Design Considerations - The eight separation modes selected for evaluation are shown in Figure 5.15-12. Attention is called to modes E and F, which involve a 600 foot separation altitude; it is above this altitude that a parachute was found to be necessary in the weight optimization studies. For anlaysis purposes it becomes a convenient marker to employ when

INDEPENDENT DATA PACKAGE DERIVED MISSION CONSTRAINTS

- Mars landing between 6 February 1974 and 16 April 1974
- Landing site within 10° North and 40° South Latitude with 8° S Latitude as nominal
- Maximum communication distance of 1.9 AU
- Availability of 210 foot antenna and DSN receiving channel for landed operations.
- Direct S-Band telecommunication link
- Minimum 150° antenna beamwidth
- Maximum 24 hr mission duration
- Design weight goal of 100 lb

Figure 5.15-11

IDP SEPARATION MODES

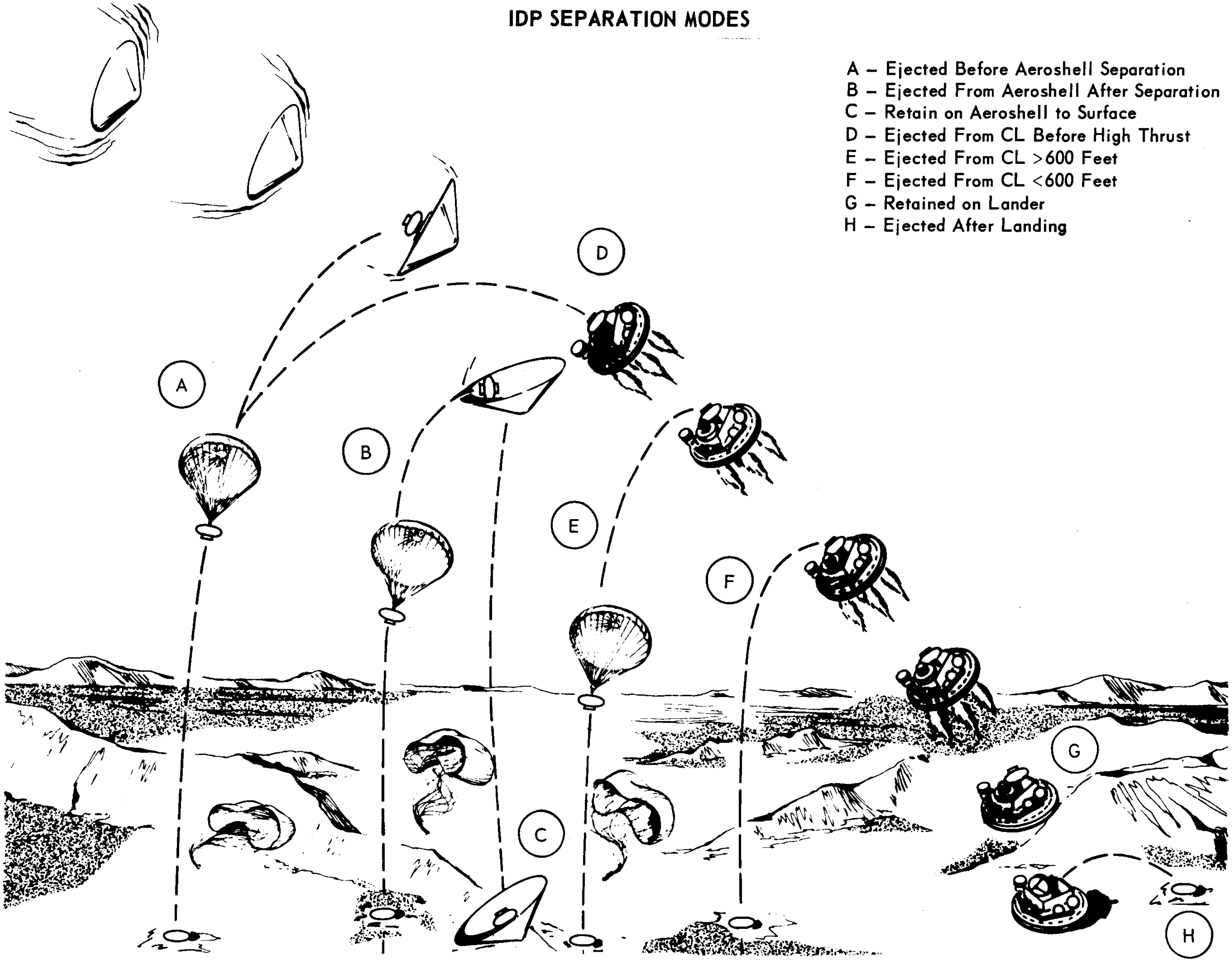

A – Ejected Before Aeroshell Separation
B – Ejected From Aeroshell After Separation
C – Retain on Aeroshell to Surface
D – Ejected From CL Before High Thrust
E – Ejected From CL >600 Feet
F – Ejected From CL <600 Feet
G – Retained on Lander
H – Ejected After Landing

Figure 5.15–12

categorizing separation mode candidates.

The results of the separation mode evaluation relative to performance are shown in Figure 5.15-13. The initial column in the table identifies a set of significant parameters; a weighting factor from 1 to 10 is assigned to each. Subsequent columns rate each separation mode from 1 to 8 in proportion to its influence on the subject parameter. The total performance score for each separation mode examined appears at the bottom of the respective columns. The higher the score the more desirable the mode. Separation modes with low scores generally involve an aerodynamic decelerator; greater impact limiter requirements; greater weight and burial risk; poorer payload-to-weight ratio characteristics; and difficult configuration, power, and control requirements. These "penalties" were imposed by design requirements to withstand high impact velocities; high altitude separation and exposure to high velocity Martian surface winds were in turn the main contributors to these velocities. For the high scoring separation modes the reverse of the aforementioned observations was true. In summary, performance and design considerations were seen to favor late separation or no separation at all.

IDP/Lander Reliability Considerations - The reliability analysis reflected a trend opposite to that of the performance evaluation, i.e., early separation appeared to be the more favorable design approach.

This conclusion was based on an evaluation of five discrete separation mode categories. The separation intervals examined were:

(1) Prior to Aeroshell separation and motor ignition.
(2) Between motor ignition and 600 feet altitude.
(3) Between 600 feet altitude and thrust termination.
(4) Between thrust termination and impact.
(5) After impact.

A typical evaluation of the reliability of obtaining data from either the IDP or the Surface Laboratory for case (1) is shown in Figure 5.15-14. The approach is representative of the analyses conducted for each of the cases denoted above. Figure 5.15-15 presents the composite results and identifies the corresponding separation mode cases. The final column of the referenced figure identifies the probability of achieving a successful transmission to Earth of at least one set of critical surface environment data via the lander or IDP. Note that the probability of mission success is improved by early separation of the IDP.

PERFORMANCE EVALUATION OF IDP SEPARATION MODES

EVALUATION FACTOR	WEIGHTING FACTOR	SEPARATION MODE * RATING (1-8) X WEIGHTING FACTOR							
		A	B	C	D	E	F	G	H
Aerodynamic Decelerator Requirements	10	10	10	80	10	10	80	80	80
Impact Limiter Requirements	9	27	27	9–63	27	27	45	72	63
Sep. Distance on Surface	6	48	42	42	36	30		18	6
IDP Surface Burial	4	4	4	24	4	4	12	32	24
IDP Attitude (Descent & Impact)	3	24	24	9–24	24	24	3	3	6
Sep. Dyns. on Lander	2	12	14	14	12	4	2	16	14
Sep. Dyns. on IDP	2	10	12	16	10	2	2	16	6
Descent Environment	5	20	25	35	30	5	5	40	30
Lander Operation	7	56	42	49	42	21	14	7	21
Lander Mass Properties Change	3	24	21	21	18	6	3	15	12
Lander/IDP Interface	2	6	2	10	6	6	10	16	10
IDP Weight	6	12	12	12–42	6	6	24	48	42
IDP Separation	3	3	18	24	15	9	9	24	12
IDP Configuration	7	7	14	16	7	7	28	49	35
Science Subassembly	4	4	8	8	12	20	24	32	28
CDR Subassembly	10	80	80	10	80	80	70	10	60
TM Subassembly	8	32	32	48	32	32	48	40	24
Power and Control Subassembly	2	2	2	14		4	8	60	10
Total Performance Score		381	384	441–540	373	297	405	534	483

* A Ejected from Capsule before Aeroshell separation
B Ejected from Aeroshell after Aeroshell separation
C Retained on Aeroshell to surface
D Ejected from Capsule before first high thrust
E Ejected from Capsule during thrust above 600 feet
F Ejected from Capsule during thrust below 600 feet
G Retained on Lander to surface
H Ejected from Lander after landing

Figure 5.15–13

TYPICAL VOYAGER CAPSULE MISSION RELIABILITY ANALYSIS WITH INDEPENDENT DATA PACKAGE (IDP) DEPLOYED PRIOR TO AEROSHELL SEPARATION

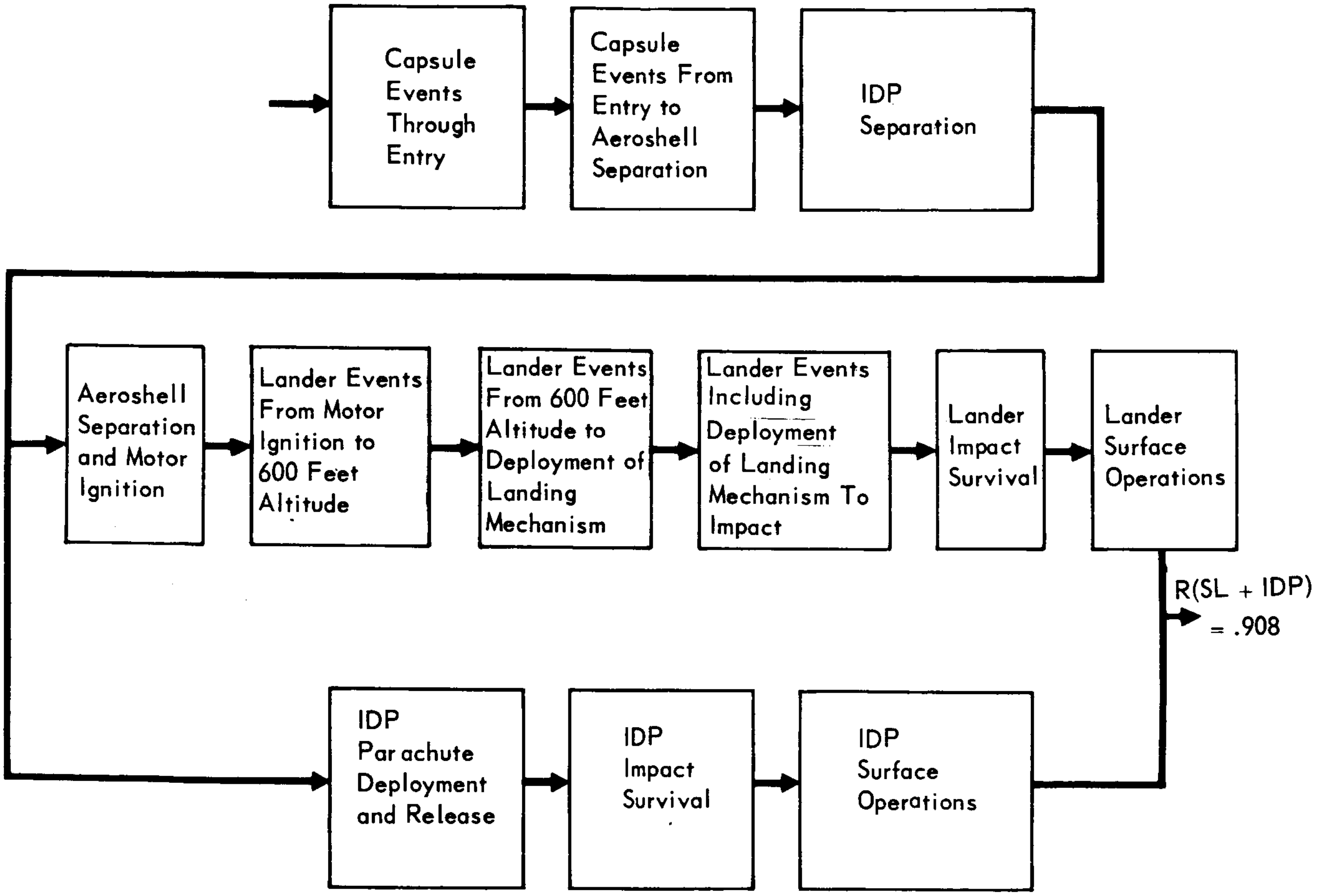
Capsule Events Through Entry
Capsule Events From Entry to Aeroshell Separation
IDP Separation
Aeroshell Separation and Motor Ignition
Lander Events From Motor Ignition to 600 Feet Altitude
Lander Events From 600 Feet Altitude to Deployment of Landing Mechanism
Lander Events Including Deployment of Landing Mechanism To Impact
Lander Impact Survival
Lander Surface Operations
R(SL + IDP) = .908
IDP Parachute Deployment and Release
IDP Impact Survival
IDP Surface Operations

Figure 5.15-14

RELIABILITY COMPARISON OF IDP SEPARATION MODES

SEPARATION TIME	SEPARATION MODE	RELIABILITY OF SL + IDP MISSION
1. IDP Separation Prior to Aeroshell Separation and Terminal Propulsion Ignition	A	0.908
2. IDP Separation at Any Point Between Motor Ignition and 600 Feet Altitude	B D E	0.810
3. IDP Separation at Any Point Between 600 Feet Altitude and Thrust Termination.	F	0.811
4. IDP Separation at Any Point Between Thrust Termination and Impact.	G	0.805
5. IDP Separation After Capsule Impact.	H	0.802

Figure 5.15–15

Conclusions - A composite look at the performance and reliability evaluations is presented in Figure 5.15-16. The composite score for each separation mode was computed as the product of performance score times reliability and then normalized relative to separation mode A. The result appears in the last column of the referenced table; the higher the rating the more desirable is the separation mode.

The rating scores are seen to fall into three general classes:

a. Ejection from Aeroshell near CL separation (A & B)

b. Ejection from CL after Aeroshell separation (D, E & F).

c. Retention through landing (G & H).

The cases of ejection from the CL after Aeroshell separation received relatively low ratings and were, therefore, eliminated from further consideration. Ejection of the IDP from the Aeroshell near CL separation and retention through landing; however, received nearly equal ratings. To resolve this dichotomy, independence was selected as the overriding factor governing preferred concept selection, since it is this objective which is fundamental to the IDP concept.

Thus, although mode H (the separation after landing case) represented the easier performance and design requirement, its low reliability assessment was not consistent with basic IDP purposes. Hence, the high reliability mode A separation (ejection prior to Aeroshell/CB separation) was selected as the preferred design concept.

It should be noted that these conclusions were drawn prior to the incorporation of a parachute into the CB descent system. Although the presence of this parachute does not change the basic tenor of the conclusions drawn herein, it does dictate that close consideration would need to be given to potential parachute system interactions to effect a high reliability IDP/CB system performance.

5.15.2.2 Critical Data Recording (CDR) - The monitoring of critical CB engineering data with the IDP prior to IDP/CB separation was examined to ascertain the merit of incorporating this design feature into the IDP baseline configuration. The approach taken was to (1) adopt a CDR measurement priority by mission phase; (2) identify likely measurement candidates within each phase; and (3) summarize CDR data loads associated with each measurement set. IDP data storage limitations and interface access restrictions were then evaluated to obtain a final recommendation on CDR bit allocation and utilization.

CDR monitoring is placed in perspective by briefly reviewing the purpose of VOYAGER 1973 IDP. The primary purpose of the IDP is to provide independent capa-

IDP SEPARATION MODE COMPOSITE PERFORMANCE AND RELIABILITY SCORE

SEPARATION MODE	PERFORMANCE SCORE	RELIABILITY EVALUATION	COMPOSITE SCORE	NORMALIZED COMPOSITE SCORE	SEPARATION CLASS
A	381	.908	346	1.0 (Ref)	I
B	384	.908	349	1.05	
C	441-540	–	–	–	
D	373	.906	338	0.98	II
E	297	.810	241	0.70	
F	405	.811	328	0.96	
G	534	.805	430	1.25	III
H	483	.802	387	1.12	

Figure 5.15-16

bility to obtain specific planetary environment information, thereby, improving the probability of mission success. Its secondary objective is to provide internal IDP diagnostic measurements to facilitate the interpretation of subsequent transmitted data. Finally, its tertiary objective is to provide engineering measurements yielding diagnostic data relating to a mission landing failure caused by lander system malfunction or by environments exceeding expectations. CDR monitoring requirements originate from satisfying the latter purpose.

The CDR mission phase measurement priorities were established in accord with the basic mission constraints and requirements. The measurements ranked in their judged order of importance are:

(1) CBS performance during high velocity entry.
(2) CBS performance during terminal descent.
(3) Pre-impact planetary surface environment data.
(4) Capsule system performance during de-orbit cruise.
(5) Post-impact planetary environment data.
(6) Pre-impact SLS status evaluation.
(7) Post-impact SLS status evaluation.
(8) Post-impact SLS performance evaluation.

CDR data, as discussed herein, is restricted to the first two priority categories identified above. It is these functions which are most sensitive to the unknown nature of the Martian environment and, therefore, represent the most hazardous phase of the mission.

For the critical descent phases, an initial set of measurement parameters was first established. Typical estimates of parameter ranges, types, numbers of measurements, accuracy, minimum sampling and total bits were also made. These parameters were then classified by their position in the descent profile (pre-separation, separation, descent, or final descent) and ranked by priority within each class. It was apparent that the later the IDP separated from the lander, the greater would be the potential critical data load. Conversely, the data capacity and interface complexity of the IDP are grossly limited by its inherent simplicity. It was, therefore, concluded that (1) only minimal CDR measurements occurring early in the descent sequence could be made; and (2) these measurements must be multiplexed and properly digitized external to the IDP prior to storage to minimize landed payload weight and interface complexities. With these constraints, critical data monitoring was considered feasible. A typical group of CDR measurements is given in Figure 5.15-17. The critical data load in this

TYPICAL CDR MEASUREMENTS LIST

NAME	NO. OF MEAS.	BITS PER MEAS.	BITS PER SAMPLE	NUMBER OF SAMPLES		TOTAL DATA	
				MIN.	MAX.	MIN.	MAX.
Terminal Propulsion Pressure	1	5	5	1	2	5	10
CB Battery Volts	4	7	28	1/4	3/4	7	21
CB Temperatures	6	5	30	1/3	2/3	10	20
Radar Altitude	1	8	8	1	2	8	16
Radar AGC	1	6	6	1	2	6	12
Radar Doppler Transmitter Power	1	4	4	1	2	4	8
Radar Range Transmitter Power	1	4	4	1	2	4	8
Radar Range	1	4	4	1	2	4	8
Radar Velocity	1	4	4	1	2	4	8
Aeroshell Release	4	1	4	1	2	4	8
Terminal Propulsion Ignition	7	1	7	1	2	7	14
Integrating Accelerometer	1	7	7	1	2	7	14
Heat Shield Temperature	1	4	4	1	3	4	12
Events	10	1	10	1	2	10	20
CDR Subtotal	40					84	179

Figure 5.15-17

example varies from 84 to 179 bits. The preferred design concept allocates 90 bits or slightly over 10% of the total data storage capacity for CDR monitoring functions.

5.15.3 Environmental Measurement Studies - The 1969 Mariner Mars probe will make some gross readings of the atmospheric profile parameters. While these derived data may minimize the uncertainties now prominent in the entry and descent problems, they will provide little on the static and dynamic characteristics of the surface environment. However, it is the near-surface atmosphere and subsurface environments which will figure strongly in (1) the search for past and present life forms, and (2) the determination of the environment to be withstood by future lander payloads. To offset the possibility of a lander catastrophe with the concurrent possibility of no data return from the investment, the inclusion of an Independent Data Package becomes a necessary consideration.

There are two basic reasons for generation of primary atmospheric data separately from the Surface Laboratory; these are:

a. In the event of failure of a 1973 soft lander, we must retain some assurance of receiving basic atmospheric environmental data with which to solve engineering problems inherent in subsequent surface missions (1975, 1977, 1979).

b. To assure the generation of atmospheric data of the maximum purity (away from retro-rocket contamination and thermal effects and from dynamic air flow disturbances near the lander), all fundamental atmospheric measurements should be made by an IDP as far from the Surface Laboratory as possible.

Because VOYAGER 1973 represents an initial landing and a first opportunity to sample the surface meteorological elements, it is logical to concentrate upon just the following basic elements:

a. Surface atmospheric pressure (average)
b. Near-surface atmospheric temperature
c. Near-surface atmospheric composition
    - o Water vapor
    - o Non-aqueous gases

The instrument selection criteria are presented in the subsequent paragraphs of this section. A summary of the characteristics of the selected instrument complement is presented in Figure 5.15-18.

5.15.3.1 Surface Atmospheric Pressure Measurement - Occultation studies and

INDEPENDENT DATA PACKAGE INSTRUMENT CHARACTERISTICS

CHARACTERISTICS	MEASUREMENT				
	PRESSURE	TEMPERATURE	WIND VELOCITY	ATMOSPHERE COMPOSITION	WATER VAPOR
INSTRUMENT	VIBRATING DIAPHRAGM TRANSDUCER	PLATINUM RESISTANCE THERMOM.	HOT WIRE ANEMOMETER	GAS CHROMATOGRAPH	HYGROSCOPIC AL_2O_3-A_u SENSOR
Weight (lb)					
Transducer	0.2	<0.1	<0.1		0.1
Electronics	0.4	0.3	0.4		0.5
Total	0.6	0.4	0.5	3.4	0.6
Volume ($in.^3$)					
Transducer	3.0	1.0	1.0		1.0
Electronics	6.0	3.0	4.0		8.0
Total	9.0	4.0	5.0	75	9.0
Power (watts)	0.5	0.3	0.5	4.0	0.5
Thermal Control (Operating)	0°C–65°C	0°C–65°C	0°C–65°C	Columns and Detectors ±3°C	0°C–65°C
Transducer Location	Interior	Deployed	Deployed	Interior	Interior
Measurement Range	0–50 mbs	–170°C→+90°C	0–260 ft/sec	10^2-10^6 ppm	Partial pressure $10^{-6} \rightarrow 40$ mb
Sensitivity	0.4 mb	2°C	1 ft/sec	10 ppm	0.1 ppm
No. of Samples	5	5	4	2	4
Bits/Sample	7	7	7	200	7
Total Data Bits	35	35	28	400	28

Figure 5.15–18

spectroscopic readings place the mean Mars surface pressure at between 4 and 16 mbars. Experimental uncertainties expand this range to from 2 to 30 mbars. The various atmospheres shown for Mars (VM-1 through VM-10) show surface pressures from 5 to 20 mbars. In addition, a seasonal variation of from 20% to 30% appears probable. Thus, it appears that an instrument working range of from 0 to 50 mbars is reasonable.

It is apparent that we are to attempt pressure measurements in a region between normal elastic cell methods and the realm of vacuum measuring instruments such as the Pirani gage. The Bourdon tube is good only to about 15 mbars (lower limit), the bellows type to about 1 mbar (but with temperature difficulties), while the evacuated diaphragm and cell combination has both temperature and sensitivity difficulties at the pressure and temperature levels which are expected.

Alternatives - NASA-Ames has developed a very promising stretched metal diaphragm type of transducer for low pressure measurement. The diaphragm is located between two parallel conducting walls and is electrostatically driven at its mechanically resonant frequency. The electrostatic power required to maintain an equilibrium vibration at a given amplitude is a function of the atmospheric pressure and gas properties. A dc excitation voltage is applied to the transducer through a precision voltage divider and current limiter. Applied in series with the dc voltage is a sinusoidal ac voltage whose frequency is adjusted for maintenance of the peak transducer output. As the pressure being measured is varied, the deflection of the vibrating diaphragm is also varied to maintain a constant amplitude of vibration.

This unit is presently undergoing further development to achieve a flight design. The unit's high accuracy, lack of requirements for reference pressures, inherent ruggedness, and generally good environmental operation are strong points in its favor for this application. The sensitivity of the transducer to atmospheric composition has been evaluated but requires additional effort. If an effect is demonstrated to exist, the transducer may have to be calibrated after data from the atmospheric composition experiments has been received.

A similar variable-capacitance type of unit is also available commercially from a number of companies including Rosemount Engineering and Lion Research. First estimates however indicate that these units possess a lesser sensitivity and linearity in the lower pressure ranges than do the vibrating diaphragm units. The variable capacitance units also are heavier, larger, and have higher power requirements. It is necessary that the signal electronics for these units be mounted integrally with the transducer to alleviate the influence of variations in line impedance on calibration.

Recommendation - The vibrating diaphragm pressure transducer mounted within the payload should be used to measure atmospheric pressure.

5.15.3.2 Near-Surface Atmospheric Temperature Measurement - The term "near-surface" is defined by the largest vertical dimension of any lander equipment as planned during the VOYAGER series. This means that we are interested in (approximately) the lowest six feet of the Mars atmosphere. Unfortunately, it is this layer of the atmosphere which will undergo the widest variations of temperature, as well as of some other properties. In the case of any planet with essentially clear areas in its atmosphere, the surface atmosphere interface will exert a powerful influence on the near surface environment.

Similarly, at the cessation of insolation the upper few millimeters of the solid surface will radiate thermally at a rapid rate; simultaneously the energy required to maintain the local wind structure will have dropped to zero, and a steep inversion (positive vertical thermal gradient with altitude) will form. The thickness of the inversion layer is not known at this time and is problematical, but it most probably will exceed the height of the lander and its equipment. Therefore there will exist: (1) a positive (upward) thermal gradient along the vertical axis of the lander, and (2) no easily measurable relationship between the temperature at a point on the lander and the normal lapse rate level at some higher altitude.

The thermal gradient parallel to the Z axis of the lander may be either positive or negative with respect to altitude, depending for sign and magnitude upon the time of the Martian day and upon wind conditions. The thermal picture is important to the operation of equipment, to life environment, and to knowledge of planetary meteorology. It is therefore important to measure the near-surface air temperature at frequent intervals.

In terms of accuracy, low weight, simplicity and uniformity (unit to unit), it is pointless to consider any unit but the platinum thermometer. This type of unit can be expected to maintain its calibration to within close limits over the desired two years, and will cover the expected range of + 50°C to -120°C without trouble.

The sensor itself consists of a length of platinum wire wound on a high dielectric frame of low specific heat. A constant voltage is applied across the terminals; measurement of the resistance, which is a function of its temperature, constitutes the reading. The measuring current must be kept very low; otherwise the element becomes a hot wire anemometer.

To obtain accurate temperature measurements, the sensor must be as completely thermally isolated from all heat sources and sinks as possible. It must be completely exposed to the free air but shielded from surface radiation and solar insolation. Also, it must be deployed sufficiently far from the IDP body that heated eddies from the IDP surface do not influence the temperatures being measured. These requirements are provided for in the preliminary design by deploying the temperature sensor on an extendable mast; multiple radiation shields with supports of low thermal conductance are provided above and below.

Recommendation - A deployed platimum resistance thermometer should be used to measure atmospheric temperature.

5.15.3.3 Near-Surface Wind Velocity - It is desired to know the wind speed near and above the Martian surface for several reasons:

a. To ascertain the near surface speed in order to compute the sand and silt carrying power and particle kinetic energy and therefore the abrasion which a long term Surface Laboratory must withstand.
b. To compute the wind stress which a long term Capsule must withstand.
c. To be able to compute the drag and wind profiles near the surface to assist in the interpretation of planetary meteorology.

A solution to the first two problems may be provided directly by a few fixed height measurements of near surface wind velocity. The third problem requires the wind velocity to be sampled simultaneously at two altitudes; however, even with just reading at a known height, theoretical values may be calculated. Thus, it is desirable to include an anemometer in the IDP instrument complement.

There are several types of anemometers in normal use, such as the cup, drag force sphere, acoustic, and hot wire. However, the combination of low pressure, low temperature, and dust rather effectively rules out the use of the first three. Therefore, the unit recommended at this time is a hot wire anemometer of the Hastings - Raydist type. This is a heated thermocouple device and is self-compensating with respect to air temperature fluctuations. In principle, the device is a low voltage bridge circuit with two noble metal thermocouples used as sensing elements; these thermocouples are heated with alternating current. A change of atmospheric flow past the probe changes the temperature of the thermocouples; this results in a change of the dc output. A third thermocouple is in the dc recorder circuit, but is unheated. Any transient effects due to change of temperature are cancelled out, since the active and reference thermocouples generate equal and opposite EMF's.

The unit would be deployed from the instrument payload and made omni-directional in the horizontal plane by placing above and below it, at suitable distances, protective plates; these plates would allow unimpeded wind flow and secondarily serve as radiation shields for the temperature sensor.

Recommendation - A deployed hot wire anemometer is the recommended instrument for wind velocity determination.

5.15.3.4 Near-Surface Atmospheric Composition - One of the several primary questions concerning the atmosphere of Mars is that of the composition. Many attempts have been made to analyze this atmosphere spectroscopically from Earth, but the only results to date have been the positive identification of CO_2 and the rather questionable identification of water vapor. No other identification has been found to be possible. But the partial pressures deduced from these findings are not sufficient to account for the total pressure as deduced from the occulatation experiment and by other conclusions. Thus, further surface-based composition determinations are necessary to extend and confirm existing data. An accurate determination of atmospheric composition will be helpful in the determination of the existence of life (past or present) and will aid in the interpretation of other composition dependent measurements (e.g, wind and pressure).

There are a number of ways to conduct an atmospheric analysis. These are (1) spectroscopic methods which are not sufficiently quantitative, (2) gas chromatographic methods which are excellent for preselected determinations, (3) mass spectroscopic methods which are excellent for scanning a predetermined mass range in which the constituents are unknown, and (4) specific element or compound detectors which, although satisfactory, require space and power beyond that available. Thus, the candidate quantitative instruments are the mass spectrometer and the gas chromatograph. A mass spectrometer for the atomic mass range of interest, however has a weight, shape factor and power consumption which exceed the practical limitations of an IDP. A gas chromatograph can be designed to be very light, require small volume, use little power, and yet produce sensitive quantitative and qualitative analyses of the major gases present in the Mars atmosphere. Moreover, these chromatograms can be telemetered to Earth with a relatively low number of data bits. These advantages make the instrument particularly attractive for use in the IDP where very severe weight, volume, power and data transmission limitations are imposed.

The gas chromatograph consists of the following basic elements: helium carrier gas supply and pressure regulator; an atmospheric sample valve and injector; two column sections where the gas constituents are separated; a detector; and an electronic data processing module. The output of the thermal conductivity detector is a simple dc voltage which increases when a second gas is present in the helium carrier. If this voltage is examined as a function of time, a series of sharp peaks is obtained. The area under each peak and the time at which maximum amplitude occurs is all the data that is needed to analyze the chromatogram. Data readout may be obtained with a simple gated integrator. The peak areas are proportional to the concentrations of the components in the mixture. The time of appearance of each component is a function of the chemical structure and is used for identification.

A hardened device of this nature has been built by JPL and its major components have been demonstrated to be capable of surviving 10,000 g_E impacts. It is estimated that a similar flight model could be packaged in a volume of 75 in^3 and would weigh 3.4 pounds.

Intake to the instrument would be via a tube wound in a helix concentric with the extendable atmospheric sensor mast. Prior to porting, this intake would be directly vented to the atmosphere; following porting, the intake would be extended together with the atmospheric sensor mast, thereby, allowing better access to an uncontaminated environment.

The instrument would have a dynamic range of from 10^2 to 10^6 ppm and would detect CO, CO_2, N_2, O_2, A, NO_n, SO_n, and possibly some hydrocarbons.

Recommendation - A gas chromatograph is the recommended instrument for atmospheric composition determination.

5.15.3.5 Near-Surface Water Vapor Detection - The objective of this instrument is to obtain some measure of the water vapor content of the Martian atmosphere in the vicinity of the planetary surface. The existence and concentration of water vapor will be very important to future estimates of the kind of life possible on Mars and of the probability of life. Such information would also be of great use in evaluating the kind and extent of weathering processes which possibly exist.

The measurement of humidity, with any real accuracy, is a difficult thing even under controlled laboratory conditions. The available evidence indicates only about 14 ± 7 microns of water exist in the Martian atmosphere. At the temperatures prevailing during much of the diurnal cycle, the detection of these minute amounts of water vapor will be difficult. The problem is further compounded by the requirement that the selected instrument be compact, sterilizable, and able to survive high impact.

Alternatives - In general, the methods of water vapor may be treated in two areas: (1) the measurement of humidity above 0°C, and (2) the detection of water vapor below 0°C - usually by frost point. The laboratory determinations above freezing are usually made with gravimetric measurements if accuracy is desired. The frost point determinations are made with a cooled mirror plus an optical system to detect electronically the formation of frost cloudiness; forst temperature is sampled in the mirror surface by thermocouple. The equipment required for these determinations is voluminous, however, and obviously impractical for the IDP.

The measurement of humidity by hygroscopic acquisition, with resulting change of electrical characteristics of a prepared element (sensor) is used extensively for ordinary temperatures and pressures; these are generally accurate to within 2-5%. This is sufficient for most purposes. The behavior of most hygroscopic elements, however, deteriorates rapidly with increasing ΔT below 0°C. In most cases the time lag constant becomes very large, and the utility of the element degrades badly. The time lag increase for Mars may be estimated very roughly by comparison of the number densities for the surface atmospheres of the two planets; for comparable compositions the ratio $N_{earth}/N_{mars} = 0.55 \times 10^2$, or the time lag for equilibrium over a hygroscopic element on Mars would be 55 times the lag for Earth. This is a minimum value; additional lag would result from the very low concentration of water vapor in the Mars atmosphere.

A candidate hygroscopic sensor is the Al_2O_3-Au element. This element consists of a thin sheet of specially anodized aluminum which develops a porous oxide coating. An outer electrode is formed by evaporation of a gold layer onto the oxide surface. The aluminum base sheet acts as the other electrode. If a fixed frequency is applied across this device it shows an impedance which is variable as a function of the absorbed water vapor. This element can measure frost points from +30°C to -110°C, or partial pressures from 40 to 10^{-6} mbars. If the total pressure lies in the range of from 4 to 20 mbars, the lowest sensitivity would possibly range from 0.1 to 0.05 ppm of water.

Another choice would be one of the various dewpoint-frost point-indicators which have been developed for military and Weather Bureau use in the Earth's atmosphere. These units are also excessively large in terms of weight and power consumption.

A qualitative measurement of water vapor present could be obtained with a P_2O_5 device. In this device a container of P_2O_5 is gently ventilated and two electrodes measure the change in vapor resistivity as a function of time. Again however, the mechanization of this device for the IDP does not appear to be practical.

Finally, the optimal device for the detection of the small amounts of water vapor thought to be present in the Mars environment would be the mass spectrometer. It is estimated that a simple tuned mass spectrometer whose design has been optimized over a limited mass range (e.g. 16 to 18 a.m.u.), could be designed for a weight allocation of 4-6 pounds. The weight and power requirements still exceed the capabilities of a 100 pound IDP.

Recommendation - The recommended detector is an Al_2O_3-Au sensing element. The hygroscopic sensing element is the only known water vapor detector device which is practical in terms of weight, size, and power for incorporation into the IDP. Since this measurement is so important to the determination of the existence of possible life forms, it is recommended that this instrument be adopted into the IDP baseline.

5.15.4 IDP Electronic Subject Studies

- The results of design studies conducted to establish the configuration of the IDP Radio Subassembly; Power and Control Subassembly; and Data Handling Subassembly are presented in this section.

5.15.4.1 Telecommunications Analysis - The derived constraints and characteristics for the IDP Telecommunication System are summarized in Figure 5.15-19.

Direct vs. Relay - In line with the basic philosophy of reliability and simplicity for the IDP telecommunications design, the direct telecommunications link was selected. Major reasons for this selection include operational simplicity, reduction of complexity in the orbiting spacecraft, and removing the need for a command receiver in the IDP. Also, studies of possible orbits indicate that it is very difficult to meet the spacecraft objectives and at the same time meet the requirements for guaranteed communications with the IDP. No new or different MDE requirements will be imposed by the Direct Link Communications since the Surface Laboratory System low-rate telecommunications link uses the identical MFSK modulation techniques.

MFSK vs. PCM/PSK - The short form design control table, Figure 5.15-20 shows that PCM/PSK modulation such as used on Mariner II and IV is not possible for the IDP. In this table two $2B_{LO}$ S-band receiver phase-lock-loop bandwidths are assumed, 1.0 Hz and 5.0 Hz. 1.0 Hz is considered to be the absolute minimum

INDEPENDENT DATA PACKAGE TELECOMMUNICATIONS
CONSTRAINTS AND CHARACTERISTICS

1. Environmental

   A. Operate in the expected Martian atmosphere and sustain the sterilization requirements as outlined in JPL Project Document PD606–4 Revision 1.

   B. Sustain a 3,100 g_E, 3 millisecond shock.

   C. Operate in temperature range of 0° C to + 65° C.

   D. Accommodate Martian surface slope angles up to plus or minus 34°.

2. Operational

   A. Two major operational alternatives are:

      (1) IDP is to operate for only 4 hours after landing, or

      (2) IDP mission is to last through a Martian night and terminate approximately 24 hours after landing.

   B. At 1973 Mars opportunity maximum communication distance is 1.9 AU (2.83×10^8 km).

   C. NASA Deep Space Net performance as detailed in Reference 5.15–1 is assumed with constraint of 210 feet diameter antenna operating in the 2–way mode and system temperature $T_s = 45 \pm 10°$ K.

   D. Transmission will be at S–band in the 2,295 MHz deep space telemetry band.

   E. Direct Mars-to-Earth link is to be employed

   F. Transmission is to occur in a period such that multi-path effects do not enter into the telecommunications design control.

   G. Omni-directional coverage will be provided using 6,110° beamwidth antennas.

   H. 16–ary MFSK modulation techniques shall be employed.

   I. It is required to transmit 800 bits nominally of data with appropriate acquisition and sync data as required. It is preferred, but not required, that the capability be included to transmit the entire data sequence at least twice.

   J. Maximum data bit error rate of 5×10^{-3} is assumed.

   K. A frequency acquisition tone and a chip sync acquisition (FSK) pair of tones must be transmitted prior to each data transmission.

   L. 20 Watt TWTA RF power source is to be employed.

   M. Data rate is to be 1.2 bps with a chip rate of 0.3 chips/second.

   N. Transmission time for an 800 bit data group and frequency acquisition tone is 18 minutes. Total transmission time for transmitting this data and acquisition tone 6 times over each of the 6 orthogonally oriented antennas is 1.8 hours.

   O. The MDE developed for the Surface Laboratory MFSK low-rate telemetry link will be utilized.

Figure 5.15–19

TELECOMMUNICATION DESIGN CONTROL TABLE (PARTIAL) – VOYAGER '73
INDEPENDENT DATA PACKAGE – DIRECT MARS TO EARTH LINK
S-BAND, 210 FT DSIF ANT., PCM/PSK MODULATION, 2.0 BPS

NO.	PARAMETER	NOM. VALUE	TOLERANCE	UNITS	SOURCE
1	Net Received Signal Power (See Figure 5.15–21)	–164.8	+6.8 –4.8	dBm	Present Design (20W, 110° Ant, etc.)
2	Receiver Noise Spectral Density, $T_s = 45°K$	–182.1	+0.9 –1.1	dBm/Hz	See Ref. 5.15–1
3	Carrier Modulation Loss	–4.1	+0.9 –1.0	dB	(Assumption)
4	Received Carrier Power	–168.9	+7.7 –5.8	dBm	Calculated Σ (1 + 3)
5	Carrier APC Noise BW., 5.0Hz	+7.1	+0.0 –0.4	dB-Hz	Calculated
6	Carrier APC Noise BW., 1.0Hz	0.0	+0.0 –0.4	dB-Hz	Calculated
	CARRIER PERFORMANCE, 5.0 Hz, $-2\ B_{LO}$				
7	Threshold SNR in $2\ B_{LO}$	+6.0	–	dB	(Assumption)
8	Threshold Carrier Power	–169.0	+0.9 –1.5	dBm	Calculated Σ (2 + 5 + 7)
9	Performance Margin	+0.1	+9.2 –6.7	dB	Calculated Σ (4 – 8)
	CARRIER PERFORMANCE, 1.0 HZ, $-2\ B_{LO}$				
10	Threshold Carrier Power	–176.1	+0.9 –1.5	dBm	Calculated Σ (2 + 6 + 7)
11	Performance Margin	+7.2	+9.2 –6.7	dB	Calculated Σ (4 – 10)
	DATA CHANNEL PERFORMANCE				
12	Modulation Loss, ($\theta_D = 0.81$)	–4.6	+0.6 –0.7	dB	Assumption
13	Received Data Subcarrier Power	–169.4	+7.4 –5.5	dBm	Calculated Σ (1 + 12)
14	Bit Rate (2.0 bps)	3.0	–	dB-bps	Assumption
15	Required STb/No ($P_{be} = 5 \times 10^{-3}$)	+7.6	+0.5 –0.5	dB	Theoretical Performance
16	Threshold Subcarrier Power	–171.5	+1.4 –1.6	dBm	Calculated Σ (2 + 14 + 15)
17	Performance Margin	+2.1	+9.0 –6.9	dB	Calculated Σ (13 – 16)

Figure 5.15–20

S-band receiver phase-lock-loop noise power bandwidth which would be technically possible by 1973. This is considerably less than the minimum 5.0 Hz bandwidth stated in JPL Engineering Planning Document #283, Rev. 2. Even with the low 1.0 Hz bandwidth, the carrier performance is seen to have a barely acceptable net margin of +0.5 dB. With the more reasonable loop bandwidth of 5.0 Hz, the net performance margin is completely out of the question, i.e., -6.6 dB. A bit rate of 2.0 bits per second is seen to give an unusable data channel net margin of -4.8 dB. A bit rate of 1.0 bit per second gives also an unusable net margin of -1.8 dB.

Telecommunications Link Design Control - This section describes the basis for selection of the IDP RF power level, modulation technique, and data rate. The Telecommunications Design Control Table, Figure 5.15-21, summarizes the RF power levels, losses, and gains discussed in the following paragraphs.

It has been shown above that PCM/PSK modulation is not possible for the IDP mission. The noncoherent M-ary method of frequency modulation is the only known technique remaining which can meet all of the requirements. The principal disadvantage in this MFSK technique is that it has not yet been used at low data rates (<2 bps) on any deep space mission.

The principal problem area in the low-rate MFSK link design is that of an efficient detection method at the DSN stations. The detection method is complicated by frequency uncertainties combined with low data rates. The IDP transmitter frequency uncertainty due to crystal oscillator drift and the 3100 g_E landing shock, is estimated to be within a range of ±2 kHz. The best detection technique, which solves the problems of acquisition and automatic frequency control, is the spectral analysis method using the recently developed digital computer Fast-Fourier Transform (FFT) programs. The use of this technique is described in detail in Volume III, Part B, Section 5.4.3, of this report.

The FFT Method is first used to find the location of the narrow band MFSK (tone spacing ≈6 Hz) spectrum within the 4 KHz uncertainty band. For a time bandwidth product (TB) of 10 the required S/N_o is $+9.5 \pm 0.5$ dB which is within the available S/N_o of +11.6 dB. A theoretical maximum time of 3.6 minutes is required for this frequency acquisition. The next operation performed by the FFT method is symbol (chip) synchronization. For an allowable worst case data detection loss of 2.0 dB the worst case available (S/N_o) of +11.6 dB permits chip synchronization within a period of ≈ 1.6 minutes. The third operation performed by the FFT method is data detection. For a TB = 7 and for a probability of bit

TELECOMMUNICATIONS DESIGN CONTROL TABLE – VOYAGER 1973
INDEPENDENT DATA PACKAGE – DIRECT MARS TO EARTH LINK
S-BAND, 210 FT ANTENNA, 16-ARY MFSK MODULATION

NO.	PARAMETER	NOM. VALUE	TOLERANCE	UNITS	SOURCE
1	Transmitter Power	+43.0	+1.0 –1.0	dBm	Initial Assumption
2	Transmitting Circuit Loss	–1.0	+0.5 –0.5	dB	Design Estimate
3	Impact Limiter Loss	–0.2	+0.2 –0.2	dB	See Note Below
4	Transmitting Antenna Gain	+3.5	+0.5 –0.5	dB	See Note Below
5	Polarization Loss	–0.2	+0.2 –0.3	dB	See Note Below
6	Transmitting Ant. Pointing Loss	–3.0	+3.0 –0.0	dB	Definition of ½ Power Beamwidth
7	Space Loss; 2,295 MHz, Nom. 1.63A.U.	–267.8	+0.3 –1.2	dB	Calculated See Note Below
8	Receiver Antenna Gain	+61.0	+1.0 –1.0	dB	See Ref. 5.15–1
9	Receiver Antenna Pointing Loss	–0.1	+0.1 –0.1	dB	
10	Net Received Signal Power, S	–164.8	+6.8 –4.8	dBm	Calculated Σ 1 thru 9
11	Receiver Noise Spectral Density, No.	–182.1	+0.9 –1.1	dBm/Hz	See Ref. 5.15–1
12	Received (S/No)	+17.3	+7.9 –5.7	dB	Calculated [10 – 11]
13	Required S/No; Bit Rate = 1.2 bps $P_{be} = 5 \times 10^{-3}$	+9.5	+3.1 –0.0	dB-Hz	Theoretical Performance
14	Performance Margin	+7.8	+8.2 –6.2	dB	Calculated [12 – 13]
15	Net Margin over Σ of Neg. Tolerances	+1.6	–	dB	Calculated [(14 Nom.) – (14 Neg. Tol.)]

Notes: ITEM 3 – This based on measurement error tolerance of ±0.4dB. Loss through dry balsa wood was found by test to be 0dB.

ITEM 4 – Crossed-slot antenna of 110° beamwidth, including losses in net efficiency, has an on-axis effective forward gain of +3.5dB.

ITEM 5 – –0.5 dB, worst case, is based on actual measured axial ratios of < 6.0dB.

ITEM 7 – Based on a latest arrival date of April 16, 1974.

Figure 5.15–21

error of less than 5×10^{-3}, the detection loss is estimated to be a worst case 1.1dB. The minimum theoretical required (S/N_0) for 16-ARv MFSK data detection at 1.2 bps and a proability of bit error of 5×10^{-3} is + 6.0 dB. The fourth function of the FFT method is that of automatic freqeuncy control (AFC) using a periodically transmitted 17th tone. This AFC is required in order to compensate for errors in the Doppler ephemeris and the errors due to IDP reference crystal oscillator drift.

In summary, the total net margin is + 1.6 dB. As a conservative approach, the acquisition tone times have been increased from the estimated values above to 4.5 minutes for frequency acquisition and to 2.5 minutes for chip sync acquisition. This gives a total acquisition time of 7.0 minutes. If it later becomes evident that the RF losses are not as great as indicated herein, the first design change should be to reduce transmitter power to a lower level. The second change would be to increase the data bit rate to achieve a shorter data transmission period.

5.15.4.2 Radio Subassembly - The functional block diagram, Figure 5.15-22, indicates the preferred design of the radio subassembly. In the following paragraphs the telecommunications link design and some of the trade-offs and hardware design problems will be discussed.

The function of the radio subassembly is to efficiently transmit the IDP data from its landed location on Mars to Earth. The radio subassembly contains the MFSK encoder, the reference crystal oscillator, the S-Band RF exciter, the RF power amplifier, a power supply, and the 6 antenna assembly.

The MFSK encoder accepts binary coded data in groups of 4 bits at a time, and generates any one of 16 tones corresponding to each possible combination of the 4 data bits. It also, upon periodic command from the data handling subassembly, generates a 17th synchronization tone called the chip sync tone.

The master crystal oscillator is the prime frequency source for the IDP. It is mounted in a shock resistant, isothermal environment. It generates the basic RF frequency for the transmitter and also is the source of bit sync and chip sync for data readout from the data handling subassembly.

The transmitter consists of the RF exciter and the RF power amplifier. The exciter output is modulated by the output of the MFSK encoder. This MFSK modulated signal is then amplified to the RF power level of 20 watts by the TWTA (Traveling Wave Tube Amplifier).

FUNCTIONAL BLOCK DIAGRAM – – I. D. P. RADIO SUBASSEMBLY

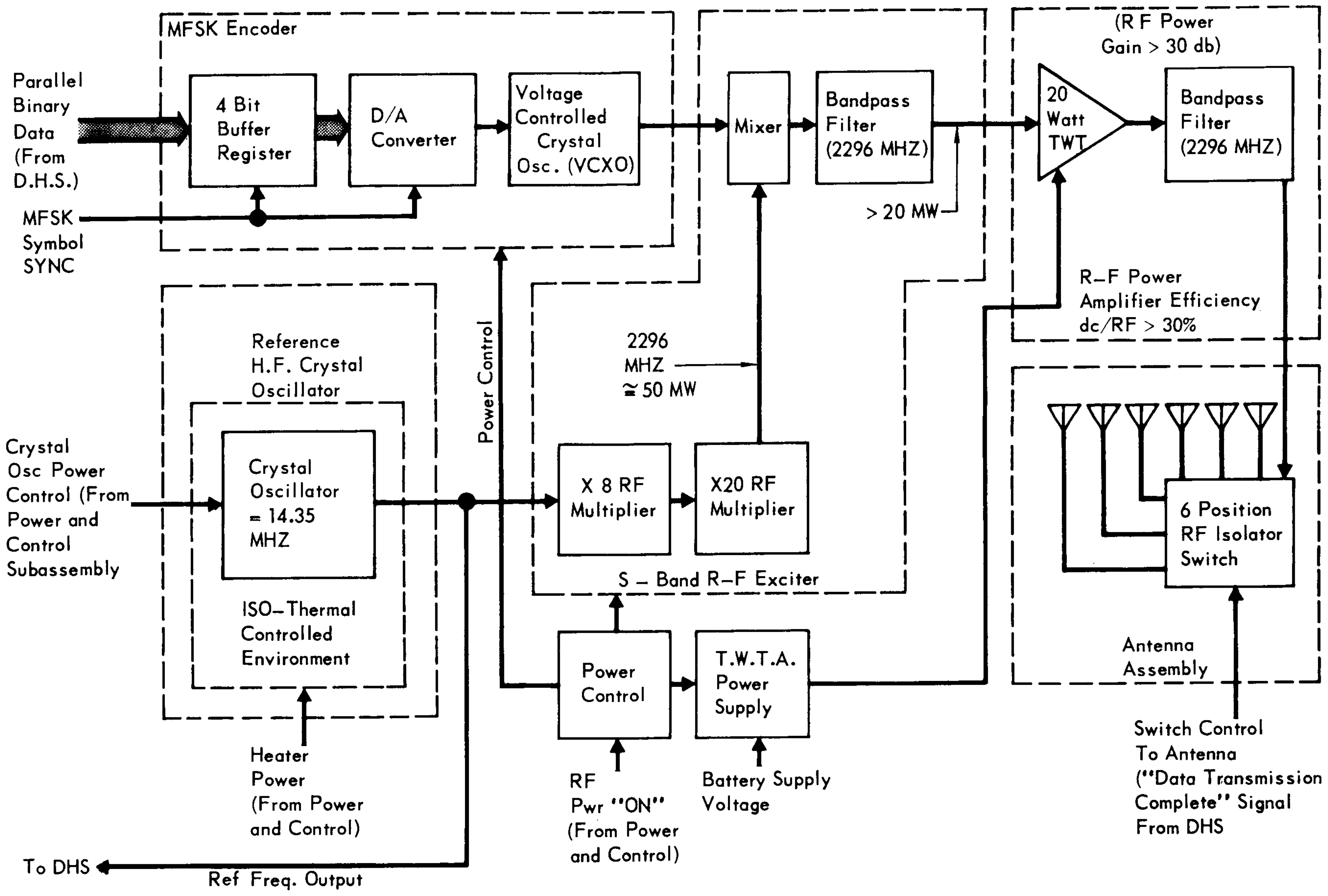
MFSK Encoder
Parallel Binary Data (From D.H.S.)
4 Bit Buffer Register
D/A Converter
Voltage Controlled Crystal Osc. (VCXO)
MFSK Symbol SYNC
Mixer
Bandpass Filter (2296 MHZ)
> 20 MW
(R F Power Gain > 30 db)
20 Watt TWT
Bandpass Filter (2296 MHZ)
R–F Power Amplifier Efficiency dc/RF > 30%
Reference H.F. Crystal Oscillator
Crystal Osc Power Control (From Power and Control Subassembly
Crystal Oscillator ≈ 14.35 MHZ
ISO–Thermal Controlled Environment
Heater Power (From Power and Control)
Power Control
2296 MHZ ≅ 50 MW
X 8 RF Multiplier
X20 RF Multiplier
S – Band R–F Exciter
Power Control
T.W.T.A. Power Supply
RF Pwr "ON" (From Power and Control)
Battery Supply Voltage
6 Position RF Isolator Switch
Antenna Assembly
Switch Control To Antenna ("Data Transmission Complete" Signal From DHS
To DHS
Ref Freq. Output

Figure 5.15–22

The antenna configuration is indicated on the block diagram, Figure 5.15-22. The mode of operation is to transmit sequentially the IDP complete data group including synchronization tones out of each of the six orthogonally positioned antennas. System design considerations imply the desirability of 4 π steradians coverage. This philosophy requires no assumptions to be made concerning the final landed orientation of the IDP on the Martian surface. It permits the use of 110°, conical shaped beam antennas with + 3.5 dB nominal gains. Although this gain would appear somewhat low for an antenna of this beamwidth, the gain figure includes the actual measured efficiency of the proposed crossed-slot antenna.

Hardware Design Problems - Hardware design problems include those of crystal oscillator instability and traveling wave tube amplifier design. The crystal oscillator design is especially difficult in the case of the IDP since the shock level of 3100 g is combined with the wide temperature variation during a Mars diurnal cycle. In order to withstand the shock, and to reduce the crystal oscillator drift as a function of changing temperature, it will be necessary to house the crystal and the oscillator and buffer stages within a shock resistant isothermal environment. It is estimated that an instability of 1×10^{-10} rms in a 1 second interval is possible based on previous Philco designs if the temperature is maintained within a few degrees. The long term drift should be less than 1×10^{-9} in a 24 hour period under these conditions. It is apparent that a traveling wave tube amplifier (TWTA) is necessary in order to efficiently generate 20 watts of RF power at S-Band. This approach presents a problem in the case of the IDP shock environment (3100 g_E). Watkins-Johnson Inc. has done the only known work to-date in implementing a shock resistant TWTA at >3000 g_E levels. Their tube, Model No. WJ-398 (22 Watts at S-Band) has been successfully tests at a 10,000 g_E peak, 1 millisecond duration shock level.

RF Switch Mechanization - A reasonable mechanization of the six-way RF antenna switch is stripline diode construction. Swtiching can be done with PIN diodes which provide approximately 1.5 ohms with 100 milliamps forward bias and 0.3 picofarads capacitance with reverse bias. A diode of this type can be used in each transmissions line to a particular antenna. Using 1/4 wave length stripline sections, these diodes can be used to switch the RF energy to any one of the six antennas.

Impact Limiter RF Loss - In order to properly evaluate the competing antenna configurations, it was necessary to know the effect of transmission of S-Band RF energy through the balsa wood impact limiter. Since no conclusive data was available, a test was initiated to determine the effect experimentally. To this end, a 12 in x 16 in x 8 in section of balsa wood, with a grain orientation and assembled configuration similar to an actual impact limiter, was fabricated and the RF attenuation at normal incidence was measured at 2,295 MHz. RF measurements were taken with the balsa wood sample pressed against the aperture of a 5 in x 7 in antenna horn. E-plane and H-plane patterns were measured with and wihtout balsa wood. Also, the measurements were made before and after a demoisturization typical of the treatment required of balsa prior to sterilization. Within an experimental error of ± 0.4 dB the dried balsa RF loss was determined to be 0 dB. This measurement is the basis for parameter 3 in the design control table, Figure 5.15-21. As a point of interest, the nondried balsa exhibited an attenuation of 1.0 dB within the same experimental error. It is expected that the dried balsa test best depicts the actual condition of the IDP limiter in a Mars environment.

Antenna Configuration - Mission configurations dictate that if a single antenna is used it must possess a conical beamwidth in excess of 150°. To achieve this coverage with a single antenna and simultaneously maintain acceptable gain and polarization decoupling losses, it is necessary that the antenna be erected above the payload ground plane. This can be best achieved by placing the antenna elements on top the extendable atmospheric sensor mast. However, the necessary RF feed lines which are small and flexible enough to be deployed through the instrument mast possess a loss characteristic of approximately 0.5 dB per foot at S-Band. This results in nearly a 2 dB net loss in transmitted power. This characteristic coupled with the inherent unreliability of a deployed antenna clearly dictates that the use of a single antenna is an undesirable solution.

The selected design approach utilizes multiple, nondeployed antennas appropriately positioned within the package envelope. Further, to circumvent the requirement for selective transmission over the upward facing antenna(s) and to guarantee communication irrespective of package orientation, the antenna beam coverage was increased to 4π steradians. Studies of the required number of antennas and their required beamwidth recommended six antennas conceptually located on the faces of a cube. A beamwidth of 110° per antenna provides complete omnidirectional coverage with a minimum 27% pattern overlap.

The data and necessary acquisition tones will be transmitted sequentially over each of the six antennas in order to accommodate wide variations in landing dispersions, surface slopes, and surface orientation.

5.15.4.3 Power and Control Subassembly - The power and control subassembly performs the two major functions of supplying and controlling power to the various IDP subassemblies and science instruments as well as generating IDP mission time and sequencing all events and data modes. A functional block diagram of this subassembly is shown in Figure 5.15-23. A listing of the power and operations control functions which are performed by the power and control subassembly are included in Figure 5.15-24.

Power Supply - The combined requirements for sterilization, 3,000 g_E impact survival, and high energy density allow a silver-zinc battery as the only practical power source for the IDP. Several studies are presently in progress to determine the best design and achievable energy density for a battery of this type. However, based on present state-of-the-art, the best specific energy that can be expected for a high impact, sterilizable, battery is 25 watt-hr/lb. For a 100 pound total IDP system weight and the instrument complement specified herein, the maximum allowable battery weight is 10 pounds. Allowing a 15% design margin in the battery capacity leaves a net usable energy of 217 watt-hours for surface operations. Examination of Figure 5.15-25 reveals that 61 watt-hours of energy are required for data measurement and housekeeping operations. Thus, 156 watt-hours of energy are available in the 10 pound battery for transmitter operation. Assuming a 22%Vdc to RF conversion efficiency in the selected 20 watt TWTA transmitter allows approximately 1.8 hours of data transmission.

The telecommunication analysis results in an estimated effective data rate of 1.2 bits/sec and an approximate frequency and sync acquisition time at the beginning of each transmission of 5 to 7 minutes. Allowing 18 minutes (or one-sixth) of the transmitters total 1.8 hour operating time for each data transmission leaves 11 minutes for actual data transmission following acquisition. This permits 800 bits of data to be transmitted at the established rate of 1.2 bits/sec.

Sequencer-Timer Programmability - A small degree of programmability is required in the sequence-timer portion of the power and control subassembly. This programmability is required in order that the IDP be adaptable to landing at different times of the Martian day. In its simplest form this would entail two stored sequences, one which would operate the IDP through a normal sequence of events with an approximate duration of 24 hours total and a second mode where an abbreviated sequence of science data would be obtained and the data transmission initiated within two hours after landing and the mission terminated within four hours after landing.

FUNCTIONAL BLOCK DIAGRAM – I. D. P. POWER AND CONTROL SUBASSEMBLY

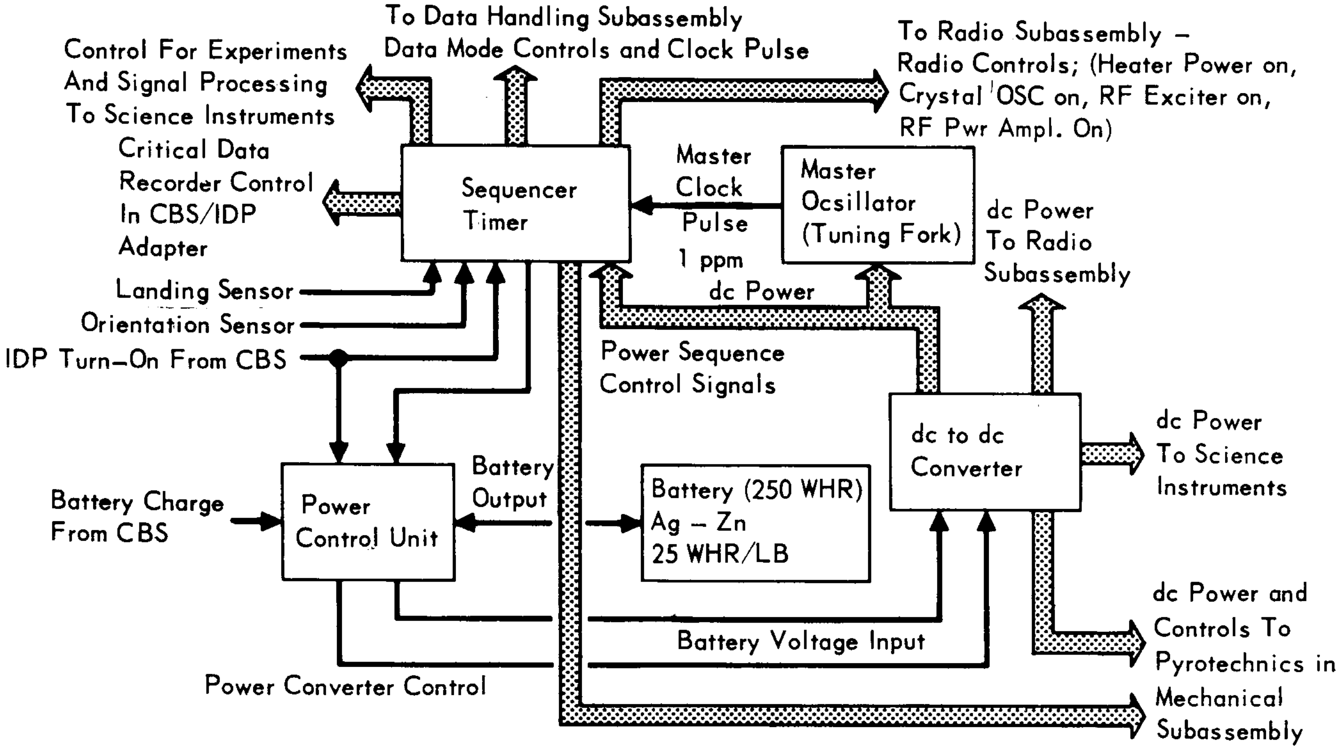

To Data Handling Subassembly
Data Mode Controls and Clock Pulse
Control For Experiments
And Signal Processing
To Science Instruments
To Radio Subassembly –
Radio Controls; (Heater Power on,
Crystal OSC on, RF Exciter on,
RF Pwr Ampl. On)
Critical Data
Recorder Control
In CBS/IDP
Adapter
Sequencer
Timer
Master
Clock
Pulse
1 ppm
Master
Ocsillator
(Tuning Fork)
dc Power
To Radio
Subassembly
dc Power
Landing Sensor
Orientation Sensor
IDP Turn–On From CBS
Power Sequence
Control Signals
dc to dc
Converter
dc Power
To Science
Instruments
Battery Charge
From CBS
Power
Control Unit
Battery
Output
Battery (250 WHR)
Ag – Zn
25 WHR/LB
dc Power and
Controls To
Pyrotechnics in
Mechanical
Subassembly
Battery Voltage Input
Power Converter Control

Figure 5.15–23

INDEPENDENT DATA PACKAGE
POWER AND CONTROL SUBASSEMBLY FUNCTIONS

- Supply power to all IDP subassemblies (TWTA excepted).
- Control turn-on and turn-off of all IDP subassemblies.
- Control charge energy from CB to maintain IDP battery at full capacity prior to IDP/CB separation.
- Respond to orientation sensor, control switchover to correct modes and deploy correct instrument mast.
- Generate IDP time.
- Sequence and control all Science Instrument operations.
- Generate critical data control functions.
- Accept Sequencer/Timer programming signals from CB to control IDP mission length (4 hr or 24 hr).
- Sequence and control Data Handling Subassembly modes and operations.
- Generate bit sync for use by the Data Handling Subassembly.

Figure 5.15–24

INDEPENDENT DATA PACKAGE POWER BUDGET
(24 HR MISSION)

ITEM	AVERAGE POWER (Watts)	OPERATING TIME (hr)	ENERGY (W h)
Instruments			
Pressure	0.5	0.4	0.2
Temperature	0.3	0.5	0.2
Wind Velocity	0.5	0.5	0.3
Gas Chromatograph	4.0	0.5	2.0
Hygroscopic Sensor	0.5	0.5	0.3
Electronics			
Sequencer/Programmer	1.0	24.0	24.0
Data Handling	1.0	24.0	24.0
CDR Monitor	1.0	0.5	0.5
Oven/Heater	0.8	12.0	9.5
Subtotal			61
Transmitter			156
Subtotal			217
15% Margin			33
Total Energy			250
Total Battery Weight @ 25 Wh /lb = 10 lb			

Figure 5.15-25

Master Oscillator Mechanization - A possible mechanization for a master oscillator is a tuning fork of the type which has been developed by American Time Products, Inc. (Bulova). This particular fork is a 400 Hz frequency standard, and it has been shock tested at a level of 2300 g_E's, for 4.0 milliseconds duration. The approximate volume of the packaged unit is 0.6 $inch^3$.

5.15.4.4 Data Handling Subassembly - A functional block diagram of the data handling subassembly (DHS) is shown in Figure 5.15-26. The primary function of the data handling subassembly is to accept and process the data as received from the various instruments and event sensors and the critical data electronics in the CB/IDP adapter and to efficiently store it in a fixed preprogrammed format within the magnetic core memory. The second function of this subassembly is to read out during the data transmission period, the contents of the memory, to intersperse appropriate sync data, and to feed this composite data and sync at a constant rate to the MFSK encoder in the radio subassembly.

Implementation - The majority of the electronics within the DHS is of a digital nature and because of the large quantity of these devices, integrated circuit techinques, large scale integration, and power gating techniques should be employed. The premium on size, weight and power also makes consideration of each of these techniques mandatory. At the present time, it is envisioned that junction type devices rather than MOS devices will be employed because of the possibility of a radiation environment due to possible use of radioisotopes in the spacecraft. Liberal use of power gating techniques must be employed in order to keep the average power dissipation low. Large scale integration techniques may be employed in certain areas when it is evident that changes will not be required.

Selection of Memory Device Type - Three types of memory devices are candidates for the IDP data storage task: magnetic cores, magnetic woven plated-wire, and magnetic thin film. Each of these devices requires approximately the same average power at this low data rate and approximately the same weight and volume. However, the magnetic woven, plated-wire memory is not suited to the incremental characteristic of the data acquisition. The magnetic thin film memory is possible a good candidate but lacks operational proof-testing. The magnetic core memory is therefore the most likely candidate since a great deal of experience has been obtained with this type of memory and 1000 bit capacity units have been tested and proved capable of withstanding the shock environment required of the IDP hardware. This core memory has no inherent problem in adapting to the

FUNCTIONAL BLOCK DIAGRAM - - IDP DATA HANDLING SUBASSEMBLY

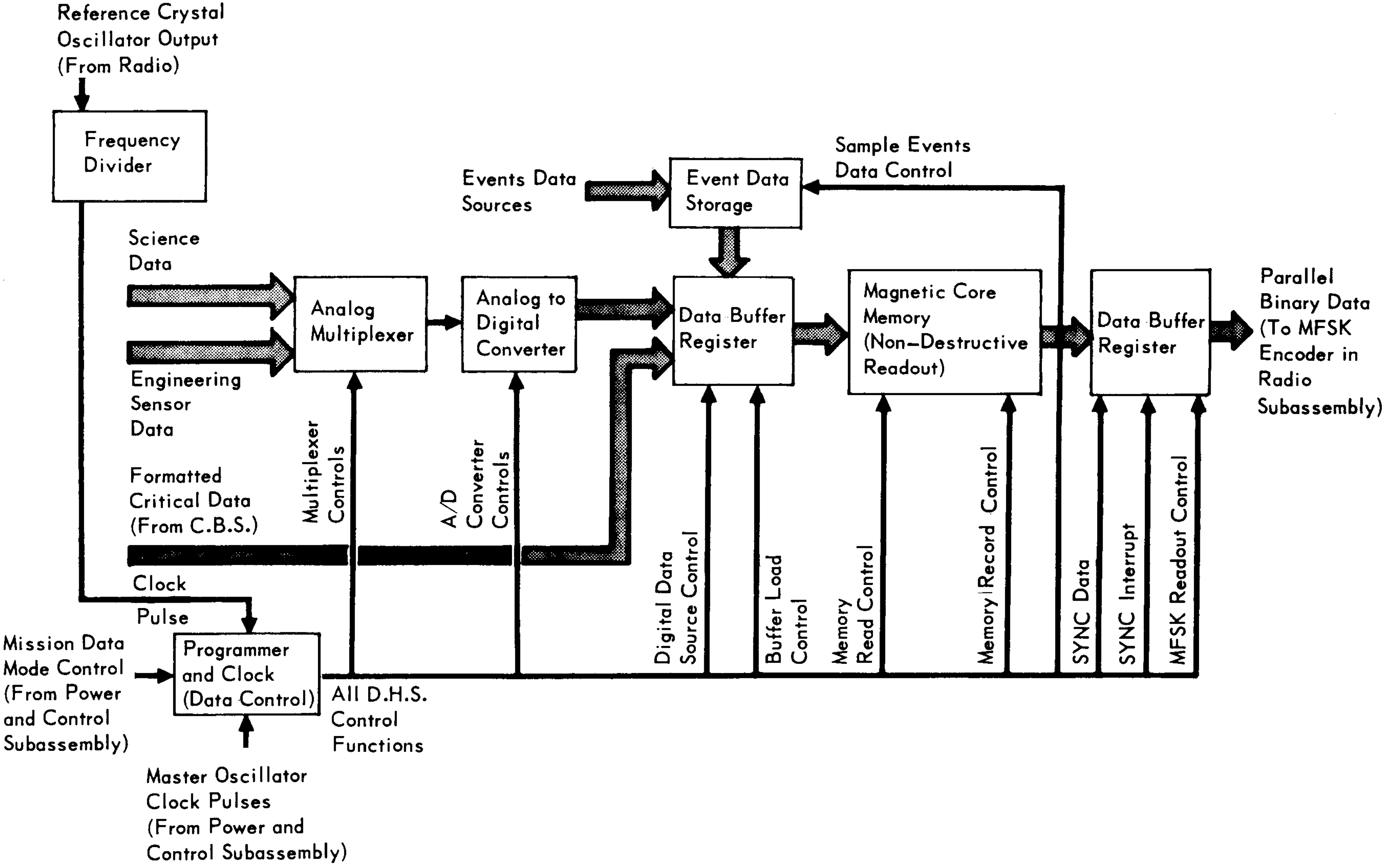
Reference Crystal Oscillator Output (From Radio)
Frequency Divider
Science Data
Engineering Sensor Data
Formatted Critical Data (From C.B.S.)
Clock Pulse
Mission Data Mode Control (From Power and Control Subassembly)
Programmer and Clock (Data Control)
Master Oscillator Clock Pulses (From Power and Control Subassembly)
All D.H.S. Control Functions
Analog Multiplexer
Multiplexer Controls
Analog to Digital Converter
A/D Converter Controls
Events Data Sources
Event Data Storage
Sample Events Data Control
Data Buffer Register
Digital Data Source Control
Buffer Load Control
Magnetic Core Memory (Non-Destructive Readout)
Memory Read Control
Memory Record Control
Data Buffer Register
SYNC Data
SYNC Interrupt
MFSK Readout Control
Parallel Binary Data (To MFSK Encoder in Radio Subassembly)

Figure 5.15-26

incremental acquisition characteristics of the IDP data.

5.15.5 IDP Mechanical Subject Studies - The following sections describe the analyses which were made to arrive at the preferred IDP mechanical configuration.

5.15.5.1 Descent Retardation - To successfully survive landing from the selected separation altitude(above 1000 feet), the IDP must be provided with an independent means of descent retardation capable of removing both the residual entry velocity of the parent vehicle and the kinetic energy of free fall. This is exemplified in Figure 5.15-27 which reveals that for separation altitudes between 1000 and 10,000 feet the IDP vertical free fall impact velocity will be between 400 and 1000 ft/sec. Since these velocities exceed the practical capabilities of passive, omnidirectional, mechanical energy absorption devices it is apparent that an auxiliary descent retardation device is required.

The two primary candidates for providing initial deceleration to the IDP are rockets and parachutes.

The rocket concept provides a closely controlled descent rate and, by careful programming, a low impact velocity. However, in order to correctly control the descent rate and impact velocity, either the properties of the Martian atmosphere and initial velocity must be known with a greater degree of accuracy than is presently available or an active descent control system must be provided. Also, an auxiliary means of stabilization is necessary to maintain proper thrust vector alignment and a sequencer/timer is required to allow proper post-separation rocket ignition.

Conversely, the parachute is adaptable to unknown initial conditions; does not require a stabilization system; is more predictable in high horizontal winds; and weighs less. Because of these advantages, it provides a higher reliability and probability of mission success. It was therefore selected for descent retardation.

Parachute System - The parachute system would consist of a pilot chute, which is used to extract the main parachute from its deployment bag; a deployment bag which stows the main parachute and its suspension and riser lines; and a main parachute which serves as a primary decelerator in controlling the descent rate of the IDP. The factors which were considered to be of prime importance in the selection of a parachute configuration were: weight, performance characteristics, reliability, and development risk. These factors are evaluated in Figure 5.15-28 for three parachute configurations representing two canopy classifications. The configurations evaluated are the ring-slot and the ring-sail canopies of the

SEPARATION ALTITUDE vs VERTICAL IMPACT VELOCITY

Independent Data Package

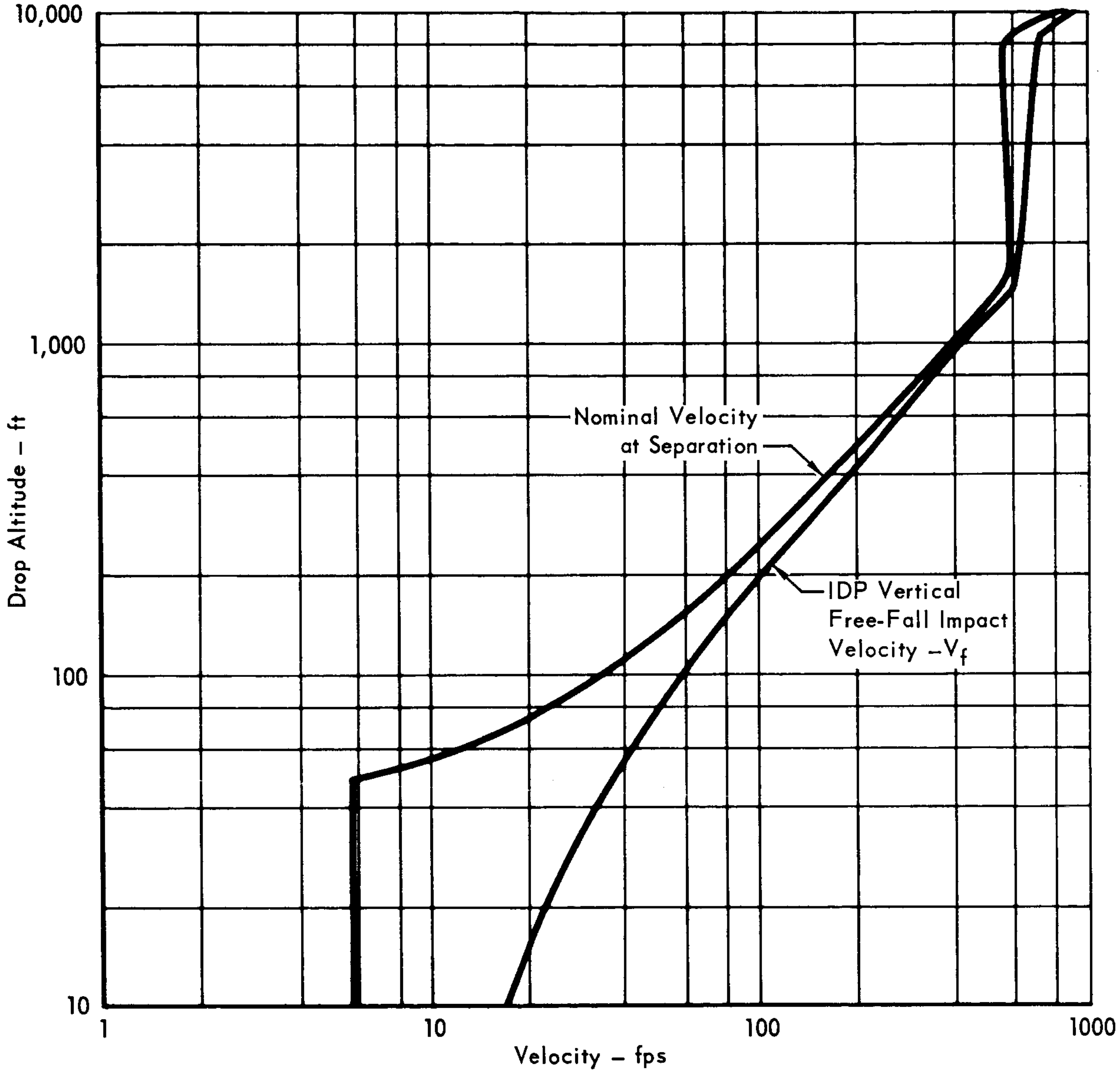

Figure 5.15–27

IDP MAIN PARACHUTE CONFIGURATION EVALUATION MATRIX

EVALUATION FACTOR	DESCENT WEIGHTING FACTOR 1–5	PARACHUTE CONFIGURATION					
		RING SLOT		RING SAIL		EXTENDED SKIRT	
		FACTOR	SCORE	FACTOR	SCORE	FACTOR	SCORE
I Weight Penalty							
Specific Drag	5	2	10	5	25	4	29
Inflation Load	2	4	8	4	8	2	4
Atmosphere	1	3	3	3	3	3	3
Sterilization	2	3	6	3	6	3	6
			27		34		25
II Performance							
Opening Shock	1	4	4	4	4	2	2
Descent Stability	1	5	4	5	5	3	3
Drag	5	3	15	5	25	4	20
			23		34		25
III Reliability							
Inflation Prob.	5	5	25	5	25	4	20
Deployment Damage Tolerance	4	4	16	3	20	3	12
Fabrication Complexity	1	4	4	3	3	4	4
Packing Damage Tolerance	2	4	8	5	10	4	8
			53		58		44
IV Development Risk							
High Speed	2	4	8	4	8	4	8
Low Density Atm.	2	2	4	2	4	1	2
Low Canopy Load	2	1	2	1	2	1	2
Configuration	3	4	12	4	12	4	12
			26		26		24
Totals			129		160		126

Figure 5.15–28

ribbon style and the extended skirt canopy of the solid textile type. These configurations were chosen because they provide good drag coefficient characteristics, reasonable stability, high reliability, and have been tested in large diameter configurations at high velocities.

The characteristics considered to be most important were specific drag, total drag, inflation probability, and deployment damage tolerance. Each of these characteristics is a primary contributor to the overall goal of low weight and high reliability. They are therefore weighted most heavily in the evaluation of Figure 5.15-28. Based on this figure, the ring-sail canopy configuration appeared to provide the most beneficial performance.* It has therefore been selected for the preliminary design weight trade studies conducted herein.

Material Selection - For the purpose of this weight trade study, the parachute canopy material was assumed to be 1.1 oz/yd nylon since it is the lightest weight material currently available and represents a conservative estimate of expected canopy weight per unit area.

The highest load which is put into the canopy material is due to the opening dynamic pressure. The relationship between the load and opening dynamic pressure can be expressed as

$$L = \frac{K\ D_o}{4}$$

where:

L = loading in pounds per inch = 42(1.1 oz/yd Nylon)

q = opening dynamic pressure in pounds per square foot

D_o = nominal diameter in feet

K = strength factor which can be expressed as:

$$K = \frac{je}{bac} = 2.7$$

where:

j = factor of safety = 1.3

e = asymmetric loading factor = 1.5

b = joint efficiency factor = .8

a = factor related to strength loss due to abrasion = .95

c = factor related to suspension line convergence angle = .95

If we compute the allowable dynamic pressure at opening using this relationship and assume a maximum 40 foot diameter canopy we obtain a loading of 18.7 lb/ft^2.

---

* Subsequent preliminary tests by NASA Langley have demonstrated that the Cross and Disk-Gap-Band parachutes of the same type may provide superior performance.

Since this capability figure exceeds the expected value of dynamic pressure at opening altitudes below 10,000 feet by a factor of from two to six times, the 1.1 oz/yd^2 material provides more than adequate design margin for the subject application; the use of lighter materials is not recommended since the systems reliability in an unknown atmosphere would be greatly compromised with only little reduction in system weight.

Deployment Conditions - It has been tacitly assumed in the foregoing discussion that parachute deployment will occur subsonically at an altitude below 10,000 feet and at a dynamic pressure less than 9 lb/ft^2.

At deployment velocities in excess of sonic the conventional ribbon type parachute canopies recommended for IDP exhibit erratic inflation tendencies, violent pulsing or "breathing" of the drag producing surface, considerably reduced drag, and failure of cloth, ribbons, and suspension lines at a fraction of their rated strength due to violent oscillation of the material. For this reason, deployment of the 20-30 foot diameter IDP canopy at velocities in excess of sonic is not recommended. If system design considerations indicate that chute deployment may occur at supersonic conditions due to encounter with an atmosphere beyond that specified by the VM models, then provision must be made in design configuration for a separate first stage decelerator specifically designed for use in the supersonic regime (e.g. a hemisflo drogue or rigid conical drogue). The weight penalty for such a first stage drogue system (for a 100 lb IDP) would be approximately 2.5 lbs. (or a 30% increase over presently envisioned subsonic chute systems. Also, deploying the parachute supersonically greatly reduces the systems reliability and is hence not a recommended design approach to be pursued further.

Parachute Analysis - An important trade-off which must be considered is the fraction of payload weight which must be devoted to the parachute in order to achieve desired vertical impact velocities. Figure 5.15-29 presents plots of canopy diameter versus weight and weight versus drag area for the three parachute configurations evaluated. This figure clearly reveals that the Ring Sail Canopy has the higher total drag per unit of weight and is hence the most efficient configuration for the applications.

NOTE: Preliminary test results by NASA Langley have revealed that this configuration may not possess reliable inflation characteristics in tenuous atmospheres; nevertheless subsequent design tradeoff data are presented for the Ring Sail Canopy since adequate preliminary design data exists for this configuration

IDP PARACHUTE DESIGN CHARACTERISTICS

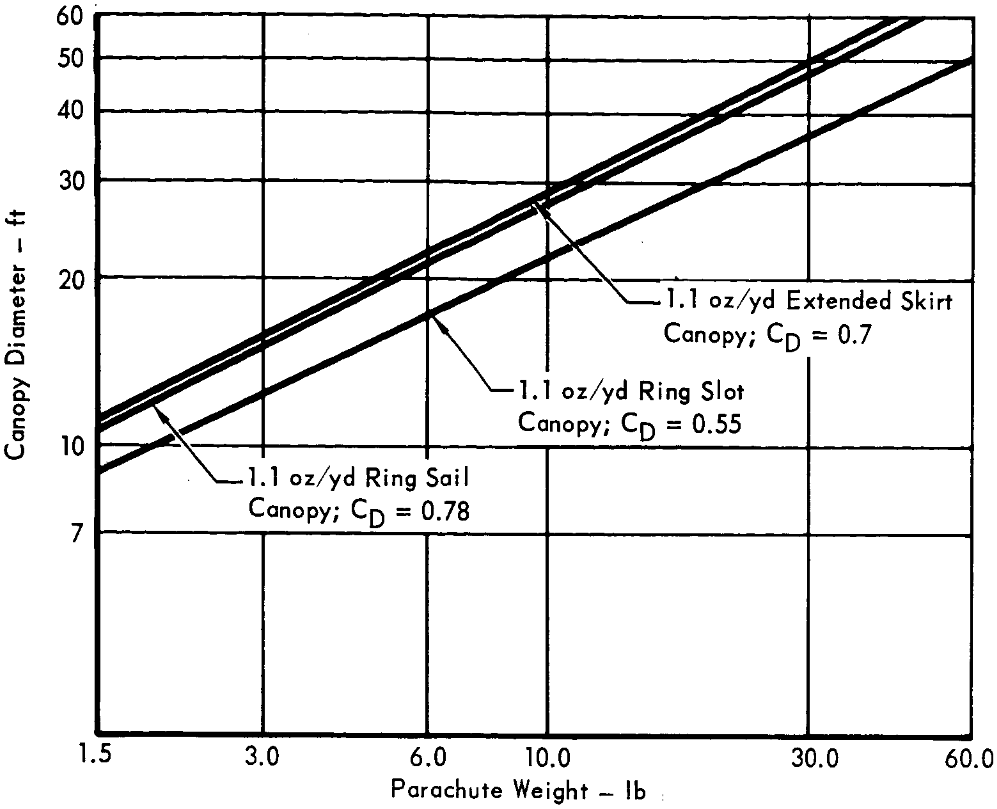

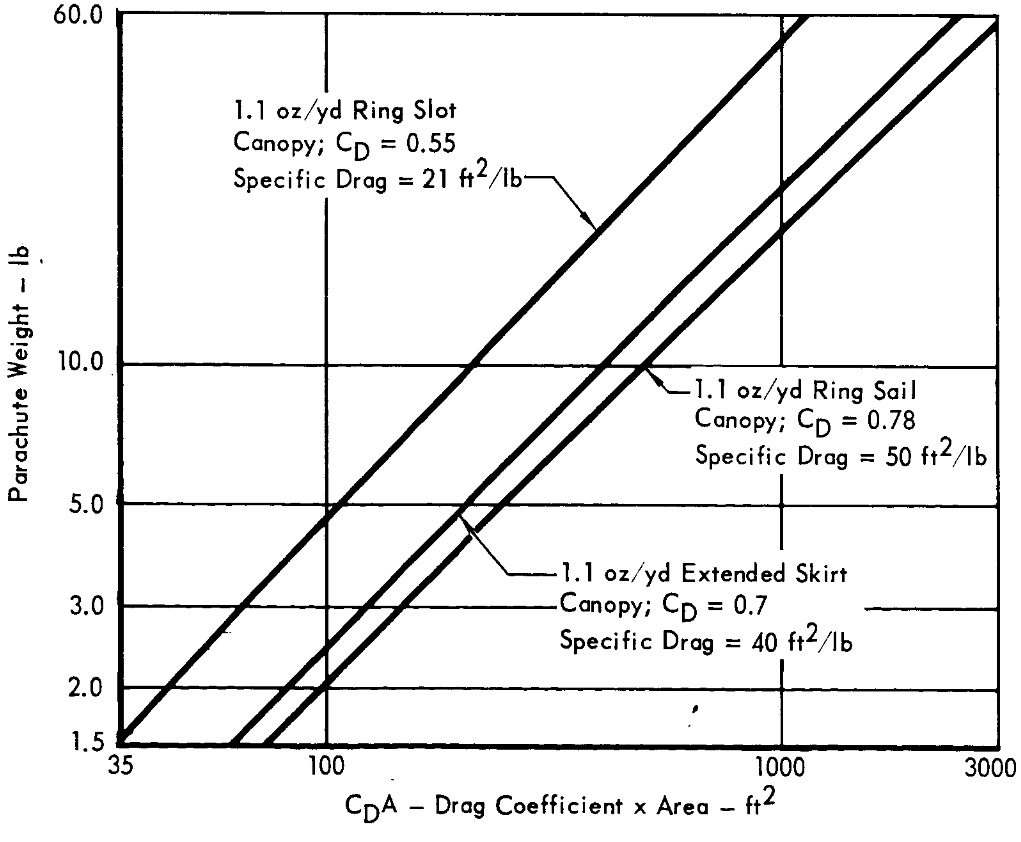

Figure 5.15–29

whereas, only meager information is available on the competitive cross and disk-gap-band parachutes presently under evaluation by NASA.

The general equation relating the drag of the parachute system and the suspended weight is:

$$1/2\ \rho\ V_v^2\ C_D A = W_T \frac{g_M}{g_E}$$

where ρ = atmospheric density in slugs per cubin foot

V_v = equilibrium descent velocity in feet per second

C_D = drag coefficient

A = nominal canopy area in square feet

$C_D A$ = drag area

W_T = total weight of the parachute system and payload in pounds.

g_M = acceleration of gravity at Martian surface in ft/sec2

g_E = acceleration of gravity at Earth's surface in ft/sec^2

Note that in the foregoing equation the drag area ($C_D A$) may also be expressed as KW_c.

$$\text{Specific Drag} = \frac{C_D A}{W_{chute}} = \text{constant}$$

The parachute weight fraction can be solved as a function of equilibrium descent velocity as follows:

$$\frac{W_c}{W_t} = \frac{2\ g_M}{V_v^2\ K g_E}$$

Since it is known that $\frac{W\ chute}{W\ total} + \frac{W\ payload}{W\ total} = 1$, we can readily plot payload weight fraction $\frac{W_P/L}{W_t}$ as a function of the equilibrium terminal descent velocity.

This data is presented in Figure 5.15-30 for the three parachute configurations considered. The atmospheric density used in determining the plots was that of the VM-7 atmosphere which yields the worst case vertical impact velocities for a given payload fraction. Any increase in atmospheric density would result in a decrease in vertical impact velocity for a given payload weight fraction. It is again apparent that the ring sail canopy configuration is the most efficient in terms of providing the highest payload weight fraction for a given terminal impact velocity. Also it is revealed that to achieve a vertical impact velocity below 100 ft/sec one must pay significant penalties in terms of payload weight fraction. It appears most practical to design the IDP for a vertical terminal impact velocity

IDP PAYLOAD FRACTION vs IMPACT VELOCITY FOR PARACHUTE DESCENT

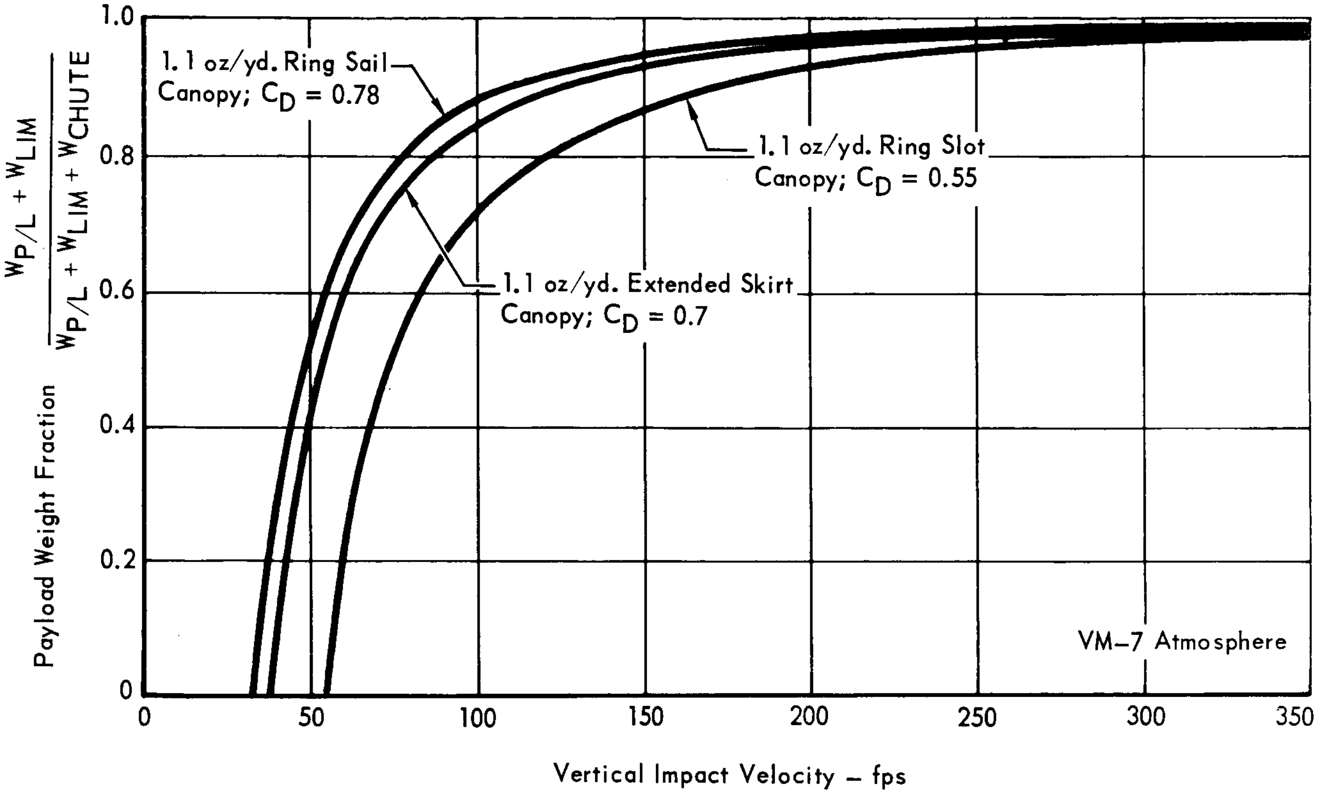

Figure 5.15-30

in the range of from 100 to 150 ft/sec; this will yield a payload weight fraction of 90 to 95 percent.

The remaining two parameters of interest are the opening shock force and the descent time. These are presented in Figure 5.15-31 as functions of the ratio, canopy area/suspended weight (A/W). The latter parameter is a constant for a given terminal descent velocity and canopy design; it possesses a value of approximately 5 (i.e. $5ft^2$ of canopy area are required per (earth) pound of suspended weight) for the 100 to 150 ft/sec velocity range of interest. Thus, for a 100 lb IDP, a 500 ft^2 (or 25 ft. diameter) parachute will be required for descent retardation. The opening shock force will be less than 50 g's and hence insignificant relative to the landing shock for the range of opening dynamic pressures anticipated (~ 10 PSF). The minimum descent time will be approximately 2 minutes for a nominal 10,000 foot deployment altitude.

Sterilization - Present requirements for sterilization qualification specify a heat soak at 130°C for three 36 hour cycles. Because of the time lag required to bring the inside of the package up to temperature, the outer portions will necessarily be soaked for longer periods of time. At these temperature and time cycles, normal nylon tends to loose some of its strength. Fortunately, other materials have been developed which exhibit good high temperature characteristics, such as Nomex (a high temperature nylon) and a series of polymide fiber textiles. These materials retain approximately 99 percent of their strength after long time soak cycles at sterilization temperatures compared with only 70 to 80 percent strength retention for nylon or dacron.

Similarly, pyrotechnics, such as reefing line cutters, should not present a design problem since there are primer materials currently available which provide satisfactory service following exposure to temperature and time cycles considerably more sever than the specified sterilization cycles. Thus, it appears that any problems which are associated with the heat sterilization cycle can be overcome with no degradation in the reliability of the parachute subsystem.

Parachute Terminal Release - To avoid post impact entanglement of the IDP in its parachute it will be necessary to separate the chute from the package at, or near, touchdown. This will require a sensor to initiate the disposal sequence. A brief investigation was therefore conducted to determine the availability of a practical solution to the problem. The following triggering devices appeared feasible and warrant further investigation.

IDP PARACHUTE OPERATIONAL CHARACTERISTICS

CANOPY AREA PER (EARTH)POUND OF SUSPENDED WEIGHT VS. IMPACT VELOCITY

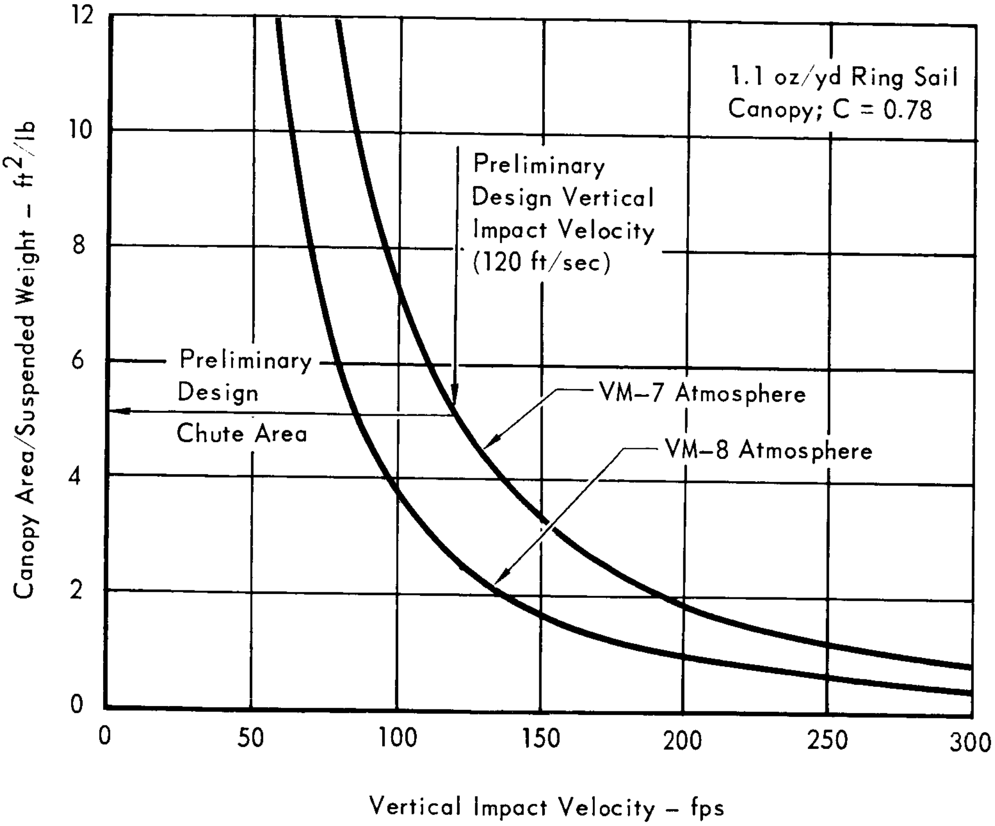

5.15-56-1

DYNAMIC PRESSURE VS. OPENING SHOCK FORCE

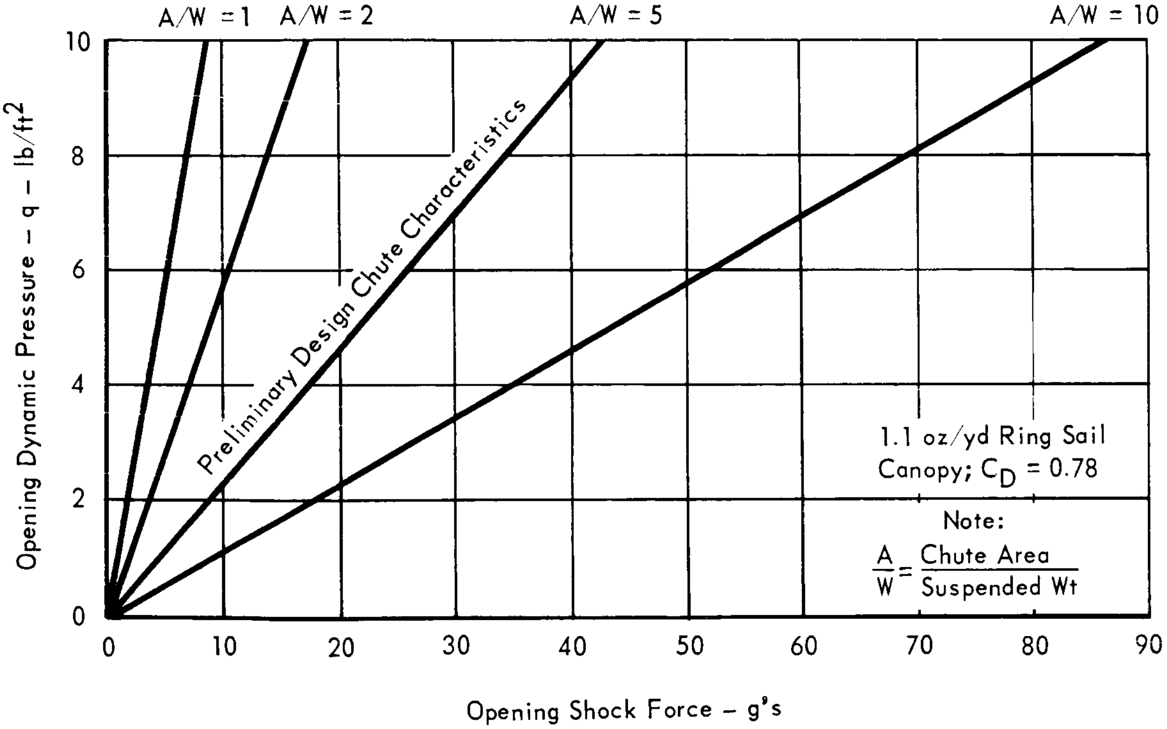

Figure 5.15-31

CHUTE FULL OPEN ALTITUDE VS. DESCENT TIME

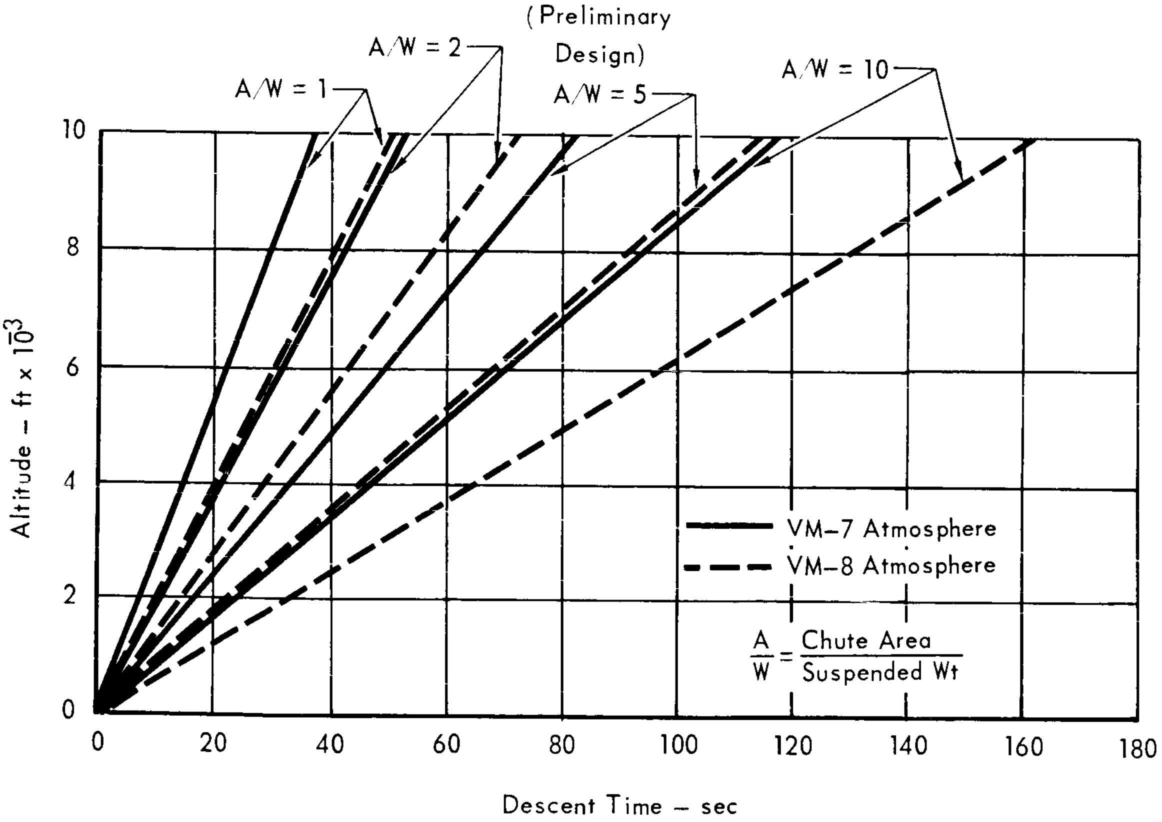

S115-56-3

a. A differentiating omnidirectional accelerometer which senses ground impact. Release at impact may, however, be too late to avoid entanglement. Also the system may pretrigger due to wind gusts or parachute opening shocks.

b. A radar altimeter such as an X-band doppler device could be mechanized for as little as 2 pounds and 1 to 2 watts. This device could produce an altitude signal accurate to within ± 100 feet.

c. Similarly, an altitude signal could be obtained from a gallium arsenide laser device presently being evaluated. Although the range of this device is presently limited to 100 feet it is anticipated that it could be extended to 200 or 300 feet in time for VOYAGER use. The current working mode weighs less than one pound and requires only milliwatts of power.

d. A fourth approach would be to use an electronic or mechanical sensor suspended beneath the IDP on a weighted line.

Conclusions

a. A parachute would provide the most reliable and light weight means for descent retardation of the IDP.

b. Terminal vertical impact velocities of 100 to 150 feet per second would provide the maximum payload weight fraction with the least expense of payload structure for impact attenuation.

c. The sterilization requirement will not compromise the performance or reliability.

5.15.5.2 Terminal Deceleration Device - Due to the wide range of uncertainty in our knowledge of Mars atmospheric and surface properties there will always be a residual terminal velocity from either a parachute or fixed impulse rocket decelerator. Thus, some form of impact attenuator will be required. To provide practical omni-directional landing protection, residual impact velocities must be held below 400 ft/sec to make efficient use of the attenuation material.

If we choose a parachute as an intermediate stage we must also assume that the IDP will be accelerated horizontally by the 220 ft/sec horizontal wind speeds of the VM-7 and -8 atmospheric models. Since we must also assume impact upon a worst case surface, oriented normal to the total velocity vector, it is apparent that an independent means of impact protection, capable of dissipating the kinetic energy of an IDP landing at velocities between 220 and 400 ft/sec, must be provided.

The obvious choice for such an application is a passive, crushable, mechanical energy absorber completely surrounding a central payload. An alternate choice would be to suspend the payload by radial cords within a large gas filled balloon; upon impact, energy would be absorbed by compressing the gas within the balloon w which in turn would rupture just as the payload came to rest. Tests by JPL have proven the feasibility oftthis approach. However, the practical payload weight fraction achievable is (perhaps) only slightly greater than the equivalent crushable (balsa) impact limiter (at 200 ft/sec) and the design is accompanied by what are considered to be difficult design mechanizations (e.g., payload release) and low operational reliability (e.g., balloon puncture, and secondary impact protection). Thus the design tradeoffs conducted herein are limited to the more reliable, proven, passive, crushable, energy dissipators. In addition, only omnidirectional devices are considered to assure adequate protection against high horizontal winds and secondary impacts.

Material Selection - Previous investigations have concluded that with a single unique exception balsa wood possesses the highest specific energy dissipation capability per pound of material. The unique exception is maraging steel honeycomb*, whose specific energy dissipation theoretically becomes competitive with 6 lb/ft^3 balsa wood at densities above approximately 26 lb/ft^3. However, it can be demonstrated that unless the average density of the 26 lb/ft^3 maraging steel material can be reduced to 6 lb/ft^3 (by the addition of local voids) without degrading its specific energy capability, the material is not competitive in terms of payload jweight fraction. Since this is not practicable, and it has additionally been demonstrated that balsa wood can survive dry heat sterilization temperatures for reasonable periods, it can be concluded that from an engineering standpoint balsa wood is the optimal material for the design of the subject IDP impact limiter.

A summary of pre-conditioning treatments conducted by JPL on 6-9 lb/ft^3 balsa wood and the effect of these treatments on the specific energy dissipation capability of a very limited number of test samples is summarized in Figure 5.15-32. Unfortunately the results of these tests are not conclusive since a wide scatter exists in the limited test data. However, the following general conclusion can be drawn:

---

* Energy Dissipating Plastic Honeycomb presently under development by General Electric (under JPL Contract 951172) may also be ultimately competitive.

RESULTS OF STERILIZATION TREATMENTS ON 6.9 TO 9.7 LB/FT^3 BALSA*

TREATMENT NUMBER	DETAILS OF TREATMENT	NUMBER OF SAMPLES	10^3 Ft Lb/Lb** Specific Energy	
			RANGE	MEAN
0	As Received	22	12.6 – 22.7	19.0
1	Held for 17 hr in a vacuum of 10^{-5} torr at room temperature	5	24.5 – 30.6	26.3
②	Held for 298 hr in air at 125°C	6	15.5 – 21.1	18.6***
3	Held for 6 hr in air at 145°C	3	19.3 – 25.6	22.1
4	Held for 108 hr in air at 145°C	3	19.9 – 30.8	25.0
5	Held for 108 hr in nitrogen at 145°C	3	23.0 – 25.9	24.5
⑥	Held for 498 hr in sealed container at 125°C	3	11.6 – 15.6	13.6
⑦	Held for 108 hr in sealed container at 145°C	3	7.7 – 14.9	11.1
8	Six 30–hr cycles at 50°C and 50% RH in an 88% Freon–12% ethylene oxide mixture	3	22.7 – 23.3	23.0
9	Treatment 1, followed by treatment 8	3	19.5 – 24.8	22.4
⑩	Held for 5 hr in nitrogen at 260°C, followed by treatment 8	2	14.6 – 16.5	15.3
11	Treatment 8, followed by six 96–hr cycles in nitrogen at 135°C	3	22.6 – 27.6	25.4
12	Treatment 1, followed by treatment 11	4	23.3 – 33.5	29.0
⑬	Held for 5 hr in nitrogen at 260°C, followed by treatment 11	2	11.9 – 19.9	15.9
14	Treatment 1, followed by one 96–hr cycle in nitrogen at 135°C	5	19.3 – 39.4	26.4
15	Treatment 1, followed by impregnation with G. E. 103 Dri-Film silicone resin	3	21.1 – 24.6	22.5
16	Treatment 1, followed by impregnation with G. E. 103 Dri-Film silicone resin, followed by 108 hr in air at 145°C	1	20.0	20.0

Notes

* JPL TR 32–1022

** At room temperature and ambient pressure

○ Treatment considered to be unacceptable

*** All samples (6) split during test indicating low transverse strength

Figure 5.15–32

a. Exposing balsa wood to ethylene oxide decontamination and short term (108 hr.) heat sterilization environments specified for VOYAGER capsule equipment does not cause a significant degradation in the materials specific energy.
b. Heating balso wood to 125°C for long times (498 hrs.) or to 260°C for short times (5 hrs.) causes a marked decrease in the materials specific energy.
c. Heating balsa wood to sterilization temperatures (without prior demoisturizatin) causes a significant decrease in specific energy.
d. Heating balsa to sterilization temperatures (145°C) causes noticeable darkening throughout the specimen.

The third item connotes that it will be necessary to demoisturize the balsa wood prior to sterilization. Demoisturization increases the specific energy absorption capability of the balsa wood (approximately 15 percent at 78°F; very little below 32°F). The shrinkage which occurs appears to be uniform and is acceptable from a design and fabrication standpoint. However, the increase in the peak/average stress ratio which occurs following demoisturization will increase the peak impact load factor slightly (perhaps 10 percent). Thus, dry heat sterilization of balsa wood is practicable if the proper precautions are taken such as vacuum demoisturization prior to sterilizaiton and a minimization of time at elevated temperature.

Analytical Model - Two omnidirectional impact limiter configurations have been studied. These are the sphere and the disk corresponding to the two preferred payload configurations evaluated during the final phases of the study.

The approach to the establishment of an analytical model for each configuration was essentially identical. Thus for brevity, the following derivations and tradeoffs are interpreted primarily in terms of a spherical balsa wood impact limiter. It was these relationships which were used in the system design weight tradeoffs of the subsequent section.

The analytical model used to predict the dynamic performance of a spherical balsa wood impact limiter assumes the balsa grain to be oriented radially and takes account of compression forces both parallel and perpendicular to the grain to determine the vertical resisting force at impact. The impacted surface is assumed to be hard and unyielding; thus, the package structure is required to dissipate all of the kinetic energy of impact.

The relating design tradeoff equations were derived based on the following series of analytical steps:

- The impact limiter vertical crushing force was expressed as a function of balsa properties, total package radius (R_T), and dimensionless stroke which is the ratio between the instantaneous distance from the sphere center to the impact plane and the initial total radius of the package.
- This function was used for computation of peak impact deceleration forces. The vertical crushing force was integrated over the total available stroke and equated to the total kinetic energy of the system at impact.
- The foregoing energy equation was solved for impact velocity capability (V) in terms of payload and limiter density (γ_P and γ_L), radial crush strength, (σ_o), tangential crush strength (σ_t), the ratio of payload diameter to total diameter (γ_p) and dimensionless limiter material stroke (i.e., available strain, $\varepsilon = 0.8$).
- The energy equation was manipulated to express payload weight fraction as a function of velocity and the foregoing variables for use in subsequent system design tradeoff of the sphere only. (Figure 5.15-33).
- The force equation was manipulated to express peak impact deceleration in Earth g's as a function of total capusle weight, payload, density, and impact velocity for the sphere. (Figure 5.15-34).

Design Tradeoffs - A specific set of design tradeoff curves for an Independent Data Package are presented in Figures 5.15-33 and 5.15-34. The charts present payload weight fraction and peak impact deceleration for a spherical capsule as functions of maximum allowable impact velocity for selected values of payload and limiter density. The 60 - 90 lb/ft^3 payload density range is representative of previous Philco-Ford high impact package designs. The 6 and 14 lb/ft^3 balsa wood densities cover the practical range of available balsa materials.

Examination of Figure 5.15-33 for payload weight fraction utilizing 6 and 14 lb/ft^3 balsa, respectively, reveals that there is little difference in payload weight fraction between the two materials. For each the payload fraction varies, nearly linearly, from 100% to zero as the velocity ranges from zero to approximately 500 ft/sec. Conversely, examination of Figure 5.15-34 for peak impact deceleration reveals that the increased stroke capability of 6 lb/ft^3 balsa reduces the landing deceleration loads by approximately 50% relative to 14 lb/ft^3 balsa. This factor coupled with the higher thermal insulative capability of 6 lb/ft^3 balsa recommends the latter minimal density balsa as the optimum material for this application. A brief examination of these trends for a disk limiter yielded similar results.

IDP GROSS PAYLOAD WEIGHT FRACTION vs TOTAL IMPACT VELOCITY FOR SPHERICAL IMPACT LIMITER

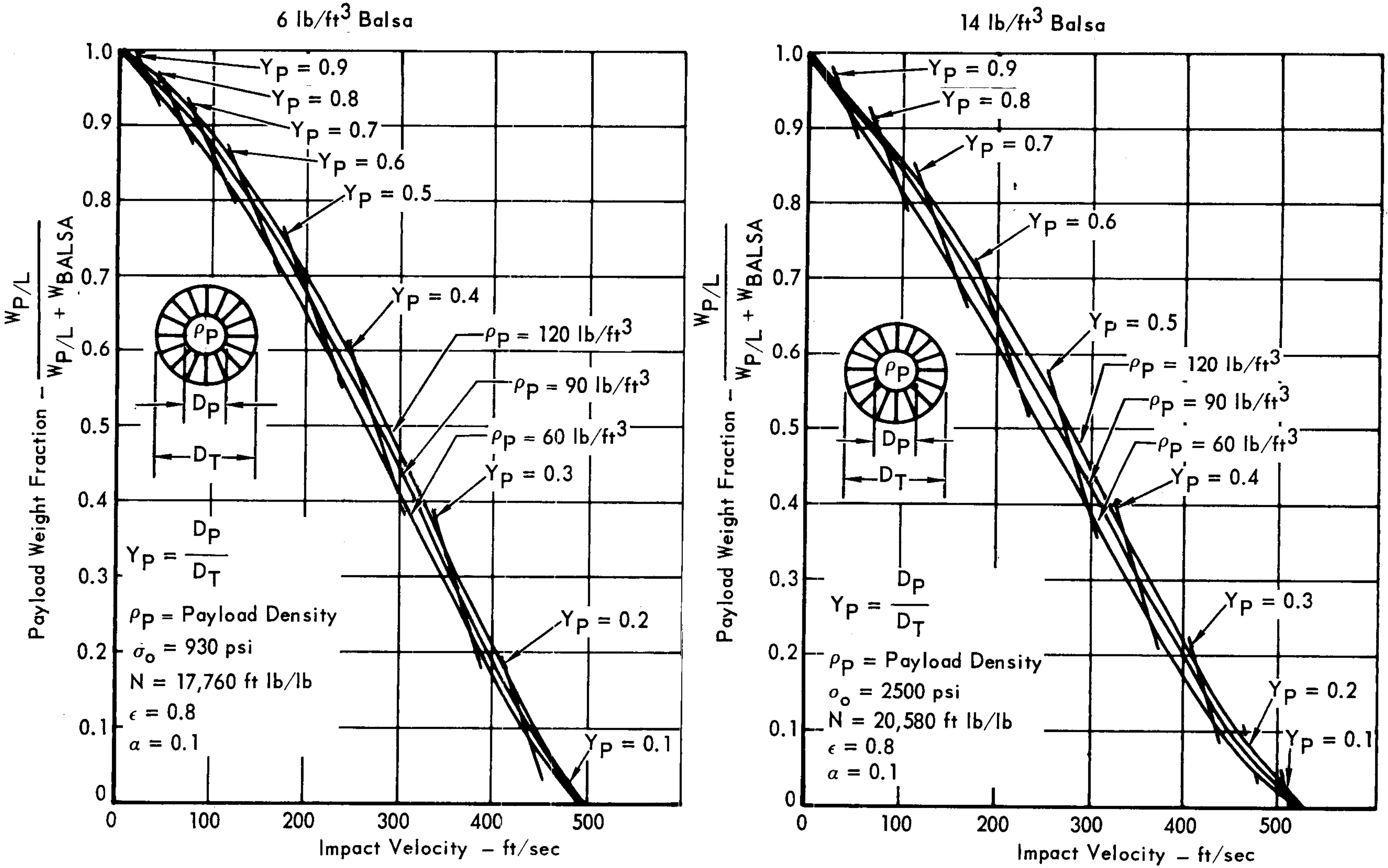
6 lb/ft³ Balsa

14 lb/ft³ Balsa

Figure 5.15-33

IDP PEAK IMPACT DECELERATION LOADS FOR SPHERICAL BALSA WOOD IMPACT LIMITER

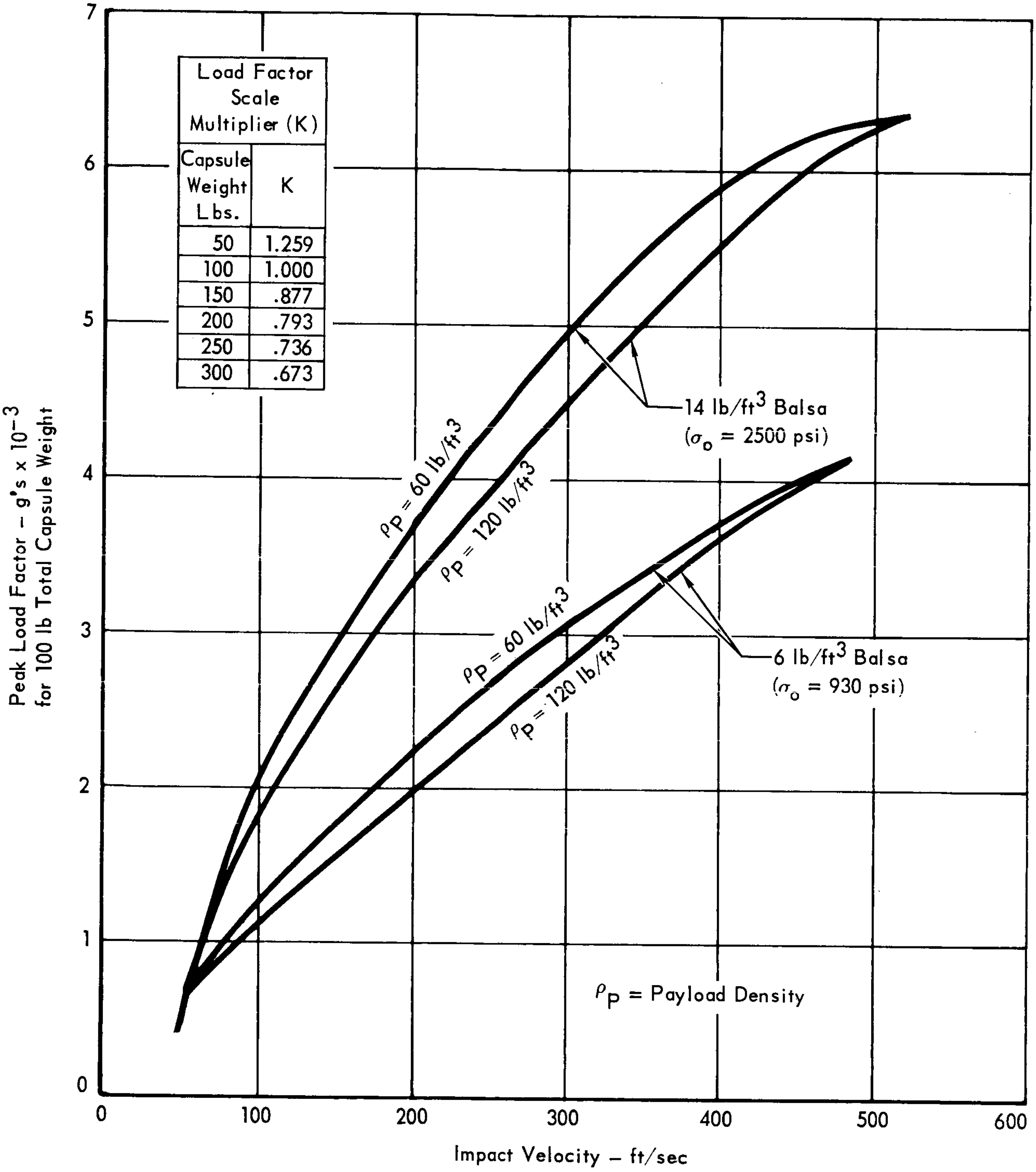

Load Factor Scale Multiplier (K)

Capsule Weight Lbs.	K
50	1.259
100	1.000
150	.877
200	.793
250	.736
300	.673

Figure 5.15-34

In fact, somewhat higher payload weight fractions were indicated based on the assumption that any disk impact limiter designed to provide adequate landing protection during either a face or edge impact will also successfully survive an oblique impact. This result appears reasonable in view of the fact that during an oblique impact the center of gravity of the disk will not be aligned with the decelerating force vector, or, if it is, it will be at such a shallow angle with respect to the impact limiter surface that lateral slippage will occur; thus a rotation will be imparted to the landing package allowing the balance of its kinetic energy to be dissipated by subsequent face impact(s).

Conclusions - A minimum six pound per cubic foot density balsa wood is the best impact limiter material for IDP. For a nominal 90 lb/ft^3 density payload with a 6 lb/ft^3 balsa impact limiter the payload weight fraction ranges, approximately linearly, from .75 to .31 as the impact velocity increases from 150 ft/sec to 350 ft/sec. Similarly, the peak impact deceleration load will range from 1700 g's to 3300 g's for a 100 pound payload and from 1300 g's to 2600 g's for a 200 pound payload.

A maximum payload weight fraction is achieved with a maximum payload density. Although the design curves of Figure 5.15-33 indicate only a 5% gain in payload weight fraction between 60 and 120 lb/ft^3 payload density, the effect is in reality much greater due to the reduced structural weight fraction within the payload which accompanies a 200 g reduction in peak impact load factor and a 50% reduction in payload volume.

Similarly, increasing the balsa density from 6 lb/ft^3 to 14 lb/ft^3 to reduce perhaps the total capsule diameter only decreases payload weight fraction about 3% according to the design curves. However, the effect is in reality much more significant due to the large increase in structural weight fraction which accompanies a 1000 to 2000 g_E increase in peak impact load factor.

Finally, the significant effect of impact velocity on payload weight fraction should be recognized. For a nominal design impact velocity of 125 ft/sec, which is a reasonable equilibrium value for parachutes, the payload weight fraction for a 90 lb/ft^3 payload, 6 lb/ft^3 balsa package is .83. For each additional 10 ft/sec of impact velocity this weight fraction is reduced approximately 2%. Thus, if impact protection for a 220 ft/sec horizontal wind velocity must be taken into account, the payload weight fraction will reduced to .56 for a 253 ft/sec total velocity, unless an alternate scheme for removing the horizontal wind component of the total impact velocity can be determined.

The effect of wind velocity on peak impact deceleration is also significant. For a 90 lb/ft^3 payload, 6 lb/ft^3 balsa package weighing 100 lb, increasing the impact velocity from 125 ft/sec to 250 ft/sec will increase the peak impact deceleration from 1700 g's to 2500 g 's.

5.15.5.3 Payload Weight Optimization - It has been concluded that due to the unknown nature of the Martian terrain and the presence of possible high horizontal surface winds it will be necessary to equip the IDP with an external balsa wood impact limiter capable of dissipating the total terminal velocity. Similarly, it has been demonstrated that in order to reduce the package's terminal velocity to a level consistent with the capabilities of omnidirectional balsa wood impact limiters (<500 ft/sec) it will be necessary to utilizing a parachute for interim descent retardation assuming IDP/CBS separation occurs above altitudes of approximately 1000 feet. The questions which remain are:

- In what combination should these devices be used to achieve a maximum payload weight fraction?
- What is the design terminal velocity condition?
- What is the influence of the assumed horiaontal wind velocity?
- Below what nominal altitude may the parachute be eliminated?

The answers to these questions are presented in the following paragraphs in terms of achievable payload weight fraction.

Parachute/Limiter/Payload Weight Trade - The net payload weight fraction for a combination parachute/limiter landing system may be expressed as follows:

$$\frac{W_{P/L}}{W_{P/L} + W_{LIM} + W_{CHUTES}} = \frac{W_{P/L} + W_{LIM}}{W_{P/L} + W_{LIM} + W_{CHUTE}} \circ \frac{W_{P/L}}{W_{P/L} + W_{LIM}}$$

$$= \begin{array}{c}\text{Parachute}\\ \text{weight fraction}\end{array} \circ \begin{array}{c}\text{Impact Limiter}\\ \text{weight fraction}\end{array}$$

where $W_{P/L}$ = payload weight

W_{LIM} = impact limiter weight

W_{CHUTE} = parachute weight

The two weight fractions on the right hand side of the equation will be recognized as the parachute and impact limiter payload weight fractions derived as a function of velocity in the preceding parts of this section. These curves and their product, representing the net payload weight fraction for a combined parachute limiter landing system are shown in Figure 5.15-35. These curves were prepared based on the assumption that the descent is made in the least dense atmosphere (VM-7) with a horizontal wind velocity of 220 feet per second all of which is transmitted to the parachute-suspended spherical payload. Impact was assumed to occur on a surface oriented normal to the total velocity vector. An examination of the referenced figure reveals that the maximum payload weight fraction which can be achieved for a parachute/limiter system is 0.52. This optimal design point occurs at a vertical descent velocity of 120 ft/sec and a total impact velocity of 250 ft/sec. These velocities were selected as the preliminary design values for the IDP configurations described herein.

The effect of assuming higher or lower horizontal winds on the maximum achievable payload weight fraction was also investigated. The result is shown in Figure 5.15-36. It may be seen that up to a 25% increase in payload weight fraction may be achieved by reducing the assumed horizontal wind velocity to zero. Conversely, if we assume a 220 ft/sec surface wind blowing down a 34° slope with an impact normal to the total velocity vector we find that the system optimizes at a vertical parachute velocity of 90 ft/sec; a total velocity of 280 ft/sec; and a payload weight fraction of 0.42. Based on engineering judgment, the practical occurrence of either of the aforementioned conditions appears remote; they were therefore dismissed as unrealistic design points.

Parachute/Limiter Trade Altitude - The gross payload weight fraction for a free falling payload with impact limiter alone will vary depending on the deployment altitude and initial velocity. This relationship is shown in Figure 5.15-37 for a nominal CBS landing profile assuming no acceleration due to horizontal winds. It will be noted that for a "limiter only" lander, the payload fraction varies from zero, for a 1000 foot separation altitude, to unity for a near surface separation. Superimposed on this plot is the previously derived constant or optimal payload weight fraction for the combined parachute/impact limiter descent retardation system.

The figure indicates that for deployment altitudes below approximately 600 feet, the impact limiter alone would provide a more favorable fraction of payload weight to total weight. Above 600 feet, the parachute-limiter combination would

IDP PAYLOAD WEIGHT FRACTION vs TOTAL IMPACT VELOCITY

(220 FT/SEC HORIZONTAL WIND)

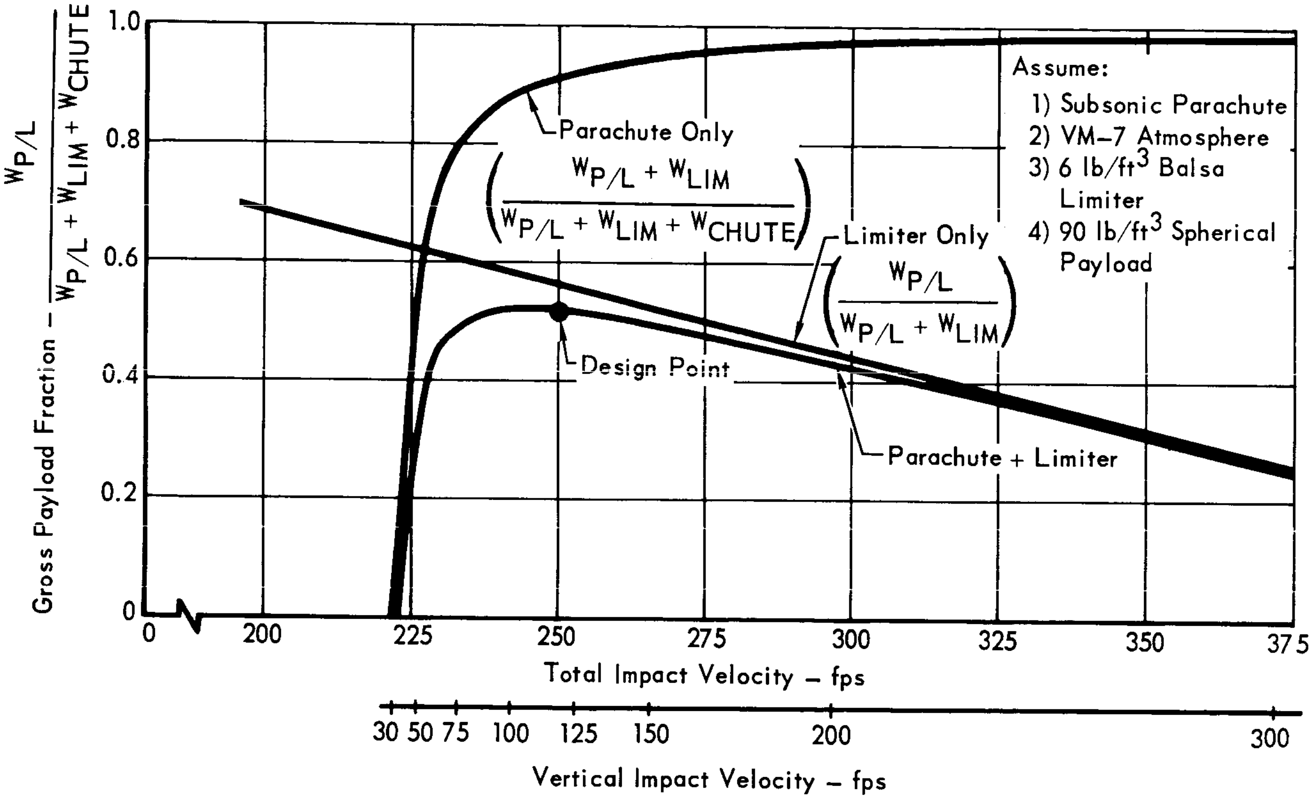

Figure 5.15-35

EFFECT OF HORIZONTAL WIND VELOCITY ON MAXIMUM IDP PAYLOAD WEIGHT FRACTION
(PARACHUTE/LIMITER LANDING SYSTEM)

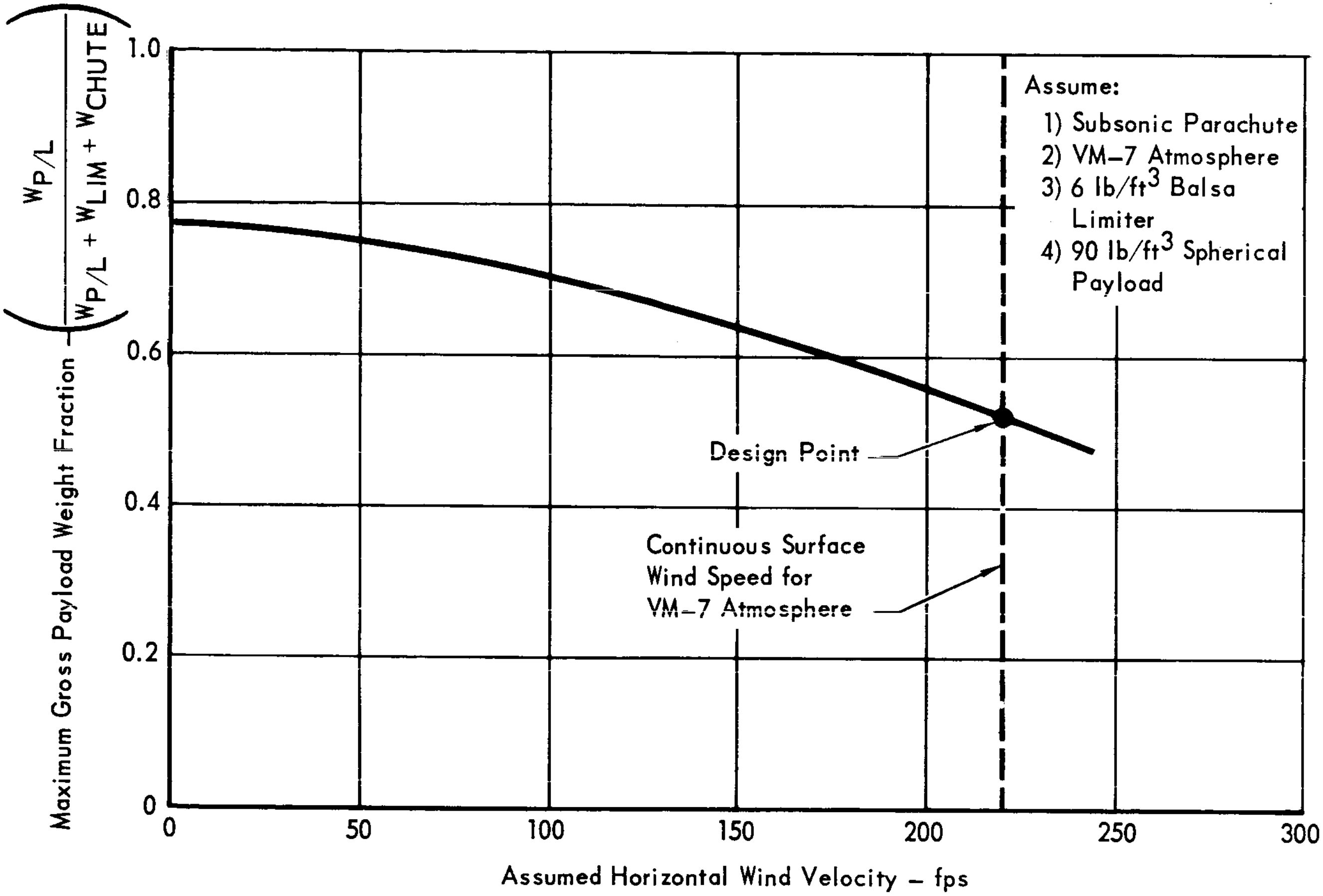

Figure 5.15-36

EFFECT OF IDP DEPLOYMENT ALTITUDE ON PAYLOAD WEIGHT FRACTION

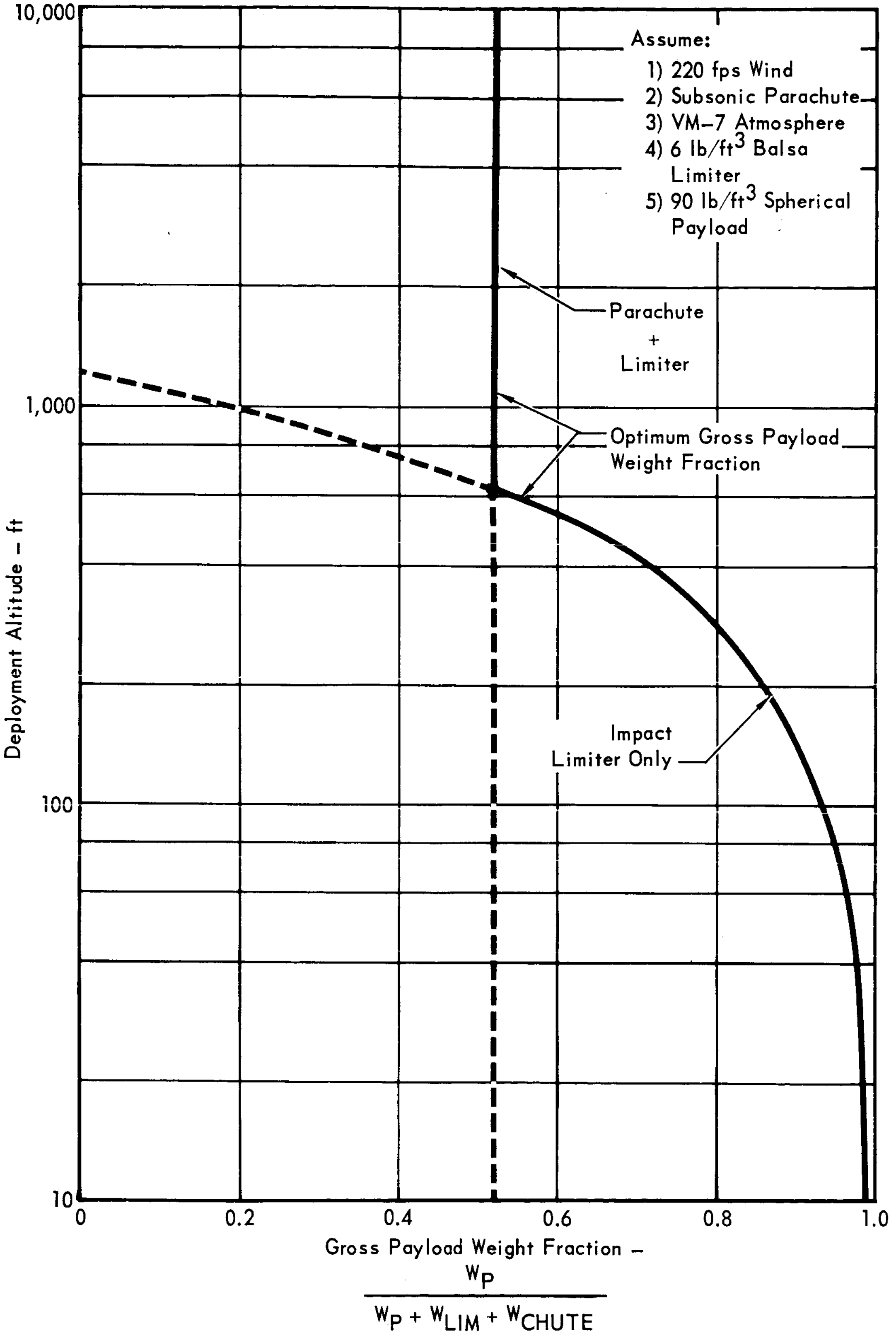

Figure 5.15-37

provide the highest fraction of payload weight. It should be noted that the VM-7 atmosphere with a horizontal wind velocity of 220 feet per second was used and that this wind velocity was assumed to be fully transmitted to the parachute suspended payload. Any horizontal velocity which might be imparted by the wind to a free falling payload was neglected since its effect on total impact velocity is only a fraction of one percent for the deployment altitudes of interest.

Conclusions

a. To maximize payload weight fraction, a parachute is required at separation altitudes above 600 feet.

b. For a parachute/limiter landing system and 220 ft/sec winds:

- The maximum payload weight fraction is 0.52.
- The optimum vertical parachute descent velocity is 120 ft/sec.
- The optimum total impact limiter design velocity is 250 ft/sec.
- The weight distribution for a spherical payload is summarized in Figure 5.15-38.
- For the optimal system the weight allocation is:

Payload	.52
Parachute	.07
Impact Limiter	.41

5.15.5.4 Configuration Selection and Evaluation - The selection of an IDP configuration was initiated by consideration of the range of possible shapes which an object to be provided with omnidirectional impact protection could assume. Considered were spheres, oblate spheroids, prolate spheroids, tetrahedrons, wedges, cylinders, disks, cubes, dumbbells, toroids, cones, truncated cones, hemispheres, pyramids, ellipsoids, and lenticular configurations. Combinations of the foregoing basic geometrical shapes were also considered.

It is apparent that from a weight efficiency standpoint the sphere offers the optimal configuration in terms of minimum structural and impact limiter weight fraction for a given landing condition. However, from an operational standpoint, it possesses the two prime liabilities of assuming a completely random orientation following impact and simultaneously offering poor inherent stability. The spherical shape therefore requires either an auxillary means of achieving post impact erection and stabilization or an omnidirectional instrument deployment, RF radiation, and stabilization capability. It is threfore attractive to examine only those alternate shapes which retain to the greated extent possible the high payload weight fraction of the sphere and additionally overcome its two basic

IDP WEIGHT DISTRIBUTION FOR PARACHUTE/LIMITER LANDING SYSTEM

(220 FT/SEC HORIZONTAL WIND)

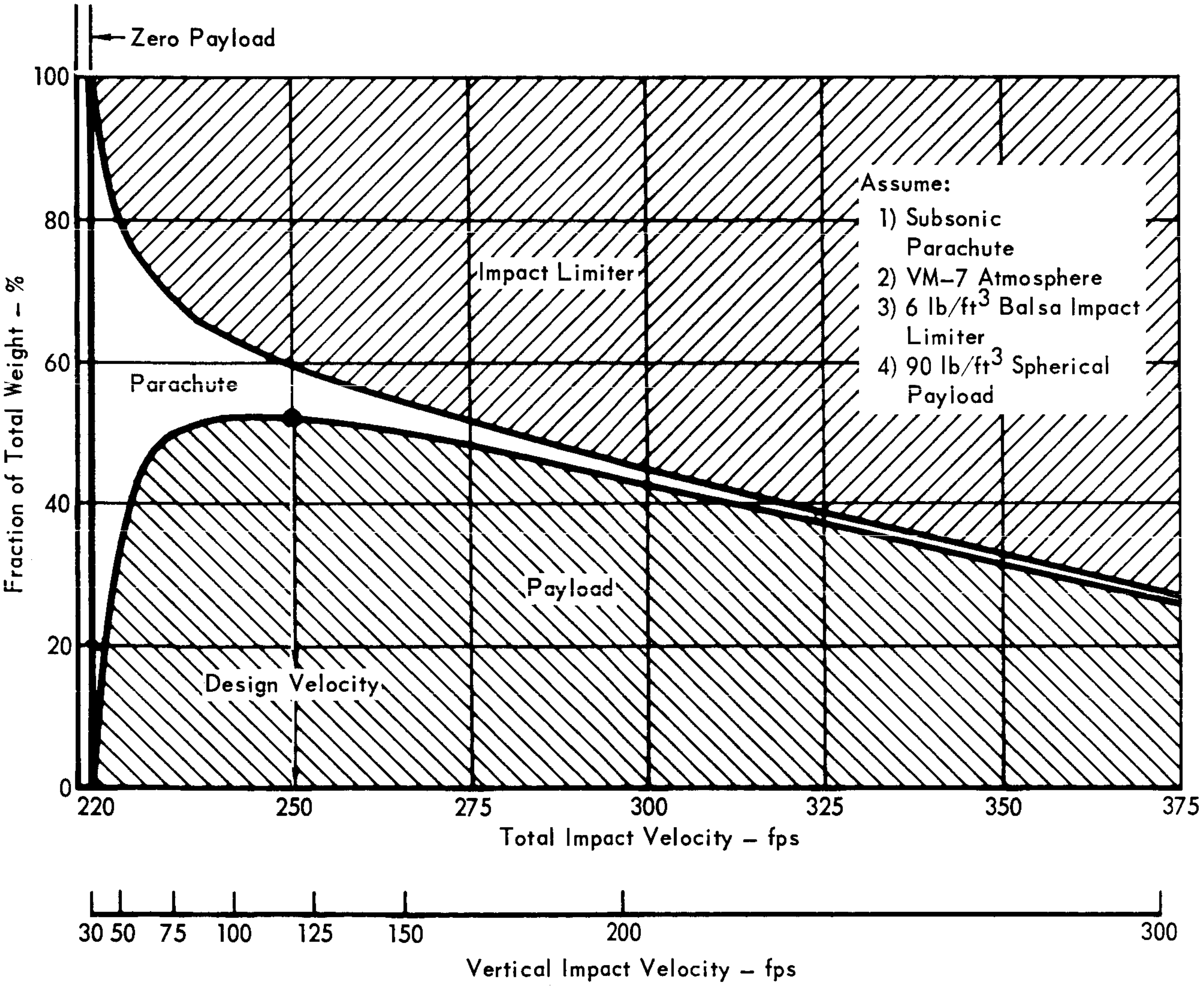

Figure 5.15-38

operational liabilities. This eliminates from further consideration shapes such as the tetrahedron, wedge, cube, cone, hemisphere, and pyramid which are relatively inefficient structurally and do not significantly reduce the degree of random package orientation or instability. Similarly, the dumbbell and torus are eliminated primarily on the basis of their structural inefficiency. This leaves the spheroids, cylinders, disks, ellipsoids, and lenticular configurations. For the purpose of preliminary concept definition, these configurations may all be grouped into the following three general categories: spheres, disks, and cylinders. The sphere provides the best payload weight efficiency; the disk provides relatively good payload weight efficiency coupled with bistable orientation and inherent stability; and the cylinder offers a possible design compromise midway between.

Candidate Configurations - The design investigation was initiated with the evaluation of nine specific configurations each of which fall into one of the three perferred shape categories enumerated above, i.e., spheres, disks and cylinders. The characteristics of this initial set of nine configurations (A through I) are presented in Figure 5.15-39. Each configuration provides for the erection of a vertical instrument sensor mast. This was considered a requirement to achieve accurate temperature and wind velocity data.

For comparison purposes a brief investigation was made of a configuration not requiring mast deployment. This approach, although attractive from a mechanical design and reliability standpoint, did not appear practical in terms of quantity and quality of scientific data. A wind velocity measurement was not feasible and temperature could be measured only at the surface of the impact limiter. Accurate interpretation of the latter measurement in terms of ambient atmospheric temperature appeared doubtful because the sensor will respond primarily to the equilibrium surface temperature of the limiter which is a small function of ambient temperature and a large function of several poorly defined parameters such as the convective heat transfer coefficient and the surface emissivity. An evaluation and ranking of the nine configurations shown in Figure 5.15-39 resulted in an initial recommendation of designs A, C, E, and I for further study.

The E or Bi-stable disk configuration ranked first in the evaluation and was therefore an obvious initial choice.

The four masted sphere and three master cylinder configurations C and I, respectively, were ranked a near second and third. In view of the close resemblance of the configurations, however, an engineering judgment was made to direct further study towards only the spherical configuration.

CANDIDATE INDEPENDENT DATA PACKAGE CONFIGURATIONS

	Sphere				Dis	
	A	B	C	D	E	F
CONFIGURATION	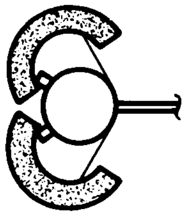	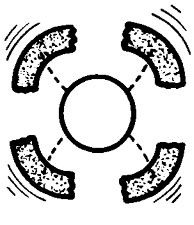	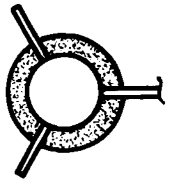	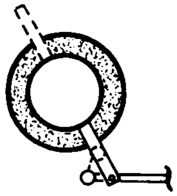	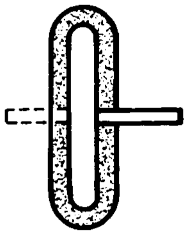	
	Clamshell Sphere With Crushable Impact Limiter	Flotation Sphere With Removable Impact Limiter and Auxiliary Legs (6)	Four Masted Sphere With Crushable Impact Limiter (4 Sets of Atmospheric Sensors)	Two Masted Sphere With Crushable Impact Limiter (2 Sets of Atmospheric Sensors	Bi-stable Disc With Top Deploying Instrument Mast (2 Sets of Atmospheric Sensors). Crushable Limiter	Bi-stable With Side Deploying Instrumen Mast (Gra Erection)
PERFORMANCE EVALUATION (1 = BEST)	2	3	3	1	1	1
	2	1	1	1	2	2
	2	1	2	3	1	3
	1	2	1	3	1	1
	1	1	1	3	1	3
	2	3	1	3	1	3
	2	1	2	2	1	2
	2	2	3	2	1	1
	2	3	1	1	1	1
	4	5	2	7	1	6
UNDESIRABLE DESIGN FEATURES	X					
		X				
		X				
			X		X	X
		X				

Figure 5.15-39

		Cylinder		Shape
	G	H	I	Designation
	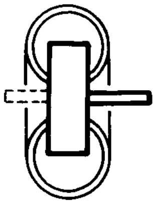	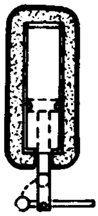	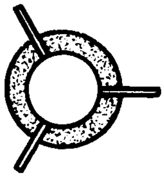	Sketch
Disc ity	Bi-stable Disc With Top Deploying Instrument Mast (2 Sets of Atmospheric Sensors). Inflatable Toroid Impact Limiter	Flotation Cylinder With Fixed Impact Limiter and End Deploying Instrument Mast (Gravity Erection)	Three Masted Cylinder With Fixed Impact Limiter (3 Sets of Atmospheric Sensors)	Description
	1	3	2	Payload Weight Fraction
	3	2	2	Impact Survival
	3	3	2	Terrain Independence
	2	3	2	Stability
	2	3	1	Data Measurement
	3	3	1	Functional Reliability
	3	2	2	Development Risk
	1	2	2	Design Flexibility
		2	1	Ease of Manufacturing
	8	9	3	Performance Ranking
				Active Payload Erection (Reduced Reliability)
				Terrain Contamination (VSL Effects)
				Limiter Removal Reqd (Poor Thermal Isolation)
	X		X	Vertical Sensing (Reduced Reliability)
		X		Flotation Required (Poor Transit Electrical Access)

5/15-73-2

The fourth ranking configuration A was the erecting or clamshell sphere. It was noted that this configuration's lower ranking was primarily attributable to the probability of its erection mechanism sustaining damage during impact and to the absence of an impact limiter following erection to serve as thermal insulation. Thus, it was decided to further pursue this design approach, but with the modification that the erection mechanism be retained within the package during impact, and , then, subsequently deployed without impact limiter removal.

The fifth ranking configuration was the flotation sphere. It however, possessed three highly undesirable design features:

a. The impact limiter required removal by pyrotechnics to effect instrument porting thereby severely contaminating the surrounding terrain.
b. The impace limiter was not retained for post-landing thermal insulation.
c. The flotation barrier greatly hampered transit access for battery charge and critical CBS data monitoring.

For these reasons further evaluation of the flotation sphere concept was terminated.

The remaining four configurations D, F, G, and H did not merit further study based primarily on their high reliance on a relatively known terrain.

Preferred Concept Definition - In review, the configurations selected for final study were the erecting sphere,A, the four masted sphere, C, and the disk, E. Several layouts of each of these configurations were prepared in an attempt to overcome their inherent design deficiencies.

The results of an evaluation conducted on the three developed configuration layouts is summarized in Figure 5.15-40. The four masted sphere rated relatively low. It was primarily deficient in the following areas:

a. Poor packaging efficiency.
b. Complex 4-mast erection.
c. Risk of atmospheric sensor contamintion during erection.
d. Poor thermal isolation by the 4 conducting masts.
e. Difficult manufacture, assembly and checkout.
f. Low adaptability to design changes due to a severely cut-up internal volume.
g. Requirement of an orientation sensor capable of resolving the uppermost of 4 masts only 110 degrees apart.

A satisfactory erecting sphere design with telescoping erecting arms stored within the package payload was prepared. In operation this configuration first rolled itself on its side by extending three legs out the top of the payload.

SUMMARY OF IDP CONFIGURATION EVALUATION

MISSION EVALUATOR	CONFIGURATION SCORE AND RANKING		
	DISK	ERECTING SPHERE	4 MASTED SPHERE
I – Design Performance (System Performance)	70.0% (1)	67.8% (2)	65.1% (3)
II – Operational Performance (Versatility and Cost)	71.3% (2)	71.5% (1)	58.8% (3)
III – Functional Reliability (Probability of Mission Success)	78.3% (2)	83.0% (1)	75.7% (3)
IV – Development Risk	81.8% (2)	83.3% (1)	70.4% (3)
Weighted Average*	75.6% (2)	77.1% (1)	68.3% (3)

*Weighting:		
	Design Performance	20%
	Operational Performance	25%
	Functional Reliability	35%
	Development Risk	20%

Figure 5.15–40

It then erected itself to a vertical orientation by a simultaneous rotation of all three legs about a point just outside the impact limiter surface. Actuation was accomplished by a single internal gas actuated piston. This configuration received a numerical rating nearly equal to that of the disk. It was rejected, however, due to the active nature of its erection and the possible interferences of an unknown terrain.

The disk configuration appeared to possess all of the advantages of the other configurations with none of their disadvantages and additionally offered:

a. Ease of manufacture.
b. Ease of assembly.
c. Ease of checkout.
d. Excellent stability.

The bi-directional orientation was accommodated by allowing selective deployment of dual atmospheric sensor modes. The necessity of erecting a single antenna to achieve the requisite 150° antenna beam coverage was circumvented by outfitting the disk with six antennas conceptually located on the six faces of a cube. This 4π steradian antenna coverage allowed a significant increase in the MSFK bit rate, the transmission of composition, water vapor, and pressure data even though porting was not achieved; and the transmission of the foregoing plus temperature and possibly wind velocity even if the capsule comes to rest on edge.

Conclusion - A disk configuration possessing bi-directional atmospheric sensor masts and six antenna providing 4π steradian coverage is the preferred preliminary design concept for the Independent Data Package.

5.15.5.5 Thermal Control Considerations - The temperature of the Martian surface is expected to range from a minimum of -190°F to a maximum of 120°F. Since the operating temperature of the Independent Data Package must be maintained between 32°F and 140°F, primarily to prevent damage and to maintain operating efficiency in the silver zinc battery, thermal control must be provided.

The IDP thermal control system is designed to maintain acceptable equipment temperatures under two extreme environmental histories:

a. A hot clear day environment characterized by a peak Mars surface temperature of 120°F at mid-day and a minimum surface temperature of -80°F just before dawn.
b. A cold, cloudy day environment characterized by a continuous -190°F day and night Mars surface temperature.

By designing the thermal control system to meet these extreme environments, the successful operation of the thermal control system with any actual Martian surface condition is assured.

The recommended IDP thermal control concept has three major elements: insulation, a heat sink, and heaters. Of these elements only heaters are not inherent in the basic IDP design concept and must be included specifically for thermal control. Insulation is required to prevent excessively low temperatures during exposure to the nighttime portion of the hot day environment and to limit the required heater power to reasonable levels during the exposure to the cold day environment. The balsa wood impact limiter has a thermal conductivity of 0.02 BTU/ft hr°F. This value compares quite favorably with the conductivities of other materials suitable for the insulation of a hard landing Mars surface capsule. Thus the impact limiter serves natrually as an IDP insulator. Of course, the performance of the insulation will be degraded locally in areas crushed during landing. It is estimated that the conductivity of the balsa wood may be increased by a factor of two in the impact area. However, using the impact limiter as the basic insulation system leads to a more efficient overall IDP design than providing a separate internal insulation blanket.

A heat sink is required to absorb the relatively high internal heat dissipation during data transmission. The heat sink damps out variations in IDP temperature during exposure to the cyclical hot day environment and reduces the required heater energy. The natural heat capacity of the IDP equipment and structure (approximately 9 BTU/°F) is sufficient for these purposes.

Heaters are required to maintain the IDP temperature at an acceptable level during exposure to the continuous -190°F cold day environment. The worst case occurs for an evening landing when the IDP may remain in the cold environment for 22 hours with an equipment dissipation averaging only 4 watts. During the relatively high dissipation data transmission period, heater power is not necessary. A total of 100 watt-hrs of heater energy are required for this design condition. Possible heat sources include electrical heaters and chemical heaters. Electric heaters are of proven reliability and are easy to use. Suitable chemical heaters are not yet available, however, there are no apparent technical barriers to their employment. It is estimated that a 100 watt-hr chemical heater would weight one pound.

Refined Temperature Control for Special Devices - The transmitter crystal oscillator and the gas chromotograph detectors and perhaps columns require temperature control within ± 5°F. Since it is impractical to control the entire payload within such narrow limits, special temperature control devices will be required for these elements. One approach would be to provide a small thermoelectric heater-cooler capable of providing steady state temperature control for any payload temperature between 32° and 140°F. A second,more economical approach, would be to use a heater only and provide temperature control near the upper operating limit of the package. This latter system would require local insulation of the critical element; a heat sink of fusinn material whose melting point is at the control temperature; and an electric heater.

SECTION 5.15 REFERENCES

5.15-1 JPL EPD 283, Revision 2, Planned Capabilities of the DSN for VOYAGER 1973, 1 January 1967